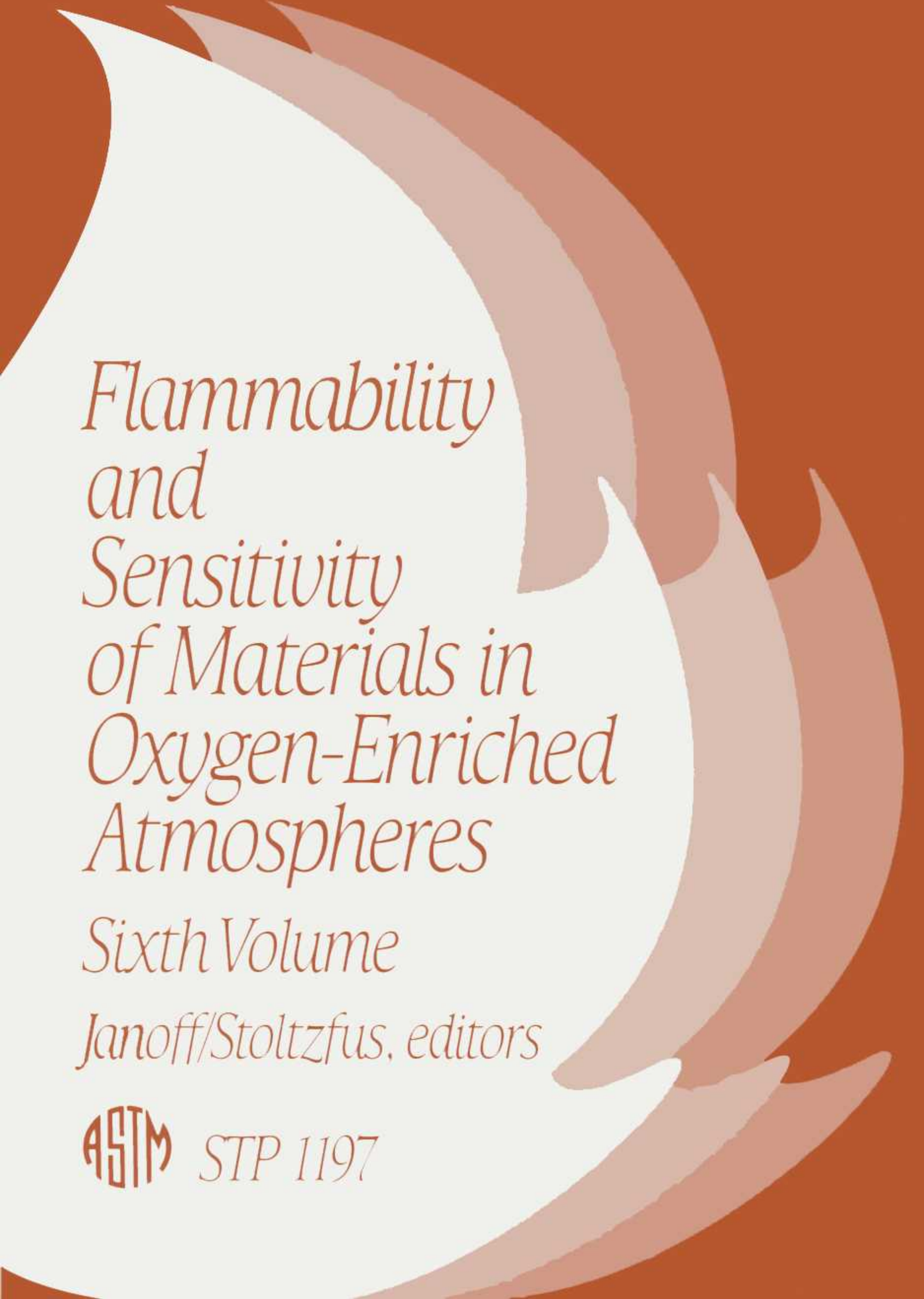

Flammability and Sensitivity of Materials in Oxygen-Enriched Atmospheres

Sixth Volume

Janoff/Stoltzfus, editors

ASTM STP 1197

STP 1197

Flammability and Sensitivity of Materials in Oxygen-Enriched Atmospheres: 6th Volume

Dwight D. Janoff and Joel M. Stoltzfus, editors

ASTM Publication Code Number (PCN)
04-011970-31

ASTM
1916 Race Street
Philadelphia, PA 19103

Library of Congress

ISBN: 0-8031-1855-4
ISSN: 0899-6652
ASTM Publication Code Number (PCN): 04-011970-31

Photocopy Rights

Authorization to photocopy items for internal or personal use, or the internal or personal use of specific clients, is granted by the AMERICAN SOCIETY FOR TESTING AND MATERIALS for users registered with the Copyright Clearance Center (CCC) Transactional Reporting Service, provided that the base fee of $2.50 per copy, plus $0.50 per page is paid directly to CCC, 27 Congress St., Salem, MA 01970; (508) 744-3350. For those organizations that have been granted a photocopy license by CCC, a separate system of payment has been arranged. The fee code for users of the Transactional Reporting Service is 0-8031-1855-4/93 $2.50 + .50.

Peer Review Policy

Each paper published in this volume was evaluated by three peer reviewers. The authors addressed all of the reviewers' comments to the satisfaction of both the technical editor(s) and the ASTM Committee on Publications.

To make technical information available as quickly as possible, the peer-reviewed papers in this publication were printed "camera-ready" as submitted by authors.

The quality of the papers in this publication reflects not only the obvious efforts of the authors and the technical editor(s), but also the work of these peer reviewers. The ASTM Committee on Publications acknowledges with appreciation their dedication and contribution to time and effort on behalf of ASTM.

Printed in Ann Arbor, MI
September 1993

Foreword

The Sixth International Symposium on Flammability and Sensitivity of Materials in Oxygen-Enriched Atmospheres was presented at Noordwijk, The Netherlands, from 11 to 13 May 1993. The symposium was sponsored by ASTM Committee G-4 on Compatibility and Sensitivity of Materials in Oxygen-Enriched Atmospheres. Kenneth McIlroy, Praxair, Inc., Linde Division, and Mike Judd, European Space Agency/ESTEC, served as cochairmen of the symposium.

Acknowledgment

The quality of papers in this publication reflects not only the obvious efforts of the authors but also the unheralded work of the reviewers. Coleman Bryan, Barry Werley, Kenneth McIlroy, Richard Paciej, Len Schoenman, Melvyn Branch, Michael Yentzen, Bill Royals, Marilyn Fritzemeier, Dwight Janoff, and Joel Stoltzfus acted as review coordinators, enlisting appropriate reviewers and ensuring that reviews were completed properly and submitted on time. The editors also wish to acknowledge Rita Hippensteel for her efficient and diligent assistance in preparing this document.

Joel M. Stoltzfus
Dwight D. Janoff

Contents

KEYNOTE ADDRESS

DEVELOPMENT AND EVALUATION OF TEST METHODS

IGNITION AND COMBUSTION OF POLYMERS

IGNITION AND COMBUSTION OF METALS

ANALYSIS OF IGNITION MECHANISMS

STRUCTURED PACKINGS FOR CRYOGENIC AIR SEPARATION PLANTS

MISCELLANEOUS

Overview

The purpose of the symposium on flammability and sensitivity of materials in oxygen-enriched atmospheres was to build upon the foundation provided by previous symposia. The aim was to:

- provide a reference text on a subject that is not widely addressed in accessible literature,
- build a reference of the concepts and practices used in designing oxygen systems,
- provide a data base to support the use of ASTM Committee G-4 guides and standards, and
- serve as a guide to Committee G-4 members in their future efforts to address the problems of oxygen-use safety.

This volume, in addition to those from previous symposia (STP 812, 910, 986, 1040, and 1111), is an important resource on the subject of the proper use of materials in oxygen-enriched environments. Committee G-4's contribution to the resources on the subject also include four standard guides (G 63, G 88, G 93, and G 94), three standard test methods (G 72, G 74, and G 86), and a fourth test method for determining the promoted ignition and combustion properties of metallic materials that is currently being balloted. The latest contribution is a Standards Technology Training course entitled "Controlling Fire Hazards in Oxygen-Handling Systems." In this course, attendees are taught to apply the available resources to improve the safety of oxygen-handling systems. We are confident that this volume will be a welcome contribution to the subject.

This STP comprises six sections. The first section presents two papers on the development and evaluation of test methods. Werley proposes an approach to more cost-effective gaseous impact testing. Sidebotham et al. presents a new test method for determining the minimum oxygen concentration to support an intraluminal flame. These papers may provide the impetus to develop new standard test methods or to modify existing ones.

The second section, which addresses the ignition and combustion of polymeric materials, comprises four papers. Wolf et al. discuss the spontaneous ignition temperatures of tracheal tube materials. This work extends previous work on oxygen index and flame spread in materials used in operating rooms. Bruley and de Richemond discuss recommendations for preventing fires in the oxygen-enriched atmospheres that may occur during surgery. The effects of diluent gases in oxygen on the flammability of polymers at high pressures is discussed by Hirsch and Bunker. They observe that at some pressure between 20.7 and 34.5 MPa, even the most burn resistant polymers become flammable in air, indicating that high-pressure air systems require enhanced safety precautions. Finally, Shelley et al. study the effect of hydrocarbon oil contamination on the ignition and combustion properties of PTFE tape in oxygen.

Seven papers comprise the third section in which data on the ignition and combustion of metals and alloys are presented and applied. These papers indicate the need for Committee G-4 to standardize the promoted combustion test method and provide a common set of definitions that can be used by experimenters in presenting their data. Steinberg et al. raise the question as to the applicability of metals flammability data obtained on earth to oxygen systems used in space. They point out that metals and alloys appear to be more flammable in a reduced-gravity environment than in a one-gravity environment. The final three papers in this section, along with the keynote address paper, discuss the application of metals ignition and combustion data to real systems; a process that requires the development and use of ones "technical judgment."

Regarding the paper on the promoted ignition-combustion behavior of carbon steel in oxygen-gas mixtures by McIlroy et al., a peer reviewer notes that these data suggest that 6-mm diameter rods of carbon steel are more flammable than 3-mm diameter rods at low pressures. This result contradicts the existing understanding of the role of dimension on metals flammability and is particularly significant if it is not the result of experimental technique.

The fourth section presents five papers in which specific ignition mechanisms are analyzed and discussed. The papers by Abbud-Madrid et al., Steinberg et al., and Shelley et al. discuss the development of models for the ignition of metals and alloys. This type of effort is absolutely necessary to identify and to begin to bridge the gaps in our understanding of the thermodynamic and kinetic processes involved in the ignition and combustion of materials. The better these processes and the parameters affecting them are understood, the more able we will be to build safer systems.

The paper by Shelley et al. concludes that polytetrafluoroethylene exhibits surface-burning. Our peer reviews have found this conclusion controversial. One reviewer does not feel the observations cited form an adequate basis to deduce surface combustion is occurring.

Structured packing materials for cryogenic air separation columns is the subject of the four papers in the fifth section. Werley et al. present a critical review of aluminum flammability data that is the cooperative result of several oxygen producers. This review, and the papers by Zawierucha et al. and Barthélémy, represent a large portion of the collective and individual work generated by a Compressed Gas Association task force.

The final section contains four papers on oxygen system safety, cleaning for oxygen systems, and a device for measuring wear and friction in high pressure oxygen. The paper on oxygen system safety by Koch represents a good "primer," offering guidance to individuals new to the subject. This paper will be appearing, in essence, as an appendix to ASTM G 88, "Standard Guide for Designing Systems for Oxygen Service."

These papers confirm that the objectives of the Symposium were met. The papers presented here (in conjunction with previous symposia volumes) provide a previously unavailable reference of oxygen system design concepts and practices. These volumes provide a data base that supports the use of ASTM Committee G-4 guides and standards. In addition, they serve as a guide to committee members in their future efforts to address the problems of safe oxygen use.

Joel M. Stoltzfus

NASA Johnson Space Center,
White Sands Test Facility, Las Cruces, NM 88004;
symposium chairman and editor.

Dwight D. Janoff

Lockheed Engineering and Sciences Company,
NASA Johnson Space Center, Houston, TX 77058;
symposium chairman and editor.

Keynote Address

Robert Lowrie[1]

OXYGEN COMPATIBILITY OF METALS AND ALLOYS

REFERENCE: Lowrie, R., "Oxygen Compatibility of Metals and Alloys," Flammability and Sensitivity of Materials in Oxygen-Enriched Atmospheres: 6th Volume, ASTM STP 1197, Dwight D. Janoff and Joel M. Stoltzfus, Eds., American Society for Testing and Materials, Philadelphia, 1993.

ABSTRACT: The oxygen compatibility of metals and alloys is highly important because they constitute the major part of most oxygen systems. The recent development of semi-standard tests for metal specimens has greatly increased our understanding of the ignitability and combustibility of commonly used metals and alloys. The results of such testing are summarized and discussed for the major alloy groups.

The need for interaction among material choice, component and system design, and operational procedures to arrive at the most economical safe solution is stressed. Some possible ways for producing metals or alloys with decreased combustibility in oxygen are suggested.

KEY WORDS: oxygen, metals, alloys, oxygen compatibility, safety, ignitability, combustibility, flammability, selection, testing, particle impact, frictional heating, promoted combustion

INTRODUCTION

Metals and alloys have always had an important role in oxygen equipment, and they will continue to do so. Historically, metals -- and from here on when I say metals for brevity I will mean metals and alloys -- have been used in all types of equipment, tools, and decorative objects because of the combinations of ductility, strength, and fabricability that can be obtained with them.

---

[1] Consultant, 2206 East Alvarado St., Fallbrook, CA 92028.

In contrast, ceramic materials, while they may have high strengths, are not ductile at ambient temperatures and are notch sensitive. Thus, they are used chiefly where the imposed stresses are low or compressive. However, the oxide ceramics have the advantage for oxygen service of being truly nonflammable.

Many polymers exhibit appreciable ductility and can be fabricated readily, but their strengths are much lower than most structural alloys. Polymers reinforced with continuous ceramic fibers can attain high strengths, and in particular, high strength-to-weight ratios in the direction parallel to the reinforcement. However, they no longer have appreciable ductility in that direction. With regard to oxygen compatibility, the polymers are generally more easily ignited than are the usual structural metals.

A comprehensive survey on compatibility of structural metals with oxygen was written by Clark and Hust (1) in 1974. The data available at that time were obtained by a number of investigators, each usually working with his own test, and none of whom tested all or nearly all of the structural metals and alloys of interest for oxygen service.

There were some considerable differences in the ranking of materials for compatibility according to different tests (Table 1). This indicated the need to match as closely as possible the test conditions with the most likely potential causes of ignition and burning in the application considered.

The work of Kirschfeld at BAM in Berlin, which was published in nine papers and summarized in Reference 5, revealed, in addition to a ranking, the importance of specimen size and oxygen pressure. Kirschfeld found the rate of burning of wire samples after promoted combustion to be approximately proportional to the square root of oxygen pressure and to be inversely proportional to the cross-sectional area of the specimen. He was able to burn small diameter wires (0.5-2 mm, 0.02-0.079 in) of all the metals except nickel. It has perhaps not been properly appreciated that the oxygen compatibility of metals decreases markedly with decreasing size. This effect has been shown again in some recent promoted combustion tests on wire mesh reported by Stoltzfus et al (34) and in tests of sheet metal packing by Dunbobbin et al (35).

How can we decide what material is appropriate for a given application? There are several nonexclusive possibilities. Is there a history of the use of a material in this or a similar part? If so, have there been failures — either leading to oxygen-fed fires, or that under different attending circumstances might have resulted in such a fire? Has testing been done on the component itself with various possible malfunctions of associated equipment? This kind of evaluation was discussed at a previous Symposium by Stradling et al (10) and is also covered in a recent NASA guide (7).

TABLE 1 OLDER OXYGEN-COMPATIBILITY RANKING OF METALS AND ALLOYS *

DEAN & THOMPSON[2] THERMAL IGN.	NIHART & SMITH[3] PROMOTED IGNITION		SIMON[4] PROMOTED IGN.	KIRSCHFELD[5] BURNING RATE	NIHART & SMITH[3] POWDER IMPACT	BAUER ET AL[6] LOX IMPACT
TO 5.5 MPa	13.8 MPa	34.5 MPa	1.65 MPa	to 22.8 MPa	0.34-0.69 MPa	1 atm
Aluminum		Gold, Silver				Silver Solder
Nickel		Nickel		Nickel		(40% Ag)
Hastelloy C						
Monel 400	Monel 400				Monel 400	
Inconel X750	Inconel 600	Yellow Brass			Monel K500	
Hastelloy X	Monel S	Inconel 600				
Hastelloy R	Tobin Bronze	Aluminum			Tobin Bronze	
Copper	Duranickel	Copper	Copper	Copper	Copper	Copper
	Ampco 15			Brass		
	Permanickel			Tin Bronze		Bronze
	Monel K500					
	Hastelloy R					
	Maraging Steel					
	Beryllium Copper					
	Elgiloy					
	Rene 41					
	Inconel X750	Inconel X750				
	Multimet					
	Hastelloy X					9% Ni Steel
	Haynes 25					
	Everdur					
310 SS				Cast Iron	Steel	
410 SS			Ferritic Cr Steel			
304 SS	18-8 SS	18-8 SS	18-8 SS		18-8 SS	18-8 SS
321 SS			Brass			
347 SS			Ni-Al Bronze	347 SS		
17-7 PH SS			Tin Bronze			
			Gun Metal			
Carbon Steel			Gray Cast Iron	Low-C Steel		
			Nodular Iron	Cobalt		
				Magnesium		
				Zinc		
	Aluminum		Aluminum	Aluminum	Aluminum	Al Alloys
Titanium			Alloy Steel			

* Most compatible material at top of column, least at bottom.

TESTS FOR METALS

What test information is available on the oxygen compatibility of the metals themselves? Testing has been less extensive for metals than for nonmetallic materials, and, until recently, there have been no generally accepted or standard tests, with the exception of heat of combustion. This latter is a very important property that measures the amount of energy available to maintain the combustion temperature by providing for the various heat transfer losses, including preheating adjacent material to continue combustion. The heats of combustion of all the common metals are well known, and those for alloys can be calculated with sufficient accuracy by summing the products of the weight fractions and the heats of combustion of the metals in the alloy (9).

Heats of combustion are given for metals and alloys in Table 6. The more combustion-resistant metals have the lower heats of combustion. However, that is not the only factor involved. Nickel has a higher heat of combustion than copper or its alloys, yet it is less easily burned. Cobalt has a slightly lower heat of combustion than nickel but burns more readily. Similarly, the stainless steels lie above the carbon steels, but they are less easily combustible.

Kirschfeld (8) suggested that it is easier to burn metals that occur as oxides with two valences, e.g. iron, cobalt, or copper, than those with only one valence state like nickel. He postulated that in the former case a heterogeneous reaction can occur but that only a homogeneous reaction can occur in the latter, unless the temperature is somehow raised to vaporize nickel and permit a vapor phase reaction. He accomplished the latter by burning nickel and aluminum wires twisted together.

In 1982, NASA funded a project to develop three tests that had been recommended by a Steering Group from NASA and industry. These were tests of promoted combustion, friction/rubbing, and particle impact ignition (14, 15, 17). NASA then used these tests to evaluate a group of metals of particular interest for aerospace applications. Subsequently, ASTM Committee G-4 assembled funding from industry to test an additional group of metals of interest for industrial use (19). Our present knowledge of the oxygen compatibility of metallic materials is based strongly upon those programs and upon additional work that they stimulated.

TEST RESULTS

A summary of the rankings of metallic materials based on the combined results of the NASA and ASTM/Industry (20) programs is included in Table 2 together with the results of recent work by McIlroy and coworkers (23, 26) and Zabrenski et al (27). The specific test results from the first two test programs are given in Tables 3, 4, and 5. Based upon all this work, I have drawn the generalized conclusions presented in the following.

TABLE 2 RECENT OXYGEN COMPATIBILITY RATINGS

ASTM/NASA[14,20] Particle Impact	ASTM/NASA[15,20] Friction/Rubbing	ASTM/NASA[17,20] Promoted Ignition	UCC Linde[23,26] Promoted Ignition	Zabrenski[27] Oxygen Index
	Nickel	Nickel	Nickel 200	
			Nichrome V	
Monel 400	Inconel 600		Monel 400	Monel 400
		Copper	Monel K500	
			Naval Brass	
		Monel 400	Copper	Copper
	Tin Bronze		90-10 Cupronickel	
Tin Bronze		Tin Bronze	70-30 Cupronickel	
Yellow Brass			Free Cutting Brass	Yellow Brass
			2% Beryllium Copper	
	Nodular Cast Iron	Yellow Brass	INCO 141 Filler	
			Inconel X-750	
		Red Brass	Admiralty Brass	
	13-4 Stainless Steel		Tin Bronze (G)	
			Tin Bronze,Gun Metal	
Inconel 600		Inconel 600	Inconel 600	Inconel 600
	Monel K500		Berylco 440	
	Monel 400		Tin Bronze, Navy M	
			Silicon Bronze	
	WC Coating		Hastelloy C-276	
	Gray Cast Iron		Stellite 6B	
	Leaded Tin Bronze	Stellite 6B	MP 35N	Stellite 6
7% Aluminum Bronze	AISI 4140 Steel		Inconel 625	
Inconel 625		Inconel 625	Hastelloy C-22	
		Waspaloy	Haynes 25	
	Hastelloy X	440C Stainless St.	Inconel 625	
		17-4PH Steel	Incoloy 825 & 65	Incoloy 800
	14-5 PH Steel	Incoloy 800	Inconel 718	
Inconel 718	Yellow Brass		Hastelloy X	
Nodular Cast Iron			Hastelloy G3	
Incoloy 800			Hastelloy G	
	Stellite 6B		Elgiloy	
			Silicon Brass	
	304 Stainless Steel		Hastelloy G-30	
	410 Stainless Steel		Hastelloy B	
	Invar 36		Carpenter 20 Cb-3	
	17-4 PH Steel		410 Stainless Steel	
316 Stainless Steel		321 Stainless Steel	430 Stainless Steel	430 Stainless
304 Stainless Steel	Nitronic 60 Steel		SAF 2205 Steel	
		316 Stainless Steel	316 Stainless Steel	304 Stainless
Nitronic 60	7% Aluminum Bronze		310 Stainless Steel	316 Stainless
		304 Stainless Steel	304 Stainless Steel	201 Stainless
13-4 Stainless Steel	Carbon Steel	Inconel 718	17-4 PH Steel	
14-5 Stainless Steel		Nodular Cast Iron	Invar	Zinc
		Nitronic 60		10% Al Bronze
		9% Nickel Steel	Carbon Steel	9% Ni Steel
	C355 Aluminum Alloy		Ni-Aluminum Bronze	1018 Steel
	SAE 11 Babbitt	7% Aluminum Bronze	Aluminum Bronzes	
	6061 Aluminum Alloy	2219 Aluminum Alloy	A356 Aluminum Alloy	
6061 Aluminum Alloy	Ti-6Al-4V	6061 Aluminum Alloy	1100 Aluminum	6061 Aluminum

TABLE 3 PROMOTED COMBUSTION TEST DATA (17, 20)

	BURNING BEHAVIOR AND RATE (in/s)			
PRESSURE (psig)	7000	2500	1000	500
Nickel	NI (6)*			
Copper	NI (2)*			
Monel 400	SE (5)*			
Tin Bronze	SE (5)			
Yellow Brass	SE (5)			
Red Brass	SE (5)			
Inconel 600		SE (3), 0.16 (1)	SE (4)	
Stellite 6B		SE (2), 0.46 (5)	SE (4)	
Inconel 625		0.39, (4)	SE (5)	
Incoloy 800		0.44 (2)	SE (1),0.38 (1)	SE (5)
Inconel 718			0.44 (4)	SE (4)
316 SS			0.44 (5)	SE (4)
304 SS		0.47 (10)		SE (10)
17-4 PH SS			0.33	SE
Ductile Iron			0.27 (1)	0.14 (1)
Nitronic 60	0.33 (1)			
9% Ni Steel			0.53 (1)	0.38 (1)
7% Al Bronze			1.10 (1)	1.09 (1)
6061 Aluminum			2.53 (4)	

Notes: NI, No ignition; SE, Self extinguished in < 2";
*, Tested at 8000 psig rather than 7000 psig.
Samples are 1/8 in. (3.17 mm) rods.
( ), Number of tests

TABLE 4 FRICTION/ RUBBING TEST DATA (20)

TEST MATERIAL		Pv PRODUCT
Stationary Sample	Rotating Sample	($W/m^2 \times 10^{-8}$)
Tin Bronze	Tin Bronze	2.1, 2.2
Ductile Cast Iron	WC-coated 4140	1.7, 1.8, 1.8
13-4 SS	13-4 SS	1.3, 1.4, 2.0
Ductile Cast Iron	Monel 400	1.3,1.3,1.5
Gray Cast Iron	410 SS	1.2[a]. 1.3, 1.5[a]
Gray Cast Iron	17-4 PH (H 1150 M)	1.2, 1.4, 1.7
Beryllium Copper	Monel 400	1.1, 1.2, 1.2
AISI 4140	Monel K-500	1.1, 1.1, 1.4
Ductile Cast Iron	410 SS	1.1, 1.2, 1.2
Ductile Cast Iron	17-4 PH (H 1150 M)	1.1, 1.1, 1.2
Monel 400	Nitronic 60	1.0, 1.4, 1.6
Bronze	Monel K-500	0.96, 1.8, 1.8
Tin Bronze	304 SS	0.95, 1.0, 1.2
Bronze	17-4 PH (H 1150 M)	0.89, 1.0
14-5 PH	14-5 PH	0.86, 1.0, 1.0
Ductile Cast Iron	Stellite 6B	0.82, 0.88, 1.1
Ductile Cast Iron	Tin Bronze	0.80, 1.4, 1.7
Bronze	410 SS	0.78, 0.93, 1.2
Stellite 6B	Stellite 6B	0.77, 0.81
Tin Bronze	Aluminum Bronze	0.77, 0.80, 0.82
304 SS	17-4 PH (H 1150 M)	0.69, 0.74, 0.86
304 SS	Beryllium Copper	0.63, 0.77, 1.2
Stellite 6B	Nitronic 60	0.65, 0.67, 0.75
Ductile Cast Iron	Nitronic 60	0.44, 0.51, 0.75
Nitronic 60	Nitronic 60	0.30, 0.35, 0.79
Aluminum Bronze	C355 Aluminum	0. 29, 0.31
Nitronic 60	17-4 PH (1150 M)	0.28, 0,44, 0.61
Babbitt on Bronze	17-4 PH (H 1150 M)	0.09, 0.10, 0.21
Babbitt on Bronze	Monel K-500	0.09, 0.16, 0.19
Babbitt on Bronze	410 SS	0.08, 0.09, 0.20

Notes: Pv product required for ignition at 6.9 MPa (1000 psi), 17,000 rpm, and a steadily increasing load, where P is pressure on original sample contact area and v is the linear velocity of the rotating sample.

a. Samples welded but did not ignite

TABLE 5 PARTICLE IMPACT TEST DATA (20)

MATERIAL	REACTION TEMPERATURE	
	(°C)	(°F)
Monel 400	>329	>625
Tin Bronze	>307	>585
Yellow Brass	>346	>655
Inconel 600	>332	>630
7% Aluminum Bronze	304	580
Inconel 625	302	575
Inconel 718	202	395
Ductile Cast Iron	202	395
Incoloy 800	196	385
316 SS	52	125
304 SS	46	115
Nitronic 60	38	100
13-4 SS, Cast	27	80
14-5 PH SS	27	80
6061 Aluminum Alloy	-34	-30

Note: Temperature of sample for ignition upon impact by a 2 mm aluminum alloy sphere traveling at ~400 m/s in oxygen at ~4 MPa (600 psi).

TABLE 6 HEATS OF COMBUSTION OF METALS AND ALLOYS

Material	$-\Delta H_c$ cal/g	Source
Beryllium (BeO)	15,865	Janaf *
Aluminum (Al_2O_3)	7,425	Janaf
Magnesium (MgO)	5,900	Janaf
Titanium (TiO_2)	4,710	Janaf
Chromium (Cr_2O_3)	2,600	Smithells *
Ferritic and Martensitic Stainless Steels	1800-2000	Calculated
Austenitic Stainless Steels	1750-1900	Calculated
Precipitation-Hardening Stainless Steels	1750-1950	Calculated
Carbon and Low Alloy Steels	1630-1850	Calculated
Iron (Fe_2O_3)	1,765	Janaf
Iron (Fe_3O_4)	1,600	Janaf
Inconel 718	1510-1655	Calculated
Inconel 600	1250-1655	Calculated
Aluminum Bronzes	1100-1400	Calculated
Zinc (ZnO)	1,270	Smithells
Cobalt (Co_3O_4)	1,225	Smithells
Tin (SnO_2)	1,170	Smithells
Monel K-500	960-1140	Calculated
Nickel (NiO)	980	Smithells
Cobalt (CoO)	970	Smithells
Monel 400	765-920	Calculated
Yellow Brass, 60Cu/40Zn	700-860	Calculated
Cartridge Brass, 70Cu/30Zn	605-790	Calculated
Red Brass, 85Cu/15Zn	460-690	Calculated
Bronze, 88Cu/10Sn/2Zn	425-655	Calculated
Copper (CuO)	585	Janaf
Copper (Cu_2O)	320	Janaf
Lead (PbO)	250	Smithells
Silver (Ag_2O)	35	Smithells

* Janaf, Reference 43; Smithells, Reference 44

Noble Metals

The noble metals (gold, silver, platinum) are virtually inert to oxygen because of their negligible heats of combustion. However, they are too expensive for any but specialty applications, e.g. plated coatings on metal O-rings or tips of labyrinth seals. Silver, silver plate, and gold plate did not react in impact tests in various liquid and gaseous oxygen environments (41).

Alloys of silver and copper, usually with some zinc and/or cadmium, are used widely for brazing components together. These so-called "silver solders" have low heats of combustion and have passed the few LOX impact tests run with them. When present as thin layers between metal surfaces, these brazing alloys should have good oxygen compatibility.

Nickel and Its Alloys

Nickel, copper, and alloys based on them are the most oxygen-compatible metallic materials available at an affordable cost for structural uses. Nickel, Inconel 600, Monel 400, and Monel K-500 were difficult both to ignite and to keep burning in the NASA tests (Tables 3, 4, 5). Other high nickel alloys containing small amounts of reactive metals (Al,Ti, Nb) and significant quantities of iron like Inconel X-750 and Inconel 718 are somewhat less difficult to ignite and burn.

McIlroy, Zawierucha and co-workers (23, 26) tested many nickel-base alloys using iron wire plus oil as the igniter. They found nickel, Nichrome V, Inconel 600, Inconel X-750, Monel 400, and Monel K-500 to be very resistant to combustion at oxygen pressures to 30.3 MPa (4400 psig) or above (Table 2).

Nickel was the only base metal tested by Kirschfeld (8) that would not burn in oxygen when in the form of a small diameter wire. This resistance to combustion persisted up to 200 atmospheres pressure of oxygen. Similarly, when NASA tested nickel wire cloth (0.18 mm, 0.007 in. diameter wire) in promoted combustion, it would not burn in oxygen at 0.77 MPa (100 psig) (34). In contrast, cloth of 0.19 mm (0.0075 in) Monel 400 wire burned, though at slow rates, in oxygen at 0.33 to 0.086 MPa (35 to 0 psig).

Copper and Its Alloys

Copper and its alloys (bronzes except aluminum bronzes, brasses, and beryllium copper) have been widely used for oxygen service and with a very good record. The NASA test data show that copper and most copper alloys are difficult to ignite by rubbing or particle impact or to burn by promoted combustion (Tables 3, 4, 5). McIlroy et al (23) conducted promoted combustion tests on copper and a dozen of its alloys (Table 2). They found most of these alloys to be resistant to burning at pressures of 30.3 to 38.6 MPa (4400 - 5600 psig).

Copper alloys are also excellent in resistance to LOX impact tests (37, 41). The work of Kirschfeld (42), however, showed that 1 mm (0.040 in) copper wire and 2 mm (0.079 in) brass wire could burn in oxygen at atmospheric pressure. NASA tested copper wire cloth (wire diameter 0.19 mm, 0.0075 in) in promoted combustion with inconsistent results. They were able to burn it in two of five tests at 0.33 MPa (35 psig) but not at 0.24, 0.43, 0.60, or 0.77 MPa (23, 50, 75, or 100 psig) (34).

Aluminum bronzes are an exception to the good oxygen compatibility of copper alloys. An aluminum bronze containing only 7% Al was very easily ignited in the NASA friction/rubbing test (Table 4). Specimens of this aluminum bronze also burned completely in oxygen at 3.45 MPa (500 psig) in the NASA promoted combustion test. McIlroy et al (23) also found in a promoted combustion test using a promoter of iron wire and hydrocarbon oil that aluminum bronzes containing from 5 to 11% Al burned much more readily than other copper alloys (Table 2). Similar promoted combustion tests were run with a steel promoter by Benning et al (21). They found that a 10.5% Al bronze would burn in commercial oxygen at pressures down to 1.15 MPa (160 psi) and that a 6.5% Al bronze had a burning threshold of 2.05 MPa (300 psi). In contrast, the 7% Al bronze alloy rated well in the NASA particle impact test (Table 5).

In view of the mainly poor test results and of the fact that aluminum bronze alloys have been involved in some oxygen pump fires, the use of aluminum bronzes in any rotating oxygen machinery or as valve seats is not recommended.

Stainless Steels

Stainless steels of various types are used in many oxygen applications: austenitic steels, AISI 304 and 316; martensitic steels, AISI 410; ferritic steels, AISI 430; precipitation hardening steels, 17-4PH; duplex steels, AISI 329. However, these steels are by no means as oxygen compatible as the better nickel and copper alloys mentioned above.

The stainless steels are mainly in the lower rankings of the alloys tested at NASA (Tables 3, 4, 5). In the promoted combustion and particle impact tests, all the stainless steels that were tested ranked near the bottoms of the lists. As examples, 304 and 316 stainless steels self-extinguished at 3.55 MPa but burned completely at 7.0 MPa (1000 psig), and Nitronic 60, a stainless steel especially formulated for galling resistance, burned completely at 3.55 MPa (500 psig).

Williams et al (22) conducted particle impact tests on 304 and 316 stainless steels. A mixture of 2g of iron powder and 3g of sand and rust was impacted on the sample at 67°C (153°F) and at pressures of 22 to 32 MPa (3175-4625 psig). Samples did not ignite at velocities of 45 m/s (148 ft/s), but 316 ignited at 51 and 54 m/s (167 and 177 ft/s) at 22 and 24 MPa (3175 and 3465 psig). These velocities were high enough to ignite the particles on impact, the likely ignition mechanism.

The behavior of stainless steels in the friction/rubbing test is much more variable, depending upon the steel, the material against which it rubs, and whether it is the rotating or stationary specimen.(Table 4). When combinations of materials are rubbed together, the more easily ignited material appears to control the limiting Pv product or energy flux (20, 24). (P is the pressure applied between the two specimens, and v is the surface velocity of the rotating specimen.)

When a stainless steel is one of the rubbing materials, it is usually the controlling material. However, it also appears that the increased cooling of a rotating specimen compared to a stationary one increases somewhat the Pv product required to ignite it.

The cast stainless steel 13-4 rubbed against itself required a high Pv product for ignition, as did 410 and 17-4PH stainless steels rotated against ductile or gray cast iron and Nitronic 60 against Monel 400. In contrast, Nitronic 60 rotated against itself or Stellite 6B or ductile cast iron had low products of Pv for ignition. Most combinations of various stainless steels with other materials had intermediate to low Pv values.

Newer data from promoted ignition tests confirm and amplify the NASA test results. McIlroy, Zawierucha, et al (23. 25. 26, 33) determined maximum pressures for resisting combustion for several stainless steels in commercially pure oxygen (99.7%) and in such oxygen diluted with further nitrogen, argon, or carbon dioxide. They added two new test chambers, one with eight times the volume and one with continuous oxygen flow. This latter proved to be a more severe test than either static test in the range of pressures where it could be used (to 3.55 MPa, 530 psig). While the flow condition may have contributed to this increased severity, the cause may also have been a different ignition system. An electrical current was passed through a steel igniter and the specimen, which significantly preheated the latter. In addition, there was no oil igniter to generate carbon dioxide and dilute the atmosphere.

For 316 stainless steel, the maximum pressure to resist combustion was 3.35 MPa (500 psig) in the small chamber, 2.65 MPa (400 psig) in the large, and 1.62 MPa (250 psig) in the flow chamber. With 20Cb-3, there was no sustained combustion in any chamber at 3.55 MPa (530 psig). Combustion did occur in both static chambers at 7.0 MPa (1030 psig).

The precipitation hardening stainless steel 17-4PH was run in all three testers in two metallurgical conditions. In the annealed state the no-burn and burn pressures were 1.03 and 1.33 MPa (165 and 208 psig). In the H-1150 hardened condition, these pressures were 2.76 and 3.35 MPa (415 and 500 psig). McIlroy and Zawierucha point out in this paper (33) that little consideration has been given to the effect of the metallurgical structure of an alloy or the concentration of minor constituents on its oxygen compatibility. Zabrenski et al (27) have reported that the burning threshold for annealed 304 stainless steel in rods of 6.4 mm (0,25 in) diameter was 5.0 MPa (725 psig), while cold worked 304 had a threshold above 10.34 MPa (1500 psig). Additional work on the effect of metallurgical condition is warranted so we may select the best condition for use.

Carbon and Low-Alloy Steels and Cast Irons

Carbon steels and low-alloy steels ignite in oxygen at temperatures somewhat below their melting points. Sato and Hirano (16) determined the autoignition temperature of a low carbon steel to be 1300°C (2372°F), apparently at pressures of 1 to 10 MPa (130 to 1435 psig). They also reported that the burning rate of that steel increased, depending upon the pressure, by 50 % to 200% as the specimen temperature increased from ambient to 1200°C (2192°F). Cast irons also ignite below their melting points, and they burn somewhat slower than steels, perhaps because of the presence of graphite burning to carbon dioxide.

The ASTM/NASA test program included a number of tests on steels and cast irons. In promoted combustion tests, ductile cast iron and a 9% nickel steel rated below the stainless steels and did not self-extinguish in oxygen at 3.35 MPa (500 psig) (Table 3). McIlroy et al (23) found in their promoted ignition tests that carbon steel and a special stainless steel SAF2205 were the only metals tested that could be ignited by a hydrocarbon oil promoter without iron wire at 6.9 MPa (1000 psig).

Tests of carbon steel by Benning and Werley (18) with their pressurized oxygen index equipment showed that a carbon steel would just burn at 1 MPa (130 psig) in a mixture of 81% oxygen and 19% nitrogen. At 6.9 MPa and 20.7 MPa (1000 and 3000 psig), the threshold composition for burning was found to be 53% oxygen and 47% nitrogen. In more recent tests in a new apparatus, Zabrenski et al (27) found the pressure threshold for promoted combustion of 1018 carbon steel, tested as 6.4 mm (0.25 in) rods to be only 0.27 MPa (25 psig). Tubing of 1018 carbon steel (6.4 mm OD and 4.6 mm ID, 0.25 in. and 0.18 in.) had a threshold of 0.1 MPa (0 psig).

In NASA friction/rubbing tests (Table 4), the ductile and gray cast irons behaved well, requiring a high Pv product for ignition when paired with rotating samples of tungsten-carbide-coated steel, Monel 400, 17-4PH, and 410 stainless steel. Jenny and Wyssmann (12) had found that ductile cast iron behaved well when rubbed by 420 stainless steel. This good behavior in rubbing may be a result of a low coefficient of friction from the graphite in the cast irons and/or the generation of carbon dioxide at the rubbing interface where it would lower the oxygen concentration. These results indicate that a cast iron compressor casing would be more resistant to ignition from rubbing than would one of steel or stainless steel.

AISI 4140 steel exhibited good resistance to ignition when Monel K-500 was rotated against it. In contrast, carbon steel run against carbon steel ignited at low Pv values.

In the NASA particle impact test, ductile cast iron ranked with the lower-rated nickel-base alloys and above the stainless steels (Table 4). No carbon or low alloy steel was subjected to this test.

However, Williams et al (22) included a carbon steel in their low velocity "particle shower" tests. They did not ignite the steel at 19.6 MPa (2855 psig), 65° C (149° F), and a gas velocity of 30.8 m/s (101 ft/s). However, they ignited the two samples tested at the same pressure, 82°C (180°F), and a velocity of 51 m/s (167 ft/s). Again, it may require ignition of the particles on impact in order to ignite the sample.

Carbon and low alloy steels and cast irons are very important and inexpensive materials of construction. It is evident, however, that care must be taken in using these materials, because they are easily ignited by promoted combustion with hydrocarbon oils, etc. and will burn vigorously at low oxygen pressures.

Aluminum and Its Alloys

Aluminum and its alloys are difficult to ignite thermally because of the highly tenacious oxide film that is usually present. They must be heated well above their melting temperatures for ignition to occur. Once ignited, however, aluminum burns violently in pressurized oxygen. Promoted ignition is a major concern with aluminum parts. Aluminum alloy 6061 ranks at the bottom in the NASA promoted combustion test. It does not self extinguish at 3.35 MPa (500 psig), the lowest pressure used, and it burns at a rate about five times that of the stainless steels (Table 3).

McIlroy et al (23) also found in their promoted combustion tests that aluminum burns completely in the pressure range of 6.9 to 11 MPa (1015 - 1610 psig). Benning et al (21) determined threshold pressures for the burning of 6061 aluminum alloy rod in oxygen of various purities. In 99.99% oxygen, the threshold is 210 kPa (15 psig), and in 99.82% oxygen with 0.18% Ar, it is 900 kPa (115 psig). This difference in threshold pressure and larger differences for higher argon contents are attributed to the accumulation of argon adjacent to the burning aluminum. This hinders the diffusion of oxygen to the combustion zone, resulting in a lower oxygen concentration there.

Aluminum alloy 6061 also ranked at the bottem of the list in NASA friction/rubbing and particle impact tests (Tables 4 and 5). In addition, impact or heavy rubbing between an aluminum part and a rusty object may cause ignition by the thermit reaction. Bauer et al (6) produced an explosion in an aluminum alloy LOX pump by injecting pieces of rusty nail into it during normal operation.

Aluminum and its alloys usually pass the LOX impact test. Austin (37), however, reported significant reaction frequencies on impact in LOX or GOX at 0.7 to 3.4 MPa (85 and 500 psig) and fewer reactions at 6.9 and 10.3 MPa (1000 and 1500 psig). This anomalous behavior has not been explained, though contamination is possible.

According to Lucas and Riehl (38), the presence of grit (silica, alumina, silicon carbide) increases considerably the frequency of reactions. Aluminum with some dyed coatings fails the LOX impact test.(41). Bryan (39) reported that aluminum samples contaminated with 4730 mg/m^2 (430 mg/ft^2) of silicone oil showed appreciable reactions in LOX impact tests and that faint reactions occurred at one tenth of that concentration of contaminant.

Disruption of the oxide film by heavy rubbing in the presence of a PCTFE oil or grease can lead to an ignition of the aluminum (40), and if this occurs in a pressurized oxygen atmosphere, an intense fire may result.

Aluminum and its alloys have been used safely in many applications in oxygen equipment. These range from air separation unit cold boxes to high pressure gas cylinders. However, these successful uses depend upon the absence of a suitable ignition source. In contrast, there have been ignitions of aluminum alloy LOX pumps, where high speed rubbing provided the ignition event.

Cobalt-base Alloys

For cobalt-base alloys, there are a few test results available. In NASA tests, Stellite 6B, a wear-resistant alloy deposited by welding, rated well in promoted combustion. It was self-extinguishing at 6.9 MPa (1000 psig), and some samples self-extinguished at 17.2 MPa (2500 psig), though others burned. McIlroy et al (23) also tested Stellite 6B and found it to be self-extinguishing in the range of 6.9 to 11.0 MPa (1000 -1600 psig). They also found much of the specimen length unburned after ignition in the range 30.3 to 38.6 MPa (440- 5600 psig). The cobalt-nickel-based alloy MP33N self-extinguished in the range 20.7 to 24.1 MPa (3000-3500 psig), but burned completely at 30.3 to 38.6 MPa. Elgiloy was moderately resistant to burning in the 6.9 to 11.1 range. Zawierucha and McIlroy (26) tested Haynes 25, a well-known alloy for high temperature applications. It resisted combustion at 13.9 MPa (2000 psig), and some burns occurred at 17.3 MPa (2500 psig). Stellite 6B ranked in the lower intermediate group in the NASA friction/rubbing test (Table 4).

Kirschfeld was only able to burn 2 mm (0.079 in) diameter cobalt wires in oxygen at pressures of at least 3.2 MPa (450 psig), and of 10 MPa (1435 psig) for 1 mm (0.040 in) wire. Thus, cobalt was much more resistant to combustion than iron in his tests, though less so than nickel.

Tin and Its Alloys

Tin and its alloys are not very oxygen compatible. NASA friction/rubbing tests of a tin-base Babbitt metal ranked it very low when specimens of Monel K-500 or hardened stainless steel were rotated against it (Table 4). Sircar et al (31) have reported low pressure thresholds for promoted combustion and for ignition by mechanical impact for tin-lead alloys. Monroe et al (11) burned a tin-base Babbitt alloy at 121°C (250°F) with ignition presumably by a small electrical spark at a fresh fracture surface.

MATERIAL CHOICE

The choice of a material or a combination of materials for a given application is seldom simple. As we have seen, almost all metallic materials can burn in oxygen under some conditions. In some cases, oxygen pressure or concentration can be kept low enough to prevent ignition or combustion. If the application allows, this is a preferred course. Frequently, however, the conditions are such that at least some of the candidate metals can burn if ignited. If so, many factors must be balanced — and there may be several alternative solutions. This selection process is discussed in ASTM Standard G 94, And I will not repeat it here. Rather, I will mention some of the factors and options and cite a few examples.

Because metals constitute the greater part of most oxygen equipment. their cost is a major consideration. Availability may also be an important constraint. Semi-fabricated forms or special components may not be available in less common and more expensive alloys. Fabrication or joining is more difficult for certain alloys. Finally, it will not do to select a material of high oxygen compatibility for a component if that material is not well suited for the application and may compromise the proper functioning of the equipment.

The application of metal test results to material choice is discussed extensively in ASTM Standard Guide G 94. This guide presents the many factors to be considered, with special emphasis on those particularly important for metals, reviews the ASTM procedure for evaluating probabilities of ignition and potential damage, and works through three examples.

Metal test results alone, however, as G 94 points out, are often inadequate for deciding on the selection of a metal for a component. Indeed, three areas of choice contribute to the safety of any oxygen equipment. These are material selection, equipment design, and procedures for operation and maintenance. I cannot do justice to the latter two here. but I will briefly highlight them.

Design is very important in determining the safety of oxygen equipment. Most metals are difficult to ignite. and design choices can greatly reduce the probability of ignition. Providing adequate clearances and/or rubbing strips of ignition-resistant materials can help prevent fires in rotating equipment. Likewise the use of sensors to detect undue vibration or temperature increases can provide extra time to shut down such equipment before an ignition occurs.

Designing for ease of cleaning allows removal of easily ignitable contaminants that might, in turn, ignite a metal part. Providing screens or filters and keeping oxygen gas velocities below critical values can greatly decrease the probability of ignition by particle impact. Carbon steel pipelines are a classic example. Once ignited, steel burns readily in oxygen at common pipeline pressures. However, pipeline fires are rare because the lines are maintained clean and the gas velocities are controlled to appropriate values.

Start-up and shut-down are the most dangerous times because conditions are not steady. Resonance peaks with the attendant danger of excessive vibration and rubbing can occur in rotating machines. High gas velocities with danger of particle impact ignition as well as adiabatic compression at dead ends can occur if care is not taken. A compressor is often started on nitrogen to check it out before oxygen is admitted. Metal wear dust formed during nitrogen operation will not be oxidized and may be pyrophoric. The change to oxygen should be gradual to slowly oxidize such material.

If less oxygen compatible materials are to be chosen, based on operating conditions and safety precautions, it is essential to be able to count on proper maintaining of that status. Regular maintenance helps to avoid mechanical failures and to preserve system cleanness, e.g. on filters or screens. It is also important to do all maintenance work on oxygen systems under clean conditions. Safety equipment --- sensors, alarms, relief valves, etc. --- needs to be checked regularly. Maintenance work must also be done safely. When a leak is to be repaired, depressurize the system before attempting any repair. Tightening a flange bolt or a valve packing nut of a system under pressure might cause an ignition --- and the operator would be directly next to it. Double block-and-bleed valve arrangements or insertion of a blind flange can prevent passage of oxygen through one leaking valve to an area being worked on.

IMPROVING ALLOYS FOR OXYGEN SERVICE

The differences in oxygen compatibility found by Zabrenski et al (27) between annealed and cold worked stainless steel and by McIlroy and Zawierucha (33) between annealed and precipitation hardened 17-4PH stainless steel have been mentioned. The presence or absence of minor phases as well as the particle size and distribution of a phase may influence the ignitability of an alloy. Heat treatments can form or dissolve, coarsen or refine such phases. Zawierucha and McIlroy (26) have cited a number of metallurgical factors that might affect the oxygen compatibility of alloys. Large changes in ignitability or combustibility are not likely to result from changes in metallurgical structire. However, a study of these effects in common alloys could help to improve our use of them in oxygen equipment.

Several investigators have reported that increasing the carbon content of iron alloys reduces their combustibility somewhat. In steels, the carbon in amounts of 0.02% to 1.2% is mainly present as carbides of iron or of alloying elements. Such carbides are hard and brittle, and they act to strengthen steels by various amounts depending upon their concentration and particle size, as determined by heat treatment. Carbides probably have little effect on the ignition of steels except perhaps by friction. With regard to combustion, the burning of carbides will produce a gas, chiefly carbon dioxide. This gas will dilute the oxygen directly adjacent to the burning metal surface. If the conditions are close to the lower limit for combustion, e.g. in pressure, concentration, or temperature, the burning may be slowed or extinguished.

In most cast irons with carbon contents of 2.2% to 4.0%, much of the carbon is present as graphite flakes or nodules, with the balance as carbides. Graphite decreases the coefficient of friction of a cast iron below that of steel at ambient conditions. A similar effect at elevated temperatures would help to explain the superior resistance to ignition of cast iron in the NASA friction/rubbing test. However, it is known that the excellent lubricating ability of graphite at ambient depends upon the presence of moisture. Thus, at high temperatures, its lubricity would be expected to decrease. It would be helpful to have the results of a NASA friction/rubbing test on cast iron in which the coefficient of friction was measured during the test, as has been done for other alloys by Stoltzfus et al (28),to clarify this situation.

In any case, the major effect may rather be that burning the large amount of carbon in a cast iron generates copious amounts of carbon oxide gases, which dilute the oxygen concentration below the limit for combustion. This may be particularly important in the friction/rubbing test where the access of oxygen to the faying surfaces is limited. It would be of interest to vary the geometry of the test specimens to allow more access, e.g. by castellating the end of one specimen.

On the assumption that the formation of carbon oxide gases during the burning of a carbon-containing metal can increase its resistance to combustion, we might consider incorporating carbon in alloys based on metals other than iron. Copper is one such possibility. Carbon is only slightly soluble in copper or in tin bronzes. This has two results. First, carbon cannot be incorporated into copper alloys by dissolution. Second, if carbon is dispersed in a copper alloy, the dispersion will be quite stable.

Powder metallurgical techniques are an obvious way to produce the dispersions we are considering. Further, for special components, the fabrication costs could be reasonable. However, if the graphite particles are not either fully surrounded or well wetted by the alloy, fine channels for gas leakage might be present. Experimentation is necessary to determine whether a problem exists and, if so, how to overcome it.

The work of Benning et al (21) suggests another similar path for developing alloys of reduced oxygen flammability. This concept is also based on reducing the concentration of oxygen at the burning interface below that needed to sustain combustion. Benning accomplished this by adding an inert gas (argon or,less effectively, nitrogen) to the atmosphere in which an aluminum alloy was burned. If the inert gas (argon, helium, nitrogen,etc.) were incorporated in the alloy as gas at high pressure in fine closed pores, it would be released directly at the combustion interface during burning.

Such a composite of gas-filled pores in an alloy could be produced by powder metallurgical methods. Standard pressing and sintering procedures could be used to produce a porous compact. This compact might then be sintered further to close the pores while in an atmoshpere of inert gas at high pressure. Alternatively, the compact could be encapsulated in a metal can, pressurized with inert gas, and then hot extruded, hot isostatically pressed, or shock consolidated. A quite different way to produce a metal/inert-gas composite would be by ion implantation of the gas.

As regards the properties of metal/gas composites, there is considerable technical literature on the behavior of fine gas bubbles in metals. Much of this is from the nuclear industry, which is concerned with the development of gas pores in reactor components and with their effects on mechanical properties.

SUMMARY

The general oxygen compatibility of metals and alloys in various situations can be measured reasonably well by tests of their resistance to promoted combustion and to ignition by rubbing or particle impact. Results of these tests are, of course, a function of oxygen pressure and concentration and of metal temperature.

However, choices of metals cannot be made solely on the basis of these tests. The metal must be appropriate for the service, it must be able to be fabricated into the component, and it must be economically affordable. Precious metals and nickel and copper alloys have the highest oxygen compatibility. However, for many applications we must use carbon, alloy, or stainless steels or aluminum alloys for the above reasons. This is possible and is done regularly and safely even though the oxygen concentration and pressure are such that these metals can burn. We accomplish this by designing, operating, and maintaining the equipment so as to avoid ignition events to the maximum possible extent and to minimize the damage from an ignition.

The effects on oxygen compatibility of many metallurgical variables have not yet been systematically explored. Such work may help us to use alloys in their most resistant conditions. Finally, the modification of metals or alloys so that during combustion they release inert gases to reduce oxygen concentration at the burning interface is suggested as a possible way to improve their resistance to combustion.

Trademarks: The following trademarks occur in the text:

International Nickel Co.,-Toronto - INCO, Inconel, Incoloy, Monel.
Haynes International, Kokomo, IN - Haynes, Stellite, Hastelloy.
Hoskins Mfg. Co., Detroit, MI - Nichrome V.

REFERENCES

1. Clark, A.F. and Hust, J.G., AIAA Journal, 12, #4, 441-454 (1974).

2. Dean, L.E. and Thompson, W.R., J. Am. Roc. Soc. 31, 917-922 (1961).

3. Nihart, G.J. and Smith, C.P., "Compatibility of Materials with 7500 psi Oxygen", AMRL-TDR-64-76, AD608260 (1964).

4. Simon, W., Stahl u. Eisen 88, 1090-1097 (1968).

5. Kirschfeld, L., Summarized by C. McKinley, CGA Oxygen Compressors and Pumps Symposium, 27-33 (1971).

6. Bauer, H., Wegener, W., and Windgassen, K.F., Cryogenics 10, 241-248 (1970).

7. Bamford, L.J. and Rucker, M.A., "Guide for Oxygen Component Qualification Tests", NASA TP-WSTF-712 (1992).

8. Kirschfeld, L., Metall. 21, 98-102 (1967).

9. Lowrie, R., Flammability and Sensitivity of Materials in Oxygen-Enriched Atmospheres: First Volume, ASTM STP 812, B. Werley, Ed., American Society for Testing and Materials, Philadelphia, 1983, 84-96.

10. Stradling, J.S.. Pippen, D.L., and Frye. G.W., ibid, 97-107.

11. Monroe, R.W., Bates, C.E., and Pears. C.D., ibid, 126-149.

12. Jenny, R. and Wyssmann, H.R.. ibid, 150-166.

13. Slusser. J.W. and Miller, K.A., ibid, 167-191.

14. Benz, F.J., Williams, R.E., and Armstrong, D., ibid, Second Volume, ASTM STP 910, M. Benning, Ed., 1985, 16-37.

15. Benz, F.J. and Stoltzfus, J.M., ibid, 38-58.

16. Sato, J. and Hirano. T., ibid, 118-134.

17. Benz, F.J., Shaw, R.C., and Homa, J.M., ibid, 135-152.

18. Benning, M.A. and Werley, B.L., ibid, 153-170.

19. Cronk, J.O., ibid, Third Volume. ASTM STP 986, D. Schroll, Ed., 21-27 (1988).

20. Stoltzfus, J.M., Homa, J.M., Williams, R.E., and Benz. F.J., ibid, 28-53.

21. Benning. M.A., Zabrenski, J.S., and Le, N.B., ibid, 54-71.

22. Williams, R.E., Benz, F.J., and McIlroy, K., ibid, pp 72-84.

23. McIlroy, K., Zawierucha, R., and Drnevich, R.F., ibid, pp 85-104.

24. Schoenman, L., Stoltzfus, J., and Kazaroff, J., ibid, pp104-133.

25. McIlroy, K. and Zawierucha, R., ibid, Fourth Volume, ASTM STP 1040, Stoltzfus, J.M., Benz, F.J., and Stradling,, J.S., Eds., 1989, pp 38-53.

26. Zawierucha, R. and McIlroy, K., ibid, pp 145-161.

27. Zabrenski, J.S., Werley, B.L., and Slusser, W., ibid, pp 178-194.

28. Stoltzfus, J.M., Benz, F.J., and Homa, J., ibid, pp 212-223.

29. Christianson, R.C. and Plante, B.A., ibid, pp 227-240.

30. Barthelemy, H., DeLode, G., and Vagnard, G., ibid, pp 267-285.

31. Sircar, S., Stoltzfus, J., and Gunaji, M., ibid, Fifth Volume, ASTM STP 1111, J. Stoltzfus and K. McIlroy, Eds., 1991, pp 260-9.

32. Zawierucha, R., McIlroy, K., and Mazzarella, R., ibid, pp 270-287.

33. McIlroy, K. and Zawierucha, R., ibid, pp 288-297.

34. Stoltzfus, J., Lowrie, R., and Gunaji, M., ibid, pp 326-337.

35. Dunbobbin, B., Hansel, J., and Werley, B., ibid, pp 338-353.

36. Boddenberg, K. and Waldmann, J., ibid, 528-545.

37. Austin, J.G., " A Survey of Compatibility of Materials with High Pressure Oxygen Service", NASA 275.03-72-11, 1972.

38. Lucas, W.R. and Riehl, W.A., ASTM Bill. 244, pp 29-34, Feb. 1960.

39. Bryan, C.J., "Final Report on the Effect of Surface Contamination on LOX Sensitivity", NASA Kennedy Space CEnter, MTB 306-71, 1971.

40. Lockhart, B.J. and Bryan, C.J., "KSC Lubricant Testing Program", NASA TN D-7372, Nov. 1973.

41. Nonmetallic Materials Design Guidelines and Test Data Book, NASA JSC 02681.

42. Kirschfeld, L., Metall. 14, 792-796, 1960.

43. JANAF Thermochemical Tables, Second Edition, NSRDS-NBS37, National Bureau of Standards, Washington, D.C., 1971.

44. Smithells. C.J., Metals Reference Book, Fifth Edition, Butterworth, London, 1976.

Development and Evaluation of Test Methods

Barry L. Werley[1]

A Perspective on Gaseous Impact Tests: Oxygen Compatibility Testing on a Budget

---

REFERENCE: Werley, B. L., "**A Perspective on Gaseous Impact Tests: Oxygen Compatibility Testing on a Budget,**" *Flammability and Sensitivity of Materials in Oxygen-Enriched Atmospheres, Sixth Volume, ASTM STP 1197*, Dwight D. Janoff amd Joel M. Stoltzfus, Eds., American Society for Testing and Materials, Philadelphia, 1993.

ABSTRACT: Gaseous impact testing has been accomplished in assorted ways dating back to at least the 1950s. ASTM Committee G-4 grappled with disparate views and melded them into ASTM G 74 in 1982. Criticized for being both too sensitive and too insensitive, recent data has unfortunately also led to calls for the test's abandonment. A historical review of the test is presented, speculation on desirable elements in an improved G 74 test are presented, and several arguments for preserving the test are presented. An attempt to analyze the test dynamic is offered. The principal virtue of the test is argued to be its potential simplicity and low cost implementation which may enable compatibility testing by smaller laboratories previously forced to rely on the data of others. A possibly unique ability to study aging effects in polymers is also cited. The greatest need in restructuring the test is argued to be the optimization of geometry to allow data to not only rank materials but to reflect worst-case real-world exposures and perhaps allow inference about materials autoignition temperatures.

KEY WORDS: fire, flammability, ignition, adiabatic compression, oxygen compatibility, gaseous impact.

Gaseous impact (GI), often referred to with some imprecision as adiabatic compression, has been implicated causally in numerous fires in oxygen systems. The basic mechanism of these fires is discussed in ASTM G 88 Standard Guide for Designing Systems for Oxygen Service.

Basically, rapidly compressed oxygen in a low surface-area-to-volume space of appreciable volume, is nearly adiabatic. Mechanical work in compressing the gas is converted into an increase in temperature that can lead to autoignition of system components. As a result, operators are universally admonished to pressurize systems slowly as a means to allow dissipation of this heat of compression.

The mechanism is important, because it is known to cause fires. ASTM Committee G 4, however, has always had difficulty in agreeing how the significance of the mechanism should be addressed experimentally and even whether or not it should be addressed.

The Committee had been aware of differing test apparatuses that had been used

[1] Hazards Research Specialist, Air Products and Chemicals, Inc., 7201 Hamilton Boulevard, Allentown, PA 18195-1501.

through the years at Airco, Rego, AGA, Circle Seal, BAM (the German testing authority) and NASA. In the 1970s, one extreme view described the test as igniting "everything." The other extreme view was expressed by NASA in the mid-1980s when the test appeared too insensitive to ignite PTFE under conditions considerably above those in which PTFE had experienced fires. Indeed, for a period, pressures in excess of 3000 psig were required to ignite PTFE. At the time of adopting ASTM G 74-82 ASTM Standard Test Method for Ignition Sensitivity of Materials to Gaseous Fluid Impact, the only active members of Committee G 4 that were conducting gaseous impact tests were NASA, AGA, and Circle Seal Inc. Among them, NASA had done the more extensive work, and so it was agreed to depict the NASA apparatus in the standard. However, test parameters were selected that were consistent with all three user's abilities

Very importantly, the standard was specified for use only in ranking materials. Although NASA used the test to evaluate materials for specific applications, some data had begun to surface suggesting that the NASA implementation was not readily reproduced and since there were differences in hardware, the conservative step of avoiding direct comparison to actual systems was taken.

More recent work has brought insight. A verbal report at the 1985 Committee G-4 symposium indicated further studies at NASA were also exhibiting reproducibility problems. The 1987 ASTM G-4 symposium includes papers on compression ignition of polymer-lined hose by Barthelemy [*1*], an overview on the BAM method by Wegener et al. [2], and further work at NASA with their configuration by Moffett et. al. [*3*]. At the 1989 symposium Schmidt et. al. [*4*] again reported on a difficulty in discriminating between different materials, but the typical apparatus of G 74, excluding test cell was also used to test PTFE-lined hoses in a report by Janoff et al. [5] with better results. And in the recent 1991 symposium, Janoff et. al [*6*] reported that geometry and other modifications to the NASA test apparatus have increased its sensitivty to the point where a correlation could be drawn between GI data and autogenous ignition temperatures, and Vagnard et. al [*7*] described the corresponding test used by L'Air Liquide.

However, at present there is no movement to generate extensive public-access databases for GI test results. There are few data in the open literature and no data in G-4's standards. Indeed, Janoff et al.[*6*] continued to call for use of the test only on actual equipment configurations and recommended that other techniques (G 72, D 4809, or chemical methods) be used for measuring autogenous ignition.

GI tests, however, may offer two excellent advantages: low cost and a potential ability to study aging effects in polymers.

A simplified, rudimentary GI test apparatus can be configured for a much smaller capital investment than most oxygen compatibility tests. In principle, one needs only a full cylinder of oxygen, a remotely operated fast-opening valve (such as a ball valve), a run of tubing and an appropriately shielded dead end--equipment within the budget of even small vendors (Fig. 1). Further, an abbreviated protocol can be conducted for a per-test cost that is also enviable of all other tests. This procedure might even be desirable merely as an alternative from which to surmise autoignition temperatures. However, with careful selection of test parameters, it may also be possible to use the GI test to select materials for real-world compression exposures. In principle, all that would be required would be to select test parameters so that a test exposure was equal to or of greater severity than would be experienced by a polymer in any real-world system. In some cases, this approach might be too conservative, because

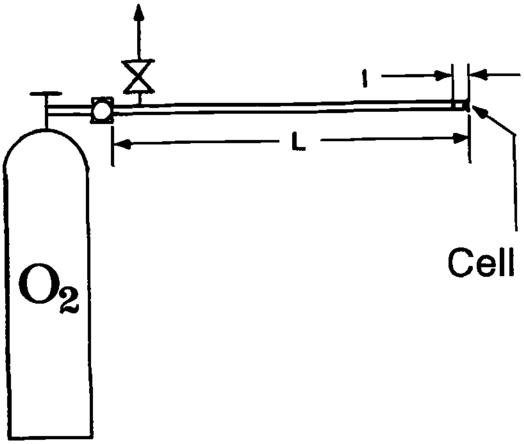

FIG. 1--*Rudimentary gaseous impact apparatus.*

many polymers, such as PTFE, are successfully used at pressures above the level at which they can be ignited by worst-case gaseous impact. However, this does not preclude use of the conservative approach at lower pressures. Indeed, since PTFE does not appear to have ignited in gaseous impact testing at less than about 1000 psig (6.9 MPa), it is worth noting that a majority of existing oxygen systems operate below this pressure, and so the test may still be useful to apply in a conservative fashion.

The potential for the GI system to study aging effects is keyed to its ability to expose a polymer to an oxygen environment in many different states of pressure and temperature, then promptly expose the polymer to gaseous impact.

In order to promote the gaseous impact test, this paper will examine and analyze the basic test dynamics, suggest methods to achieve worst-case response and propose changes that may be desirable in the interest of conservatism and safety.

Model

Rapid-compression ignition can be very reliable. Rapid compression is the exclusive ignition mechanism of the diesel internal-combustion engine. With regard to proposing a model, studies by Chase [*8*] and Wilson et al. [*9*] are pertinent.

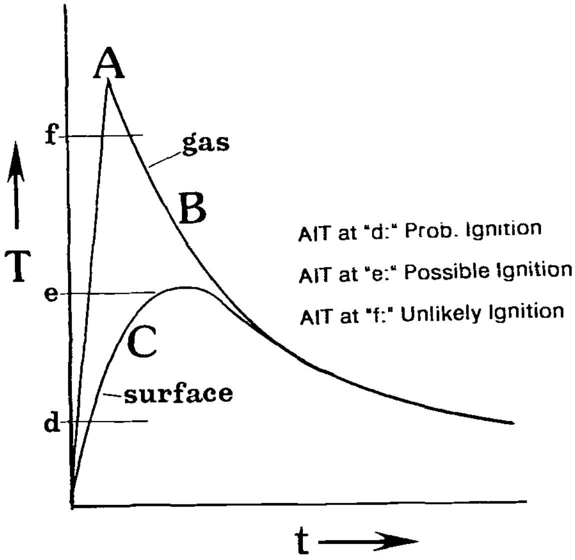

FIG. 2--*Surface temperature and gas temperature versus time.*

In an oxygen system, a likely sequence of events during gaseous impact is:

- Mechanical work used to compress the gas is converted to sensible heat exhibited as an increase in the oxygen temperature (Fig. 2, point A).

- Polymer components or oils located at the end points of the system suddenly find themselves immersed in high temperature oxygen.

- The gas begins to transfer heat to both the polymer and other surroundings. It is on a cooling curve (Fig. 2, Arc B). The polymer is on a warming curve (Fig. 2, Arc C).

- As the polymer surface warms, the gas cools and the temperatures converge. If ignition does not occur, the temperatures decay back to ambient conditions.

- If the polymer achieves an "ignition condition" before the oxygen cools below the ignition condition, then a fire of the polymer may occur. The greater the oxygen is in excess of the ignition condition when the polymer achieves the ignition condition, the more likely is a fire.

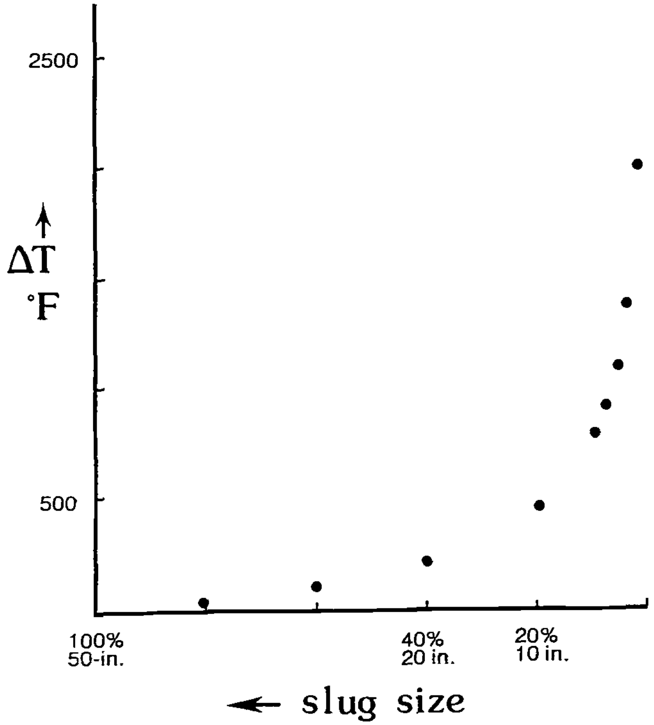

FIG. 3--*Average gas slug temperature versus boundary location.*

The "ignition condition" is not simply the autogenous ignition temperature that might be measured by G 72, for when the surface achieves the experimentally measured autoignition temperature (as measured by tests such as ASTM G 72), the bulk of the specimen is at a lower temperature that may not support combustion (akin to a flash or fire point). Conversely, for some materials, the rapid exposure of the surface to high temperature may allow ignition at a lower temperature than an AIT test might indicate, because slow heating in an AIT test may enable dissipation of volatile vapors that may appear in volume too small to establish a flammable mixture.

Janoff et al. [5] provide an analysis of the adiabatic compression equation and the size of the plug of gas of greatest temperature that can form in a worst case analysis. This worst case assumption is predicated upon:

- the initial slug of gas in the system does not mix with the incoming gas (which is cooling due to expansion).
- The slug of gas is compressed much as if a piston were acting on it.

Leslie [*10*] uses a computer program and analysis to argue that rapidly pressurized systems approximate theoretical adiabatic performance and that the above assumptions are reasonable, despite some boundary mixing that must occur. Fig. 3 depicts temperature conditions throughout the compressed slug of oxygen as a function of various stages of compression for a system of assumed uniform pressure throughout. Notice that the majority of temperature rise occurs just as the slug is reaching maximum compression (after 80% of the compression has occurred and the slug length is reduced to 20% of its initial length, the end gas temperature has experienced just 25% of the ultimate temperature rise). This is one of the features that aids the adiabaticity, since at the lower temperatures present during most of the compression, a period when the slug of gas is exposed to a much greater surface area, heat transfer is at a substantially lower rate due to a smaller differential temperature.

As a result, an extremum GI test should focus on the heat transfer properties of the end point more than the interconnecting tubing.

Important Test Parameters

Using the above model, it is worthwhile to speculate on the parameters that may be important in the design of a GI test. Among these are likely to be: system volume, specimen mounting, compression-line length, initial pressure, ignition energy dissipation, and specimen preparation, among others. These will be considered in turn.

System Volume

An increase in sensitivity observed in the NASA system as reported by Janoff [*6*] very likely was due to an increase in the internal volume of the system (by a change from 0.24-in. [0.6-cm] to 0.47-in. [1.2-cm] inside-diameter tubing). This alteration meant that the mass of hot oxygen that bathed the polymer was increased by a factor of 2.6. Therefore, the sensible heat available to warm the polymer increased by this same amount. Since the mass of available oxygen increased as the square of the tubing size, further increases in tubing size should similarly increase the sink of heat available. A secondary effect is that as the tubing size increases, the surface area per volume decreases so that the gas cooldown curve is also protracted. Hence there is a likely relationship between the test and the real world provided the diameter of the tubing in the tubing used in the test equals or exceeds the diameter of tubing used in real world systems. This conclusion assumes that the large-diameter test system can be pressurized with sufficient rapidity to be considered adiabatic.

Specimen Mounting

Since the compressed oxygen will cool most quickly near the chamber walls, the specimen in a maximal-severity test should be located centrally in the

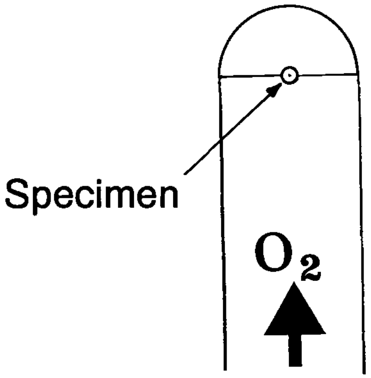

FIG. 4--*Apparatus terminations.*

compressed oxygen. This would dictate a mounting on the tubing centerline a distance at least one-half the tubing's diameter from the dead end. To minimize heat transfer the surface-area-to-volume of the dead end should be minimized, which suggests a hemispherical or spherical closure may be preferred, Fig. 4. These geometries would also help to focus reflected radiation to the specimen.

Line Length

In order for the test polymer to be fully immersed in hot oxygen gas and to minimize the influence of boundary mixing, the length of the line initially containing the oxygen to be compressed must be substantially longer than the test cell. The equation provided by Janoff et al. [5] (their equation 3) may be used to relate the minimum allowed compression-tube length, L (including the cell length), to the test cell length, l, and initial and final pressures, P_i and P_f, because one desires the final slug to more than fill the test chamber by a suitable factor. For constant-diameter tubing the equation becomes:

$$L = l\ (P_f/P_i)^{1/n} \qquad (1)$$

Where n is the ratio of specific heats of oxygen at constant pressure to constant volume.

Note that this length is a function of both the final and initial pressure. Hence, for a system that may experience 3000 psi (20.6 MPa) and have a 1-in. (2.54-cm.) long test section, the interconnecting tubing should be at least a 44-in. (1.11-m.) long line. The modified test assembly used by Janoff [7] is approximately on the boundary for this criterion. Curiously, the earlier small-bore vessel depicted in G-74 fared better in this regard but sufferred the much less favorable final compressed-slug mass. Since the new system is more severe, it suggests that bore dimension is a more critical parameter than line length.

Initial Pressure

Initial pressure downstream of the fast-opening valve should be a critical variable. Presently, G 74 specifies an initial atmospheric condition for the system prior to gaseous impact. There is at least a 10% variation in normal atmospheric pressure at various sites employing the test. Variations in initial pressure can affect the test in two ways: final temperature achieved, and amount of heat transferred. Since ignition requires the achievement of **both** the establishment of sufficient specimen temperature **and** the complex transfer of a minimum ignition energy, the optimum condition must be surmised.

Final temperature is reasonably predicted by the adiabatic compression equation in ASTM G 88, paragraph 5.2.6.1:

$$T_f = [P_f/P_i]^{(n-1)/n}T_i \tag{2}$$

where T_f and T_i are the respective final and initial absolute temperatures, P_f and P_i are the respective final and initial absolute pressures, and n is the ratio of specific heats of oxygen at constant pressure to constant volume. Fig. 3 depicts the anticipated temperature rises that are achieved when oxygen at an initial pressure of 14.7 psia (100 kPa) is compressed to a final pressure of 2400 psia (16.5 MPa).

Heat transfer is much more complex. At a 10% lower initial pressure, the final temperature is expected to be about 3% higher. However, the mass of gas compressed is 10% less. Therefore, the size of the final slug of gas is smaller and its temperature will decay much more rapidly due to heat transfer, for its sensible heat is less.

An analysis of the energy that can be transferred for a rapidly compressed gas slug is difficult. To obtain some coarse qualitative insight, one can use the expression provided by Janoff et al.'s [5] equation (4) for the thermal energy available in gas of mass, m, to cause ignition and that can be transferred to the specimen and the system, $mC_p[T_f-T_i]$. One can substitute the expression (2), above, for the final temperature, and treat the initial oxygen mass, m, as a constant multiple, K, of the initial pressure, (that is KP_i) to estimate the maximum available ignition energy as:

$$E = KC_pP_i[(P_f/P_i)^{(n-1)/n}T_i - T_i] \tag{3}$$

where C_p is the specific heat at constant final pressure, and m is the mass of gas in the final slug.

One can set the derivative of this expression to zero to identify a maximum that occurs when:

$$[P_f/P_i]^{(n-1)/n} = n \tag{4}$$

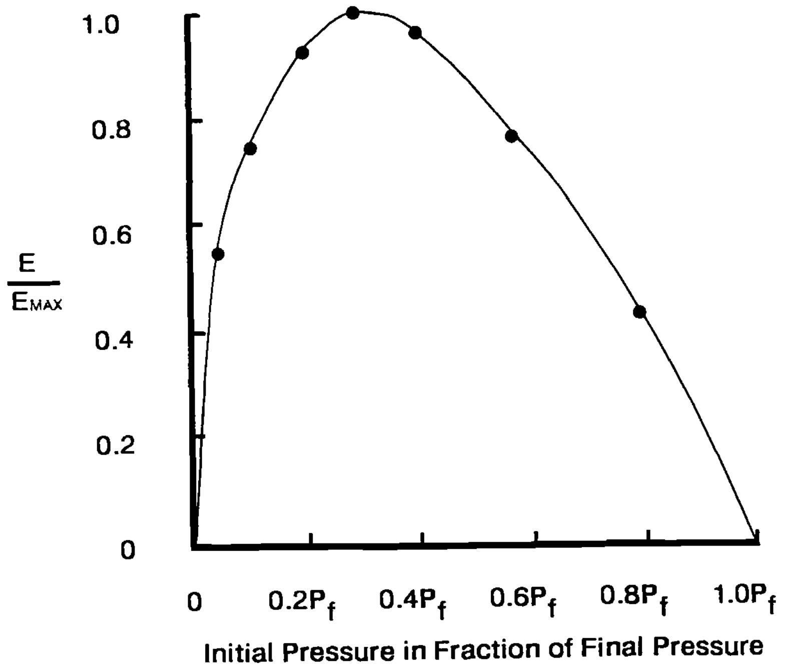

FIG. 5--*Relative ignition energy versus fractional final pressure.*

where n is the ratio of specific heats at constant pressure to constant volume.

A plot of equation (3) divided by its maximum energy point yields Figure 5 and illustrates the maximum, which occurs for oxygen when the initial pressure is approximately 30.8% of the final absolute pressure. In other words, a maximum ignition energy is available in 2400 psi (16.5 MPa) compression when the absolute initial pressure is about 739 psi (5.1 MPa). Indeed, when atmospheric pressure is increased by 10%, we have seen that a decrease in final temperature of 3% occurs, but an *increase* in available ignition energy of nearly 10% occurs. For the example in Figure 3, when initial pressure is at the level that yields maximal energy, peak temperature is reduced dramatically to only 282°F (139°C), but the energy available to heat a specimen increases to about 500% of that available at a one atmosphere starting pressure. As a result, initial pressure should be viewed as an important parameter to control.

This coarse analysis suggests that compression temperature and available ignition energy can have opposing influences and a parametric study may be needed to sort out the actual significance of each. In a laboratory test, it is easy to ensure that a suitably large slug of gas at the highest temperature is produced, but in the real world, where mixing of the compression gas with the compressing gas is more likely, the more severe circumstance may be where the initial pressure is higher than atmospheric. Indeed, in cases where the final temperatures produced are well above the autoignition temperature of the material under test, a higher initial pressure may be needed to ensure the most severe test.

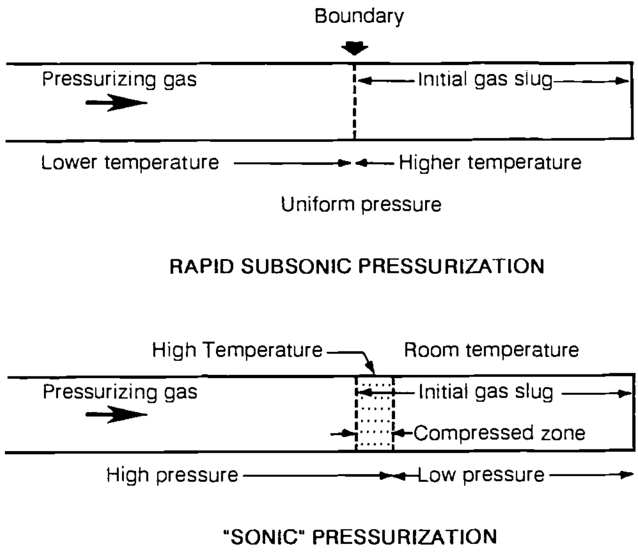

FIG. 6--*Simplified models of gaseous impact.*

Compression Wave Model

Two forms of "fast" pressurization can be considered: sonic and subsonic. In the case of a subsonic pressurization, the situation of Figure 6 (top) applies. The pressure throughout the system is considered to be uniform throughout. Hence all points downstream of the boundary are at the same temperature, having all experienced similar compression. Heat transfer is occurring throughout the system's surface.

In a sonic compression, a shock wave is moving toward the dead end, Figure 6 (bottom), applies. In this case the specimen is not exposed to elevated pressures or temperatures until the shock wave arrives (in a 44-in., 1.11-m, system it would require about 3 ms). The slug of heated oxygen forms on the front of the boundary and is at the maximum temperature for the full 3 ms. In the sonic case, a variable length slug radiates and is in heat exchange with the wall of the tubing for up to 3 ms before the specimen is exposed to any temperature increase at all.

Identifying the more severe of these two modes may require experimentation. On a shear heat transfer basis, one might surmise that because radiation is likely to be the dominant heat transfer mechanism, the shock wave mode with its high temperature slug might lose more heat than the slightly slower mode, however, it is difficult to surmise the role of the shock wave itself upon impacting the specimen.

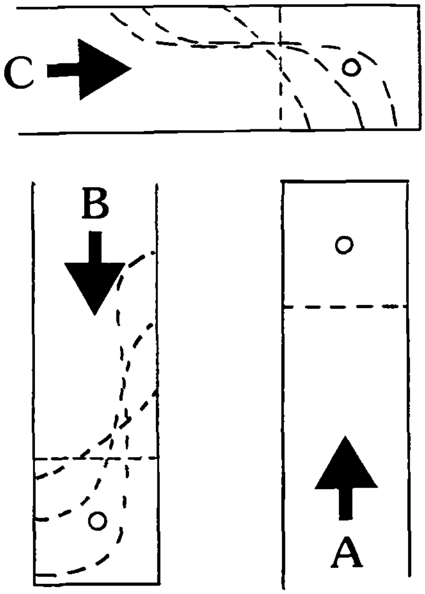

FIG. 7--*Buoyancy effects on hot gas slug.*

Energy Dissipation

When the slug of high temperature gas has been produced, heat dissipation factors become important. Two will be discussed here: adiabatic expansion and convection.

At present, the standard describes a typical test procedure in which a rapid compression is accomplished and the specimen is allowed to soak at pressure for five seconds before the system is vented. Tests of polymer-lined hoses reported by Janoff et al. [5] indicated that even at pressures well above the minimum pressure to produce ignition, up to 5 to 10 seconds could pass before burn-through occurred. As a result, the G 74 practice of venting of the pressurized gas after just 5s should be avoided, because the resulting adiabatic expansion produces cooling that might quench an ignition. Ignition in numerous materials is a process in which many steps may occur. Single pressurization cycles with protracted soak periods are likely to be most productive in the test. Since extremely fast pressurization was used in Janoff's tests, they may suggest that the role of a shock wave discussed in the previous section may not be critical.

Convection is a well known heat transfer mechanism. Convection is likely to be significant in gaseous impact tests of large-bore systems, especially when testing materials with significant induction periods (ignition delays). Simple gas buoyancy can lead to convective cooling of the test specimen. Since hot gases rise, the gaseous impact chamber should point upwards so that normal buoyancy tends to stratify the hot gas in the vicinity of the specimen, Figure 7, Part A, rather than to dissipate them, Figure 7, Parts B and C.

Specimen Preparation

Clearly, the specimen preparation should be a critical parameter. High surface-area-to-volume promotes the transfer of energy and should result in more sensitivity to gaseous impact. Porous surface areas should similarly tend to aggravate sensitivity.

Indeed, one of the areas that gaseous impact testing may be most productive is in the study of aging influences on oxygen compatibility. Two aging influences not easily studied in other equipment will be considered here: surface finish and oxygen absorption.

In the case of surface finish, most materials used in oxygen have smooth surfaces. One might expect aging to increase the surface area of a material through abrasion, cracking, etc. If one attempts to study the influence of such changes in an autoignition temperature test, such as ASTM G 72, the surface finish is unlikely to play a strong role for many materials. This is because many materials melt at temperatures well below their autoignition temperature. In the G-72 AIT test, the original surface may be modified by the slow temperature ramp that is used. In the case of G 74, the specimen surface is abruptly exposed to the high temperature and the prospect of surface feature changes are reduced.

A similar analysis suggests that oxygen absorption may be more effectively studied with gaseous impact. Irani [*11*] reports that, for example, fluorocarbon rubber (FKM) is known to absorb significant amounts of oxygen. Following a soak at pressures of 2880 psig (19.9 MPa) and return to atmospheric pressure, FKM can "inflate," and volumes can increase by as much as 100% due to absorbed oxygen. Efforts to study the influence of this absorbed oxygen are thwarted by numerous influences. The oxygen begins to diffuse out of the rubber to the atmosphere beginning upon depressurization. Also, in attempts to measure ignition temperatures, the slowly rising temperature aids in the dissipation of the absorbed oxygen so that by the time high temperatures are reached, the specially prepared material has probably returned to the condition of an unprepared elastomer.

In the case of gaseous impact testing, the elastomer can be soaked at pressure in the GI apparatus itself. It can then be depressurized momentarily and allowed just a few seconds to come to ambient temperature, and then it can be repressurized quickly with oxygen, and in the process mechanical work on the absorbed oxygen or on oxygen trapped in pores in the elastomer should drive up its temperature in a circumstance where all of the heat transfer is directly into the polymer itself. The GI test may be viewed in this case as the rapid compression of a oxygen-filled balloon.

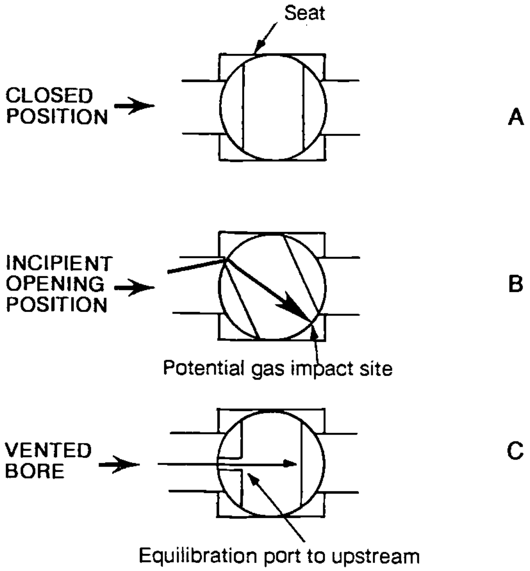

FIG. 8--*Gaseous impact in ball valves.*

Ball Valve and System Safety

Although the potential for an economical test method is alluring, there are a few aspects that raise concerns which should be addressed. Perhaps the most important is the safety in using a ball valve to rapidly pressurize the test chamber. Ball valve use with oxygen, especially at high pressure, has been discouraged, because fires have resulted upon ball valve operation.

In most instances the fires have been attributed to the rapid pressurization that occurs downstream. Since ball valves are the exact real-world components that are most often suspect, this would not appear to be a disadvantage in this case. Why spend large amounts of money on special valves to ensure opening times that will not be confronted in the real world?

Unfortunately, there are a few known cases in which the ball valve that was being opened, itself, ignited upon operation. These events have exhibited a randomness; a verbal report on one such event described at the 1991 ASTM G 4 symposium was in a system that had been in service for a protracted period. These events warrant discussion since the mechanism for them is not clear.

An hypothesis for ball-valve self ignitions can be proposed along with a protential remedy. The hypothesis presumes that the bore of the ball valve can constitute an independent system that can experience gaseous impact during ball-valve opening. Figure 8, Parts A and B, depicts a ball valve at two stages of operation: closed and imminent at "incipient" opening.

Normally, ball valves operate with upstream pressure forcing the ball into the polymer on the downstream hemisphere, establishing a seal there. Compressive force tends to be reduced in the polymer on the upstream hemisphere. As a result, in many cases, one might suspect that the upstream hemisphere might not seal and the bore of the ball might be expected to be equilibrated with the upstream system.

However, it is not inconceivable that the upstream hemisphere might also form a seal and the bore might act as an isolated chamber. For example if the ball valve is closed while in a depressurized state, or perhaps even worse, might be in a partially pressurized state, and the upstream system is then pressurized, perhaps the bore might remain at the low or intermediate pressure. Then when the ball is at its incipient opening point, Figure 8, Part B, it might just experience pressurization of the bore for a transient period just long enough to generate high temperatures in contact with the exposed polymer seat and induce its ignition. Indeed, many commercial ball valves have bores that approximate, or are larger than, the dimensions of the more sensitive GI test cells in use.

Indeed, a commercial ball valve was modified so that pressure in the bore could be measured, and with the bore depressurized, the valve was slowly opened. The bore became pressurized before any flow from the valve occurred. Further, the pressurization of the bore does not appear to have been due to manufacturing tolerance or wear, because when the valve was removed and installed in the reverse direction, the same effect was seen, Perhaps, the pressure on the ball and the force it produces on the downstream hemisphere render the downstream seal more effective. Hence, slow opening of ball valves may lessen the stress downstream but actually increase the stress in the bore.

Further, since these events of self-ignition exhibit a random nature, it may be that the worst-case condition which results in ignition is when the bore contains an intermediate pressure. In the intermediate-pressure case, the incoming gas is likely to mix with the oxygen already present in the bore. As we have seen above, the available energy to induce ignition in a case like this is a strong function of the initial downstream (bore) pressure and the simple model above suggested that the maximum energy available might result from a bore pressure as high as 30.8% of the upstream absolute pressure. Hence the ignition event might not necessarily occur until some random operation resulted in the entrapment of just the right amount of pressure to yield a severe ignition condition.

If this mechanism can be demonstrated, a simple route to eliminate it might be to vent the bore of the ball to the upstream system (as is presently done in ball valves for liquid service) and is accomplished by drilling a small hole in the upstream hemisphere, Figure 8, Part C. Such a result might upgrade the safety of a rudimentary G 74 apparatus and might also suggest ways to expand the range of acceptable ball-valve use in oxygen systems

Summary

Although several laboratories have successfully used variants of gaseous impact tests, the typical ASTM implementation and several variants of it have not proven useful due largely to insensitivity. The favorable economics of the potential test implementations and the potential value of the test in studying aging effects in polymers may warrant further work by ASTM Committee G-4 to modify and revalidate the procedure.

An optimum test may be capable of a worst-case gaseous impact, allowing its application to real world systems, and the preceding superficial analysis suggests this may demand a long and large-bore supply line, an upward mounted hemispherical test chamber, central specimen mounting, and an ability to carefully vary and control the initial pressure.

References

[*1*] Barthelemy, H., and Vagnard, G., **"Ignition of PTFE-Lined Hoses in High-Pressure Oxygen Systems: Test Results and Considerations for Safe Design and Use,"** *Flammability and Sensitivity of Materials in Oxygen-Enriched Atmospheres: Third Volume, ASTM STP 986*, D. W. Schroll, Ed., American Society for Testing and Materials, Philadelphia, 1988, pp. 289-304.

[2] Wegener, W., Binder, C., Hengstenberg, P., and Weinert, D., **"Tests to Evaluate the Suitability of Materials for Oxygen Service,"** *Flammability and Sensitivity of Materials in Oxygen-Enriched Atmospheres: Third Volume, ASTM STP 986*, D. W. Schroll, Ed., American Society for Testing and Materials, Philadelphia, 1988, pp. 268-278.

[*3*] Moffet, G. E., Pedley, M. D., Schmidt, N., Williams, R. E., Hirsch, D., and Benz, F. J., **"Ignition of Nonmetallic Materials by Impact of High-Pressure Gaseous Oxygen,"** *Flammability and Sensitivity of Materials in Oxygen-Enriched Atmospheres: Third Volume, ASTM STP 986*, D. W. Schroll, Ed., American Society for Testing and Materials, Philadelphia, 1988, pp. 218-232.

[*4*] Schmidt, N., Moffett, G. E., Pedley, M. D., and Linley, L. J., **"Ignition of Nonmetallic Materials by Impact of High Pressure Oxygen II: Evaluation of Repeatability of Pneumatic Impact Test,"** *Flammability and Sensitivity of Materials in Oxygen-Enriched Atmospheres: Fourth Volume, ASTM STP 1040*, Joel M. Stoltzfus, Frank J. Benz, and Jack S. Stradling, Editors, American Society for Testing and Materials, Philadelphia, 1989, pp. 23-37.

[*5*] Janoff, D., Bamford, L. J., Newton, B. E., and Bryan, C. J., **"Ignition of PTFE-Lined Flexible Hoses by Rapid Pressurization With Oxygen,"** *Flammability and Sensitivity of Materials in Oxygen-Enriched Atmospheres: Fourth Volume, ASTM STP 1040*, Joel M. Stoltzfus, Frank J. Benz, and Jack S. Stradling, Editors, American Society for Testing and Materials, Philadelphia, 1989, pp. 288-308.

[*6*] Janoff, D., Pedley, M. D., and Bamford, L. J., **"Ignition of Nonmetallic Materials by Impact of High Pressure Oxygen III: New Method Development,"** *Flammability and Sensitivity of Materials in Oxygen-Enriched Atmospheres: Fifth Volume, ASTM STP 1111*, Joel M. Stoltzfus and Kenneth McIlroy, Eds., American Society for Testing and Materials, Philadelphia, 1991, pp. 60-74.

[*7*] Vagnard, G., Delode, G., and Barthelemy, H., **"Test Methods and Interpretation of Results for Selecting Non-Metallic Materials for Oxygen Service,"** *Flammability and Sensitivity of Materials in Oxygen-Enriched Atmospheres: Fifth Volume, ASTM STP 1111*, Joel M. Stoltzfus and Kenneth McIlroy, Eds., American Society for Testing and Materials, Philadelphia, 1991, pp. 489-505.

[*8*] Chase, J. D., **"Evaporation and Ignition in Air of a Surface Oil Film Following Adiabatic Compression,"** *Combustion and Flame*, Vol. 10, No. 4, Dec. 1966, pp. 315-329.

[*9*] Wilson, M. P., DeSouza, F., and Presti, J., **"Oil-Air Explosion Hazards in High-Pressure Air Systems,"** Contracts NObs 4204 and 4314, General Dynamics, Groton, Conn, November, 1961.

[*10*] Leslie, I. H., **"Thermodynamic and Fluid Mechanic Analysis of Rapid Pressurization in a Dead-End Tube,"** *Flammability and Sensitivity of Materials in Oxygen-Enriched Atmospheres: Fifth Volume, ASTM STP 1111*, Joel M. Stoltzfus and Kenneth McIlroy, Eds., American Society for Testing and Materials, Philadelphia, 1991, pp. 399-413.

[*11*] Irani, R. S., Currie, J. L., Wilson, N. J., and Sanders, J., "**Dimensional Changes in Elastomers Under High-Pressure Oxygen,**" *Flammability and Sensitivity of Materials in Oxygen-Enriched Atmospheres: Third Volume, ASTM STP 986*, D. W. Schroll, Ed., American Society for Testing and Materials, Philadelphia, 1988, pp. 60-74.

George W. Sidebotham[1], James A. Cross[2], Gerald L. Wolf[3]

A TEST METHOD FOR MEASURING THE MINIMUM OXYGEN CONCENTRATION TO SUPPORT AN INTRALUMINAL FLAME

REFERENCE: Sidebotham, G. W., Cross, J. A., and Wolf, G. L., "A Test Method for Measuring the Minimum Oxygen Concentration to Support an Intraluminal Flame," Flammability and Sensitivity of Materials in Oxygen-Enriched Atmospheres: 6th Volume, ASTM STP 1197, Dwight D. Janoff and Joel M. Stoltzfus, Eds., American Society for Testing and Materials, Philadelphia, 1993.

ABSTRACT: A test method for measuring the minimum concentration to support an intraluminal flame is described. An oxidizer is flowed through a plastic tube, and an ignition source is applied to the free end of the tube. If the oxygen concentration is sufficient, a flame propagates along the inner surface of the tube, termed an intraluminal flame. The minimum concentration of oxygen, or limiting oxygen index (LOI), that will support such a flame is determined. Results are reported for polyvinyl chloride tubing and compared to those using the standard ASTM D 2863, the candle-type flammability test. In the intraluminal test, the LOI with helium as the diluent gas is lower than that with nitrogen as the diluent, in contrast to results using ASTM D 2863. The effects of buoyancy are reduced in the intraluminal test, and the results may therefore be more applicable to low gravity environments.

KEYWORDS: Flame spread, oxygen index, polyvinyl chloride, combustion, endotracheal tube fires, microgravity

---

[1] Assistant Professor of Chemical Engineering, The Cooper Union for the Advancement of Science and Art, 51 Astor Place, New York, NY 10003.

[2] Cooper Union Masters degree recipient. Currently with the Brooklyn Union Gas Company, Brooklyn, NY.

[3] Professor of Clinical Anesthesiology, State University of New York, Health Science Center at Brooklyn, 450 Clarkson Avenue, Box 6, Brooklyn, NY 11203.

INTRODUCTION

The minimum oxygen concentration that will support combustion is a useful measure of the relative flammability of solid materials in oxygen enriched atmospheres. The well known candle-type flammability test [1] was originally published in 1970 as the ASTM Standard Test Method for Measuring the Minimum Oxygen Concentration to Support Candle-like Combustion of Plastics (Oxygen Index) D 2863. The minimum oxygen concentration is also referred to as the limiting oxygen index (LOI) [2] or the critical oxygen index (COI) [3]. An alternative experimental methodology to obtain an LOI is presented in this paper.

It is emphasized that a universal LOI does not exist for a given material [3, 4]. Rather, an LOI exists for a material for a given test method. Therefore, application of standardized test results to a particular system must be made with caution. It is left to the discretion of the designer or user of a system to determine whether or not the results from the standard test accurately reflect what can be expected in the system under consideration. Even if quantitative agreement between the standard test and an application is uncertain, it is tempting to speculate that qualitative trends are preserved: if material A is less flammable than material B in the LOI test, then A is less flammable than B in any system. The results reported here suggest that even qualitative agreement can be suspect.

The present work is an outgrowth of research into operating room fire safety problems [5]. The accidental ignition of endotracheal tubes during surgery by surgical lasers, electrosurgical units and electrocautery continues to pose a fire risk in the oxygen-enriched environment of the mouth or airway. In an effort to understand this endotracheal tube fire problem, a simple experiment was developed. Results of this experiment and a discussion of the flame mechanisms are reported in reference [6]. Briefly, an oxidizer is flowed through a plastic tube and an ignition source is applied to the open end of the tube. A flame, termed an intraluminal flame, is observed to propagate along the inside surface of the tube at a measurable speed. It was concluded that this intraluminal flame spread process characterizes endotracheal tube fires.

For a given oxygen concentration, there exist flow limits: if the flow rate of oxidizer is too great or too small, an intraluminal flame cannot be established. As the oxygen concentration is reduced, the rate of flame spread decreases and the flow limits narrow until a limiting oxygen concentration is reached below which an intraluminal flame cannot be established. The results of such tests then represent an alternative measure of the limiting oxygen index. Results from this test are reported and compared to those obtained by the standard ASTM D 2863 method.

EXPERIMENTAL

A brief description of the experimental approach used to determine the limits of intraluminal flame spread in polyvinyl chloride tubing is reported here. Further details can be found in reference [7].

Gaseous flows were obtained from compressed gas cylinders. Flow rates were regulated by mass flow controllers, calibrated with a soap bubble meter. In the present study, various sizes of Clear-flo polyvinyl chloride tubing, obtained from New Age Industries, were used. Data has not yet been obtained for other materials. The ignition source was a pilot flame obtained by flowing natural gas through a small copper tube to yield a diffusion flame approximately 1 cm in height.

To perform the test, a section of tubing, sufficiently long to guarantee fully developed flow, was connected to the oxidizer source. The downstream end was horizontal, open to the atmosphere, and loosely supported by a clamp, allowing the tube to hang cantilevered approximately 15 cm from the clamp. The tube was marked on the outside with a greaseless pen at known intervals, typically 5 cm. A fixed flow rate of oxidizer (oxygen plus diluent) was delivered to the test specimen. The ignition source was applied to the free end after sufficient time was allowed to flush the system. The flame event was successful if an intraluminal flame propagated for at least 5 cm, or survived at least 3 minutes. This criterion is the same as that in ASTM D 2863.

If an event occurred, the oxygen concentration was decreased by either lowering the oxygen flow rate (with fixed diluent flow), or by increasing the diluent flow (with fixed oxygen flow). The test was repeated until a flame did not satisfy the criterion for a successful event.

There was concern that the oxygen concentration in the vicinity of the free end was lowered due to mixing with ambient air. To investigate this effect, tests were performed in which the ignition source was inserted approximately 3 cm into the tube instead of being applied to the free end. The results were not affected by how the ignition source was applied.

A complication of the test was encountered in determining the upper flow limit in some cases. At high oxygen concentrations, it was observed that a flame could be anchored outside of the free end, and slowly consume the entire tube, yielding an apparent flame spread rate. This "free end flame" was considered to be stabilized outside of the flame by a complex recirculation pattern that existed outside the tube. However, the leading edge of this flame never entered into the tube, and is not considered an intraluminal flame. This complication did not occur near the limiting oxygen concentration.

The conventional candle-type ASTM (D 2863) was performed on the same material to allow comparison with the present intraluminal flame test. Following Simpson, et al. [4], the test was adapted to a tube material and other diluents. The flame spread in this test was observed to occur on the outside surface of the tube.

RESULTS

Figure 1 shows the intraluminal flame spread rate as a function of oxidizer velocity for 50% O2 mixtures (by volume) in nitrogen and helium. The techniques used to generate these data are described in reference [6]. In both cases, there is a lower flow limit, and upper flow limit, and a peak in the flame spread rate. It is apparent that helium yields a much higher peak flame spread rate than nitrogen. However, beyond the flame spread rate peak, the

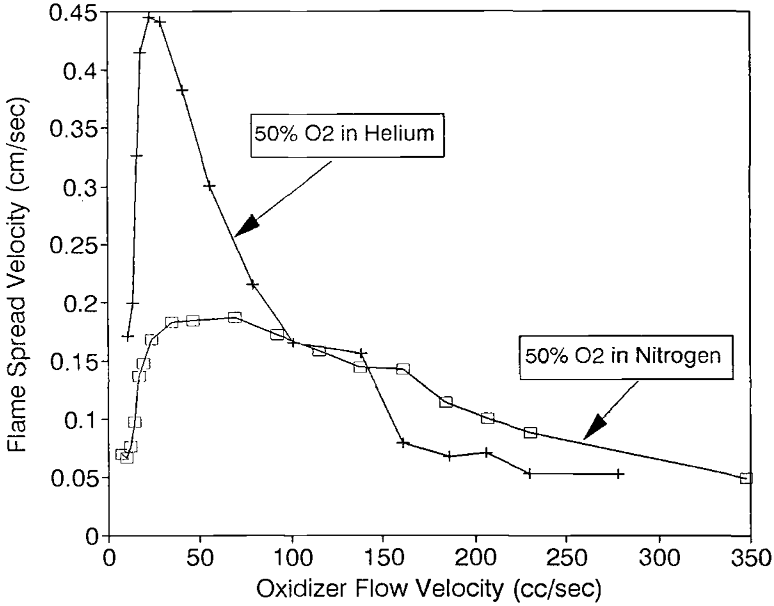

Figure 1 -- Intraluminal flame spread rate versus oxidizer flow velocity for 50 vol% oxygen in two diluent gases. 3.2 mm inner diameter, 6.4 mm outer diameter polyvinyl chloride tubing was used.

rate of decay of flame spread rate with increasing oxidizer flow is also much larger for helium. Therefore, the upper flow limit occurs at a lower total oxidizer flow for helium. For other oxygen concentrations, the shapes of the curves are similar, but the limits are wider for higher oxygen concentrations, and shallower for lower oxygen concentrations. Flammability maps, which indicate flammable and non-flammable regions, can be constructed using data of this type.

Figure 2 shows a conceptual diagram of a flammability map, in which flammable regions are separated from non-flammable regions. The oxygen concentration is plotted against the total oxidizer flow rate (or flow velocity) in the tube. For a given oxygen concentration, low flow and high flow limits exist. These limits approach each other as the oxygen concentration is reduced until they meet. The oxygen concentration below which intraluminal flames cannot be established is the limiting oxygen index for intraluminal flame propagation.

The flammable region is separated into two parts. Region A represents intraluminal flame propagation, while region B represents the so-called "free end flames" that were stabilized outside the free end of the tube. For all cases investigated here, the onset of these flames occurred at higher oxygen concentrations than the LOI, and therefore did not interfere with the attainment of the LOI.

The non-flammable region is separated into three parts. Regions C and D represents regions with sufficient oxygen concentration, but are below the lower flow limit, or above the upper flow limit respectively. Region E represents regions in which the oxygen concentration is sufficiently low that intraluminal flames cannot be established for any flow rate.

Figure 3 shows a typical flammability map in which the oxygen concentration is plotted against the oxidizer velocity (total flow rate divided by the area). Conditions that yielded intraluminal flames are reported with one symbol, and conditions which did not yield flames are reported as another symbol. The limiting oxygen index is the lowest oxygen concentration for which a flame existed, and occurs at a particular flow velocity. For every tube material, tube geometry and diluent type, a flammability map similar to Figure 3 must be developed to yield the LOI.

Experience dictated that the lower flow limit was easily and reproducibly obtained. To isolate the lower flow limit, it was most convenient to fix the diluent flow rate, and to vary the oxygen flow rate. In this manner, successive tests yielded points along a line roughly perpendicular to the lower flow limit line. In principle,

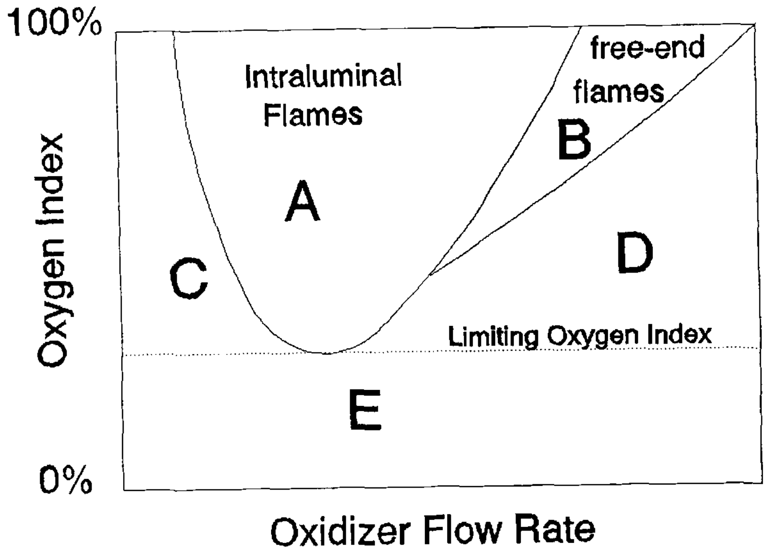

Figure 2 -- Schematic representation of a flammability map.

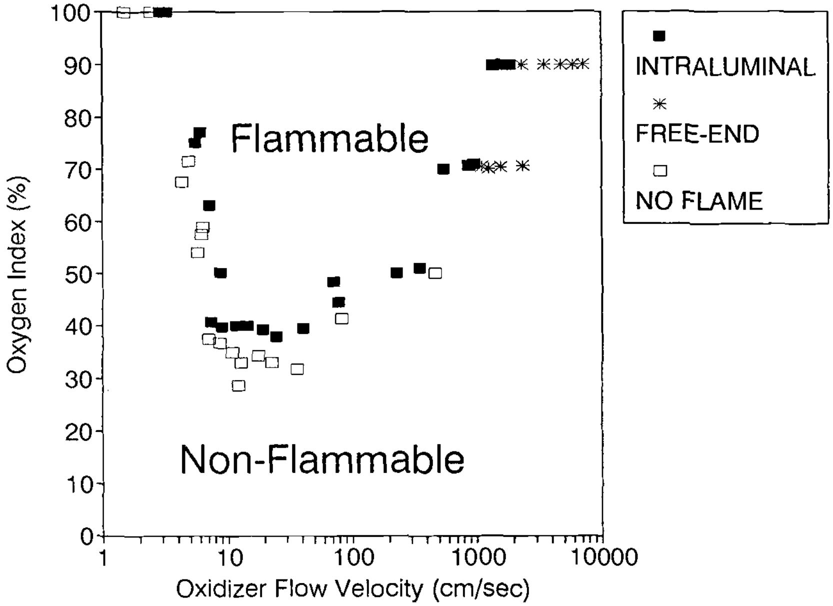

Figure 3 -- Typical flammability map. 3.2 mm inner diameter, 6.4 outer diameter tubing. Nitrogen is the diluent gas. Data points indicate the type of flame observed for conditions tested.

the upper flow limit could similarly be most conveniently obtained by fixing the oxidizer flow and varying the diluent flow. However, since the magnitude of the slope of the lower flow limit was much steeper than that of the upper flow limit, it was found that this approach was not necessary to find the LOI.

Figure 4 shows the effect of the inner diameter on the LOI for four different diluents. It is apparent that the LOI decreases with increasing tube inner diameter for the intraluminal flame test. The LOI obtained with helium is consistently lower than that obtained with nitrogen. This result suggests that nitrogen is a more effective flame suppressant than helium. Carbon dioxide (CO2) yielded the highest LOI, and argon yielded the lowest LOI.

The conventional candle-type flammability test (ASTM D 2863) was performed on the same material using nitrogen and helium as diluents. The LOI was found to be weakly dependent on size for the candle type test. The average LOI was 24.2 for nitrogen mixtures, and 30.2 for helium mixtures. This trend of greater values of LOI when helium is used as compared to nitrogen is consistent with that reported by Werley [4] and Simpson et al. [5], and suggests that helium is a more effective diluent at suppressing flame spread, in contrast to the conclusion using the intraluminal test. The results with carbon dioxide and argon using the candle-type test [4] are consistent with those found in the present study.

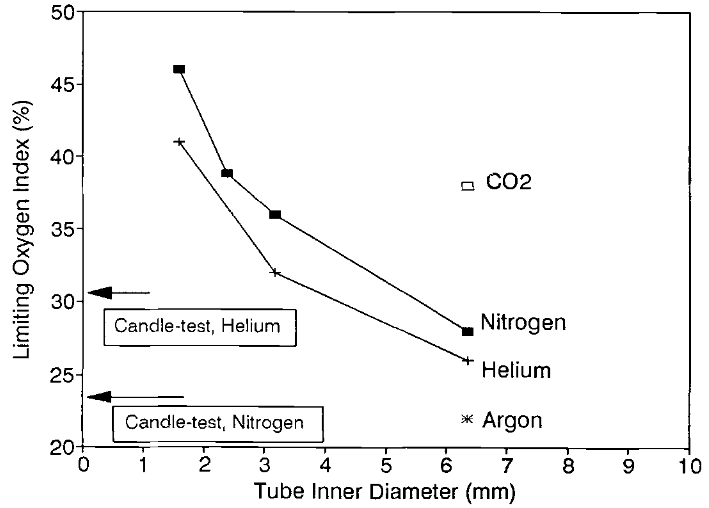

Figure 4 -- Limiting oxygen index as a function of tube inner diameter. Four different inerts were tested. Results from ASTM D 2863 are indicated for nitrogen and helium.

DISCUSSION

In order to understand the trends observed in the intraluminal LOI test, it is helpful to reconsider the mechanisms of flame spread, discussed by Glassman [2], as applied to intraluminal flame spread [6]. A schematic of the intraluminal flame spreading process is shown in Figure 5. The bulk of the flame is a gas phase diffusion flame in which the gaseous fuel is obtained by gasification of the solid fuel. The energy for gasification comes from heat conducted through the gaseous fuel vapor to the solid fuel. There is a quenching layer between the flame and the solid fuel because the solid fuel vaporizes at a much lower temperature than that at the diffusion flame surface. Inside the quenching layer and near the leading edge of the flame, fuel and oxidizer mix. Therefore, the leading edge is a pre-mixed flame which propagates toward the opposed flow at a distance from the solid fuel, termed the quenching distance.

At low flows, the flame spread rate increases with increasing oxidizer flow because of the increase in fuel gasification rate associated with the improved heat transfer rate from the hot flame gases to the solid fuel. However, as the oxidizer flow rate is increased, the spreading flame must propagate against a stronger opposed flow. Eventually,

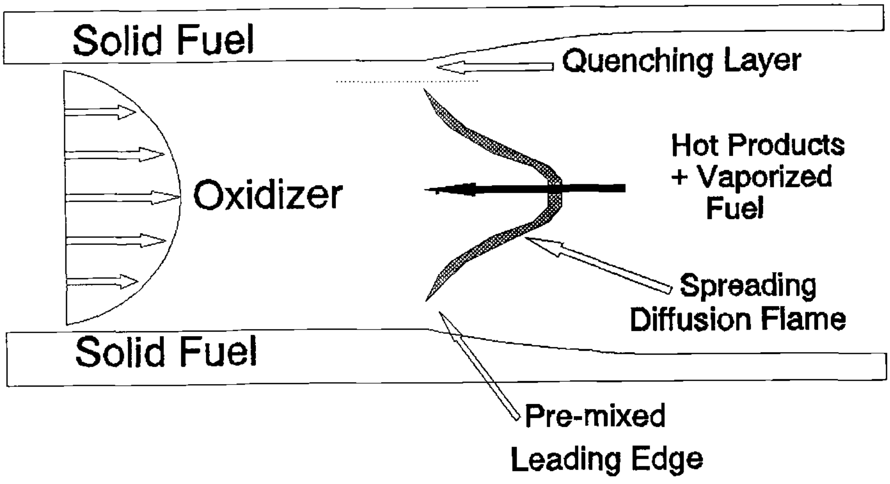

Figure 5 -- Schematic of an intraluminal flame. The flame is spreading from right to left as indicated by the solid arrow. The fuel is thinner downstream of the flame because of fuel vaporization.

this latter effect dominates the former, and the flame spread rate in the laboratory reference frame is observed to peak, then decrease with increasing oxidizer flow. Ultimately, the opposed flow rate at the quenching distance is greater than the leading edge pre-mixed flame speed, and the flame cannot enter into the tube. This effect then yields the upper flow limit, or "blow-out" limit.

Helium vs. Nitrogen

Helium has a much higher thermal diffusivity, hence higher quenching distance, than nitrogen[*]. Therefore, since the velocity profile is parabolic, the velocity at the quenching distance is larger for helium than for nitrogen for the same oxidizer flow velocity. An intraluminal flame with helium as the inert is more sensitive to an increase in flow velocity.

Helium has a lower specific heat than nitrogen, hence higher flame temperatures, than nitrogen. Therefore, since the leading edge pre-mixed speed increases strongly with temperature, the flame spread rate for helium is greater than that for nitrogen for low opposed flow rates (where the effects of the opposing flow are not dominant).

Buoyancy Effects

The effects of natural convection, or buoyancy, on flame spread help explain the difference between the standard candle-type test and the intraluminal flame test. For opposed flow flame spread with an oxidizer of infinite extent, the flame can induce a flow into the flame [2]. The hot gases produced by the flame have a low density, and therefore experience a buoyant upward acceleration. To conserve mass, these rising gases are replaced by fresh gas. As a result, the spreading flame experiences an induced opposed flow even in a quiescent atmosphere. When the forced flow is much less than that generated by natural convection, the flame spread rate is independent of the forced flow. This result is experimentally verified for flame spread over flat plates [2]. Further, for these experiments, a low flow limit of flame spread has never been reported.

In contrast, for intraluminal flames, the flame does not propagate into an oxidizer of infinite extent. Hot

---

[*] The depth of the quenching layer is related to heat conduction. The magnitude of the quenching distance is proportional to the thermal diffusivity of the gas (the thermal conductivity divided by the density and the specific heat), which varies approximately with the inverse square root of the molecular weight.

gases generated in the flame have no place to rise in the confines of the tube. Therefore, there is no induced flow due to buoyant effects, and the only flow rate the flame experiences is the forced flow supplied through the tube. Indeed, as the oxidizer flow rate decreases, the flame spread rate decreases until the lower flow limit is reached. The only previous reports of low flow limits of flame spread are those in microgravity experiments [8].

The candle-type flammability test yields results for LOI which are insensitive to forced flow within the oxidizer flow range dictated (provided there is no mixing of ambient air [3]). It is thus argued that the flow field in the vicinity of the burning sample is controlled by buoyant effects. A plausible explanation for higher LOIs in helium compared to nitrogen is that with the larger quenching distance, and induced buoyant flow rate, the leading edge of the helium flame experiences a higher opposed velocity.

Application to Other Material Geometries

While the intraluminal flammability test is well suited to tube geometries of transparent materials, it may be possible to extend the test to solid materials which are not in tubular form. For example, holes of a given size can be drilled into a plate of plexiglass to simulate a tube geometry, and an oxidizer flowed through the holes. Alternatively, the flame spread between two sheets of plexiglass through which an oxidizer flows can be attempted. If the test is to be extended to opaque materials, a method of flame detection must be identified.

CONCLUSIONS

1) The minimum oxygen concentration which will support an intraluminal can be measured easily and reproducibly.
2) In comparing the effects of nitrogen versus helium, opposite trends are observed with the intraluminal test as compared to the standard ASTM test. The intraluminal test is considered to be more relevant to the endotracheal tube fire problem.
3) The results of the test depend on the inner diameter of the tube. This dependence must be further understood prior to proposing a standard test method.
4) In principle, adaptations of the intraluminal test can be applied to any solid material which can be tested using the standard candle-type test.
5) The effects of buoyancy are much less important in the intraluminal flammability test than they are in the candle-type test. Therefore, the intraluminal flame test may be useful for low gravity applications.

ACKNOWLEDGEMENTS

The authors would like to thank Robert Aftel for assistance with many experiments, Ron Adner for obtaining the data with carbon dioxide and argon, and to four high school students, Jeannette Cooper, Steven Kovach, Xiao Yang Li and Wei Lian Su, who obtained nitrogen data as part of a summer research internship program at the Cooper Union.

REFERENCES

[1] Fenimore, C.P. and Martin, F.J., "Candle-Type Test for Flammability of Polymers," Modern Plastics, MOPLA, Vol. 43, November 1966, p. 141.

[2] Glassman, I., "Combustion Fundamentals of Low Volatility Materials in Oxygen-Enriched Atmospheres," Flammability and Sensitivity of Materials in Oxygen-Enriched Atmospheres, ASTM STP 1111, Joel M. Stoltzfus and Kenneth McIlroy, Eds., American Society for Testing and Materials, Philadelphia, 1991.

[3] Wharton, R.K., "An Assessment of the Critical Oxygen Index Test as a Measure of Material Flammability," Flammability and Sensitivity of Materials in Oxygen-Enriched Atmospheres, ASTM STP 986, D.W. Schroll, Ed., American Society for Testing and Materials, Philadelphia, 1987.

[4] Werley, B.L. "An Oxygen Index Update," Flammability and Sensitivity of Materials in Oxygen-Enriched Atmospheres, ASTM STP 986, D.W. Schroll, Ed., American Society for Testing and Materials, Philadelphia, 1988.

[5] Simpson, J.I., Wolf, G.L., and Schiff, G.A., "The Oxidant O2 (Helium) Index of Flammability of Endotracheal Tubes," Flammability and Sensitivity of Materials in Oxygen-Enriched Atmospheres, ASTM STP 1040, Joel M. Stoltzfus, Frank J. Benz, and Jack S. Stradling, Eds., American Society for Testing and Materials, Philadelphia, 1989.

[6] Sidebotham, G.W., Wolf, G.L., Stern, J. and Aftel, R. "Endotracheal Tube Fires: A Flame Spread Phenomenon," Flammability and Sensitivity of Materials in Oxygen-Enriched Atmospheres, ASTM STP 1111, Joel M. Stoltzfus and Kenneth McIlroy, Eds., American Society for Testing and Materials, Philadelphia, 1991.

[7] Cross, J.A., "Effects of Intraluminal Helium and Nitrogen on Flammability Characteristics of Polyvinyl Chloride Tubes with Application to the Tracheal Tube Fire Problem," Masters of Engineering thesis, The Cooper Union, New York, NY, May 1991.

[8] Olson, S.L., "Mechanisms of Microgravity Flame Spread Over a Thin Solid Fuel: Oxygen and Opposed Flow Effects," Combustion Science and Technology, Vol. 76, pp. 233-249, 1991.

Ignition and Combustion of Polymers

Gerald L. Wolf[1], J. Gary McGuire[2], Philip F. Nolan[3], George W. Sidebotham[4]

SPONTANEOUS IGNITION TEMPERATURE OF TRACHEAL TUBES

REFERENCE: Wolf, G. L., McGuire, J. G., Nolan, P. F., and Sidebotham, G. W., "Spontaneous Ignition Temperature of Tracheal Tubes," Flammability and Sensitivity of Materials in Oxygen-Enriched Atmospheres: 6th Volume, ASTM STP 1197, Dwight D. Janoff and Joel M. Stoltzfus, Eds., American Society for Testing and Materials, Philadelphia, 1993.

ABSTRACT: Operating room fires continue to be reported in the medical literature. To simulate operating room conditions, a high pressure spontaneous ignition apparatus was redesigned to allow for the determination of spontaneous ignition temperature of tracheal tubes in 100% oxygen at atmospheric pressure. Pure oxygen flowed through a test chamber at 100 cm^3/min, and a temperature ramp rate of 10°C/min was used. Sample temperature, chamber temperature, chamber pressure and elapsed time were stored on-line by computer. The experimental ignition temperature was observed as a spike in sample temperature-time plot.

---

[1] Professor of Clinical Anesthesiology, State University of New York, Health Science Center at Brooklyn, Box 6, 450 Clarkson Avenue, Brooklyn, New York, 11203.

[2] Consultant Safety Engineer, SRC Consultants, Ltd., Woolston, Cheshire, U.K.

[3] Professor, Department of Chemical Engineering, South Bank University, 103 Borough Road, London, SE1 0AA, U.K.

[4] Assistant Professor of Chemical Engineering, The Cooper Union for the Advancement of Science and Art, 51 Astor Place, New York, New York, 10003.

Five samples each of poly (vinyl chloride), red rubber and silicone rubber tracheal tubes were analyzed for spontaneous ignition temperature, which were determined to be 428°C, 371°C, 381°C, respectively.

It was concluded that the small differences in spontaneous ignition temperature for the various tracheal tube materials has little clinical relevance to the tubes chosen for the particular surgical procedure.

KEYWORDS: combustion, polyvinyl chloride, red rubber, silicon rubber, spontaneous ignition temperature, tracheal tube fires.

INTRODUCTION

Operating room fires continue to be reported in the medical literature. Head and neck surgical procedures in which a laser[1] or electrosurgical apparatus[2] is used during the administration of an oxygen enriched anesthetic atmosphere to the patient via a polymer tracheal tube create a particularly hazardous situation. This study extends the previous work on oxygen index[3] and flame spread[4] to the area of spontaneous ignition temperature (SIT) of tracheal tubes manufactured of polyvinyl chloride (PVC), red rubber (RR), and silicone rubber (SR).

EXPERIMENTAL METHOD

In order to obtain data relevant to operating room conditions, a high pressure SIT apparatus was modified to allow for the determination of SIT for tracheal tube materials in 100% oxygen at ambient pressure. The apparatus is based on that previously described by Swindells, Nolan and Wharton[5].

Figure 1 is a diagrammatic representation of the experimental arrangement. Pure oxygen flows from tanks pressurized at 136 bar (13.6 M Pa), and subsequently reduced to 3.4 bar (0.34 M Pa). Flow is controlled by a needle valve downstream from the regulator, and flow rate through the test chamber is determined at an outlet 50-cm^3 bubble flowmeter with the aid of a stop watch. A mercury-manometer-calibrated pressure transducer upstream monitors the pressure within the test chamber. A 1 kW coil heater wound spirally and circumferentially around the test chamber provides ramped heating within the chamber, and the test chamber/heating coil unit is overwrapped with ceramic insulation padding and is placed into a metal container. An externally adjustable relief valve set at 3.4 bar (0.34 M Pa) releases possible inadvertent

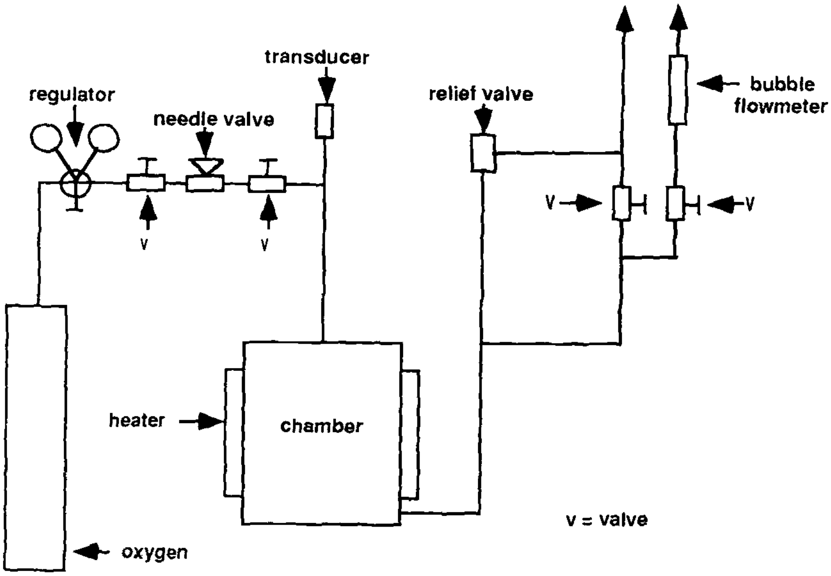

FIG. 1 - - EXPERIMENTAL SETUP

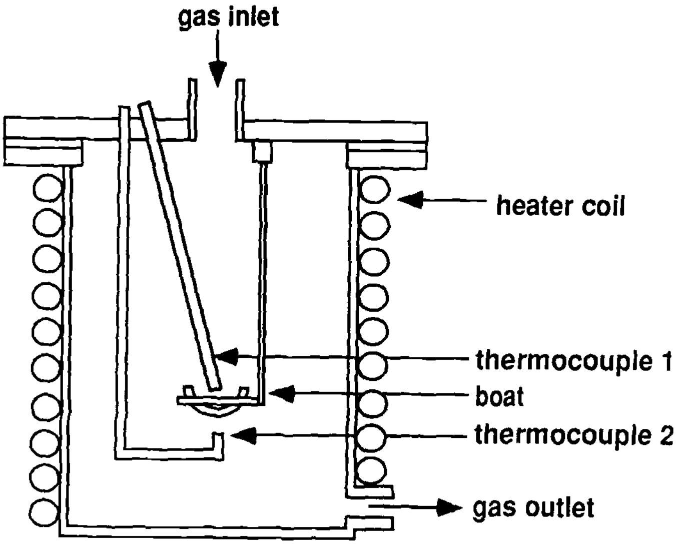

FIG. 2 - - TEST CHAMBER

explosive pressure buildup. Following flow determinations, the bubble flowmeter is bypassed and the exiting gas flow vented to atmosphere.

Figure 2 illustrates the test chamber. The chamber is manufactured from a cylindrical section of stainless steel of 3-mm wall thickness, 50-mm internal diameter, and 150-mm height. A welded-top rim with interposed copper gasket tapped to receive bolts secures a lid to the test chamber containing an inlet gas fitting, a sample boat holder, and two thermocouples (TC). The sample boat, 1.5 mm thick borosilicate glass and hemispherical in shape with an inner diameter of 1.0 cm, is supported during the test within the sample holder loop.

Samples are prepared by sectioning a segment of tube wall into 1-mm^3 sections and washing the sections in trichloro trifluoroethane solvent to remove any surface grease and contaminants. A weighed sample of 150 mg +/- 2 mg is placed into the boro silicate boat. The boat is placed in the loop of the sample boat holder, placed into the stainless steel cylindrical test chamber, and sealed by lid, gasket and bolts. Nickel coated 1-mm diameter chromel-alumel thermocouples were chosen. Thermocouple 1, positioned 1 mm above the sample, senses sample temperature. Thermocouple 2, positioned 1 mm below the sample boat, senses test chamber temperature.

A flow of 100% oxygen is established through the chamber at 100 cm^3/min, and a temperature ramp rate of 10^0C/min is obtained by voltage surges to the heating coil controlled by a voltage regulator and controller with serial computer interfacing to TC2. Data from TC1, TC2, pressure transducer, and elapsed time are constantly monitored in graphic display by a computer. All experimental data is stored to disk and downloaded to a spreadsheet program for storage, analysis and presentation. Experimental ignition temperature is observed as a spike in the recording from TC1 and analysis of digital data.

Industrial grade PVC was initially tested, followed by testing of tracheal tubes samples manufactured of PVC, RR and SR.

The statistical significance of differences between industrial grade PVC tubing at low and high pressure were analyzed by a t-test with $p<0.01$ considered significant. The statistical significance of differences between tracheal tube samples manufactured of PVC, RR and SR were tested by one-way analysis of variance with Bonferroni corrcted t-tests for pairwise comparisons (overall $p<0.01$, $p<0.003$ considered significant for pairwise tests).

The tests were performed in the High Pressure Cells of the Fire and Explosion Unit of the Chemical Engineering Department of the South Bank University, London, U. K. The High Pressure Cells are reinforced concrete laboratory cubicles designed to contain possible fire and explosion events, vent explosively expanding gases safely while trapping debris, and allow rapid exit of personnel.

RESULTS

Prior to testing tracheal tube samples, samples of industrial grade polyvinyl chloride tubing were studied to establish the reliability of, and gain confidence in, the test apparatus. During initial testing the SIT of industrial grade PVC clustered at two temperatures as presented in Table 1.

TABLE 1--SIT for Industrial Grade PVC

PVC	n	SIT	Standard Deviation
	5	257°C	+/- 0.5°C
	5	397°C	+/- 6.0°C

On review of the data, it is evident that there was an inadvertent pressure build-up in some experiments. When pressure within the test chamber exceeded 1.2 bar abs (0.12 M Pa), SIT was 257°C, and when pressure within the chamber was below 1.2 bar abs (0.12 M Pa), the SIT was 397°C. Corrections were then made in the system to eliminate pressure increases during an experiment.

Five samples each of polymeric polyvinyl chloride (PVC), red rubber (RR), and silicon rubber (SR) tracheal tubes were then analyzed for SIT. Results are presented in Table 2.

TABLE 2--SIT for Tracheal Tubes

Material	n	SIT	Standard Deviation
PVC	5	428°C	+/- 0.6°C
RR	5	371°C	+/- 0.7°C
SR	5	381°C	+/- 14.1°C

Figures 3, 4, and 5 are typical temperature-time plots of the data obtained. Experimental ignition temperature is recorded as the take off point of the temperature spike indicating ignition of the specimen. Ignition of the test specimen was confirmed by examining the contents of the sample boat on disassembling the test chamber after ignition. Aborting the ramped temperature prior to ignition spike and examining the test specimen consistently revealed no ash.

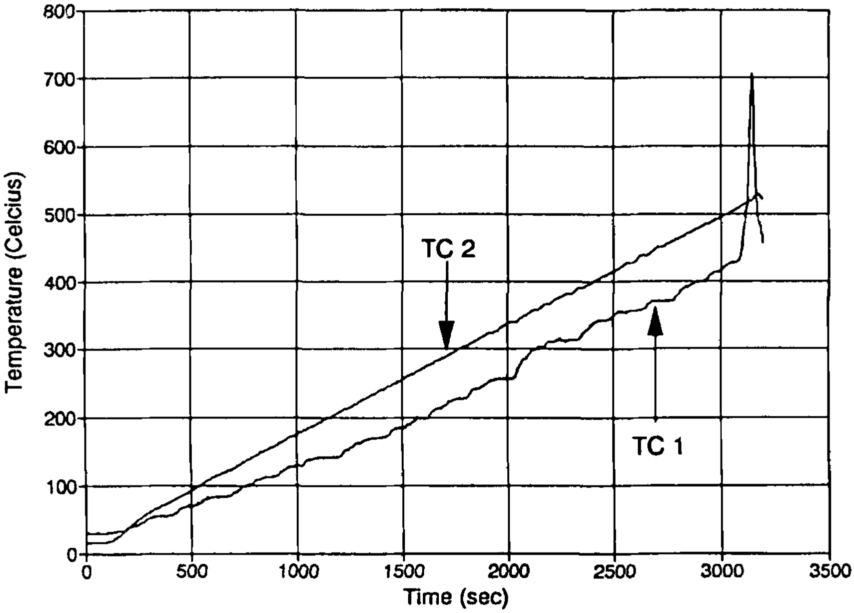

FIGURE 3
PVC

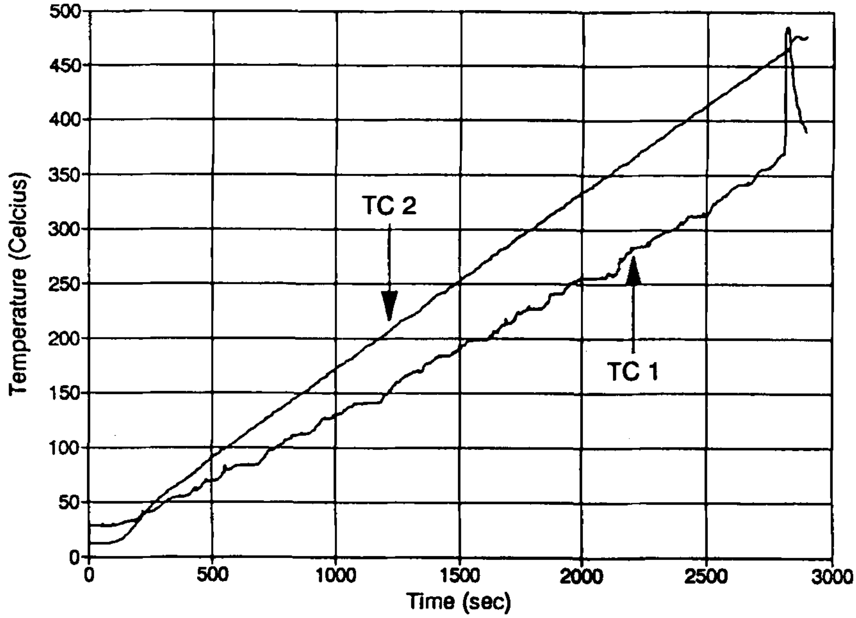

FIGURE 4
RR

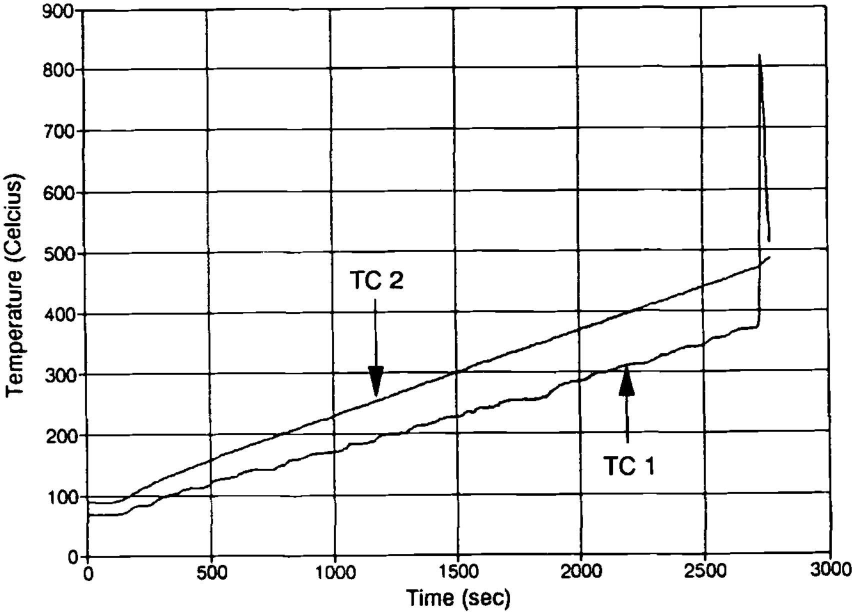

FIGURE 5
SR

Thermocouple 1, positioned 1 mm above the sample and taken to represent sample temperature records a lower temperature than thermocouple 2, positioned 1 mm below the sample boat. This difference indicates non-uniform temperature within the test chamber. Attempts to more efficiently circulate gases within the test chamber by insertion of a magnetic stirrer proved unsuccessful, since uncoupling of the internal ceramic magnet with the external magnet occurred on approaching the Curie point of the internal magnet.

The difference between industrial grade PVC tubing at low and high pressure was significant at $p < 2.85X10^{11}$. Analysis of variance between tracheal tube samples manufactured of PVC, RR and SR was significant at $p < 0.000\ 000\ 2$ ($F = 56.6$), with the difference between PVC and RR significant at $p < 0.000\ 01$, and the difference between PVC and SR significant at $p < 0.000\ 08$. The difference between RR and SR was not statistically significant ($p = 0.087$).

DISCUSSION

This study was undertaken to expand the database relevant to the airway fire problem in order to provide information as to choice of materials, to facilitate modeling of the problem, and ultimately attain the as yet elusive goal of solving the clinical conundrum of the application of ignition energy in an oxygen enriched atmosphere in the presence of a potential fuel.

The SIT is but one of many combustion data points relevant to choice of materials for a specific use in a specific environment. Other information such as heat of combustion, thermal conductivity, specific heat, oxygen index and flame spread must also be considered.

It is interesting to note that the data presented herein rank the tracheal tube materials in similar ranking to the findings obtained in oxygen index determinations previously reported[3]. Poly (vinyl chloride) has the highest SIT and highest oxygen index. Silicone rubber and red rubber have similar SIT's and similar oxygen indices.

The temperature achieved when a typical surgical laser is applied to materials far exceeds these SIT values[1]. Therefore, the difference in SIT observed has little clinical relevance.

Studies on PVC pyrolysis in inert gas[6] reveal liberation of complex mixtures of monomer and chain fragments, along with fragments not related to the original chain. Heating PVC to 220°C-280°C decreases the mass by 60% by dehydrohalogenation (96% of products released below 350°C are hydrogen chloride). Further heating to between 400°C-450°C results in further pyrolysis to 80% mass loss by the fracture of the carbon polymer chain, and release of carbon chains and ring structures. In greatest abundance are ethylene, propylene, and benzene, totalling 45% of released products between 400°C-450°C. The effect on SIT of 1.2 bar abs (0.12 M Pa) pressure was an unexpected finding. At less than 1.2 bar abs(0.12 M Pa) the ramped temperature passes through the dehydrohalogenation phase without ignition, with ignition on release of depolymerization products at 397°C. Redesign of the test apparatus maintained pressure at less than 1.2 bar abs (0.12 M Pa) and yielded consistent results. It is interesting to speculate that the ignition mechanism operating in hyperbaric conditions is dehydrohalogenation based, and that the ignition mechanism at ambient conditions is based on the ignition of volatiles such as ethylene, propylene, and benzene. Further studies with controlled, pressurized systems would be necessary to fully understand these effects.

---

[1] Pearce, J. A., Professor of Electrical and Computer Engineering, and Biomedical Engineering, University of Texas, Austin, Texas. Personal Communication.

CONCLUSION

We conclude that the SIT of tracheal tube materials is well within the hazard range of potential operating room ignition sources. Moreover the differences in SIT between the various tracheal tube materials do not offer clinically relevant advantages between materials.

REFERENCES

[1] Sosis, M. B., "Airway Fire During CO_2 Laser Surgery Using a Xomed Endotracheal Tube." Anesthesiology, Vol. 72, 1990, pp. 747-749.

[2] Bailey, M. K., Bromley, H. R., Allison, J. G., Conroy, J. M., and Krzyzaniak, W., "Electrocautery-Induced Airway Fire During Tracheotomy." Anesth. Analg., Vol. 71, 1990, pp. 702-704.

[3] Wolf, G. L., and Simpson, J .I., "Oxidant O_2 and Oxidant N_2O Indices of Flammability and their Additive Effect." Flammability and Sensitivity of Materials in Oxygen Enriched Atmospheres. Third Volume, ASTM STP 986, D. W. Schroll, Ed., American Society for Testing and Materials, Philadelphia, Pa., 1988, pp. 420-426.

[4] Sidebotham, G. W., Wolf, G. L., Stern, J., and Aftel, R. M. "Endotracheal Tube Fires, A Flame Spread Phenomenon." Flammability and Sensitivity of Materials in Oxygen-Enriched Atmospheres: Fifth Volume, ASTM STP 1111, Joel M. Stoltzfus and Kenneth McIlroy, Eds., ASTM, Philadelphia, Pa., 1991, pp. 168-178.

[5] Swindells, I., Nolan, P. F., and Wharton, R. K., "Spontaneous Ignition Temperatures of Nonmetals in Gaseous Oxygen." Flammability and Sensitivity of Materials in Oxygen-Enriched Atmospheres: Third Volume, ASTM STP 986, D.W. Schroll, Ed., ASTM, Philadelphia, Pa., 1988, pp. 206-217.

[6] Stromberg, R. R., Strauss, S., and Achhammer, B. G., Journal of Polymer Science, Vol. 35, 1959, p. 353.

Albert L. de Richemond[1] and Mark E. Bruley[2]

INSIDIOUS IATROGENIC OXYGEN-ENRICHED ATMOSPHERES AS A CAUSE OF SURGICAL FIRES

REFERENCE: de Richemond, A. L. and Bruley, M. E., "Insidious Iatrogenic Oxygen-Enriched Atmospheres as a Cause of Surgical Fires," Flammability and Sensitivity of Materials in Oxygen-Enriched Atmospheres: 6th Volume, ASTM STP 1197, Dwight D. Janoff and Joel M. Stoltzfus, Eds., American Society for Testing and Materials, Philadelphia, 1993.

ABSTRACT: During many surgeries, the risks of fire exist because heat sources (e.g., electrosurgical probes, lasers) are used close to fuels (e.g., tracheal tubes, body hair, surgical drapes) in oxygen-enriched atmospheres (OEA). When the OEA is recognized as a hazard, precautions are taken to reduce the risk, e.g., minimizing oxygen concentration prior to use of electrosurgery.

However, some actions of the surgical team can lead to one of two types of OEAs that are not readily recognized by, or apparent to, the surgical team as a hazard. One type involves entering a body cavity that contains an OEA, during tracheostomy for example. The other type has an OEA developing around the surgical site as can happen when a misplaced or leaking breathing circuit is under the surgical drapes. With regrettable frequency in these cases, a surgical fire results.

This paper discusses several cases of fire during surgery that involved insidious oxygen-enriched atmospheres. Recommendations to prevent and to deal with such fires are also presented.

KEY WORDS: anesthesia, electrosurgery, oxygen, precautions, pulse oximetry surgical fires surgery.

---

[1] Mr. de Richemond is a senior project engineer with ECRI, 5200 Butler Pike, Plymouth Meeting, PA 19462, USA.

[2] Mr. Bruley is the director of the accident and forensic investigations group for ECRI, 5200 Butler Pike, Plymouth Meeting, PA 19462, USA.

Case 1. Fatal Infant Surgery Fire.

A two week old, 1 kg infant underwent minor surgery in a neonatal intensive care unit (NICU) procedure room for repair of a cardiovascular defect. While in the NICU, the infant was ventilator dependant. The ventilator breathing circuit used in the NICU was an open-ended, single limb type and exhausted oxygen at its exhalation valve located at the tracheal tube connector next to the infant's mouth. For the surgery, this breathing circuit was used during delivery of anesthesia and exhausted approximately 11 liters per minute beneath the surgical drapes. The infant had been draped with four cotton huck towels placed on the left chest and then covered by disposable polypropylene surgical drapes. Oxygen flowed beneath the drapes and welled up past the edges of the drape fenestration at the surgical site for about five minutes prior to the initial cold scalpel incision. After the incision, a small bleeder was cauterized with an electrosurgical needle electrode. Upon cauterization, a cotton gauze surgical sponge held next to the incision, the huck towels, the disposable drapes, and the linens and blankets upon which the infant lay burst into flames. The fire enveloped the infant, causing second and third degree burns over 60% of its body. The intense fire on and around the infant had lasted only five to eight seconds. The infant died a few hours after the fire. Use of a double limb breathing circuit that would have exhausted the oxygen well away from the draped patient would have prevented the OEA that was responsible for this fire.

INTRODUCTION

The above case illustrates the severity of oxygen-enriched surgical fires. During many surgeries, the risks of fire exist because heat sources (e.g., electrosurgical probes, lasers) are used close to fuels (e.g., tracheal tubes, body hair, surgical drapes) in oxygen-enrich atmospheres (OEA) [1,2,3,4]. For example, electrosurgery uses an electric current or arc to cut or cauterize tissue. The arc or the resulting hot electrosurgical probe tip can easily ignite many materials in room air and OEA. The electrosurgical procedure can also create tissue embers which carry sufficient energy in OEA to ignite some materials upon which they land. Tissue on the heated probe tip can flame, and the radiant heat from this flame, in an OEA, can also ignite materials with fine surface fibers.

These risks are masked by other perceptions about the devices. With electrosurgery, an electrical current path is needed before heating can occur, and a split second activation in an OEA can be sufficient to ignite drapes, towels, breathing circuits, and other fuels found in the surgical operating room. Wet or electrically resistant materials commonly used in surgery are not easily ignited in room air, and the perceived risk of fire is low. However, the end of the probe tip used to apply the current to the tissue can become red hot, retaining considerable heat for up to several seconds after the current is stopped, and can ignite materials if misplaced during this short time. An electrically insulating holster, packed with most electrosurgical probes, should be used to hold the probe within the surgical field when it is not in use. Holster use prevents accidental probe activation and contact with flammable materials. Holster use, combined with activating the probe only when it is in view in the surgical field, can help minimize the risk of a fire. However, safety protocols and device safety instructions are not always followed, sometimes with disastrous results.

Oxygen is often used in high concentrations to allow a patient to better tolerate surgery. A recent trend in anesthesia has been to administer high oxygen concentrations regardless of the patient's need. Pulse oximetry can allow the anesthesiologist to monitor the patient's oxygen need and titrate the oxygen concentration in the breathing gas mixture accordingly. In many cases during anesthesia, nitrous oxide, an analgesic agent and oxidizer, is mixed with oxygen; nitrous oxide is often, mistakenly, not considered as contributing to an OEA. In most cases, the OEA is contained within the circle breathing system of the anesthesia machine or is exhausted to a safe location away from the patient. When the OEA is recognized as a hazard, precautions are taken to reduce the risk, e.g., minimizing oxygen concentration shortly prior to use of electrosurgery or lasers. However, leaks in the breathing circuit or poor placement of ventilation equipment can create OEAs in unexpected spaces or at unrealized times.

With regrettable frequency in these cases, some actions of the surgical team can ignite materials and cause a surgical fire. To illustrate how these fires occur, presented below are several cases of surgical fires that we have investigated wherein an unrealized OEA led to a surgical fire. Recommendations to prevent such fires are also presented.

Case 2. Tracheostomy Fire

A patient with chronic obstructive pulmonary disease had been intubated with a tracheal tube for several days and was receiving ventilator support with 100% oxygen. During surgery to implant a tracheostomy tube for long-term ventilatory support and oxygen therapy, the surgeon used an electrosurgery probe (appropriately so) to dissect down to the trachea. Rather than switch to a scalpel or scissors to cut through the cartilaginous tracheal rings, he proceeded with the electrosurgical probe. He assumed that the cuff of the tracheal tube was distal to the incision site. However, unknown to the surgeon, the tube had moved promixally in the trachea, placing the cuff immediately beneath the incision site but not visible through the wall of the trachea. The surgeon unknowingly placed the hot, sparking probe close to the flammable plastic tube in a 100% oxygen atmosphere. His first cut through the tracheal rings was uneventful, but with the second cut, flames erupted from the incision site. The tracheal tube was immediately disconnected from the oxygen source, and this apparently put out the fire, but a subsequent breath forced through the breathing circuit cause the flames to again burst forth. Water was then poured into the incision site, a breath of 100% oxygen given, and the fire returned. At this point the surgical team realized that the tube, not the patient, was burning and removed the burning, melted tube. Water was finally injected into the tracheal tube and the incision site and successfully extinguished the fire. Unfortunately, the fire had charcoalized the patient's trachea, and he died a few weeks after the incident after sloughing much of his airway.

Case 3. Misplaced Oxygen Source.

A nine day old infant needed emergency surgery to implant cannulae in blood vessels in her neck to enable extracorporeal membrane oxygenation of her blood to so enable her lungs to further develop. The infant was brought to the hospital by emergency personnel who used a portable oxygen tank and bag mask to deliver oxygen to her. She was transferred to the hospital's oxygen supply and bag mask. During intubation, the mask, with 100% oxygen still flowing, was placed next to the infant. The infant was prepared for surgery, draped with cotton huck towels and a surgical drape, and surgery commenced. In the first few minutes of surgery, an electrosurgical probe was used to stop bleeding from some small blood vessels. The probe was placed aside on the surgical drape. About twenty minutes later, the probe was again used and flamed upon activation. Oxygen from the initially-used mask had been flowing throughout the surgery, had enriched the space beneath the drapes, and was welling out of the fenestration of the drapes. When the blood and tissue fragments adherent to the electrosurgical probe were heated in the OEA, they ignited and in turn ignited the fine hair (lanugo) on the infant's neck along with the nap on the cotton huck towels. With a whoosh, this ignition chain spread the fire underneath the drapes to the blanket, mattress, and oxygen mask in what has been called surface fiber flame propagation [1]. Quick action by the surgical team removed most of the burning materials on and around the infant, extinguished the fire with sterile saline solution, and saved the infant who suffered only minor burns.

Case 4. Mustache Fire

A man with a large bushy mustache was undergoing dental surgery with analgesia of 25% oxygen and 75% nitrous oxide administered through a nasal mask. This gas mixture created an OEA in and around the mask and around the mustache. During use of a dental bur, a small incandescent spark, possibly a bur tooth or piece of dental filling, arced out of the patient's mouth and landed in the mustache, igniting it. The burning hair instantly ignited the nasal mask, and the fire quickly travelled inside the breathing circuit tubing toward the anesthesia machine before being extinguished. The man lost his mustache and was severely burned about his nose and cheeks. Had the patient's mustache been coated with a water base surgical jelly prior to surgery, it would not have ignited.

Case 5. Facial fire

A bearded patient was receiving supplemental oxygen through a mask that had been trimmed by cutting off the portion over the bridge of the nose. This modification allowed oxygen introduced at the mask bottom to blow directly into the surgical site. The surgical site was defined with cotton huck towels as a 4 cm by 12 cm fenestration over the eyes and covered the trimmed mask. The surgeon used scissors to trim growths from the patient's eyelids and then used a needle tip electrosurgical probe to cauterize the bleeding. A small tissue ember from the probe tip incandesced in the oxygen streaming from the fenestration and landed on the oxygen-enriched towels which immediately burst into flame along with the patient's facial hair and the oxygen mask. The burning materials were quickly removed and the fire extinguished, but the patient suffered second degree burns over much of the face.

Case 6. Leaky Oxygen Valve

During head and neck surgery on a spontaneously breathing patient, the surgical team followed a fire-safe procedure by stopping supplemental oxygen flow to the patient about a minute prior to using electrosurgery. This normally allows oxygen to dissipate significantly and thus reduces the ignition risk.

However, when fully closed, the oxygen valve on the anesthesia machine had 300 cc/min leak because of wear. This small leak was enough to maintain an OEA around the surgical site. When the electrosurgical probe was activated, it ignited the surgical drapes which were quickly removed from the patient who suffered minor burns.

Case 7. Lung Resection

During surgery to remove a portion of the patient's lung, the surgeon was blotting blood with a dry cotton gauze surgical sponge while cauterizing oozing blood vessels with an electrosurgery probe. The patient was receiving 100% oxygen which was leaking from the resected lung into the deep chest incision. The sponge became oxygen-enriched and, upon contact with the electrosurgical probe, burst into flame. The surgeon tossed the burning sponge to the floor where it was quickly stamped out. Fortunately, the flaming sponge did not ignite the surgical drapes or the gowns of the surgical team.

DISCUSSION

In the cases presented above, an unrealized oxygen-enriched atmosphere allowed easy ignition of fuels commonly present during surgery. Fires involving oxygen are outside the realm of most people's experience, including clinicians. Indeed, the fires described above astonished the medical personnel involved with the ease with which they started, the size of their flames, the rapidity of their spread, and amount of material that became involved. This explains part of the reason these fires occurred, ignorance of the presence and associated risks of OEA.

But those reasons alone are not the entire explanation. There is no formal reporting of surgical fire incidents. However, ECRI operates and maintains the world's largest database of reported medical device related accidents and actively investigates reported surgical fires. With over 19 million surgeries performed each year in the United States [5], we estimate that only about 100 surgical fires occur. Of these, about 10% or less result in serious injury or death.

Most surgical teams are used to doing their work in a certain routine manner, reasoning that. "We've always done it this way and never had a problem." But in each of the above cases a small seemingly insignificant event set the stage for the catastrophe in the presence of a confluence of predisposing conditions related to oxidizer, ignition source, and fuels. It is the small, hard-to-discern difference from routine that allows catastrophe.

For example, in the Tracheostomy Fire, the surgeon was young and heavily used electrosurgery for most procedures; older surgeons commonly use a scalpel or scissors to enter the airway. The surgeons' routines were slightly different and the former presents more of a fire risk during tracheostomy. Emergency surgery is not routine, but following routine techniques like removing unneeded devices from the area around the could have prevented the Misplaced Oxygen Source fire. The patient in the Facial Fire did not need 100% oxygen beneath the towels, but it was common practice. Switching to air or stopping the oxygen before using electrosurgery should have been part of the routine in that case, but the risk was not recognized. Recognizing that an OEA can occur and taking precautionary measures before hand will minimize the risk of fire. Take the mustache fire for example; large bushy mustaches are not too common, but a simple technique, coating the mustache with water-based surgical jelly before the surgery, could have prevented the fire had it been recognized that hair easily ignites and burns ferociously in an OEA.

But surgical routine can also minimize the likelihood of small changes and the impact of their occurrence. Routine use of pulse oximetry can reduce the need for high oxygen concentration throughout the procedure and the attendant risk of OEA. (Paradoxically, some anesthesiologists administer excessive oxygen in an attempt to, unnecessarily, keep the patient's monitored blood oxygen level near 100% saturation.) Thorough routine maintenance may have caught the Leaky Oxygen Valve and prevented that fire.

If a surgical fire occurs, whether on or in the patient, the surgical team must react with speed and decisiveness to control the fire and save the patient. Especially in surgical fires involving OEA, seconds count in catching the fire before it becomes vigorously established. Based on our investigations [4], we recommend the following three actions be done in rapid succession to fight a surgical fire:

1. Stop the flow of breathing gases to the patient.

2. Remove the burning materials from the patient.

3. Care for the patient.

In step one, stopping the breathing gases seems contrary to helping the patient. But should the oxygen and or nitrous oxide be involved in the fire, stopping the flow of these gases will reduce the intensity of the fire. Also, the surgical team may need to evacuate the patient. To do this, the patient must be disconnected from the anesthesia machine and will require manual ventilation. The anesthesiologist can most effectively do this step.

Step two requires rapidly removing the burning material. The surgeon is usually in the best position to rip the flaming drapes from the patient or pull the burning tracheal tube from the patient's throat. The longer the material is on or in the patient, the more damage the fire will do to the patient through heating or production of toxic chemicals. A few moment's hesitation may allow the fire to grow enough to present a risk of igniting the gowns of the surgical team or equipment in the operating room.

Once the burning material is away from the patient, the surgical nurses must extinguish the fire. As is typical in OEA fires, other material around the patient will be burning. Some have advocated throwing a fire blanket over the burning patient. This is wrong; the blanket will trap heat, smoke, and flame around the patient causing him more severe injury, the fire may continue to burn, and possibly involve the blanket, especially if and OEA is present, and ventilation or control of bleeding cannot be accomplished to help care for the patient. We recommend use of a Halon or carbon dioxide fire extinguisher as the most effective means of extinguishing surgical fires on the patient if the burning materials cannot be removed. They can be discharged directly onto the patient with little risk of added patient injury. Bottled sterile saline solution has also been used to good effect.

With the fire being dealt with by the surgical nurses, the surgeon and anesthesiologist must move quickly to care for the patient, the third step. This will involve re-establishing patient ventilation, control of bleeding, tending to other surgical needs, and possible evacuation of the patient of the to another operating room or safe area to complete the surgery. Operating tables are heavy and cumbersome to move especially in an operating room crowded with yelling people, many devices, and burning materials.

Unless the surgical team has reviewed, or better, practiced what to do in the event of a surgical fire, evacuation may not be possible and other injury and more severe damage may result. We advocate that surgical teams learn about and practice fighting surgical fires.

CONCLUSION

A surgical fire will often involve an oxygen-enriched atmosphere and will place the patient and surgical staff at risk. Several such cases were presented above and means of minimizing or preventing such events were discussed. The following three step procedure for fighting a surgical fire was described. In rapid succession:

- Stop the flow of breathing gases to the patient.

- Remove the burning materials from the patient.

- Care for the patient.

REFERENCES

[1] Bruley, M. E. and Lavanchy, C., "Oxygen-Enriched Fires During Surgery of the Head and Neck," Symposium on Flammability and Sensitivity of Materials in Oxygen-Enriched Atmospheres: Fourth Volume, ASTM STP 1040, Joel Stoltzfus, Frank J. Benz, and Jack S. Stradling, Eds., American Society for Testing and Materials, Philadelphia, 1989.

[2] de Richemond, A. L., "Laser Resistant Endotracheal Tubes -- Protection Against Oxygen Enriched Airway Fires During Surgery?" Flammability and Sensitivity of Materials in Oxygen-Enriched Atmospheres: Fifth Volume, ASTM STP 1111, Joel M. Stolztfus & Kenneth Mc Ilroy, Eds., American Society for Testing and Materials, Philadelphia, 1991.

[3] de Richemond, A. L. and Bruley, M. E., "Head and Neck Surgical Fires," in Eisley, D. W. Ed., Complications in Head and Neck Surgery, Mosby YearBook, 1992.

[4] ECRI, A Surgical Fires Primer, Health Devices, 21(1) Jan 1992.

[5] Rutkow, I. M., "Surgical Operations in the United States: 1979 to 1984," Surgery, 101(2), Feb 1987, pp 192-200.

David B. Hirsch[1] and Radel L. Bunker[2]

EFFECTS OF DILUENTS ON FLAMMABILITY OF NONMETALS IN HIGH-PRESSURE OXYGEN MIXTURES

REFERENCE: Hirsch, D. B. and Bunker, R. L., "Effects of Diluents on Flammability of Nonmetals in High-Pressure Oxygen Mixtures," Flammability and Sensitivity of Materials in Oxygen-Enriched Atmospheres: 6th Volume, ASTM STP 1197, Dwight D. Janoff and Joel M. Stoltzfus, Eds., American Society for Testing and Materials, Philadelphia, 1993.

ABSTRACT: NASA White Sands Test Facility recently investigated the effects of diluents on flammability of nonmetals. Downward-flame propagation flammability tests were conducted on Teflon PTFE, Kel-F 81, and Viton samples, using helium, nitrogen, argon, and neon diluents. The tests were conducted at 6.9 MPa (1000 psia), 20.7 MPa (3000 psia), and 34.5 MPa (5000 psia) using various diluent/oxygen mixtures. The test objective was to determine the minimum diluent concentration required to extinguish the burning sample. The data indicated that at pressures of 6.9 MPa (1000 psia) and higher, the materials tested (which are among the most commonly used nonmetals in oxygen systems) would burn even in low-oxygen concentrations. Large quantities of diluents, approximately 60 percent and higher, were required to prevent sustained combustion. Helium was the most effective diluent for preventing flame propagation, followed by nitrogen, neon, and argon. The effectiveness of helium could be explained by its high thermal conductivity, which could have resulted in reduced heat-feedback to the burning material. For a given pressure increase, the increase in diluent concentration required for sample extinguishment was higher for Teflon PTFE and Kel-F 81 than for Viton. At some pressure between 20.7 MPa (3000 psia) and 34.5 MPa (5000 psia), Teflon PTFE and Kel-F 81 became flammable in air, indicating that high-pressure air systems require careful selection of appropriate nonmetallic materials and design considerations to avoid ignition sources.

KEYWORDS: polymers, nonmetals, diluents, flammability, combustion.

INTRODUCTION

Life-support systems designed for Space Shuttle and Space Station Freedom will use nonmetallic materials in high-pressure oxygen systems. When exposed to ignition sources, most nonmetals ignite and burn in oxygen environments. Burning nonmetals in high-pressure oxygen systems could cause catastrophic system failures. Adding small quantities of

---

[1] Senior Engineer, Lockheed-ESC, NASA White Sands Test Facility, P. O. Drawer MM, Las Cruces, NM 88004.

[2] Aerospace Engineer, NASA-JSC, White Sands Test Facility, P. O. Drawer MM, Las Cruces, NM 88004.

nontoxic diluent gases to oxygen might prevent burning of nonmetals in high-pressure oxygen systems. NASA White Sands Test Facility (WSTF) recently investigated the possibility of using nontoxic diluent gases in high-pressure oxygen systems to reduce the ignition or combustion of nonmetallic materials.

A literature review was conducted on the effects of diluents on combustion of nonmetals [1]. The review indicated that diluents affect the ignition and flame-spread rates in diluent/oxygen mixtures because of the diluent effects on the thermal conductivity, specific heat, and diffusivity of the mixtures. Helium, which has a higher thermal conductivity than nitrogen, was found to be a better inhibitor of ignition processes. Nitrogen/oxygen mixtures, which have higher heat capacities and lower diffusivities than helium/oxygen mixtures, generally result in lower flame rates. The literature review indicated that information pertaining to combustion of nonmetals at high pressures was scarce.

EXPERIMENTAL APPROACH

To determine the effects of diluent/oxygen mixtures on combustion of nonmetals, downward-flame propagation flammability tests were conducted on test samples using various diluent concentrations. The test logic was to determine the minimum diluent concentration (MDC) in a diluent/oxygen mixture required for sample self-extinguishment at 6.9 MPa (1000 psia), 20.7 MPa (3000 psia), and 34.5 MPa (5000 psia).

During testing, if the test sample failed to self-extinguish, then the diluent concentration was increased for the following test. However, if the sample self-extinguished, then the diluent concentration was decreased for the following test. The test samples were considered self-extinguished when their measured burn lengths were less than 6.4 cm (2.5 in). The results were confirmed by performing a total of three tests at the MDC at which the samples self-extinguished.

TEST MATERIALS AND SAMPLE PREPARATION

Helium, nitrogen, argon, and neon were the diluent gases used during testing. These gases are classified as simple asphyxiants, with no specific toxic effects [2]; however, because of their low molecular weight, helium/oxygen mixtures distort vocal communication.

Three nonmetals, which are used extensively in high-pressure oxygen systems, were used in this evaluation: Teflon PTFE[1], Kel-F 81[2], and Viton[1].

The nonmetallic samples were cylindrical rods of 0.32 cm (0.13 in) nominal diameter and 7.6-cm (3.0-in) long. Prior to tests, the Teflon PTFE and Kel-F 81 samples were washed in a warm solution of a mild detergent in deionized water, rinsed with deionized water, and blown dry with filtered, water- and oil-free nitrogen. The Viton samples were blown-dry with filtered, water- and oil-free nitrogen.

TEST APPARATUS

The test chamber consisted of a cylindrical stainless steel chamber fitted with a copper liner (Fig. 1). The chamber had an internal volume of 12.4-liters (760-in^3), which ensured that no more

---

[1] Trademark of E.I. DuPont De Nemours and Company Incorporated, Wilmington, Delaware

[2] Trademark of 3M Company, St. Paul, Minnesota

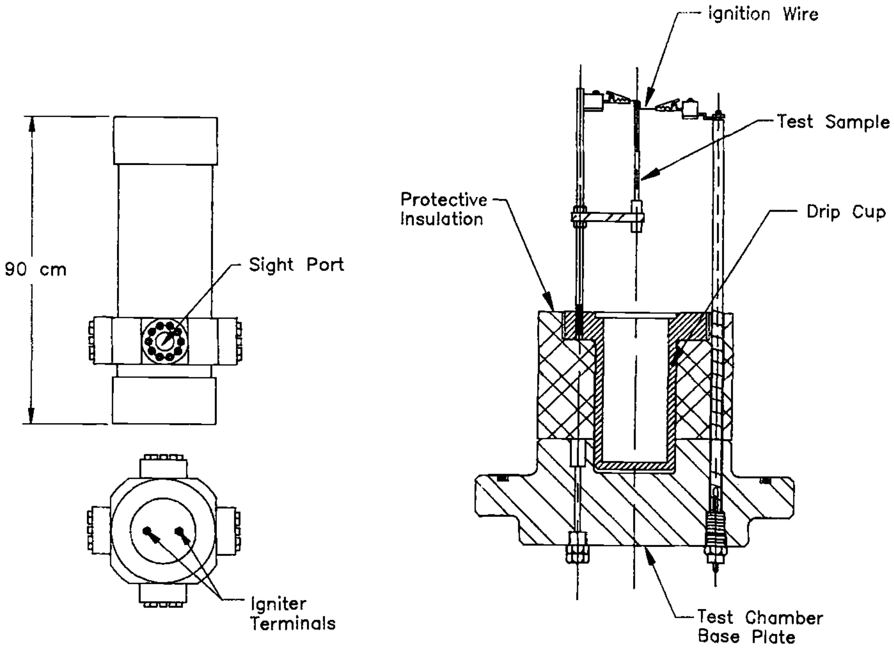

(a) (b)

FIG. 1--Schematic of Test Chamber
(a) Exterior (b) Interior

than 5 percent of the initial oxygen was consumed during combustion of the samples at the lowest oxygen concentration and test pressure. The chamber contained four 5.1-cm (2.0-in) diameter sight ports near the lower end of the chamber that were used for observing the combustion event. Test samples were positioned vertically in the test chamber and supported at the bottom with a sample holder mounted on the lower base plate. Premixed and preanalyzed test gas was supplied to the test chamber from pressurized cylinders.

The test chamber was instrumented with a pressure transducer and fitted with electrical feedthroughs for ignition. The ignition of samples was achieved by electrically heating a 20-AWG nickel-chromium bare wire wrapped 2.5 turns around the upper 0.32-cm (0.13-in) end of the sample. The electrical supply to the ignition wire was a voltage source capable of providing 16 amps root mean square (RMS).

TEST PROCEDURES AND CONDITIONS

Each sample was installed in the test chamber, and the ignition wire was mounted on the upper end of the sample. The test chamber was purged with the test gas, and the required test atmosphere was established. Power was applied to the igniter wire until sample ignition was achieved. Combustion of the sample was observed and video-recorded. After each test, the chamber was vented, and the sample was removed. Burn lengths for each sample were measured as the difference between the pretest and the posttest sample lengths.

The tests were conducted at 6.9 MPa (1000 psia) and 20.7 MPa (3000 psia) on Teflon PTFE, Kel-F 81, and Viton using the helium, nitrogen, and argon diluents. Limited studies were conducted at 34.5 MPa (5000 psia) on Teflon PTFE and Kel-F 81 using the nitrogen diluent and at 6.9 MPa (1000 psia) on Teflon PTFE using the neon diluent.

RESULTS AND DISCUSSION

The MDCs in the diluent/oxygen mixtures required for sample self-extinguishment are presented in Figs. 2, 3, and 4. The data indicate that large quantities of diluents, approximately 60 percent and higher, were required to prevent flame propagation.

Helium was the most effective diluent for preventing flame propagation, followed by nitrogen and then argon. At 6.9 MPa (1000 psia), neon was as effective as nitrogen for preventing flame propagation on Teflon PTFE. The differences between diluents regarding their effectiveness for preventing flame propagation decreased with increasing pressures. At 6.9 MPa (1000 psia), the average difference between the MDC of the most and least effective diluent was 14 percent; at 20.7 MPa (3000 psia), the average difference was only 8 percent.

The effect of pressure on the MDC was greater for materials that had lower MDC values at ambient pressure. Increasing the pressure from ambient to 20.7 MPa (3000 psia) resulted in a MDC increase from 0 percent to 79 percent for Teflon PTFE and Kel-F 81; the same pressure increase resulted in a MDC increase from 39.5 percent to 76 percent for Viton.

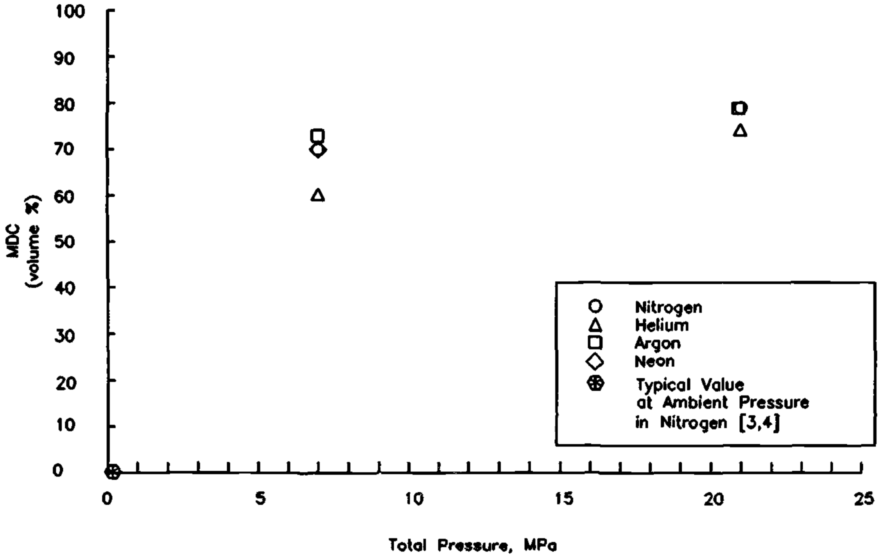

FIG. 2--Minimum Diluent Concentration in Diluent/Oxygen Mixtures Required for Teflon PTFE Self-Extinguishment

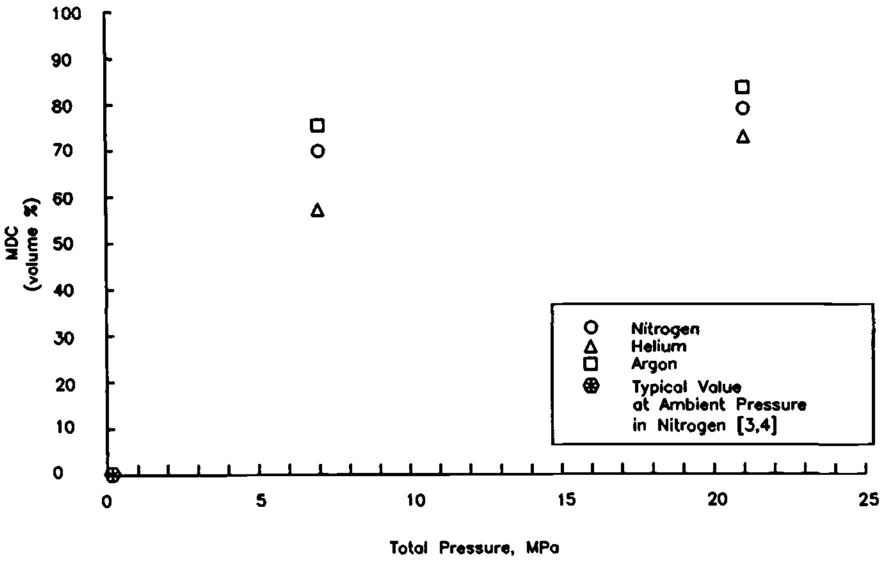

FIG. 3--Minimum Diluent Concentration in Diluent/Oxygen Mixtures Required for KEL-F 81 Self-Extinguishment.

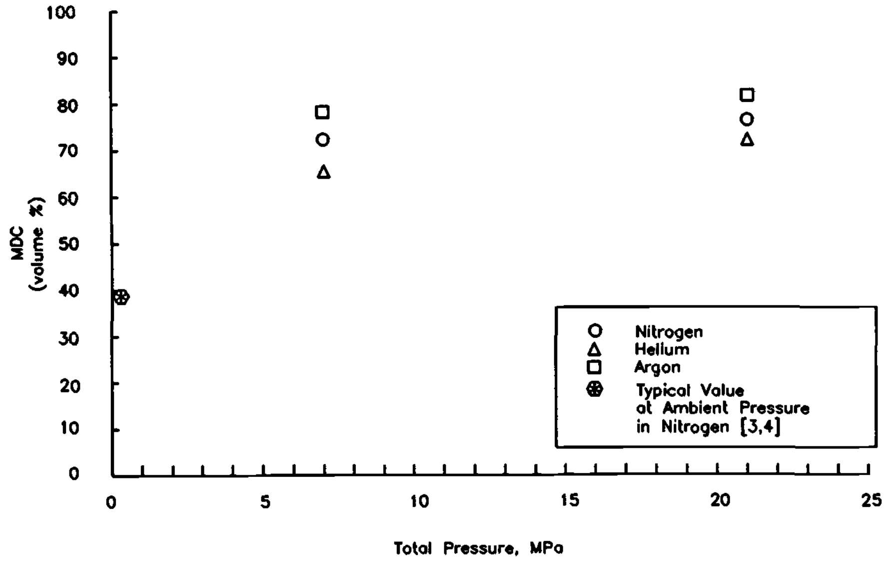

FIG. 4--Minimum Diluent Concentration in Diluent/Oxygen Mixtures Required for Viton Self-Extinguishment.

A similar effect was observed in a study of the effect of pressure on the oxygen index, where the effect of pressure on the oxygen index was found to be greater for materials with higher oxygen index values at ambient pressures [3]. The tests conducted by Benning were limited to maximum pressures of 2 MPa (290 psia).

The limited number of tests performed at 34.5 MPa (5000 psia) with Teflon PTFE and Kel-F 81 resulted in complete combustion of samples in environments of 19-percent oxygen and 81-percent nitrogen. This indicates that at some pressure between 20.7 MPa (3000 psia) and 34.5 MPa (5000 psia) these materials became flammable in air.

CONCLUSIONS AND RECOMMENDATIONS

The data indicate that at pressures of 6.9 MPa (1000 psia) and higher the most commonly used nonmetals in oxygen systems would burn even in environments having low-oxygen concentrations. Large quantities of diluents, approximately 60 percent and higher, were required to prevent flame propagation. Helium was the most effective diluent for preventing flame propagation, followed by nitrogen, neon, and argon. The effectiveness of helium could be explained by its high thermal conductivity, which could have resulted in reduced heat-feedback to the burning material. The differences between the diluents regarding their effectiveness for preventing flame propagation decreased with increasing pressures.

Among the diluents tested, only nitrogen and helium have practical applicability; argon is less efficient for preventing flame propagation than nitrogen, and although neon is equally efficient for preventing flame propagation as nitrogen, neon is much more expensive than nitrogen. Nitrogen is physiologically acceptable in nitrogen/oxygen mixtures; however the partial pressure of oxygen must remain above the level which causes hypoxia. Helium/oxygen mixtures are used safely in diving atmospheres [5], indicating that short-term exposures to helium is physiologically acceptable; however, the partial pressure of oxygen must remain above the level which causes hypoxia. The physiological effects of long-term exposure to helium/oxygen mixtures with high helium content are unknown. If intended for breathing, the helium/oxygen or nitrogen/oxygen mixtures with MDC values would not cause hypoxia as long as these mixtures were regulated to ambient pressure [2,6,7].

Nonmetals considered nonflammable in air at ambient pressures could ignite and burn in air at pressures greater than 20.7 MPa (3000 psia), indicating that high-pressure air systems require very careful selection of appropriate nonmetallic materials and design considerations to avoid ignition sources. Based on these results, high-pressure air systems above 20.7 MPa (3000 psia) need to be evaluated and possibly treated as high-pressure oxygen systems from the standpoint of propagation of combustion after ignition. Other materials currently used for high-pressure air systems should be evaluated for ignition and combustion propagation. Based on the results from the high-pressure tests, helium should be tested at low pressures to evaluate for possible fire extinguishment applications.

REFERENCES

[1] Hirsch, D. B., R. L. Bunker, and D. Janoff. "Effects of Oxygen Concentration, Diluents, and Pressure on Ignition and Flame-Spread Rates of Nonmetals." Flammability and Sensitivity of Materials in Oxygen-Enriched Atmospheres: Volume 5, ASTM STP 1111, J. M. Stoltzfus and K. McIlroy, Eds., Philadelphia: American Society for Testing and Materials, 1991.

[2] Sax, N. I. Dangerous Properties of Industrial Materials. New York: Van Nostrand Reinhold Company, 1968.

[3] Benning, M. A. "Measurement of Oxygen Index at Elevated Pressures." Flammability and Sensitivity of Materials in Oxygen-Enriched Atmospheres: Volume 1, ASTM STP 812, B. L. Werley, Ed., Philadelphia: American Society for Testing and Materials, 1983.

[4] Ikeda, G. K. "Oxygen Index Tests to Evaluate the Suitability of a Given Material for Oxygen Service." Flammability and Sensitivity of Materials in Oxygen-Enriched Atmospheres: Volume 1, ASTM STP 812, B. L. Werley, Ed., Philadelphia: American Society for Testing and Materials, 1983.

[5] Friedman, R. and K. R. Sacksteder. "Science and Technology Issues in Spacecraft Fire Safety." NASA Technical Memorandum 88933, AIAA-87-0467. Prepared for the 25th Aerospace Sciences Meeting sponsored by the American Institute of Aeronautics and Astronautics, Reno, Nevada, January 12-15, 1987.

[6] Kimzey, J. H. "Flammable and Toxic Materials in the Oxygen Atmosphere of Manned Spacecraft." NASA Technical Note TN D-3415. Washington, D.C.: NASA, May 1968.

[7] Carhart, H. W. "Inerting and Atmospheres." Ohio: Spacecraft Fire Safety Workshop, NASA Lewis Research Center, August 20-21, 1986.

Shelley, R.M.[1], Janoff, D. D.[2], and Pedley, M. D.[3]

EFFECT OF HYDROCARBON OIL CONTAMINATION ON THE IGNITION AND COMBUSTION PROPERTIES OF PTFE TAPE IN OXYGEN

REFERENCE: Shelley, R. M., Janoff, D., and Pedley, M. D., "Effect of Hydrocarbon Oil Contamination on the Ignition and Combustion Properties of PTFE Tape in Oxygen," Flammability and Sensitivity of Materials in Oxygen-Enriched Atmospheres: Sixth Volume, ASTM STP 1197, D. Janoff and J. M. Stoltzfus, Eds., American Society for Testing and Materials, Philadelphia, 1993.

ABSTRACT: Testing was conducted to determine and compare the sensitivities of two oxygen test methods for detecting the presence of hydrocarbon oil contamination on polytetrafluorethylene tape. Ambient pressure mechanical impact tests were conducted, using ASTM Test Method for Compatibility of Materials with Liquid Oxygen (Impact Sensitivity Threshold and Pass-Fail Techniques) (ASTM D 2512); the tests determined the effect of contaminant concentration on the minimum impact energy for ignition. In the other test method, developed at the NASA Johnson Space Center White Sands Test Facility, the contaminated tape was heated using a pyrolysis furnace in flowing, gaseous oxygen. The presence of hydrocarbons in the gaseous oxygen stream was detected by fourier transform infrared spectroscopy (FTIR). This test method also determined the autoignition temperature of the contaminated tape. The test results showed that FTIR of the gases from the pyrolysis furnace is significantly more sensitive than liquid oxygen mechanical impact tests for detecting the presence of contamination. However, the autoignition temperature determined in the pyrolysis furnace is far less sensitive to the presence of hydrocarbon oil contaminants than liquid oxygen mechanical impact tests. Additional testing was conducted using a modified pneumatic impact test system (ASTM Test Method for Ignition Sensitivity to Materials to Gaseous Fluid Impact [ASTM G 74]), to study the effect of hydrocarbon contamination on the ignition process.

KEYWORDS: polytetrafluoroethylene, tape, hydrocarbon contaminant, mechanical impact test, pneumatic impact test, fourier transform infrared spectroscopy pyrolysis furnace, ignition, combustion, autoignition temperature

---

[1] Senior Scientist, Lockheed-ESC, NASA Johnson Space Center White Sands Test Facility, P. O. Drawer MM, Las Cruces, NM 88004.

[2] Principal Scientist, Lockheed-ESC, 2400 NASA Road One, Houston, TX 77058.

[3] Section Head of Nonmetallic Materials, NASA Johnson Space Center, Houston, TX 77058.

Polytetrafluoroethylene (PTFE) antiseize tape is used to seal various types of aerospace fittings in high-pressure oxygen systems at the NASA Johnson Space Center (JSC). The tape is produced by the extrusion of fine PTFE paste. PTFE powder is blended with a kerosene-based lubricant to form a paste and then extruded through dies. After extruding, the lubricant is driven off to leave pure PTFE. Each batch of tape is tested for reactivity using the ASTM Test Method for Compatibility of Materials with Liquid Oxygen (Impact Sensitivity Threshold and Pass-Fail Techniques) (ASTM D 2512), or the Test Method for Determining the Ignition Sensitivity of Materials to Mechanical Impact in Pressurized Oxygen Environments (ASTM G 86). The tape almost invariably passes these tests at the 98 J energy level, which is consistent with it being pure PTFE [1].

Recently, one batch of tape did not pass the ASTM G 86 test at the 98 J energy level and ambient temperature for a pressure of 69 MPa. Because of the reported poor repeatability of the test [2], it was questionable whether the failure resulted from the greater reactivity of this particular batch, or the variability in the test. Since the tape was reported by the manufacturer to be pure PTFE, hydrocarbon contamination either left over from the manufacturing process or introduced during handling was a possible source of the batch difference. The batch that failed the mechanical impact test was evaluated using the fourier transform infrared spectroscopy (FTIR) pyrolysis furnace [3]. The data showed that no significant hydrocarbon contamination was present, and that the sample behavior was characteristic of PTFE. Based on the FTIR results and the acceptable performance of the tape in the ASTM G 86 test at the 82 J energy level for the same temperature and pressure, the previously questionable batch of tape was accepted for use in high-pressure oxygen.

Because of these events, an investigation was initiated to determine whether the FTIR pyrolysis furnace could be used as a batch qualification test for the PTFE tape. Further, since the primary concern was hydrocarbon contamination, the effects of hydrocarbon oil contamination on the pyrolysis, ignition, and combustion behavior of PTFE tape were investigated. To use the FTIR pyrolysis furnace for batch acceptance of the PTFE tape, it had to be demonstrated that the FTIR pyrolysis furnace was more sensitive to contamination than the mechanical impact test. This was done by contaminating the tape with known levels of contamination and performing both tests. The autoignition temperature (AIT) was also measured using the FTIR pyrolysis furnace at various contaminant levels. Additional testing was conducted, using a modified pneumatic impact test system (ASTM Test Method for Ignition Sensitivity to Materials to Gaseous Fluid Impact [ASTM G 74]), to study the effect of hydrocarbon contamination on the ignition process.

EXPERIMENTAL APPROACH

Samples of PTFE tape about 1.25 cm wide and approximately 0.01 cm thick were contaminated with a hydrocarbon oil to known levels. The contaminated tape samples and a control group of clean samples were tested by the mechanical impact test in ambient-pressure liquid oxygen (LO_2) (ASTM D 2512), the FTIR pyrolysis furnace, and the modified pneumatic impact test at an impact pressure of 17 MPa. The mechanical impact test measured the effect of contamination on the ignition frequency (ASTM D 2512 was used rather than ASTM G 86, because its sensitivity to reactive materials is similar and the test is significantly less expensive). The FTIR pyrolysis furnace test investigated the effect of contamination on the temperature at which pyrolysis products and products associated with combustion are evolved. The modified pneumatic impact test investigated the effect of contamination on the ignition pressure and burning characteristics.

EXPERIMENTAL PROCEDURE

Contaminating Samples with Oil

All PTFE tape test samples were used directly from the roll and handled only with clean disposable gloves. Oil was placed on all samples (except the control samples) with a microsyringe at a single location to give worst-case conditions. The oil was then folded inside the tape.

Mechanical Impact Testing

Mechanical impact testing was developed in the late 1950's [4] and is currently used by NASA as a standard test for screening materials for use in LO_2 (NHB 8060.1 test 13 part 1, ASTM D 2512) and gaseous oxygen (GO_2) (NHB 8060.1 test 13 part 2, ASTM G 86) [5]. NHB 8060.1 test 13, part 1, was developed to assess the suitability of polymeric materials for use in ambient pressure LO_2. A plummet is dropped onto a striker pin resting on a disc-shaped sample that is immersed in LO_2. The test is valuable for gross screening of materials compatibility with oxygen; however, reproducibility problems arise because of poor detection sensitivity with many materials [2]. NHB 8060.1 test 13, part 2, is the GO_2 mechanical impact [5]; similar reproducibility problems occur with this test.

Unpressurized LO_2 mechanical impact testing was conducted on samples of the contaminated PTFE tape. Seven contamination levels between 0 and 3900 mg/m^2 were selected for the tests. The impact energy was 98 J. For each impact, a 100-mg sample of contaminated tape was folded over so it could fit in the 1.3-cm-diameter sample holder; before folding, the samples were approximately 1.3 cm square. 20 samples were impacted in each test. One or more reactions from the 20 samples constituted failure of the test. Uncontaminated PTFE tape usually shows no reaction [1].

FTIR Pyrolysis Furnace Testing

In the FTIR pyrolysis furnace, the sample is mounted in a ceramic combustion boat in a quartz tube [3]. The sample is heated by a pyrolysis furnace. Gas flows past the sample in the quartz tube at ambient pressure with a predetermined flow rate. An infrared beam is passed through CaF_2 windows in the quartz tube downstream of the sample, and gases emitted from the sample as it is heated are detected with a detector attached to a portable FTIR unit. Each test sample of contaminated tape weighed approximately 1000 mg and was folded over itself so that it was 2.5 cm long. The test gas was high-purity oxygen (less than 100-ppm impurities) at flow rates of 150 scc/min at ambient pressure. The heating rate was 10 °C/min. FTIR traces and video coverage were obtained during heating.

It has been noted that PTFE produces negligible gases until the 350 - 400 °C range is reached [3]; this is in contrast to hydrocarbons, which produce detectable species at 200 °C or less. The testing described here used the low-temperature gas emission of hydrocarbons to differentiate clean tape from contaminated tape. The detection limit was determined by performing at least three tests at each level of contaminant. The interval weight of contaminant was 3.66 mg/m^2.

Pneumatic Impact Testing

Pneumatic impact testing (ASTM G 74) was developed to simulate rapid pressurization of materials by valve action. The sample is placed in a low-pressure sample chamber, then high-pressure oxygen from an accumulator (68 MPa) is released into the sample chamber. The sample ignites when sufficient heat transfers to it from adiabatic compression of the gas. Results from pneumatic impact testing have, like the mechanical impact test results, had reproducibility problems [6].

The equipment used in this testing is modified from that used in ASTM G 74; a light-optics pipe is placed next to a sapphire window so light emissions are detected during an ignition event. A quartz light pipe (0.32-cm outside diameter) bonded within a stainless steel tube (0.64-cm outside diameter) is used. During operation, the radiation emitted from the sample is transmitted via the light pipe to a silicon photodiode viewing the exit port through the sapphire window. The system uses an optional fiber-optic cable to transmit the radiation signatures to the photodiode or an emission spectrometer. The radiant energy measured with the photodiode is recorded as a function of time with a LeCroy high-speed data acquisition system; this allows data to be collected in milliseconds. The testing with this modified equipment was conducted at a constant impact pressure and no attempt was made to determine reaction threshold pressures as in ASTM G 74.

The detector indicates temperature increases associated with the radiative emission from the test system and sample; this is easily detectable with the light optics pipe as a sharp increase in the millivoltage output. Because the silicon photodiode has a cutoff response to wavelengths longer than 1.1 µm, the detector is not sensitive to the radiant energy of the sample chamber for temperatures under 500 K. Flame temperatures in excess of this threshold are easily distinguished from the system temperature or the radiant heat produced from slowly reacting materials.

Seven 100-mg samples of clean tape and seven 100-mg samples of PTFE tape contaminated with 5 mg of oil were wrapped around the threads of a screw and tested in the dead-end configuration for pneumatic impact (Fig. 1). The test pressure was 17 MPa and the pressurization rate was 33.3 MPa/ms. The maximum light intensity, burn time, pressure at ignition, and time at ignition were collected.

Maximum light intensity is the maximum intensity detected by the light pipe of the emitted radiation during combustion; burn time is the time for which visible radiation was detected during combustion of the sample; pressure at ignition is the pressure, obtained from data traces, at the time that light emission is first detected; time at ignition is the time (from initial pressurization) at which light emission is first detected.

MATERIALS

The PTFE tape was supplied by Plastomer Products, New Town,3 PA. It was made according to MIL-T-27730A [7], size II from DuPont PTFE grade T-60 powder. The tape was supplied in rolls 660 cm long by 1.25 cm wide; its weight was 1000 mg per 107 cm length. PTFE is a highly crystalline plastic with a melting point of 327 °C and a specific gravity of 2.17 g/cm^3.

The contaminant hydrocarbon oil was DTE 25, supplied by Mobil Oil Company. This oil has a specific gravity of 0.885 and a viscosity of 46 centipoise at 40 °C.

RESULTS

Mechanical Impact

Table 1 shows the number of reactions in 20 impacts for contamination levels between 0 and 3900 mg/m^2 oil. The contaminated samples began reacting at an oil film level of 260 mg/m^2, indicating that the reaction threshold is somewhere between 130 and 260 mg/m^2.

FTIR Pyrolysis Furnace

FTIR pyrolysis furnace traces show that the oil affects the temperature at which gaseous oxidation products are detected, at contamination levels as low as 11 mg/m^2. Fig. 2 shows spectra measured at temperatures of (a) 280 °C, (b) 320 °C, and (c) 340 °C at the 11 mg/m^2 contamination level.

Fig. 3 shows spectra measured at temperatures of (a) 260 °C, (b) 280 °C, and (c) 285 °C at the 2600-mg/m^2 contamination level. This figure shows stages leading to the ignition of the tape sample.

The detection limit for the concentration of oil on the tape was 11 mg/m^2. The minimum concentration of oil at which the AIT of the tape was depressed was 2400 mg/m^2 (65 mg/1000 mg PTFE tape). This AIT was 285 °C, which was the same as the pure oil; the AIT of the clean PTFE tape was 525 °C. A summary of the temperatures at which gaseous products are detected is given in Tables 2 and 3 for contaminated and clean tape.

Pneumatic Impact

The hydrocarbon contaminant did not affect the pressure or the time at which the tape ignited. However, the contamination caused the samples to burn longer and with more intensity. The results of the pneumatic impact testing are shown in Table 4.

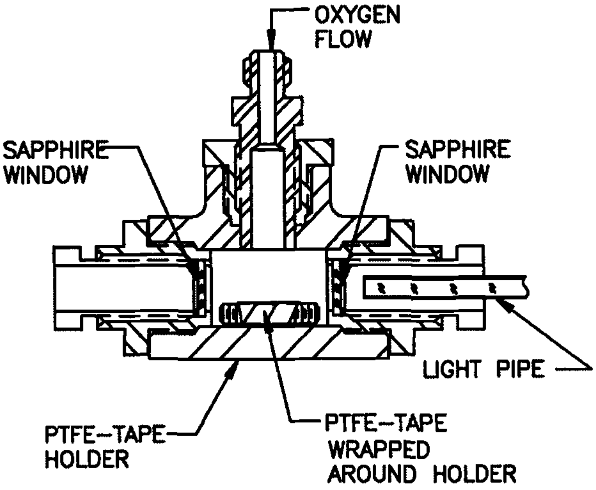

Fig.1--PTFE tape sample in dead-end configuration pneumatic impact test system.

DISCUSSION

The contamination level detected with the mechanical impact test was 260 mg/m^2 and with the FTIR pyrolysis furnace, was 11 mg/m^2. These can be compared with the standard NASA oil film specification for oxygen systems of 11 mg/m^2 and the Compressed Gas Association specification of 1100 mg/m^2 [8,9]. The pyrolysis furnace can measure to the NASA specification while the LO_2 mechanical impact test can only measure greater than an order of magnitude above the specification. Previous studies have shown that hydrocarbon oils are reactive at concentrations above 65 mg/m^2 [10]. (Ignition of such contaminants at these concentrations never resulted in ignition of hardware components; however, the tests were conducted in all-metallic systems). Thus, the mechanical impact test may not be able to detect a potentially reactive sample, whereas the pyrolysis furnace can.

The depression of the AIT (requiring a minimum oil level of 2400 mg/m^2) had poor sensitivity to the oil level and is probably not a good method of determining contamination. The insensitivity of the AIT measurement could be because a lot of the oil contamination may have evolved degradation products at the slow heating rate of 10 °C per minute, leading to a small quantity of contaminant remaining at the time of ignition.

The pneumatic impact data showed no effect of the oil on the pressure or time at which ignition started. These results are not unexpected, because the concentration of oil on the tape was approximately 1800 mg/m^2 (50 mg/1000 mg PTFE tape), lower than the minimum concentration of oil at which the AIT was depressed in the FTIR pyrolysis furnace. However, they do suggest that the presence of even

Table 1--Mechanical impact test results.

Contamination Level, mg/m^2	Number of mechanical impact reactions (20 Impacts at Each Level)
0	0
130	0
260	1
520	6
780	8
1300	5
3900	13

TABLE 2 —PTFE tape contaminated with Mobil DTE 25 oil tested with FTIR spectrometer.

Temperature, °C	Gaseous products
<175	Nothing Detectable
175	Hydrocarbons
260	Hydrocarbons, CO_2, $C_xH_yO_z$
280	Hydrocarbons, CO_2, $C_xH_yO_z$, CO, H_2O
285	Ignition
>285	Hydrocarbons, CO_2, $C_xH_yO_z$, CO, HF, COF_2, CF_4, SiF_4

TABLE 3—Clean PTFE tested with FTIR spectrometer.

Temperature, °C	Gaseous products
327	Nothing Detectable
<390	Nothing Detectable
450	CO_2, COF_2
520	CO_2, COF_2, CF_4, SiF_4
525	Ignition
610	CO_2, CO, COF_2, CF_4, SiF_4
660	SiF_4

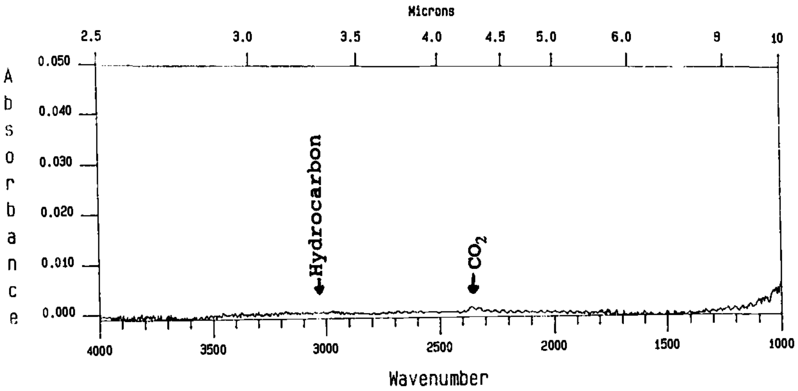

(a) 280 °C.

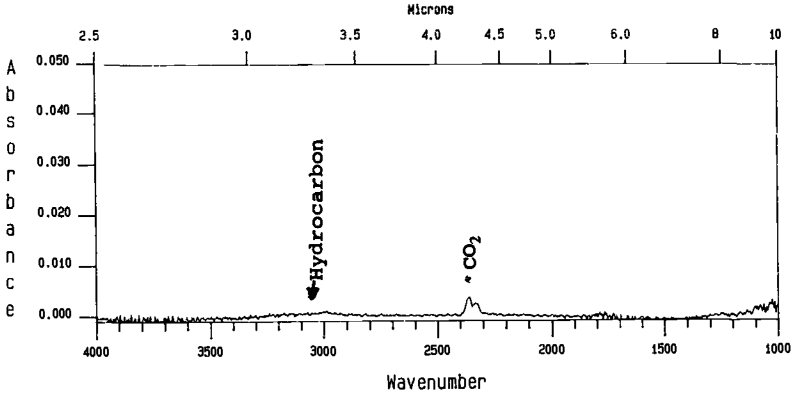

(b) 320 °C.

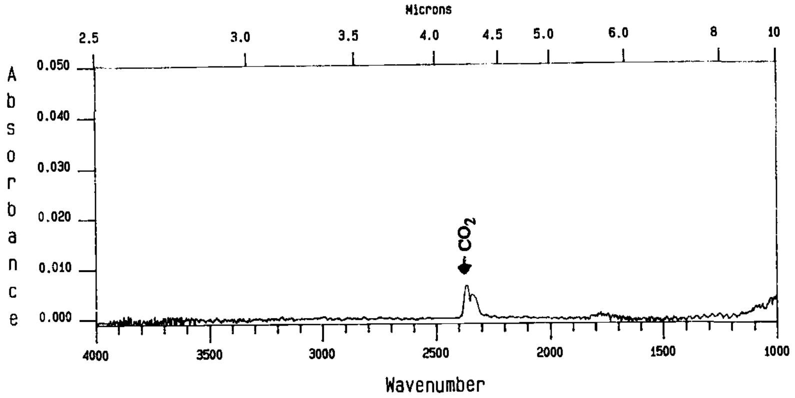

(c) 340 °C.

Fig. 2--FTIR spectra for samples at the 11-mg/m^2 contamination level

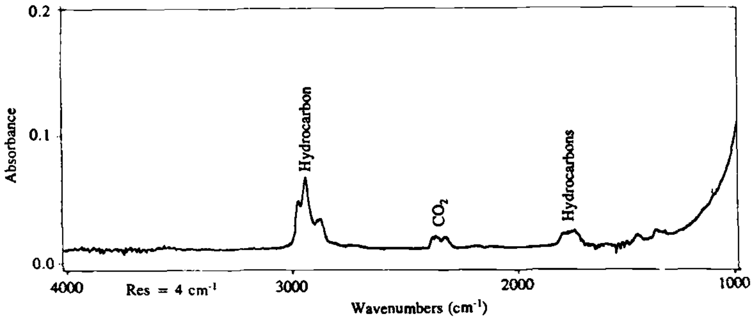

(a) 260°C

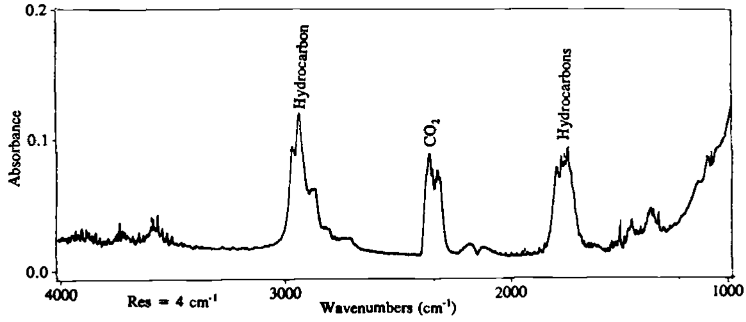

(b) 280°C

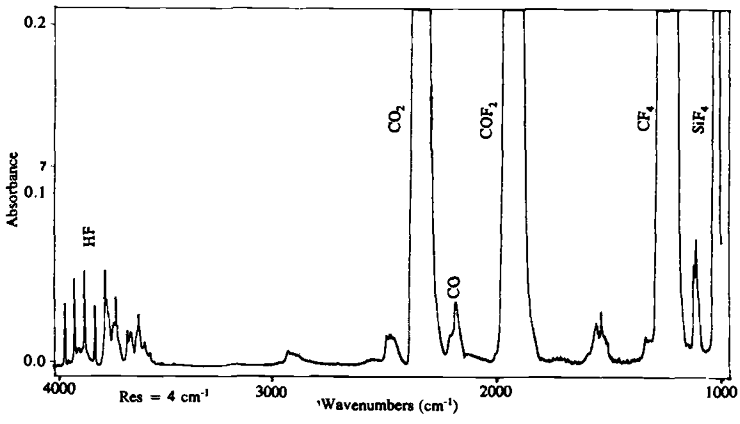

(c) 285°C

Fig. 3--FTIR spectra for samples at the 2600-mg/m^2 contamination level.

Table 4--Pneumatic impact test results.

Sample	Maximum light intensity[a], mV	Burn time[b], ms	Ignition pressure[c], MPa	Ignition time[d], ms
CLEAN	.52	658	11.2	76
CLEAN	0.81	755	11.0	76
CLEAN	1.01	529	14.3	106
CLEAN	1.31	890	9.7	66
CLEAN	1.56	600	12.9	91
CLEAN	1.76	624	11.9	82
CLEAN	2.05	752	12.2	82
AVERAGE	1.28	687	11.9	88
5 mg OIL	1.19	926	7.0	48
5 mg OIL	1.90	655	12.2	86
5 mg OIL	2.19	1058	9.9	66
5 mg OIL	2.24	1348	14.9	113
5 mg OIL	2.25	976	8.5	56
5 mg OIL	3.09	1093	13.3	93
5 mg OIL	5.88	1213	15.9	213
AVERAGE	2.68	1038	11.7	96

[a] Maximum peak signal obtained from the light pipe trace
[b] Time for which light was detected during a reaction
[c] Pressure at which light was first detected
[d] Time after initial pressurization at which light was first detected

quite high concentrations of oil contaminants does not promote ignition of PTFE tape by adiabatic compression heating. Random variation of the data was large. The AIT of oil is around 285 °C compared with over 500 °C for PTFE. A difference would be expected if larger amounts of oil were used.

The oil-contaminated samples burned longer and had higher intensity light emissions than the clean tape. The burn time was found to be in proportion to the total heat of combustion of the sample (ΔH_c PTFE + ΔH_c oil). The average heat dissipation rate was found to be around 0.75 J/ms for both the oil-contaminated and clean tapes.

Pure PTFE ranks highly amongst other polymers when standard oxygen tests are performed on it (mechanical impact, autoignition temperature, oxygen index). The reasons for its relative stability in oxygen are many. The following paragraphs discuss the stability of PTFE and why the addition of hydrocarbon oil contamination would decrease that resistance to ignition and combustion in oxygen systems.

PTFE has a high chain stiffness of the molecule, which arises from the larger size of the fluorine atom compared with hydrogen (as in linear polyethylene). This high chain stiffness results in the low ΔS_m, and provides PTFE with a high melt rigidity (melt viscosity 10^{10}-10^{11} p at 350 °C). Contributing to the high melt viscosity is the high weight average molecular weight, typically in the range 400,000 to 9,000,000 atomic mass units. As a result of the high molecular weight, PTFE, like most polymers, does not volatilize; degradation must occur prior to the formation of any vapor phase products. The degradation products of PTFE begin to evolve at 350-450 °C; the type of products and evolution temperature from this testing agree, in general, with the literature [11]. The products found for PTFE degradation are summarized in Table 3.

The reaction products can be explained by the following mechanisms [12]:

$$\underset{\text{PTFE}}{(CF_2)_n} \rightarrow (CF_2)_{n-x} + \underset{\text{CARBENE RADICALS}}{xCF_2:} \qquad (1)$$

These difluorocarbene radicals would normally combine to form tetrafluoroethylene in the absence of oxygen. When oxygen is present, CF_2 radicals react with O_2 to form carbonyl fluoride (COF_2), followed by a decomposition reaction:

$$2CF_2: + O_2 \rightarrow 2COF_2 \qquad (2)$$

$$2COF_2 \rightarrow CO_2 + CF_4 \qquad (3)$$

The reaction products from Equations 2 and 3 were observed in testing. The difluorocarbene radicals are reaction intermediates, having only a transient existence because of the low energy barrier to their conversion into products. Carbenes are bent molecules and are either singlet species with paired electrons (having anti-parallel spins) or triplet species with two single electrons (having parallel spins) [13,14,15,16,17,18,19,20]. Reactions with oxygen will be different dependent on whether triplet or singlet species are produced [14]. The species type was not investigated in this work.

The SiF_4 may be explained by the formation of HF from COF_2 and trace water in the system [21] as follows:

$$COF_2 + H_2O \rightarrow CO_2 + 2HF$$

The HF subsequently reacts with the quartz tube in the reaction

$$4HF + SiO_2 \rightarrow 2H_2O + SiF_4$$

The absence of detectable concentrations of difluorocarbene radicals and tetrafluoroethylene molecules in the combustion gases suggests that the limiting reaction in the combustion of PTFE under the given experimental conditions is that described in Equation 1. Errede [22] showed that the mechanism in Equation 1 occurs because the bond at the chain end is different and weaker than the rest of the chain bonds and is more easily broken. If the carbenes are formed only at chain ends, the concentration of carbenes should be proportional to the number density of chain ends in the PTFE; this number is higher for lower molecular weights. The dependence on molecular weight would not be so strong for hydrocarbons because of the large number of defects in the chain and the resulting random chain scission mechanism of degradation; that is to say, the degradation does not take place solely at the chain ends.

We suggest that batch differences in PTFE arise from contamination or other low molecular weight volatiles that will evolve at appreciably lower temperatures than products from pure PTFE. These tests showed that batch differences arising from contamination are detectable with the FTIR pyrolysis furnace. The effect of varying molecular weight (and thus the number of chain ends) on the reactivity of different batches of PTFE was not studied in this program, but would be an interesting direction for future work.

FUTURE WORK

From discussion of the oxidation and combustion mechanisms of PTFE, a potential source of batch variation in PTFE is molecular weight difference. As noted above, further investigation of this proposed mechanism would be of value for understanding batch variations in PTFE. It would also be valuable to extend this approach to other materials to determine whether batch variations caused by contamination or variations in the chemistry can be detected. The FTIR furnace appears to be the most promising tool for such studies. It should be possible to study the effect of varying the PTFE molecular weight on the temperature at which carbonyl fluoride starts to become detectable. Another possible approach is to lower the oxygen pressure or concentration to reach a level where difluorocarbenes or C_2F_4 molecules are just detectable and determine the effect of PTFE molecular weight on their concentration.

Additional mechanical impact testing should be conducted to verify that these results also apply to the pressurized GO_2 test. Further pneumatic impact testing should be conducted to determine if a difference in the AIT may be seen if larger amounts of oil are used. A difference is expected, based on the FTIR furnace data. Testing the effects of different levels of oil contamination on polymeric materials in the system previously used to obtain threshold contaminant levels for ignition [10] would also be of value to establish oil levels required to promote ignition and verify the high numbers found for PTFE in this study.

CONCLUSIONS

The FTIR pyrolysis furnace is more sensitive than the ambient pressure LO_2 mechanical impact test and the pneumatic impact test for detecting contaminated PTFE tape. The FTIR spectrum is sensitive to contaminant levels as low as 11 mg/m^2; however, the AIT measured in the FTIR furnace is not affected by oil until the sample is grossly contaminated. The FTIR furnace appears to be a promising tool for screening batches of materials for oxygen compatibility. However, additional testing is required to verify that it is sensitive to batch variations caused by differences in the materials chemistry as well as to variations caused by contamination.

REFERENCES

[1] Vagnard, G., Delode, G., and Barthelemy, H., "Test Methods and Interpretation of Results for Selecting Non-Metallic Materials for Oxygen Service," Flammability and Sensitivity of Materials in Oxygen-Enriched Atmospheres: Fifth Volume, ASTM STP 1111, J. M. Stoltzfus and K. McIlroy, Eds., American Society for Testing and Materials, Philadelphia, PA, 1991, pp. 489-505.

[2] Moffett, G. E., Schmidt, N. E., Pedley, M. D., and Linley, L. J., "An Evaluation of the Liquid Oxygen Mechanical Impact Test," Flammability and Sensitivity of Materials in Oxygen-Enriched Atmospheres: Fourth Volume, ASTM STP 1040, J. M. Stoltzfus, F. J. Benz, and J. S. Stradling, Eds., American Society for Testing and Materials, Philadelphia, 1989, pp. 11-22.

[3] Tapphorn, R. M., Shelley, R., and Benz, F. J., "Test Developments for Polymers in Oxygen-Enriched Environments," Flammability and Sensitivity of Materials in Oxygen-Enriched Atmospheres: Fifth Volume, ASTM STP 1111, J. M. Stoltzfus and K. McIlroy, Eds., American Society for Testing and Materials, Philadelphia, 1991, pp.43-59.

[4] Lucas, W. R., and Riehl, W. A., ASTM Bulletin, ASTBA, No. 244, February 1960, pp. 29-34.

[5] "Mechanical Impact for Materials in Ambient Pressure LOX (Test 13A)," and "Mechanical Impact for Materials in Variable Pressure LOX and GOX (Test 13B)," NHB 8060.1C, Flammability, Odor, Offgassing, and Compatibility Requirements and Test Procedures for Materials in Environments that Support Combustion, Office of Safety and Mission Quality, NASA, 1991.

[6] Lockhart, B. J., Hampton, M. D., and Bryan, C. J., "The Oxygen Sensitivity/ Compatibility of Several Materials by Different Test Methods," Flammability and Sensitivity of Materials in Oxygen-Enriched Atmospheres: Fourth Volume, ASTM STP 1040, J. M. Stoltzfus, F. J. Benz, and J. S. Stradling, Eds., American Society for Testing and Materials, Philadelphia, 1989, pp. 93-105.

[7] MIL-T-27730A. "Tape Antiseize PTFE with Dispenser," US Government Printing Office, p. 64.

[8] Werley, B. L., "Oil Film Hazards in Oxygen Systems," Flammability and Sensitivity of Materials in Oxygen-Enriched Atmospheres: ASTM STP 812, B. L. Werley, Ed., American Society for Testing and Materials, 1983, pp. 108-112.

[9] NASA JSCM 5322B, Contamination Control Requirements Manual. NASA Johnson Space Center, November (1982).

[10] Pedley, M. D., Pao, J., Bamford, L., Williams, R. E., and Plante, B., "Ignition of Contaminants by Impact of High-Pressure Oxygen," Flammability and Sensitivity of Materials in Oxygen-Enriched Atmospheres: Third Volume, ASTM STP 986, D. W. Schroll, Ed., American Society for Testing and Materials, Philadelphia, PA, 1987, pp. 305-317.

[11] Jellinek, H. H. G., Degradation of Vinyl Polymers, Academic Press, Inc., 1955.

[12] Morisaki, S., "Simultaneous Thermogravimetry-Mass Spectrometry and Pyrolysis-Gas Chromatography of Fluorocarbon Polymers," Thermochimica Acta, 25, 1978, pp. 171-183.

[13] Wasserman, E., Kuck, V. J., Hutton, R. S., Anderson, E. D., and Yager, W. A., "^{13}C Hyperfine Interactions of Geometry of Methylene," Letter to editor, Journal of Chemical Physics, Vol. 54, No 9, May 1971, pp. 4120-4121.

[14] Harrison, J. F., "The Structure of Methylene," Accounts of Chemical Research, Vol 7, 1974, pp. 378-384.

[15] Margrave, J. L., Sharp, K. G., Wilson, P. W., "The Dihalides of Group IVB Elements," Fort. Chem. Forsch, Vol 26, 1972, pp. 1-35.

[16] Wasserman, E., Yager, W. A., and Kuck, V. J., "EPR of CH_2: A Substantially Bent and Partially Rotating Ground State Triplet," Chemical Physics Letters, Volume 7, No. 4, 1970, pp. 409-413.

[17] Hay, P. J., Hunt, W. J., and Goddard, W. A., "Generalized Valence Bond Wave Functions for the Low-Lying States of Methylene," Chemical Physics Letters, Volume 13, No. 1, 1972, pp. 30-35.

[18] Kirmse, W., Carbene Chemistry, Academic Press, 1964.

[19] Kirmse, W., Progress in Organic Chemistry, 6, 1964, pp. 164-213.

[20] Closs, G. L., Topological Stereochemistry, 3, 1968, pp. 193-235.

[21] Paciorek, K. L., and Zun, L. B., "Fundamental Ignition Study for Material Fire Safety Improvement," Final Report, Part 1, Contract NASW-1921, NASA, Dynamic Science, 1970.

[22] Errede, L. A., "The Application of Simple Equations for Calculating Bond Dissociation Energies to Thermal Degradation of Fluorocarbons," Thermal Degradation of Fluorocarbons, Vol 27, October 1962, pp. 3425-3430.

Ignition and Combustion of Metals

Kenneth McIlroy[1], Joseph Million[1] and Robert Zawierucha[1]

PROMOTED IGNITION-COMBUSTION BEHAVIOR OF CARBON STEEL IN OXYGEN GAS MIXTURES

REFERENCE: McIlroy, K., Million, J., and Zawierucha, R., "Promoted Ignition-Combustion Behavior of Carbon Steel in Oxygen Gas Mixtures," Flammability and Sensitivity of Materials in Oxygen-Enriched Atmospheres: 6th Volume, ASTM STP 1197, Dwight D. Janoff and Joel M. Stoltzfus, Eds., American Society for Testing and Materials, Philadelphia, 1993.

ABSTRACT: Promoted ignition-combustion is a term which has been used to describe a situation where a substance with poor oxygen compatibility ignites and supports the combustion of a more resistant material. Previous papers on the subject in recent years have reported on the investigation of this phenomenon as it related to carbon steel, stainless steels and a number of engineering alloys. However, the bulk of these investigations have involved relatively high pressures.

Carbon steel is a common alloy used in the construction of equipment used in industrial gas applications. Yet, promoted ignition-combustion test data on carbon steel samples showing the effects of variables such as test pressure, oxygen purity, temperatures, section size, promoter types, etc. on promoted ignition-combustion behavior are scarce; particularly, at low pressures.

In this investigation, the promoted-ignition combustion behavior of carbon steel was studied in oxygen-nitrogen gas mixtures over the pressure range of 0.118 MPa to 0.446 MPa with oxygen purities ranging from 70% to 99.7%. Comparative tests were made using 3.175 mm and 6.35 mm diameter rods at pressures up to 0.273 MPa. Over the pressure and purity ranges tested, there was little difference due to size effects. Carbon steel burns occurred at pressures as low as 0.118 MPa with oxygen purities of 95% and above, in the promoted ignition-combustion tests.

KEY WORDS: Promoted Ignition-Combustion, Carbon Steel, Oxygen

---

[1] Engineering Associate, Senior Chemist, and Manager, respectively, Materials Engineering Laboratory, Praxair Inc., Linde Division, P.O. Box 44, Tonawanda, NY 14151-0044

INTRODUCTION

Carbon steel is extensively utilized in the industrial gas business for oxygen services. Although, it has occasionally been involved in various incidents where components have burned, the historic service experience has been excellent. Careful design, well established cleaning procedures for oxygen service and system maintenance have been key factors in the industry's safety record.

Within the past six years there have been a number of new oxygen applications which necessitated development of new data bases. New metals ignition-combustion test techniques were introduced which are still in the process of evolution. Much of the previous work which has been reported has involved engineering alloys other than carbon steel, 99.7% nominal oxygen purity and relatively high pressures in the range of 3.55 MPa to 34.58 MPa. In this regard, References 1 through 4 are examples.

Oxygen services may involve relatively low pressures, and reduced purity levels in various applications or air separation processes as well as materials that are not exotic. References 5 through 7 are noteworthy in that they present data pertinent to flammability tendencies under conditions of reduced purity or pressures for carbon steel and aluminum. However, for carbon steel, relatively little attention has been given to the low pressure end of the service range i.e. pressures of 0.446 MPa and less.

In this paper, data presented to address this deficiency were generated using a flow tester. Oxygen purities ranged between 70% and 99.7%. Various promoters as well as several different thicknesses were used in the investigation.

EXPERIMENTAL

Test Specimens

The specimens used had nominal dimensions of 3.175 mm diameter by 98.4 mm length or 6.25 mm diameter by 98.4 mm length. Typically, the 3.175 mm diameter has been used by the authors and NASA in past investigations [1-4, 7, 9]. The larger diameter rods were included to allow comparison with the smaller diameter and selected literature data.

Material Chemistry

The carbon steel used in the experimental program was commercially available welding rod. The chemical analyses of the material are as follows:

Table I - Alloy Chemical Analysis Data

Composition by Weight	3.175 mm Rods	6.25 mm Rods
% C	0.05	0.03
% Mn	1.09	0.35
% Si	0.52	0.01
% S	0.09	0.014
% P	0.01	0.005
% Cu	0.03	0.01
% Al	0.076	0.01
% Ti	0.057	0.01
% Zr	0.043	0.01
% Fe	98.034	99.551
Calculated Heat of Combustion, Calories/Gram	1802	1768

Oxygen-Nitrogen Gas Mixtures

The gases were obtained in specially premixed cylinders with nominal oxygen concentrations ranging between 70% and 99.7% oxygen.

Test Apparatus

The test apparatus which will be referred to as the "flow tester" essentially is a pressurized oxygen index tester. Other pressurized oxygen index experiments are described in References 6 through 8.

The flow tester was selected to test the combustion behavior of selected alloys in flowing oxygen gas mixtures at specific pressures which may be considerably lower than practical in static testers without oxygen starvation effects.

The gas is regulated to the desired pressure and the gas is throttled to achieve a flow of 20 standard liters per minute through the system. The volumetric flow selection was based on test work reported on in Reference 7. In this configuration, the gas velocity is calculated to be 25.4 mm/second at 0.8 MPa and 100 mm/second at 0.27 MPa. Thus, the gas flow is low but sufficient to provide oxygen for the rod in the combustion zone.

The flow tester used in this study is a second generation design. It has a broader base section which allows better clearance of the test sample and the grounded chamber wall. Figure 1 shows the second generation flow tester with the broader base in schematic form. Note that this vessel also has the capability to conduct flammability tests at cryogenic temperatures, or with sample types other than rods.

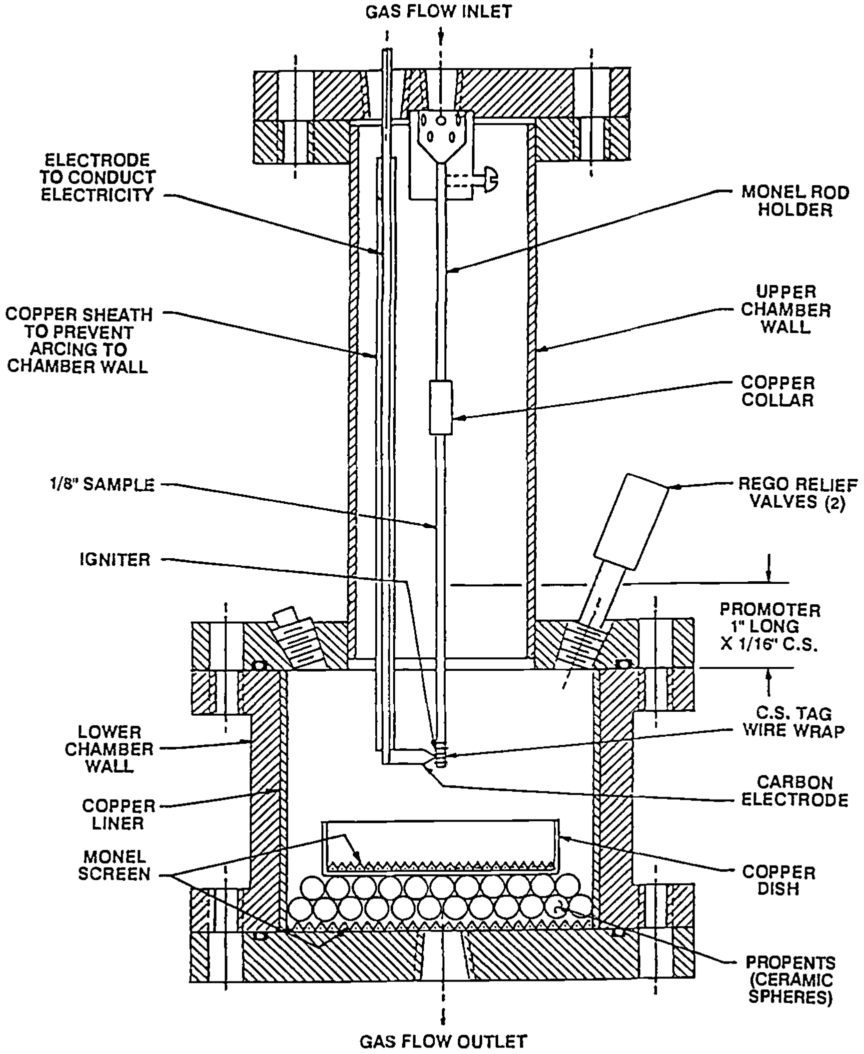

FIG. 1 -- Schematic of Second Generation Flow Tester Based upon Pressurized Oxygen Index Concept.

Promoter

In early test work, Reference 7, a carbon steel collar was used as the promoter. The collar was and is an excellent choice for promoting combustion of hard-to-combust alloys at higher pressures. The promoter is, of course, ignited by an electric arc. Since the metal to be tested is carbon steel, the thick carbon steel collar was difficult if not impossible to ignite in reduced oxygen purity environments; particularly at low pressures.

In this paper, Pyrofuze(R), an aluminum-palladium exothermic composite (manufactured by Pyrofuze Corporation, Mt. Vernon, NY) and carbon steel wire were evaluated as promoters.

The nominal weight and thickness of the Pyrofuze(R) wire was 0.074g and 0.4 mm, respectively. The corresponding carbon steel wire promoter was 0.15 g and 0.4 mm.

Criteria for Evaluation

Criteria are extensively discussed in an earlier paper, Reference 9. Recent Praxair investigations have defined a burn when less than 70% of the 98.4 mm sample remains intact after ignition. This criteria allows 30% of the sample to be melted/ignited and a sufficient length remains to develop steady state combustion. The burn length corresponding to 30% is 2.95 cm.

A burn criterion of 30% of the sample melted/ignited corresponds to an upper shelf criterion with respect to the Promoted Ignition-Combustion Curve described in Reference 9 and shown in Figure 2. It is also possible to use other criteria such as a 100% burn criterion which reflects a "lower shelf behavior" from the flammability standpoint. In this investigation, data is reported using both 30% and 100% burn criteria.

RESULTS AND OBSERVATIONS

Burn Criterion 30%, 3.175 mm Rods

Figure 3 shows flammability data for 3.175 mm carbon steel rods over the 0.119 MPa to 0.446 MPa range in oxygen-nitrogen gas mixtures using both Pyrofuze(R) and carbon steel promoters. The data is shown using the 30% burn criterion or upper shelf definition for the burn/no burn threshold.

A key observation is the number of burns that occurred at low pressures and at purities less than 99.7%. Burns were not expected at pressures less than 0.27 MPa even at 99.7% purity based upon data presented in Reference 8.

At the lowest pressure of 0.119 MPa, the carbon steel rods burned irrespective of promoter at an oxygen purity of 95% and above. At the 90% and 80% oxygen purity levels, the difference in severity between the Pyrofuze(R) and carbon

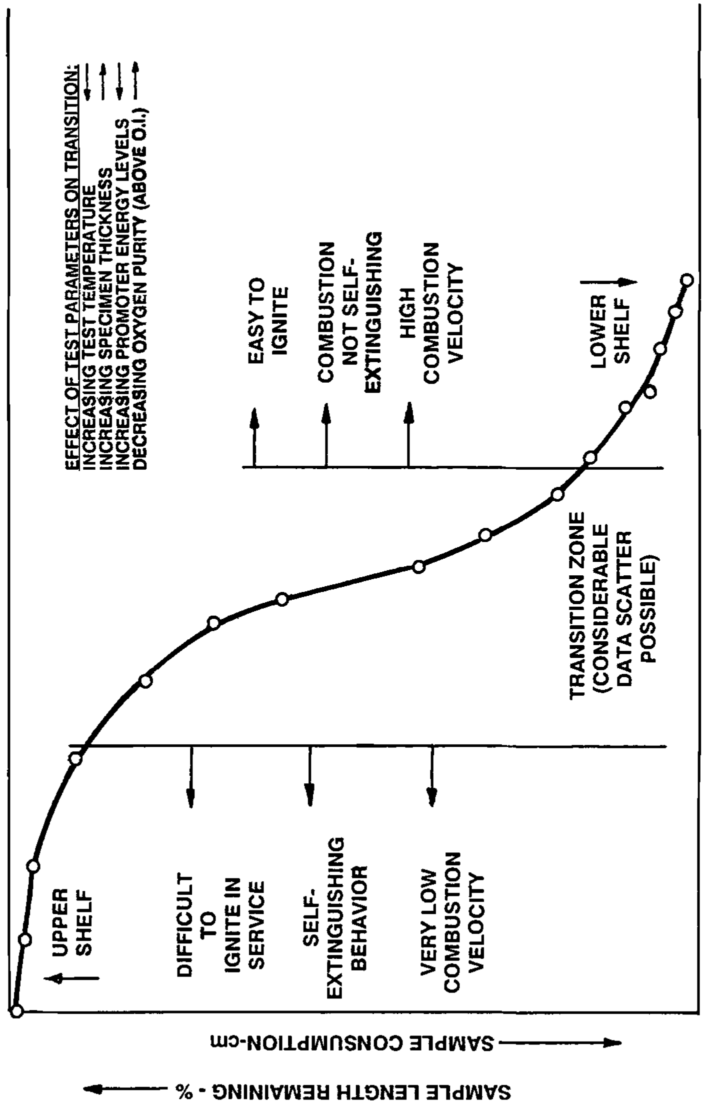

FIG. 2 -- Schematic of the Promoted Ignition-Combustion Transition (PICT).

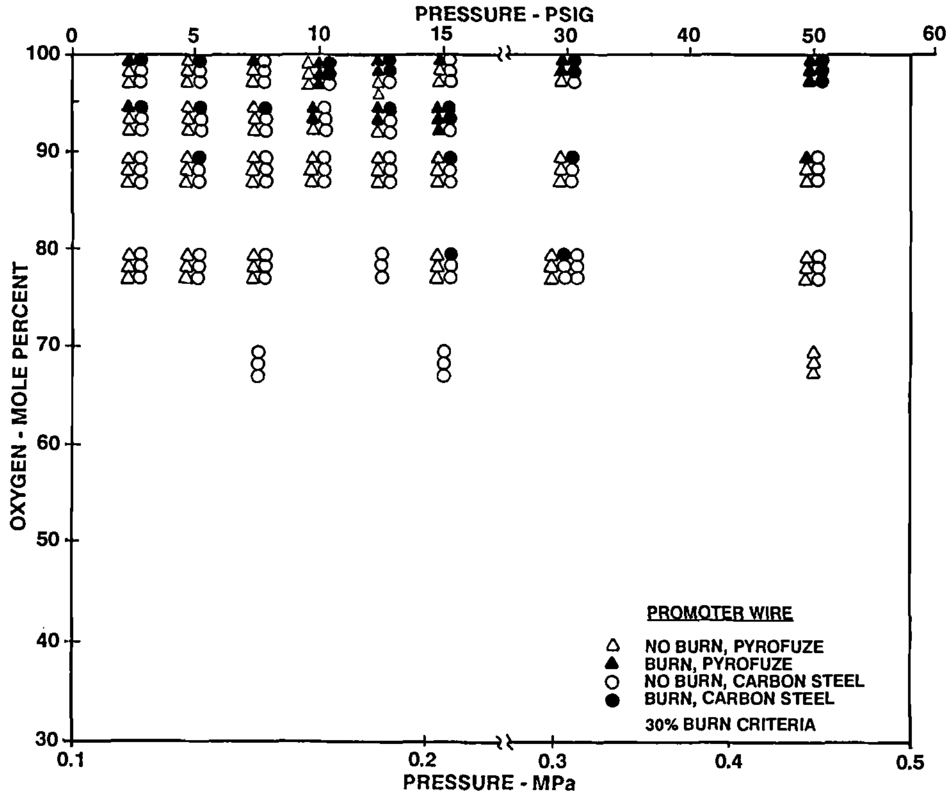

FIG. 3 -- Flammability Data for 3.175 mm Diameter Carbon Steel Rods in Oxygen-Nitrogen Gas Mixtures as Functions of Oxygen Purity and Pressure, Using Pyrofuze and Carbon Steel Wire Promoters and 30% Burn Criteria.

steel promoters is evident. However, any difference between the two promoters is not easily discernible at the 95% and 99.7% purity levels.

Burn Criterion 100%, 3.175 mm Rods

Figure 4 shows the flammability data for carbon steel rods over the 0.119 MPa to 0.446 MPa range in oxygen-nitrogen gas mixtures using both Pyrofuze(R) and carbon steel promoters. In this instance, the data is interpreted using the 100% burn criterion or lower shelf definition for the burn/no burn threshold. The difference in the severity of the carbon steel and Pyrofuze(R) promoters is minimal up to a test pressure of 0.273 MPa. Above that pressure, the Pyrofuze(R) promoter is more severe.

If Figures 3 and 4 are compared, it is apparent that the carbon steel burn/no burn threshold using Pyrofuze(R) promoter would be similar irrespective of which burn criteria is used. However, with carbon steel wire promoter, the 100% burn criteria would tend to give a higher burn/no burn threshold over the tested pressure range.

6.25 mm Rod Data

Figure 5 shows the flammability data for 6.25mm carbon steel rods over the pressure range of 0.119 MPa to 0.273 MPa using carbon steel wire as the promoter. In this instance, utilization of either the 30% or 100% burn criteria gave the same interpretation of what a burn was since the samples burned completely if they burned. Once the 6.25 mm diameter rods were ignited, there was a pronounced tendency for the rods to keep burning and not arrest.

At oxygen purities of 90% and above, the bulk of the carbon steel data shows burn behavior for 6.25 mm rods. Only at oxygen purities of 80% and below did carbon steel cease to exhibit burn behavior at pressures up to 0.273 MPa. The data of Zabrenski [8] indicated a burn/no burn threshold of 0.273 MPa for carbon steel using 6.25 mm rods presumably at an oxygen purity of 99.7%. In contrast, a burn at 0.119 MPa occurred in this investigation with a 6.25 mm carbon steel rod at an oxygen purity of 99.7%.

DISCUSSION

The test work in this investigation determined the effect of different promotor types and burn criteria on the burn/no burn threshold for carbon steel at relatively low pressures with 3.175 mm diameter rods. There is no clear cut difference across the board in severity between the two types. The choice of burn criteria might affect a severity rating. Carbon steel wire promoters obviously are cheaper.

The investigation also showed the effects of rod diameter. Once ignited, the 6.25 mm rods showed a greater

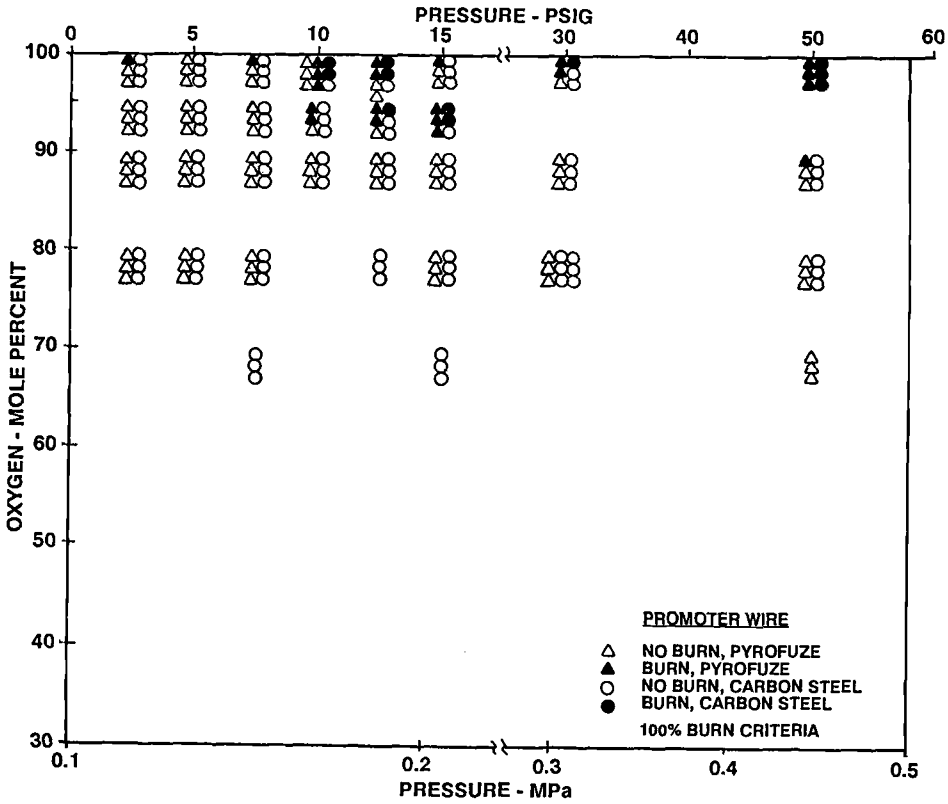

FIG. 4 -- Flammability Data for 3.175 mm Diameter Carbon Steel Rods in Oxygen-Nitrogen Gas Mixtures as Functions of Oxygen Purity and Pressure, Using Pyrofuze and Carbon Steel Wire Promoters and 100% Burn Criteria.

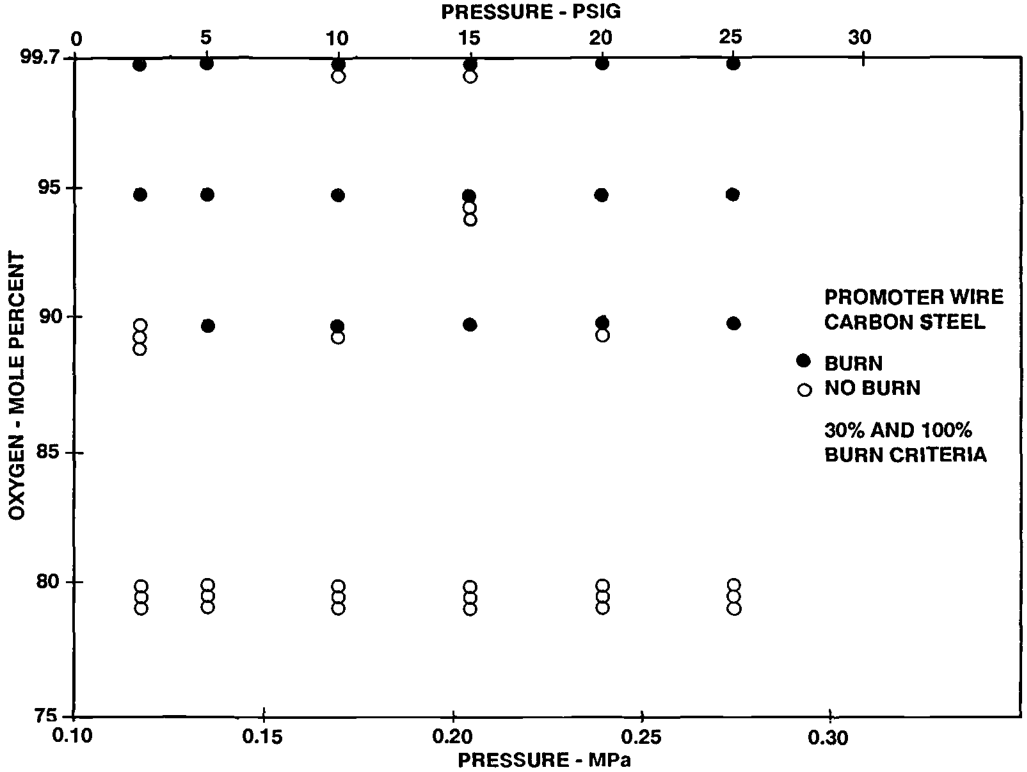

FIG. 5 -- Flammability Data for 6.25 mm Diameter Carbon Steel Rods in Oxygen-Nitrogen Gas Mixtures as Functions of Oxygen Purity and Pressure.

tendency to keep burning rather than arrest as compared to the 3.175 mm diameter rods. Thus, there was no difference in results if 30% or 100% burn criteria were used. It is worth noting that there were chemistry differences between the two rod sizes which could have affected combustion propagation somewhat. Nevertheless, the thicker specimen did shift the burn/no burn threshold to higher purity levels over the tested pressure range.

A noteworthy result was the burn behavior of carbon steel in 99.7% oxygen at pressures as low as 0.119 MPa for both the 3.175 mm and 6.25 mm diameter rods. This is in contrast to the data of Zabrenski which reported a burn threshold of 0.273 MPa for 6.25 mm diameter carbon steel rods.

Figure 6 shows previous carbon steel flammability data abstracted from Reference 7 for 3.175 mm diameter carbon steel rods using carbon steel collars as the promoter. Inspection of this data along with data from other tests with the current work indicated that a composite, Figure 7, could be created which also shows the carbon steel burn/no burn threshold from our investigation over the pressure range of 0.118 MPa to 34.475 MPa. The composite flammability curve remedies the data deficiency which has existed. It indicates that carbon steel is more flammable in oxygen than reported in other investigations but still shows carbon steel to be nonflammable over a substantial envelope of oxygen purity and pressure.

SUMMARY

The promoted ignition - combustion behavior of carbon steel rods was investigated at pressures up to 0.446 MPa in oxygen-nitrogen gas mixtures ranging from 70% to 99.7% using carbon steel wire and pyrofuze promoters.

At the highest oxygen purity of 99.7% carbon steel rods were consumed in promoted ignition-combustion tests at pressures as low as 0.119 MPa irrespective of rod diameter or promoter type. Carbon steel wire promoter appeared to be more severe than Pyrofuze(R) in these tests.

The tendency for carbon steel samples to burn was primarily a function of pressure and purity. As pressures increased, the oxygen content required for combustion continued to drop. At a test pressure of 0.446 MPa the minimum oxygen content to sustain combustion was 70% using a 30% (29.5 mm) burn criteria for 3.175 mm rods.

In the low pressure range that was investigated, the 6.25 mm rod samples were somewhat more flammable than the 3.175 mm samples as measured by the oxygen content required to support combustion over the test pressures evaluated; however, it must be acknowledged that there were chemistry differences between the two diameter rods. This result is contrary to that of previous experimenters. However, even

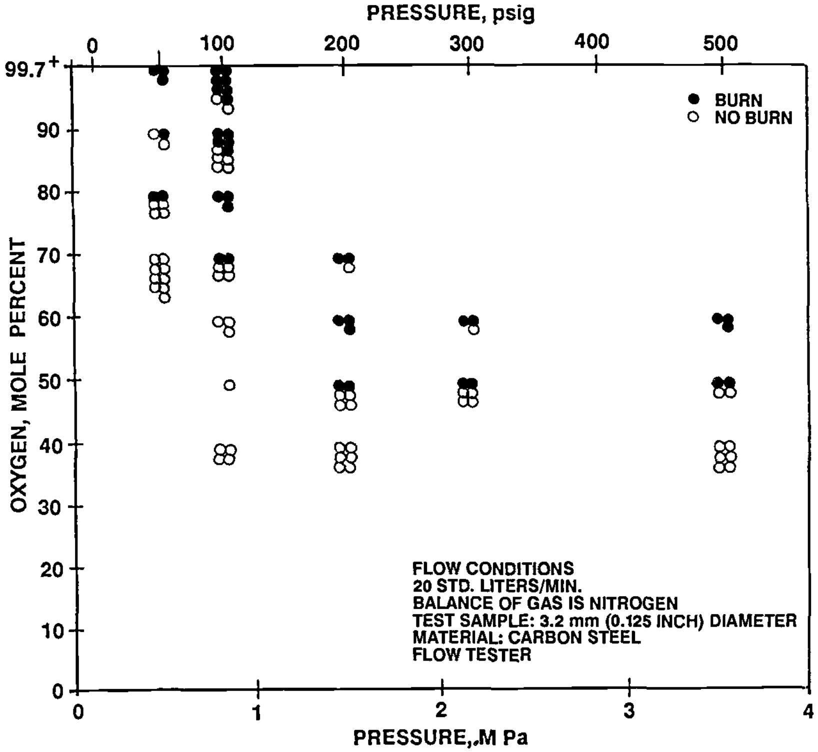

FIG. 6 - Carbon steel flammability as a function of oxygen purity and gas pressure (flow tester).(7)

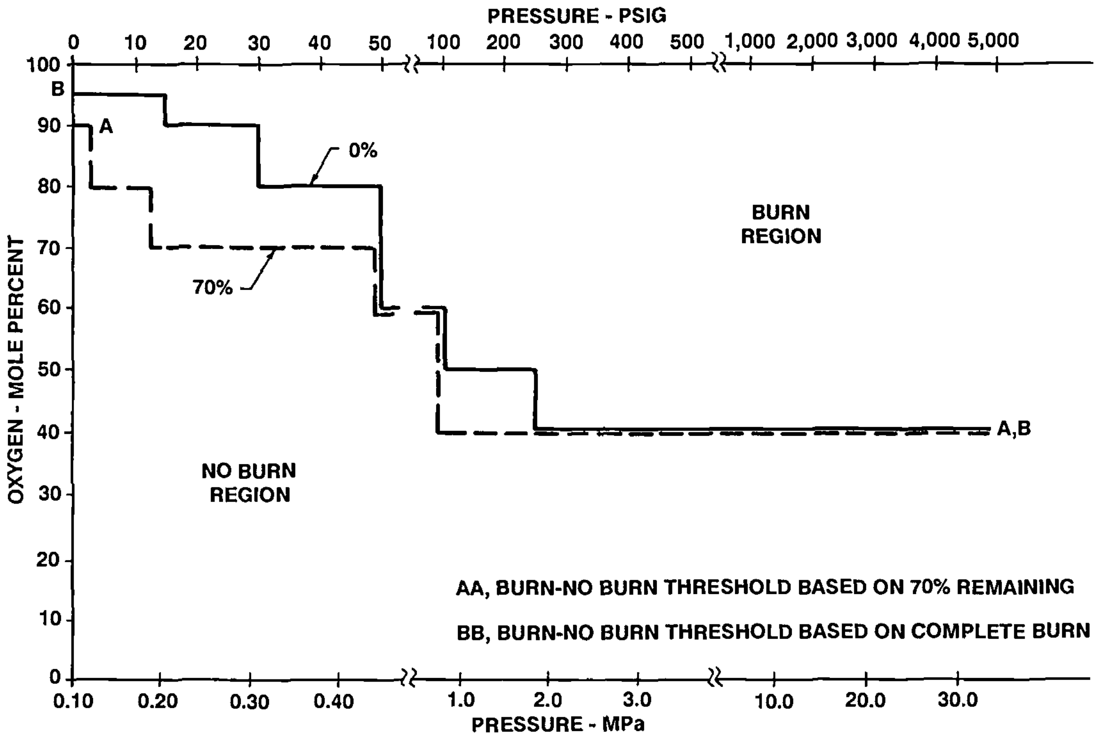

FIG. 7 -- Flammability Envelopes for 3.175 mm Diameter Carbon Steel Rods.

the large diameter samples proved to be combustible at relatively low pressures in oxygen with purity of 90% or more.

A future test program will examine apparent anomolies that appear in this study.

As a consequence of this investigation and other investigations, it was possible to construct a schematic of the burn/no burn curve for 3.175 mm diameter carbon steel rods over the pressure range of 0.118 MPa to 34.475 MPa with oxygen purity ranging from 40% to 99.7%.

ACKNOWLEDGEMENT

The authors wish to acknowledge the contribution by J. A. Hasbrouck in conducting the test work.

REFERENCES

[1] Benz, F. J., Shaw, R. C., and Homa, J. M., "Burn Propagation Rates of Metals and Alloys in Gaseous Oxygen", ASTM Symposium on Flammability and Sensitivity of Materials in Oxygen-Enriched Atmospheres, Washington, DC, 24 April, 1985, STP 910, American Society for Testing and Materials, Philadelphia, 1986, pp. 135-152.

[2] Zawierucha, R., Drnevich, R. F., McIlroy, K., and Knecht, P., "Material Compatibility and Systems Considerations in Thermal EOR Environments Containing High-Pressure Oxygen", SPE/DOE Fifth Symposium on Enhanced Oil Recovery of The Society of Petroleum Engineers and The Department of Energy, Tulsa, OK, April 20-23, 1986.

[3] McIlroy, K., Zawierucha, R., and Drnevich, R. F., "Promoted Ignition Behavior of Engineering Alloys in High-Pressure Oxygen", Flammability and Sensitivity of Materials in Oxygen-Enriched Atmospheres: Third Volume, ASTM STP 986, D. W. Schroll, Ed., American Society of Testing and Materials, Philadelphia, PA 1988, pp. 85-104.

[4] Stoltzfus, J. M., Homa, J. M., Williams, R. E., and Benz, F. J., "ASTM Committee G-4 Metals Flammability Test Program: Data and Discussion", Flammability and Sensitivity of Materials in Oxygen-Enriched Atmospheres: Third Volume, ASTM STP 986, D. W. Schroll, Ed., American Society for Testing and Materials, Philadelphia, 1988, pp. 28-53.

[5] Benning, M. A. and Werley, B. L., "The Flammability of Carbon Steel as Determined by Pressurized Oxygen Index Measurements", ASTM Symposium on Flammability and Sensitivity of Materials in Oxygen-Enriched Atmospheres, Washington, DC, 24 April, 1985, STP 910, American Society for Testing and Materials, Philadelphia, 1986, pp. 153-170.

[6] Benning, M. A., Zabrenski, J. S., and Le, N. B., "The Flammability of Aluminum Alloys and Aluminum Bronzes as Measured by Pressurized Oxygen Index", Flammability and Sensitivity of Materials in Oxygen-Enriched Atmospheres, ASTM STP 986, D. W. Schroll, Ed., American Society for Testing and Materials, Philadelphia, 1988, pp. 54-71.

[7] McIlroy, K. and Zawierucha, R., "The Effects of Testing Methodology on the Promoted Ignition-Combustion Behavior of Carbon Steel and 316L Stainless Steel in Oxygen Gas Mixtures", Flammability and Sensitivity of Materials in Oxygen Enriched Atmospheres: Fourth Volume, ASTM STP 1040, J. M. Stoltzfus, F. J. Benz and J. S. Stradling, Editors, American Society for Testing and Materials, Philadelphia 1989, pp. 38-53.

[8] Zabrenski, J. S., Werley, B. L. and Slusser, J. W., "Pressurized Flammability Limits of Metals", Flammability and Sensitivity of Materials in Oxygen Enriched Atmospheres: Fourth Volume, ASTM STP 1040, J. M. Stoltzfus, F. J. Benz and J. S. Stradling, Editors, American Society for Testing and Materials, Philadelphia, 1989, pp. 178-194.

[9] Zawierucha, R., McIlroy, K. and Mazzarella, R. B., "Promoted Ignition-Combustion Behavior of Selected Hastelloys in Oxygen Gas Mixture", Flammability and Sensitivity of Materials in Oxygen Enriched Atmospheres: Fifth Volume, ASTM 1111, J. M. Stolzfus and K. McIlroy, Editors, American Society for Testing and Materials, pp. 270-287.

Coleman J. Bryan,[1] Joel M. Stoltzfus,[2] and Mohan V. Gunaji[3]

AN ASSESSMENT OF THE FLAMMABILITY HAZARD OF SEVERAL CORROSION RESISTANT METAL ALLOYS

REFERENCE: Bryan, C. J., Stoltzfus, J. M., and Gunaji, M. V., "An Assessment of the Flammability Hazard of Several Corrosion Resistant Metal Alloys," Flammability and Sensitivity of Materials in Oxygen-Enriched Atmospheres: 6th Volume, ASTM STP 1197, Dwight D. Janoff and Joel M. Stoltzfus, Eds., American Society for Testing and Materials, Philadelphia, 1993.

ABSTRACT: The Space Shuttle launch environment at the John F. Kennedy Space Center is extremely corrosive. Recent corrosion studies have identified Hastelloy B-2, Haynes Alloy C-230, Hastelloy C-22, Hastelloy C-276, Hastelloy G-30, and Inconel 625 as being very resistant to this launch environment. Since several corrosion related problems have been encountered in the launch support oxygen systems, especially the expansion bellows in the liquid oxygen vacuum jacketed lines, it was decided to evaluate the flammability of these alloys in oxygen. Therefore, the NASA White Sands Test Facility was requested to evaluate the ignition susceptibility of these alloys using particle impact, frictional heating, and promoted combustion tests. These tests indicated that the corrosion resistant alloys were more ignition resistant than the materials in the existing systems. Hastelloy C-22 expansion bellows installed in the Orbiter Fuel Cell Servicing System have performed satisfactorily since installation in 1989.

KEYWORDS: oxygen, particle impact, metals, safety, frictional heating, flame propagation, flammability, promoted combustion, Inconel, Hastelloy, compatibility

---

[1] Chief, Failure Analysis and Materials Evaluation Branch, John F. Kennedy Space Center, FL 32899.

[2] Aerospace Technology Engineer, White Sands Test Facility, Las Cruces, NM 88004.

[3] Mechanical Engineer, Lockheed-ESC, White Sands Test Facility, Las Cruces, NM 88004.

INTRODUCTION

The gaseous oxygen (GOX) system used to support the Space Transportation System (Space Shuttle) at the National Aeronautics and Space Administration's John F. Kennedy Space Center (KSC) was originally designed in the 1960's for support of the Apollo program. The system was designed to supply 41.2 MPa (6000 psi) GOX at a flow rate of 30 m/s (100 ft/s) using components, piping, and tubing fabricated from 300 series stainless steel. A hazard assessment of this system was recently made and reported at the Fifth International Symposium on the Flammability and Sensitivity of Materials in Oxygen-Enriched Atmospheres [1].

Large quantities of hydrochloric acid are generated by the solid rocket motors during the launch of the Space Shuttle. This, in addition to the normal subtropical marine environment, has resulted in measured pH values below 1 on the launch structures. Several corrosion related problems have been encountered in the launch support oxygen systems, especially in the expansion bellows in the liquid oxygen vacuum jacketed lines. Recent corrosion studies have identified Hastelloy B-2, Hastelloy C-230, Hastelloy C-22, Hastelloy C-276, Hastelloy G-30 and Inconel 625 as being very resistant to this launch environment. Therefore, it was decided to evaluate the flammability characteristics of these alloys in oxygen. Accordingly, the Johnson Space Center's White Sands Test Facility (WSTF) was requested to evaluate the ignition susceptibility of these alloys in pressurized oxygen using particle impact, frictional heating, and promoted combustion tests.

EXPERIMENTAL

Materials

The materials evaluated in this investigation are described in Table 1. The actual composition of the alloys was not determined.

TABLE 1 -- Alloys tested.

Alloy	UNS Number
Hastelloy B-2[A]	N10665
Haynes Alloy C-230[A]	N06230
Hastelloy C-276[A]	N10276
Hastelloy C-22[A]	N06022
Hastelloy G-30[A]	N06030
Inconel 625[B]	N06625

[A]Registered trademark of the Cabot Corporation
[B]Registered trademark of the International Nickel Co.

Test Methods

Frictional heating--The frictional heating test was developed approximately 12 years ago by WSTF. The test system has been previously described in detail [2]. It consists of a cylindrical pressure chamber containing an inner cavity through which a rotating shaft extends via a series of bearings and seals. The shaft is connected to a drive motor/transmission assembly that is capable of turning the shaft at rotational speeds from 1000 to 20,000 rpm. The other end of the shaft is connected to a pneumatically actuated cylinder, which allows axial movement of the shaft and provides the capability of applying a normal load of up to 4450 N (1000 lbf). The rotating test specimen is mounted on the shaft and the stationary test specimen is affixed to the test chamber. The rotating test specimen has a surface velocity of approximately 20 m/s (67 ft/s) when the shaft turns at 17,000 rpm. The contact surface area was 1.83 cm^2 (0.283 in^2).

In this test program, the objective was to rank the relative ignition resistance of the metals by using the product of the apparent contact pressure (P) and the linear surface velocity (V) required for ignition to occur. The apparent contact pressure is the normal force applied to the test specimen divided by the initial cross-section area of the specimens. The tests were conducted at a pressure of 6.9 MPa (1000 psi) with a ramp load profile of 3.4 kg/s (7.5 lb/s) or 1.86 kg/s-cm^2 (26.5 lb/s-in^2). The rotary test sample was rotated at 17,000 ± 200 rpm. Three tests were conducted on each metal pair, using new test specimens each time.

Flame propagation--These tests were conducted using the WSTF High-Pressure Promoted Combustion Facility. The test system has been described previously in detail and comprises a test chamber, an oxygen supply system, an accumulator (sized to ensure that no more than 10 percent of the available oxygen can be consumed during a test), and pressure and temperature (thermopiles) indicators [2]. The test sample was a rod fabricated from the required test alloy with a length of 13.3 ± 1 cm and a diameter of 0.32 ± 0.01 cm.

In each test, an aluminum promoter was installed on the bottom of the test sample. The sample with attached promoter was mounted in the sample holder and placed in the test chamber. An Al-Pd igniter wire was connected to the promoter and the feed-through connections inside the chamber. The test chamber was sealed and filled with GOX to 7 MPa and then vented to the atmosphere. This procedure was repeated three times to flush the air from the test chamber. The chamber was then filled with GOX and the pressure adjusted to the desired test pressure. The leak rate was then checked to ensure that it was not excessive, and the data acquisition system was activated. Current was applied to the ignitor from a 28-volt power supply until ignition occurred.

When the sample either self-extinguished or was completely consumed, the chamber was vented to ambient pressure, and then opened to examine the test specimen. The linear propagation rate was calculated using the data gathered by the thermopiles during the test. Tests were performed at ten pressures beginning at 6.9 MPa (1000 psi), with pressure being incremented in steps of 6.9 MPa, and ending at 69 MPa (10000 psi). Three tests were conducted on each alloy at each pressure.

Particle impact--These tests were conducted using the WSTF Particle Impact Test Facility. The subsonic particle impact chamber, sample geometry, and oxygen high-flow test system used in these evaluations was previously described [3]. Five-gram samples of an iron powder/inert particle mix [3] were injected into the oxygen stream flowing from 55 to 60 m/s at 28 MPa (4000 psi) and 325K.

The target specimens were fabricated from bar stock. Each specimen was cleaned in soapy water, rinsed with deionized water, blown dry with gaseous nitrogen, and sealed in PTFE bags. Plastic gloves were used to handle the specimens during installation. For each test, the orifice sized for the test velocity was installed with a specimen into the orifice holder. The heat exchanger was activated and the iron powder was loaded into the injector. The test conditions were entered into the microprocessor, and all the instrumentation, including the video equipment, was activated. Oxygen flow was initiated, and after test conditions were reached, the microprocessor was commanded to inject the particles. The microprocessor stopped the flow of oxygen five seconds later. The test specimen was removed and visually examined for evidence of ignition. Three tests were conducted on each alloy at each condition.

RESULTS

Frictional Heating

Table 2 shows the PV (W/m^2) products for the tests conducted on the different metals pairs. The lowest value of the range in PV product was used to determine the relative ranking of metal pairs. For metals evaluated by this test, the higher the PV product, the greater the resistance to ignition in the test system. In most tests only one of the test samples burned, either the stationary or rotary, with no identifiable trend.

Flame Propagation

The threshold burning pressure of each alloy is presented in Table 3. At the present time there are no ASTM standard criteria for the pass/fail rating of samples in this combustion test. For the purposes of this paper, the threshold burning pressure was defined as the lowest pressure at which at least one of the test specimens was completely consumed or was consumed to the point at which the sample holder terminated the propagation by acting as a heat sink. This is consistent with the threshold criteria in the proposed ASTM combustion test for metallic materials in oxygen-enriched atmospheres under development. Zawierucha, et al. chose a minimum burn length of 2.95 cm, 30 percent of the specimen length, as the criterion for the determination of the threshold burning pressure in tests conducted on metallic materials using a hyrdrocarbon/iron-wire promoter [6,7].

TABLE 2 -- Relative ranking of the metal pairs for resistance to ignition by frictional heating at 17000 rpm and GOX pressure of 6.9 MPa (1000 psi).

Material Pair		PV Product	Rank
Rotary	Stationary	(W/m^2 x 10^{-8})	
Hastelloy C-22	Hastelloy C-22	2.00 - 2.99	1
Inconel 625	Inconel 625	1.62 - 1.73	2
Hastelloy B-2	Hastelloy B-2	1.61 - 2.16	3
Hastelloy C-22	Monel K-500	1.58 - 3.72	4
Hastelloy C-276	Monel K-500	1.41 - 2.70	5
Haynes Alloy C-230	Haynes Alloy C-230	1.40 - 1.82	6
Hastelloy G-30	Monel K-500	1.34 - 1.62	7
Hastelloy C-276	Hastelloy C-276	1.21 - 2.82	8
Inconel 625	Monel K-500	0.94 - 2.00	9
Hastelloy C-22	17-4 PH SS	0.92 - 1.00	10
Hastelloy G-30	Hastelloy G-30	0.90 - 1.28	11
Hastelloy C-276	17-4 PH SS	0.89 - 1.10	12
Hastelloy G-30	17-4 PH SS	0.84 - 1.02	13
Inconel 625	17-4 PH SS	0.64 - 1.09	14

TABLE 3 -- Threshold burning pressures of metals tested.

Material	Threshold Pressure			
	This Work		Previous Work	
	(MPa)	(psi)	(MPa)	(psi)
Hastelloy C-22	34.5	5000	13.8	2000 [7]
Hastelloy C-276	20.7	3000	20.7	1750 [7]
Inconel 625	17.2	2500	13.8	2000 [6]
Hastelloy G-30	6.9	1000	5.2	750 [7]
Hastelloy B-2	6.9	1000	Not Tested	

Particle Impact

There was no evidence of either particle or specimen ignition for any of these corrosion resistant alloys.

DISCUSSION

The results from the frictional heating tests revealed that Hastelloy C-22 on Hastelloy C-22 was very resistant to ignition. The PV product of 2.00 is almost 50 percent higher than that of Monel 400 on Monel 400 and Monel K-500 on Monel K-500 [4]. Previous testing has shown no large differences from one alloy pair to another as long one of the pair was a stainless steel. This finding agreed with the data in this study where the stainless steel evaluated was 17-4 PH.

The promoted ignition tests in this study revealed that Hastelloy C-22 had the highest minimum burning pressure and that the Hastelloy alloys G-30 and B-2 had the lowest threshold burning pressures. All the alloys evaluated in this study were found to have higher threshold burning pressures than the 303, 304, 316, 17-4 PH stainless steel alloys used in the KSC oxygen systems [1]. The 30 percent criterion of Zawieruch et al. would obviously provide a more conservative ranking of materials as shown in Table 3. However, there is a difference in the promoters in that may influence the results also. The Zawierucha group chose their hydrocarbon/iron-wire promoter based on consideration of the proposed use of the materials. The proposed ASTM test method notes that polymeric, the great majority of which are hydrocarbon based materials, promoters may be used, but that the combustion products may affect the results via contamination of the test media. Many copper based alloys have been found to have significantly higher threshold burning pressures, but are not suitable for use in the highly corrosive acidic environment found in launch operations at the KSC.

None of the corrosion resistant alloys evaluated in this study ignited in the particle impact test.

CONCLUSIONS

The six alloys evaluated in this study were all found to be more resistant to ignition than the stainless steel alloys currently used in oxygen systems at the KSC. Stainless steel expansion bellows for vacuum jacketed cryogenic lines are being replaced with bellows fabricated from Hastelloy C-22. Thus far, the Hastelloy C-22 bellows that have been in service for over 36 months exhibit no signs of corrosion; whereas the previously used 316 stainless steel bellows failed approximately every 18 months.

ACKNOWLEDGMENTS

This paper was prepared under the sponsorship of the National Aeronautics and Space Administration. Neither the U. S. government nor any person acting on behalf of the U. S. government assumes any liability resulting from the use of the information contained in this paper, or warrants that such use will be free from privately owned rights. The use of company trademarks or trade names does not constitute an endorsement of these materials, but only to simplify their identification.

REFERENCES

[1] Bryan, C. J., Stoltzfus, J. M., and Gunaji, M. V., "An Assessment of the Metals Flammability Hazard in the Kennedy Space Center Oxygen System," Flammability and Sensitivity of Materials in Oxygen-Enriched Atmospheres: Fifth Volume, ASTM STP 1111, J. M. Stoltzfus and K. McIlroy, Eds., American Society for Testing and Materials. Philadelphia, 1988, pp. 453-462.

[2] Stoltzfus, J. M., Homa, J. M., Williams, R. E., and Benz, F. J., "ASTM Committee G-4 Metals Flammability Test Program: Data and Discussion," Flammability and Sensitivity of Materials in Oxygen-Enriched Atmospheres: Third Volume, ASTM STP 986, D. W. Schroll, Ed., American Society for Testing and Materials. Philadelphia, 1988, pp. 28-53.

[3] Williams, R. E., Benz, F. J., and McIlroy, K., "Ignition of Steel Alloys by Impact of Low-Velocity Iron/Inert Particles in Gaseous Oxygen," Flammability and Sensitivity of Materials in Oxygen-Enriched Atmospheres: Third Volume, ASTM STP 986, D. W. Schroll, Ed., American Society for Testing and Materials. Philadelphia, 1988, pp. 72-84.

[4] Benz, F. J., and Stoltzfus, J. M., "Ignition of Metals and Alloys in Gaseous Oxygen by Frictional Heating," Flammability and Sensitivity of Materials in Oxygen-Enriched Atmospheres: Second Volume, ASTM STP 910, M. A. Benning, Ed., American Society for Testing and Materials, 1986, pp. 38-58.

[5] Benz, F. J., Shaw, R. C., and Homa, J. M., "Ignition of Metals and Alloys in Gaseous Oxygen by Frictional Heating," Flammability and Sensitivity of Materials in Oxygen-Enriched Atmospheres: Second Volume, ASTM STP 910, M. A. Benning, Ed., American Society for Testing and Materials, 1986, pp. 135-152.

[6] Zawierucha, R., and McIlroy, K., "Promoted ignition-Combustion Behavior of Selected Engineering alloys in Oxygen Gas Mixtures," Flammability and Sensitivity of Materials in Oxygen-Enriched Atmospheres: Fourth Volume, ASTM STP 1040, J. M. Stoltzfus, F. J. Benz, and J. S. Stradlingn, Editors, American Society for Testing and Materials. Philadelphia, 1988, pp. 145-161.

[7] Zawierucha, R., McIlroy, K., and Mazzarella, R. B., "Promoted ignition-Combustion Behavior of Selected Hastelloys^{TM} in Oxygen Gas Mixtures," Flammability and Sensitivity of Materials in Oxygen-Enriched Atmospheres: Fifth Volume, ASTM STP 1111, J. M. Stoltzfus and K. McIlroy, Eds., American Society for Testing and Materials. Philadelphia, 1988, pp. 270-287.

James L. Schadler[1] and Joel M. Stoltzfus[2]

PRESSURIZED FLAMMABILITY LIMITS OF SELECTED SINTERED FILTER MATERIALS IN HIGH-PRESSURE GASEOUS OXYGEN

REFERENCE: Schadler, J. L. and Stoltzfus, J. M., "Pressurized Flammability Limits of Selected Sintered Filter Materials in High-Pressure Gaseous Oxygen," Flammability and Sensitivity of Materials in Oxygen-Enriched Atmospheres: 6th Volume, ASTM STP 1197, Dwight D. Janoff and Joel M. Stoltzfus, Eds., American Society for Testing and Materials, Philadelphia, 1993.

ABSTRACT: Previous promoted combustion tests have demonstrated that the threshold pressure (the minimum oxygen pressure required to self-sustain combustion) of various engineering alloys is dependent on the configuration of the sample. Monel 400, when configured as a 3.2-mm (0.13-in.) -diameter rod, has a threshold pressure 500 times greater than when configured as a 60 x 60 wire mesh constructed of 0.19-mm (0.0075-in.) -diameter wire. Sintered filter elements, often used in oxygen systems, have finely divided construction (a high surface to volume ratio) similar to a wire mesh configuration. This similarity raises the question whether the threshold pressure data for the 3.2-mm (0.13-in.) -diameter rod, the wire mesh, or neither should be used for various alloys configured as sintered filter elements.

This study was conducted on three engineering alloys configured similar to sintered filter elements. Monel 400 powder, 316L stainless steel (SS316L) powder, and three types of tin-bronze powder were sintered into rods ranging in diameter from 3.2 to 6.3 mm (0.13 to .25 in.), with pore sizes representative of 3- to 150-μm-rated filters. Each sample was mounted vertically in a 12.4 liter (757 in.^{3}) vessel and ignited at the bottom using an aluminum-palladium igniter wire. For each sample a threshold pressure was determined.

The test results indicated that the sintered Monel 400 and the sintered SS316L have threshold pressures closer to the wire mesh than 3.2-mm (0.13-in.) -diameter solid rods. As tested, the Monel had a threshold pressure of 0.69 MPa (100 psig) and the SS316L had a threshold pressure of White Sands Test Facility ambient, 82 kPa (12 psia). Except for two grades of A type sintered tin-bronze, all the sintered tin-bronzes had threshold pressures above 68.9 MPa (10 000 psig). Grade 153A and grade 103A had threshold pressures of 68.9 MPa (10 000 psig) and 37.9 MPa (5 500 psig), respectively. The results indicate that P or HP types of sintered tin-bronze filter elements are preferred for use in oxygen systems.

KEYWORDS: promoted combustion, threshold pressure, filters, metal powders, sample configuration, sintered metal

---

[1] Principal Engineer, Lockheed-ESC, White Sands Test Facility, P. O. Drawer MM, Las Cruces, NM 88004.

[2] Project Manager, NASA, White Sands Test Facility, P. O. Drawer MM, Las Cruces, NM 88004.

A critical parameter required to evaluate the safety of gaseous oxygen systems is the threshold pressure (the minimum oxygen pressure required to sustain combustion) of the materials in the system [1,2,3,4,5]. Promoted combustion testing has demonstrated that the threshold pressure of a material is dependent on the configuration of the sample [6,7,8]. This was demonstrated at White Sands Test Facility (WSTF) by testing different engineering alloys configured as rods whose diameters increased in steps along the rods' longitudinal axes [7]. For 316L stainless steel (SS316L) the 3.2-mm (0.13-in.) -diameter portion of the rod partially burned at 3.45 MPa (500 psig), and supported sustained combustion at 6.89 MPa (1 000 psig). The 4.8-mm (0.19-in.) -diameter portion of the rod had not sustained combustion at 3.45 MPa (500 psig), had partially sustained combustion at 6.89 MPa (1 000 psig), and had sustained combustion at 20.7 MPa (3 000 psig). Similarly the 6.3-mm (0.25-in.) -diameter portion of the rod had not sustained combustion at 3.45 MPa (500 psig) or 6.89 MPa (1 000 psig), and had sustained combustion at 20.7 MPa (3 000 psig). Later testing showed that when SS316L is configured as a 60 x 60 wire mesh constructed of 0.19-mm (0.0075-in.) -diameter wire, it sustains combustion at less than 89 kPa (13 psia) [8].

Filters in oxygen systems often contain a filtering element made from sintered metal powders. The filter elements are available in many sizes and shapes and are commonly made of 300 series stainless steel, various types and grades of tin-bronze, and, less common but available, Monel 400. While the filter elements are constructed of engineering alloys whose threshold pressures are known in some configurations, the sintered filter elements' high surface-to-volume ratio raises the question of which threshold pressure should be used.

Using promoted combustion testing techniques, the threshold pressure for three different materials, SS316L, Monel 400 and various types and grades of tin-bronze were determined. The results provide direction in selecting filters for use in oxygen systems.

EXPERIMENTAL

Samples were procured which represent the common sintered elements: three types of tin-bronze, SS316L, and Monel 400. Monel 400, while less common as a filter material than the other two materials, was tested because it is often used in oxygen systems and has demonstrated a strong dependence on configuration with regard to its threshold pressure [7,8].

All samples were manufactured according to standard sintered filter manufacturing processes. No binders or materials, other than the primary metals, are present in any of the samples. The size of the samples was dictated by availability. Fig. 1 shows the sample configuration of each of the three types of tin-bronze, the Monel 400, and the SS316L samples. The Monel 400 and SS316L samples' dimensions were not the optimum choice since they are inconsistent with regard to a single sample size among the test population. However, the dimensional variations between the samples is felt to be less important than the expected major difference between the threshold pressure of sintered filter material and the same material configured as a wire or solid rod.

The SS316L (UNS S31603, by weight percent 16-18 Cr, 10-14 Ni, 0.03 C, 2.0 Mn, 1.0 Si, 0.045 P, 0.030 S, 2-3 Mo, balance Fe) samples were circular cross section rods, 4.7 mm (0.18 in.) in diameter and 5.8 cm (2.3 in.) long. The SS316L powder used in manufacturing the rods had a particle size of -20 +30 Tyler mesh (particles sit on a mesh with a 600μm x 600μm opening but fall through a 800μm x 800μm opening). The SS316L sintered rods represented a 25 - 35μm filter rating.

The Monel 400 (UNS NO4400, by weight percent 0.02 AL, 0.04 C, 30.61 Cu, 1.87 Fe, 1.02 Mn, 66.29 Ni, 0.004 S, 0.15 Si) samples were elliptical cross section rods, 7.6 cm (3.0 in.) long, with a major axis of 4.0 mm (0.16 in.) and a minor axis of 3.6 mm (0.14 in.). The Monel

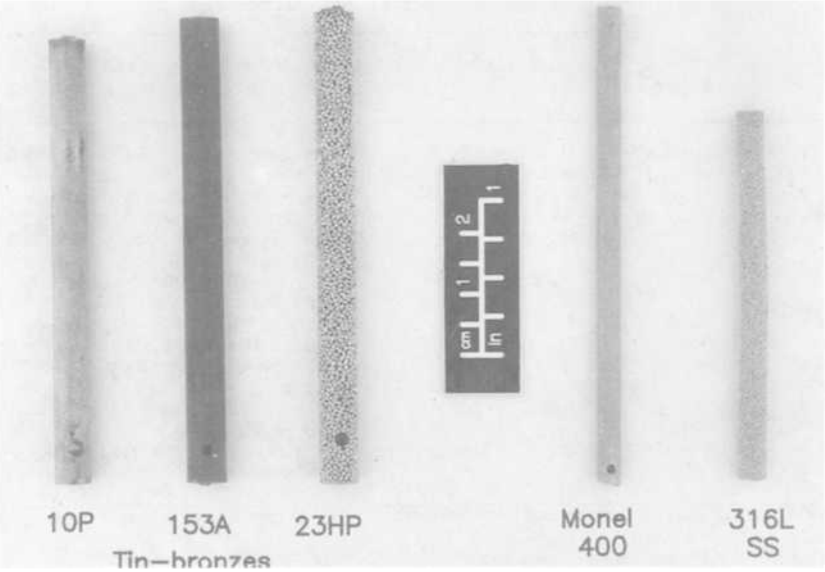

FIG. 1--Sample configurations.

400 powder used in manufacturing the rods had a particle size of -100 Tyler mesh (particles fall through a 147μm x 147μm opening). The Monel 400 sintered rods represented a 5μm-10μm filter rating.

The three types of tin-bronze powders used in filter manufacturing cover a total of 16 grades of powder. Test samples bracketed each grade of the commonly available tin-bronze filter powders. Table 1 lists the tin-bronze powders that were tested. All the tin-bronze samples, regardless of type or grade, were circular cross section rods of 6.3 mm (.25 in.) diameter by 7.6 cm (3.0 in.) long.

The HP grades of filter powders are made by tin coating rounded, cut copper wire. Before sintering, each particle consists of a solid copper core coated with a thin layer of tin. Upon sintering, the tin bonds the particles together and diffuses into the copper to form a bronze coating. The HP grades are the coarsest filter powders. Filters rated from 32μm-150μm are made from the HP type of tin-bronze powders.

The A grades of filter powders are made by tin coating atomized particles of copper. Like the HP type powders, the tin bonds the particles together and diffuses into the copper, forming bronze, during the sintering process. The A grades of filter powders are finer than the HP grades and used to make filters rated between 10μm-44μm.

The P grades of filter powders are made by atomizing pre-alloyed bronze. This results in particles that are almost perfectly spherical in shape and uniform in composition, throughout. Sintering is accomplished using the same method as the other types of powders, heating the powders in a mold under little or no pressure while necks between particles form. The P type of filter powder is used in filters rated from 3μm-80μm.

TABLE 1--Tin-bronze filter powders.

Filter Rating[a]	Grade and Type	% Tin[b]	Particle Size Sieve Analysis[c,d,e]
3 - 4	10P	9.5 - 10.5	25% max +325, 75% min -325
10 - 15	153A	9.5 - 10.5	2% max +150, 30 - 60% +200, 35 - 65% +325, 10% max -325
17 - 24	103A	9.25 - 10.5	2% max +100, 20 - 40% +150, 40% max +325, 35 - 55% +200, 10% max -325
24 - 40	90P	9.5 - 10.5	3% max +50, 90% min +100, 10% max +150
30 - 44	61A	9.5 - 10.5	2% max +60, 40 - 70% +80, 30 - 60% +100, 10% max +150
32 - 44	68HP	6.0 - 8.0	1.5% max +50, 95% min +60, 5% max +70
60 - 80	250P	9.5 - 10.5	5% max +20, 90 - 60% +30, 10 - 40% +40
86 -150	23HP	3.5 - 4.5	2% max +20, 97% min +30, 3% max +40

[a] Filter Rating is approximately one-third the pore size of the sintered material.
[b] By weight, the remainder is copper.
[c] Before sintering, powder specification
[d] Reference [9].
[e] USA Standard Sieve, ASTM Specification E11.

It should be noted that the metal powders used in the Monel 400 and the SS316L samples are similar in particle shape to each other, although the Monel 400 particles are much smaller, and both are a different shape than the basic spherical shape of the tin-bronze powders. Figs. 2a and 2b illustrate the differences in particle shape and size. Particular manufacturing requirements of sintered powders dictate the use of the irregular shaped particles in the Monel 400 and SS316L.[3]

TEST SYSTEM DESCRIPTION

The tests were conducted in the WSTF High Pressure Promoted Combustion test facility [7]. The test system consisted of the 12.4 liter (757 in.^{3}) test chamber, a 68.9 MPa (10 000 psig) oxygen supply system, pressure recording equipment, and a 60 frame per second video recorder. The video recorder was used to record sample combustion and burn velocities by looking through one of the test chamber's 5-cm (2.0-in.) -diameter sapphire windows. The samples were suspended vertically and ignited at the bottom using multiple wraps of 0.40-mm (0.016-in.) aluminum-palladium wire. A post-test inspection of each unburnt sample verified that multiple wraps of the aluminum-palladium wire would have suffient energy to cause ignition. Each sample was grooved or had a small drilled hole to prevent the wrapped igniter from falling off.

---

[3] Phone conversation with William J. Ullrich, Senior Metallurgist, Alcan Powders and Pigments, Division of Alcan Aluminum Corporation, Union, New Jersey, September 10, 1992.

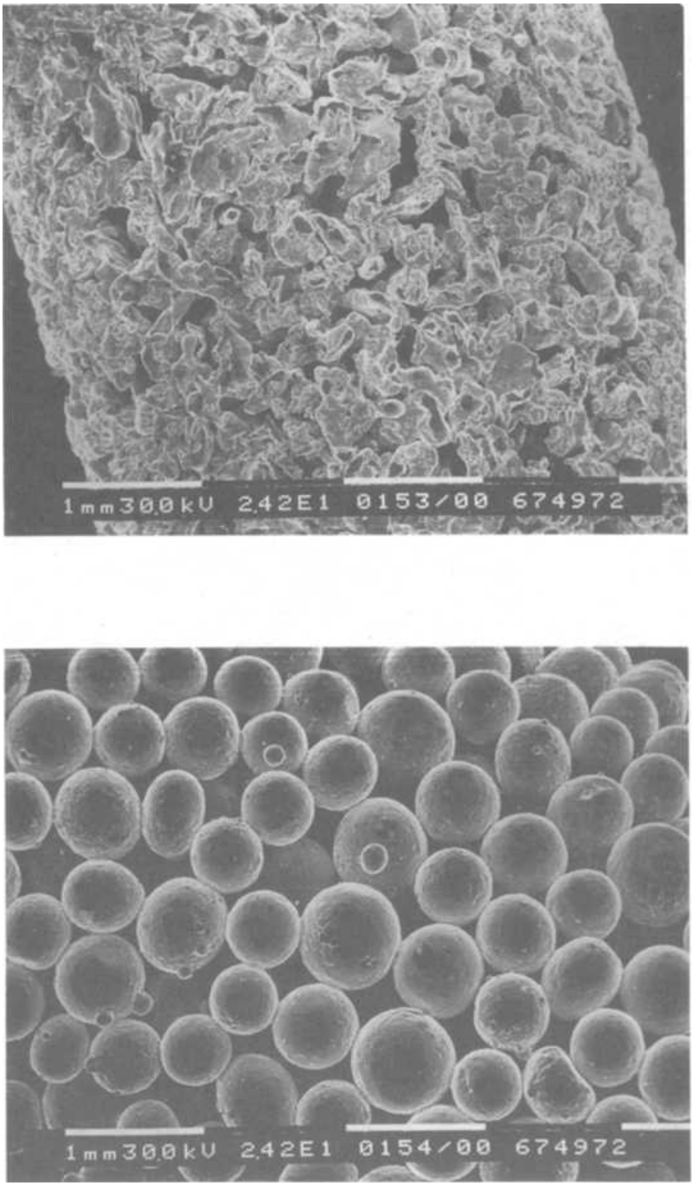

Fig. 2a--Surface photomicrographs of sintered material surfaces; (top) SS316L, (bottom) Tin-bronze - 10P.

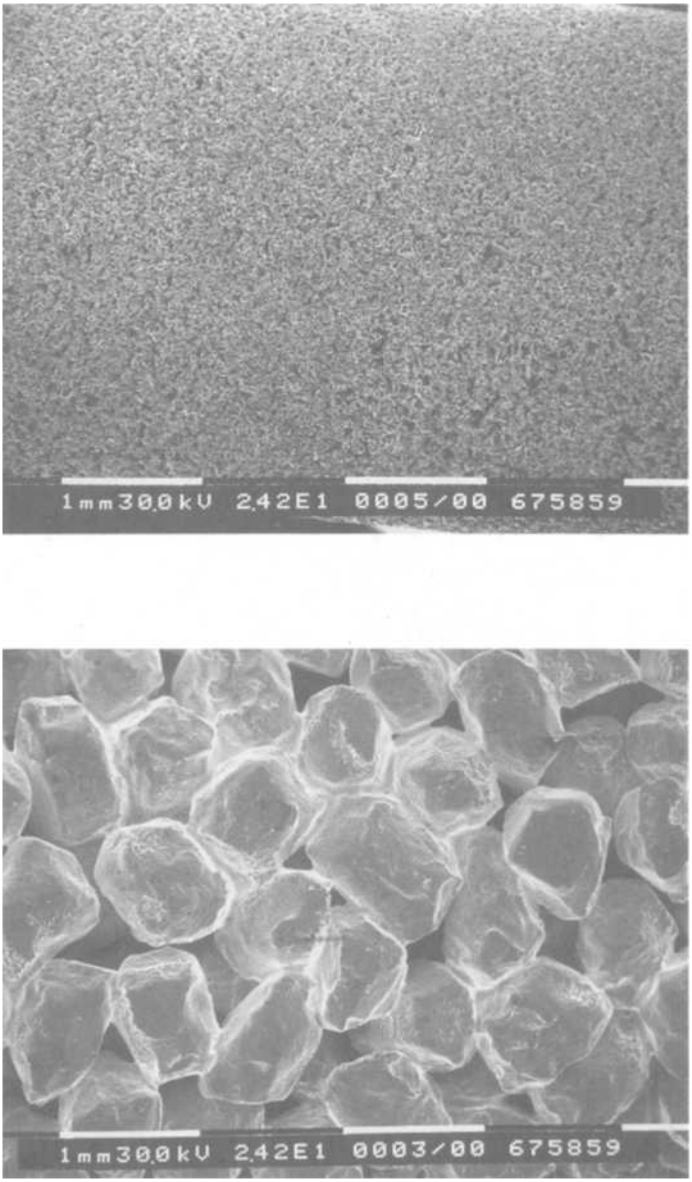

Fig. 2b--Surface photomicrographs of sintered material surfaces; (top) Monel 400, (bottom) Tin-bronze - 23HP.

PROCEDURE

The samples were prepared for test by drilling or grooving an end for igniter retention, washing in soapy, deionized water for five minutes, rinsing in deionized water, and blowing dry with filtered nitrogen. Because the porosity of the samples caused them to hold moisture, they were dried an additional 16 hours in 38° C (100° F) air at ambient pressure. Comparative vacuum bake-out experiments were conducted on each sample type to ensure that the 16 hour drying time was sufficient to remove all moisture from the samples. Once clean and dry, the samples were individually bagged for storage until tested. Prepared samples were handled with gloves only.

Just prior to testing, a sample was removed from its bag, the igniter was installed, and the sample was mounted vertically in the chamber. After mounting the sample, the igniter leads were hooked up, the chamber was sealed, and the system was prepared for testing. Prior to pressurizing to the test pressure, the chamber was purged three times by filling with 3.45 MPa (500 psig) oxygen and venting to ambient. After purging, the chamber was stabilized at the test pressure, the data acquisition equipment was turned on, and the igniter was initiated. After the test was complete, the chamber was vented, purged, and opened, allowing the sample's posttest condition to be recorded. The burn velocities were estimated by measurements taken from the video playback.

RESULTS AND DISCUSSION

After testing, each sample was classified into one of four categories: no ignition occurred, ignition but no sustained combustion occurred, partial sustained combustion [greater than 1.3-cm (0.50-in.) sample melted or gone] occurred, or sustained combustion (sample burned up to holder) occurred. In practice, a strong ignition is desirable to ensure that sustained combustion occurs if the test pressure is just above the threshold limit [6]. The ignition/no ignition determination was made by defining ignition as the formation of a solidified partial ball of molten metal on the end of the test sample. This molten ball was used as evidence that, if the sample was flammable at the test pressure, it had sufficient ignition energy to allow sustained combustion [10,11]. Fig. 3 illustrates what was deemed a positive ignition. In some tests the igniter fired, as evidenced by the video, but the sample failed to ignite (no posttest molten residue). A no-ignition condition resulted in a retest with a new sample. With the Monel 400 samples that did not burn, no well-defined molten ball was found on the end of the posttest sample. This was true even though a posttest video review showed that ignition of the sample had occurred. This lack of the normal postignition indicator was attributed to the sintered Monel's unusual burning characteristics.

The threshold pressure found in any particular test series should be understood as the minimum pressure, among those pressures tested, required to support sustained combustion under the test conditions. It must not be used as the threshold pressure under all conditions. [6] While this series of tests used an igniter arrangement judged to be sufficient to assure ignition, it is assumed that a different ignition method may exist which yields a lower threshold pressure. Additionally, these tests were done in quiescent oxygen, and the results, particularly the burn velocities, could be substantially different if the tests were conducted with oxygen flowing through the samples.

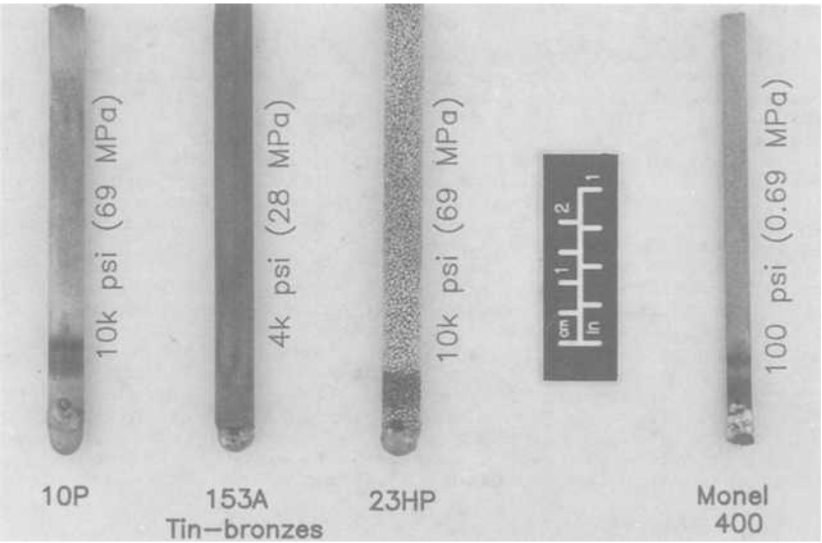

FIG. 3--Ignition without sustained combustion.

The test results are shown in Fig. 4. Both grades of type HP (used in filter rated 32μm-150μm) tin-bronze and all three grades of type P (used in filters rated 3μm-80μm) tin-bronze had threshold pressures greater than 68.9 MPa (10 000 psig). In contrast, type A tin-bronze had a threshold pressure that was dependent on the grade of type A powder that composed the sample. The larger particle grade, 61A (used in filters rated 30μm-44μm), had a threshold pressure greater than 68.9 MPa (10 000 psig). The smaller particle grades, 153A (used in filters rated 10μm-15μm) and 103A (used in filters rated 17μm-24μm), had threshold pressures less than 68.9 MPa (10 000 psig). Grade 153A completely burned at test pressures at or above 37.9 MPa (5 500 psig) but did not sustain combustion at 27.6 MPa (4 000 psig). Grade 103A sustained combustion at 68.9 MPa (10 000 psig) but did not sustain combustion at 58.6 MPa (8 500 psig).

The burn velocities of the tin-bronzes appeared more dependent on the particle size than on the test pressures. The finer particles had a greater burn velocity, even at lower pressures. Grade 153A had a burn velocity of 0.95 cm/s (0.37 in./s) at 37.9 MPa (5 500 psig) while the coarser 103A had a burn velocity of 0.83 cm/s (0.33 in./s) at 68.9 MPa (10 000 psig). (Firm conclusions, based on the burn velocities, are not drawn because the data are tainted by the lack of a tolerance on the burn velocity measurements. The tolerance is undeterminable given the small number of tests run.)

The SS316L sample sustained combustion at all three test pressures: WSTF ambient [82 kPa (12 psia)], 0.35 MPa (50 psig), and 0.69 MPa (100 psig). In all tests the sintered SS316L samples were consumed, in a manner expected for SS316L, which burns as a liquid [10].

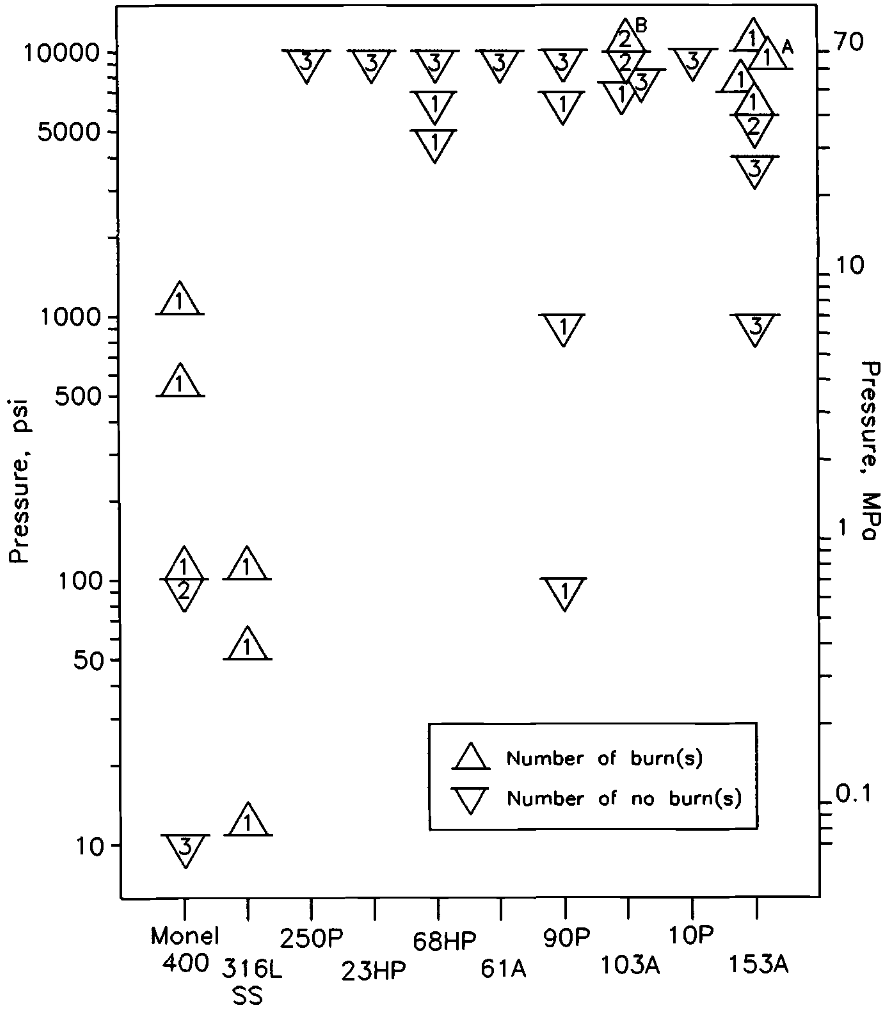

A. Sample self extinguished after 1.73 inch (4.4 cm)
B. One sample self extinguished after 1 inch (2.5 cm)

FIG. 4--Results of promoted combustion testing of sintered filter materials.

For the alloy SS316L, the method of burning, the cyclic forming, dropping off and reforming of a molten ball on the samples end appears to be consistent whether the material is configured as a solid rod, a sintered rod, or a wire mesh [6,7,8]. The burn velocity was unavailable for the ambient pressure test, 0.46 cm/s (0.18 in./s) for the 0.69 MPa (100 psig) test and 0.46 cm/s (0.18 in./s) for the 0.35 MPa (50 psig) test.

At 6.89 MPa (1 000 psig) the Monel 400 sample was completely consumed in a combustion process equivalent to the one previously described for the tin-bronze and SS316L samples. At 82 kPa (12 psig) the Monel 400 samples would not sustain combustion. At test pressures of 3.45 MPa (500 psig), and 0.69 MPa (100 psig) the reactions of the Monel 400 samples were unusual. *Fig.* 5, shows the exterior of a rod after sustained combustion at 0.69 MPa (100 psig). The figure shows that the posttest sample was rough and oxidized when compared with the pretest sample. This is the same posttest condition as the rod tested at 3.45 MPa (500 psig). The video tapes of the 0.69 MPa (100 psig) and 3.45 MPa (500 psig) tests show a band of glowing metal on the rod's circumference moving up the rod from the ignited end. No metal dripped off the rod during the 0.69 MPa (100 psig) test, but a single large drop fell from the rod during the 3.45 MPa (500 psig) test. The drop removed 1.27 cm (0.50 in.) of the sample.

Velocity measurements of the Monel 400 6.89 MPa (1 000 psig) test showed that the rod was consumed at 0.28 cm/s (0.11 in./s), much slower than the SS316L or tin-bronze burn velocities. The burn velocity of the Monel 400 during the 3.45 MPa (500 psig) test was 0.40 cm/s (0.16 in./s) and appeared consistent before and after the drop of molten Monel 400 fell off. A burn velocity of 0.19 cm/s (0.07 in./s) was estimated for the 0.69 MPa (100 psig) test. This dip in the burn velocity may be an artifact of the velocity measurement technique or could represent a non-linear relationship between test pressure and burn velocity. A dip in the burn velocity as a function of pressure has been reported

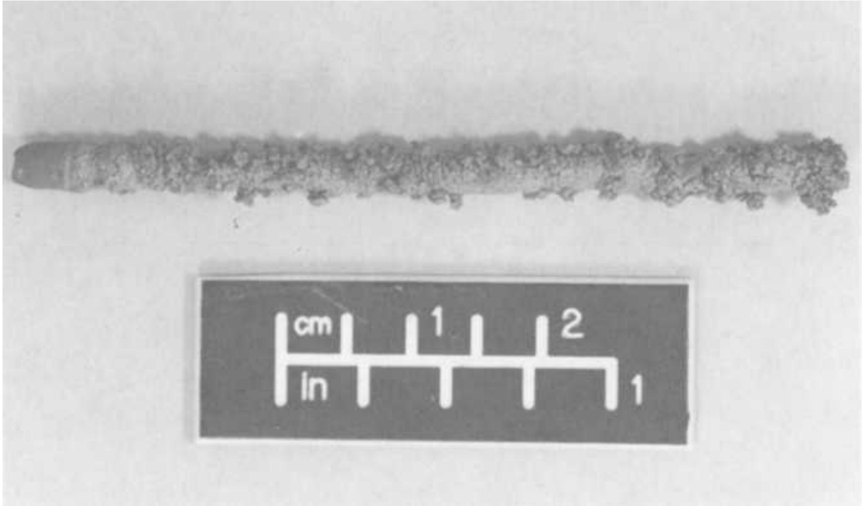

FIG. 5--Monel rod after 3.45 MPa (500 psig) test.

by Sato [12] for aluminum rods. In the report Sato shows the dip in the aluminum burn velocity was at pressures below 3.45 MPa (500 psig) and more pronounced as the surface-to-volume ratio increased as rod diameter decreased from 3 mm to 1 mm (0.12 to 0.04 in.)

Monel 400, configured as a 60 x 60 wire mesh constructed of 0.19-mm (0.0075-in.) -diameter wire rolled into a loose, hollow cylinder, burned in previous testing [8] at WSTF ambient threshold pressure. This ambient pressure burning was described as a molten, burning ball which repeatedly grew and fell from the bottom of the sample, as expected of a metal which burns as a liquid. Fig. 6 shows that the inner core of the sintered Monel 400 sample was melted. Energy-dispersive X-ray spectroscopic analysis shows a copper enrichment of the exterior of the rod.

Table 2 shows a comparison of the test results of 3.2-mm (0.13-in.) -diameter rods, wire meshes, and sintered rods. For Monel 400 and SS316L, it appears that the sintered rods behave more similarly to the wire meshes than to the 3.2-mm (0.13-in.) -diameter rods. No comparison can be made to the tin-bronzes because no wire mesh data are available in the literature. Further tests should be run to determine the flammability of the tin-bronze wire meshes. Also note that the Monel 400 and SS316L sintered materials were tested as smaller diameter rods [3.6 x 4.1-mm (0.14 x 0.16-in.) elliptical cross section for the Monel 400 and 4.7-mm (0.19-in.) diameter for the SS316L] than the sintered tin-bronze rods, 6.3 mm (0.25 in.) in diameter. Further testing should be conducted on smaller diameter sintered tin-bronze rods to determine how the size of the rod effects the threshold pressure.

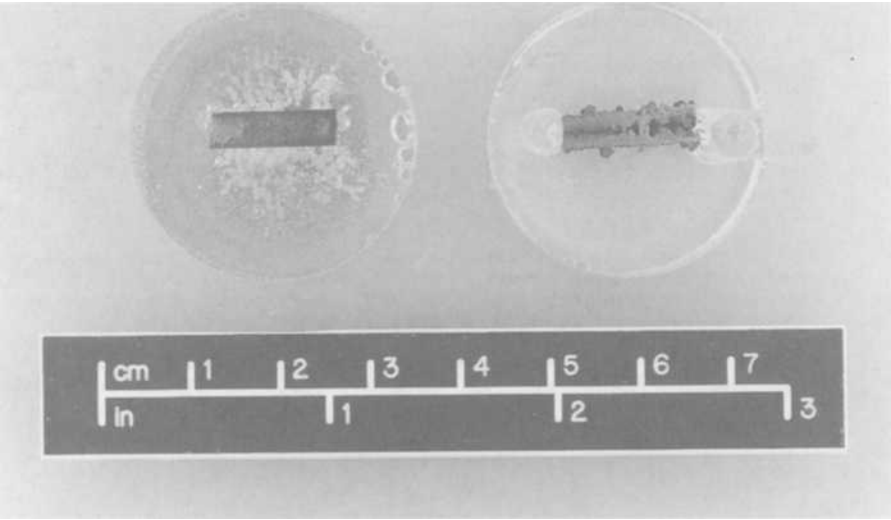

FIG. 6--Cross-sectional views of Monel 400 rod.

Table 2--Threshold pressure comparison between sintered, solid and wire mesh.

Material	Threshold Pressure, MPa (psig) 3.2 mm (0.13 in.) Solid Rod MPa		Wire Mesh kPa		Sintered	
Monel 400	>68.9	(10 000)[a]	82	(12.4)[b]	0.69 MPa	(100)
(-100 Tyler mesh particle size)						
SS316L	6.9	(1 000)[a]	82	(12.4)[b]	82.0 kPa	(12.4)
(-20 +30 Tyler mesh particle size)						
Tin-Bronzes[e]	>48.3	(7 000)[c]	ND[d]			
10P	...	...	...	...	>68.9 MPa	(10 000)
90P	...	...	...	...	>68.9 MPa	(10 000)
250P	...	...	...	...	>68.9 MPa	(10 000)
153A	...	...	...	...	37.9 MPa	(5 500)
103A	...	...	...	...	68.9 MPa	(10 000)
61A	...	...	...	...	>68.9 MPa	(10 000)
68HP	...	...	...	...	>68.9 MPa	(10 000)
23HP	...	...	...	...	>68.9 MPa	(10 000)

[a] Steinberg [7]

[b] Stoltzfus [8], 60 x 60 mesh, 0.19-mm (0.0075-in.) -diameter wire

[c] Stoltzfus [5], tin-bronze tested was by weight percent 10-12 Pb, 88-90 Cu, maximum test pressure 48.3 MPa (7 000 psig)

[d] ND = No Data

[e] Particle size is grade and type dependent, see Table 1.

CONCLUSIONS

The following conclusions were made:

- The threshold pressure of Monel 400 and SS316L when configured in sintered rods is much lower than the same alloy in solid 3.2-mm (0.13-in.) -diameter rods.
- When configured as sintered 6.3-mm (0.25-in.) -diameter rods, all grades of type HP and P tin-bronze filter powders (used in filters rated 3μm-150μm) have threshold pressures above 68.9 MPa (10 000 psig).
- When configured as sintered 6.3-mm (0.25-in.) -diameter rods, type A tin-bronze filter powders have threshold pressures which decrease from greater than 68.9 MPa (10 000 psig) for grade 61A (used in filters rated 30μm-44μm) to less than 37.9 MPa (5 500 psig) for grade 153A (used in filters rated 10μm-15μm).
- Sintered tin-bronze filters, made of type P or HP powders, appear to be the best choice for oxygen systems at pressures up to 68.9 MPa (10 000 psig).

ACKNOWLEDGEMENTS

The authors are grateful to Frank Benz, NASA-White Sands Test Facility Laboratories Chief, for making discretionary funds available to conduct this testing. The authors also thank Mott Metallurgical Corporation, Pat Kavanagh of Avenger, Lanny Pease of Powder-Tech Associates, and William Ullrich of Alcan Powders and Pigments for technical help and timely responses to our requests for samples.

REFERENCES

[1] ASTM, Standard Guide for Evaluating Metals for Oxygen Service, G94-90, American Society for Testing and Materials, Philadelphia, PA, 1990.

[2] Compressed Gas Association, Industrial Practices for Gaseous Oxygen Transmission and Distribution Piping System, CGA Pamphlet G-4.4, Arlington, VA, 1987.

[3] NFPA 53M, Fire Hazards in Oxygen-Enriched Atmospheres, 1990 Edition, Quincy, MA, February 5, 1990.

[4] ASTM Committee G4.05, Fire Hazards in Oxygen Systems: ASTM Standards Technology Training Coursebook, Second Edition, B. L. Werley, Ed., American Society for Testing and Materials, Philadelphia, PA, 1991.

[5] Stoltzfus, J. M., Homa, J. M., Williams, R. E., and Benz, F. J., "ASTM Committee G-4 Metals Flammability Test Program: Data and Discussion," Flammability and Sensitivity of Materials in Oxygen-Enriched Atmospheres: Vol. 3, ASTM STP 986, D. W. Schroll, Ed., American Society for Testing and Materials, Philadelphia, PA, 1988, pp 28-53.

[6] Zabrenski, J.S., Werley, B. L., and Slusser, J. W., "Pressurized Flammability Limits of Metals," Flammability and Sensitivity of Materials in Oxygen-Enriched Atmospheres: Vol. 5, ASTM STP 1040, Joel Stoltzfus, Frank J. Benz, and Jack S. Stradling, Eds., American Society for Testing and Materials, Philadelphia, PA, 1989.

[7] Steinberg, T. A., Rucker, M. A., and Beeson, H. D., "Promoted Combustion of Nine Structural Metals in High-Pressure Gaseous Oxygen; A Comparison of Ranking Methods," Symposium on Flammability and Sensitivity of Materials in Oxygen-Enriched Atmospheres: Vol. 4, ASTM STP 1040, Joel Stoltzfus, Frank J. Benz, and Jack S. Stradling, Eds., American Society for Testing and Materials, Philadelphia, PA, 1989.

[8] Stoltzfus, J. M., Lowrie, R., and Gunaji, M. V., "Burn Propagation Behavior of Wire Mesh Made from Several Alloys," Flammability and Sensitivity of Materials in Oxygen-Enriched Atmospheres: Vol. 5, ASTM STP 1040, Joel Stoltzfus and Kenneth McIlroy, Eds., American Society for Testing and Materials, Philadelphia, PA, 1991.

[9] Alcan. *Bronze Filter Powders*. Alcan Powders and Pigments, Division of Alcan Aluminum Corporation, Union, New Jersey.

[10] Benz, F., Steinberg, T. A., and Janoff, D., "Combustion of 316 Stainless Steel In High-Pressure Gaseous Oxygen," Symposium on Flammability and Sensitivity of Materials in Oxygen-Enriched Atmospheres: Vol. 4, ASTM STP 1040, Joel Stoltzfus, Frank J. Benz, and Jack S. Stradling, Eds., American Society for Testing and Materials, Philadelphia, PA, 1989.

[11] Sato, J. and Hirano, T., "Fire Spread Limits Along Metal Pieces In Oxygen," Flammability and Sensitivity of Materials in Oxygen-Enriched Atmospheres: Vol. 3, ASTM STP 986, D. W. Schroll, Eds., American Society for Testing and Materials, Philadelphia, PA, 1988.

[12] Sato, S. "Fire Spread Rates Along Cylindrical Metal Rods in High Pressure Oxygen," Flammability and Sensitivity of Materials in Oxygen-Enriched Atmospheres: Vol. 4, ASTM STP 1040, Joel Stoltzfus, Frank J. Benz, and Jack S. Stradling, Eds., American Society for Testing and Materials, Philadelphia, PA, 1989.

Theodore A. Steinberg,[1] D. Bruce Wilson,[1] and Frank J. Benz[2]

MICROGRAVITY AND NORMAL GRAVITY COMBUSTION OF METALS AND ALLOYS IN HIGH PRESSURE OXYGEN

REFERENCE: Steinberg, T. A., Wilson, D. B., and Benz, F. J., "Microgravity and Normal Gravity Combustion of Metals and Alloys in High Pressure Oxygen," Flammability and Sensitivity of Materials in Oxygen-Enriched Atmospheres: 6th Volume, ASTM STP 1197, Dwight D. Janoff and Joel M. Stoltzfus, Eds., American Society for Testing and Materials, Philadelphia, 1993.

ABSTRACT: The NASA White Sands Test Facility has completed an extensive test program aimed at evaluating the burning characteristics of metals and alloys in microgravity environments. The metals and alloys burned in 100% oxygen include rods of 2219 aluminum, 316 stainless steel, copper, nickel 200, Monel K-500, zinc, magnesium, tungsten, iron, and titanium. Sheets and meshes of 316 stainless steel were also tested to study configuration effects. All metals and alloys tested supported combustion in the absence of gravity which indicates surface tension induced circulation is sufficient to ensure fuel/oxidizer mixing. The microgravity combustion of 316 stainless steel volatilized the chromium or chromium oxide, a result that does not occur in similar normal gravity tests. In microgravity the melting surface no longer remains horizontal but becomes slanted and the molten ball obtains a spherical shape and is often observed to precess around the rod. As in normal gravity, during the microgravity burning of the rods, the regression rate of the melting surface increases with either increasing oxygen pressure or decreasing rod diameter. In microgravity, however, the regression rate of the melting surface is significantly faster than in similar normal gravity tests. Metals and alloys considered nonflammable in normal gravity up to oxygen pressures of 68.9 MPa burned at significantly lower pressures in microgravity and configurations not considered flammable in normal gravity readily burned under similar microgravity conditions. These observations are consistent with the conclusion, due to retention of the molten material during microgravity burning, that the temperature in the molten ball in microgravity is greater than in normal gravity.

KEYWORDS: metal combustion, alloy combustion, microgravity metal combustion, microgravity alloy combustion, gravity effects.

INTRODUCTION

The present document used by NASA to qualify materials for use in spacecraft environments, the NASA Handbook (NHB) 8060.1C, contains a test (Test 17) addressing the use of metals [1]. Test 17 requires the promoted combustion test of 30.48-cm- (12 in.) long, 0.32-cm-diameter

---

[1] Principal Scientists, Lockheed-ESC, White Sands Test Facility, P.O. Drawer MM, Las Cruces, NM 88004.

[2] Laboratory Chief, NASA, White Sands Test Facility, P.O. Drawer MM, Las Cruces, NM 88004.

cylindrical rods in 100% gaseous oxygen. The metallic material is considered flammable if one out of five samples burns at least 15.24 cm.

Test 17 is a qualitative test that is based on a selected burn length and only requires results obtained from normal gravity metals combustion tests. The application of Test 17 flammability data obtained in normal gravity and used for selecting materials for use in microgravity is of great concern. White Sands Test Facility (WSTF) has become a center for the study of the combustion characteristics of metallic materials. WSTF performed metals tests at Lewis Research Center's (LeRC) small drop tower to determine the applicability of normal gravity metals combustion test results when applied to microgravity environments.

Until recently, no data on the flammability (either relative or absolute) of metals in microgravity has been presented. Additionally, no work has been done to ascertain the applicability of using normal gravity metals flammability data in the qualification of these metals for use in microgravity environments. This work is essential to assure the safety of space vehicles and inhabitants is not compromised by the inappropriate application of normal gravity metals flammability data to microgravity environments. This paper gives a summary of the microgravity metals work that has been completed, to date, as well as presents new results on the similarities and differences between the normal gravity and microgravity combustion of metals and alloys.

BACKGROUND

Except for the low temperature solid phase oxidation that most metals exhibit, the most distinctive aspect of the combustion of metallic materials is the two phases in which combustion can occur; either liquid phase or vapor phase. Most metallic materials used in the design of oxygen systems burn in the liquid phase. Various proposed criteria concerning the apriori prediction of the phase of combustion of metallic materials and their validity is discussed elsewhere [2].

Metal combustion testing has been performed by Hirano and Sato et al., [3-10] and workers at WSTF [11-13]. These researchers studied combustion propagation along cylindrical metallic rods. Various rod diameters and oxygen pressures were investigated. The conclusions from these tests were that, in normal gravity, some metallic materials are flammable and this combustion is dependant on rod diameter and oxygen pressure. As the oxygen pressure decreases, or the rod diameter increases, the melting surface (the surface between the solid rod and the molten ball) regression rate of the rod decreases and combustion eventually extinguishes. The pressure where combustion (for 0.32-cm-diameter rods) is no longer supported is called the threshold pressure. Hirano et al., [7] and Benz et al., [11] suggested that the rate determining step for the combustion process, in normal gravity, is oxygen availability and oxygen mixing in a molten mass that forms on, and attaches to, the rod. This conclusion would imply that, in the molten mass, molten metal is in excess, not oxygen. Current research at WSTF [13,14], however, looking specifically at oxygen intake into the molten mass formed on a burning iron rod, implies that there is excess oxygen in the molten mass and oxygen availability is not limiting the combustion process for iron.

To investigate the relationship between gravity and the metal combustion process, Steinberg [13,15,16] initiated a test program to use the LeRC to perform short duration microgravity tests. To date, these tests are the only ones which demonstrate the effects of gravity on the combustion of metals and alloys.

EXPERIMENTAL

A brief summary of the test apparatus, materials, igniter, and facilities is given. A more thorough description is given in references [13,15,16].

Facilities

The normal gravity combustion tests were conducted at WSTF in Las Cruces, New Mexico, and the microgravity combustion tests were conducted at the 2.2 s drop tower facility at the NASA LeRC in Cleveland, Ohio. The LeRC drop tower is approximately 27-m high (with a drop height of 24 m) and provides accelerations between 10^{-4} and 10^{-5} gravities, which were produced when the test apparatus was in free-fall inside a drag shield. The same test apparatus was used for both the normal gravity and the microgravity testing.

Test Apparatus

Construction of a unique remotely operated, durable test apparatus was necessary to perform the LeRC drop tests. The test apparatus consisted of a pressure vessel (combustion chamber), power supply, data acquisition and control system (DACS), signal conditioners, instrumentation for oxygen pressure and temperature, view port, high speed camera, and extinguishment system. The volume of the chamber used was 650.1 +/- 6.55 cm^3 (which ensured less than 3% of the available oxygen was consumed during a test). During a test the DACS would control all test apparatus settings and store accumulated test data for post-test downloading.

Materials

The oxygen used at both WSTF and LeRC was 99.5% pure (min.), and the test pressures were varied from 0.1 MPa (14 psia) to 8.6 MPa (1250 psia). The rods were 2219 aluminum, 316 stainless steel, copper, nickel 200, Monel K-500, zinc, magnesium, tungsten, iron, and titanium. Sheets and meshes of 316 stainless steel were also tested. Table 1 gives the compositions of the metals and alloys burned.

Igniter

All experiments in normal gravity and microgravity were ignited with small quantities of aluminum-palladium wire wrapped around the bottom of a sample. This wire was ignited by resistive heating and had negligible effects on the oxygen surroundings [12].

RESULTS AND DISCUSSION

New results and discussion are presented. For comparison, a summary of results reported elsewhere [13-16] is given. Fig. 1 shows a typical growth-and-detachment cycle for a molten ball burning on a 0.32-cm-diameter cylindrical iron rod in normal gravity at 6.89 MPa (1000 psia). As the molten ball grows, melting of the solid rod occurs (via energy transfer from the combustion process), and the melting surface moves upward. This process proceeds, in normal gravity, until the molten ball detaches from the solid rod (when the gravitational force becomes larger than the surface tension and adhesion force) and a new molten ball forms.

Fig. 2 shows the equivalent combustion experiment, in microgravity, as shown in Fig. 1. The last frame of Fig. 2 shows the

TABLE 1--Compositions of metals and alloys tested.

Metal	Chemical Composition (by Weight Percent)															
	Al	C	Cr	Cu	Fe	Mg	Mn	Mo	N	Ni	O	P	S	Si	Ti	W	Zn
Iron[1]			<50	<100	bal[2]		<100			<100		<100					
316 Stainless Steel			17.3	0.04	bal	1.59		2.16		12.2		0.03	0.004	0.61			
2219 Aluminum	bal			6.3	0.3	0.02	0.3						0.2		0.06		
Titanium		0.01			0.03				0.006		0.06				bal		
Mild Steel (SS41)[3]	0.07				bal		0.37					0.05	0.05	0.013			
Copper[1]				bal		10				300				50			
Nickel 200		0.02			0.04		0.20			bal			0.006	0.01			
Monel K-500	2.6	0.25		29.0	2.0		1.5			bal			0.01	0.5	0.5		
Zinc[1]				5		2								1		bal	
Magnesium				0.02	0.05	bal	0.01			0.001							
Tungsten[1]	7		4	<1	4	<1	<1	<8		1				<1		bal	

[1] These values are given in parts per million (ppm).
[2] bal refers to balance, that is, the balance of the metal is of this element.
[3] This metal was burned by Sato [10].

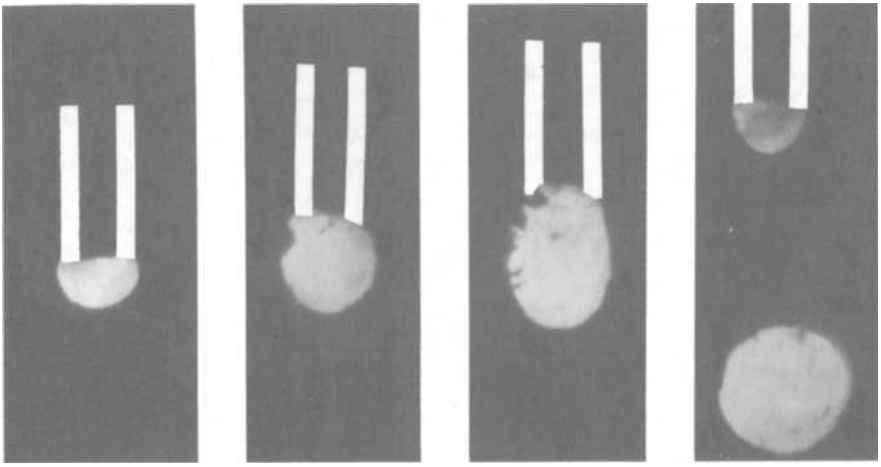

FIG. 1--Typical growth and detachment of molten ball formed on burning iron rod (0.32-cm-diameter) at 6.9 MPa oxygen pressure in normal gravity. (The white lines were added to the photographs to show the boundaries of the rod.)

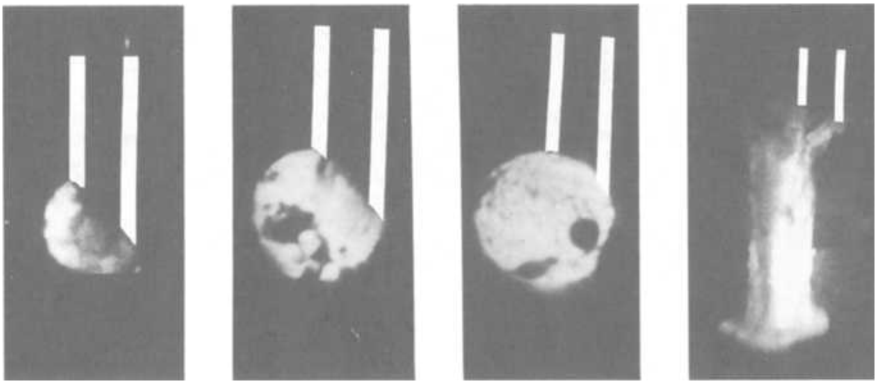

FIG. 2--Combustion of iron rod (0.32-cm-diameter) at 6.9 MPa oxygen pressure in microgravity (and detachment of molten ball due to impact at test conclusion).

effect of impact of the test apparatus at the conclusion of a drop. Upon impact, for most materials, the rod was not extinguished but, now in normal gravity, continued to propagate the combustion until the entire rod was consumed. For the system shown in Fig. 2, the drop time of 2.2 s would correspond to approximately five growth-and-detachment cycles in normal gravity. But as Fig. 2 shows, no detachment of the molten mass occurs, and the increasing size of the molten mass accurately reflects the accumulation of material in the molten mass.

At the beginning of testing it was not clear whether metals would support combustion in the absence of gravity. It was immediately determined that all the metals tested do support combustion under microgravity conditions similar to conditions supporting combustion in normal gravity. This result indicates that surface tension induced circulation in the molten mass is sufficient to ensure mixing of fuel and oxidizer and continue propagation of the burning event in the absence of buoyancy. Experiments that had the rod (iron) ignited in the middle of the sample, clearly showed the free end of the rod swinging with this surface tension induced circulation as it was drawn into the molten ball.

Obvious visual changes in the burning of the rods occurred when the gravitational force was reduced. These changes include a) the shape of the molten mass changes from a teardrop in normal gravity to a sphere in microgravity, b) the change of the melting surface from a circular section, in normal gravity, to a conical section in microgravity (which results in a larger attachment area), and c) the molten ball, in microgravity, is often observed to precess around the rod as it burns. These changes are shown schematically in Fig. 3 which also allows a qualitative comparison between the normal gravity and microgravity combustion of cylindrical rods.

All metals tested (as cylindrical rods), above the threshold pressures obtained for these metals in normal gravity, burned for the entire duration of the drop. The relationships between rod diameter, oxygen pressure, and melting surface regression rate have been shown to be consistent, for the iron system, in microgravity environments, though the magnitude of the regression rate is significantly larger in microgravity than in normal gravity. The microgravity regression rate of the melting surface is calculated by representing the melting surface by a slanted line defined by the intersection of the molten ball and the solid rod (Fig. 3). The midpoint of this line is monitored as the melting surface progresses up the rod, to determine the microgravity regression rate. The dependency of the regression rate of the melting surface on rod diameter and oxygen pressure for the iron system, both in normal gravity and microgravity, is shown in Fig. 4. Similar trends are exhibited by the other metallic materials tested in cylindrical rod configuration. These test results emphasize a significant difference between the normal gravity and microgravity combustion, that is, microgravity greatly increases the regression rate of the melting surface for similar experimental conditions. As Fig. 4 shows, the regression rate of the melting surface is two to three times faster in microgravity for the 1-mm-diameter rods, and one and one-half to two times faster for the 2-mm- and 3-mm-diameter rods.

Though Fig. 4 is for the iron system, calculations show similar increases in regression rates of the melting surface in microgravity for other metallic materials burned in this study. For example, in normal gravity the regression rate of the melting surface for 0.32-cm-diameter 316 stainless steel rods, at approximately 6.3 MPa (914 psia), has been reported as 13.2 mm/s [3,10], 11.0 mm/s [11,17], and 9.0 mm/s [18]. In microgravity the regression rate of the melting surface for 316 stainless steel at 6.3 MPa is 24.4 mm/s, about double the fastest rate reported in normal gravity. For aluminum, the regression rate of the melting surface in normal gravity at 1.9 MPa and 2.6 MPa has been reported [10] to be 32 mm/s and 29 mm/s, respectively. In microgravity

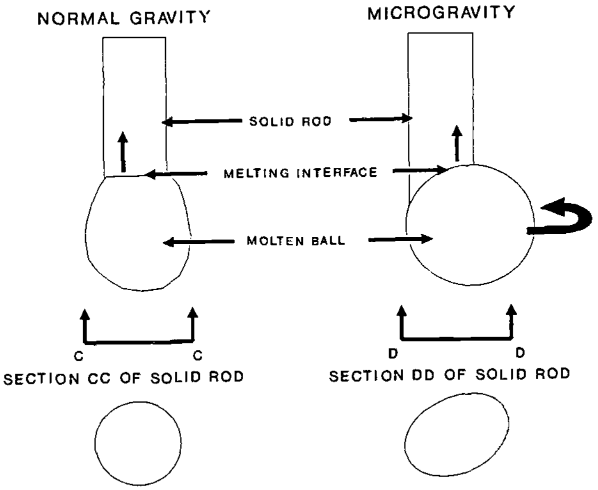

FIG. 3--Comparison of burning rods between normal gravity and microgravity.

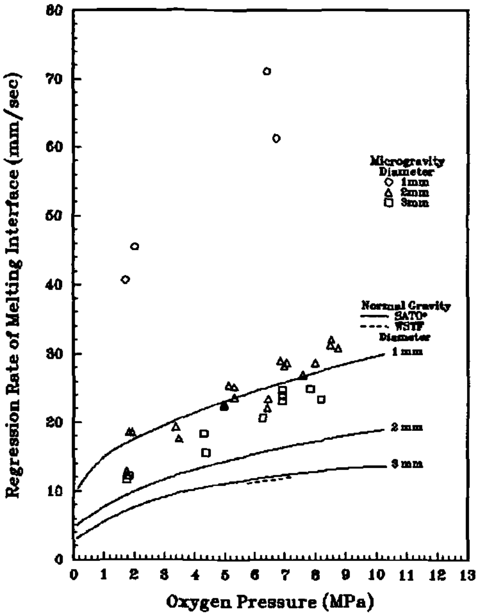

FIG. 4--Comparison of regression rate of melting surface between normal gravity (mild steel and iron) and microgravity (iron) as a function of oxygen pressure and rod diameter.

the regression rate of the melting surface for 2219 aluminum, at these pressures, is 167.4 mm/s and 182.9 mm/s, respectively, more than five times the normal gravity regression rate. These observed increases in the regression rates of the melting surface during microgravity combustion can be attributed to an increase in the temperature of the molten mass due to retention of all the molten mass (no detachment) as well as the larger attachment area between the molten mass and the solid rod.

The burning of 0.32-cm-diameter rods of 316 stainless steel, in microgravity (and normal gravity), were qualitatively identical to the burning of iron rods, that is, increased regression rate of the melting surface, intense circulation of the molten ball, precessing of the ball about the rod, etc. A significant difference, however, was that, after the experiment, the chamber was coated in a fine olive-green powder. The powder was collected, analyzed (x-ray diffraction) and determined to be chromium oxide (Cr_2O_3). This phenomena does not occur in similar experiments with 316 stainless steel in normal gravity. Consistent with the observed increases in the regression rates of the melting surface during microgravity combustion, the volatilization of the chromium or chromium oxide can be due to an increase in the temperature of the molten mass.

Fig. 5a shows the combustion of a 0.32-cm-diameter 2219 aluminum rod at 2.7 MPa oxygen pressure. The combustion zone is similar in shape, growth, and progression up the rod as is seen with 316 stainless steel and iron, but the total luminosity is significantly greater as is the quantity of volatile products surrounding the combustion zone.

The combustion of bulk titanium in normal gravity exhibits three regular and very repeatable stages for specimens of similar dimensions [20,21]. Initially is an ignition and heating-up stage followed by vigorous expulsion of particles, and finally quiescent burning similar to 316 stainless steel and iron. Fig. 5b shows the microgravity combustion of a 0.32-cm-diameter titanium rod at 0.1 MPa oxygen pressure during the particle expulsion stage. It was observed, in microgravity, that the period and onset of these three stages is different than in normal gravity; the first stage is very rapid and the expulsion stage is of longer duration and starts earlier. Due to the short test time, it was not determined if other anomalies would be present if the tests were conducted for longer times. Also, the number of tests conducted did not allow determination if these three stages were regular and repeatable.

Zinc, magnesium, and tungsten rods (0.32-cm-diameter) were also burned under microgravity conditions. In normal gravity the combustion of these metals is accompanied by the volatilization of either the oxide or metal, that is, after a test the chamber is coated with either a fine powder or flakes of the oxide. The same phenomena occurred during the microgravity combustion of these materials. Regression rates of the melting surface were not obtainable due to these volatilized species.

Copper, nickel 200, and Monel K-500 are three metallic materials that have been determined to be unable to support upward combustion in normal gravity of 0.32-cm-diameter rods in 100% oxygen up to a pressure of 68.9 MPa (10,000 psia). In microgravity, these three metallic materials all burned at the relatively low oxygen pressure of 6.9 MPa (1000 psia). The combustion of these metallic materials in microgravity propagated because the formed combustion zone would not detach as occurs in similar combustion in normal gravity. Since the molten mass does not detach in microgravity, additional energy that is lost during the normal gravity burning of these materials at these conditions, is available to propagate the burning in microgravity, that is, energy is not lost at a faster rate then it is generated. Figs. 5c and 5d show the burning copper and nickel 200, respectively. The test time of 2.2 s did not allow adequate time to permit propagation of the burning event for a significant distance along the nickel 200 or Monel K-500 rods. For the copper rods, a regression rate of the melting surface of 9.7 mm/s and 24.1 mm/s was obtained for oxygen pressures of 6.9 MPa and 8.1 MPa, respectively.

Different shapes were burned in microgravity to compare configurational effects with similar tests conducted in normal gravity. Fig. 6a shows the microgravity burning of a 316 stainless steel wire mesh (1.7 MPa) rolled into the shape of a cylinder, and Fig. 6b shows the microgravity burning of a 316 stainless steel sheet (6.9 MPa). In normal gravity the combustion of these meshes visually appears identical to the burning of cylindrical rods (except for the calculated regression rates). The photograph of the 316 stainless steel mesh (Fig. 6a) shows a capillary effect as the molten material is drawn up the center cavity prior to melting through, acquiring new material and growing. This implies, in normal gravity, the buoyant effect is large enough to prevent the capillary effect. In normal gravity, 316 stainless steel sheets extinguished at this pressure, due to residual thermal energy being lost at a faster rate than it is generated as the molten mass detaches. In microgravity, the sheets burned until the samples were completely consumed due to the lack of removal of molten material from the reaction zone. Several of the tests with the sheets appeared to show the combustion zone progressing along the surface prior to completely melting and burning of the underlying material. It should be noted that the combustion of both the 316 stainless steel meshes and sheets resulted in the deposit of the fine green powder that also occurred during the combustion of the 316 stainless steel rods.

The results of these experiments show that some of the results of normal gravity Test 17 tests are applicable to microgravity environments. These would include the relationships between the regression rate of the melting surface and the oxygen pressure and rod diameter, that is, in normal gravity and microgravity, as the oxygen pressure is decreased or rod diameter increased, the regression rate of the melting surface decreases. A difference however, between the normal gravity and microgravity burning is the increased regression rate of the melting surface in microgravity. T'ien [22] hypothesized that a reversal in the absolute flammability of materials at different gravity levels is possible due to heat transfer effects, but this work is the first experimental evidence that supports this hypothesis. Configurations (sheets) and metallics (copper, nickel 200, Monel K-500) that are nonflammable in normal gravity become flammable in microgravity; a result both scientifically interesting and with serious implications in regards to fire safety and the applicability of normal gravity test results to microgravity environments.

CONCLUSIONS

Many metals and alloys readily burn in both normal gravity and microgravity. All metals and alloys tested support combustion in the absence of gravity which indicates surface tension induced circulation is sufficient to ensure mixing of the fuel and oxidizer in the molten ball formed. Changes that occur during the microgravity burning of rods would include the molten ball changing to a sphere, the melting surface no longer remaining horizontal, and the precessing of the molten ball around the rod. An increase in the regression rate of the melting surface with either increasing oxygen pressure or decreasing rod diameter occurs both in normal gravity and microgravity, but the regression rate of the melting surface is significantly greater in microgravity. The microgravity combustion of 316 stainless steel volatilized the chromium or chromium oxide, a result that does not occur in similar normal gravity tests. Metals and alloys considered nonflammable in normal gravity tests up to oxygen pressures of 68.9 MPa burned at significantly lower pressures in microgravity and configurations not flammable in normal gravity become flammable in

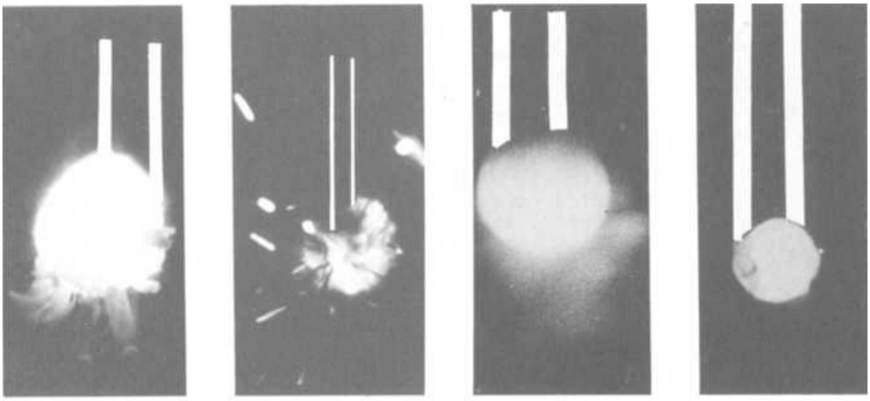

A B C D

FIG. 5--Microgravity combustion in oxygen of 0.32-cm-diameter rods of a) 2219 aluminum at 2.7 MPa, b) titanium at 0.1 MPa, c) copper at 6.9 MPa, and d) nickel 200 at 6.9 MPa.

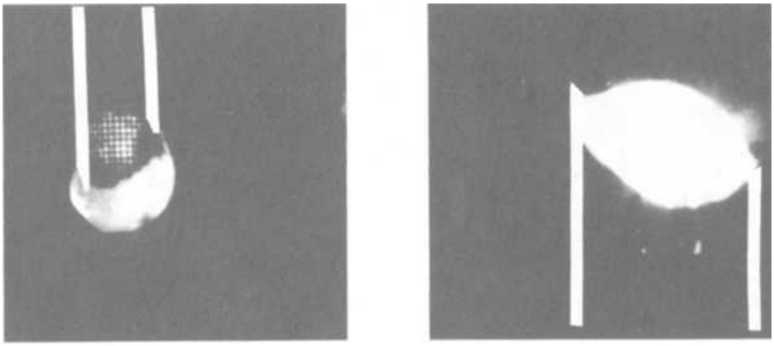

A B

FIG. 6--Microgravity combustion in oxygen of 316 stainless steel a) mesh (24 × 24 strands per cm, 0.019-cm-diameter strand), and b) sheet (1.3-cm-wide, 2.5-cm-long, 0.1-cm-thick) at 6.9 MPa.

microgravity, that is, a reversal in flammability occurs. These observations are consistent with the conclusion, due to retention of the molten material during microgravity burning, that the temperature in the molten ball in microgravity is greater than in normal gravity.

Owing to the short microgravity time available at LeRC, however, no comparison could be made between Test 17 qualifications performed in normal gravity and microgravity. These results indicate that the application of normal gravity tests results to material selections for microgravity environments, without further work, especially new configurations and metals and alloys considered nonflammable in normal gravity, would be premature and possibly hazardous.

FUTURE WORK

The largest problem with the LeRC facility used in this investigation was the short test duration (2.2 s). For materials that ignite and burn easily, the two seconds of test time did not allow qualification according to the requirements in Test 17, that is, 15.2 cm of burn for a 0.32-cm-diameter rod. Testing is therefore required in a microgravity environment of longer duration to study the combustion process of metallic materials and to better determine the applicability of normal gravity Test 17 flammability data to microgravity environments. For the faster burning metallic materials, longer tests are needed to see if the trends shown during the short duration tests will continue or whether differences will occur.

It has been shown that at a pressure of 6.9 MPa in normal gravity [14] and over the pressure range of 1.7 MPa to 8.6 MPa in microgravity [15] the combustion of iron is accompanied by the intake of an excess (above stoichiometric requirements), amount of oxygen into the formed molten mass. A first-order lumped parameter model to obtain mechanistic parameters for the liquid phase combustion occurring in the molten mass formed on a cylindrical iron rod has been proposed [19]. The model will permit comparison of kinetic parameters with corresponding normal gravity models. Presently, the model is more appropriate for application in reduced gravity environments because the excess entrapped oxygen in the formed molten mass does not offgas back to the gaseous surroundings during a test (since the molten ball does not detach). In normal gravity, the detachment of the molten mass complicates model solution because the iron oxide slag that accumulates on the chamber bottom offgasses the entrapped oxygen back to the gas-phase. The effects of the oxygen offgassing from the product slag were significant enough that they can not be ignored in normal gravity modeling.

Testing is being conducted to determine the quantity of oxygen in the molten mass above the stoichiometric requirements for complete combustion. This testing is also being performed in an effort to determine the way the oxygen is bound in the molten ball, that is, as diatomic oxygen, monatomic oxygen, oxide (what type), etc.

Testing of various configurations, other metals and alloys, including both those flammable and nonflammable in normal gravity is also proposed for future work. The characterization of the regression rate of the melting surface for these materials would also be performed. The microgravity testing of the metallic materials closer to their threshold pressures obtained in normal gravity is also proposed, as well as the testing below the obtained normal gravity threshold pressures.

REFERENCES

[1] "Flammability, Odor, Offgassing, and Compatibility Requirements and Test Procedures for Materials in Environments that Support Combustion," NHB 88060.1C, Test 17, NASA, Washington, DC, April 1991, pp. 4-58.

[2] Steinberg, T. A., Wilson, D. B., and Benz, F. J., "The Combustion Phase of Burning Metals," Combustion and Flame, Vol. 91, 1992, pp. 200-208.

[3] Sato, J., and Hirano, T., "Behavior of Fire Spreading Along High Temperature Mild Steel and Aluminum Cylinders in Oxygen," Flammability and Sensitivity of Materials in Oxygen Enriched Atmospheres: Second Volume, ASTM STP 910, M. A. Benning, ed., American Society of Testing and Materials, Philadelphia, 1986, pp. 118-134.

[4] Hirano, T., Sato, K., Sato, J., "An Analysis of Upward Fire Spread Along Metal Pieces," Fire Dynamics and Heat Transfer - HTD, Vol. 25, J. G. Quintiere, R. L. Alpert, and R. A. Altenkirch, eds., New York, ASME, 1983.

[5] Hirano, T., Sato, K., Sato, Y., Sato, J., "Prediction of Metal Fire Spread in High Pressure Oxygen," Combustion Science and Technology, Vol. 32, 1983, pp. 137-159.

[6] Sato, J., Sato, K., Hirano, T., "Fire Spread Mechanisms Along Steel Cylinders in High Pressure Oxygen," Combustion and Flame, Vol. 51, 1983, pp. 279-287.

[7] Hirano, T., Sato, Y., Sato, K., Sato, J., "The Rate Determining Process of Iron Oxidation at Combustion in High Pressure Oxygen," Oxidation Communications, 6, NOSI-4, 1984, pp. 113-124.

[8] Sato, K., Sato, Y., Tsuno, T., Nakamuta, Y., Hirano, T., Sato, J., "Metal Combustion in High Pressure Oxygen Atmosphere Detailed Observation of Burning Region Behavior by Using High Speed Photography," 15th International Congress on High Speed Photography and Photonics, SPIE Vol. 384, San Diego, 1982, pp. 828-832.

[9] Sato, K., Hirano, T., Sato, J., "Behavior of Fires Spreading Over Structural Metal Pieces in High Pressure Oxygen," ASME - JSME Thermal Engineering Joint Conference Proceedings, Vol. 4, 1983, pp. 311-316.

[10] Sato, J., "Fire Spread Rates Along Cylindrical Metal Rods in High Pressure Oxygen," Flammability and Sensitivity of Materials in Oxygen Enriched Atmospheres: Fourth Volume, ASTM STP 1040, Stoltzfus, F. J. Benz, and J. Stradling, Eds., American Society of Testing and Materials, Philadelphia, 1989, pp. 162-177.

[11] Benz, F. J., Steinberg, T. A., Janoff, D., "Combustion of 316 Stainless Steel in High-Pressure Gaseous Oxygen," Flammability and Sensitivity of Materials in Oxygen-Enriched Atmospheres: Fourth Volume, ASTM STP 1040, J. Stoltzfus, F. J. Benz, and J. Stradling, Eds., American Society for Testing and Materials, Philadelphia, 1989, pp. 195-211.

[12] Steinberg, T. A., Rucker, M. A., Beeson, H. D., "Promoted Combustion of Nine Structural Metals in High-Pressure Gaseous Oxygen; A Comparison of Ranking Methods," Flammability and Sensitivity of Materials in Oxygen-Enriched Atmospheres: Fourth Volume, ASTM STP 1040, J. Stoltzfus, F. J. Benz, and J. Stradling, Eds., American Society for Testing and Materials, Philadelphia, 1989, pp. 54-75.

[13] Steinberg, T. A., Metals Combustion at High Oxygen Pressure in Normal and Reduced Gravity: Model and Experiment, Ph.D. Dissertation, New Mexico State University, Las Cruces, New Mexico, May, 1990, University Microfilms, Inc., Ann Arbor, Michigan, 91-01023, 51-08B, Dissertation Abstracts, pg. 4021.

[14] Steinberg, T. A., Mulholland, G. P., Wilson, D. B., Benz, F. J., "The Combustion of Iron in High Pressure Oxygen," Combustion and Flame 89:221-228 (1992).

[15] Steinberg, T. A., Wilson, D. B., and Benz, F. J., "The Burning of Metals and Alloys in Microgravity," Combustion and Flame 88:309-320 (1992).

[16] Steinberg, T. A., Benz, F. J., "Iron Combustion in Microgravity," Flammability and Sensitivity of Materials in Oxygen-Enriched Atmospheres: Fifth Volume, ASTM STP 1111, J. M. Stoltzfus and K. McIlroy, Eds., American Society for Testing and Materials, Philadelphia, 1991, pp. 298-312.

[17] Benz, F. J., Shaw, R. C., and Homa, J. M., "Burn Propagation Rates of Metals and Alloys in Gaseous Oxygen," Flammability and Sensitivity of Materials in Oxygen-Enriched Atmospheres: Second Volume, ASTM STP 910, M. A. Benning, Ed., American Society for Testing and Materials, Philadelphia, 1986, pp. 135-152.

[18] McIlroy, K., Zawierucha, R., and Drnevich, R. F., "Promoted Ignition Behavior of Engineering Alloys in High-Pressure Oxygen," Flammability and Sensitivity of Materials in Oxygen Enriched Atmospheres: Third Volume, ASTM STP 986, D. W. Schroll, ed., American Society of Testing and Materials, Philadelphia, 1988, pp. 85-104.

[19] Steinberg, T. A., Wilson, D. B., Benz, F. J., "A Model For Liquid Phase Burning Metals," in preparation (to be submitted to Combustion and Flame).

[20] Clark, A. F., Moulder, J. C., and Runyan, C. C., Fifteenth Symposium (International) on Combustion, The Combustion Institute, Pittsburgh, 1974, pp. 489-499.

[21] Runyan, C. C., Moulder, J. C., and Clark, A. F., Combustion and Flame, 23:129-133 (1974).

[22] T'ien, J. S., "The Possibility of a Reversal of Material Flammability From Normal Gravity to Microgravity." Presented at the International Microgravity Combustion Workshop, January 25-26, 1989, Cleveland, Ohio.

Mohan V. Gunaji[1] and Joel M. Stoltzfus[2]

REVIEW OF FRICTIONAL HEATING TEST RESULTS IN OXYGEN-ENRICHED ENVIRONMENTS

REFERENCE: Gunaji, M. V. and Stoltzfus, J. M., "Review of Frictional Heating Test Results in Oxygen-Enriched Environments," Flammability and Sensitivity of Materials in Oxygen-Enriched Atmospheres: 6th Volume, ASTM STP 1197, Dwight D. Janoff and Joel M. Stoltzfus, Eds., American Society for Testing and Materials, Philadelphia, 1993.

ABSTRACT: Friction is a known ignition source for metals and polymers in oxygen systems. This paper provides a review of the test results currently in the literature and an update of frictional ignition tests recently conducted at WSTF. Most of the results are presented in terms of the Pv product required for ignition (Pv_{ign}), where *P* is the normal load divided by the rubbing area and *v* is the relative linear velocity between the samples. Rankings based on Pv_{ign} are presented for similar and dissimilar pairs of metal alloy test samples. A comparison of the Pv_{ign} in liquid oxygen (LOX) and the PV_{ign} in gaseous oxygen (GOX) indicates that materials are approximately three to four times more difficult to ignite in LOX than in GOX. A discussion of the application of the data to material selection is also presented.

KEYWORDS: Oxygen, metals, alloys, ignition by friction, frictional heating tests, ranking, Pv_{ign}

INTRODUCTION

As described in the ASTM "Standard Guide for Evaluating Metals for Oxygen Service" (ASTM G-94), bearing materials and other metal alloys burn in oxygen-enriched environments. A test method was developed at the NASA Johnson Space Center White Sands Test Facility to evaluate the ignition of metals by friction [1,2,3,4,5]. This paper is a review of the literature on ignition due to friction, and it also provides an update on results of some recent frictional heating tests.

LITERATURE REVIEW

Oxygen-system equipment was designed in the past according to the following design rules [5]:

- Assure high mechanical reliability of the compressor.
- Wherever possible, use low velocities and low gas temperatures.

---

[1] Principal Engineer, Lockheed-ESC, White Sands Test Facility, P.O. Drawe MM, Las Cruces, NM 88004.

[2] Project Manager, NASA, White Sands Test Facility, P.O. Drawer MM, Las Cruces, NM 88004.

- Select materials proven to have favorable ignition and combustion characteristics.
- Ensure that the system is clean, to minimize ignition sources.

When mechanical components rub together, heat is generated by friction. This friction in oxygen-enriched environments has been reported as the cause of many fires [1,2,3,4,5,6]. Benz and Stoltzfus [1] report that ignition of metals by friction has troubled the designers and users of pumps, compressors, and various other oxygen-system components. The frictional heating system was developed to determine whether metals and alloys will ignite when their surfaces rub in an oxygen environment. Benz and Stoltzfus [1] described the energetics during the rubbing process as

$$\frac{dq_{acc}}{dt} = \dot{Q}_{RX}+\dot{Q}_{fric}-\dot{Q}_{L}-\dot{Q}_{W} \tag{1}$$

The energy balance given in Equation 1 shows that the rate of heat accumulation (dq_{acc}/dt) is a function of the rate of heat generated due to oxidation (Q_{RX}); the rate of frictional energy $(\dot{Q}_{fric})$ generated at the rubbing surface; the rate of energy loss by conduction, convection, and radiation $(\dot{Q}_{N})$; and the rate of energy loss by work (Q_{L}), such as permanent deformation of the material.

Benz and Stoltzfus also developed a ranking criteria for materials in the same study, which is currently being used by researchers. This ranking criteria is based on the Pv product required for ignition (Pv_{ign}) where P is the normal load divided by the rubbing area and v is the relative linear velocity between the samples. The Pv_{ign} is a measure of a material's resistance to ignition and is dependent on P, v, the particular alloy, oxygen pressure, and oxygen concentration. Benz and Stoltzfus also indicate that the coefficient of friction decreases as the temperature of the sample increases.

According to Adamson [8], the coefficient of friction should increase as the contact pressure is increased. The effect of chamber oxygen pressure on the Pv_{ign} was studied by Benz and Stoltzfus [1]. The results indicate that as the oxygen pressure was increased, the Pv_{ign} decreased until it reached a minimum, and then as the oxygen pressure was increased further, the Pv_{ign} increased. The rate of decreasing and increasing was a function of the material. They speculated that the increase in Pv_{ign} after the minimum was reached was due to increased convective heat loss at higher chamber pressures.

Stoltzfus et al. [6] and Bryan et al. [10] evaluated the Pv_{ign} for dissimilar pairs of materials. Stoltzfus et al. suggested a more general ranking criteria to include the coefficient of friction, μ. This criteria was the μPv product. The propensity of a material to convert mechanical energy to thermal energy is given by

$$Q_f = Pv\mu A = \omega L \tag{2}$$

where

Q_f = rate of frictional energy generated (W)
A = initial cross-sectional area of the sample (m^2)
L = torque (N-m),
P = contact pressure (N/m^2)
v = linear surface velocity (m/s)
ω = angular velocity (rad/s)
μ = coefficient of friction

Equation 2 suggests that the generation of thermal energy is dependent on μ. Stoltzfus et al. [2] compared the ranking of several alloys based on the Pv_{ign} and the μPv_{ign}. The comparison suggested that for environments where frictional heating is a dominant ignition mechanism, metals and alloys must be selected based on frictional heating test results and the Pv_{ign} ranking criteria rather than the μPv_{ign}. This selection criteria is because the susceptibility to ignition is dependent on the ability to convert mechanical energy to thermal energy and the quantity of thermal energy required to heat the material to its ignition temperature. The Pv_{ign} is a measure of these properties of the material.

Schoenman et al. [4] reported ignition of metals from the rubbing of hydrostatic bearings and turbine blade tips operating in a high-pressure oxygen environment. Frictional heating tests were conducted at pressures of 1 to 300 atm and surface speeds of 10 to 33 m/s in gaseous oxygen. The candidate materials were selected based on structural requirements, suitability for cryogenic application, previous experience, and their calculated burn factor. The burn factor was the heat of formation of the most stable oxide of the material, divided by the material's heat absorption capability.

Zhu et al. [12] analyzed the frictional heating data and tried to develop a model to provide a theoretical understanding of the various fundamental physical processes occurring, such as heat and mass transfer, chemical reactions, and metallurgical transformation. A good understanding of these processes would lead to improvements of the frictional heating test and a better interpretation of the data to aid in the design of oxygen systems. Zhu et al. [12] suggest that the transient heating of the test sample is due to heat generated by friction and heat losses are due to convective cooling. They also concluded that for the materials evaluated (carbon steel and Monel K-500), the test data did not indicate that the actual oxygen pressure had a significant effect on the coefficient of friction.

Yuen [13] developed a data reduction program and an ignition model for the analysis of the data generated by frictional heating. Based on the transient temperature data measured on the stationary sample, the model predicted the effective friction coefficient, activation energy and reactive flux constant for different metals/alloys at various test conditions. Bryan et al. [10] assessed the metals flammability hazard in high-pressure oxygen systems at the NASA Kennedy Space Center. They ranked metals based on the resistance to ignition, measured as the product of the apparent contact pressure P and the linear surface velocity v required for ignition. They found that as the Pv_{ign} increases, the resistance to friction-induced ignition increases.

Gunaji et al. [9] used the frictional heating test system to study surface modifications of Monel K-500 as a means of reducing friction and wear in high-pressure oxygen. This study revealed that even though some observations could be made from the data generated using the frictional heating test apparatus, a different test method must be developed if a more sensitive assessment of the effects of surface treatment on the tribological characteristics is required. Their study emphasized that the test system is reliable for ignition comparisons (relative ranking of materials), but is not reliable for wear data unless it is modified.

TEST SYSTEM DESCRIPTION

The GOX frictional heating apparatus (Fig. 1) described here is the same as that described by Benz and Stoltzfus [1]. It consists of a high-pressure test chamber (Fig. 2), an electrical motor and transmission assembly, and a pneumatic actuation cylinder. The high-pressure test chamber, fabricated of Monel 400, consists of a cylindrical chamber with a replaceable nickel sleeve inside. The chamber contains a rotating shaft that extends through the chamber via a series of bearings and seals. The shaft is connected at one end to a drive motor/transmission assembly capable of rotating the shaft up to 30 000 rpm. The other end of the shaft is connected to a pneumatically actuated cylinder, which allows axial movement of the shaft to apply up to 4 450 N (1 000 lbf) normal load on the test specimens. The rotating

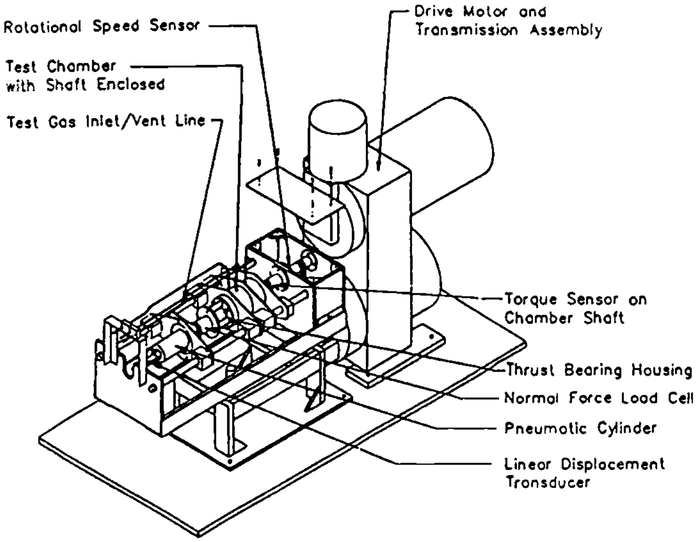

FIG. 1--Frictional heating test system

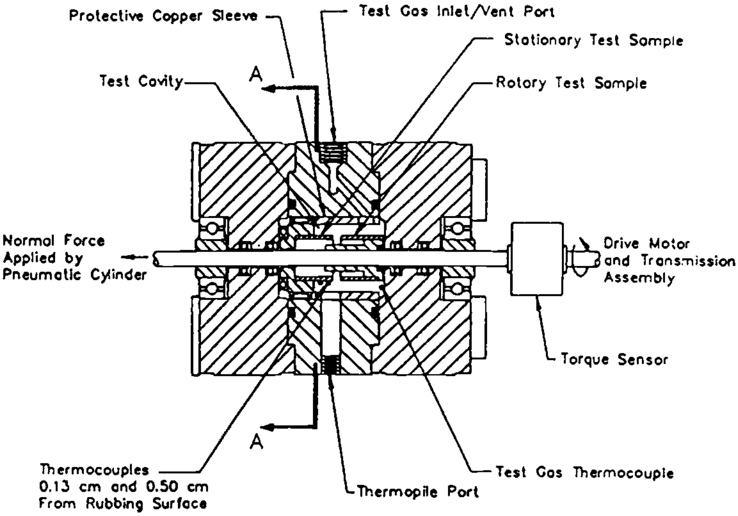

FIG. 2--High-pressure test chamber for frictional heating test system.

test specimen is mounted on the shaft, and the stationary test specimen is affixed to the test chamber.

The LOX frictional heating test system is similar to the GOX frictional heating test system, except that it is configured vertically and has a fluid piping system for the liquid oxygen.

REVIEW AND UPDATE OF RESULTS

The typical results of the frictional heating tests for some commonly used alloys are shown in Table 1 and Table 2. Table 1 shows the Pv_{ign}'s when the rotary and stationary samples are the same alloy, while Table 2 shows the Pv_{ign}'s when the rotary and stationary samples are of dissimilar alloys. Tables 1 and 2 also show the relative ranking of the materials for resistance to ignition by friction. The ranking is based on the lowest Pv_{ign} in 3 tests with each metal pair. Stoltzfus et al. [7] suggest that the reason for the range of Pv_{ign}'s is not known, but is speculated to be due to the formation and destruction of the oxides on the rubbing surface and the different heat transfer conditions between the stationary and rotary samples. When stationary and rotary samples are dissimilar, the metal that is least resistant to ignition by frictional heating tends to control the ignition threshold.

Table 3 shows the comparison of data from the GOX and LOX systems; this comparison indicates that the Pv_{ign} is greater in LOX than in GOX. It is hypothesized that LOX causes greater convective cooling in the chamber than does GOX. For melting and ignition of the samples to occur, the frictional heat generated at the interface of the samples must therefore be greater in LOX than in GOX.

TABLE 1--Friction ignition test data for similar pairs of test specimens.[a]

Test materials		Pv product at ignition	
Stator	Rotor	$W/m^2 \times 10^{-8}$	(lbf/in^2 × ft/min x 10^{-6})
Inconel MA 754	Inconel MA 754	3.96 - 4.12*	11.30 - 11.75[d]
Haynes 214	Haynes 214	3.05 - 3.15	8.73 - 8.98[d]
Inconel MA 758	Inconel MA 758	2.64 - 3.42	7.53 - 9.76
Nickel 200	Nickel 200	2.29 - 3.39	6.50 - 9.66[b]
Tin Bronze	Tin Bronze	2.15 - 2.29	6.15 - 6.55[c]
Hastelloy C-22	Hastelloy C-22	2.00 - 2.99	5.72 - 8.52[e]
Inconel 600	Inconel 600	2.00 - 2.91	5.70 - 8.30[b]
Inconel MA 6000	Inconel MA 6000	1.99 - 2.66	5.68 - 7.59[d]

[a] 2.5-cm (1-in.)-diameter by 0.25-cm (0.1-in.) wall by 2-cm (0.8-in.) specimens rotated axially and horizontally in stagnant 6.9 MPa (1 000 psia), aviator's breathing grade oxygen. *v* is the specimen linear velocity of 22 m/s (72.2 ft/s), and P is the specimen contact pressure at ignition (Loading force/initial contact area). Tests were conducted by keeping *v* constant and increasing *P* at a rate of 35 N/s (7.86 lbf/s) until ignition.

* This material did not ignite at these Pv products.

[b] [2]

[c] [7]

[d] [3]

[e] [4]

All unreferenced data is from previously unpublished frictional heating tests performed at NASA White Sands Test Facility.

TABLE 1 (Cont'd)--Friction ignition test data for similar pairs of test specimens.[a]

Test materials		Pv product at ignition	
Stator	Rotor	$W/m^2 \times 10^{-8}$	($lbf/in^2 \times ft/min \times 10^{-6}$)
Glidcop Al-25	Glidcop Al-25	1.95 - 3.59	5.56 - 10.24
NASA-Z	NASA-Z	1.77 - 2.63	5.05 - 7.52
Cu Zr	Cu Zr	1.68 - 3.19	4.81 - 9.11
Inconel 625	Inconel 625	1.63 - 1.73	4.65 - 4.94
Hastelloy B-2	Hastelloy B-2	1.61 - 2.16	4.60 - 6.12[e]
Waspaloy	Waspaloy	1.55 - 2.56	4.45 - 7.05[d]
Monel 400	Monel 400	1.44 - 1.56	4.12 - 4.46[b]
Haynes Alloy 230	Haynes Alloy 230	1.40 - 2.19	4.00 - 6.24[d,c]
Monel K-500	Monel K-500	1.37 - 1.64	3.91 - 4.68[b]
13-4 PH	13-4 PH	1.31 - 2.06	3.74 - 5.88[c]
Hastelloy C-276	Hastelloy C-276	1.21 - 2.82	3.45 - 8.06[e]
Incoloy 903	Incoloy 903	1.20 - 1.44	3.41 - 4.11[d]
Inconel 718	Inconel 718	1.10 - 1.19	3.13 - 3.37[d]
17-4 PH (H 900)	17-4 PH (H 900)	1.00 - 1.21	2.87 - 3.45
Yellow Brass	Yellow Brass	0.97 - 1.22	2.77 - 3.49
Hastelloy X	Hastelloy X	0.93 - 1.05	2.66 - 3.02[b]
Hastelloy G30	Hastelloy G30	0.91 - 1.29	2.58 - 3.68[e]
14-5 PH	14-5 PH	0.88 - 1.04	2.51 - 2.96
304 SS	304 SS	0.85 - 1.20	2.33 - 3.41[d]
17-4 PH	17-4 PH	0.85 - 1.07	2.42 - 3.05
Inconel 706	Inconel 706	0.81 - 1.21	2.33 - 3.51
303 SS	303 SS	0.78 - 0.91	2.25 - 2.60
Stellite 6	Stellite 6	0.79 - 0.82	2.25 - 2.35
Brass CDA 360	Brass CDA 360	0.70 - 1.19	1.98 - 3.41[b]
17-4 PH (Condition A)	17-4 PH (Condition A)	0.61 - 1.05	1.75 -2.99
Invar 36	Invar 36	0.60 - 0.94	1.71 - 2.68[b]
Incoloy MA 956	Incoloy MA 956	0.53 - 0.75	1.67 - 2.02
316 SS	316 SS	0.53 - 0.86	1.50 - 2.50[a]
440 C Stainless Steel	440 C Stainless Steel	0.42 - 0.80	1.19 - 2.28[d]
Nitronic 60	Nitronic 60	0.29 - 0.78	0.82 - 2.22
Incoloy 909	Incoloy 909	0.29 - 1.15	0.85 - 3.30[d]
Aluminum 6061-T6	Aluminum 6061-T6	0.061	0.18[b]
Ti-6Al-4V	Ti-6Al-4V	0.0035	0.01[b]

[a] 2.5-cm (1-in.)-diameter by 0.25-cm (0.1-in.) wall by 2-cm (0.8-in.) specimens rotated axially and horizontally in stagnant 6.9 MPa (1 000 psia), aviator's breathing grade oxygen. *v* is the specimen linear velocity of 22 m/s (72.2 ft/s) and P is the specimen contact pressure at ignition (Loading force/initial contact area). Tests were conducted by keeping *v* constant and increasing *P* at a rate of 35 N/s (7.86 lbf/s) until ignition.

* This material did not ignite at these Pv products.

[b] [2]

[c] [7]

[d] [3]

[e] [4]

All unreferenced data is from previously unpublished frictional heating tests performed at NASA White Sands Test Facility.

TABLE 2--Friction ignition test data for dissimilar pairs of test specimens.[a]

Test materials		Pv product at ignition	
Stator	Rotor	$W/m^2 \times 10^{-8}$	($lbf/in^2 \times ft/min \times 10^{-6}$)
Monel K-500	Hastelloy C-22	1.57 - 3.72	4.51 - 10.61
Monel K-500	Hastelloy C-276	1.41 - 2.70	4.00 - 7.70
Monel K-500	Hastelloy G30	1.34 - 1.62	3.81 - 3.87
Ductile cast iron	Monel 400	1.28 - 1.45	3.65 - 4.13[a]
Gray cast iron	410 SS	1.19 - 1.48	3.39 - 4.24[a]
Gray cast iron	17-4 PH (H 1150 M)	1.17 - 1.66	3.35 - 4.75[b]
Cu Be	Monel 400	1.10 - 1.20	3.14 - 3.42
Ductile cast iron	410 SS	1.10 - 1.23	3.12 - 3.43[b]
AISI 4140	Monel K-500	1.09 - 1.35	3.10 - 3.85[b]
Ductile cast iron	17-4 PH (H 1150 M)	1.09 - 1.17	3.00 - 3.35[b]
Monel 400	Nitronic 60	1.03 - 1.69	2.93 - 4.78[c]
Inconel 718	17-4 PH SS	1.02 - 1.12	2.91 - 3.20[c]
Bronze	Monel K-500	0.99 - 1.84	2.82 - 5.26[b]
Tin bronze	304 SS	0.97 - 1.25	2.78 - 3.56[b]
Monel K-500	Inconel 625	0.93 - 2.00	2.67 - 5.70
17-4 PH SS	Hastelloy C-22	0.93 - 1.00	2.65 - 2.86
Monel K-500	304 SS	0.92 - 1.13	2.63 - 3.24[c]
Inconel 718	304 SS	0.90 - 1.18	2.58 - 3.37[c]
17-4 PH SS	Hastelloy C-276	0.89 - 1.10	2.55 - 3.14
Bronze	17-4 PH (H 1150 M)	0.89 - 1.02	2.55 - 2.90[b]
316 SS	303 SS	0.89 - 0.90	2.53 - 2.57[c]
Inconel 718	316 SS	0.86 - 0.96	2.44 - 2.73[c]
Monel 400	304 SS	0.85 - 0.94	2.43 - 2.69[c]
17-4 PH SS	Hastelloy G30	0.84 - 1.02	2.41 - 2.90
Monel K-500	303 SS	0.84 - 1.00	2.41 - 2.88
Ductile cast iron	Stellite 6	0.84 - 1.16	2.39 - 3.32[b]
Cu Zr	316 SS	0.83 - 0.90	2.39 - 2.58
Ductile cast iron	Tin bronze	0.81 - 1.69	2.32 - 4.82[b]
Monel K-500	17-4 PH SS	0.80 - 1.00	2.27 - 2.39[c]
Bronze	410 SS	0.79 - 1.20	2.25 - 3.60[b]
304 SS	303 SS	0.77 - 0.78	2.21 - 2.26[c]
Tin bronze	Aluminum bronze	0.77 - 0.84	2.20 - 2.38[b]
316 SS	17-4 PH SS	0.77 - 0.85	2.18 - 2.41[c]
Monel 400	303 SS	0.76 - 0.93	2.17 - 2.67[c]
304 SS	17-4 PH SS	0.75 - 1.09	2.14 - 3.12[c]
Inconel 718	303 SS	0.75 - 0.86	2.14 - 2.48[c]
Monel K-500	316 SS	0.73 - 0.91	2.10 - 2.61[c]
316 SS	304 SS	0.68 - 0.91	1.93 - 2.60[c]
Stellite 6	Nitronic 60	0.66 - 0.77	1.90 - 2.18[b]
Monel 400	17-4 PH SS	0.66 - 1.53	1.89 - 4.38[c]
303 SS	17-4 PH SS	0.65 - 0.88	1.86 - 2.51
17-4 PH SS	Inconel 625	0.64 - 1.09	1.83 - 3.11
304 SS	Cu Be	0.63 - 1.24	1.81 - 3.54
Monel 400	316 SS	0.62 - 0.91	1.75 - 2.59

[a] Tests were conducted by keeping *v* constant at 22 m/s (72.2 ft/s) and increasing *P* at a rate of 35 N/s (7.86 lbf/s) until ignition.

[b] [7]

[c] [4]

All unreferenced data is from previously unpublished frictional heating tests performed at NASA White Sands Test Facility.

TABLE 2 (Cont'd)--Friction ignition test data for dissimilar pairs of test specimens.[a]

Test materials		Pv product at ignition	
Stator	Rotor	W/m^2 × 10^{-8}	(lbf/in^2 × ft/min × 10^{-6})
Ductile Cast iron	Nitronic 60	0.44 - 0.75	1.25 - 2.15[b]
Aluminum bronze	C355 Aluminum	0.30 - 0.32	0.85 - 0.91[b]
Nitronic 60	17-4 PH (H 1150 M)	0.28 - 0.61	0.80 - 1.75[b]
Babbitt on bronze	17-4 PH (H 1150 M)	0.09 - 0.21	0.25 - 0.60[b]
Babbitt on bronze	Monel K-500	0.09 - 0.19	0.25 - 0.55[b]
Babbitt on bronze	410 SS	0.08 - 0.09	0.24 - 0.27[b]

[a]Tests were conducted by keeping *v* constant at 22 m/s (72.2 ft/s) and increasing *P* at a rate of 35 N/s (7.86 lbf/s) until ignition.

[b] [7]

[c] [4]

All unreferenced data is from previously unpublished frictional heating tests performed at NASA White Sands Test Facility.

TABLE 3--Comparison of frictional heating tests in LOX and GOX.

Material		PV product (W/m^2 × 10^{-8})		Reaction	
Stationary	Rotary	GOX	LOX	GOX	LOX
Inconel 718	Inconel 718	0.96 - 1.18	3.85	Yes	Yes
Monel K-500	Monel K-500	1.37 - 1.69	4.15 - 4.23	Yes	No
Inco MA754	Inco MA754	3.96 - 4.12	3.29 - 4.03	No	No
Haynes 214	Haynes 214	3.05	3.79 - 4.09	Yes	No
AMS 6278	AMS 6278	1.82	3.34	Yes	Yes
Al 6061T6	Al 6061T6	0.48	...	Yes	...
Al 2219	Al 2219	...	1.72	...	Yes
Monel K-500	Kel-F	...	0.23 - 0.45*	...	No
Monel K-500	Vespel SP21	...	1.52	...	Yes

* Sample deformation before ignition

DISCUSSION

The data in Tables 1 through 3 are useful for many applications, such as selecting materials for bearings for use in oxygen and hazards analyses in design of oxygen systems.

Hydrodynamic bearings experience unavoidable rubbing when starting and stopping; this rubbing causes heating due to friction. The materials selected for hydrodynamic foil bearing applications must withstand this severe operational condition when starting and stopping without ignition. The approach to selecting materials for bearings for use in oxygen would be to first determine the use conditions and then to perform tests to evaluate the performance of the materials under these conditions [11]. The tests could be material, configurational, and component tests. The material tests such as the frictional heating test determine the materials ignition resistance using standard samples. The configurational tests determine the behavior of the materials using test fixtures and conditions approximating configuration and conditions in actual use. The component tests verify the component and sometimes serve as acceptance tests using the actual hardware. Tests were conducted in a standard frictional heating apparatus with samples made of coated and uncoated Inconel 718 and Inconel X750. It was determined that the coating did not adversely affect the Pv_{ign}. Additionally, tests were conducted by using the loads and speeds closely resembling use conditions. No ignitions were observed. However, because the standard test samples were bulkier than the actual foil bearings, component tests are required if the materials are to be used.

An example of how the above approach was used was given by Dees et al. [11]. The frictional heating test was used for Space Suit HIP Rotator Bearing material analysis. The bearing consists of a bearing ring and race element made of Ti-6Al-4V, 440C stainless steel balls, Vespel SP-1 or Delrin spacer balls, and polyurethane environmental and lip seals. Failure of one or more ball bearings could result in an ignition induced by the friction of the bearing assembly materials. The data represented in Table 1 indicate that Ti-6Al-4V is susceptible to ignition at relatively low Pv's. Further tests conducted at 57.2 kPa (8.3 psia) at low rubbing velocities to simulate actual bearing dynamics resulted in ignition of the samples.

The risk of fire hazards in oxygen systems can be assessed by a hazard analysis. The hazard analysis involves identifying the ignition sources (rubbing, particle impact, mechanical impact, kindling chain etc.) and identifying design parameters such as gas pressure, gas temperature, flow velocity, geometrical configurations, material selection. To ensure a safe design, it is very important that the hazard analysis is done before designing the system. Quantifying probabilities for the ignition sources is difficult, but a qualitative approach will help design safe oxygen systems. In a hazard analysis on oxygen systems where friction is a credible ignition source, the use conditions can be estimated and then if the Pv estimated from the use conditions is greater than the Pv_{ign}, it can be assumed that frictional ignition may be possible in the system.

SUMMARY

Frictional heating test results were reviewed and examples of how the data could be applied for selecting materials for oxygen use when friction was a credible ignition source were given. The frictional heating test system performs well (gives repeatable results) when evaluating susceptibility to ignition by friction, but does not perform well for extracting tribological characteristics (coefficient of friction and wear). The resistance to ignition as measured with Pv products required for ignition in LOX is three to four times the resistance to ignition in GOX.

REFERENCES

[1] Benz, F. J. and Stoltzfus, J. M., "Ignition of Metals and Alloys in Gaseous Oxygen by Frictional Heating," Flammability and Sensitivity of Materials in Oxygen-Enriched Atmospheres, Vol. 2, ASTM STP 910, M. A. Benning, Ed., American Society For Testing Materials, Philadelphia, PA, 1986, pp. 38-58.

[2] Stoltzfus, J. M., Benz, F. J., and Homa, J., "The Pv Product Required for the Frictional Ignition of Alloys," Flammability and Sensitivity of Materials in Oxygen-Enriched Atmospheres, Vol. 4, ASTM STP 1040, J. M. Stoltzfus, F. J. Benz, and J. S. Stradling, Eds. American Society For Testing Materials, Philadelphia, PA, 1989, pp. 212-213.

[3] Gunaji, M. V., "KSC Metals Flammability Test: Frictional Heating," Special Test Data Report # 90-24221, NASA Johnson Space Center White Sands Test Facility, NM, 1990.

[4] Schoenman, L., Stoltzfus, J., and Kazaroff, J., "Friction-Induced Ignition of Metals in High-Pressure Oxygen." Flammability and Sensitivity of Materials in Oxygen-Enriched Atmospheres, Vol. 3, ASTM STP 986, M. A. Benning, Ed., American Society For Testing Materials, Philadelphia, PA, 1987, pp. 105-133.

[5] Jenny, R., and Wyssmann, H., "Friction-Induced Ignition in Oxygen." Flammability and Sensitivity of Materials in Oxygen-Enriched Atmospheres, Vol. 2, ASTM STP 812, B. Werley, Ed., American Society For Testing Materials, Philadelphia, PA, 1983, pp. 150-166.

[6] Stoltzfus, J. M., Homa, J. M., Williams, R. E. and Benz, F. J., "ASTM Committee G-4 Metals Flammability Test Program: Data and Discussion," Flammability and Sensitivity of Materials in Oxygen-Enriched Atmospheres, Vol. 3, ASTM STP 986, D. W. Schroll, Ed., American Society For Testing Materials, Philadelphia, PA, 1988, pp. 28-53.

[7] Stoltzfus J. M. and Gunaji, M. V., "Test Methods For Determining The Suitability of Metal Alloys For Use in Oxygen-Enriched Environments". Technology 2001, The Second National Technology Transfer Conference and Exposition, Vol. 1, NASA Conference Publication 3136, San Jose, CA., Dec 3-5, 1991, pp. 183-192.

[8] Adamson, A. W., Physical Chemistry of Surfaces, 3rd ed. John Wiley & Son, New York, 1973.

[9] Gunaji, M. V., Stoltzfus, J. M., Schoenman, L., and Kazaroff, J., "Surface Modification of Monel K-500 as a Means of Reducing Friction and Wear in High-Pressure Oxygen," Symposium on Flammability and Sensitivity of Materials in Oxygen-Enriched Atmospheres, Vol. 4, ASTM STP 1040, Joel M. Stoltzfus, Frank Benz, and Jack Stradling, Eds., American Society For Testing Materials, Philadelphia, PA, 1989, pp. 332-346.

[10] Bryan, C. J., Stoltzfus, J. M., and Gunaji M. V., "An Assessment of the Metals Flammability Hazard in the Kennedy Space Center Oxygen Systems," Flammability and Sensitivity of Materials in Oxygen-Enriched Atmospheres, Vol. 5, ASTM STP 1111, Joel M. Stoltzfus and Kenneth McIlroy, Eds., American Society For Testing Materials, Philadelphia, PA, 1991, pp. 453-462.

[11] Dees, J., Peterson, J., and Stoltzfus J. M. "Selection of Materials for Bearing Applications in Oxygen," 1992 Conference on Advanced Earth-to-Orbit Propulsion Technology, University of Alabama, AL, May 19-21, 1992.

[12] Zhu, S. H., Stoltzfus, J. M., Benz, F. J., and Yuen, W. W., "Modeling and Data Analysis of the NASA-WSTF Frictional Heating Apparatus: Effects of Test Parameters on Friction Coefficient," Flammability and Sensitivity of Materials in Oxygen-Enriched Atmospheres, Vol. 3, ASTM STP 986, Edited by D. W. Schroll, American Society For Testing Materials, Philadelphia, PA, 1988, pp. 172-187.

[13] Yuen , W. W., "Modelling and Data Evaluation of the WSTF Frictional Heating Test Facility," Flammability and Sensitivity of Materials in Oxygen-Enriched Atmospheres, Vol. 4, ASTM STP 1040, Joel M. Stoltzfus, Frank J. Benz, and Jack Stradling, Eds. American Society For Testing Materials, Philadelphia, PA, 1989, pp. 76-90.

Michael J. Yentzen[1]

Evaluation of Bronze Alloys for use as Wear Ring Material in Liquid Oxygen Pump

REFERENCE: Yentzen, M. J., "Evaluation of Bronze Alloys for Use as Wear Ring Material in Liquid Oxygen Pump," Flammability and Sensitivity of Materials in Oxygen-Enriched Atmospheres: 6th Volume, ASTM STP 1197, Dwight D. Janoff and Joel M. Stoltzfus, Eds., American Society for Testing and Materials, Philadelphia, 1993.

ABSTRACT: The selection of materials for wear parts in oxygen pumps or compressors is critical from an oxygen compatibility perspective because the function of the part is to absorb frictional energy. Part of this energy is absorbed by the sample as heat and can cause ignition of the material. There is little data on the compatibility of bronze alloys typically used for wear parts in oxygen systems, so it is difficult to ensure that the most compatible materials are used.

This paper discusses frictional heating test data obtained for seven bronze alloys which could be used in certain applications as wear parts. A test apparatus developed by the NASA test facility at White Sands to determine the resistance of materials to ignition by friction was used to obtain the data. The bronzes evaluated were selected based on the ability to function mechanically in the intended application and the anticipated resistance to ignition by friction. The alloys were ranked according to the resulting pressure-velocity (PV) product. This factor serves as a measure of the load required for ignition given a constant sample load rate, a constant gaseous oxygen pressure, and a constant sample rotational velocity. Factors influencing the test results including sample composition, material properties, and test procedures are addressed. A simple theoretical description of the phenomenon of ignition by friction is presented to explain the effects that the proposed variables may have on the PV product.

KEY WORDS: bronze alloys, friction, ignition, frictional heating test, wear ring, liquid oxygen pump.

---

[1] Materials Engineer, Propulsion Test Operations, National Aeronautics and Space Administration, John C. Stennis Space Center, MS 39529

To determine the theoretical value of Q_{ig}, the integral in Equation 1 is evaluated with respect to time from t=0 to the time of ignition. The modes of heat generation are specified by the Q subscript, but the modes of heat loss are lumped into one heading. Q_{loss} includes the heat required to melt the material, the heat absorbed or generated during phase changes, the heat loss from convective cooling, the heat loss from conduction, and the radiant heat loss.

Since all the Q values on the right side of the equation are time dependent material specific properties, it should be possible to calculate the Q_{ig} value for various materials and material combinations. In addition it has been shown that for most metals or alloys there is a certain sample temperature above which the oxidation reaction becomes self-accelerating [1]. In the case of the frictional heating test, this correlates to the ignition temperature of the material. This value is proportional to Q_{ig} plus an offset value to correct for the initial sample temperature. Since Q_{ig} is a sum of heat generation rates and losses, it is a time dependent variable which is proportional to the power transferred to the sample interface as heat. For a given sample material the ignition temperature is proportional to the net applied power if the initial interface temperature is specified. This ignition temperature is independent of how the energy is applied to heat the samples or how fast the temperature rise occurs. Jenny and Wyssmann provided a coherent discussion to demonstrate how a higher initial sample temperature decreases the power required for ignition but does not affect the ignition temperature. They also have used this simple energy input model to predict ignition times and temperatures for various material pairs [2].

Several macroscopic properties including composition, coefficient of friction, and compression strength will be discussed in terms of how they affect the PV product of the sample couple. These factors were selected based on their apparent relation to the Q_{ig} value from Eq 1. For example, compositional differences may affect the resulting PV product of a test by changing the Q_{ox}, Q_{fric}, or Q_{loss} of the material. The coefficient of friction will obviously influence the PV product by affecting the Q_{fric} portion of Equation 1. The compression strength of the material will influence the rate of energy consumption by work required to deform the sample. This value, designated as Q_w, was included by Stoltzfus et al. [3] and Benz and Stoltzfus [4] in their equations defining the rate of heat accumulation in the samples. Even though it may be a significant factor in calculating the time required for ignition, it was not included in Equation 1 because it is a mechanical and not a thermodynamic value.

EXPERIMENTAL

Material Selection

Six bronze alloys were selected as possible replacements for the C94300 high-leaded tin bronze that is currently being used for wear parts in the liquid oxygen transfer pump. These materials (Table 1) were selected primarily on the basis of their suitability to the application as wear components. The coefficients of thermal expansion

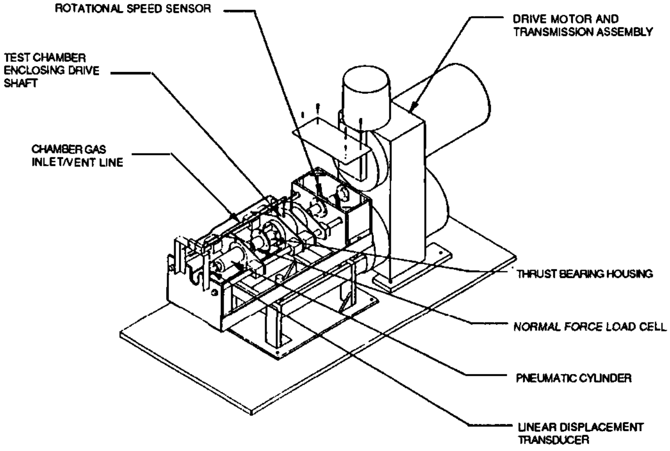

FIG. 1--Frictional Heating Test Apparatus

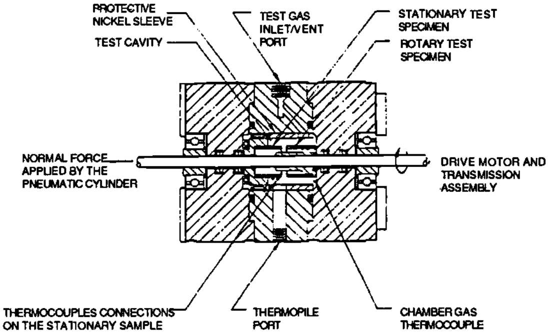

FIG. 2--Frictional Heating Test Chamber

sample was mounted on a rotating shaft connected to a 15 hp electric motor capable of rotational speeds from 1 000 to 20 000 rpm. The other sample was mounted in the test chamber. A normal load was applied to the sample couple by using a pneumatic cylinder to translate the stationary sample toward the drive motor assembly. The test parameters used were the standard ones established by Benz and Stoltzfus [5]. This was done so that the PV products could be compared to previous data collected at WSTF. The rotational velocity of the sample was approximately 17 000 rpm. This translates into an average linear velocity of approximately 20.3 m/s (66.8 ft./s) at the middle of the sample surface. The operating speed of the pump is 3 600 rpm and the cover wear ring outer diameter is approximately 15.5 cm (6.1 in.). This correlates to a maximum linear velocity of 29.2 m/s (96.1 ft./s) where the inside of the impeller may strike the cover wear ring. The case wear ring inner diameter is approximately 16.8 cm (6.6 in.). This gives a maximum linear velocity of 31.7 m/s (104.3 ft./s) where the outside of the impeller may strike the case wear ring. The similarity between these velocities and the linear velocity at the surface of the test specimens enabled a close approximation of the actual operating environment while still adhering to standard test conditions.

The load ramp rate used was approximately 31.1 N/s (7 lbf/s). The chamber was pressurized with gaseous oxygen at 6.9 MPa (1 000 psia). There was no method for controlling the chamber temperature, but it was recorded prior to testing and monitored throughout the test using a sheathed thermocouple. Temperatures were also measured at two spots on the stationary sample using thermocouples. A thermopile was used to detect changes in radiated heat from the sample interface. The normal load was measured by a 4 450 ± 22 N (1 000 ± 5 lbf) load cell, and the torque from the sample couple was measured by an 890 ± 5 N (202 ± 1 lbf) load cell. Axial displacement of the stationary sample on the drive shaft was measured using a linear displacement transducer with an accuracy of ± 0.013 cm (0.005 in). The rotational speed was measured by an rpm indicator with an accuracy of ± 3%. The pressure in the gas chamber was measured using a 68.9 ± 0.7 MPa (10 000 ± 100 psia) digital Bourdon tube gauge. The pressure in the pneumatic cylinder was measured by a strain gauge transducer with a measurement capability of 6.9 ± 0.07 MPa (1 000 ± 10 psia).

Sample Preparation

Two of the materials (C93200 and C93600) tested were purchased as continuously cast rods. The other five materials were sand castings. In addition to the bronze alloys, several rods of annealed 304 stainless steel were purchased for the tests. Nine test specimens (Fig. 3) were machined from each bronze rod, and twenty seven specimens were machined from the stainless steel rods. This allowed three tests for each bronze sample as both the rotary and stationary sample and three tests for each bronze as stationary sample coupled with a rotary sample of 304 stainless steel. The 304 stainless steel/bronze tests were designed to emulate the actual use configuration of the wear parts since the pump impeller is made from 304 stainless steel. Three additional tests with 304 stainless steel as both the rotary and stationary samples were performed to correlate the data accumulated at MSFC with previous test results from WSTF.

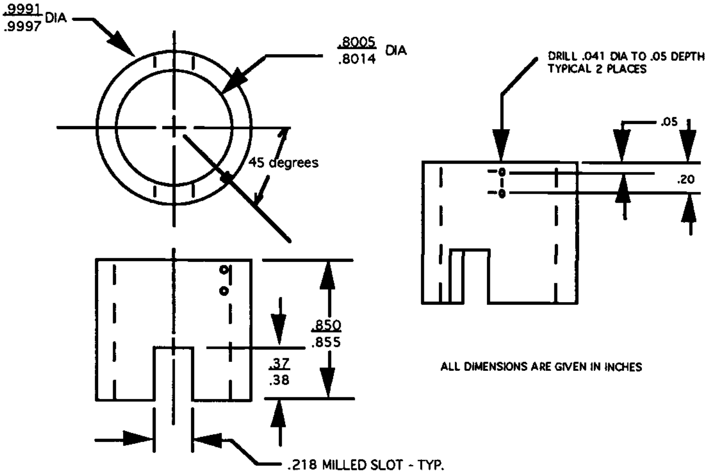

FIG. 3--Frictional Heating Sample Specifications

RESULTS

PV Products

The PV products (Table 2) were calculated by taking the load value at the point of ignition dividing it by the initial cross sectional area of the sample and multiplying it by the average velocity at the surface of the specimen. The ignition point is marked by a dramatic increase in the displacement reading usually matched by a peak temperature measurement from the thermocouple mounted nearest to the sample surface. The ranking of the alloys based on the ss/bronze tests differed significantly from the ranking based on the bronze/bronze tests especially for the C86400 manganese bronze and the C95200 aluminum bronze. These two alloys, which performed poorly in the bronze/bronze tests, ranked first and third highest in the ss/bronze tests. One possible explanation is that the coefficient of friction for these alloys is significantly higher when rubbing them against themselves than when rubbing them against 304 stainless steel.

TABLE 2--PV Products Required for Ignition[a]

Alloy UNS	Minimum PV Product Required for Ignition ($x10^{-8}$ W/m^2)		
	304 ss/bronze test	bronze/bronze test	
C90700	.98	1.88	
C90300	1.14	1.81	
C93200	1.48	1.56	
C94300	1.09	1.24	
C93600	.57	1.17	
C95200	1.39	.99	2 tests only
C86400	3.40	.83	

[a] Samples were listed in descending order of bronze/bronze PV product.

DISCUSSION

Coefficients of Friction

For a rotating hollow cylinder the coefficient of kinetic friction may be derived by the following equation [6]:

$$\mu_k = \frac{3}{2}\frac{M}{P}\frac{R_2^2 - R_1^2}{R_2^3 - R_1^3} \qquad (2)$$

where

μ_k = the coefficient of kinetic friction,
M = the axial moment (torque) applied to the cylinder, Nm,
P = the normal force exerted on the cylinder, N,
R_2 = the outer radius of the cylinder, m, and
R_1 = the inner radius of the cylinder, m.

The coefficients of friction were calculated by using the average torque value and average normal load for every tenth of a second during the second prior to ignition unless otherwise noted. The results are shown in Table 3.

TABLE 3--Average Coefficient of Friction Values[a]

	Average Coefficient of Kinetic Friction (μ_k)		
Alloy	304 ss/bronze test	Alloy	bronze/bronze test
C86400	.005[b] 2 tests	C90700	.013
C93200	.007	C90300	.015
C95200	.009 2 tests	C93200[c]	.011 2 tests
C90300	.004 2 tests	C94300	.024 2 tests
C94300	.015 2 tests	C93600	.020 2 tests
C90700	.012 1 test	C95200	.026 2 tests
C93600	.009	C86400	.043

[a] Samples were listed in descending order of PV product for each test.

[b] Calculated by using the data for the ten seconds prior to reaching the maximum load (one data point per second).

[c] Data for one of the two tests was taken during the second prior to reaching the maximum load.

In general, the coefficient of kinetic friction calculated from the bronze/bronze test data can be correlated to the PV product of the test. This trend, which shows a decrease in PV product as the coefficient of kinetic friction increases, indicates that the coefficient of kinetic friction is one of the most important factors in determining the PV product required for ignition for bronze/bronze tests. The significant exception to this trend is the C93200 bronze. The coefficient of friction for the C93200 during the bronze/bronze test was averaged down by one test during which the sample did not ignite. This test achieved an exceptionally high PV product; however the PV product was not reflected in the rankings because the alloys were ranked by the minimum PV product required for ignition. The ss/bronze tests do not show an apparent correlation between the PV product ranking and the coefficient of friction values. This would seem to indicate that the Q_{frict} value is not as important in ss/bronze tests as it is for bronze/bronze tests. The large increase in μ_k values for the C86400 and C95200 alloys during the bronze/bronze tests as compared to the ss/bronze tests may explain the low PV products for bronze/bronze tests; however, the C90300 alloy experienced a comparable increase in μ_k during the ss/bronze test as compared to the bronze/bronze test while achieving a higher PV product.

Since a good correlation between the μ_k and the PV product exists for bronze/bronze tests, it would seem to provide an ideal method for ranking the resistance to frictional ignition of at least some alloys without actually performing frictional heating tests. This would be possible if the μ_k values calculated by the frictional heating test could be correlated to the μ values determined by ordinary methods; however, this relationship seems unlikely for two reasons. First, ordinary methods for determining μ are not conducted in pressurized GOX. The formation of oxides will definitely affect the value of μ and variations in the pressure of the oxygen may change the relative values of μ for different materials. In addition, such high loads are reached during the frictional heating test that the μ_k measurement may be more representative of galling than controlled frictional rubbing typically conducted at relatively modest loads.

Effect of Ramping Load on Ignition Data

One possible misleading result which could occur during the frictional heating test is an increase in the PV product due to mechanical deformation of the material. Equation 1, from the Theoretical section, reflects the heat generated from the power applied to the sample couple interface; however, it does not consider the effect of the applied load on the physical condition of the sample material. The use of a constant load tends to minimize the effects of mechanical properties on the time required for ignition determined by the frictional heating test. This occurs because little time is required to reach the predetermined testing load during a constant-load test. Furthermore, the load utilized during the constant load tests performed by Jenny and Wyssmann [2] was much lower than the load which is reached when testing most samples using the standard WSTF load ramp rate. Therefore, if deformation does occur during the constant load test, it is less significant than the sample compression which is caused by a typical ramping load frictional heating test.

This theory may help explain the conflicting results regarding the ranking of tin bronze and gray cast iron reported by Jenny and Wyssmann compared to the ranking by Stoltzfus et al. Jenny and Wyssmann found that a gray cast iron/stainless steel pair required a much higher critical load for a specific ignition time than a C90700 tin bronze pair [2]; however, Stoltzfus et. al. found that the C90700 tin bronze required an average PV product of 2.15×10^8 W/m^2 while a gray cast iron/410 stainless steel pair required an average PV product of 1.35x10^{8} W/m^{2} [3]. Jenny and Wyssmann's test configuration used a constant load whereas Stoltzfus et al. used a ramping load. Since C90700 tin bronze has a lower compressive strength (89.7 MPa) [7] than gray cast iron (568.4 MPa - 1284.0 MPa) [8] and assuming that the temperature dependence on their mechanical properties is similar, then it is reasonable to conclude that for a given maximum load and temperature the tin bronze will deform more than the gray cast iron. The effect of this deformation would be more pronounced when applying higher loads as in the case of the 1 931 N (434 lbf) load achieved by WSTF while igniting a C90700 couple (PV product of 2.15x10^{8} W/m^{2}) than it would when using the relatively small constant load (approximately 500 N (112 lbf)) that Jenny and Wyssmann used for their C90700 tin bronze tests. Stress values at failure could not be compared because the dimensions of the Jenny and Wyssmann test samples were not available. However, it appears from photographs of the test apparatus that the stressed area is larger in the Jenny and Wyssmann samples than the WSTF samples. This would produce a greater difference between the stress values after they are calculated from the load values, adding more support to the theory that the mechanical properties of a test sample may affect its PV product during a ramping load test.

Even though the compressive strength of the C90700 tin bronze was not exceeded, this does not mean that significant plastic deformation of the sample could not have occurred. The compressive strength data is provided at ambient temperature - higher temperature compression data could not be found; however, an appreciable drop in the compressive strength would be expected at higher temperatures. The temperature dependence of compressive strength data is discussed later in the mechanical properties section.

Another instance in which the choice of constant versus ramping load rates may affect test results occurs when the rates of heat generation and loss are strongly dependent on the thickness of the oxide layer present on the sample. A ramping load may disrupt all oxide layers or it may selectively disrupt certain metal oxides. In either case this will produce rates of heat generation and loss which may differ from those produced by a constant load test. In this way, the material rankings determined by a ramping load test may not be comparable to the relative results of a constant load test.

Mechanical Properties

The maximum load which can be obtained using the WSTF frictional heating apparatus is 4 450 N (1 000 lbf) resulting in a maximum pressure of approximately 24.7 MPa (3 576 psi) (assuming a constant cross sectional area). The compressive strengths of the alloys at .001" permanent set (Table 4) are at least 75.9 MPa (11 000 psi), so the maximum stress generated should not be enough to deform the samples significantly under compression; however, the compressive strength of these alloys should decrease dramatically as a function of temperature. In general, yield strength, tensile strength, and modulus of elasticity decrease at higher temperatures [9]. By analogy, it can be assumed that compression strength usually decreases with an increase in temperature as well. The reduction in compressive strength at higher temperatures could be sufficient at higher loads to cause the bronzes to mechanically deform during testing. Further investigation into the temperature dependence of the compressive strengths of these seven alloys could be used to verify this conclusion.

TABLE 4--Displacement During Friction Test and Compressive Strength[a]

Alloy UNS	Average Displacement cm (in)		Compressive Strength at .001″	
	ss/bronze	bronze/bronze	MPa	psi
C94300	.20 (.080)[b]	.10 (.041)	75.9	11 000
C90300	.21 (.083)	.23 (.092)	89.7	13 000
C90700	.21 (.084)	.23 (.090)	89.7	13 000
C93200	.24 (.094)	.09 (.036)	xx.x	xx xxx[c]
C93600	.23 (.090)	.06 (.025)	xx.x	xx xxx[d]
C86400	.80 (.316)[e]	.02 (.007)	150.0	22 000
C95200	.41 (.162)	.01 (.004)	186.3	27 000

[a] Compressive strength data was supplied by the vendor or taken from the Ninth Edition of the ASM Handbook (Vol.2).

[b,e] Tabular data from only two tests were used to calculate these displacement values.

[c,d] Data for .1″ compressive strength identifies that these alloys are ranked appropriately on the table; however, no data on .001″ compressive strength could be found.

The average displacement values were calculated from the tabular data generated by the linear displacement transducer. The net displacement from each test was calculated by subtracting the initial linear displacement value from the final linear displacement taken .1 seconds prior to ignition. These values were averaged from at least two tests (during two tests the linear transducer did not function properly) to obtain the average displacement values given in Table 4. These values indicate the actual linear translation of the test couple, so they may represent displacement caused by mechanical deformation (both plastic and elastic), sample wear, and volumetric changes of the sample materials (due to oxidation, phase changes, or thermal expansion).

In order to determine if significant mechanical deformation of the specimens had occurred, the average displacement for each material combination was compared to the compressive strength of the bronze alloy (Table 4). The data shows that there is a relationship between the compressive strength of the alloy and the resulting displacement derived from the bronze/bronze frictional heating test data. This correlation between displacement and mechanical properties implies that sample deformation has occurred to some extent. All the bronzes confirm this relationship except the C94300 leaded bronze. The reason for this apparent anomaly is unknown, but it may relate to the fact that the displacement value is an indication of sample wear as well as sample deformation (i.e. the C90300 and C90700 tin bronzes could have experienced significantly more wear than the C94300 high-leaded bronze which might help to explain the difference in displacement values).

The displacement data calculated from the ss/bronze tests do not correlate well to the compressive strengths of the materials. This might be explained in part by the fact that load values attained in the ss/bronze tests in most cases were much lower than those reached during the bronze/bronze tests. This occurred because the most of the alloys ignited at a lower PV product during the ss/bronze tests. The two exceptions to this tendency are C86400 and C95200 which experienced a significant increase in displacement values during the ss/bronze tests as compared to the bronze/bronze tests. This could be explained by the fact that the displacement values also measures sample wear; consequently, it is assumed that for these two materials the majority of the displacement occurs as a result of sample wear and not mechanical deformation.

Composition

Since the solubility of lead in copper is low (only 0.05 wt.% at 954° C [10]), the microstructure of a cast copper-lead alloy consists of lead globules in a copper matrix. During rubbing these globules serve as the source of a thin film of lead which helps to lubricate the bearing surface. Since the maximum solubility of Pb in solid Sn is 2.5 wt.% and the maximum solubility of Sn in solid Pb is 19 wt.% [11], the copper-tin-lead alloys contain a similar microstructure consisting of lead spheroids dispersed in a Cu-Sn matrix. The effect of this high lead content on the resulting PV product was not fully understood. On one hand it might increase the PV product by decreasing the rate of heat generated by friction; however, since a film of lead is formed at the surface of the interface, the high lead content might lower the ignition temperature of the material and consequently lower the PV product.

With few exceptions, the PV products from the bronze/bronze frictional heating tests followed the anticipated results based on composition. The C86400 manganese bronze yielded a lower than anticipated PV product in the bronze/bronze frictional heating tests; however, it did not ignite in three tests when rubbed by 304 stainless steel. This unexpected result may be explained in part by the high coefficient of friction measured for the C86400 alloy when tested with itself. This produced a large Q_{frict} term which achieved Q_{ig} in a very short time resulting in a very small PV product. The large displacement value achieved by the C86400 without ignition when tested with 304 stainless steel along with the fact that the displacement appears to be relatively linear suggests that the C86400 sample experiences an alternating process of controlled oxidation and wear. A visual inspection of the post test sample also indicates that a considerable amount of sample wear has occurred.

The C90700 and C90300 tin bronze tests resulted in the highest minimum PV products. The slightly higher PV product achieved by the C90700 alloy as compared to the C90300 bronze may be the result of the addition of tin in place of the four percent zinc. The C90300 tin bronze has a higher PV product than the C93200 leaded tin bronze in bronze/bronze tests but the reverse is true for ss/bronze tests. This implies that the addition of seven percent lead in place of copper improves the ignition properties when rubbed against 304 stainless steel or that it adversely affects the ignition properties when rubbed against itself.

The C94300 leaded bronze yields a higher PV product than the C93600 leaded bronze in both the ss/bronze and the bronze/bronze tests. This result indicates that increasing the lead content from twelve percent to twenty-five percent improves the PV product of the material. This higher PV product may be the result of a decrease in the compressive strength of the higher lead alloy. The information from Table 4 which indicates that the C94300 bronze experienced approximately one and one-half times the displacement that the C93600 alloy experienced during the bronze/bronze frictional heating tests tends to imply that the reduction in compressive strength is at least partially responsible for the increase in the PV product.

CONCLUSIONS

For the alloys tested there was good correlation between the PV product and the coefficient of friction for the bronze/bronze test series; however, the values of the coefficient of friction calculated for the ss/bronze tests did not demonstrate a similar relationship. The change in μ_k values between the ss/bronze tests and the bronze/bronze tests explained some of the differences in rankings between the two series; however, a complete explanation was not achieved.

The most significant compositional effect seemed to be the lead content. In general, the two tin bronzes which contained less than .5% lead (C90300 and C90700) achieved a higher PV product than the leaded tin bronzes in bronze/bronze tests; however, during the ss/bronze tests the tin bronzes ignited at lower PV products than the C93200 leaded bronze. This is difficult to explain based on the current information. More PV product data on similar and dissimilar test couples of varying compositions is needed to properly evaluate this result. In the interim it is reasonable to conclude that the tin bronzes with minimal lead content will be more resistant to ignition by friction than the leaded bronzes in bronze on bronze rubbing applications; however, a moderate amount of lead may increase the relative ignition of bronzes when rubbed by stainless steels. From a comparison of the C93200 alloy (7% Pb) to the C90300 alloy (0% Pb), it was recognized that the addition of seven percent lead to a tin bronze alloy containing virtually no lead resulted in a lower PV product in bronze/bronze tests and a higher PV product in ss/bronze tests. From a comparison of the C94300 alloy (25% Pb) to the C93600 alloy (12% Pb), it was also demonstrated that increasing the lead content from twelve percent to twenty-five percent increases the PV product in both ss/bronze tests and bronze/bronze tests. Displacement data indicated that this might be caused at least part by the lower compressive strength of the C94300 alloy compared to the C93600 alloy. An inverse relationship between the compressive strengths of the alloys and the resultant PV products in the bronze/bronze series offered additional support for the suggestion that the compressive strengths of the alloys could have influenced the PV product rankings.

RECOMMENDATIONS

As the PV products from the ss/bronze and bronze/bronze tests suggest, the relative resistance to ignition by friction of any alloy depends significantly on the material against which the test alloy is rubbed. Since the current application calls for a material to be used as a wear ring in combination with a 304 stainless steel impeller, the minimum PV products for the ss/bronze frictional heating test are most useful. To provide a basis for comparison, the actual PV products at the case and cover wear rings were calculated after several assumptions were made. A previous study on the LOX pump bearings had determined that the maximum radial load on the bearings was 110 N (25 lbf). This would generate a maximum load of the same magnitude between the impeller and case or cover wear rings should the impeller become slightly unbalanced, so 110 N (25 lbf) was used as the contact force between the impeller and the wear rings. CAD drawings of the impeller and wear ring interfaces indicated that the contact area was almost one-half of the total interface area. One-fourth of the area was used in the PV product calculations to ensure that a conservative contact stress was calculated. The contact stresses of the case and cover wear rings were calculated to be 29 578 Pa (4.3 psig) and 35 921 Pa (5.2 psig) respectively. Using the previously calculated surface velocities, the PV products for the case and cover wear rings was found to be $.0094 \times 10^8$ W/m^2 and $.0105 \times 10^8$ W/m^2 respectively. Comparing the actual PV product results from the ss/bronze tests indicates that all of the alloys tested would provide adequate protection against ignition during normal operation of the pump; however, other factors such as bronze/bronze PV products and combustion properties were considered in order to provide a subjective assessment of the relative merits of the alloys for use in the specified application.

The C86400 manganese bronze did not ignite during the three frictional heating tests with 304 stainless steel; however, it ignited at the lowest PV products when rubbed against itself. Since it tested so poorly in bronze/bronze tests and because the results are not completely understood, the C86400 alloy would not be the primary choice for the LOX pump application. The C93200 leaded bronze yielded the second highest PV product in ss/bronze and the third highest PV product in bronze/bronze tests. Because of the consistently high PV product ranking for both tests, the C93200 leaded bronze would be the first choice for the LOX pump wear ring application. The C90300 tin bronze and the C95200 aluminum bronze could be considered suitable materials for frictional applications where 304 stainless steel is the rubbing material. Aluminum bronzes are normally avoided due to their ability to support self-sustained combustion in GOX even at relatively low pressures; however, 304 stainless steel will also support combustion in low pressure GOX environments. The current material (C94300 high-leaded tin bronze) when rubbed against 304 stainless steel achieved a respectable PV product when compared to the other alloys tested. This along with the significant service history indicates that the most reasonable course of action is to keep using the material until other factors such as cost or availability concerns provide the impetus for changing materials.

REFERENCES

[1] Kubashewski, O. and Hopkins, B.E., Oxidation of Metals and Alloys, Academic Press Inc., 1962, pg.42.

[2] Jenny, R., and Wyssmann, H., "Friction-Induced Ignition in Oxygen," Flammability and Sensitivity of Materials in Oxygen-Enriched Atmospheres, ASTM STP 812, B.L. Werley, Ed., American Society for Testing and Materials, 1983, pp. 150-166.

[3] Stoltzfus, J.M., Homa, J.M., Williams, R.E., and Benz, F.J.,"ASTM Committee G-4 Metals Flammability Test Program: Data and Discussion," Flammability and Sensitivity of Materials in Oxygen-Enriched Atmospheres: Third Volume, ASTM STP 986, D.W. Schroll, Ed., American Society for Testing and Materials, Philadelphia, 1988, pp. 37-46.

[4] McIlroy, K., Zawierucha, R., and Drnevich, R.F.,"Promoted Ignition Behavior of Engineering Alloys in High-Pressure Oxygen," Flammability and Sensitivity of Materials in Oxygen- Enriched Atmospheres: Third Volume, ASTM STP 986, D.W. Schroll, Ed., American Society for Testing and Materials, Philadelphia, 1988, pp. 85-104.

[5] Benz, F.J. and Stoltzfus, J.M., "Ignition of Metals and Alloys in Gaseous Oxygen by Frictional Heating," Flammability and Sensitivity of Materials in Oxygen-Enriched Atmospheres: Second Volume, ASTM STP 910, M.A. Benning, Ed., American Society for Testing and Materials, Philadelphia, 1986, pp. 38-58.

[6] Beer, F.P. and Johnston, E.R., *Vector Mechanics for Engineers: Statics*, B.J. Clark, Lynn E. Contrucci, and James W. Bradley, Eds., McGraw Hill, 1972, pg.17.

[7] The Metals Handbook, Volume 2, Properties and Selection:Nonferrous Alloys and Pure Metals, ASM International, 1988, pg.418.

[8] The Metals Handbook, Volume 1, Properties and Selection:Irons and Steels, ASM International, 1988, pg.19.

[9] Askeland, Donald R., The Science and Engineering of Materials, PWS Publishers, 1984, pg.132.

[10] West, E.G., *Copper and Its Alloys*, E.G. West, Ed., Halsted Press, 1982, pg. 94.

[11] Sircar, S., Stoltzfus, J.M., and Gunaji, M.V., "The Relative Ignitability and Flammability of Lead-Tin Binary Alloys in Oxygen," Flammability and Sensitivity of Materials in Oxygen-Enriched Atmospheres: Fifth Volume, ASTM STP 1111, Joel Stoltzfus and Kenneth McIlroy, Eds., American Society for Testing and Materials, Philadelphia, 1991, pp. 260-269.

Peter W. Krag[1] and H. Rob Henson[2]

MATERIALS SELECTION FOR SULFIDE PRESSURE OXIDATION AUTOCLAVES

REFERENCE: Krag, P. W. and Henson, H. R., "Materials Selection for Sulfide Pressure Oxidation Autoclaves," Flammability and Sensitivity of Materials in Oxygen-Enriched Atmospheres: 6th Volume, ASTM STP 1197, Dwight D. Janoff and Joel M. Stoltzfus, Eds., American Society for Testing and Materials, Philadelphia, 1993.

ABSTRACT: Titanium and its alloys offer superior corrosion resistance in the oxidizing sulfuric acid environments present in sulfide pressure leaching operations. Their use is limited due to their pyrophoricity in high-pressure oxygen environments. We investigated the ignition resistance of several titanium alloys in oxygen using a tensile rupture technique. A commercial titanium alloy, niobium-55 wt. % titanium (Nb-55 Ti), was found not to ignite at pressure and temperature conditions under which Grade 2 titanium and other standard titanium alloys ignite. The decreased ignitability of titanium when alloyed with niobium is discussed in terms of a burn factor (the ratio of heat of oxidation to thermal diffusivity) and alloy microstructure. Nb-55 Ti, selected for its corrosion resistance, mechanical properties and reduced pyrophoricity compared to standard titanium alloys, has been successfully used in sulfide pressure oxidation equipment.

KEYWORDS: gold, pressure oxidation, autoclaves, titanium, niobium, ignition testing, oxygen, flammability

---

[1] Senior Engineer, Bechtel Corporation, P. O. Box 193965, San Francisco, CA 94119

[2] Corrosion Specialist, Teledyne Wah Chang Albany, P. O. Box 460, Albany, OR 97321

Tonnage oxygen has recently found new uses in extractive metallurgy, such as copper flash smelting, BOF steel processes, and sulfide pressure leaching operations. To some extent construction materials in these process systems must be compatible with high-pressure oxygen, but they must meet other mechanical, chemical and economic constraints as well. Pressure oxidation leaching of sulfide minerals generates a vapor and slurry which are highly corrosive to materials conventionally used for oxygen handling equipment, such as brasses or Monels®. Thus other cost-effective ignition resistant alloys, which additionally display requisite corrosion resistance and strength, must be sought. Although titanium and its alloys offer complete corrosion resistance in oxidizing sulfuric acid environments, their use is limited due to their pyrophoricity; several accidents attributed to titanium equipment have been described in technical literature, and other, minor incidents occur regularly [1,2]. We describe an application of a commercial titanium alloy, niobium-55 wt.% titanium (Nb-55 Ti), with suitable mechanical properties, corrosion resistance similar to Grade 2 titanium, and featuring a significantly reduced field of ignition conditions.

INTRODUCTION

Certain gold ores and concentrates, zinc concentrates, and nickel mattes can be effectively treated by aqueous pressure oxidation. In this unit operation, a sulfide-containing pulp is leached under oxygen sparge, oxidizing sulfide ion to elemental sulfur or sulfate ion, and liberating the desired metal values. A class of refractory gold ores become amenable to standard cyanidation processing if first treated by pressure oxidation; gold-containing pyrite grains are converted to hematite and aqueous sulfate, liberating the gold. Nominal operating conditions for several pressure oxidation installations are summarized in Table 1. The corrosion environment in these autoclaves is severe. The vessels are typically constructed of lead-lined steel, with two courses of acid refractory brick. However, materials selection for ancillary equipment such as oxygen injectors, impellers and vent lines is difficult. Hastelloy C276®, Inconel 625® and Ferralium 255® provide less than six months of service [3]. Corrosion rate data were obtained from test coupons placed in the vapor space of an operating autoclave at the Getchell Mine of FirstMiss Gold [4]. In tests extending up to 125 days, a nil corrosion rate was measured for titanium Grades 2, 5 and 12, ziroconium alloys Zr 702 and Zr4, niobium and tantalum. Coupons of Nb-55 Ti have been exposed in the autoclave vapor space for periods up to 180 days without measurable weight change.

TABLE 1--Operating conditions for pressure oxidation autoclaves.

	P_T, kPa	T, °C	Po_2, kPa
Au			
Am. Barrick-Goldstrike [5]	2900	225	345
Homestake-McGlaughlin [6]	1000	160-180	140-280
FirstMiss-Getchell [6]	3200	210	700
METBA-Olympias [6]	1800	190	650
Sao Bento [6]	1600	190	450
Renison Goldfields Porgera [7]	1600	190	450
Placer Dome-Campbell [8]	2100	190	850
Nerco-Con [9]	2800	210	920
Zn			
Falconbridge Kidd Creek [1]	1200	150	700
Cominco-Trail [10]	1150	150	650
Ni			
Sherritt-Gordon [11]	1100	120-160	<350

Despite this impressive corrosion resistance, the pyrophoricity of titanium and its alloys limits their application. The frequently-cited data on titanium ignition is that of Littman, Church and Kinderman [12,13]. They conducted a series of experiments in which titanium samples of various geometries were fractured in high pressure oxygen mixtures over a range of temperatures. Several more-recent works have reported the high burn rate of titanium under specific conditions, but not in connection with a systematic attempt to describe a set of ignition conditions [14-16]. Other approaches to defining ignition susceptibility under various oxygen pressure-temperature conditions include determining threshhold promoter energies [17] or PV product in friction testing [18] under various conditions. A mechanical rupture technique similar to that of Littman et al. [12] was selected because it offered a ready comparison to available data for titanium alloys, and simulated a feasible ignition mechanism for the application.

EXPERIMENTAL

A high strain rate tensile machine was assembled with a pull-through autoclave to allow creating fracture surfaces under oxygen pressure. The equipment is illustrated in Figure 1. The Tinius-Olsen tensile machine, fitted with Teflon®-coated steel pull rods, provided constant strain rates at loads up to 5000 lb_f (691 N). The six-inch (0.14 m) Cortest Hastelloy C276® autoclave had Teflon® seal rings to electrically insulate the tensile specimen, and was fitted with upper and lower copper hearths to contain the molten metal which occasionally resulted from the ignition of broken samples. Samples were heated by electrical resistance using a welding power supply. A calibration curve relating current to sample temperature was developed using a 1/32" (0.8 mm) Type K thermocouple cemented to a tensile sample of each alloy tested. The autoclave was pressurized with Air Products industrial grade oxygen (min. 99.5% O_2) and pressure monitored by an Autoclave Engineers 0-5 000 psi (35.2 MPa) pressure transducer. The 1/8" (0.2 mm) round tensile specimens were machined from commercial Nb-55 Ti rod and Grade 2 titanium.

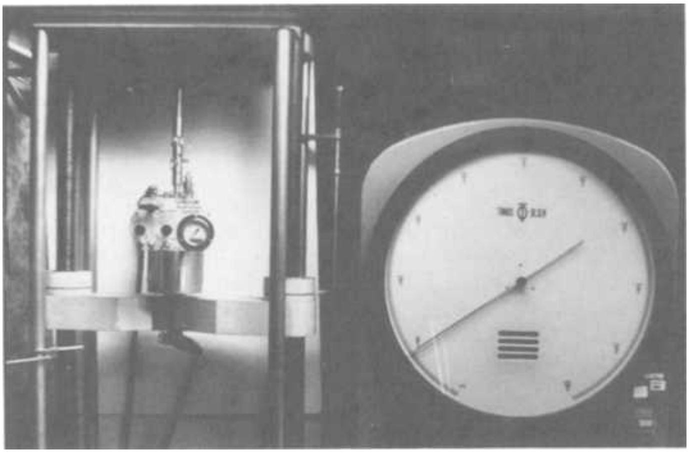

FIG. 1--Ignition testing apparatus.

Combustion rates of several reactive metal alloys in pure oxygen were measured using the promoted ignition of suspended 0.125" (0.2 mm) rods. The apparatus has been described previously [18]; results were kindly made available to us by NASA White Sands Test Facility personnel, and are published here with their permission. The thermal diffusivity of Nb-55 Ti was measured by a commercial laboratory[3].

---

[3] D. P. H. Hasselman, 601 Rainbow Ridge, Blacksburg, VA 24060

RESULTS

Three levels of fracture/ignition behavior were observed, and are illustrated in Figure 2 (a)-(c). Figure 2 (b) shows a Nb-55 Ti fracture surface with a single molten droplet; the source of heat to melt the alloy can only be metal oxidation, but the amount of heat generated was insufficient to ignite the entire sample. This condition represents incipient ignition. Ignition typically led to complete combustion of the titanium samples, which released enough heat to melt the stainless steel sample holders. The field of conditions for ignition of Grade 2 titanium and Nb-55 Ti are shown in Figure 3. The titanium curve, taken from Littman et al. [12], was bracketed at 200°C. Alloying with niobium substantially increases the threshold oxygen pressure for ignition at a given temperature. The burn rate data (Table 2) demonstrate that the niobium alloy burns significantly slower than standard titanium alloys, and at a rate comparable to that of Alloy C®, a proprietary titanium-vanadium-chromium alloy developed by United Technologies specifically for ignition/combustion resistance in aerospace applications [19]. Even at ambient oxygen partial pressures, ignition resistant titanium alloys burn rapidly.

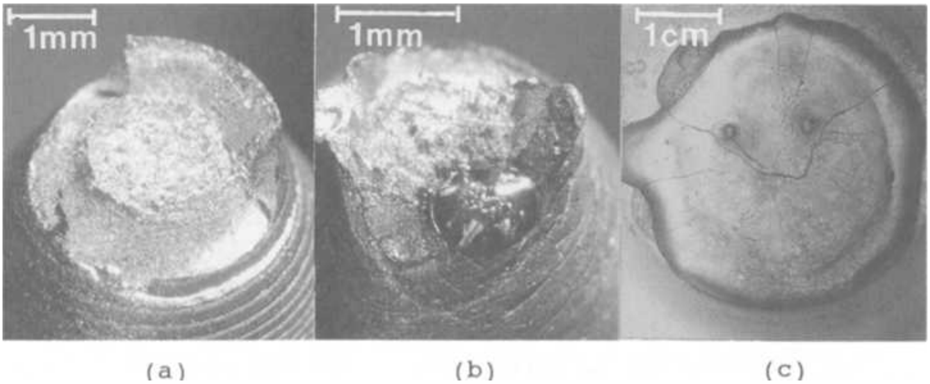

(a) (b) (c)

FIG. 2--Typical Nb-55 Ti fracture/ignition surfaces. a. No ignition. b. Incipient ignition. c. Ignition.

DISCUSSION

In this application, oxygen compatibility and metal ignition are only factors in materials selection to the extent that they limit the range of alloys considered in solving corrosion problems. The corrosion rates of materials generally used for ancillary equipment around autoclaves are known to be high, although completely corrosion resistant materials are available. Although using titanium alloys could eliminate downtime attributable to replacement of corroded vent lines, impellers, and oxygen injectors, this solution has posed an unacceptable fire hazard. Consideration of metal ignition mechanisms leading to the development of ignition-resistant alloys is germane.

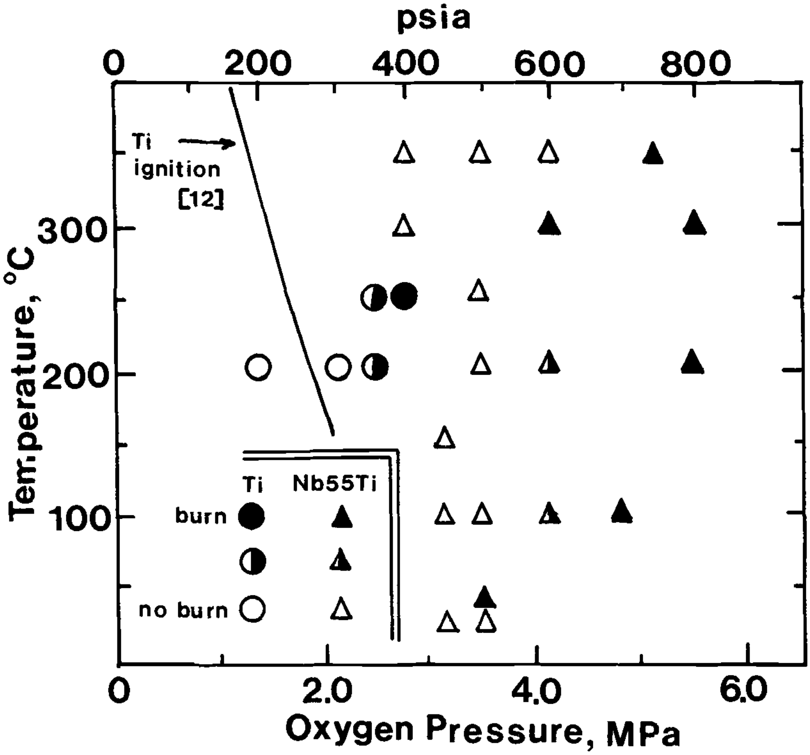

FIG. 3--Ignition conditions for Ti and Nb-55 Ti.

We shall address ignition behavior of Nb-55 Ti in terms of thermophysical properties and microstructure. Ignition behavior of metals has been correlated with a burn factor, defined as the ratio of heat of oxidation to thermal diffusivity [20]. This factor arises from models of ignition in which heat released from a site of incipient ignition is dissipated internally, rather than by evaporation of the metal. Titanium alloys of improved ignition resistance might therefore be sought by alloying to decrease heat of oxidation or increase thermal diffusivity. On a mass basis, among metals showing extensive solubility in titanium, niobium has the lowest heat of oxidation; in a crude approximation, it should therefore be most effective in lowering heat of oxidation. In addition, the thermal diffusivity of Nb-55 Ti is significantly higher than that of Grade 5 titanium. The burn factors for several engineering alloys were calculated using methods established previously [17,20], and are presented in Table 3, along with corrosion rates measured in an operating autoclave [4]. This burn factor was unable to predict the comparative ignition behavior of Grade 2 titanium and Nb-55 Ti, nor does it predict the similarity of ignition conditions for Grade 2 and Grade 5 titanium [12].

TABLE 2--Combustion rate of titanium alloys in pure oxygen.

Alloy	Test Pressure kPa O_2	Combustion Rate mm/sec
Ti	7	5.8
"	14	8.4
"	27	6.4
"	55	7.7
"	85	7.6
"	172	14.5
"	172	12.4
"	687	29.5
Ti-6-4	7	5.8
"	14	6.1
"	27	9.7
"	137	11.4
"	137	10.7
"	137	10.4
"	137	11.7
Nb-55Ti	137	8.1
Nb-55Ti	687	23.4
Alloy C®	137	7.4
"	137	7.1
"	137	7.9

Metal ignition must also be considered from the standpoint of alloy microstructure. Niobium is a beta stabilizer in titanium, forming a single-phase β alloy at 55 wt.% Ti-45 wt.% Nb. Single-phase β microstructure is important for ignition resistance, because expansion of prior α grains on the thermally-induced α/β transformation disrupts any formed ignition-inhibiting oxide layer. Cracks in the oxide layer over α grains will serve as a diffusion path for oxygen; the oxide layer over β grains will remain intact on heating from an incipient ignition site, and continue to provide ignition resistance. The simple metallurgy of the binary alloy also helps in forming operations. The single-phase alloy is mechanically stable, avoiding the strain-induced martensite transformation which occurs below 40 wt.% niobium [21]. The dynamic Young's modulus of niobium-titanium alloys has been reported by several authors, and Nb-55 Ti falls into one of two minima, having a modulus of about 62 GPa [22]. The alloy can therefore be easily worked into plate, rod or tube by conventional techniques. Figure 4 compares the mechanical properties of Grade 2 titanium with those of wrought, annealed Nb-55 Ti, showing the superior high temperature strength of the alloy.

TABLE 3--Burn factor and corrosion rate for selected alloys.

Alloy	Thermal Diffusivity $m^2s^{-1}x10^6$	Heat of Combustion MJ/kg	Burn Factor $TJsm^{-2}kg^{-1}$	Corrosion Rate mm/y
SS310	3.56	7.782	2.186	2.77
SS316	4.06	7.782	1.917	4.62
Sanicro 28®	3.19	7.155	2.243	1.07
Ferralium 255®	3.67	8.075	2.200	1.58
Hastelloy C4®	2.88	6.389	2.218	1.75
Hastelloy C22®	2.70	6.004	2.224	2.69
Hastelloy G3®	2.72	6.381	2.346	3.56
Hastelloy G30®	1.92	6.945	3.617	0.58
Hastelloy C276®	3.42	5.732	1.676	4.62
Inconel 617®	3.87	6.150	1.589	3.48
Inconel 625®	2.83	6.025	2.129	1.22
Inconel 690®	3.89	6.389	1.642	2.18
Incoloy 825®	3.11	6.757	2.173	1.90
Ti Grade 2	7.6	19.71	2.593	nil
Ti Grade 5	2.90	20.21	6.969	nil
Nb	22.8	10.245	0.449	nil
Ta	23.2	5.648	0.243	nil
Zr 702	12.15	11.90	0.979	nil
WC103	11.4	9.958	0.874	nil
Nb129Y	26.1	9.288	0.356	nil
Nb-55Ti	4.30	15.44	3.59	nil

A vent line was fabricated from 2" Sch. 40 Nb-55 Ti pipe, and was installed on an operating autoclave at the Getchell Mine of FirstMiss Gold in August 1991. This piping was previously fabricated from Ferralium 255®, and had typically required replacement every few months due to erosion corrosion. For the Nb-55 Ti pipe, there was no detectable loss of wall thickness, as assessed by ultrasonic inspection, in August 1992, after one year of service. This alloy has been found to be cost-effective, and sufficiently ignition-resistant for use in some parts of pressure oxidation autoclaves.

CONCLUSION

Materials selection for pressure oxidation autoclaves involves balancing of corrosion resistance, pyrophoricity and fabricability. Operators of these plants have typically chosen to avoid the fire hazard inherent in use of titanium alloys and utilize materials with inferior corrosion resistance, paying increased maintenance cost and lost production. Niobium-titanium alloys are resistant to both crevice and general corrosion in sulphide pressure oxidation environments, and are highly fabricable and weldable. Furthermore, they are ignition resistant compared to standard titanium alloys. Typical operating conditions for sulfide pressure oxidation autoclaves lie below established ignition conditions for standard titanium alloys, but accidents have occurred. Niobium-titanium offers an increased margin of

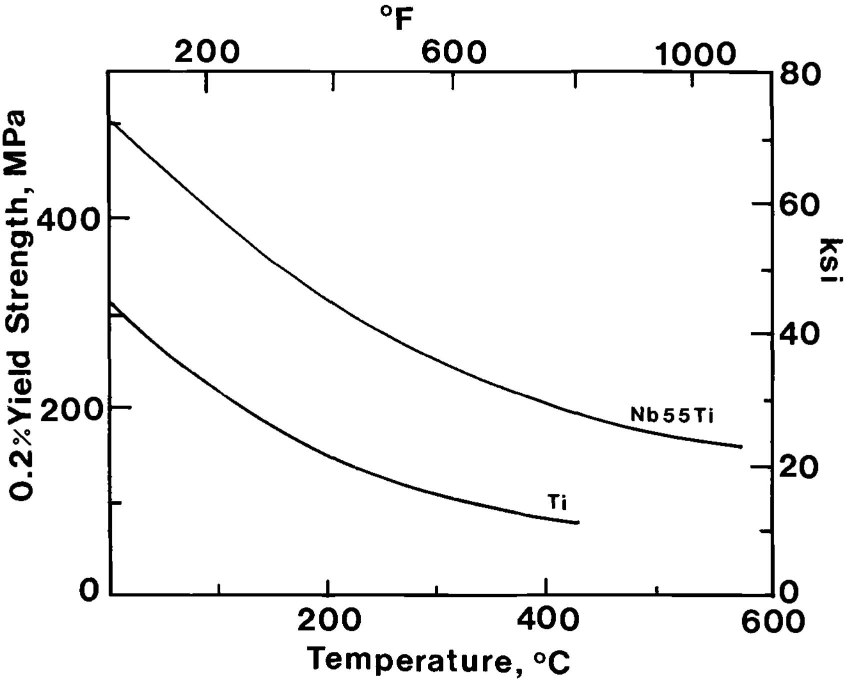

FIG. 4--Typical yield strength of Nb-55 Ti.

safety to autoclave operators seeking to lower maintenance costs and increase production rates with corrosion resistant titanium alloys.

REFERENCES

[1] Mollison, A. C. and G. W. Moore. "Sulphide Pressure Leaching at Kidd Creek". in T. S. Mackey and R. D. Prengaman, eds., Lead-Zinc '90. Warrendale, PA: TMS, 1990, pp 277-291.

[2] Gulyas, J. W. and K. D. Lunde, eds. Risk Management in Pressure Oxidation. Vancouver, CAN: Fluor Daniel Wright, 1989.

[3] Thomas, K. "Alkaline and Acid Autoclaving of Refractory Gold Ores". J. Metals, Vol. 43, No. 2, February 1990, pp. 16-19.

[4] Krag, P. and R. Henson. "An Ignition-resistant Titanium Alloy for Acid Pressure Oxidation Applications". Randol Gold Forum Vancouver '92. Golden, CO: Randol International, 1992, pp. 201-204.

[5] Thomas, K. G., H. Pieterse, R. Williams, K. S. Fraser and J. R. Goode. "The Goldstrike Autoclave Plant Design, Commissioning and Operation". in Fuerstenau, M.C. and J.L. Hendrix, eds., Advances in Gold and Silver Processing. Littleton, CO: SME, 1990, pp. 181-191.

[6] Berezowsky, R.M.G.S. and D. R. Weir. "Refractory Gold: The Role of Pressure Oxidation". in Bhappu, R. B. and R. J. Harden, eds., Gold Forum of Technology and Practices - World Gold '89. Littleton, CO: SME, 1990, pp. 295-314.

[7] Weir, D. R., J. A. King and P. C. Robinson. "Preconcentration and Pressure Oxidation of Porgera Refractory Gold Ore". Minerals and Metallurgical Processing, Vol. 3, No. 4, November 1986, pp. 201-208.

[8] Frostiak, J. and B. Haugrud. "Start-up and Operation of Placer Dome's Campbell Mine Gold Pressure Oxidation Plant". Mining Engineering, Vol. 44, No. 8, August 1992, pp. 991-993.

[9] Maltby, P. "Development of Aqueous Pressure Oxidation at the Nerco Con Mine, N.W.T., Canada". Randol Gold Forum Vancouver '92. Golden, CO: Randol International, 1992, pp. 197-200.

[10] Parker, E. G. "Oxidative Pressure Leaching of Zinc Concentrates". CIM Bulletin, Vol. 74, No. 829, May 1981, pp. 145-150.

[11] Berezowsky, R.M.G.S., M. J. Collins, D.G.E. Kerfoot and N. Torres. "The Commercial Status of Pressure Leaching Technology". J. Metals, Vol. 43, No. 2, February 1990, pp. 9-15.

[12] Littman, F. E., F. M. Church and E. M. Kinderman. "A Study of Metal Ignitions. I. The Spontaneous Ignition of Titanium". J. Less-Common Metals, Vol. 3, 1961, pp. 367-378.

[13] Riehl, W. A., C. F. Key and J. B. Gayle. "Reactivity of Titanium with Oxygen". NASA Technical Report TR-180, 1963, 113 pp.

[14] Sircar, S., H. Gabel, J. Stoltzfus, and F. Benz. "The Analysis of Metals Combustion Using a Real-time Gravimetric Technique". in Stoltzfus, J. and K. McIlroy, eds., Flammability and Sensitivity of Materials in Oxygen-Enriched Environments: Fifth Volume, ASTM STP 1111, 1991, pp. 313-325.

[15] Zabrenski, J. S., B. L. Werley and J. W. Slusser. "Pressurized Flammability Limits of Metals". in Stoltzfus, J., F. J. Benz and J. S. Stradling, eds., Flammability and Sensitivity of Materials in Oxygen-Enriched Atmospheres: Fourth Volume, ASTM STP 1040, 1989, pp. 178-194.

[16] Sato, J. "Fire Spread Rates along Cylindrical Metal Rods in High Pressure Oxygen". in Stoltzfus, J., F. J. Benz and J. S. Stradling, eds., Flammability and Sensitivity of Materials in Oxygen-Enriched Atmospheres: Fourth Volume, ASTM STP 1040, 1989, pp. 162-177.

[17] McIlroy, K., R. Zawierucha and R. F. Drnevich. "Promoted Ignition Behavior of Engineering Alloys in High-Pressure Oxygen". in D. W. Schroll, ed., Flammability and Sensitivity of Materials in Oxygen-Enriched Atmospheres: Third Volume, ASTM STP 986, 1988, pp. 85-104.

[18] Stoltzfus, J. M., J. H. Homa, R. E. Williams and F. J. Benz. "ASTM Committee G-4 Metals Flammability Test Program: Data and Discussion". in D. W. Schroll, ed., Flammability and Sensitivity of Materials in Oxygen-Enriched Atmospheres: Third Volume, ASTM STP 986, 1988, pp. 28-53.

[19] Berczik, D. M. "High Strength Nonburning Beta Titanium Alloy". UK Patent Application GB 2,238,057A, 1991.

[20] Schoenman, L., J. Stoltzfus and J. Kazaroff. "Friction-Induced Ignition of Metals in High-Pressure Oxygen". in D. W. Schroll, ed., Flammability and Sensitivity of Materials in Oxygen-Enriched Atmospheres: Third Volume, ASTM STP 986, 1988, pp. 105-133.

[21] Berger, L. W., D. N. Williams and R. I. Jaffee. "Mechanical Properties and Heat Treatment of Titanium-Niobium Alloys". Transactions of ASM, Vol. 50, 1958, pp. 384-397.

[22] Collings, E. W. "The Dynamic Modulus of Titanium-Niobium", in Timmerhaus, K. D. and A. F. Clark, ed., Applied Superconductivity, Metallurgy, and Physics of Titanium Alloys. Vol. 1: Fundamentals. The International Cryogenics Monograph Series, 1986, pp. 198-201.

Analysis of Ignition Mechanisms

Theodore A. Steinberg,[1] D. Bruce Wilson,[1] and Frank J. Benz[2]

MODELING OF AL AND MG IGNITERS USED IN THE PROMOTED COMBUSTION OF METALS AND ALLOYS IN HIGH PRESSURE OXYGEN

REFERENCE: Steinberg, T. A., Wilson, D. B., and Benz, F. J., "Modeling of Al and Mg Igniters Used in the Promoted Combustion of Metals and Alloys in High Pressure Oxygen," Flammability and Sensitivity of Materials in Oxygen-Enriched Atmospheres: 6th Volume, ASTM STP 1197, Dwight D. Janoff and Joel M. Stoltzfus, Eds., American Society for Testing and Materials, Philadelphia, 1993.

ABSTRACT: NASA determines flammability of metal and alloy samples in high pressure oxygen by Test 17 of NHB 8060.1C. An aluminum or magnesium promoter, releasing at least 3.0 kJ, is used as the sample ignition source. This ignition system is modelled using lumped-parameter mathematical equations and solved using the MATLAB computer code. Model parameters were obtained from the combustion of Al and Mg promoters on copper rods in the standard flammability instrument system. The copper rod is non-flammable under test conditions, that is, pure oxygen pressures of 3.44, 6.89, 20.7, 34.4 and 68.9 MPa. At test conditions, both aluminum and magnesium alloyed with the copper rod and burned in liquid phase reactions. The following heterogenous kinetic reaction rate functions were obtained:

$$\text{for } Al\text{:}\quad R_{Al} = \frac{0.102\ Po_2}{1. + 0.186\ Po_2}\ ,\ g/m^2s$$

$$\text{for } Mg\text{:}\quad R_{Mg} = \frac{0.067\ Po_2}{1. + 0.146\ Po_2}\ ,\ g/m^2s.$$

The model is validated by comparing 'time-to-ignition' values for iron samples with measured experimental time-to-ignition for this material. Model predictions are between -5 to +28% of measured values. This work also provides 'burn-rates' for bulk aluminum and magnesium as functions of oxygen pressure.

KEYWORDS: metal ignition model, kinetic reaction rate Al/Mg, liquid phase metal combustion, time-to-ignition.

Nomenclature

A	area, m^2
C_p	specific heat, J/g K
h_c	convective heat transfer coefficient, J/m^2 K s
fl	mixing function
k	thermal conductivity, J/m s K
k_r	reaction rate constant, g/m^2 s
K_{eq}	adsorption/desorption equilibrium constant, MPa^{-1}

---

[1] Principal scientists, Lockheed-ESC, White Sands Test Facility, P. O. Drawer MM, Las Cruces, NM 88004.

[2] Laboratory Chief, NASA, White Sands Test Facility, P. O. Drawer MM, Las Cruces, NM 88004.

L	length, cm
m	mass, g
P	pressure, MPa
R	reaction rate, g/m^2 s
S	surface area, m^2
T	temperature, K
t	time, s

Greek Symbols

ϵ	emissivity
λ	enthalpy of fusion, J/g
σ	Stefan-Boltzman constant, J/m^2 K^4 s

Subscripts

I	refers to subsystem I (promoter)
Ic	refers to part of burning promoter subject to free convection
Ir	refers to part of burning promoter subject to radiative losses
II	refers to subsystem II (rod core)
III	refers to subsystem III (rod segment)
IV	refers to subsystem IV (rod segment)
o	ambient conditions
V	refers to subsystem V (oxygen)
x	cross section of rod

INTRODUCTION

One of the tests used by NASA for evaluating the flammability, in high pressure oxygen, of metals and alloys is promoted combustion of cylindrical rods (NHB 8060.1C, Test 17) [1]. The normal sequence for this experiment is that a metallic ignition promoter (aluminum or magnesium disc, Fig. 1a) is press-fitted to the end of a 30.4-cm-long, 0.32-cm-diameter metal or alloy rod test sample. This promoter is ignited by aluminum-palladium wire and the burning promoter ignites the sample rod. The sample metal or alloy can melt without igniting, partially burn and extinguish, or burn completely. The experimental system used and detailed test procedures are described in Reference [2]. To be considered 'flammable' by the NASA test, the metal or alloy must burn 15.2 cm for one-out-of-five samples at maximum use oxygen pressure. Ambient temperature, rod diameter, and oxygen pressure are parameters of the tests.

When copper is the sample material, the conditions of the standard test, that is, 100% oxygen at 3.44, 6.89, 20.7, 34.4 or 68.9 MPa and ambient temperature, do not result in ignition of the copper rod. Rather, these experiments provide information on aluminum and magnesium combustion. A macroscopic burn rate for the metal promoter as a function of oxygen pressure can be obtained and verified using a lumped-parameter system model for these experiments. Figure 1a shows the promoter-ignition disc on the test rod, the definition of the appropriate subsystems for analysis, Fig. 1b, and the lumping network equivalent, Fig. 1c [3,4].

EXPERIMENTAL OBSERVATIONS/RESULTS

The model schematic of Fig. 1b is based on the experimental results as shown in Fig. 2a for aluminum promoters and Fig. 2b for magnesium promoters. The burned promoter metal oxide is still attached to the rod and the rod shows two distinct bands of discolorations, with similar discoloration bands for each of the five different experimental pressures. This discoloration is a qualitative measure of the temperature of this portion of the rod at the end of an experiment. Figure 2 shows that the rod temperature profile was a function of oxygen pressure.

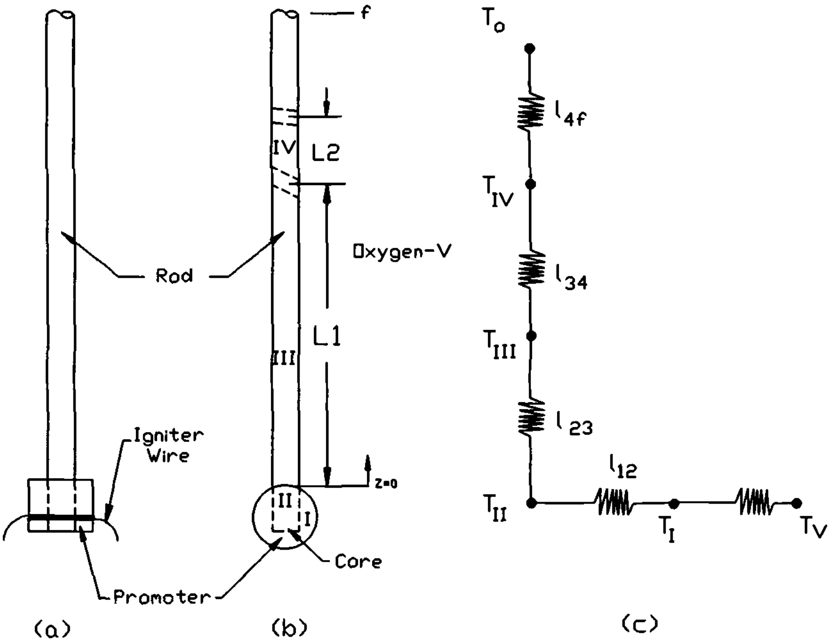

FIG. 1--Al/Mg promoter system schematic; a) promoter on rod, 2) the subsystems for analysis and c) the lumping network equivalent.

Figure 3a and 3b are representative cross sections of two burned promoters attached to the sample rods. These cross sections show that the copper rod within the promoter (Subsystem II of Fig. 1b) reached the melting temperature of copper but did not fall (detach) from the rod. These figures also indicate that the burning of the metallic promoter resulted in vigorous mixing of the material in the burning metal. SEM/x ray and Auger analysis of these cross-sections confirm the mixing of molten metal oxide, melted copper, and melted metal (aluminum or magnesium).[3,4] These analyses show stoichiometric binary alloys have solidified, that is, Mg_2Cu and AlCu were formed. Complete combustion of all the promoter metal did not occur, therefore, the model analysis will require a parameter for the extent of reaction. Oxides of the promoter material plus the stoichiometric compounds were distributed throughout region I of Fig. 1b. Aluminum and magnesium each have only one stable solid oxide, $Al_2O_3(s)$ and MgO(s), respectively, and the SEM/x ray analysis confirmed uniform oxygen distribution in the combustion

---

[3] Bank. S., LESC memorandum, private communication, March 1991.

[4] Hornung, S., LESC memorandum, private communication, October 1992.

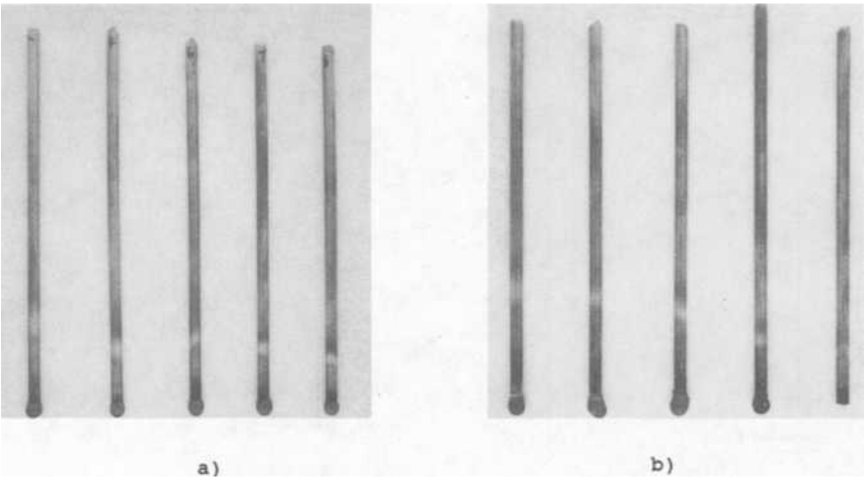

FIG. 2--Results of test on copper rod with a) aluminum promoter and b) magnesium promoter. The test pressures are (from left to right) 3.44, 6.89, 20.7, 34.4, and 68.9 MPa, respectively.

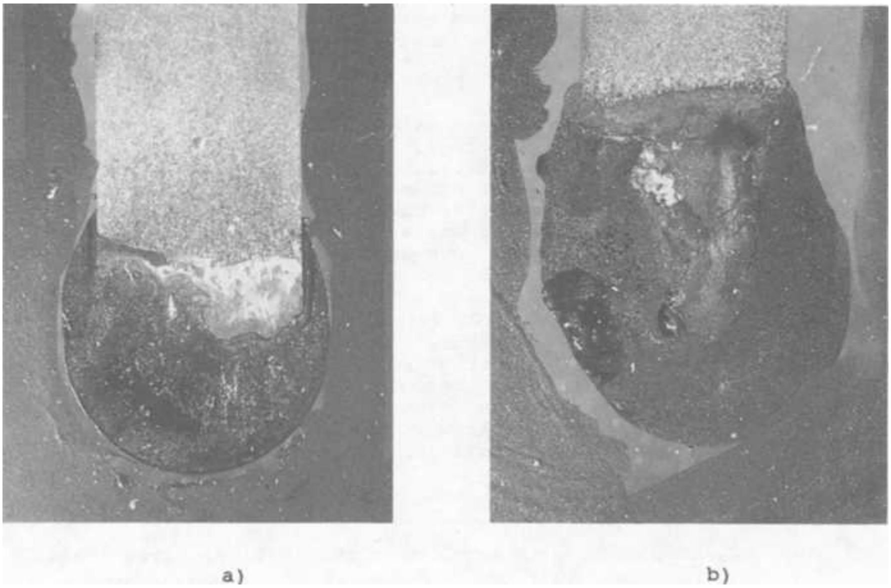

FIG. 3--Residual promoter mass on copper rod; a) aluminum promoter at 68.9 MPa, and b) magnesium promoter at 20.7 MPa.

products and gave component ratios consistent with the reaction stoichiometry.

Each experimental run was recorded by video camera. This video tape was used to measure the burn time for a given promoter mass. Average values of burn time for each promoter for each oxygen pressure are recorded in Table 1. Table 1 also gives the experimental values L1 and L2 (see Fig. 1b), which are the markings shown on the copper rods. A second set of experiments was conducted using an aluminum promoter on an iron rod (0.32-cm diameter, 15.1-cm long). At all five test pressures and for all samples, the Al promoter ignited the rod and the rod burned completely. Again a video camera recorded these events and this film was used to measure the time-to-ignition. The time-to-ignition data for the iron samples are recorded in Table 2.

TABLE 1--Average burn-time data for Al/Mg promoters on copper rods.

Promoter Material	Pressure (MPa)	Average Burn-Time (s)	L1 (cm)	L2 (cm)
Al	3.44	1.41	1.86	0.74
	6.89	0.98	1.24	0.56
	20.7	0.73	1.52	0.48
	34.4	0.60	1.26	0.36
	68.9	0.60	1.08	0.32
Mg	3.44	1.83	2.66	0.68
	6.89	1.17	2.56	0.48
	20.7	0.93	2.08	0.48
	34.4	0.63	1.44	0.36

TABLE 2--Time-to-ignition for iron with aluminum promoter.

Test Number	Pressure (MPa)	Time-To-Ignition of Rod (sec)
1	3.44	0.28
2	3.44	0.25
3	3.44	0.27
4	6.89	0.18
5	6.89	0.25
6	6.89	0.27
7	20.7	0.20
8	20.7	0.22
9	20.7	0.20
10	34.4	0.13
11	34.4	0.17
12	34.4	0.12

MODEL ANALYSIS

Each subsystem of Fig. 1b is described in terms of mass and enthalpy conservation balances. The lumped-parameter assumption reduces the equations to first-order, non-linear differential equations. The resulting model equations are suitable for solution by the MATLAB computer code [5].

SUBSYSTEM I - THE PROMOTER

The following assumptions are made for modelling the combustion of the promoter:

1. The subsystem is assumed spherical; surface area is calculated based on final volume.
2. The molten volume is based on the density of the liquid metal. The molten mass is well mixed.
3. Combustion is heterogenous and the reaction rate will be modelled in terms of a Langmuir-Hinshelwood-Hougen-Watson (LHHW) rate equation [6].
4. Thermodynamic and transport properties will be weighted averages of the metal and metal oxide. The enthalpy of reaction will correspond to the sum of $\Delta_R H$ for the set of reactions which occur, that is, the products of reaction are $Al_2O_3(l)$, $AlO(v)$, and $AlO_2(v)$ for the aluminum system and $MgO(l)$ and $MgO(v)$ for the magnesium system.
5. Radiative transport from the molten ball is to the containment vessel.
6. Thermal energy transfer to Subsystem II is by conduction.

The mass balance for the metal in the promoter is [6]:

$$\frac{dm_i(t)}{dt} = -\frac{k_r \, Po_2}{1 + K_{eq} \, Po_2} \cdot S \cdot f1 \equiv R_i \cdot S \cdot f1 \tag{1}$$

The enthalpy balance for the promoter is:

$$\begin{aligned} \bar{m}_I \, \bar{C}_{pI} \frac{dT_I(t)}{dt} = {} & |<\Delta_R H^\circ> \cdot R_i \cdot S \cdot f1| - \frac{\bar{k}_I(t) A_{II}}{\ell_{12}} (T_I(t) - T_{II}(t)) \\ & - \epsilon \sigma A_{Ir} (T_I^4(t) - T_o^4) - h_c A_{Ic} (T_I(t) - T_V(t)) \end{aligned} \tag{2}$$

SUBSYSTEM II - THE SAMPLE ROD CORE (WITHIN THE PROMOTER)

The following assumptions are made for modelling the sample rod core:

1. Mass is constant. The rod core melts but does not react.
2. Thermal energy transfer occurs only by conduction.
3. Thermodynamic properties will be mean values.

The enthalpy balance for the sample rod core is:

$$m_{II}\,\bar{C}_{pII}\,\frac{dT_{II}(t)}{dt} = \frac{\bar{k}_I(t)A_{II}}{\ell_{12}}\,(T_I(t) - T_{II}(t)) - \frac{\bar{k}_{II}A_x}{\ell_{23}}\,(T_{II}(t) - T_{III}(t)) - \dot{m}_{II}\,\lambda_{II}\,\delta(T_{II}(t) - T_{IIm}) \tag{3}$$

SUBSYSTEM III AND IV - THE SAMPLE ROD

As shown on Fig. 2, there are two regions of discoloration of the samples which result from the combustion of the promoter. The following assumption apply to the model for these subsystems:

1. No oxidation of the sample rod occurs.
2. Thermal energy transfer to these subsections occurs only by conduction through the rod.
3. Thermodynamic properties will be mean values.
4. The rod discoloration is a function of temperature only i.e. each band of color on the sample rod is the same temperature for all five experiments.

The enthalpy balance of Subsystem III is:

$$m_{III}\,\bar{C}_{pIII}\,\frac{dT_{III}(t)}{dt} = \frac{\bar{k}_{II}A_x}{\ell_{23}}\,(T_{II}(t) - T_{III}(t)) - \frac{\bar{k}_{III}A_x}{\ell_{34}}\,(T_{III}(t) - T_{IV}(t)) \tag{4}$$

The enthalpy balance for Subsystem IV is:

$$m_{IV}\,\bar{C}_{pIV}\,\frac{dT_{IV}(t)}{dt} = \frac{\bar{k}_{III}A_x}{\ell_{34}}\,(T_{III}(t) - T_{IV}(t)) - \frac{\bar{k}_{IV}A_x}{\ell_{4f}}\,(T_{IV}(t) - T_o) \tag{5}$$

The temperature condition for the rod subsystem is:

$$T_{III}\,(L_1,P_1) = T_{III}\,(L_1,P_2) = T_{III}\,(L_1,P_3) = T_{III}\,(L_1,P_4) = T_{III}\,(L_1,P_5) \tag{6}$$

and

$$T_{IV}(L_1+L_2,P_1) = T_{IV}(L_1+L_2,P_2) = T_{IV}(L_1+L_2,P_3) = T_{IV}(L_1+L_2,P_4) = T_{IV}(L_1+L_2,P_5) \tag{7}$$

SUBSYSTEM V - THE GASEOUS OXYGEN

The following assumptions apply to the model of the oxygen:

1. Oxygen is transparent to infra-red radiation [7].
2. Thermal energy transfer is by free convection from the burning molten mass.
3. Thermodynamic properties will be mean values.
4. Mass of oxygen is constant, e.g. less than 3% of total oxygen is consumed by combustion.

The subsystem V enthalpy balance is:

$$m_V \bar{C}_{pV} \frac{dT_V(t)}{dt} = h_c A_{Ic} (T_I(t) - T_V(t)) \qquad (8)$$

There are six dependent variables in the model, $m_I(t)$, $T_I(t)$, $T_{II}(t)$, $T_{III}(t)$, $T_{IV}(t)$, and $T_V(t)$. All thermodynamic and transport properties are available from standard references. The adjustable parameters are k_r, K_{eq}, h_c, f1 and ϵ. The thermal conductivity and specific heat of the rod, for the different segments, are assumed to be equal, that is, $C_{pII}=C_{pIII}=C_{pIV}$, and $k_{II}=k_{III}=k_{IV}$.

DISCUSSION

Realistic validation of a mathematical model suggests that the number of adjustable parameters be reduced as much as possible by reference to other independent experimental data or from available published correlations. The physical evidence confirms that the combustion of both aluminum and magnesium occurred in the liquid phase; however this photographic evidence also showed that volatile reaction products were produced. (This was further confirmed by physical evidence of a fine powder in the combustion chamber after a test.) The amount of these products would vary with the system pressure. Equations 9 and 10 shows the possible stoichiometry for the aluminum and magnesium systems, respectively.

$$(2x+y+z)Al(l) + (3/2x+1/2y+z)O_2(g) \rightarrow xAl_2O_3(l) + yAlO(v) + zAlO_2(v) \qquad (9)$$

$$(x+y)Mg(l) + (x/2+y/2)O_2 \rightarrow xMgO(l) + yMgO(v) \qquad (10)$$

The average enthalpy value, $<\Delta_R H^o>$, in Eq. 2, is based on Gordon-McBride computer calculations for the distribution of product species as a function of temperature and pressure.

Equation 1 has three parameters, k_r, K_{eq}, and f1. f1 reflects the mixing of the molten metal oxide, the molten promoter metal, and the melting copper of the rod. As the copper mixes into the molten mass it has a quenching effect on the reaction and complete combustion of all the metal in the promoter does not occur. f1 is defined as a parabolic function (shown in Table 3).

The free convection heat transfer coefficient, h_c (Eq. 8) can be estimated from published correlations [8]. In Table 3 are the calculated values from the appropriate correlation. The variation shown is a result of the increasing oxygen pressure. These values (as a function of pressure) were then used in solving the model. The h_c parameter was not adjusted. The fourth parameter needed for model solution is the emissivity of the molten burning metal. There were no specific values found in the literature for burning aluminum and magnesium. While the temperature of the molten ball will vary as the extent of reaction changes [9], a constant value of emissivity was used. The value used was 0.3 [10].

The MATLAB routine used to solve the promoter combustion model requires that the vector of first-order differential equations be in state space form [11]. Table 4 lists the state-space form of the model equations solved by the MATLAB program, where the C's are used for conciseness to specify constants.

In Eq. 1, the reaction rate, R_i, is modelled to have the two parameters k_r and K_{eq}. The analysis of the molten mass (Fig. 3) indicates that about 10% residual promoter metal was not burned. Therefore, the modelling analysis was to solve the system equations

TABLE 3--Al/Mg promoter model parameter values.

Pressure (MPa)	Emissivity	Free Convection Heat Transfer h_c ($J/s\ K\ cm^2$)	Mixing Function Function $f1=(1-(t/\tau)^2)$ τ*
		Al Promoter	
3.44	0.3	0.04	1.41
6.89	0.3	0.07	0.98
20.7	0.3	0.19	0.73
34.4	0.3	0.31	0.60
68.9	0.3	0.76	0.60
		Mg Promoter	
3.44	0.3	0.04	1.83
6.89	0.3	0.07	1.17
20.7	0.3	0.19	0.93
34.4	0.3	0.31	0.63

*Experimental measurement

TABLE 4--State-space model equations.

$$
\begin{aligned}
dm_I(t)/dt &= R_i \cdot S \cdot (1-(t/\tau)^2) \\
dT_I(t)/dt &= -\ (C_3 + C_5)\ T_I(t) - C_4\ T_I^4(t) + C_3\ T_{II}\ (t) \\
&\quad + C_5\ T_V(t) - (C_6\ T_I(t) + C_7)\ dm_I/dt + C_4\ T_o^4 \\
dT_{II}(t)/dt &= C_2\ T_I(t) - (C_1 + C_2)\ T_{II}(t) + C_1\ T_{III}(t) - Q \\
dT_{III}(t)/dt &= C_8\ T_{II}(t) - (C_8 + C_9)\ T_{III}(t) + C_9\ T_{IV}(t) \\
dT_{IV}(t)/dt &= C_{10}\ T_{III}(t) - (C_{10} + C_{11})\ T_{IV}(t) + C_{11}\ T_o \\
dT_V(t)/dt &= C_{12}\ T_I(t) - C_{12}\ T_{IV}(t)
\end{aligned}
$$

using R_i as the only adjustable parameter to achieve 90% combustion and the temperature equalities shown by Eq.'s 6 and 7. After obtaining the five R_i values (one for each pressure), the k_r and K_{eq} will be determined.

Table 5 lists Al/Mg promoter metal property values as well as the constant thermodynamic values used. In addition, values for all in the state-space equations' constants are given for both promoter metals.

Table 6 are the calculated temperature values for Subsystems III and IV as represented by Eq. 6 and Eq. 7. The aluminum promoter shows that the five temperature values (that is, for the five oxygen pressures of the experiments) coincide over the normalized time of the experiments. Similar calculated temperature values are obtained for the magnesium promoter. The corresponding R_i values for the aluminum system for oxygen pressures of 3.4, 6.9, 20.7, 34.0, and 69.0 MPa are 0.2135, 0.3085, 0.413, 0.505 and 0.51 g/m^2, respectively. For the magnesium system, the corresponding R_i values, for oxygen pressures of 3.4, 6.9, 20.7, 34.0, and 69.0 MPa are 0.152, 0.24, 0.30, and 0.44 g/m^2,

TABLE 5--Al/Mg promoter properties.

Material	Density (293 K) kg/m^3	Total Weight g	Heat Capacity J/kg K	Latent Heat of Fusion J/g	Thermal Conductivity J/m s K	Melting Temp K	Standard Heat of Combustion(1) kJ/g	Auto-ignition Temp.[14] K
Al	2702	0.224	903	396.8	237	933	30.03	>1000
Mg	1740	0.208	1024	348.0	156	923	24.74	900
Cu	8890	...	380	206.7	388	1358	...	...
Fe	7897	...	452	245.9	73	1808	...	...

Parameter Values for Aluminum and Magnesium Promoters

Press. (MPa)	C_1	C_2°	C_3°	C_4°	C_5°	C_6	C_7	C_8	C_9	C_{10}	C_{11}	C_{12}	U_1
						Aluminum							
3.4	1.2	2.5	8.	1.14E-11ϵ	2.h	3.12	5.12E4	0.51	0.48	1.17	0.53	0.02h	544/τ
6.9	1.2	2.0	8.	1.14E-11ϵ	2.h	3.12	5.42E4	0.57	0.65	2.28	0.73	0.01h	544/τ
20.7	1.4	2.0	8.	1.14E-11ϵ	2.h	3.12	5.22E4	1.0	1.08	2.35	0.84	0.004h	544/τ
34.	1.6	2.35	8.	1.14E-11ϵ	2.h	3.12	5.2E4	1.0	1.1	3.75	1.21	0.002h	544/τ
69	2.4	2.5	8.	1.14E-11ϵ	2.h	3.12	5.7E4	1.1	1.2	4.5	3.5	0.001h	544/τ
						Magnesium							
3.4	1.2	3.0	8.85	1.18E-11ϵ	1.67h	2.86	6.4E4	0.27	0.26	1.02	0.59	0.022h	544/τ
6.9	1.35	3.5	8.85	1.18E-11ϵ	1.67h	2.86	6.45E4	0.29	0.29	1.54	0.84	0.011h	544/τ
20.7	1.42	3.0	8.85	1.18E-11ϵ	1.67h	2.86	6.45E4	0.41	0.43	1.82	0.84	0.004h	544/τ
34.	1.84	3.0	8.85	1.18E-11ϵ	1.67h	2.86	6.4E4	0.77	0.88	2.69	1.20	0.002h	544/τ
						Iron							
3.4	4.0	12.	8.0	1.14E-11ϵ	2.01h	3.12	5.12E4	18.0	1.72	1.72	1.72	0.02h	544/τ
6.9	4.0	12.	8.0	1.14E-11ϵ	2.01h	3.12	5.42E4	18.0	1.72	1.72	1.72	0.01h	544/τ
20.7	4.0	12.	8.0	1.14E-11ϵ	2.01h	3.12	5.22E4	18.0	1.72	1.72	1.72	0.004h	544/τ
34.	4.0	12.	8.0	1.14E-11ϵ	2.01h	3.12	5.2E4	18.0	1.72	1.72	1.72	0.002h	544/τ

where f1 = $(1 - (t/\tau)^2)$ - pseudo thermal diffusivity; $h \equiv h_c$ free convection heat transfer coefficient; $\epsilon \equiv$ emissivity.

TABLE 6--Subsystem III and IV temperatures (K).

	Al - SS III					Al - SS IV				
	pressure, MPa					pressure, MPa				
t/τ	3.4	6.8	20.7	34.0	69.0	3.4	6.8	20.7	34.0	69.0
0.1	307	304	303	302	300	300	300	300	300	300
0.3	370	344	342	340	343	310	308	306	306	308
0.5	456	417	440	427	427	333	330	327	330	334
0.7	585	526	539	526	550	389	372	369	373	383
0.9	685	614	650	638	656	441	433	425	432	438
1.0	724	659	699	694	705	470	465	455	468	468

	Mg - SS III				Mg - SS IV			
	Pressure, MPa				Pressure, MPa			
t/τ	3.4	6.8	20.7	34.0	3.4	6.8	20.7	34.0
0.1	308	304	304	302	300	300	300	300
0.3	368	347	345	344	310	306	306	306
0.5	464	440	424	433	337	328	326	329
0.7	580	540	526	550	387	370	364	366
0.9	670	641	625	661	442	421	414	422
1.0	713	689	672	722	469	450	441	457

respectively. These values of R_i were fitted (least squares) to the LHHW model of heterogeneous reaction rate (Eq. 1).

The equations are:

$$\text{for } Al\text{:}\quad R_{Al} = \frac{0.102\, P_{O_2}}{1. + 0.186\, P_{O_2}},\ g/m^2s, \tag{11}$$

and

$$\text{for } Mg\text{:}\quad R_{Mg} = \frac{0.067\, P_{O_2}}{1. + 0.146\, P_{O_2}},\ g/m^2s. \tag{12}$$

The reaction rate equations are validated against experimental times for an aluminum promoter on an iron rod (Table 7). This model adjusted distances L1 and L2 of Fig. 1b to coincide with the rod just above the promoter metal. Ignition of the rod occurs when the rod core (Subsystem II) reaches the melting temperature for iron, 1800 K. Parameter values for the model analysis are given in Table 5 [12].

TABLE 7--Time-to-ignition comparison for iron.

	Time-to-Ignition, sec.		
Pressure, MPa	<Experimental>	Calculated	Deviation, %
3.44	0.27	0.32	18.0
6.89	0.23	0.24	4.3
20.7	0.21	0.20	-4.8
34.4	0.14	0.18	28.0

The values of the constants (state-space equations, Table 4) for the iron system do not vary from pressure-to-pressure except for the changing enthalpy of reaction, that is, C_7 of Table 4. The calculated values are given in Table 7. As shown in Table 7, the variation of the calculated time-to-ignition for iron is from -5 to 28% when compared to the experimental values. Equations 11 and 12, therefore, provide a reasonable macroscopic reaction rate as a function of oxygen pressure for aluminum and magnesium, respectively.

CONCLUSIONS

A standard metal flammability experiment has been used to study the combustion kinetics of aluminum and magnesium as a function of oxygen pressure at the end of a copper rod. The kinetic parameters have been validated for these materials by computer modeling of the experimental system. The model, a lumped parameter, non-linear set of first order differential equations obtained from mass and enthalpy balances was solved by the MATLAB code. This approach was efficient and consistent with the experimental data available.

At the test conditions, this work provides functional expressions for the burning of aluminum and magnesium over the oxygen pressure range of 3.44 MPa to 68.9 MPa. It confirms that free convection heat transfer correlations provide reasonable values for the experimental conditions, that is, metal combustion at high oxygen pressure. A value of emissivity of 0.3 for the burning metal is consistent with the model.

The Auger and SEM/x ray measurements are adequate for determining extent of reaction and the mixing of the molten promoter material and the copper rod core. Further instrumentation of this system to provide a measurement of the copper rod temperature is warranted and is in progress. Future experiments will focus on the mixing function. With these additional experimental measurements this model will be used to determine kinetic parameters describing the temperature of Al and Mg in oxygen reactions.

REFERENCES

[1] "Flammability, Odor, Offgassing, and Compatibility Requirements and Test Procedures for Materials in Environments that Support Combustion," NHB 88060.1C, Test 17, NASA, Washington, D.C., April 1991, pg 4-58.

[2] Steinberg, T. A., Rucker, M. A., and Beeson, H. D., "Promoted Combustion of Nine Structural Metals in High-Pressure Gaseous Oxygen; A Comparison of Ranking Methods," Flammability and Sensitivity of Materials in Oxygen-Enriched Atmospheres: Fourth Volume, ASTM STP 1040, Joel M. Stoltzfus, Frank J. Benz, and Jack S. Stradling, Eds., American Society for Testing and Materials, Philadelphia, 1989, pp. 54-75.

[3] Himmelblau, D. M. and Bischoff, K. B. Process Analysis and Simulation in Deterministic Systems, John Wiley and Sons, New York, 1971, pp. 31.

[4] Sage, A. P. and Melson, J. L., System Identification, Academic Press, New York, 1971, pg. 2.

[5] PRO-MATLAB User's Guide, The Mat Works, Inc., South Natick, Massachusetts., 1990.

[6] Froment, G. F. and Bischoff, K. B., Chemical Reactor Analysis and Design, John Wiley and Sons, New York, 1979, pp. 90.

[7] Herzberg, G., Molecular Spectra and Molecular Structure, Vol. 1., Second Edition, New York, NY, 1950.

[8] Incropera, F. P. and deWitt, D. P, Fundamentals of Heat and Mass Transfer, 2nd Edition, John Wiley and Sons, New York, 1983, pp. 426-433.

[9] Steinberg, T. A., Wilson, D. B., and Benz, F. J., "The Combustion Phase of Burning Metals," Combust. Flame, 91, 1992, pp. 200-208.

[10] Metals Reference Book, Volume III, Colin J. Smithells, Ed., Plenum Press, New York, 1967.

[11] Swisher, G. M., Introduction to Linear Systems Analysis, Matrix Publishers, Inc., Champaign, ILL., 1976, pp. 8.

[12] Monroe, R. W., Bates, C. E., and Pears, C. D. "Metal Combustion in High-Pressure Flowing Oxygen." Flammability and Sensitivity of Materials in Oxygen-Enriched Atmospheres, ASTM STP 812, B. L. Werley, Ed., American Society for Testing Materials, 1983, pp. 126-149.

Thomas J. Feiereisen[1], Melvyn C. Branch[2], Angel Abbud-Madrid[3] and John W. Daily[4]

GRAVITY AND PRESSURE EFFECTS ON THE STEADY-STATE TEMPERATURE OF HEATED METAL SPECIMENS IN A PURE OXYGEN ATMOSPHERE

REFERENCE: Feiereisen, T. J., Branch, M. C., Abbud-Madrid, A., and Daily, J. W., "Gravity and Pressure Effects on the Steady-State Temperature of Heated Metal Specimens in a Pure Oxygen Atmosphere," Flammability and Sensitivity of Materials in Oxygen-Enriched Atmospheres: 6th Volume, ASTM STP 1197, Dwight D. Janoff and Joel M. Stoltzfus, Eds., American Society for Testing and Materials, Philadelphia, 1993.

ABSTRACT: A fundamental description of the heat transfer mechanisms leading to the combustion of metals in a pure oxygen atmosphere over a range of levels of gravity is important in understanding spacecraft fire safety. In this study, a new method of metal specimen heating to the point of combustion by focused optical radiation was used. A computational model of the laboratory combustion chamber and specimen heating was developed. Accuracy of the computational software was evaluated with two test cases comparing calculated output with experimental data from the literature. Model accuracy was evaluated by comparing computational output with experimental data at 1.0 *g* and 0.1 MPa. A range of gravity from 0.0 *g* to 10.0 *g* and a range of pressure from 0.01 MPa to 1.0 MPa was then explored. The results indicated that for a constant input heat flux on the specimen, convection heat transfer increased and asymptotically approached a limit for both the increased gravity case and increased pressure case. This limit in convection heat transfer caused a limit in minimum specimen temperature regardless of gravity field magnitude or chamber pressure within the ranges studied. In addition, it has been shown computationally that the microgravity laminar free convection environment can be simulated in the terrestrial laboratory by reducing the ambient pressure.

KEY WORDS: microgravity combustion, combustion of bulk metals, free convection, computer modeling, oxygen environment

---

[1]Research Assistant, [2]Professor, [3]Research Assistant, [4]Professor; all authors are at the Center for Combustion Research, Department of Mechanical Engineering, University of Colorado, Boulder, CO 80309-0427

INTRODUCTION

The objectives of this study are to investigate the effect of gravity and pressure (each independently) on the steady-state temperature and the modes of heat transfer for bulk metal specimens subject to high heat flux in a pure oxygen atmosphere. Interest in the combustion of bulk structural metals in an oxygen-enriched atmosphere has grown in regard to spacecraft fire safety. Spacecraft utilize many pressure vessels containing oxidizers and oxygen. Most structural metals, when exposed to a threshold oxygen partial pressure and sufficient temperature, will ignite and burn vigorously until either the metal is consumed or the oxygen partial pressure falls below threshold.

There are three phases of metal combustion; heat-up, ignition and combustion. At standard gravity, studies have been done to explore the heat-up phase [1] and the ignition/combustion phases [2 - 4]. In the microgravity environment, some initial work has been done to explore the combustion phase [5], but the heat-up and ignition phases have been largely ignored. The absence of data on the heat-up and ignition phases is due to the method of ignition of bulk metals in previous combustion experiments. In most experiments, a metal/hydrocarbon igniter was used to ignite bulk metal specimens. This technique, while efficient for studying the combustion phase, is far too rapid to study the heat-up phase and produces too many contaminants to study the ignition phase. An ignition method consisting of a high heat flux radiant light source focused on bulk metal specimens extends the heat-up time and eliminates metal/hydrocarbon igniter contaminants allowing unimpeded study of both phases.

In the following sections, a description of the experimental apparatus is presented. A summary of software verification by comparing calculated output of two classical free convection cases to experimental data found in the literature is given. Modeling of the experimental apparatus of this study is then described including a comparison of calculated temperature output and experimental temperature data obtained in the laboratory. Results and a discussion follow describing the effect of gravity and the effect of pressure on the steady-state temperature of the metal specimen. The relationship between gravity and pressure is also described.

EXPERIMENTAL APPARATUS AND PROCEDURE

The experimental combustion system being modeled is shown in Figure 1. The experimental apparatus consists of a stainless steel cylindrical combustion chamber about 15 cm in diameter and 25 cm high. An oxygen-enriched atmosphere that can vary from near vacuum to 10 atmospheres (1.0 MPa) is contained within the sealed chamber. Cylindrical bulk metal specimens, 6 mm in diameter and 5 mm high, are placed on the ceramic base pedestal. The study described in this paper specifically considers iron specimens. The top surface of the metal specimens are irradiated through a quartz window located in the top of the chamber by a non-coherent, continuous spectrum radiation source located outside the chamber. The radiation source is a 1000 W (input) xenon arc lamp with broad band output in the ultraviolet, visible and near-infrared range. The non-coherent, collimated beam from the source was passed through a lens and focused to a spot roughly the same diameter as the metal specimens. Energy absorption by the oxygen from the beam was calculated as negligible. Thermocouples were used to obtain temperature

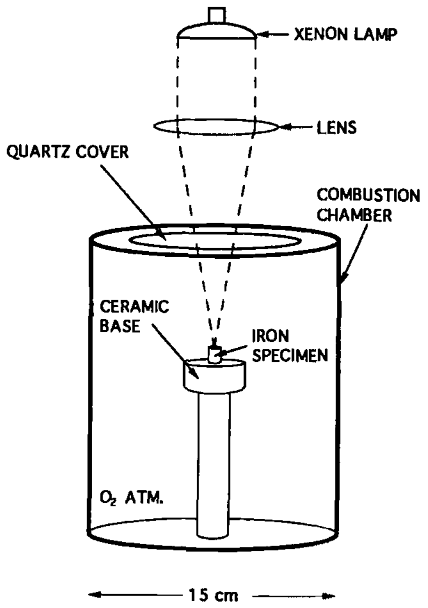

Figure 1. Experimental set-up showing combustion chamber, light source and specimen placement

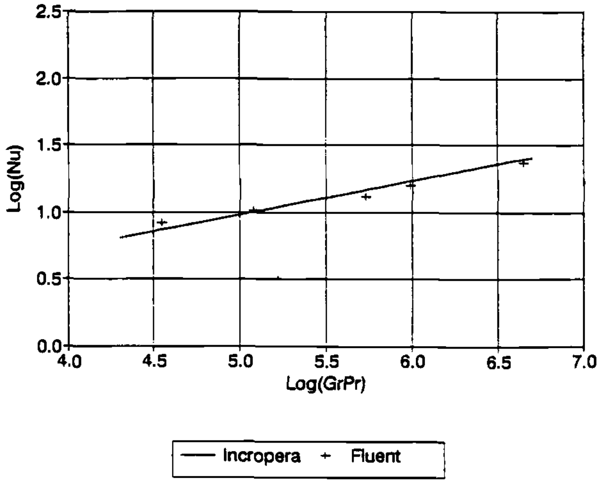

Figure 2. Fluent output comparison to that found in the literature (Incropera) for free convection from a horizontal disk

information during the heat-up phase and the beginning of the ignition phase. Temperature output information ceased at the time of ignition due to the destruction of the thermocouples.

With the combustion chamber sealed and pressurized, the radiation source was adjusted until the focused spot was directly on the metal specimen top surface. The temperature of the specimen was recorded until failure of the thermocouple occurred. The entire process, heat-up, ignition and combustion was also recorded on video tape. A typical observation of a test run for iron specimens is as follows:

0-15 seconds: discoloration, visible expansion of the specimen

15-20 seconds: rapid oxide formation, localized melting

20+ seconds: ignition and vigorous, sputtering combustion

Once combustion was initiated, it would continue for 1-2 seconds until all the metal was consumed.

SOFTWARE VERIFICATION

The computational software used in this study was Fluent [6]. This is an interactive fluid dynamics and heat transfer software package developed by Fluent Inc. Two test cases were run to verify the accuracy of the free convection calculation of the software by comparing software output to experimental data found in the literature. The first case was free convection heat transfer from a horizontal disk and the second case was free convection heat transfer from a vertical wall. Both test cases contain elements of the experiment described in this study. A comparison of both calculated results was made to experimentally-determined relations found in Incropera and DeWitt [7]. Only laminar free convection, Grashof*Prandtl number (GrPr) <~ 1.0E+9, was investigated because the entire scope of the experiments lie within the laminar region.

Variation of GrPr in both test cases was accomplished by varying the characteristic length (disk diameter or wall height, symbolized as d). The Nusselt number (Nu) was evaluated and the results displayed on a log(Nu) as a function of log(GrPr) plot. It should be noted that the computational results were a minor function of grid resolution. As grid resolution increased, the computational results approached a constant. This verification exercise as well as the study described in this paper used a high resolution grid (~1 mm square cell size) to minimize this effect.

Figure 2 shows the comparison of the computational data to the experimentally-determined relation for the horizontal disk. The computational results tend to over-predict the experimental relation at the lower values of GrPr and to under-predict the experimental relation at the higher values of GrPr. However, the variation throughout the range of interest is not more than 13%. Figure 3 shows the comparison of the experimental data to the experimentally-determined relation for the vertical wall. The computational results tend to over-predict the experimental relation over the entire range of interest. In this case, the variation is no more than 12%.

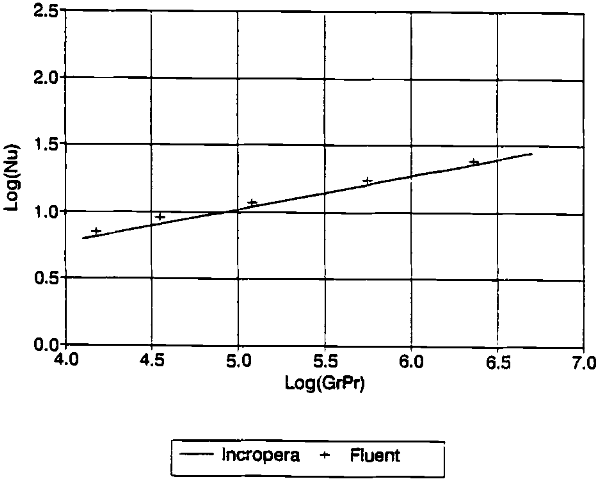

Figure 3. Fluent output comparison to that found in the literature (Incropera) for free convection from a vertical wall

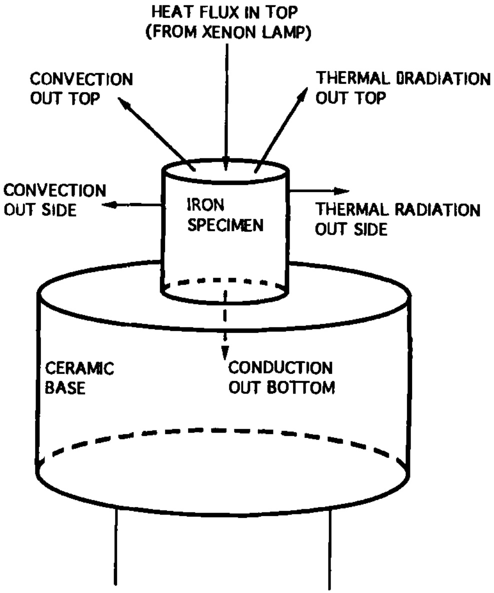

Figure 4. Metal specimen heat transfer modes included in the computational model

The agreement between computational and experimental data seen here is very good considering the complexities of modeling convection heat transfer and the complexities of obtaining reliable experimental convection data. Conduction heat transfer and radiation heat transfer are more well-understood and the modeling of both in the study described in this paper was straight-forward. The largest source of error was computation of the convection heat transfer and this component of error was quantified at no more than 13%.

COMPUTATIONAL MODEL

A diagram of the bulk metal specimen indicating the heat transfer modes included in the computational model is shown in Figure 4. Heat flux from a xenon lamp is input at the top surface. Heat losses include thermal radiation out the top, thermal radiation out the side, conduction out the bottom (including contact resistance between the metal and ceramic), convection out the side and convection out the top.

An axisymmetric, finite difference grid of the metal specimen and the combustion chamber is shown in Figure 5. The top of the ceramic pedestal base is located at the bottom center of the grid with the cylindrical specimen on top of that. The boundaries (exclusive of the ceramic base) are free pressure boundaries allowing oxygen at chamber ambient pressure and temperature to enter the domain and exit the domain as needed to maintain a mass balance. The chamber walls and the region near the walls were excluded from this model because previous iterations of the model indicated very little fluid activity near the chamber walls. Most fluid activity was in the center of the chamber. By eliminating the region near the walls and going to an open domain, the center of the chamber could be modeled in greater detail while keeping computing time to a minimum. The domain included in this model is 8.0 cm diameter and 8.0 cm high. The metal specimen is 6 mm in diameter, 5 mm high and encompasses 6 cells across the diameter and 5 cells in height whereas the entire open domain contains 38 cells across the diameter and 33 in height. Idealization of the system reduces the number of physical processes that are modeled. Secondary physical processes such as specimen expansion and oxide formation are not modeled. All the computational studies described in this paper do not consider oxygen-metal reactions.

Oxygen is considered a perfect gas over the entire range of temperature and pressure investigated and solids are unaffected by changes in pressure so the fluid and metal properties were input as functions of temperature only. Metal surface properties were idealized as constant. The study described in this paper considered only iron as the metal specimen. Similar heat transfer and temperature trends can be expected with most metals and gases under similar conditions. Ceramic properties were nearly constant over the temperature range considered in this study and were input as such. An estimate of contact resistance between the metal specimen and the ceramic base of 20% of the thermal conductivity of the ceramic was used.

The maximum GrPr over the range of temperature, pressure and gravity was calculated at about 3.0E+4. The critical GrPr number is 1.0E+9 so the fluid in the combustion chamber remains well within the laminar regime and no turbulence models were invoked.

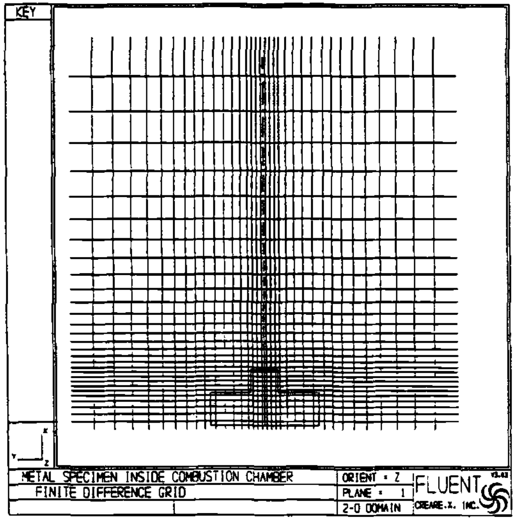

Figure 5. Finite difference grid for the combustion chamber and metal specimen

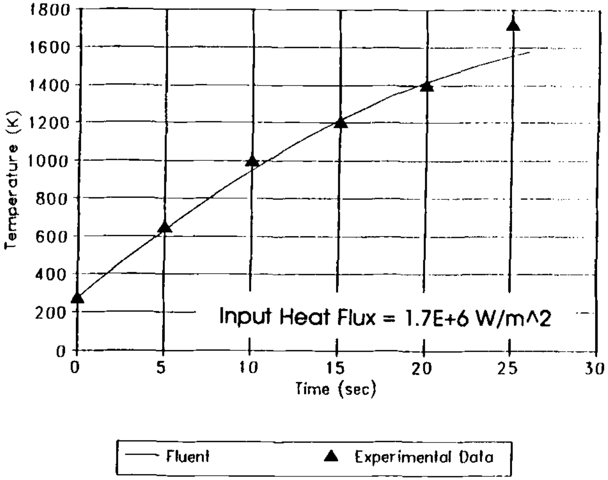

Figure 6. Metal specimen transient temperature comparison between computational output and experimental data

input flux used to heat a metal specimen was not known because the xenon lamp output, focused spot size and spot placement were only approximately known. An estimate of the specimen input flux was made by adjusting the model input flux until the measured temperature data matched the model temperature data. By this method, the average heat flux was determined to be 1.7E+6 W/m^2. A comparison between the experimental data and the model data is shown in Figure 6. The agreement between the experimental data and the model data is quite good in both trend and magnitude up to about 20 seconds and about 1400 K. Beyond that point, the experimental data diverges from the model data because the surface reactions of combustion begin to drive the temperature of the metal specimen. The computational model does not include surface reactions and therefore only continues to rise asymptotically to some steady-state level.

A steady-state (heat input equals heat transfer from the specimen) test case with gravity = 1.0 *g* and pressure = 0.1 MPa was run with a reduced heat flux (1.1E+6 W/m^2) to obtain realistic pre-ignition metal temperatures. Steady-state temperature distribution is displayed in Figure 7 to obtain a qualitative understanding of the temperature distribution in the fluid. This temperature distribution is what one would expect for buoyancy induced flow. Contrast this temperature distribution with the temperature distribution of Figure 8 obtained at 0.0 *g*. We see that the convection plume ceases to exist at 0.0 *g* and the fluid merely conducts the heat away without fluid movement.

The transient model temperature data match with the experimental data and the steady-state temperature distribution as expected provides confidence that the model is actually describing the experimental system. An investigation of the temperature and heat transfer mode variation as a function of both gravity and pressure was conducted with the steady-state model to eliminate time as an additional variable.

RESULTS AND DISCUSSION

Effect of Gravity:

A plot of metal specimen steady-state temperature as a function of gravity for a pressure of 0.1 MPa is given in Figure 9. The specimen temperature is highest (1577 K) at 0.0 *g* and decreases with increasing gravity reaching 1498 K at 10.0 *g*. The largest influence of gravity on the specimen steady-state temperature occurs between 0.0 *g* and 1.0 *g* with 38% of the temperature drop occurring by 1.0 *g*. The temperature appears to be approaching a limit asymptotically.

The reason for this temperature behavior can be explained by the steady-state heat transfer component as a function of gravity plot of Figure 10. The conduction heat loss is nearly constant over the entire range of gravity but the convection heat loss increases with increasing gravity. This behavior is almost intuitive but what is not intuitive is the asymptotic manner of the convection heat transfer with increasing gravity. One notes an increase from 5.5 W at 0.0 *g* to 9.2 W at 10.0 *g* with 38% of that increase occurring between 0.0 *g* and 1.0 *g* thus accounting for the specimen temperature drop over the range of gravity investigated. There appears to be a limit to the magnitude of convection heat transfer regardless of the strength of the gravity field beyond a certain level (not ascertained in this study). The asymptotic behavior of the steady-state specimen temperature as a function of

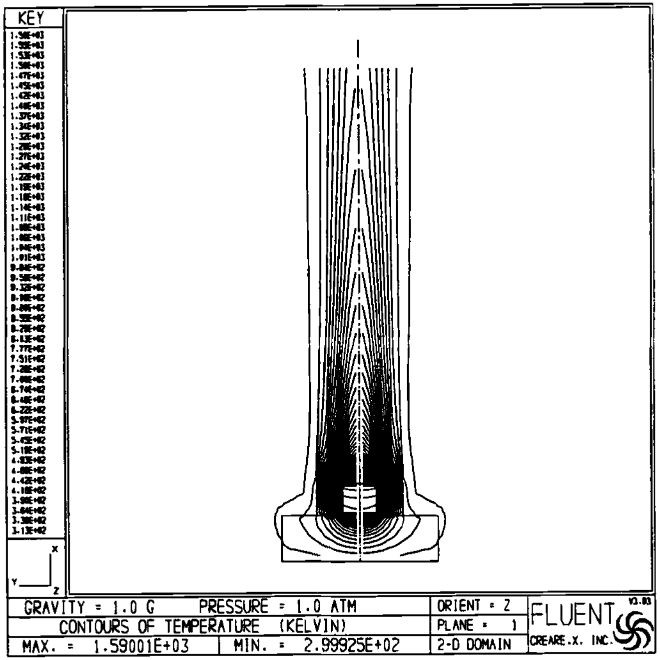

Figure 7. Steady-state temperature distribution in the domain for gravity = 1.0 g and pressure = 0.10 MPa

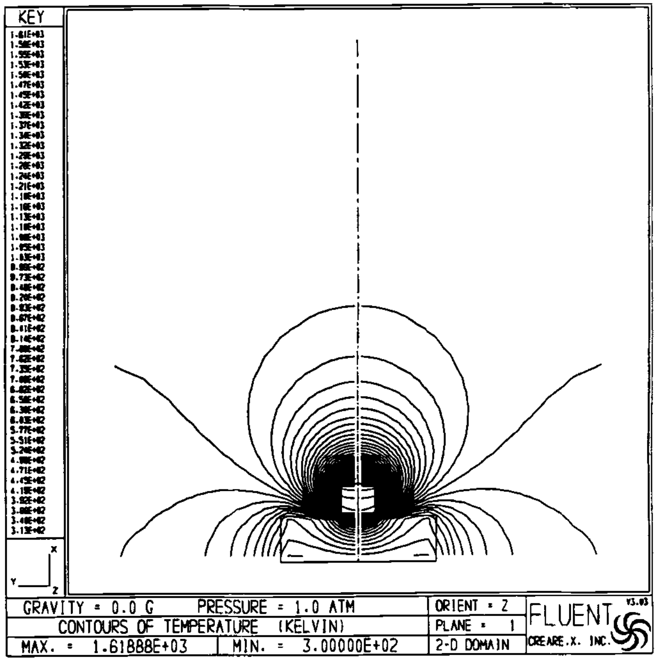

Figure 8. Steady-state temperature distribution in the domain for gravity = 0.0 g and pressure = 0.10 MPa

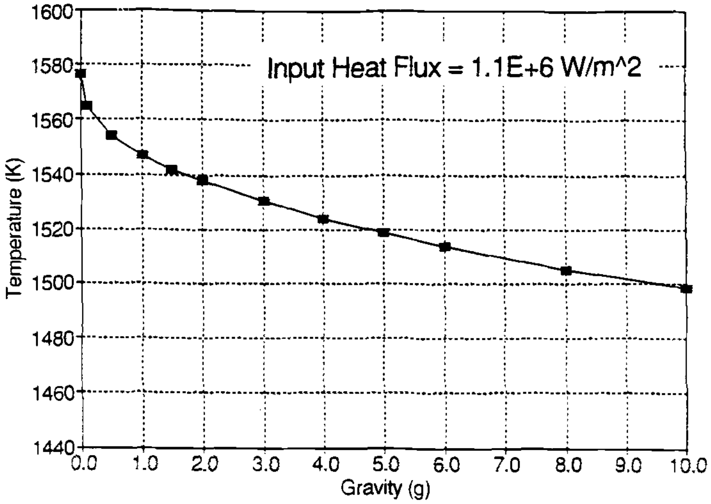

Figure 9. Metal specimen steady-state temperature (averaged) as a function of gravity (at 1.0 atmosphere)

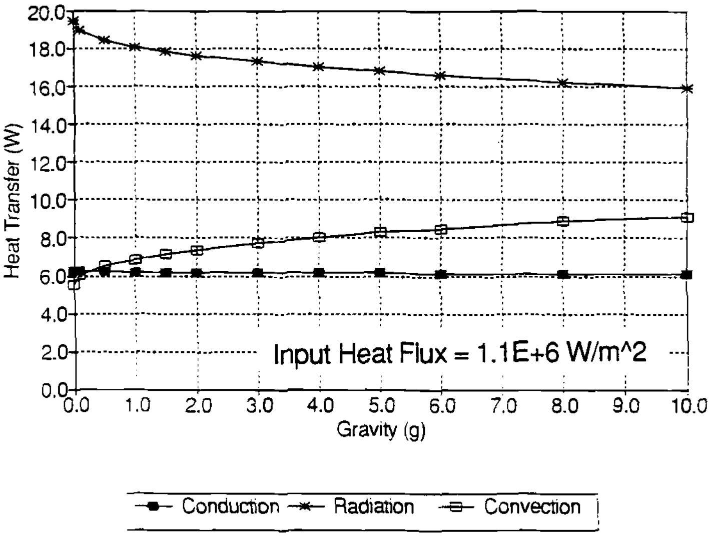

Figure 10. Metal steady-state heat transfer component as a function of gravity (at 1.0 atmosphere)

gravity is explained through the variation in fluid thermal conductivity (k) as the fluid steady-state temperature varies over the range of gravity explored. With increased gravity, the driving force of convection is increased. The result is a greater movement of fluid through the domain of interest with fluid entering the domain at ambient temperature. The quicker the fluid moves through the domain, the less it heats up and therefore, the surrounding fluid temperature does not get as high as when fluid remains within the domain of interest longer. As one would expect, Nusselt number continues to increase with increased gravity (41% increase between 0.0 *g* and 5.0 *g*). At the same time, thermal conductivity of the fluid is decreased with decreased surrounding fluid steady-state temperature (17% decrease between 0.0 *g* and 5.0 *g*). The net result is that these two opposing effects counter each other based on the heat transfer relation:

$$h = \frac{Nu * k}{d} \tag{1}$$

The heat transfer coefficient moderates with increasing gravity causing the steady-state specimen temperature to approach a constant value in the gravity range studied.

Effect of Pressure:

A plot of metal specimen steady-state temperature as a function of pressure at 1.0 *g* is given in Figure 11. The specimen temperature is highest (1570 K) at low pressure (0.015 MPa) and decreases with increasing pressure. A fairly linear relationship exists between the pressure and the specimen steady-state temperature between low pressure and about 0.3 MPa. The temperature then bottoms out at 1475 K by about 0.5 MPa pressure and remains there regardless of the pressure increase up to at least 1.0 MPa. There is some indication from Figure 11 that the steady-state temperature may actually increase again at higher pressure.

This temperature behavior can be explained by the steady-state heat transfer component as a function of pressure plot of Figure 12. The conduction heat loss is again nearly constant over the entire range of pressure but the convection heat loss increases with increasing pressure. Again, this behavior is almost intuitive but what is unexpected is the plateau behavior in the convection heat transfer beyond about 0.5 MPa. One notes an increase in convection heat transfer from 5.8 W to 10.0 W between 0.0 MPa and 0.5 MPa but no increase beyond that thus accounting for the drop in temperature in that range of pressure. There is a limit to the magnitude of convection loss regardless of the chamber pressure beyond about 0.5 MPa and up to at least 1.0 MPa. The asymptotic behavior of the steady-state specimen temperature as a function of pressure can be explained in a manner similar as that for the case where gravity was a variable. The driving force of convection is enhanced at increased pressure due to the higher density of the fluid in contact with the metal specimen. This in turn drives more fluid through the domain of interest with that fluid entering at ambient temperature. At increased pressure, the steady-state temperature of the surrounding fluid is decreased. As in the gravity as a variable case, Nusselt number is increased at increased pressure (278% increase between 0.015 MPa and 0.5 MPa). At the same time, thermal conductivity is decreased with the decreased steady-state temperature caused by the increased pressure (38% decrease between 0.015 MPa and 0.5 MPa). The net result again is that these two opposing

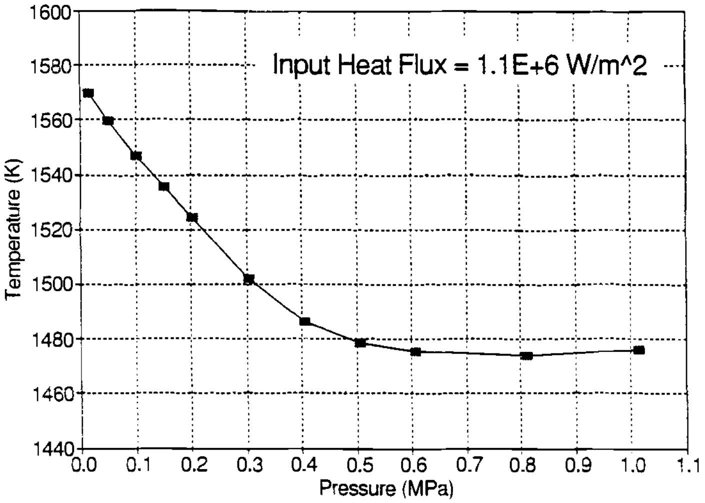

Figure 11. Metal specimen steady-state temperature (averaged) as a function of pressure (at 1.0 gravity)

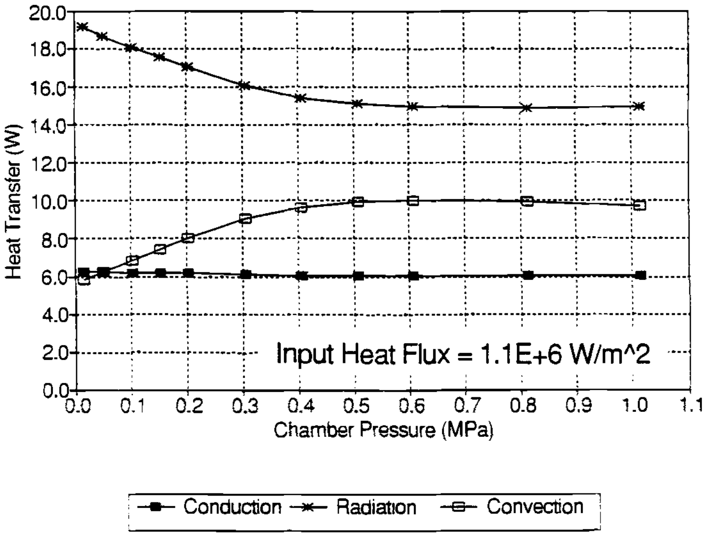

Figure 12. Metal steady-state heat transfer component as a function of pressure (at 1.0 gravity)

effects tend to counter each other based on Equation 1. and the heat transfer coefficient moderates with increased pressure. This in turn causes the steady-state specimen temperature to approach a constant value in the pressure range studied.

Relationship between Gravity and Pressure

Compare the specimen temperature as a function of gravity curve (Figure 9) and specimen temperature as a function of pressure curve (Figure 11). The parabolic character of the temperature as a function of gravity curve (gravity <~ 2.0 g) and the linear character of the temperature as a function of pressure (pressure <~ 0.3 MPa) suggests a relationship between these two curves. That relationship is that buoyancy scales like pressure squared times gravity (p^2g), [8]. This would indicate that the microgravity laminar free convection environment can be simulated at 1.0 *g* simply by manipulating the ambient pressure. A check of this hypothesis was conducted computationally. A model simulation was run with 0.01 *g* and 0.1 MPa with the temperature distribution results given in Figure 13. We see a wide, weak plume above the metal specimen as opposed to the narrow, strong plume presented in the temperature distribution plot of Figure 7. Based on the p^2g relationship, we would expect to find a very similar temperature distribution in the domain for a gravity of 1.0 *g* and pressure of 0.01 MPa (conditions easily produced in the terrestrial laboratory). Figure 14 is that temperature distribution for 1.0 *g* and 0.01 MPa. Comparing Figure 13 and Figure 14, we see that both temperature distributions are very similar. The temperature distributions are so similar that, for these two cases, the temperature at each corresponding cell between analyses differs by less than 1 °K. Clearly, the microgravity environment for laminar free convection can be simulated by simply manipulating the ambient pressure according to the relationship buoyancy scales like p^2g.

CONCLUSIONS

Several conclusions can be drawn from this work. At a constant heat flux input and at steady-state:

- Specimen temperature decreases with increasing gravity but appears to approach a limit. In this study, the steady-state temperature dropped from 1577 K to 1498 K between 0.0 *g* and 10.0 *g* with 38% of that drop occurring between 0.0 *g* and 1.0 *g*.
- Convection heat transfer increases with increasing gravity. In this study, convection heat transfer increased from 5.5 W to 9.2 W between 0.0 *g* and 10.0 *g* with 38% of that increase occurring between 0.0 *g* and 1.0 *g* thus accounting for the behavior of the specimen temperature.
- Specimen temperature decreases with increasing pressure but also appears to approach a limit. In this study, the steady-state temperature dropped from 1570 K to about 1475 K between 0.015 MPa and 0.5 MPa and stays nearly constant beyond 0.5 MPa.
- Convection heat transfer increases with increasing pressure. In this study, convection heat transfer increased from 5.8 W to 10.0 W between 0.015 MPa and 0.5 MPa and then remained nearly constant

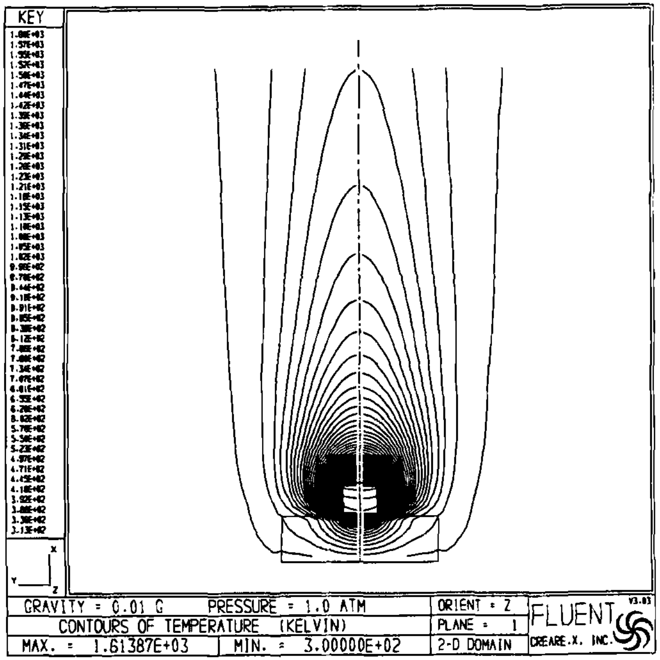

Figure 13. Steady-state temperature distribution in the domain for gravity = 0.01 g and pressure = 0.10 MPa

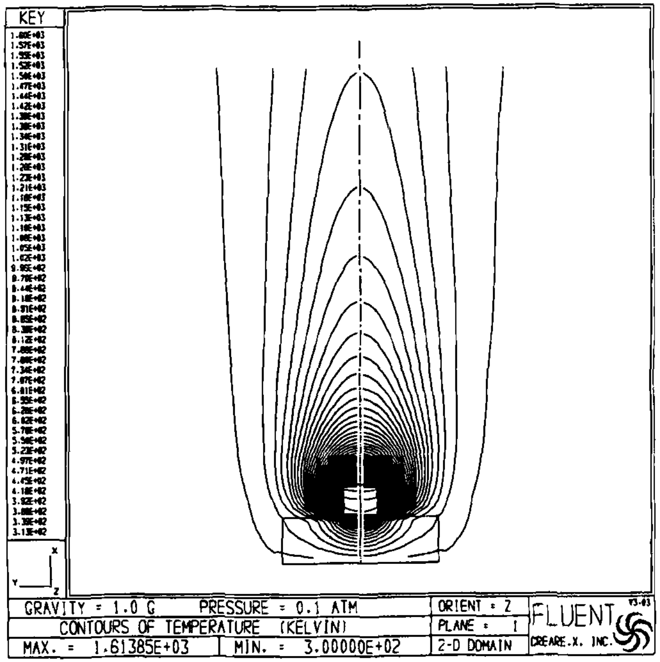

Figure 14. Steady-state temperature distribution in the domain for gravity = 1.0 g and pressure = 0.01 MPa

beyond 0.5 MPa thus accounting for the behavior of the specimen temperature.

- Asymptotic behavior of all curves is due to a balance being struck between the increased buoyant forces and the decreased thermal conductivity of the fluid over the range of variables studied.

In addition:

- Bulk metals may be easier to ignite in the microgravity environment due to the reduced rate of convection heat transfer in the microgravity environment.
- Ignition energy is relatively insensitive to pressure above 0.5 MPa (until at least 1.0 MPa)
- Microgravity laminar free convection experiments may be simulated with low pressure at 1.0 *g* (from buoyancy scales like p^2g).

ACKNOWLEDGMENT

This work is sponsored by the National Aeronautics and Space Administration, Grant NASA-NAG3-1257

REFERENCES

[1] Gebhart, B., "Transient Natural Convection from Vertical Elements," Journal of Heat Transfer, February, 1961, pp. 61-70

[2] Mellor, A. M. and Glassman, I., "A Physical Criterion for Metal Combustion," Pyrodynamics, Vol. 3, 1965, pp. 43-64

[3] Sullivan, H. F. and Glassman, I., "Vapor-Phase Diffusion Flames in the Combustion of Magnesium, Calcium and Strontium," Combustion Science and Technology, Vol. 4, 1972, pp. 241-256

[4] Nguyen, K. and Branch, M. C., "Ignition Temperature of Bulk 6061 Aluminum, 302 Stainless Steel and 1018 Carbon Steel in Oxygen," Combustion Science and Technology, Vol. 53, 1987, pp. 277-288

[5] Steinberg, T. A. and Wilson, D. B., "The Burning of Metals and Alloys in Microgravity," Combustion and Flame, Vol. 88, 1992, pp. 309-320

[6] Fluent Computational Fluid Dynamics Software, Version 3.03, Fluent Inc., Lebanon, New Hampshire, 1991

[7] Incropera, F. P. and DeWitt, D. P., Introduction to Heat Transfer, 2nd ed., John Wiley and Sons, New York, 1990, pp. 500, 506

[8] Mortazavi, S., Sunderland, P. B., Jurng, J., Faeth, G. M., "Structure and Soot Properties of Non-Buoyant Laminar Round-Jet Diffusion Flames," Proceedings from the Second International Microgravity Combustion Workshop, NASA Lewis Research Center, Cleveland, Ohio, September 15-17, 1992

Angel Abbud-Madrid[1], Melvyn C. Branch[2], Thomas J. Feiereisen[3] and John W. Daily[4]

IGNITION OF BULK METALS BY A CONTINUOUS RADIATION SOURCE IN A PURE OXYGEN ATMOSPHERE

REFERENCE: Abbud-Madrid, A., Branch, M. C., Feiereisen, T. J., and Daily, J. W., "Ignition of Bulk Metals by a Continuous Radiation Source in a Pure Oxygen Atmosphere," Flammability and Sensitivity of Materials in Oxygen-Enriched Atmospheres: 6th Volume, ASTM STP 1197, Dwight D. Janoff and Joel M. Stoltzfus, Eds., American Society for Testing and Materials, Philadelphia, 1993.

ABSTRACT: The present work investigates the mechanisms that lead to ignition and subsequent self-sustained combustion of bulk metals. To this effect, an experimental study isolating the ignition process was conducted with the novel feature of using a short-arc lamp as a non-coherent, continuous radiation source. A 1000 W xenon arc lamp was used to irradiate the top surface of a cylindrical metal specimen 5 mm in diameter and 5 mm high in a quiescent pure-oxygen (O_2) environment at an absolute pressure of 0.1 MPa. Measurement of surface temperature histories and a qualitative visual record of the ignition process and the subsequent self-sustained combustion event were obtained. Iron (Fe), titanium (Ti), zirconium (Zr), magnesium (Mg), zinc (Zn), tin (Sn), copper (Cu) and aluminum (Al) specimens were investigated. All metals exhibited ignition and sustained combustion except with the aluminum sample. Ignition temperatures below, above or in the range of the metal melting point were found. Ignition and combustion of copper rods at 0.1 MPa in normal gravity conditions revealed the dramatic effect of sample geometry, experimental configuration and ignition source on the ignitability and flammability of bulk metals.

KEYWORDS: bulk metals, ignition, combustion, radiative heating, continuous radiation source, oxygen, iron, titanium, zirconium, magnesium, zinc, tin, copper, aluminum.

---

[1] Research Assistant, [2] Professor, [3] Research Assistant and [4] Professor, Center for Combustion Research, Mechanical Engineering Department, University of Colorado, Boulder, CO 80309-0427.

INTRODUCTION

Early research on combustion of metals was motivated by the knowledge of the large heat release and corresponding high temperatures associated with metal-oxygen reactions. The advent of space flight brought about an increased interest in the ignition and combustion of metallic particles as additives in solid rocket propellants. More recently, attention has been given to the flammability properties of bulk, structural metals due to the high number of accidents involving burning metal components in high-pressure oxygen systems [1].

Less attention has been given to the ignition phenomena of bulk metals, i.e., the mechanisms that lead to a self-sustaining exothermic reaction. As with combustion studies, the majority of the early work was concentrated on the ignition of finely divided powders [2,3]. These studies showed that when fine metallic particles without an oxide coating were quickly exposed to air, ignition occurred due to the pyrophoric reaction. Recently there has been a growing interest on studying the ignition of bulk, structural metals. The promoted ignition test developed by the NASA White Sands Test Facility [4] utilizes easily ignitable metals or hydrocarbons to ignite a cylindrical metal rod on the bottom end for upward propagation studies. This method has the disadvantages of the contaminating effect of the reaction between the ignition source material and the metal sample, and the poor estimate of the ignition energy transferred to the metal.

Non-intrusive techniques have also been used to determine ignition behavior. Brzustowski and Glassman [5] explored ignition by direct electric heating of metal wires and ribbons. The ignition point was determined by the balance of the rate of heat produced and the rate of heat removed from the metal sample. Bransford and Clark [6] used a carbon dioxide (CO_2) laser to ignite metals and alloys. They defined the ignition point by monitoring the mass as a function of time. A large mass increase was found at this point due to accelerated oxidation. Nguyen and Branch [7] utilized a CO_2 laser and a two-color pyrometer to determine the surface temperature of aluminum, 302 stainless steel and 1018 carbon steel specimens. Ignition was defined as the point at which there exists an abrupt change in the slope of the light intensity curve detected by the pyrometer.

These three studies show the importance of utilizing a non-intrusive ignition source which also provides a close estimate of the heat input flux. Nevertheless, it is evident from the results of these investigations that there is a lack of common agreement regarding the definition of an ignition point. The difficulty of providing an accurate ignition model is complicated by factors such as: metal type, oxygen pressure, formation of protective oxide layers, experimental apparatus and configuration, gravitational force and sample size. As a consequence, there is a strong need to provide a fundamental study that identifies all the important variables that characterize the ignition phenomena.

The following work represents a preliminary study that is part of a broader research effort aimed at providing further insight into this multi-variable dependent phenomena by looking at the effects of gravity on the ignition behavior of metals. Studies conducted under microgravity conditions provide simplified boundary conditions since buoyancy is removed and make possible the identification of fundamental ignition mechanisms. The scope of this preliminary experimental study includes the use of a continuous radiation ignition source, the measurement of surface temperature of a variety of metals and a qualitative observation of the ignition phenomena at normal gravity.

OBJECTIVES AND APPROACH

The specific objectives of this investigation include: a) a feasibility study for the use of a continuous radiation source for metal ignition, b) testing and characterization of the ignition behavior of a variety of metals and c) building a preliminary experimental database of ignition of metals under normal gravity conditions.

The advantage of using a continuous radiation light source lies primarily on its non-intrusive character and on the nature of its spectral distribution. A short-arc lamp provides broadband radiation in the ultraviolet, visible and near-infrared regions (in the 200-1200 nm range); since the absorptivity of metals increases significantly with decreasing wavelength within this spectral range, this feature will in turn result in a decreased input power requirement. The flexibility, ruggedness and low-weight properties of these lamps make them also very attractive for future experiments on high-speed centrifuges (for elevated gravity environments) and zero-gravity simulators (for reduced gravity experiments).

The metals tested in this investigation, iron (Fe), titanium (Ti), zirconium (Zr), magnesium (Mg), zinc (Zn), tin (Sn), copper (Cu) and aluminum (Al) were selected because of their importance as elements of structural metals and their simple chemical composition (pure metals instead of multi-component alloys to avoid complication in future morphology and spectroscopic studies). In addition, these specimens exhibit a wide range of melting and boiling temperatures, heats of combustion, oxide formation processes and adiabatic flame temperatures. Copper was selected since no reported cases of copper rod burning at normal gravity were found in the literature (copper wire mesh of 0.19 mm diameter has been burned by Stoltzfus, et. al. [8] and copper rods of 3.2 mm diameter have been burned under microgravity conditions by Steinberg, et. al. [9]). Table 1 gives the chemical composition of all the metals tested in this investigation. The experimental approach consisted in providing surface temperature profiles, ignition temperature values and a qualitative record of the heating, ignition and combustion stages of the metal specimen.

EXPERIMENTAL APPARATUS AND PROCEDURES

The experimental system is shown in Figure 1. The radiation source selected consisted of a 1000 W xenon short-arc lamp with 250 W of broadband output radiation power (with approximately 42% of output power between 800-1200 nm and the rest between 200-800 nm).

The high-intensity, non-coherent light comes out of the lamp in a highly collimated beam (4° half-angle) and is then intercepted by an aspheric lens (8 cm diameter, 6 cm focal length) which provides the maximum light collection efficiency for the available focal length under these conditions. The beam is then focused down to a 5 mm spot on the top surface of a metal sample providing approximately a 1 MW/m^2 power density. The cylindrical metal specimen is 5 mm in diameter and 5 mm in height and rests on top of a circular refractory brick base which isolates the metal sample from heat conduction to its supporting pedestal. These components (lens, specimen and pedestal) are located inside a 4.5 L stainless steel cylindrical chamber which permits input radiation through a 10 cm diameter, 2 cm thick quartz window. Visual access is provided by three side quartz windows. A pure oxygen environment (99.5% (min) O_2) is provided in all tests at an absolute pressure of 0.1 MPa. The absorption of radiation by O_2 at this pressure

TABLE 1 -- Chemical composition of metals tested

Metal	Chemical composition (in parts per million, ppm)													
	Ag	Al	As	Bi	C	Ca	Cd	Cu	Cr	Fe	Hf	In	Mg	Mn
Aluminum		bal[1]				13		12		<77			17	
Copper	1		10	2				bal		2			1	
Iron	42									bal			2	1
Magnesium		100				150		20		50			bal	50
Tin	0.1			0.1		0.1		0.2		0.5		2	0.5	
Titanium					30					100				
Zinc	8			<1			<2	50					2	
Zirconium		2						10	2	50	35			

	N	Na	Ni	O	P	Pb	S	Sb	Si	Sn	Ti	W	Zn	Zr
Aluminum									<72					
Copper			30			3		20	5	5				
Iron		55	40		10		67		4	5			8	
Magnesium			10			50			50	10			100	
Tin						1		2		bal				
Titanium	80			100							bal			
Zinc						3			2	1			bal	
Zirconium									<25		2	2		bal

[1] bal refers to the balance of the chemical composition of this element.

and spectral range is negligible. The chamber pressure is monitored by a solid-state piezoresistive pressure transducer. The specimen surface temperature is measured by a Platinum-Platinum/10% Rh (0.1 mm diameter) thermocouple located in the center of the sample at approximately 0.5 mm below the top surface. The thermocouple leads are shielded by insulating ceramic tubing and are introduced to the centerline of the sample from one side of the top surface. Visual observations are recorded with a video camera with appropriate filtering equipment.

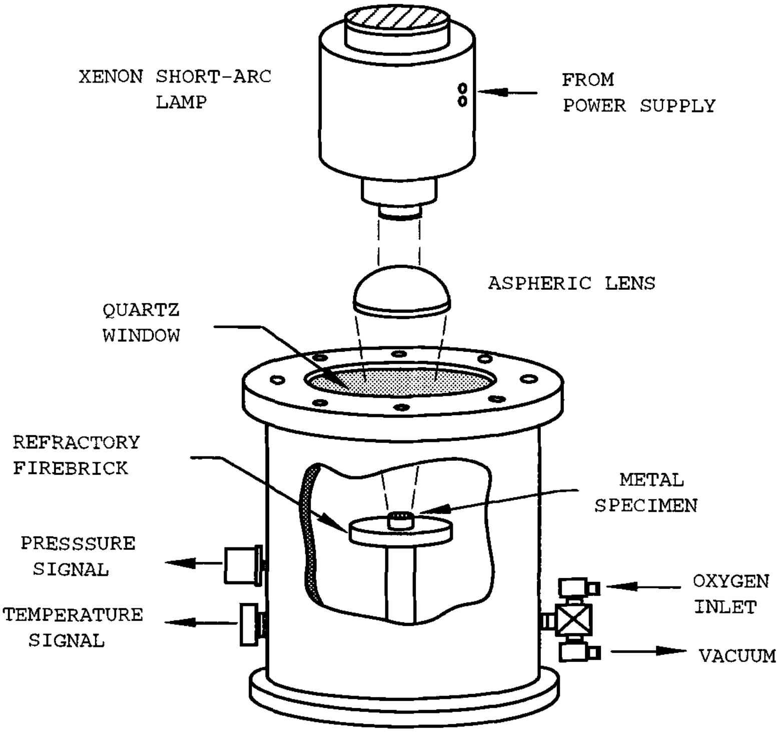

FIG. 1 -- Experimental Apparatus

Prior to the experimental run, the metal sample is thoroughly cleaned and placed on top of the refractory firebrick. Care is taken to assure that the thermocouple makes good contact with the metal by checking electrical continuity. After closing the combustion chamber, three evacuation and filling cycles are executed to provide a pure-oxygen atmosphere inside the vessel. The lamp is turned on to the desired output power and the light beam is focused on top of the metal specimen. Immediately after ignition the lamp is turned off to remove all external heating to the sample. The experiment is monitored throughout by temperature and pressure displays, a temperature chart recorder and the video camera. After complete combustion, the final pressure is recorded to quantify oxygen consumption. A minimum of 5 samples of each metal are tested to ensure experimental repeatability.

RESULTS AND DISCUSSION

Initial testing of the short-arc lamp performance was done with simple heating and melting experiments with the different metals in air at atmospheric conditions. Melting was successfully achieved in all cases in time periods ranging from 15 to 30 seconds. The lamp was then tested for radiant ignition of metal samples in a pure-oxygen atmosphere. All metals, except Al, exhibited ignition and combustion within the same time period as with the melting tests. Having proved the effectiveness of the radiation source for sample ignition, multiple tests were performed with all the aforementioned metals. The results obtained are summarized in the next three sections.

Qualitative Observations

A visual record of all successful experimental runs revealed the existence of three important and distinctive phases:

a) The heating period started with a sudden thermal expansion of the top surface of the specimen after radiation was applied. Surface structure changes were also detected by the variation of the radiation characteristics of the sample. These surface changes are related to the allotropic nature of some metals in the solid phase and the metal oxide layer formation.

b) The ignition phase was characterized by rapid oxidation and a noticeable increase in energy release evidenced by the intense radiation emitted from the reaction zone.

c) The combustion event varied in speed and strength among the different metals tested. In the case of iron, titanium, and zirconium, a well defined self-sustained propagation of the reaction zone at the top surface was accompanied by a violent exothermic reaction including random outward expelling of small particles. The detection of intense luminosity was due to the high temperatures (3000-4000 K) reached in the reaction zone.

For magnesium and zinc the combustion phase evolved much faster with the generation of a fine oxide powder that formed a dust cloud which deposited uniformly on the walls and windows of the combustion chamber. This behavior may suggest the existence of volatile metal or metal oxide products.

A marked difference in reaction intensity and combustion behavior was observed with copper as described in the Special Cases section.

Temperature Profiles

Temperature records also revealed uniquely the existence of the heating, ignition and combustion stages. Figures 2 and 3 show the temperature histories of all the metal specimens studied at 0.1 MPa. In all cases there is a steep rise in surface temperature in the first second of heating caused by the sudden flux of radiant energy from the light source. This increase in temperature in turn generates conductive, convective and radiative heat transfer from the upper surface of the sample that significantly lowers the rate of temperature increase. In the case of Fe, Ti and Zr (Fig. 2) this rate continues monotonically until a point of inflection is reached in the curve after which the temperature vs. time slope rapidly increases again.

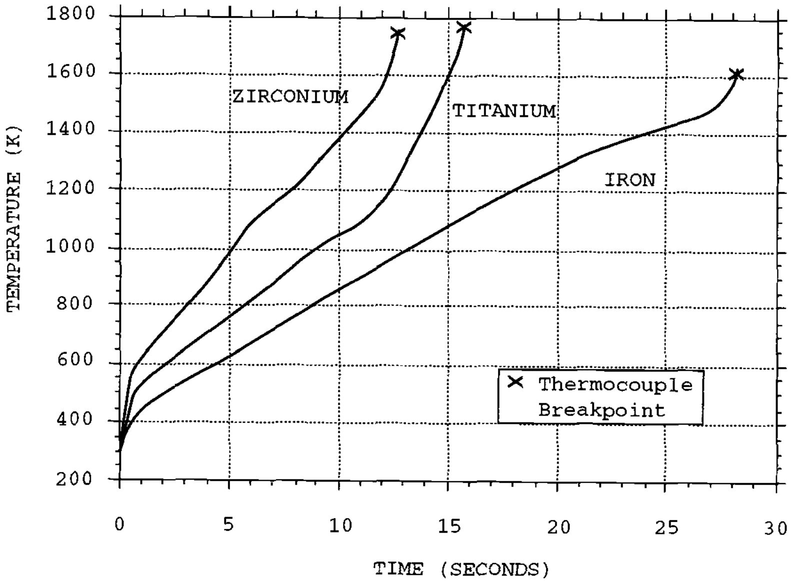

FIG. 2 -- Temperature vs. time behavior of iron (Fe), titanium (Ti) and zirconium (Zr).

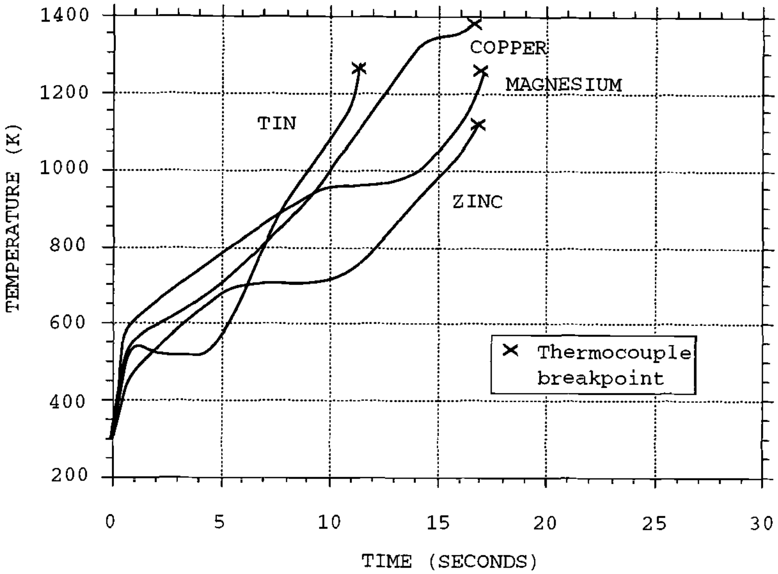

FIG. 3 -- Temperature vs. time behavior of tin (Sn), zinc (Zn), magnesium (Mg) and copper (Cu).

This transition point is identified as the temperature at which the heat generated by the metal oxidation first exceeds the heat lost through conduction, convection and radiation. This temperature is defined in this investigation as the ignition temperature of the metal sample. For Fe, Ti and Zr the ignition temperature occurs below their melting point.

Beyond the ignition temperature, the metal specimen is driven into a thermal runaway region as a consequence of the exponential dependence of the reaction rate on temperature. The acceleration of the reaction rate ultimately leads to the exothermic, self-sustained combustion event. At this stage, the temperature drastically increases to values in the range of 3000-4000 K depending on the metal type where it stays throughout the combustion phase. As shown in Figure 2, the thermocouples are unable to follow the temperature increase in this last stage because their maximum operating temperature is around 1750 K. A small but noticeable change in the slope around 1100 K can also be detected in the case of Ti and Zr samples. This change corresponds to a solid phase transition on both metals (Ti at 1155 K and Zr at 1135 K). The latent heat associated with this crystal structure change from an hexagonal close-packed structure to a body-centered cubic lattice (4.4 kJ/mol for Ti and 3.9 kJ/mol for Zr) is responsible for the slope change in the temperature profiles. The similar behavior encountered in the heating, ignition and combustion phases of Ti and Zr may be related to both metals being elements of Group IVb in the periodic table.

Figure 3 shows the temperature histories for the Sn, Zn, Mg and Cu samples. In contrast with the results from Figure 2, these profiles show an intermediate plateau which corresponds to the solid-liquid phase transition point. The heat released by oxidation at this point is still lower than the heat lost by the specimen and the temperature continues to increase almost exclusively by the radiant flux from the xenon lamp. Eventually the ignition temperature is reached and the molten metal confined by the outside oxide layer bursts out and exothermically reacts with the oxygen gas. In the case of Mg and Zn the ignition temperature is so close to the boiling temperature of the metal that there is probably volatilization of the metal or the oxide product, explaining the existence of the metal oxide particle cloud that forms after ignition. This combustion behavior has been observed before with Mg, Zn and Al rods using the pressurized oxygen index apparatus [10]. For copper, its ignition temperature coincides with the melting temperature of the metal.

Table 2 shows the heat of combustion, melting, ignition, and adiabatic flame temperatures at 0.1 MPa of the different metals used in this investigation. In the case of Fe, Ti and Zr it is evident that the ignition temperature is always below the melting temperature of the metal, whereas the opposite is true for Mg, Zn and Sn.

Special cases

The following cases represent two noteworthy examples of different behavior from the previously mentioned results.

a) Aluminum. All ignition tests performed on aluminum were unsuccessful. This metal proved to be very difficult to ignite due to the formation of a highly insulating oxide layer that prevented the molten metal inside to come into contact with the surrounding oxygen atmosphere. The existence of this protective oxide layer has been confirmed by other studies [5,7,11].

TABLE 2 -- Heats of combustion, melting, ignition and adiabatic flame temperatures at 0.1 MPa of the metals studied.

Metal Specimen	Heat of Combustion (kJ/mol)[a]	Melting Temperature (K)[b]	Ignition Temperature (K)[c]	Adiabatic Flame Temp. (K)[d]
Aluminum	1656	933	2327	4005
Titanium	1520	1939	1670	3993
Zirconium	1097	2125	1555	4278
Tin	738	504	1156	...
Magnesium	601	923	1250	3432
Zinc	432	692	1060	...
Iron	272	1809	1470	3400
Copper	156	1358	1360	...

[a] From JANAF Tables [12]. The heats of combustion correspond to the following metal/metal oxide system: Al/Al_2O_3, Ti/Ti_2O_3, Zr/ZrO_2, Sn/SnO_2, Mg/MgO, Zn/ZnO, Fe/FeO, Cu/CuO

[b] From JANAF Tables [12].

[c] From this investigation, except for Al from Brzustowski, et. al. [5]

[d] From Steinberg, et. al. [13]

Table 2 shows that the ignition temperature of Al is much higher than the melting temperature of the metal and it actually corresponds to the melting point of the metal oxide (Al_2O_3). Prolonged heating was applied to induce ignition in the metal sample, but the surface temperature reached a steady-state value below the melting point of the metal oxide.

b) Copper. A very interesting and unexpected result of this investigation was the ignition and combustion of copper samples by radiant heating. Previous work [4,10] has classified copper rods as non-flammable even at the highest possible pressure (69.5 MPa in some cases) due to the sudden extinction of the sample after ignition on upward propagation studies at normal gravity using the promoted combustion test (with 3.2 mm diameter rods). Under our experimental configuration, clear evidence of ignition and subsequent downward propagation on copper specimens (5 mm diameter rods) was obtained at a pure oxygen pressure of 0.1 MPa. In contrast with the other metals studied, copper exhibited a smooth combustion phase characterized by a slow regression rate with a low-luminosity reaction zone. This behavior may be due to the low heat of combustion of copper (see Table 1) in the presence of high heat losses by conduction, convection and radiation. This in turn results in a low flame temperature and a slow reaction rate that give the observed slow regression rate and low luminosity. This same argument may explain the difficulty of burning copper rods in the upward propagation mode at normal gravity. Under the upward propagation configuration, the detachment of the first molten ball from the vertical rod removes the thermal mass that preheats the solid metal in front of it and causes a rapid cooling of the reaction zone (where the low heat of reaction is unable to overcome heat losses) with self-extinguishment following afterwards. Since this growth-and-detachment event is absent under microgravity conditions and convective heat transfer losses are significantly reduced, successful upward propagation tests with 3.2 mm diameter copper rods at oxygen pressures as low as 6.9 MPa have been obtained in low-gravity combustion experiments [9].

Several tests with different specimen lengths (up to 30 mm) were successfully carried out to provide unmistakable evidence of self-propagation and complete oxidation of the sample. In all cases the lamp was turned off after ignition to remove all external heat transfer to the sample. In addition, all tests showed a noticeable decrease in oxygen pressure after the experiment (2-4%) providing further indication of complete metal oxidation.

CONCLUSIONS

This study has proved the effectiveness of using a non-coherent, continuous radiation source for metal ignition. In addition, ignition and combustion tests were performed on different metal specimens, including Fe, Ti, Zr, Mg, Zn, Sn and Cu. Qualitative observations and temperature profiles have revealed the existence of the heating, ignition and combustion stages. These zones are characterized by well-defined surface structure changes, surface temperature behavior, luminosity and chemical activity. Values of ignition temperature (defined here as the point of inflection in the temperature vs. time curve) below (as in Fe, Ti and Zr), above (as in Sn, Zn and Mg) and in the range of the melting point of the metal (as in Cu) were obtained from the temperature records. Evidence of the ignition and self-sustained downward propagation of copper rod specimens at 0.1 MPa under normal gravity conditions revealed the dramatic effect of sample geometry, experimental configuration and ignition source on the ignitability and flammability of metals. As these results indicate, care must be exercised when using the promoted combustion test to establish general flammability criteria of metals.

The experimental work is being complemented by modeling studies which include the effects of conduction, convection and radiation heat transfer in the solid specimen and the surrounding gas [14]. The computational model explores the effects of gravity (0.0 *g* to 10.0 *g*) and pressure (0.015 MPa to 1 MPa) on the heating phase of the metal sample under non-oxidizing conditions. The heat transfer studies are designed to help evaluate the energy balance on the specimen during heating prior to ignition.

Future work will focus on completing ground-based experiments with different types of metals, surface morphology studies and spectroscopic measurements. These results will be later compared with experiments done under high and low gravity conditions.

ACKNOWLEDGMENTS

This work was supported by the National Aeronautics and Space Administration, Lewis Research Center, Grant NASA-NAG3-1257. We acknowledge the contributions and helpful discussions of Ted Steinberg at the NASA White Sands Testing Facility.

REFERENCES

[1] Clark, A. F. and Hust, J. G., "A Review of the Compatibility of Structural Materials with Oxygen," AIAA Journal, Vol. 12, No. 4, 1974, pp. 441-454.

[2] Markstein, G. H., "Combustion of Metals," AIAA Journal, Vol. 1, No. 3, 1963, pp. 550-562.

[3] Friedman, R. and Macek, A., "Ignition and Combustion of Aluminum Particles in Hot Ambient Gases," Combustion and Flame, Vol. 6, 1962, pp. 9-19.

[4] Stoltzfus, J. M., Homa, J. M., Williams, R. E., and Benz, F. J., "ASTM Committee G-4 Metals Flammability Test Program: Data and Discussion," Flammability and Sensitivity of Materials in Oxygen-Enriched Atmospheres: Third Volume, ASTM STP 986, D.W. Schroll, Ed., American Society for Testing and Materials, Philadelphia, 1988, pp. 28-53.

[5] Brzustowski, T. A., and Glassman, I., "Vapor-Phase Diffusion Flames in the Combustion of Magnesium and Aluminum: II. Experimental Observations in Oxygen Atmospheres," in Heterogeneous Combustion, Wolfhard, H. G., Glassman, I., and Green, L., Jr., (eds.), Academic Press, New York, 1964, pp. 117-158.

[6] Bransford, J. W. and Clark, A. F., "Laser-Initiated Combustion Studies of Selected Aluminum, Copper, Iron, and Nickel Alloys," NBSIR 81-1647, Natl. Bur. Stds., 1981.

[7] Nguyen, K., and Branch, M. C., "Ignition Temperature of Bulk 6061 Aluminum, 302 Stainless Steel and 1018 Carbon Steel in Oxygen," Combustion Science and Technology, Vol. 53, 1987, pp. 277-288.

[8] Stoltzfus, J. M., Lowrie, R., and Gunaji, M. V., "Burn Propagation Behavior of Wire Mesh Made from Several Alloys," Flammability and Sensitivity of Materials in Oxygen-Enriched Atmospheres: Fifth Volume, ASTM STP 1111, Joel M. Stoltzfus and Kenneth McIlroy, Editors, American Society for Testing and Materials, Philadelphia, PA., 1991, pp. 326-337.

[9] Steinberg, T. A., Wilson D. B., and Benz, F. J., "Metals Combustion in Normal Gravity and Microgravity," Second International Microgravity Combustion Workshop, September 15-17, 1992, NASA-Lewis Research Center, Cleveland, Ohio.

[10] Zabrenski, J. S., Werley, B. L., and Slusser, J. W., "Pressurized Flammability Limits of Metals," Flammability and Sensitivity of Materials in Oxygen-Enriched Atmospheres: Fourth Volume, ASTM STP 1040, Joel M. Stoltzfus, Frank J. Benz, and Jack S. Stradling, Editors, American Society for Testing and Materials, Philadelphia, PA., 1989, pp. 178-194.

[11] Merzhanov, A. G., Grigorjev, M. and Gal'chenko, Y. A., "Aluminum Ignition," Combustion and Flame, Vol. 29, 1977, pp. 1-14.

[12] JANAF Thermochemical Tables, 3rd ed.(D. R. Lide, Jr., Editor.), American Chemical Society and American Institute of Physics, New York, Vol. 14, 1985.

[13] Steinberg, T. A., and Wilson D. B., "The Combustion Phase of Burning Metals," Combustion and Flame, Vol. 91, 1992, pp. 200-208.

[14] Feiereisen, T. J., Branch, M. C., Abbud-Madrid, A., and Daily, J. W., "Gravity and Pressure Effects on the Steady-State Temperature of Heated Metal Specimens in a Pure Oxygen Atmosphere," Flammability and Sensitivity of Materials in Oxygen-Enriched Atmospheres, ASTM STP 1197, Dwight D. Janoff, and Joel M. Stoltzfus, Eds., American Society for Testing and Materials, Philadelphia, 1993 (in press).

Richard M. Shelley,[1] D. Bruce Wilson,[1] and Harold Beeson[2]

COMBUSTION CHARACTERISTICS OF POLYMERS AS IGNITION PROMOTERS

REFERENCE: Shelley, R. M., Wilson, D. B., and Beeson, H., "Combustion Characteristics of Polymers as Ignition Promoters," Flammability and Sensitivity of Materials in Oxygen-Enriched Atmospheres: 6th Volume, ASTM STP 1197, Dwight D. Janoff and Joel M. Stoltzfus, Eds., American Society for Testing and Materials, Philadelphia, 1993.

ABSTRACT: Four polymers, which were high density polyethylene (HDPE), polytetrafluoroethylene (PTFE), unfilled polyimide (PI), and graphite-filled polyimide (GPI), were burned in high pressure oxygen over the range 0.7 to 69 MPa. Three metallic materials were used as support rods: aluminum 2216, stainless steel 316, and pure copper. Flame characteristics of the polymers are described, as well as the polymer potential for igniting the metal support.

HDPE burns at all pressures with a diffusion flame, PTFE burns at all pressures as a surface burner, PI and GPI are combined surface and diffusion flame burners. Flame compositions and temperatures were estimated based on computer calculations (Gordon McBride) and experimental melting characteristics of the aluminum rods.

KEYWORDS: Polymer combustion, metal ignition, polymer flames, flammability, polyethylene, polytetrafluoroethylene, polyimide.

INTRODUCTION

ASTM guide G63 [1] for evaluating nonmetallic materials for oxygen service is concerned primarily with properties associated with the susceptibility to ignition and fire propagation. The design engineer is concerned primarily with these events and also with the potential for ignition of adjacent metallic structural components. Currently, while extensive experience is available for systems operating at less than 20.7 MPa, there is relatively little experience with oxygen systems operated at greater than 20.7 MPa. Actual performance tests are recommended for such systems [2].

Hazard assessment of new oxygen systems without performance testing requires appropriate mechanisms and their parameters (i.e. rate-controlling regime). These are not available for polymers operating in high pressure oxygen. This paper reports the analysis of polymer combustion in an experimental configuration characteristic of a standard flammability test [3,4]. Tests were conducted over the pressure range 0.7 - 69 MPa. Characteristic properties for the polymers are given in Table 1.

---

[1] Senior scientist and staff scientist, respectively, Lockheed-ESC, White Sands Test Facility, P. O. Drawer MM, Las Cruces, NM 88004.

[2] Special Projects Director, NASA, White Sands Test Facility, P. O. Drawer MM, Las Cruces, NM 88004.

TABLE 1--Polymer properties.

Materials	Monomer Formula	Total Sample Weight, g	Auto-ignition Temp, K [7]	Heat of Comb. J/g [7]	Decomposition Products [6]
HDPE	C_2H_4	0.58	498	46,500	$C_xH_yO_z$, CO, CO_2, H_2O
PTFE CO_2,	C_2F_4	1.38	785-800	5,325	CO, CF_4, COF_2
PI	$C_{22}H_{10}N_3O_5$	1.01	835	...	HCN, CO, $C_xH_yO_z$, CO_2, HN_3, H_2O
GPI	$C_{22}H_{10}N_3O_5$	1.05	835	26,065	HCN, CO, $C_xH_yO_z$, CO_2, HN_3, H_2O

EXPERIMENTAL APPROACH AND METHOD

Polymers were placed at the bottom end of 15 cm (6")long, 0.3 cm (⅛") diameter aluminum 2219 rods and ignited by aluminum-palladium wire in the same configuration as the upward propagation promoted combustion test described by Steinberg et al [5], all polymers were burned to completion. Each experimental run was recorded on video tape. The video tape recording provided a measure of burn-time for each polymer, when ignition of the rod occurred, and a measure of ignition time. Length of burning witness marks on the rod, and analysis of flame type from video stills were obtained from the data.

All materials were tested for promoted combustion at 3.4, 6.4, 21, 34, and 69 MPa. The polyimides sometimes ignited the aluminum rod; a result that was undesirable because there could be no analysis of data from the remaining rod. Vespel SP1 had consequently to be omitted from testing at or above 20.7 MPa; results were obtained for PI at 34 MPa using copper rods. To investigate further the difference between the filled and unfilled polyimide Vespels, the polymers were tested, additionally, at 0.7 and 2.1 MPa.

Measurements of pressure were made to the nearest 0.35 MPa at 2.1 MPa or greater pressures. At pressures below 2.1 MPa pressures were measured to the nearest 0.035 MPa. Times were measured and reported to the nearest 0.10 second. Lengths were measured to the nearest 0.01 cm and reported to the nearest 0.10 cm. Masses were measured to the nearest 10^{-5}g.

A tube furnace/fourier transform infra red (FTIR) [6] apparatus was used to obtain gaseous products of the polymers. Models generated from the above data were used to predict the polymers behavior when promoting combustion in 316 stainless steel.

EXPERIMENTAL MATERIALS

Promoters of all the polymers were 1.3-cm (½-inch) diameter and 0.64-cm (¼-inch) high cylinders with a circumferential groove machined in for the igniter wire. Previous testing was performed with polyethylene, PTFE, and GPI promoters and aluminum 2219 and stainless rods; recent testing performed with PI and GPI was performed with aluminum 2219 and pure copper rods.

Polyethylene data was obtained from previous testing and was known to be high density polyethylene (HDPE), but the specific grade was unknown. Although the exact material was not specified, the data were considered to be of scientific value to include in this work.

The polytetrafluoroethylene or PTFE (Dupont Teflon grade 8A) is a highly crystalline fully fluorinated, carbon-based polymer of density 2.17 g/cc and melting point 600 K (327° C.)

PI and GPI are polyimide resins manufactured by DuPont. PI (Vespel SP1) is an unfilled base resin and GPI (Vespel SP21) is a 15% by weight graphite filled resin.

The rod materials were aluminum 2219 and stainless steel 316.

RESULTS

Figures 1 through 4 are sketches of each of the burning polymers (taken from the video recording). Each sketch shows the flame characteristic of each type of polymer. Fig. 1 shows the predominantly diffusion type flame characteristic of burning HDPE. The flame was separated from the sample surface. Fig. 2 shows the surface burning characteristic of PTFE. Fig. 3 is PI and 4 is GPI. Both show surface burning as well as a diffusion flame. All polymers combustion regimes will be described further in the discussion section.

Figs. 5a and 5b show that the experimental system produced reproducible results. Each figure shows the aluminum rods and characteristic flame markings of the rods. Fig. 5a was PI combustion and Fig. 5b corresponded to combustion of GPI. The rods show that melting of aluminum occurred, indicating a temperature of 933 K was reached, however the aluminum oxide skin remained intact and ignition of the rod did not occur.

Fig. 6 shows an aluminum rod from the combustion of HDPE for different oxygen pressures. The flame markings are clearly similar and will be discussed later. Table 2 summarizes the average values for important variables for these tests.

Fig. 7 shows the aluminum rod from the combustion of PTFE for each of five different oxygen pressures. The absence of flame markings on the rods are consistent with surface burning. Table 3 summarizes average values for important variables from these tests.

Fig. 8 shows the aluminum rods from the combustion of PI for each of the different pressures. The flame markings are clearly similar and this is consistent with the flame characteristics as shown in Figs. 3 and 4. Figures 5a and 5b compare PI and GPI at 2.1 MPa.

Tables 4 and 5 summarize average values for important variables for these PI and GPI tests.

Table 6 reports the result of flammability experiments conducted using HDPE, PTFE, and GPI on 316 stainless steel rods (0.3125-cm diameter). The table indicates whether the standard polymer disc ignited the stainless steel.

DISCUSSION

The experimental results, i.e. flame photographs, burn times, rod markings, and times to ignition, provide the basis for the discussion of qualifying the polymers combustion characteristics. The ability to extrapolate these experimental results depends on obtaining fundamental mechanism parameters, (reaction rate parameters and thermal energy transfer parameters). Parameter values are obtained through model analysis [8]; however, the model should be appropriate for the data available for verification and for the intended use of the model. The system is a burning polymer disc and the metallic rod to which it is attached. A general model schematic for discussion is shown in Fig. 9 This model divides the flame zone into two distinct regions on the aluminum rod (a core region and an oxide region). Hence the following discussion concerns the aluminum rod. The first step in modelling a

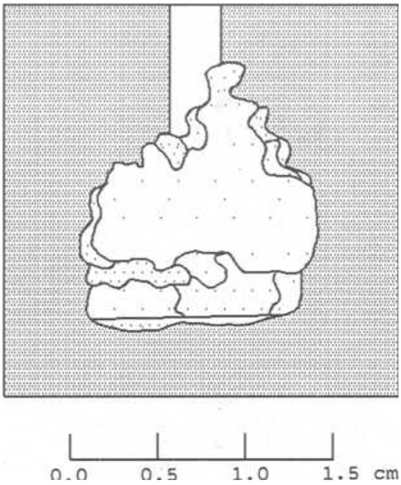

FIG. 1--HDPE burning at 3.4 MPA in pure oxygen ignited by pyrofuse.

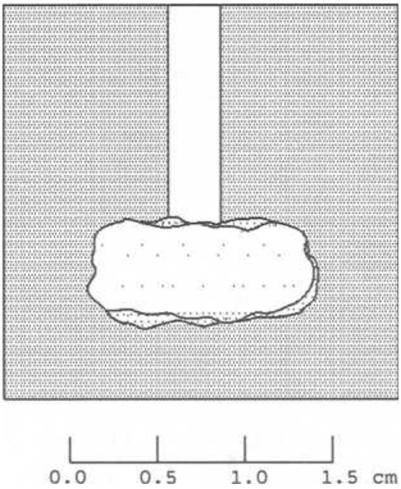

FIG. 2--PTFE burning at 3.4 MPA in pure oxygen ignited by pyrofuse.

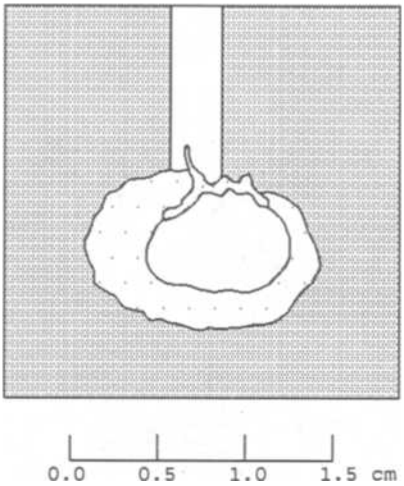

FIG. 3--PI burning at 3.4 MPA in pure oxygen ignited by pyrofuse.

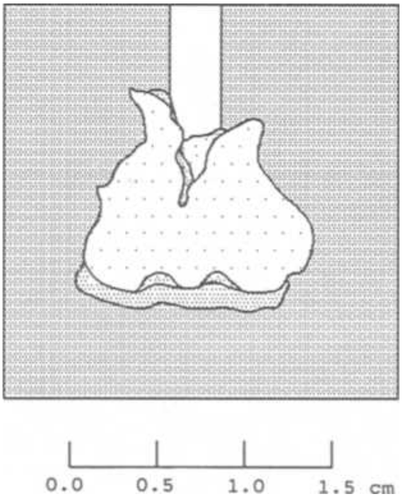

FIG. 4--GPI burning at 3.4 MPA in pure oxygen ignited by pyrofuse.

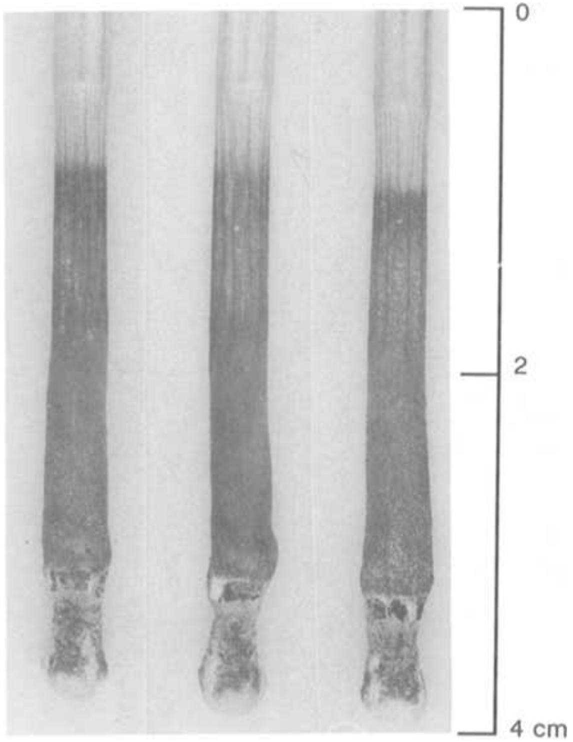

FIG. 5a--Six-inch aluminum rods after combustion of PI at 2.1 MPa oxygen.

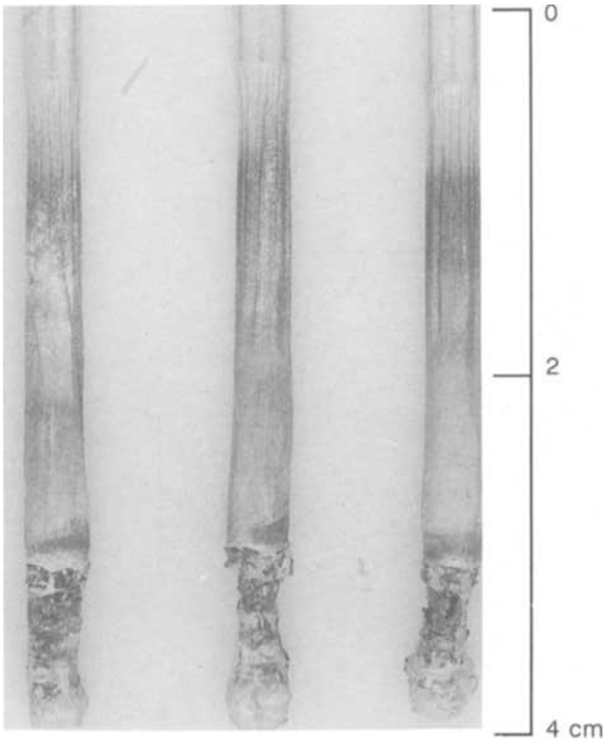

FIG. 5b--Six-inch aluminum rods after combustion of GPI at 2.1 MPa oxygen.

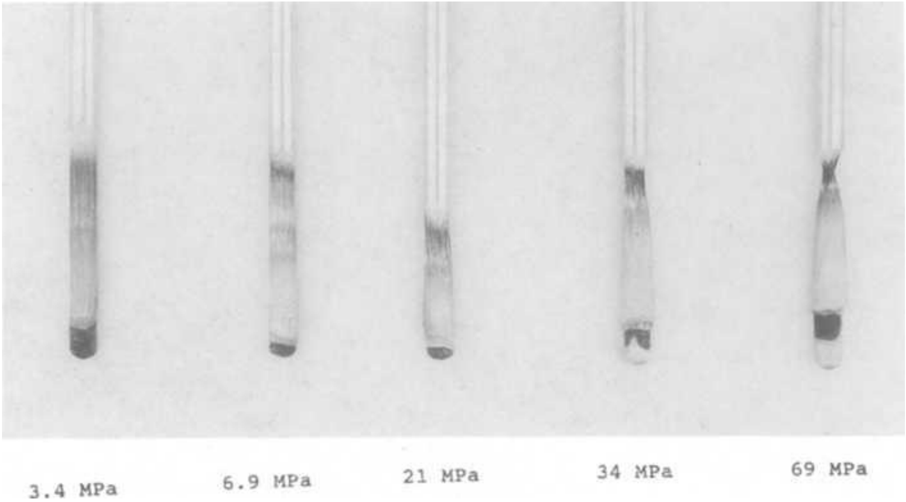

FIG. 6--Combustion of HDPE on aluminum rods as a function of oxygen pressure.

reacting system is to determine the balanced stoichiometric chemical equations. Table 1 shows the chemical formulae for the monomeric units of each polymer as well as identifying combustion products that have been identified experimentally [6]. The experiments, however, measured the composition external to the flame zone as shown in Fig. 1-4 and 9.

While HDPE and PTFE have simple monomer units, it is well established that a complete description of the kinetic mechanism of a simple hydrocarbon combustion can involve more than forty elementary reactions [9,10]. It is apparent that without extensive in-situ measurement of all the chemical species throughout the flame, the application of a distributed parameter (partial differential equation) model is excessive. Rather a reduced form of model should be attempted. There are general procedures available for simplifying chemical kinetics based on knowledge of the complete dynamic kinetic mechanisms [10]. These schemes represent the thermodynamic state of fluid in terms of four or five variables (rather than the forty or more required by the detailed mechanism). These current approaches are based on the partial

TABLE 2--Summary of HDPE experiments.

Press. Mpa	Burn Time sec	Mass Burn. Rate g/sec	Heat Release Rate J/sec	Heat Affected Zone Length 1,L1 cm	Heat Affected Zone Length 2,L2 cm	Mass Change of rod %
3.4	28.8	.02	936.5	1.1	1.2	+0.01
6.8	20.1	.03	1341.8	0.9	1.2	-0.2
20.4	9.9	.06	2724.2	0.8	0.7	+0.2
34.0	5.2	.11	5186.5	1.4	0.7	+0.01
69.0	3.8	.15	7097.4	1.4	0.5	+0.01

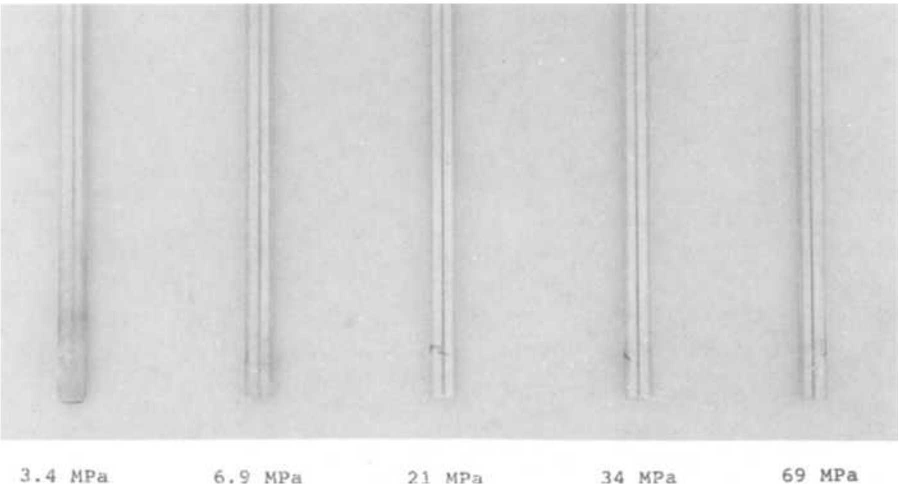

FIG. 7--PTFE on aluminum rods as a function of oxygen pressure.

equilibrium and steady state assumptions, yet require the complete mechanism to develop the reduced model. These complete mechanisms are not available for polymer combustion in high pressure oxygen.

The experimental results of this work do provide the data necessary to develop a simplified lumped parameter model, e.g. Fig. 9. Examining the aluminum rods of Figs. 5 through 8 shows that there are two distinct zones within the flame: a smooth slightly expanded or bulging zone (A of Fig. 9); and a zone where the aluminum oxide has wrinkled, owing to the drainage of molten aluminum in the core (B of Fig. 9). The aluminum oxide film has remained intact. Had the aluminum oxide film broken during the burning of the polymer the molten aluminum would have likely ignited (this occurred in one test at 69 MPa). An estimate for the temperature of each zone can be made based on partial equilibrium for the chemical reactions and the melting temperatures of aluminum (933 K) and aluminum oxide (2327 K). The melting and drainage of aluminum inside the aluminum oxide skin indicates that the flame temperature must be greater than 933 K. Very thin films of aluminum oxide are amorphous and hence would be expected to stretch or contract

TABLE 3--Summary of PTFE experiments.

Press. Mpa	Burn Time sec	Mass Burn Rate g/sec	Heat Release Rate J/sec	Heat Affected Zone		Mass Change of Al rod %
				Length 1, L1 cm	Length 2,L2 cm	
3.4	17.7	.078	415.7	0.9	...	+0.001
6.9	12.2	.113	603.2	0.2	...	+0.002
20.4	7.0	.197	1051.3	0	...	+0.003
34.0	5.4	.256	1362.8	0	...	+0.004
69.0	4.3	.321	1711.4	0	...	+0.005

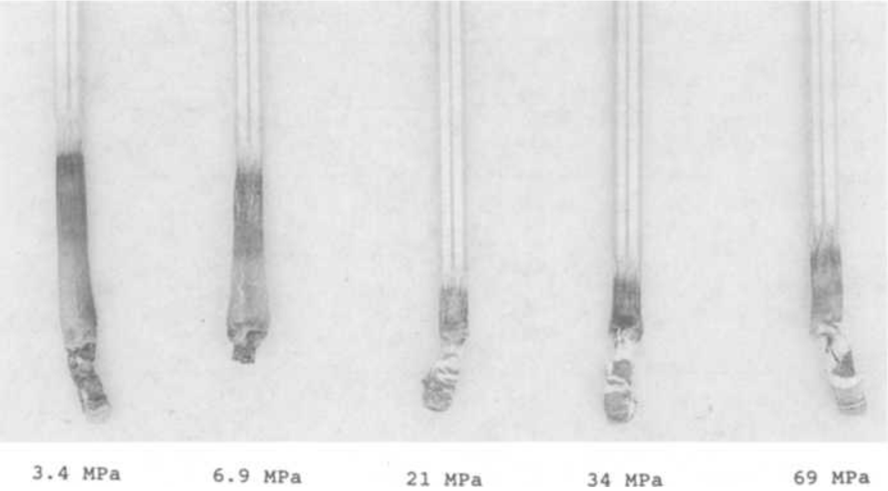

FIG. 8--PI on aluminum rods as a function of oxygen pressure.

if the temperature were close to the melting point of 2327 K. Each type of polymer used in these experiments will be discussed in terms of the simplified model shown in Fig. 9.

The HDPE flame of Fig. 1 shows that it resembles a true diffusion flame. The markings of the aluminum rods shown in Fig. 6 have two very distinct flame zones. Table 2 reports the length of each zone for the HDPE flame. In addition, Table 2 reports the change in weight for the aluminum rods. This measurement confirms two facts: no apparent volatilization of aluminum occurred, and all the polymer was consumed. These facts were further confirmed by Auger analysis of the surface rod, showing that carbon was not incorporated into the oxide matrix.[3]

Table 7 gives partial equilibrium compositions for the two flame zones for HDPE. These compositions and the corresponding temperatures were calculated using the Gordon-McBride computer code [11]. The computations are based on zone A (Fig. 9) being fuel rich and zone B

TABLE 4--Summary of PI experiments.

Press. Mpa	Burn Time sec	Mass Burn Rate g/sec	Heat Release Rate cal/sec	Heat Affected Zone Length 1,L1 cm	Heat Affected Zone Length 2,L2 cm	Mass Change of Al rod %
0.7	69	.015	381.5	1.9	0.78	-0.1
2.1	31	.033	849.2	2.1	0.78	-0.1
3.4	23.5	.043	1120.2	2.4	0.62	+0.001
6.9	13.7	.074	1921.6	...	...	...
34.0	8	.126	3290.7	...	...	...

---

[3] Bahk, S., private communication, WSTF, October 1991.

TABLE 5--Summary of GPI experiments.

Press. Mpa	Burn Time sec	Mass Burn Rate g/sec	Heat Release Rate cal/sec	Heat Affected Zone Length 1,L1 cm	Length 2,L2 cm	Mass Change of rod %
0.7	70.7	.015	387.1	2.2	0.9	-0.2
2.1	39.7	.026	689.4	2.1	0.8	-0.2
3.4	30.3	.035	903.2	1.7	0.8	+0.02
6.8	17.5	.060	1563.9	0.8	1.1	-0.1
20.6	9.8	.107	2792.7	0.6	0.6	-0.1
34.0	7.2	.146	3801.0	0.7	0.7	+0.01
69	5.4	.194	5068.2	0.8	0.9	+0.1

TABLE 6--Ignition of 316 stainless steel by the polymer promoters.

	HDPE		PTFE		GPI	
Pressure	Ign. # of Tests	Times sec	Ign. # of Tests	Times sec	Ign. # of Tests	Times sec
3.4	0/3	...	0/3	...	3/3[b]	22
6.9	1/3[a]	13.5	0/3	...	3/3[c]	14
20.4	3/3	4.5	0/3	...	0/3	...
34.0	1/3	2.2	0/3	...	0/3	...
69.0	1/3	1.8	0/3	...	0/3	...

[a] 60% burn
[b] 25% burn
[c] 75% burn

having excess oxygen, with temperatures that correspond to providing sufficient thermal energy transfer to achieve the melting conditions of aluminum and aluminum oxide described above.

The species shown for zone A were used as the feed stream to zone B and should correspond to species identified experimentally as listed in Table 1 for HDPE and they are consistent. The flame markings on the aluminum rods provide one further fact for discussion and this is the relative length of each zone and the total flame length. As seen in Fig. 3, and reported in Table 2 the shortest flame for zone A and overall occurs at about 20.4 MPa. If the gases of the flame zone are treated as ideal gases and the temperatures of Table 7 are used for each zone, then there should be a steady decline in the length of the flame zone over the experimental region. This is not the case and since oxygen is essentially ideal for these temperatures and pressures, the non-ideality of the combustion gases must come from the actual species present in the zones of the flame. The partial equilibrium calculations are used to identify all the free radical or intermediate species that can occur in hydrocarbon flames [9]. Those species identified in Table 7 are non-ideal (based on compressibility factors) for the temperature ranges identified. Tables 7 through 9 give the compositions

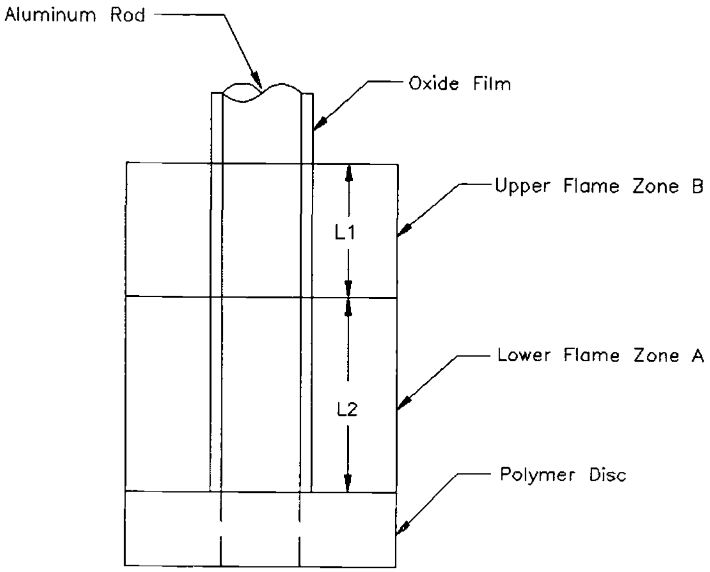

FIG. 9--Burn regions on the test rod.

in mole fractions of the indicated flame zones at different pressures.

Table 8 gives the corresponding Gordon McBride calculations for PTFE. Since Fig. 1b shows that PTFE burns as a surface burner there is essentially no flame zone. This is confirmed by the absence of rod markings as shown in Fig. 7. Note there does appear to be a very limited zone at the lower pressures 3.4 and 6.9 MPa, as shown in Table 3. The latter is within the length of the polymer disc and both can be attributed to the last part of the polymer burn and can be the result of conduction within the rod. The negligible weight change supports the observation of the complete burn of the polymer and no vaporization of aluminum. The Gordon-McBride temperatures would correspond to a surface temperatures and the product gases must be essentially fully oxidized, i.e. thermodynamically stable for the temperature and pressure. Further they must correspond to the species experimentally identified as given in Table 1. There is correspondence with all these requirements for the Table 8 species and values.

Examination of Figs. 3 through 5 and 8, plus the sample weights shown in Table 1 indicate sufficient similarities between PI and GPI that will be discussed as one category of polymer, ie both show surface burning as well as diffusion flames. At the low pressures, the rod markings are similar to those of HDPE, while at the higher pressures the rods show significant distortions, and for PI the aluminum rod was ignited at 6.8 and 34 MPa. While the weight changes are not consistent, values from Table 4 and 5 indicate that there was not significant volatilization and the mass balance indicates complete polymer burn.

Table 9 shows the Gordon Mc-Bride calculations for the zone A and B compositions and temperatures. Similar considerations as occur for HDPE flames also must apply to the PI/GPI flames, and also the additional surface burning. Comparison of Figs. 1 through 4 shows that HDPE retains its original shape throughout the burn while the surface burning of PI/GPI changes the polymer shape, collapsing it into a char

TABLE 7--Equilibrium compositions of flame zones - HDPE.

Species	Pressure (MPa)				
	3.44	6.89	20.4	34.4	68.9
	Mole fractions of flame zone A				
	Temperature (K)				
	2022	2034	2070	2098	2149
CH_2O	...[a]	...	...	...	...
CH_4	0.002	0.003	0.009	0.014	0.022
CO	0.499	0.499	0.498	0.497	0.495
CO_2	...	0.001	0.002	0.003	0.004
C_2H_2	...	...	...	...	...
H_2	0.496	0.493	0.482	0.474	0.458
H_2O	0.002	0.003	0.008	0.012	0.019
	Mole fractions of flame zone B				
	Temperature (K)				
	3003	3045	3106	3130	3159
CO	0.014	0.012	0.008	0.007	0.006
CO_2	0.186	0.189	0.194	0.200	0.198
H_2	0.003	0.003	0.002	0.002	0.002
H_2O	0.178	0.180	0.184	0.186	0.188
O	0.015	0.012	0.008	0.007	0.006
OH	0.038	0.036	0.031	0.029	0.026
O_2	0.565	0.568	0.572	0.574	0.575

burn adjacent to the rod. The compositions of PI/GPI show that the same non-ideal species in flame zone A plus the thermodynamically stable species corresponding to the experimental observations for zone B as shown in Table 1.

TABLE 8--Equilibrium compositions of the flame for PTFE.

Species	Pressure (MPa)				
	3.44	6.9	20.4	34.4	68.9
	Mole fraction				
	Temperature (K)				
	1770	1780	1790	1793	1795
CF_4	0.021	0.021	0.021	0.022	0.022
COF_2	0.042	0.043	0.043	0.043	0.043
CO_2	0.023	0.023	0.022	0.022	0.022
F, FO, FO_2, F_2	<0.005	<0.003	<0.002	<0.001	<0.001
O_2	0.91	0.91	0.91	0.91	0.91

TABLE 9--Equilibrium compositions of flame zones - GPI.

	Pressure (MPa)				
Species	3.44	6.89	20.4	34.4	68.9
	Mole fractions of flame zone A				
	Temperature (K)				
	2265	2269	2282	2293	2316
CH_4	0.001	0.001	0.004	0.007	0.012
CO	0.574	0.574	0.576	0.577	0.58
CO_2	...	...	0.001	0.001	0.002
C_2H_2	0.001	0.001	0.001	0.001	0.002
HCN	0.003	0.003	0.003	0.003	0.003
H_2	0.299	0.298	0.293	0.288	0.278
H_2O	...	0.001	0.002	0.003	0.005
NH_3	...	...	...	...	...
N_2	0.016	0.016	0.016	0.016	0.016
C(GR)	0.106	0.106	0.105	0.104	0.102
	Mole fractions of flame zone B				
	Temperature (K)				
	2093	2961	3047	3089	3140
CO	0.034	0.034	0.028	0.025	0.022
CO_2	0.230	0.235	0.243	0.247	0.252
H_2	0.005	0.004	0.003	0.003	0.002
H_2O	0.095	0.096	0.099	0.101	0.103
NO	0.005	0.006	0.006	0.006	0.006
N_2	0.004	0.004	0.004	0.004	0.004
O	0.032	0.028	0.023	0.019	0.016
OH	0.039	0.038	0.036	0.034	0.032
O_2	0.551	0.554	0.558	0.560	0.563

Further confirmation of the characterization of the nature of the combustion of the four polymers can be shown by a qualitative analysis of the reaction rate measured by the average change of mass with time, as a function of total oxygen pressure. Combustion occurring in a diffusion flame would fit a "power law" reaction rate model; while combustion occurring on a surface would fit a "Langmuir-Hirschelwood-Houger-Watson" (LHHW) reaction rate model [12]. Tables 2 through 5 give the mass burning rate (g/s) as a function of oxygen pressure for the four polymers. Table 10 summarizes the goodness-of-fit of these functions, as measure by the regression coefficient.

As shown in Table 10, the limited data do not distinguish between the two models with respect to using regression coefficients as a criterion. HDPE appears to have a region where the surface is engulfed by flame. This is a result of the method of ignition, i.e. the polymer was ignited at the bottom and the sides would have ignited. The analysis does not clearly distinguish between surface combustion and homogeneous combustion for PTFE, the flame zone shown in Fig. 1b and the failure to ignite 316 stainless steel (Table 6) at any pressure do not suggest that the burning of PTFE occurs at the surface.

Validation that the qualitative analyses of partial equilibrium calculations of these polymers burning in high pressure oxygen is

TABLE 10--Comparison of reaction rate burn modes.

	Power Law		LHHW	
	Eq. for Mass Loss	Regression Coeff.	Eq. for Mass Loss	Regression Coeff.
HDPE	$0.0082P_{O2}^{0.7}$	0.993	$\frac{0.0065P_{O2}}{1+1040P_{O2}}$	0.980
PTFE	$0.044P_{O2}^{0.5}$	0.997	$\frac{0.025P_{O2}}{1+107P_{O2}}$	0.992
PI	$0.019P_{O2}^{0.7}$	0.999	$\frac{0.025P_{O2}}{1+400P_{O2}}$	0.997
GPI	$0.018P_{O2}^{0.6}$	0.998	$\frac{0.023P_{O2}}{1+410P_{O2}}$	0.97

consistent with experimental observation is provided in Table 6, experiments used 316 stainless instead of aluminum 2219. If it is assumed that the ignition temperature is the melting temperature of stainless steel, about 1800 K, then the confirmation can be based on the energy available (Tables 2 through 5) and the temperatures of the flames, in Tables 7 through 9.

Firstly, PTFE did not ignite any of the stainless rods. As a surface burner thermal energy transfer from PTFE to the rod must occur by radiant transfer or free convection. Model calculations show that, for the duration of PTFE sample burns, sufficient energy is not transferred to the stainless steel rod to reach the melting temperature, hence ignition did not occur at any pressure.

Examination of the HDPE and GPI results of Table 6 show that GPI ignited the stainless steel at 3.4 and 6.8 MPa pressures while HDPE ignited the material at 20.4, 34, and 69 MPa. Comparison of the thermal energy available (per unit time) between HDPE and GPI, Tables 2 and 5, for each pressure combined with the temperature values given in Tables 7 and 9, confirms that the flame model is consistent with the absence of stainless steel ignitions.

The ignition of 316 stainless steel by these polymers can be summarized as shown in Fig. 10, where a macroscopic (pseudo average)

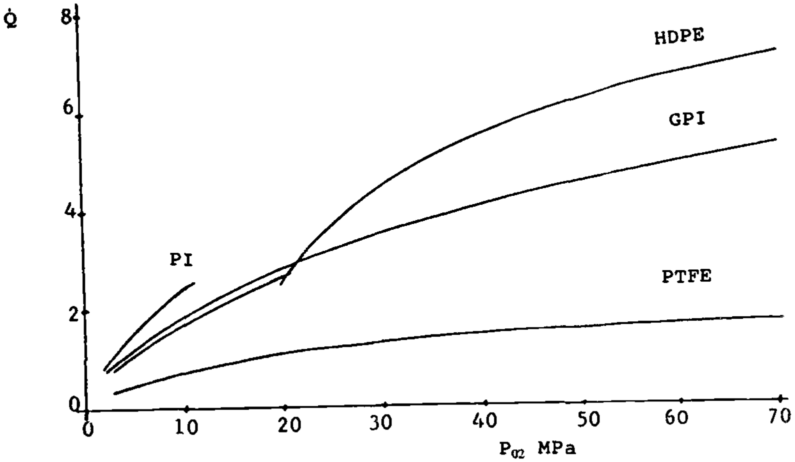

FIG. 10--Rate of thermal energy ($\dot{Q}$) as a function of pressure.

rate of thermal energy generation, $\dot{Q}$, as a function of oxygen pressure is plotted. The values of $\dot{Q}$ are taken from Tables 2 through 5. This figure clearly shows that the very low $\dot{Q}$ for PTFE does not transfer sufficient thermal energy to the 316 stainless steel to raise its temperature to above 1600 K, the melting temperature, above which ignition is typically observed. PI and GPI at the lower pressures have $\dot{Q}$ values greater than HDPE and this is reversed at higher pressures. These are consistent with PI and GPI igniting 316 stainless steel at the lower pressures (Table 6) where HDPE does not. This is reversed at the higher pressures above 3.4 MPa in the experimental data, and above 20 MPa in the model in Fig. 10. PI also ignited the aluminum rods as reported in Table 4.

CONCLUSIONS

Burning characteristics of polymers HDPE, PTFE and PI/GPI in high pressure oxygen have been examined. experiments were conducted using NASA standard flammability tests for metallic materials. Under the test conditions where the polymer discs were supported on aluminum rods, the resulting markings or absence of markings on the rods by the flame or the lack thereof suggested that a simplified model consisting of two zones within the flame would provide a reasonable description. Further the melting point of aluminum and aluminum oxide places bounds on the respective flame zone temperatures. Confirmation of the flame model was achieved by comparison with experiments conducted with stainless steel rods.

HDPE burns at all test pressures with a diffusion flame and will ignite the stainless steel rods at the higher test pressures (oxygen pressures of 20.4 MPa and above). PTFE burns as a surface burner and did not ignite 316 stainless steel at any test pressure. PI and GPI exhibit similar burning characteristics being both surface and diffusion type burners. GPI ignited stainless steel at the lower test pressures of 4.4 and 6.8 MPa; PI ignited the aluminum rods at pressures above 34 MPa.

REFERENCES

[1] ASTM G63-87, "Standard Guide for Evaluating Nonmetallic Materials for Oxygen Service", American Society for Testing and Materials, 1991.

[2] Oxygen Safety Handbook, Stoltzfus, J.M., Beeson H., and Benz, F., Editors, NASA White Sands Test Facility, Las Cruces NM (to be published).

[3] Benz, F.J., Shaw R.C., and Homa, J.M., "Burn Propagation Rates of Metals and Alloys in Gaseous Oxygen", Flammability and Sensitivity of Materials in Oxygen Enriched Atmospheres, ASTM STP 910, M.A., Benning, Ed, American Society of Testing and Materials, Philadelphia, 1986, pp. 2135-152.

[4] Flammability, Odor, and Offgassing and Compatibility Requirements and Test Procedures for Materials in Environments that Support Combustion, NASA NHB8060.1C, Washington, April 1991.

[5] Steinberg, T.A., Rucker, M.A., and Beeson, H.D., "Promoted Combustion of Nine Structural Metals in High Pressure Gaseous Oxygen: A Comparison of Ranking Methods", Symposium on Flammability and Sensitivity of Materials in Oxygen Enriched Atmospheres: Fourth Volume, ASTM STP 1040, Joel M. Stoltzfus, Frank J. Benz, and Jack S. Stradling, Editors, American Society for Testing and Materials, Philadelphia, 1989.

[6] Tapphorn, R. M., Shelley, R., and Benz, F., "Test Developments for Polymers in Oxygen-Enriched Environments," Flammability and Sensitivity of Materials in Oxygen-Enriched Atmospheres: Fifth Volume, ASTM STP 1111, Joel M. Stoltzfus and Kenneth McIlroy, Eds., American Society for Testing and Materials, Philadelphia, 1991.

[7] Ikeda, G. K., "Oxygen Index Tests to Evaluate the Suitability of a Given Material for Oxygen Service," Flammability and Sensitivity of Materials in Oxygen Enriched Atmospheres: First Volume, ASTM STP 812, B. L. Werley, Ed., American Society for Testing and Materials, Philadelphia, 1983, pp 56-57.

[8] Himmelblau, D. M., Bischoff, K. B., "Process Analysis and Simulation: Deterministic Systems", John Wiley and Sons, New York, 1971, pp 88-91.

[9] Pitz, W. J., and Westbrook, C. K., "Chemical Kinetics of the High Pressure Oxidation of n-Butane and its Relation to Engine Knock", Combustion and Flame, 63: 1086, pp 113-133.

[10] Maas, U., and Pope, S.B., "Simplifying Chemical Kinetics: Intrinsic Low dimensional Manifolds in Composition Space", Combustion and Flame, 88; 1992, pp 239-264.

[11] Gordon, S., and B. J. McBride. "Computer Program for Calculation of Complex Chemical Equilibrium Compositions, Rocket Performance, Incident and Reflected Shocks, and Chapman-Jouguet Detonations." NASA SP-273, National Aeronautics and Space Administrations, Washington, DC, 1971.

[12] Froment, G.F., and Bischoff, K.B., "Chemical Reactor Analysis and Design." John Wiley and Sons, New York, 1979, pp. 90.

Richard M. Shelley[1], Rollin Christianson[2], and Joel M. Stoltzfus[3]

EVALUATION OF BUNA N IGNITION HAZARD IN GASEOUS OXYGEN

REFERENCE: Shelley, R. M., Christianson, R., and Stoltzfus, J. M., "Evaluation of Buna N Ignition Hazard in Gaseous Oxygen," Flammability and Sensitivity of Materials in Oxygen-Enriched Atmospheres: 6th Volume, ASTM STP 1197, Dwight D. Janoff and Joel M. Stoltzfus, Eds., American Society for Testing and Materials, Philadelphia, 1993.

ABSTRACT: The NASA Johnson Space Center White Sands Test Facility (WSTF) evaluated the ignition hazards of a section of Buna N rubber suspected to be lodged in a gaseous oxygen system. A configuration simulation tester was used to test for the minimum mass of Buna N required to cause an ignition hazard, which meant ignition of the Inconel 718 metal structures of the oxygen system. High-density polyethylene (HDPE), a comparison material with a higher heat of combustion than Buna N, was also tested. Analytical techniques were performed on the Buna N rubber and the HDPE to investigate the polymer-to-metal ignition process. The minimum weight required to cause ignition in the Inconel 718 was 1.5 mg, which was more than the 0.1 - 0.2 mg of contaminant found in the oxygen system. HDPE had a lower propensity to ignite the Inconel 718 even though it has a much higher heat of combustion than Buna N; this result was explained in terms of the different structures of the two polymers. Additional testing was conducted to examine the differences of two different batches of Buna N at 10 ± 0.5-mg samples. Buna N was found to be batch sensitive in its ignition performance; batch differences were more easily discernible by analytical techniques.

KEYWORDS: Buna N, high-density polyethylene, fourier transform infrared tube furnace apparatus, differential scanning calorimeter light-pipe, thermal gravimetric analysis, ignition hazard simulation.

A piece of Buna N polymer was found lodged in a gaseous oxygen (GO_2) system, constructed primarily of Inconel 718 metal. The weight of the Buna N polymer contamination in the GO_2 system was estimated to be 0.1 - 0.2 mg. Promoted combustion of a metal by a polymer can occur in oxygen systems [1], but it was not known if this small amount of contamination could ignite the Inconel 718.

The primary objective of this evaluation was to assess the ignition hazard of the Buna N polymer contaminant in a GO_2 system. The secondary objective was to better understand the polymer-to-metal ignition process.

To evaluate the ignition hazard of the Buna N polymer contaminant, a simulation of the Buna N hazard was conducted using a configuration

---

[1] Senior Scientist, Lockheed-ESC, White Sands Test Facility, P. O. Drawer MM, Las Cruces, NM 88004.

[2] Principal Engineer, Lockheed-ESC, White Sands Test Facility, P. O. Drawer MM, Las Cruces, NM 88004.

[3] Project Manager, NASA, White Sands Test Facility, P. O. Drawer MM, Las Cruces, NM 88004.

simulation tester. High-density polyethylene (HDPE), a comparison material with a higher heat-of-combustion than Buna N, was also tested in the hazard simulator. To assess the polymer-to-metal ignition process, Buna N and HDPE were tested using a fourier transform infrared (FTIR) tube furnace apparatus, differential scanning calorimeter (DSC) light pipe, and thermal gravimetric analysis (TGA).

TEST SYSTEMS AND PROCEDURES

Ignition Hazard Simulation

The test apparatus consisted of a high-temperature, high-pressure, high-mass flow rate oxygen heat exchanger to supply the test fluid to a special configuration simulation tester, shown in Fig. 1. The heat exchanger was designed to supply oxygen to the simulator under conditions duplicating those that existed in the GO_2 system under analysis. The tester was designed to simulate, as closely as possible, the piece of Buna N lodged in an Inconel 718 component in the GO_2 system. To simulate worst-case conditions during the evaluation, a temperature of 260 - 315°C (500 - 600°F) and a pressure of 27.6 - 34.5 MPa (4 000 - 5 000 psia) were achieved at the maximum pressurization rate possible with the equipment, with a mass flow rate of approximately 0.91 kg/sec (2 lb/sec). The ignition source for the sample was the temperature imparted to the polymer from the flow of hot oxygen gas.

The tester configuration sandwiched a section of polymer between two Inconel 718 plates (0.79-cm [0.31-inch thick]) and exposed the polymer to the rapid heating from the pressurized oxygen source, as shown in Fig. 2. The center regions of the plates had holes to allow fluid passage around the polymer sample, while retaining the sample as it was subjected to the severe flow conditions. The Buna N was ignited by raising the temperature and pressure. For each polymer, a minimum of three tests was conducted in each weight range, which was arbitrarily chosen (these weights varied). Additional tests were conducted if clarification of the results was required. A complete burn of Inconel 718 plate(s) by the polymers refers to the Inconel 718 being ignited and consumed.

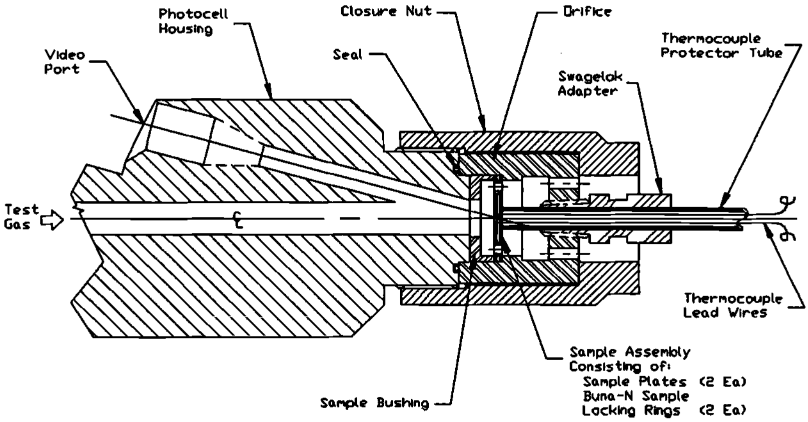

FIG. 1--Configuration simulation tester.

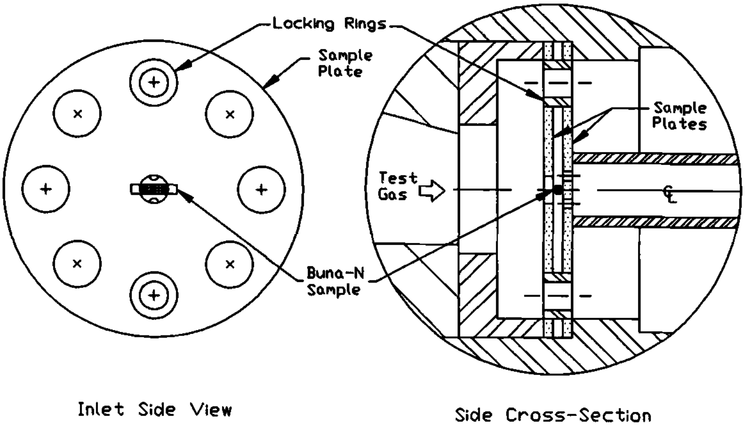

FIG. 2--Buna N sample holder.

The ignition of the polymer and Inconel 718 samples was recorded by high-speed video. Video was taken on the upstream side of the center of the test specimen through the video port shown in Fig. 1. The polymer sample, if any was remaining, and the Inconel 718 plates were visually examined after the tests. The gas temperature and pressure at the time of the ignition were deduced from test parameters monitored during the test.

FTIR Tube Furnace

Testing with the FTIR tube furnace was conducted to examine pyrolysis products and the autoignition temperature (AIT) of the polymers to obtain analytical information on the polymer-to-metal ignition process. The test system consists of a tube furnace, a quartz sampling tube, a metered gas source, and an FTIR spectrometer. This apparatus is discussed in detail elsewhere [2]. The oxygen flow rate used was 150 cm^3/min at ambient pressures, with a heating rate of 10°C/min. Video was taken of the sample, and combustion gases were analyzed by taking FTIR traces over time intervals. A sample of 250 mg was tested. A 10-mg sample was also tested as a comparison.

DSC Light Pipe

DSC light-pipe testing was conducted to confirm AIT results from the FTIR tube furnace and to obtain exotherms and endotherms during pyrolysis and combustion. A detailed description of the apparatus is given elsewhere [2]. The DSC light-pipe tests investigated ignition properties of the polymers in 100-percent oxygen. The following parameters were varied: flow rate, sample mass, heating rate, and age of the Buna N rubber. The flow rate was 0.1 - 2.0 liter/min, the sample mass was 5 - 50 mg, and the heating rate was 5 - 20°C/min.

TGA

TGA was performed to obtain weight-loss information on the Buna N as a function of temperature in oxygen. An Omnitherm TGA 1500 was used for the thermal gravimetric analysis [3]. The sample size of the Buna N analyzed was 5 mg, and the heating rate was 10°C/min. Testing of HDPE was not performed, because the purpose of this test was to determine BUNA N batch variability.

TEST MATERIALS

Metals

The two round Inconel 718 metal plates used in this evaluation were connected by copper locking rings (Fig. 3a). Inconel 718 has the following composition by weight percent: Ni 53, Fe 19, Cr 19, Al 0.4, Mo 3, Nb 5, Ti 0.5. The Inconel 718 metal burns incompletely at 3.5 MPa (500 psia) and completely at 20.7 MPa (3 000 psia) or higher [4]. The metal plates were ultrasonically cleaned in Freon 113 prior to the evaluation.

Polymers

The Buna N and HDPE polymers were cleaned with isopropyl alcohol and water and dried prior to the evaluation. The o-ring and section of Buna N contaminant (indicative of the size of the actual Buna N contaminant) are shown in Fig. 3b. The formula for the base polymer of Buna N is as follows:

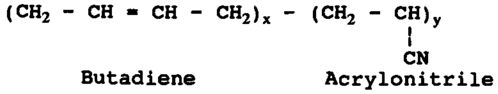

$$(CH_2 - CH = CH - CH_2)_x - (CH_2 - \underset{\displaystyle CN}{\underset{|}{CH}})_y$$

The values of *x* and *y* can vary, giving different weight percentage values of acrylonitrile monomer for different grades of material. The acrylonitrile content affects the properties of the compound markedly.

The specification of the Buna N rubber is stated in MIL-P-5315B [5]. The MIL-P-5315 B covers hydrocarbon-fuel-resistant o-ring material for use in aircraft and engine fuel systems. The specification also requires excellent resistance to temperatures of -46°C (-50°F) or below. The batch of Buna N rubber that was in the GO_2 system was made by National O-Ring, was supplied by JSC Houston, had a nominal Shore A hardness of 65, was cured in the first quarter of 1984 (1Q84), and had an expiration date of 1Q89. Ingredients of the Buna N compounds are listed in Table 1.

Insufficient Buna N material remained of the original batch, so additional material had to be obtained for testing. Some of the additional Buna N material was made by National O-Ring, was supplied by NASA Johnson Space Center White Sands Test Facility (WSTF) stores, and has a specific gravity of 1.28 g/cc, a nominal Shore A hardness of 65, a compound number C69, a batch number 61311, and a cure date of 3Q77. The rest of the Buna N material was made by National O-Ring, was supplied by Federal Mogul, and had a specific gravity of 1.26 g/cc, a nominal Shore A hardness of 65, a compound number C69, and a cure date of 2Q89.

The HDPE was made by Quantum, was supplied by WSTF stores, and had a specific gravity of 0.943 g/cc and a melt flow index of 7 grams per 10 min (10 kg at 190°C).

RESULTS AND DISCUSSION

Ignition Hazard Simulation

Tables 2 and 3 show the Buna N and HDPE ignition test data. Fig. 3c shows an Inconel 718 assembly that was thoroughly ignited. The minimum weight of the Buna N materials found to ignite the Inconel 718 was 1.5 mg, which is greater than the 0.1 - 0.2 mg in the GO_2 system under investigation. The 20-mg Buna N sample, cured in 3Q77, ignited the Inconel 718 metal consistently. The same amount of material from the 2Q89 batch ignited but only eroded the metal. None of the three HDPE samples, which produced more heat from combustion than the Buna N samples, caused ignition of the Inconel 718 metal.

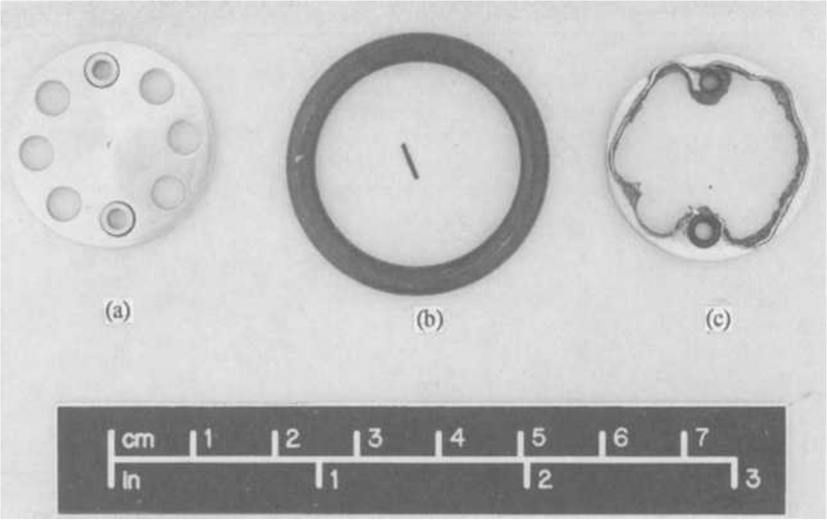

FIG. 3--Buna N polymer and Inconel 718 plate: (a) Inconel 718 plate with locking rings, (b) Buna N polymer and section of polymer contaminant, and (c) ignited Inconel 718 plate.

TABLE 1--Contents of Buna N material[a].

Ingredient	Parts by Weight
Paracril 1880 (20% acrylonitrile base polymer, Uniroyal Chemical Co.)	100
Sulphur MB (vulcanizing agent)	<5
ZMT-1 (antioxidant)	<2
Zinc oxide (accelerator activator and reinforcing filler)	5
Stearic acid (part of sulfur vulcanizing system)	1
FEF N550 carbon black (reinforcing filler)	60
MT N990 carbon black (reinforcing filler)	50
DBEEA (processing aid)	25
DBES (processing aid)	25
MBTS (delayed action semi ultra accelerator)	<5
TMETD (ultra accelerator and vulcanizing agent)	<5
Identification Pigment	Trace

[a] Compound C69

TABLE 2--Ignition of Inconel 718 by polymers.

Sample Weight Range (mg)	Number of Tests	Heat of Combustion for Sample Weight Range (J)	Number of Inconel 718 Ignitions
		Buna N	
0.28 - 1.3	7	9.6 - 45.6	0
1.5 - 1.6	3	52.3 - 56.1	1
3.6 - 4.5	14	125.6 - 157.4	4
9.8 - 10.5	12	342.9 - 367.2	7
18.9 - 21.0	6	661.1 - 734.8	4
		HDPE	
20.0	3	933.7	0

TABLE 3--Ignition of Buna N.

Sample Weight (mg)	Effects on Inconel 718 Plate(s)
	Batch 3Q77
9.8	Partial burn, charring
10.0	Complete burn[a], charring
10.2	No burn, charring
10.3	No burn, charring
10.4	No burn, charring
10.4	Partial burn, charring
	Batch 2Q89
9.9	Complete burn penetrating plates over large area
9.9	Partial burn, no charring
10.0	Partial burn, light charring
10.2	Partial burn, light charring
10.3	No burn, light charring
10.5	No burn, light charring

[a] Complete burn means the Inconel 718 plate(s) ignited and were consumed.

Additional testing was conducted to examine the effect of the two Buna N batches using 10 ± 0.5-mg samples. There were no marked differences in the ignition performances of the polymers when in contact with the Inconel 718; however, the 3Q77 samples were observed to produce more char than the 2Q89 samples.

FTIR

Typical FTIR traces prior to ignition for Buna N and HDPE are shown in Figs. 4 and 5. The gaseous products given off during heating of HDPE are given in Table 4. Buna N gave off such a large amount of soot or char prior to combustion that the sample was not visible when the charring occurred. The Buna N sample ignited with an initial burst or "pop" and after a few seconds burned with a glow. HDPE gave off a white, waxy material when heated, and ignited and burned with a candle-like flame.

The AIT of both Buna N compounds at both sample sizes were consistently around 480°C. The AIT of HDPE was 295°C for the 250 mg sample size and around 480°C for the 10-mg sample size.

DSC Light Pipe

Figs. 6 and 7 show typical DSC light-pipe thermograms of the heat and temperature for the Buna N and HDPE. The DSC light-pipe results indicate that the Buna N ignited in 478 - 525°C (892 - 977°F) in 100-percent oxygen at ambient pressure (12.4 psia). The effect of decreasing the flow rate from 2.0 to 0.1 liters/min was apparent in an increase of AIT by about 15°C (27°F). Sample weight decrease from 50 mg to 5 mg resulted in a decrease in AIT of 16°C (28.8°F). A change in the heating rate from 20°C/min to 5°C/min resulted in a decrease in AIT by about 35°C (63°F) (Fig. 8). The effect of pressure change will be investigated in future tests. Both batches of Buna N materials produced similar results in the DSC light pipe.

TGA

Analyses of the TGA traces for the two Buna N rubbers show that the two batches of Buna N materials were indistinguishable when using TGA. Both Buna N rubbers produced two weight losses: 5 - 10 percent at approximately 250°C (482°F) and 35 - 40 percent at approximately 420°C (788°F).

CORRELATION OF TESTS

The AIT test results obtained with the FTIR spectrometer system and the DSC light-pipe unit for the Buna N materials tested show good correlation with each system and with the AIT values recorded in

TABLE 4--HDPE tested with FTIR spectrometer[a].

Temperature		Gaseous Products[b]	DSC Features
(°C)	(°F)		
135	275	Nothing detectable	Melting point
200	392	Nothing detectable	Pre-exotherm
250	482	$C_xH_yO_z$, CO_2, CO	Beginning of exotherm
275	527	$C_xH_yO_z\uparrow$, $CO_2\uparrow$, CO↑, H_2O	Plateau of exotherm
295	563	Ignition	"
300	572	$C_xH_yO_z\uparrow$, $CO_2\uparrow$, CO↑, H_2O	"
485	905	$C_xH_yO_z\downarrow$ $CO_2\uparrow$, CO↑, H_2O	"

[a] HDPE (Quantum, LR 720), 250-mg samples, 10 K/minute, 150-sccm oxygen

[b] ↑Quantity increasing at that temperature; ↓Quantity decreasing at that temperature

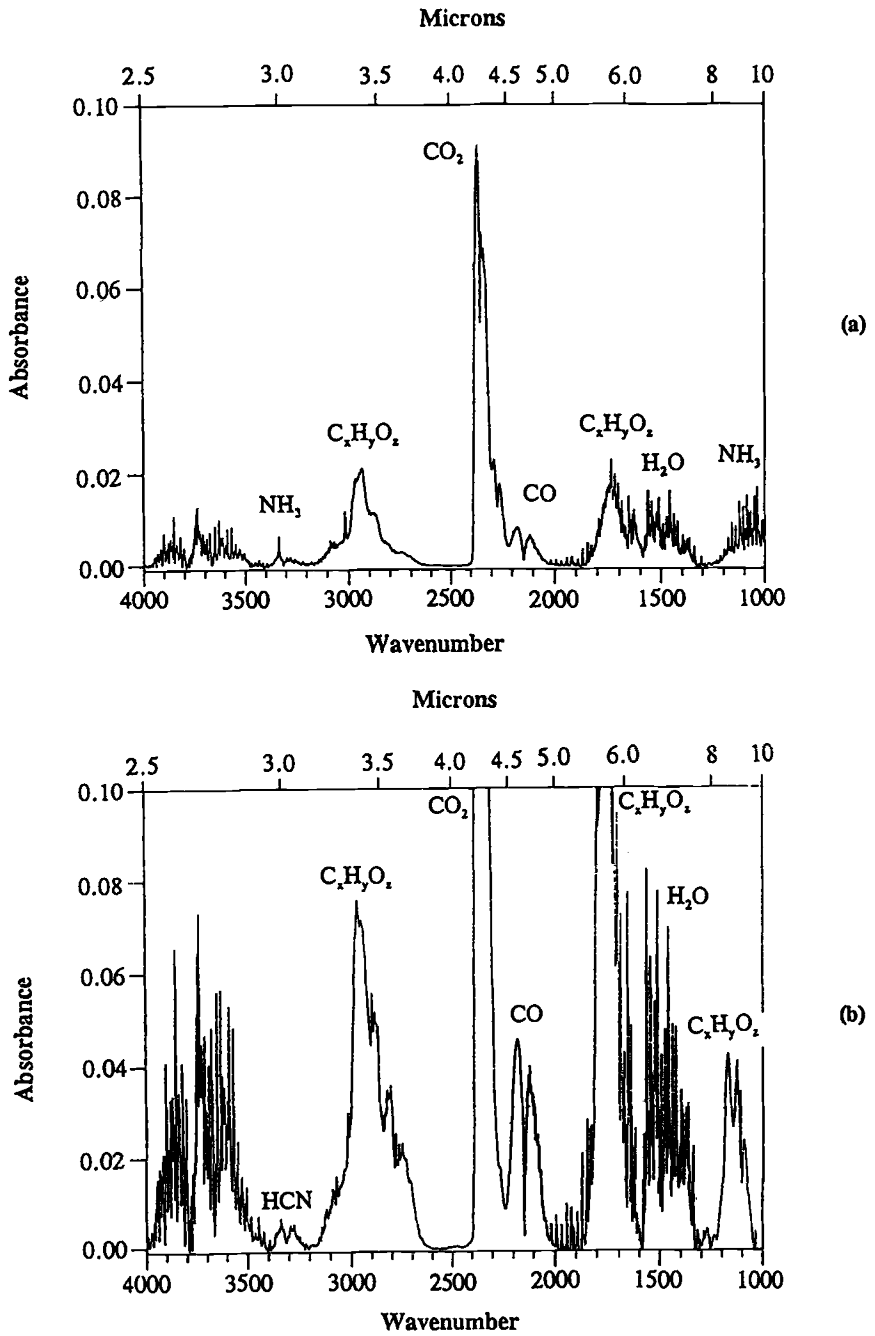

FIG. 4--FTIR absorbance spectra of Buna N at 400°C for (a) batch 3Q77 and (b) batch 2Q89.

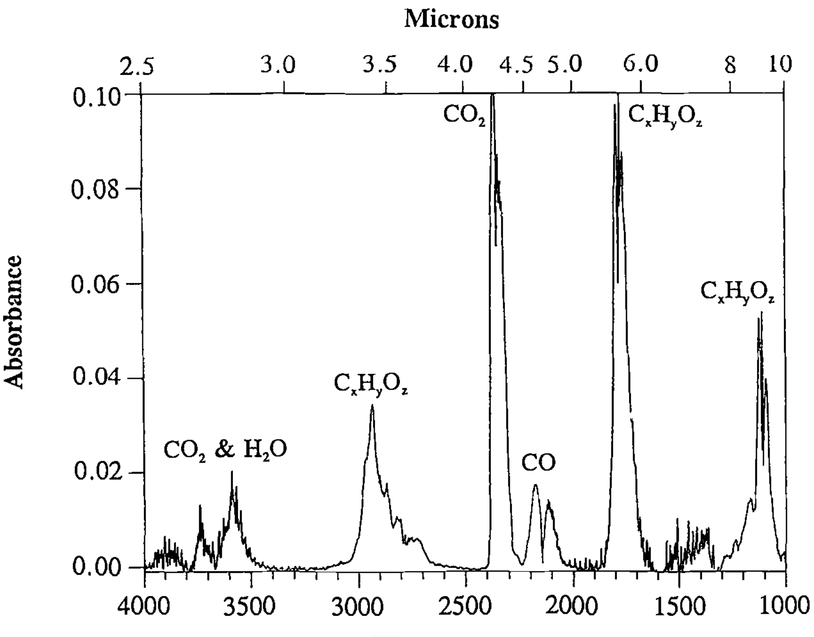

FIG. 5--FTIR absorbance spectra of HDPE prior to ignition.

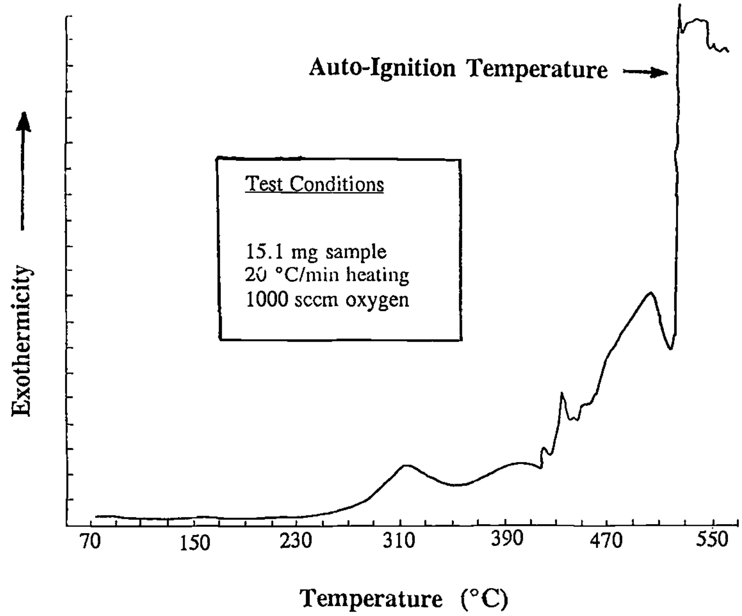

FIG. 6--DSC light-pipe trace for Buna N.

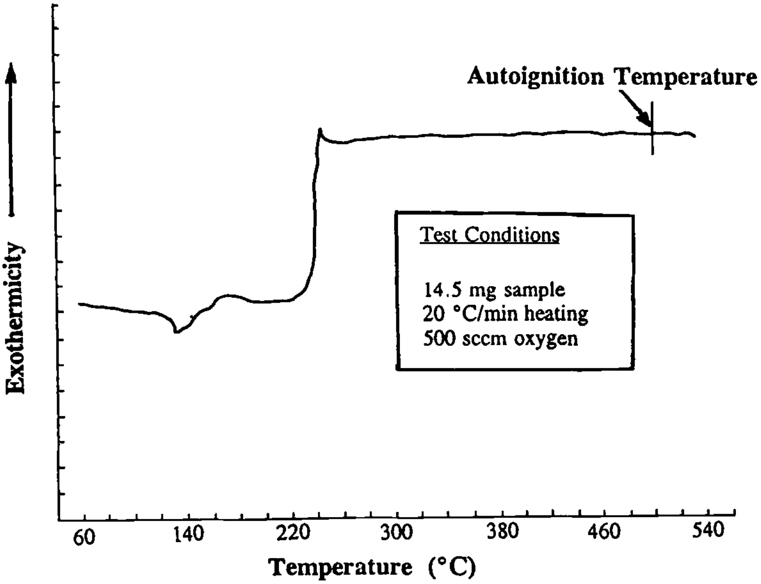

FIG. 7--DSC light-pipe trace for HDPE.

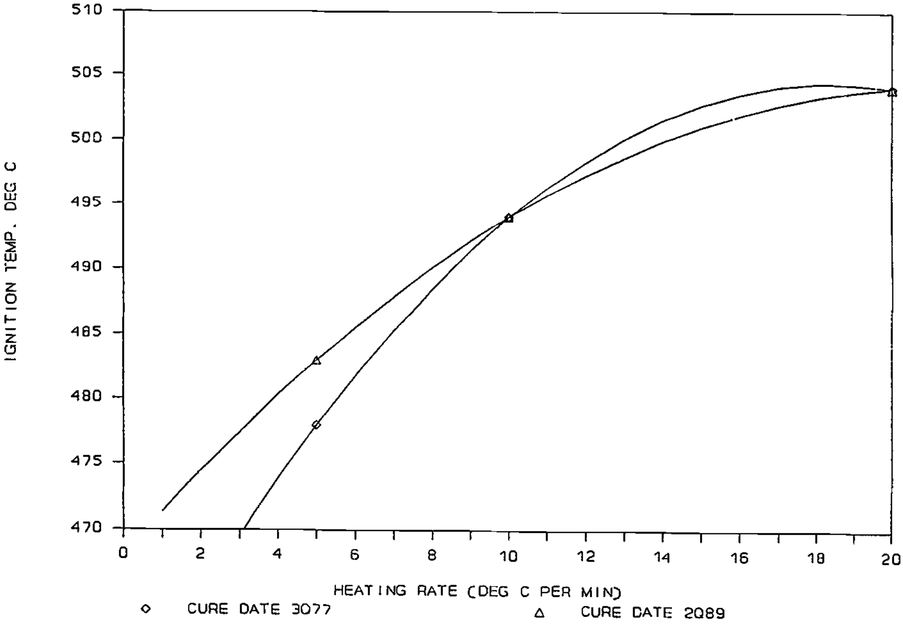

FIG. 8--Effect of heating rate on ignition.

Table 5. The slightly low AIT value obtained with the FTIR spectrometer system is attributed to the lower oxygen flow rate used in the FTIR tests compared with the DSC light-pipe tests.

HDPE does not show the same correlation as Buna N. The AIT measured for HDPE with the DSC light-pipe system is significantly higher than the accepted value [6] or the AIT measured with the FTIR spectrometer system for large sample masses. This is attributed to the dependency of the AIT on the surface-to-mass configuration of the molten HDPE, as described by Tapphorn et al [2].

The most significant difference between the two Buna N batches (as indicated by FTIR spectral analysis) is that measurable concentrations of ammonia (350°C to 475°C [662°F to 887°F]) are produced with the pyrolytic decomposition of the 3Q77 sample, while the 2Q89 sample produced almost no ammonia. The 2Q89 sample also produces lower concentrations of $C_xH_yO_z$ for comparable temperatures than the 3Q77; significant concentrations of $C_xH_yO_z$ products are still observed in the 2Q89 sample after ignition.

In addition, when directly comparing six 10-mg samples of each batch tested in the modified particle impact tester, the 3Q77 batch produced more char on the metal. The amount of carbon black was assumed to be the same (from TGA and specific gravity measurements) in each sample, so char formation must have occurred. The acrylonitrile part of the Buna N (see Section 5.2) is prone to cyclization [7]; in fact, this is the first stage to producing carbon fibers, in which a ladder polymer is formed. The second stage occurs at higher temperatures and involves eliminating anything that is not carbon from the chain (including nitrogen); this could be the source of the ammonia.

The absence of ammonia in the decomposition of the 2Q89 batch may indicate a lower weight percentage of the acrylonitrile base polymer or a different copolymer configuration compared with the 3Q77 batch. Qualitative analyses (identification of pyrolytic products) of the absorbance spectra as a function of sample temperature are given in Table 6 for HDPE and Buna N.

According to Table 6, the HDPE is much easier to ignite and apparently should produce more energy than the Buna N, because the HDPE has a higher heat of combustion; however, the HDPE did not ignite the

TABLE 5--Buna N tested with FTIR spectrometer[a].

Temperature		Gaseous Products[b]	DSC Features
(°C)	(°F)		
<150	<302	Nothing detectable	
150	302	$C_xH_yO_z$, CO_2, H_2O	Pre-exotherm
250	482	$C_xH_yO_z$, CO_2, CO, H_2O, COS, CS_2	1st exotherm
310	590	$C_xH_yO_z\uparrow$, $CO_2\uparrow$, CO↑, H_2O COS↓, $CS_2\downarrow$	Peak of exotherm
340	644	$C_xH_yO_z$, CO_2, CO, H_2O	
350	662	$C_xH_yO_z$, CO_2, CO, H_2O, NH_3	2nd exotherm
380	716	$C_xH_yO_z$, CO_2, CO, H_2O, NH_3 HCN	
400	752	$C_xH_yO_z$, CO_2, CO, H_2O, $NH_3\downarrow$ HCN↓	
475	887	$C_xH_yO_z\uparrow$, $CO_2\uparrow$, CO↑, $H_2O\uparrow$	Ignition

[a] Buna N (National O-ring compound C69), 250-mg samples, 10 K/minute, 150-sccm oxygen

[b] ↑Quantity increasing at that temperature; ↓Quantity decreasing at that temperature

TABLE 6--Ignition and combustion properties of materials, and AITs measured with new methods and equipment.

Mater.	Oxygen Index[a]	Heat of Combustion[a] (cal/g)	AIT[a]		FTIR Spectrometer AIT		DSC/Photodiode Detector AIT	
			(°C)	(°F)	(°C)	(°F)	(°C)	(°F)
Buna N	22	8355	489	912	480	896	494	921
HDPE	<17.5	11154	226	439	295	563	469	876

[a] [8]

[b] 250-mg samples, 10 K/minute, 150-sccm oxygen, 85.5 kPa (12.4 psia)

[c] 15-mg samples, 10 K/minute, 1 000-sccm oxygen, 85.5 kPa (12.4 psia)

metal whereas the Buna N did. The HDPE above its melting point (135°C [275°F]) is less dimensionally stable than the Buna N; the Buna N is crosslinked (with sulfur) and is more dimensionally stable. The Buna N would be expected to hold its position longer than the HDPE melt, which becomes less viscous with increased temperature. Thus, heat transfer to the metal (related to heat of combustion/contact surface area) remains constant for the Buna N but decreases with temperature for HDPE.

The HDPE burnt with a candle-like flame characteristic of a vapor flame. The FTIR furnace also showed that the precombustion gases consisted largely of $C_xH_yO_z$, a vapor-phase product that is oxidizable. Both Buna N materials ignited vigorously with a small flame (vapor-phase burning), which then turned into a glowing (nonvapor-phase) type burning. Again, both Buna N polymers showed $C_xH_yO_z$ in the precombustion gases. The initial vapor-phase burning is considered to be a kindling for the nonvapor-phase burning; the nonvapor-phase burning is thought to correspond to burning of the carbon black in Buna N. The effect of filler will be investigated in another work.

CONCLUSIONS

The Buna N polymer ignited the Inconel 718 in the modified configuration simulation tester. The lowest weight of the Buna N polymer that ignited the metal was 1.5 mg, which was more than the size range (0.1 - 0.2 mg) found in the GO_2 system under investigation. Results indicate that the suspected section of Buna N is a minimal hazard in the GO_2 system, because the minimum weight of the Buna N necessary to ignite the Inconel 718 was not within the specified range.

None of the three HDPE samples ignited the Inconel 718 in the modified configuration simulation tester. Thus, HDPE contamination in a GO_2 system may, under certain circumstances, be safer than Buna N contamination. This conclusion contradicts previous beliefs that the material performances are based on the measured values of oxygen index, AIT, and heat of combustion.

Based on the test results obtained to better understand the polymer-to-metal ignition process, the Buna N polymers were found to ignite metals better than the HDPE polymers because of the shape retention and possibly the carbon black filler that the Buna N rubber contains.

REFERENCES

[1] Benning, M. A., and Werley, B. L., "The Flammability of Carbon Steel as Determined by Pressurized Oxygen Index Measurements." Flammability and Sensitivity of Materials in Oxygen-Enriched Atmospheres: Volume 2, ASTM STP 910, M. A. Benning, Ed., American Society for Testing and Materials, Philadelphia, 1986, pp. 153-170.

[2] Tapphorn, R. M., Shelley, R., and Benz, F.J., "Test Developments for Polymers in Oxygen-Enriched Environments," Symposium on Flammability and Sensitivity of Materials in Oxygen-Enriched Atmospheres: Volume 5, ASTM STP 1111, J. M. Stoltzfus and K. McIlroy, Eds, American Society for Testing and Materials, Philadelphia, 1991, pp 43-59.

[3] Omnitherm Corporation. TGA 1000/1500 Instruction Manual, Omnitherm, 1990.

[4] Steinberg, T. A., Rucker, M. A., and Beeson, H. D., "Promoted Combustion of Nine Structural Metals in High-Pressure Gaseous Oxygen; A Comparison of Ranking Methods," Symposium on Flammability and Sensitivity of Materials in Oxygen-Enriched Atmospheres: Volume 4, ASTM STP 1040, J. M. Stoltzfus, F. J. Benz, and J. S. Stradling, Eds, American Society for Testing and Materials, Philadelphia, 1989.

[5] Department of Defense, Packing, Preformed, Hydrocarbon Fuel Resistant, MIL-P-5315B, US Government Printing Office, 1964.

[6] Bryan, C. J., and R. Lowrie, "Comparative Results of Autogenous Ignition Temperature Measurements by ASTM G72 and Pressurized Scanning Calorimetry in Gaseous Oxygen," Flammability and Sensitivity of Materials in Oxygen-Enriched Atmospheres: Volume 2, ASTM STP 910, M. A. Benning, Ed., American Society for Testing and Materials, Philadelphia, 1986, pp. 108-117.

[7] Society of Plastics Engineers, Handbook of Composites, Van Nostrand Reinhold, New York, 1982.

[8] Ikeda, G. K., "Oxygen Index Tests to Evaluate the Suitability of a Given Material for Oxygen Service," Flammability and Sensitivity of Materials in Oxygen-Enriched Atmospheres: Volume 1, ASTM STP 812, B. L. Werley, Ed., American Society for Testing and Materials, Philadelphia, 1983, pp. 56-57.

Structured Packings for Cryogenic Air Separation Plants

Robert Zawierucha[1], Joseph F. Million[1], Scott L. Cooper[1], Kenneth McIlroy[1], and Jay R. Martin[1]

COMPATIBILITY OF ALUMINUM PACKING WITH OXYGEN ENVIRONMENTS UNDER SIMULATED OPERATING CONDITIONS

REFERENCE: Zawierucha, R., Million, J. F., Cooper, S. L., McIlroy, K., and Martin, J. R., "Compatibility of Aluminum Packing with Oxygen Environments Under Simulated Operating Conditions," Flammability and Sensitivity of Materials in Oxygen-Enriched Atmospheres: 6th Volume, ASTM STP 1197, Dwight D. Janoff and Joel M. Stoltzfus, Eds., American Society for Testing and Materials, Philadelphia, 1993.

ABSTRACT: High surface area aluminum structured packings are possible components in cryogenic distillation columns used for air separation. Recently published literature has reported on the occurrence of strong energy releases involving aluminum structured packing which was subjected to flammability tests in the presence of liquid oxygen using strong thermite and magnesium promoters, under conditions which may not be typical of operating conditions in a cryogenic distillation column.

An experimental program was conducted to determine the compatibility of aluminum packing under test conditions which more closely simulated actual column operating conditions. The effects of various thermite, magnesium, hydrocarbon and metal promoters were evaluated in LOX/GOX environments with a nominal oxygen purity of 99.9% at pressures up to 0.17 MPa.

A major finding was that aluminum packing which was "irrigated" with LOX but not immersed in LOX did not experience severe energy releases in flammability tests up to a maximum pressure of 0.17 MPa at a nominal oxygen purity of 99.9%. This simulated column operating conditions. Elimination of packing "irrigation" and immersion of the aluminum packing at one end in LOX resulted in a severe energy release in one test conducted at 0.16 MPa. The latter result verified recent literature reports but was not considered representative of packing operating conditions.

Of particular interest in this paper are details and schematics of a pressurized test vessel which was designed for the program. This test apparatus is capable of providing various combinations of packing immersion and irrigation, thereby simulating actual operating conditions.

KEY WORDS: Aluminum Packing, Metals Flammability, Oxygen, Cryogenic Distillation Columns

---

[1] Manager, Senior Chemist, Consultant, Engineering Associate and Director respectively, Research and Development, Praxair, Inc., Linde Division, P.O. Box 44, Tonawanda, NY 14151-0044

INTRODUCTION

It is believed that high surface area structured packing will find increasing use in the cryogenic distillation of air because it can result in systems that consume less energy than conventional distillation tray technology. Packings are typically fabricated from corrugated sheets of thin metal which have high surface area to metal volume ratios.

Typical commercial packings have thicknesses on the order of 0.2mm-0.25mm, although these dimensions should not be considered limiting. Packing could be used in distillation columns in oxygen concentrations of part per million levels to 99.9+%. At the higher oxygen purities, packing might be used at absolute pressures on the order of 0.17 MPa-0.20 MPa maximum.

In normal service, packing is utilized in countercurrent service with liquid flowing downward concurrent to the upward vapor flow. This concept is referred to as "irrigation." Cryogenic packing is not normally submerged in liquid oxygen or used without "irrigation." Packing is not likely to be submerged in liquid oxygen even if the column liquid is totally released into the sump. However, unless prohibited by standard operating procedures, the lower end of a packed cryogenic distillation column might be inadvertently submerged during a start up. It is believed that the preceding factors should be considered when devising compatibility tests of packing.

A significant aspect in the design of oxygen systems is the flammability and combustion of materials. Aluminum, a preferred material for packing based upon economics, is known to be flammable and combustible in oxygen. However, long term experience within the industrial gas business has resulted in a successful history of aluminum usage with only a few scattered incidents despite the huge amounts of aluminum utilized.

Concerns about the suitability of aluminum packing for cryogenic distillation columns stem from two recent publications. Reference 1 indicated that aluminum would burn under conditions found in a distillation column and in its test data supported the substitution of cuprous materials. The test data were based upon the use of strips as opposed to actual packing.

The second publication, Reference 2, to a large extent, presented flammability data based upon actual packing samples. When tested in the form of actual packing, aluminum was found to be susceptible to combustion propagation at oxygen concentrations in excess of 97.4%. Some of the tests resulted in violent energy releases i.e. explosions; possibly, detonations. Copper packing was recommended for environments with a purity of >97.4%.

Design, manufacturing and QC practices largely based upon a great deal of experience and common sense have been developed through the years which have allowed the industry to utilize flammable materials. However, the potential impact of detonations is a subject that is difficult to deal with in the design of process equipment.

The basic question that has evolved in response to Reference 2 is the following: How valid is the test method and the results obtained described therein to the use of aluminum packing in cryogenic distillation columns? This paper presents experiments generated during the 1989-1991 time period to assess the suitability of aluminum packing for cryogenic distillation columns.

EVOLUTION OF TEST CONCEPT

General

The "Slusser-Miller Extended Fire Triangle" from Reference 3 which has been modified to include purity and phase on the oxygen leg is considered to be a useful starting point for the discussion. It is shown in Figure 1. For a fire to occur, fuel, oxygen and an ignition mechanism have to be present simultaneously.

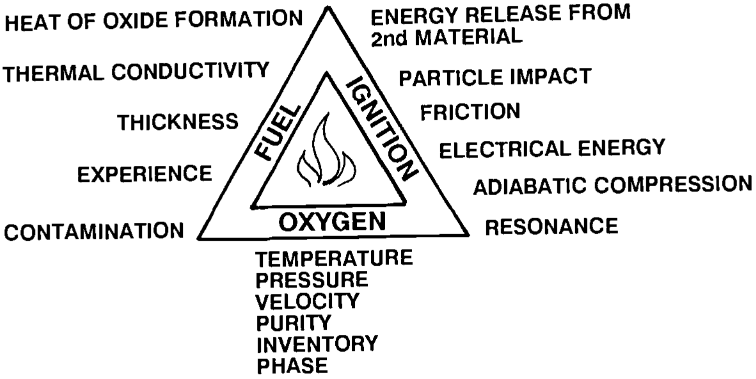

Figure 1. The Slusser-Miller Fire Triangle with modifications.

We can now discuss the fuel, oxygen and ignition mechanism variables, how they interrelate and affect the choice of testing procedure which may be used.

The Fuel Leg

All materials in an air separation plant have to be considered as fuels. Generally, the lower the heat of combustion, the better. Unfortunately, in contrast to metals such as copper and nickel, aluminum has a high heat of combustion which makes it an excellent fuel. High thermal conductivity helps to mitigate the use of aluminum as it allows the energy from an ignition event to be dispersed. The thin cross-section of aluminum packing is an adverse factor which is offset by extensive industry experience with thin cross-sections in components such as Brazed Aluminum Heat Exchangers (BAHX).

Despite attempts to remove them, oxygen systems may contain contaminants of various forms. When contaminants are considered, hydrocarbons come to mind immediately when oxygen compatibility is discussed. Hydrocarbons may be introduced from the atmosphere in the form of species such as acetylene, methane, ethane or propane. The inadvertent concentration of atmospheric hydrocarbons is generally considered to be the cause of most incidents in cryogenic distillation columns.

Manufacturing residues, solvents, greases, etc. or wear products from gaskets, seals, etc. are also sources of hydrocarbon contaminants. In addition, other contaminants such as metal filings, corrosion products or halogenated hydrocarbons may be inadvertently left or introduced into a system. Contaminants are therefore a factor of considerable significance in the design of a compatibility test or the identification of a failure mechanism involving oxygen systems.

The Oxygen Leg

In the oxygen leg, we are dealing in the aluminum packing application with cryogenic temperatures, relatively low pressures, at least in the high purity regions, and relatively low velocities. The inventory consists of a liquid film on the surface of the packing, a gas phase surrounding the packing and a liquid oxygen pool below the level of the packing. Oxygen purity may range from relatively low oxygen concentrations to 99.99+% in the high purity areas. The oxygen phase aspects are crucial to the test design. A key aspect of oxygen purity is that it increases the severity of energy releases of many contaminants within a system.

With respect to the liquid pool, the aluminum packing will usually be above it even if the column contents are "dumped" into the sump. Furthermore, in the event this happens, the liquid pool oxygen purity will be reduced. Only during start-up conditions is it possible to submerge the lower end of the packing and this can be prevented by operating procedures.

The Ignition Mechanism Leg

Operating conditions within a cryogenic distillation column are such that most ignition mechanisms are eliminated. Of the various ignition mechanisms, the only one which is pertinent to packed columns is "Energy Release From A Second Material." This mechanism is also known as "Promoted Ignition." This is the mechanism in which contaminants play a role. The promoter that has been selected for a promoted ignition-combustion test should be related to potential contaminants within a system. However, this may not always be the case for "pure" flammability studies or if physical characteristics prevent the use of a preferred promoter in a test. Cleaning obviously reduces the potential for such a mechanism, but may not completely eliminate it.

Test Concept Selection

Consideration of the fuel-ignition mechanism-oxygen variables as they relate to a packed column leads to the general observation that a promoted ignition-combustion test is the appropriate concept to apply to the flammability testing of aluminum packing. Likely contaminants to be used as promoters include: hydrocarbons, small metal particles and other residues including corrosion products which may be encountered in an air separation plant. The corrosion products could be metal oxides that are easily reduced by aluminum at elevated temperatures.

To be meaningful, the test sample has to be tested in the environment of interest. Reference 4 shows the effect of oxygen purity on aluminum combustion; therefore, high purity oxygen is required. However, Reference 4 also questions the suitability of hydrocarbons as promoters. The nature of the application requires a flowing liquid film on the surface of the test article, the presence of oxygen vapor and a proximity to a liquid oxygen pool; although, not necessarily immersion. These requirements suggest the use of actual packing samples as opposed to strips or rods.

A major concern relates to the energy level of the promoter relative to the size of the packing sample. It should be reasonable, a concept not easily definable. A second concern relates to the magnitude of the energy release which occurs in the event that ignition and combustion takes place. It should be safely contained.

Categories of Promoted Ignition-Combustion Tests

There are three general categories of promoted ignition-combustion packing tests that were conducted in this investigation; identified as follows:

1.) Single packing element - atmospheric pressure.
2.) Multiple packing element - atmospheric pressure.
3.) Single packing element - pressurized.

Concurrent with the above, flammability tests were also made of Brazed Aluminum Heat Exchanger (BAHX) samples. However, this test work will be treated in the future as a separate item in another paper.

SINGLE PACKING ELEMENT - ATMOSPHERIC PRESSURE TESTS

Objective

The major purpose of the single packing element tests was to assess promoter effects and not necessarily duplicate actual packing conditions. It was also to provide more confidence in conducting tests with multiple elements under simulated process conditions.

Apparatus

The test apparatus for the single element packing test is shown in Figure 2. It was a copper test vessel with copper end caps. Nominal dimensions of the vessel were 112 mm diameter x 127 mm height x 2.5 mm wall.

Ceramic spacers were placed on the bottom of the vessel to keep the packing off the bottom. Feed throughs for a thermocouple to determine the liquid level and the ignition circuit were provided as well as a drain at the bottom of the vessel.

Aluminum Packing Element

The packing element was 3003 aluminum with a nominal dimension of 95.25mm diameter x 76.2mm height. Foil with a nominal thickness of 0.25mm was used to make up the circular samples. Figure 3 shows a typical sample after completion of a test. The

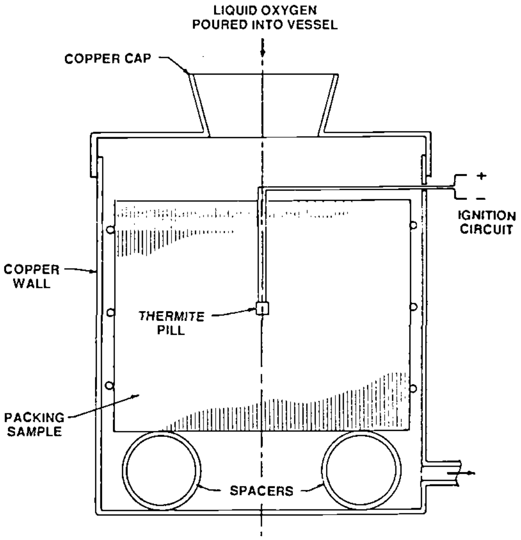

Figure 2. Schematic of test apparatus for single element - unpressurized tests.

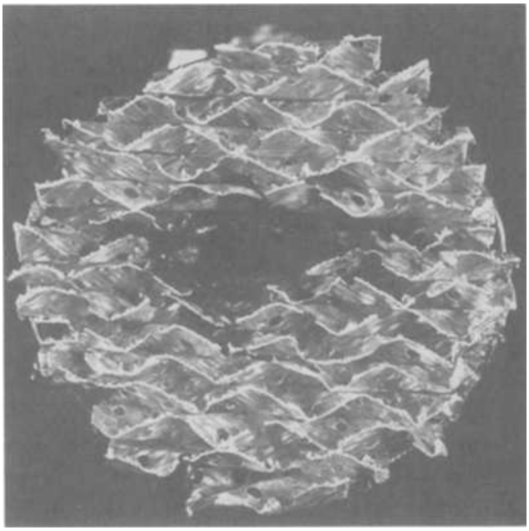

Figure 3. Photomacrograph of packing element after atmospheric ignition test in GOX/LOX using 1g thermite + 5g Mobil 600 oil and 0.13g steel wire as promoter.

weight range of the packing sample was 56.70 g to 72.12 g prior to test.

Test Environments

Air, gaseous oxygen and liquid oxygen were used in this series of tests. The analyzed oxygen purities of the gaseous oxygen (GOX) and liquid oxygen were 99.83% and 99.88% respectively. The oxygen used in these tests was commercial product and not made up specifically for the tests.

Promoters

The purpose of this testing phase was to a large extent to determine the effects various promoters had on the packing samples and select "reasonable promoters for follow-on tests in other test phases." The following promoters were used:

1.) 1g, 2g, or 4g thermite.
2.) 1g thermite + 0.13g steel wire.
3.) 1g thermite + 0.5g Mobil 600 oil.
4.) 1g thermite + 0.5g Mobil 600 oil
+ 0.13g steel wire.

Test Procedures

The various promoters were placed in the interior of the individual packing samples. Thermite was encapsulated. Where steel wire was used, it was wrapped around the thermite. Mobil 600 oil, where it was used, was spread on the thermite and adjacent packing material.

Tests ignited in air were not done in the copper test vessel so that the energy release without the presence of GOX and LOX could be observed. For the single GOX test, the sample was placed in the copper vessel and subjected to an extensive purge; then ignited.

For the LOX/GOX tests, the copper vessel with the test sample within was filled to the top with LOX. When the liquid level dropped, so that the promoter was in the vapor phase, it was ignited.

Results

In all, 10 tests were conducted in this phase. The results are tabulated in Table I. No explosions or serious combustion propagation occurred. Weight changes were considered to be insignificant; however, weights were affected by various adhering remnants of promoter and combustion products.

Figure 3, which was referred to previously, shows the sample from test number 10. It experienced the largest volumetric loss of packing materials though little weight change.

TABLE I -- RESULTS OF SINGLE PACKING FLAMMABILITY TESTS - ATMOSPHERIC PRESSURE

TEST NO.	ENVIRONMENT	PROMOTER	PACKING WEIGHT (g)		RESULT
			BEFORE	AFTER	
1	AIR	1g THERMITE	61.83	61.81	NO EXPLOSION/ PROPAGATION
2	AIR	1g THERMITE + 0.13g STEEL WIRE	66.83	66.92	NO EXPLOSION/ PROPAGATION
3	GOX	1g THERMITE	72.12	71.98	NO EXPLOSION/ PROPAGATION
4	LOX/GOX*	1g THERMITE	65.09	65.29	NO EXPLOSION/ PROPAGATION
5	LOX/GOX*	1g THERMITE	56.70	56.72	NO EXPLOSION/ PROPAGATION
6	LOX/GOX*	1g THERMITE + 0.13g STEEL WIRE	65.99	65.81	NO EXPLOSION/ PROPAGATION
7	LOX/GOX*	2g THERMITE	63.23	63.20	NO EXPLOSION/ PROPAGATION
8	LOX/GOX*	4g THERMITE	65.58	65.33	NO EXPLOSION/ PROPAGATION
9	LOX/GOX*	1g THERMITE + 0.5g MOBIL 600 OIL	71.57	71.58	NO EXPLOSION/ PROPAGATION
10	LOX/GOX*	1g THERMITE + 5g MOBIL OIL + 0.13g STEEL WIRE	67.90	65.77	NO EXPLOSION, MOST SEVERELY DAMAGED

* IGNITION IN VAPOR PHASE JUST ABOVE LOX/GOX BOUNDARY

Remarks

Taken as a group, the results were considered to be very encouraging. The results indicated a high potential for combustion arrest if ignition occurred, even with the use of strong promoters. There was no indication of any explosive tendencies in this test series. The test results created more confidence in the potential results which might be obtained with multiple elements and under process conditions.

MULTIPLE PACKING ELEMENT - ATMOSPHERIC PRESSURE TESTS

Objectives

One objective was to provide a sample configuration more typical of the stacking arrangement in an actual distillation column. A second objective was to evaluate the effects of irrigation and continued LOX flow after an ignition event. The third objective was to evaluate the effects of packing immersion in LOX while irrigated during a promoted ignition event.

Apparatus

Figure 4 is a schematic of the test apparatus used in the multiple packing element tests. In the upper right hand corner of Figure 4, is an insulated LOX vessel with nominal internal dimensions of 152mm diameter x 305mm height. The LOX level in this vessel is determined by a float. Copper tubing with an in-line valve connects the LOX reservoir to a cruciform distributor in the top of the simulated packed column in the lower left hand corner of the figure.

The simulated packed column is a copper pipe with a nominal diameter of 112mm, height of 610mm, and thickness of 2.54mm. It sits on a gravel bed in a tray. If it is desired to have a pool of LOX at the base of the column, a perforated copper cap with holes drilled to set the depth of the LOX pool can be placed at the bottom of the copper pipe. Otherwise, LOX which enters through the top will flow into the gravel after it flows down and irrigates the packing samples.

Typically, four packing samples are used in this apparatus. Tests may be conducted with the bottom element at least 76mm above the gravel or immersed in LOX to a depth of 12mm - 19mm.

Aluminum Packing Elements

Each individual packing element had the same exterior dimensions as the packing elements cited previously. The packing material was aluminum alloy 3003. In this series of tests the packing foil had nominal thicknesses of 0.20mm and 0.25mm. The weight range was 62.67g to 80.6g.

The bottom of the four packing elements contained the promoter in the approximate center of the sample. A thermocouple was placed in the packing element immediately above it.

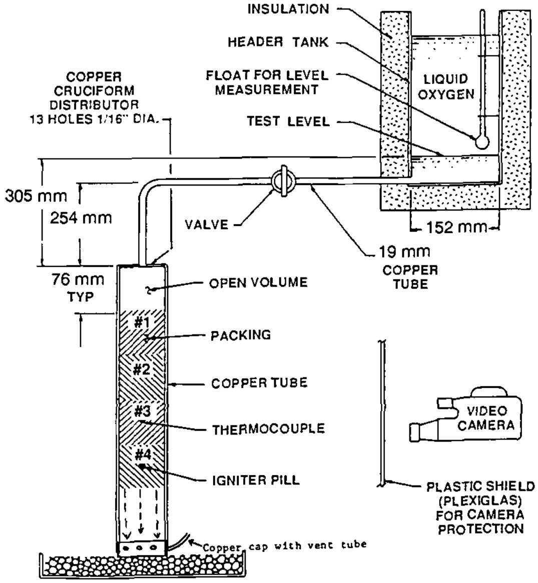

Figure 4. Schematic of the test apparatus for multiple element tests - atmospheric pressure - irrigated.

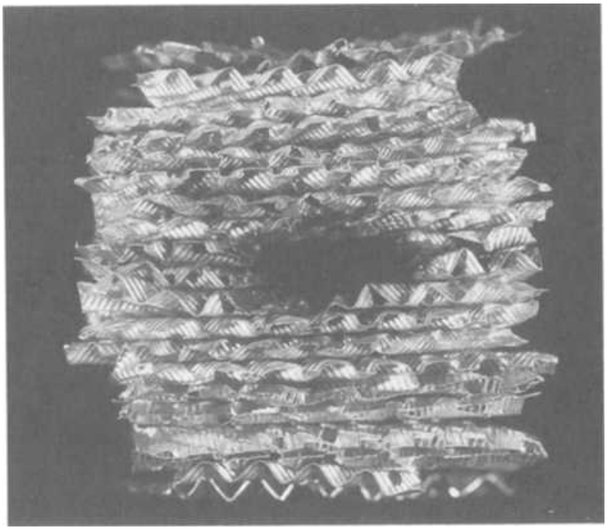

Figure 5. Photomacrograph of bottom packing element after atmospheric promoted ignition test, irrigated, using 2g thermite as promoter.

Test Environments

Commercial LOX with analyzed purities of 99.88% and 99.9% were used in this series of tests. These were not synthetic mixtures.

Ignitor

Pyrofuze^R, an Al-Pd composite, which generates an exothermic reaction when resistance heated, was used as the ignitor. The ignitor was in direct contact with the promoter.

Promoters

The following promoters were utilized in this phase and placed in the center of the bottom packing elements:

1.) 1g, 2g or 3g thermite.
2.) 1g, 2g or 3g thermite + 0.5-0.8g Mobil 600 oil.
3.) 1g thermite + 2g 1:1 mix of CuO/Al powder + 0.2g Mg ribbon.

Some of the stronger promoters were used in a deliberate attempt to induce explosions after weaker promoters failed to do so. The CuO/Al combination is also a thermite although Fe_2O_3/Al mixes are more commonly thought of when the term thermite is mentioned.

Test Procedures

The LOX reservoir was filled to the top and allowed to flow through the tubing through the cruciform which distributed LOX into the upper packing sample. LOX then flowed down through the four packing samples into the gravel bed in the case of a test where the bottom packing was not submerged or into a LOX pool if a submerged test was run.

The LOX was allowed to flow out of the reservoir until the float reached a level which corresponded to the desired flow velocity required in a column. This meant that approximately 75% of the reservoir had been depleted of LOX.

At this time, the ignitor was set off in the bottom packing element. After ignition, LOX continued to flow through the test apparatus thereby irrigating the packing and passed by the ignitor site into the gravel or into the LOX pool.

Results

Table II shows the results obtained in the promoted ignition tests of multiple packing elements which were irrigated by LOX but not immersed in LOX at the lower end. Table III shows similar results for tests in which the bottom element was immersed in LOX.

TABLE II - ALUMINUM PACKING FLAMMABILITY TEST RESULTS
MULTIPLE PACKING ELEMENTS - ATMOSPHERIC PRESSURE - NO LOX IMMERSION

TEST NO.	IGNITOR	PROMOTER	LOX IMMERS.[2]	LOX IRRIG.	OXYGEN PURITY	PACKING WEIGHT [1] (g)		RESULT
						BEFORE	AFTER	
11	PYROFUZE	1 g THERMITE	NO	YES	99.9	79.4	79.7	NO PROPAGATION NO EXPLOSION
12	PYROFUZE	2 g THERMITE	NO	YES	99.9	78.5	79.5	NO PROPAGATION NO EXPLOSION
13	PYROFUZE	3 g THERMITE	NO	YES	99.9	77.4	77.7	NO PROPAGATION NO EXPLOSION
14	PYROFUZE	1 g THERMITE 0.6 g OIL	NO	YES	99.9	77.2	77.1	NO PROPAGATION NO EXPLOSION
15	PYROFUZE	2 g THERMITE 0.5 g OIL	NO	YES	99.9	80.6	81.4	NO PROPAGATION NO EXPLOSION
16	PYROFUZE	3 g THERMITE 0.8 g OIL	NO	YES	99.9	79.9	80.5	NO PROPAGATION NO EXPLOSION
17	PYROFUZE	1 g THERMITE	NO	YES	98.88	62.67	62.65	NO PROPAGATION NO EXPLOSTION
18	PYROFUZE	1 g THERMITE	NO	YES	98.88	69.93	71.07	NO PROPAGATION NO EXPLOSION

[1] WEIGHTS ARE FOR BOTTOM ELEMENT CONTAINING IGNITOR AND PROMOTER.

[2] BOTTOM PACKING ELEMENT IS AT LEAST 76MM ABOVE GRAVEL BED BELOW TEST APPARATUS.

TABLE III -- ALUMINUM PACKING FLAMMABILITY TESTS
MULTIPLE PACKING ELEMENTS - ATMOSPHERIC PRESSURE - LOX IMMERSION

TEST NO.	IGNITOR	PROMOTER	LOX IMMER.[2]	LOX IRRIG.	OXYGEN PURITY	PACKING WEIGHT[1] (g)		RESULT
						BEFORE	AFTER	
19	PYROFUZE	1 g THERMITE	12mm-19mm	YES	99.9	77.4	77.7	NO PROPAGATION NO EXPLOSION
20	PYROFUZE	2 g THERMITE	12mm-19mm	YES	99.9	79.7	79.8	NO PROPAGATION NO EXPLOSION
21	PYROFUZE	3 g THERMITE	12mm-19mm	YES	99.9	78.9	78.9	NO PROPAGATION NO EXPLOSION
22	PYROFUZE	1 g THERMITE 0.5 g OIL	12mm-19mm	YES	99.9	79.6	79.9	NO PROPAGATION NO EXPLOSION
23	PYROFUZE	1 g THERMITE 2 g 1:1 CU O/AL POWDER MIX MAGNESIUM RIBBON	12mm-19mm	YES	99.9	78.8	78.8	NO PROPAGATION NO EXPLOSION

[1] THE WEIGHTS GIVEN ARE FOR THE BOTTOM PACKING ELEMENTS WHICH CONTAINED IGNITOR AND PROMOTER.
[2] LOWER PORTION OF THE BOTTOM PACKING ELEMENT IS IMMERSED IN LOX TO A DEPTH OF 12mm-19mm.

Some of the tests were quite energetic and provided vivid visual displays due to the quantity of promoter utilized. However, in no case was there significant combustion propagation or an explosion. The weight gain-loss data showed negligible gains or losses irrespective of promoter type. Figure 5 shows a selected bottom packing element from test number 12.

Remarks

As did the test results obtained with the single tests, the experimental results obtained with the multiple element tests were considered very encouraging. The data indicated a high potential for combustion arrest if a promoted ignition event occurred even if strong energetic promoters were used. There was no evidence of severe combustion propagation or explosive tendencies although some of the visual displays caused by the strong promoters were quite impressive.

SINGLE PACKING ELEMENT - PRESSURIZED TESTS

Objectives

The major objective of this phase was to obtain promoted ignition-combustion data of aluminum packing at typical operating pressures in relatively high purity oxygen under conditions typical of packed column operation i.e. packing irrigated not immersed in LOX and pressurized. A second objective was an investigation of promoted-ignition behavior under conditions reportedly associated with the violent energy releases reported in Reference 2.

It should be noted that none of the data in this paper described to this point verified the results reported in Reference 2 regarding detonations or violent energy releases; hence, pressure was considered to be a variable worth investigating.

Test Apparatus, Early Tester

Figure 6 is a schematic of the pressurized tester utilized at the outset to characterize the promoted ignition-combustion tester of aluminum packing. The device was of all copper construction and did not have an irrigation capability. LOX is introduced into the tester via a resevoir on the top after a ball valve is opened. Upon reaching the bottom, the LOX will flash off and after multiple introductions of LOX, will cool the vessel down and also purge it.

The single packing element sits on ceramic tubes which keep it off the base but submerged in LOX to a depth of 25mm to 38mm. Thermocouples at various locations identify the depth of the LOX and establish the liquid-vapor interface. When closed off, the vessel pressurizes via vaporization of the LOX and desired pressure is maintained by a back pressure relief valve.

The lower vessel contains ports for the ignitor circuit, pressure transducer and an oxygen analyzer in addition to the thermocouple ports. The diameter of the upper portion is approximately 102mm with a height of approximately 914mm. The diameter of the bottom pot is approximately 229mm with a height of 178mm.

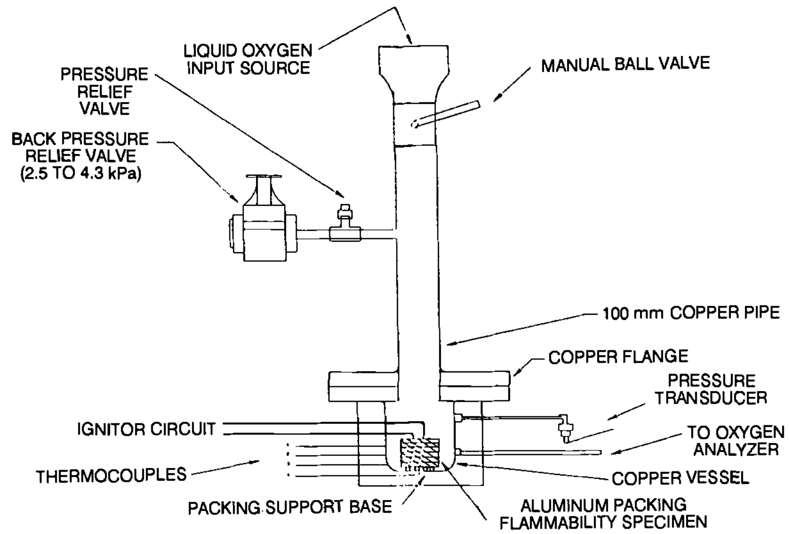

Figure 6. Schematic of single element pressurized tester, LOX immersion, no packing irrigation.

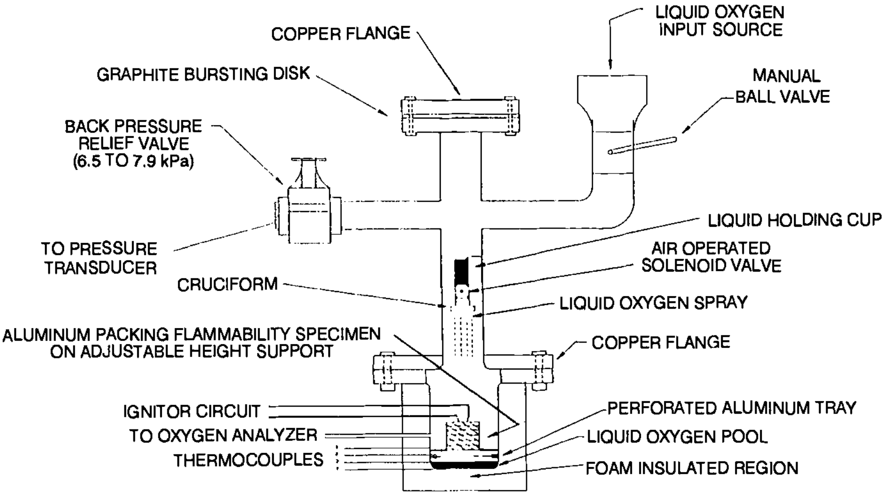

Figure 7. Schematic of single element pressurized tester, variable height above LOX, packing irrigation.

Test Apparatus, Later Model

Figure 7 is a schematic of the later single element pressurized tester which has the capability to irrigate a single element packing specimen at service pressure during a promoted ignition-combustion test. This vessel is also of copper construction. Major differences between it and the earlier pressurized tester are as follows:

1.) A larger graphite burst disc to relieve internal pressure quickly in the event of a severe energy release.

2.) An internal liquid holding cup which holds sufficient LOX to enable a perforated cruciform to generate a spray for 15-45 seconds during the promoted ignition test to "irrigate" the test specimen.

3.) The aluminum packing specimen sits on a perforated aluminum tray which has an adjustable height above the LOX pool.

4.) The base of the device is insulated to prevent excessive flash off and promote quiescence in the LOX pool.

5.) A back pressure relief valve with a higher rating allows higher internal pressures to be reached.

In contrast to the earlier test approach, LOX is introduced from a cryogenic storage vessel to the bowl via a flex hose which runs through an explosion proof wall. The manual ball valve admitting LOX into the vessel is activated remotely with a lanyard. After multiple introductions of LOX, the vessel is cooled down and purged.

Pressure within the vessel is maintained via a back pressure relief valve. LOX level is monitored via thermocouples. The packing sample is always above the LOX pool.

Aluminum Packing Samples

These are identical to the single element packing specimens including ignitor/promoter placement described earlier in the paper for the other test phases, except the thickness was always 0.20mm. Weights ranged from 77.6 to 79.4 grams.

Test Environments

The LOX utilized was of commercial origin and had an analyzed oxygen purity levels of 98.7% for the "early tester" and 99.9% for the later tester.

Test pressures ranged from 0.136 MPa to 0.17 MPa.

Ignitor

Pyrofuze$^{(R)}$ wire was utilized as the ignitor based upon its satisfactory performance in earlier test phases.

Promoters

Promoters utilized in this phase included the following:

1.) 1g, 2g or 3g of thermite.
2.) 1g thermite + 0.2g Mg ribbon.

Test Procedures

To a large extent the conduct of the tests can be inferred from the description of the two test vessels. It should be emphasized that in both cases, there is a considerable effort expended in purging the vessel and cooling it down. This is done to insure that oxygen purities are at a high level consistent with the original LOX purity.

The major difference between the two testers, is that in the original pressure tester the packing sample is partially submerged and not irrigated while in the later tester the sample is above the LOX pool and irrigated. There is a window of up to 45 seconds when packing irrigation occurs within which ignition can occur. After that time, the sample will not be irrigated due to depletion of the LOX reservoir internal to the pressurized tester.

Results

Table IV lists the promoted ignition data obtained with the early model of the pressurized single packing element flammability tester. No packing weight data are available; however, it is believed that the samples were in the range of 70g - 80g. The tester was in existence for three tests. An explosion destroyed the test apparatus on the third test, No. 26. Most of the packing sample was consumed in the incident. This result confirmed the observation made in Reference 2 that aluminum packing partially submerged in LOX and not irrigated may explode if subjected to a promoted ignition event in high purity gaseous oxygen.

TABLE IV -- RESULTS OF ALUMINUM PACKING FLAMMABILITY TESTS, SINGLE PACKING ELEMENT, PRESSURIZED, LOX IMMERSION, NO IRRIGATION

TEST NO.	IGNITOR	PROMOTER	PRES. MPa	LOX IMMER.	LOX IRRIG.	OXY. PUR.	RESULT
24	PYROFUZE	1g THERMITE	0.136	25mm-38mm	NO	98.7%	NO PROPAGATION NO EXPLOSION
25	PYROFUZE	2g THERMITE	0.136	25mm-38mm	NO	98.7%	NO PROPAGATION NO EXPLOSION
26	PYROFUZE	3g THERMITE	0.157	25mm-38mm	NO	98.7%	EXPLOSION

This confirmation came at a considerable cost with respect to test equipment and there was no incentive to repeat the test under the exact same conditions which were not considered to be representative of packed column operation.

Table V lists the results of promoted ignition-combustion tests conducted on aluminum packing that was "irrigated," above a LOX pool and ignited in gaseous oxygen with a purity of 99.9% and pressures up to 0.17 MPa. No explosions or runaway combustion occurred. All of the samples were more or less intact resembling Figures 3 and 5 from earlier tests. No significant changes were noted in the weight gain-loss data.

Tests 31 through 39 utilized 1g thermite plus 0.2g Mg as the promoter. It can be argued that thermite, an Al-Fe_2O_3 mix, is a reasonable simulation of ferrous corrosion products and aluminum dust which might be found in an air separation plant if it is not properly cleaned. Mg additions to a promoter mixture cannot be justified with that argument. Reference 2 utilized Mg additions to enhance the severity of the promoted ignition event. It was considered desirable to demonstrate the survivability of the aluminum packing with a strong promoter and allow the data to be directly compared to Reference 2. Therefore, Mg additions were made to the promoter mixture.

Remarks

Results obtained in this test series were significant. The tests conducted under conditions not representative of packed column operation generated one violent energy release; thereby, confirming the results of Reference 2. However, flammability tests conducted under conditions representative of packed column operation did not result in any violent energy releases or significant combustion propagation.

DISCUSSION

This paper and Reference 2 can be contrasted with technical papers such as References 4 and 5 in that not only is the flammability of an aluminum alloy in an oxygen environment an issue but also whether or not there is a possibility of an explosion or violent energy release. A key aspect of both this paper and Reference 2 is that they deal with LOX in contrast to gaseous oxygen, which is the medium of most metal flammability studies.

The use of aluminum in oxygen environments is extensive with an excellent safety record. There have been several scattered incidents of aluminum-LOX reactions which resulted in violent energy releases of which Reference 6 is a prime example. Systematic promoted ignition tests of aluminum with LOX to determine those mechanism by which violent energy releases occur are relatively scarce despite these incidents. Technical concerns and questions raised in Reference 6 are still valid.

In this investigation, a violent energy release of the type reported in Reference 2 was generated under specific conditions not related to normal operation of an aluminum packed column. These included the following:

1.) Partial immersion of the aluminum packing in high purity LOX.
2.) Non-irrigation of the aluminum packing.

TABLE V - RESULTS OF ALUMINUM PACKING FLAMMABILITY TESTS
SINGLE PACKING ELEMENT, PRESSURIZED, LOX IMMERSION, NO IRRIGATION

TEST NO.	IGNITOR	PROMOTER	PRESSURE MPa	LOX IMM.	LOX IRRIG.	OXYGEN PURITY	PACKING WEIGHT (g)		RESULT
							BEFORE	AFTER	
27	PYROFUZE	1g THERM.	0.136	NO	YES	99.9%	79.3	79.5	NO PROPAGATION NO EXPLOSION
28	PYROFUZE	1g THERM.	0.136	NO	YES	99.9%	77.6	77.9	NO PROPAGATION NO EXPLOSION
29	PYROFUZE	1g THERM.	0.136	NO	YES	99.9%	79.3	79.6	NO PROPAGATION NO EXPLOSION
30	PYROFUZE	1g THERM.	0.136	NO	YES	99.9%	79.3	79.7	NO PROPAGATION NO EXPLOSION
31	PYROFUZE	1g THERM. 0.2g Mg	0.136	NO	YES	99.9%	79.3	79.5	NO PROPAGATION NO EXPLOSION
32	PYROFUZE	1g THERM. 0.2g Mg	0.136	NO	YES	99.9%	79.4	79.5	NO PROPAGATION NO EXPLOSION
33	PYROFUZE	1g THERM. 0.2g Mg	0.136	NO	YES	99.9%	79.3	79.5	NO PROPAGATION NO EXPLOSION
34	PYROFUZE	1g THERM. 0.2g Mg	0.136	NO	YES	99.9%	78.2	78.5	NO PROPAGATION NO EXPLOSION
35	PYROFUZE	1g THERM. 0.2g Mg	0.17	NO	YES	99.9%	77.7	78.1	NO PROPAGATION NO EXPLOSION
36	PYROFUZE	1g THERM. 0.2g Mg	0.17	NO	YES	99.9%	78.9	79.6	NO PROPAGATION NO EXPLOSION
37	PYROFUZE	1g THERM. 0.2g Mg	0.17	NO	YES	99.9%	79.8	80.1	NO PROPAGATION NO EXPLOSION
38	PYROFUZE	1g THERM. 0.2g Mg	0.17	NO	YES	99.9%	79.4	79.1	NO PROPAGATION NO EXPLOSION
39	PYROFUZE	1g THERM. 0.2g Mg	0.17	NO	YES	99.9%	73.8	75.5	NO PROPAGATION NO EXPLOSION

Furthermore, a strong metal-metal oxide promoter had to be used to ignite the packing.

In contrast, when the aluminum packing samples were irrigated and not immersed in LOX, promoted ignition did not result in extensive combustion propagation or explosions even if strong metal-metal oxide promoters were used in high purity oxygen and at pressures up to 0.17 MPa.

Stoltzfus et al [7] makes a case that geometry is an important factor in the flammability of a component. Brzustowski [8] has identified different combustion mechanisms for aluminum in oxygen which vary depending upon both pressure and purity. One can infer from these investigations, as well as those currently dealing with aluminum packing that sample geometry and test conditions that simulate column process conditions as closely as possible are very important considerations.

This investigation utilized a number of different promoters. Generally, it is believed that there is a consensus in the industrial gas business that hydrocarbon accumulations of species such as acetylene, methane, ethane and propane have been the major cause of incidents in air separation distillation columns. Other hydrocarbon contaminants related to manufacturing residues are also possible, as are accumulations of species such as halocarbons, metals, metal oxides, etc. if cleaning is not done properly.

The use of hydrocarbons in promoted ignition-combustion tests can be criticized as Reference 5 does. It suggests that hydrocarbon combustion products may inhibit the combustion process. However, hydrocarbon accumulations are still likely to be a major contaminant of concern in oxygen applications.

Irrespective of which promoter is utilized for test work, one implication is the same. A promoted ignition-combustion test implies that contaminant buildup is of concern. Proper cleaning, ongoing analysis of contamination buildup and removal of combustible contaminants which could result in a promoted ignition-combustion scenario are necessary for the successful operation of high surface area structured packings.

SUMMARY

This investigation confirmed that it is possible to generate a violent energy release in a promoted ignition test of aluminum packing when it is immersed in 98.7% purity LOX and not irrigated at a test pressure of 0.157MPa. This condition is not typical of aluminum packing operation.

Aluminum packing did not combust or explode when it was subjected to promoted ignition tests with strong promoters when irrigated with LOX and not partially submerged in LOX. In these tests, the LOX purity was 99.9% and maximum pressure was 0.17 MPa. These test conditions are considered representative of packing operation.

Experimental approaches to characterize the transition of metals from ignition to combustion to explosions in LOX environments are suitable areas for future work.

Flammability tests of packing used for cryogenic distillation tests should be conducted under test conditions that approximate actual operating conditions as closely as possible.

Further work to clarify issues regarding the selection of promoters representative of conditions in air separation plants, distribution equipment and auxiliary equipment is desirable.

ACKNOWLEDGEMENTS

The authors wish to acknowledge the contribution by J. A. Hasbrouck and R. F. Alessi in participating in the test work.

REFERENCES:

[1] Bennett, D.L., Ludwig, J.P., Patrylak, A.J. and Zabrenski, J.S., "Suitable Distillation Column Packing for the Cryogenic Separation of Air", United States Patent #4,813,988, March 21, 1989.

[2] Dunbobbin, B.R., Hansel, J.G., and Werley, B.L., "Oxygen Compatibility of High-Surface Area Materials", Flammability and Sensitivity of Materials in Oxygen Enriched Atmospheres: Fifth Volume, ASTM STP 1111, Joel M. Stoltzfus and Kenneth McIlroy, Editors, American Society for Testing and Materials, Philadelphia, 1991, pp 338-353.

[3] Slusser, J.W. and Miller, K.A., "Selection of Metals for Gaseous Oxygen Service", Flammability and Sensitivity of Materials in Oxygen-Enriched Atmospheres: ASTM STP 812, Barry L. Werley, Editor, American Society for Testing and Materials, Philadelphia 1983, pp 167-191.

[4] Zabrenski, J.S., Werley, B.L., and Slusser, J.W., "Pressurized Flammability Limits of Metals", Flammability and Sensitivity of Materials in Oxygen-Enriched Atmospheres: Fourth Volume, ASTM STP 1040, Joel M. Stoltzfus, Frank J. Benz and Jack S. Stradling, Editors, American Society for Testing and Materials, Philadelphia, 1989, pp 178-194.

[5] Benning, M.A., Zabrenski, J.S., and Le, N.B., "The Flammability of Aluminum Alloys and Aluminum Bronzes as Measured by Pressurized Oxygen Index," Flammability and Sensitivity of Materials in Oxygen-Enriched Atmospheres: ASTM STP 986, D.W. Schroll, Ed., American Society for Testing and Materials, Philadelphia, 1988, pp 54-71.

[6] National Traffic Safety Board, "Highway Accident Report: Liquified Oxygen Tank Truck Explosion Followed by Fires in Brooklyn, New York, May 30, 1970," Report NTSB-HAR-71-6, May 12, 1971.

[7] Stoltzfus, J.M., Lowrie, R. and Gunaji, M.V., "Burn Propagation Behavior of Wire Mesh Made From Several Alloys," Flammability and Sensitivity of Materials in Oxygen-Enriched Atmospheres: Fifth Volume, ASTM STP 1111, Joel M. Stoltzfus and Kenneth McIlroy, Eds., American Society for Testing and Materials, Philadelphia, 1991, pp 326-337.

[8] Brzustowski, T.A., "Vapor Phase Diffusion Flames in the Combustion of Magnesium and Aluminum," PhD. Dissertation, Princeton University, 1963.

H. M. Barthélémy (1)

COMPATIBILITY OF ALUMINIUM PACKINGS WITH OXYGEN - TEST RESULTS UNDER SIMULATED OPERATING CONDITIONS

REFERENCE: Barthélémy, H.M., "**Compatibility Of Aluminium Packing With Oxygen. Test Results Under Simulated Operating Conditions**", Flammability and Sensitivity of Materials in Oxygen-Enriched Atmospheres : Sixth Volume, ASTM STP 1197, Dwight D. Janoff and Joel M. Stoltzfus, Eds., American Society for Testing and Materials, Philadelphia, 1993.

ABSTRACT: Metallic structured packings are used more and more in the cryogenic distillation of air because it results in systems that consume less energy than the conventional distillation tray technology employed before. These packings are normally manufactured from corrugated sheets of thin metal. Aluminium alloys are known to be the best candidate metal for these corrugated sheets because of their good properties at cryogenic temperatures excellent formability, light weight and low cost. The purpose of this investigation was to recheck the oxygen compatibility of aluminium structured packing under simulated operating conditions. First, a series of tests were performed using simplified testing conditions to identify the important parameters, such as oxygen purity, energy supplied (type and level), and oil contamination. These tests were carried out in gaseous, liquid and gaseous/liquid oxygen environments. A second series of tests was performed under simulated operating conditions, reproducing, in particular, the irrigation conditions found in normal service. These tests have confirmed the compatibility of aluminium packings with oxygen under actual operating conditions and confirmed the choice of this material for structured packing.

KEYWORDS: Oxygen compatibility, aluminium, combustion propagation, structured packing, air separation, flammability.

Metallic structured packing is used more and more in the cryogenic distillation of air because it results in systems that consume less energy than the conventional distillation tray technology previously employed. Packings are normally manufactured from corrugated sheets of thin metal. Aluminium alloys are known to be the best candidate metals for these corrugated sheets because of their good properties at cryogenic temperatures, formability, light weight and low cost. This is why aluminium structured packings have been successfully used in air distillation columns for almost 10 years

---

1-Materials Manager, Air Liquide, DDE, 75 quai d'Orsay 75007 Paris France.

Recently, the oxygen compatibility of these aluminium packings was questioned by B.R. Dunbobbin et al. [1]. They concluded that, "above the threshold for propagation of aluminium, above 97.4 % (gaseous oxygen above a liquid pool), aluminium may not be desirable because its damage potential is so much greater and because the prospect of shock-wave production in liquid oxygen is particularly undesirable".

The purpose of this investigation was to recheck the oxygen compatibility of aluminium structural packing under simulated operating conditions. This was done because Dunbobbin tests [1] were performed in conditions very different from the actual operating conditions.

LITERATURE REVIEW

The flammability of aluminium and aluminium alloys is addressed in numerous technical papers and reports. Recently a task force of the gas industries (Compressed Gas Association) decided to review this item. Following this review a paper was prepared to be presented at this ASTM conference [2]. This paper should be considered before addressing the oxygen compatibility of aluminium structural packings.

EXPERIMENTAL TECHNIQUE AND APPARATUS

The goals of this experimental program were, first to check tests results presented by Dunbobbin [1] and to investigate carefully the conditions where unacceptable behaviour of aluminium in oxygen atmosphere was found, second, to check under simulated operating conditions, in reproducing, in particular the irrigation condition found in normal service and to determine, what could be the consequence of an ignition.

Tests On Immersed Packing Elements

These tests were performed first in order to check results presented by Dunbobbin [1], where it was established that the worst conditions are when aluminium packing samples are partially immersed in liquid oxygen (LOX) of high purity and when top ignition i.e. in gaseous oxygen (GOX) is used. They were also performed to identify the most important parameters that need to be taken into consideration.

For these tests the following testing conditions were used :

- Packing samples : they were made of 3003 aluminium alloy (AA) and composed of 7 metallic sheets 0.2 mm in thickness ; the size of these samples was 150 mm in height and 40 mm x 40 mm in cross section. The weight of the samples was approximately 32 grams. These samples were very similar to the "long specimen" used by Dunbobbin.

- Ignitor : the same ignitors as Dunbobbin were also used ; they mainly consisted of thermite pills (1-3 grams) and very often Magnesium ribbon (0.24 g as per Dunbobbin tests) was added. According to Dunbobbin, 1 g of thermite releases about 1850 calories and 0.24 g of magnesium releases about 1400 calories. To ignite the thermite a Nichrome electric wire was used.

- Test vessel : a thin copper vessel was used (0.5 mm in thickness, OD = 200 mm, Height = 220 mm). This vessel had a thick copper base heated by gaseous nitrogen (GN) circulation to increase oxygen boiling. The intensity of oxygen boiling was assumed by Dunbobbin to be an important parameter to increase intensity of reactions between aluminium and oxygen. Fig. 1 shows a schematic of this vessel and the packing element in it.

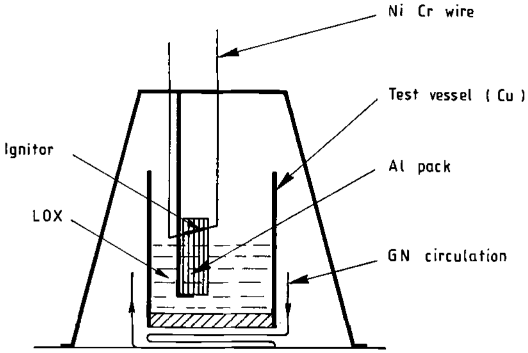

Fig. 1 - Tests on immersed packing elements - Principle

- Oxygen purity : three different grades of oxygen purities were used ; liquid oxygen from ultra pure electrolytic source (E), this oxygen typically corresponds to purity of 99.999 + %, this oxygen also contains no trace of argon often suspected to inhibit the Al/O_2 reaction ; liquid oxygen from a current cryogenic air separation plant (P), this oxygen typically corresponds to purity of 99.8 + % ; and oxygen from a cryogenic air separation plant specially designed and operated to produce high purity oxygen (HP) ; this oxygen typically corresponded to purity of 99.99 + %. GOX was also analysed just before ignition with a Servomex paramagnetic analyser. Because of the sensitivity of this type of analyser (normally ± 0.1 %) and because of the difficulty to perfectly purge the relative long pipeline for gas sampling before each ignition, analysis results of the GOX given in Table 1 should be considered as approximate (underestimated).

- Experimental procedure : tests were performed at atmospheric pressure; the test vessel was first purged with high purity GOX then filled with liquid oxygen just below the thermite ignitor (it was found that immersion of thermite in LOX before the test can lead to malfunction of this ignitor). A vigorous boiling of LOX was insured by GN (see Fig. 1) during 5 to 10 min to ensure good purity of the GOX phase which was checked as before ; the LOX level in the test vessel was monitored and the level at time of thermite ignition is given in Table 1 ; packing samples were located at about 2 cm above the vessel bottom and a LOX level of 9.5 cm corresponded to 50 % immersion of the samples.

After the tests, the quantity of aluminium which reacted (burned or melted) was noted as was any significant damage of the test vessel ; when the test vessel was destroyed (very often fragmented in several pieces) this was noted as a very energetic reaction (VER) ; when the vessel was not significantly damaged this was noted as a simple combustion (C) or no reaction (NR) if only a small quantity of aluminium has disappeared (see Table 1 a, b and c).

TABLE 1a - Tests On Immersed Packing Samples - LOX Grade "P"

Gas Phase (1) Analysis %	LOX (2) Level (cm)	Ignitor (3)		Aluminium (4) Not Recovered %	Type (5) of Reaction	Comments
		Thermite (g)	Mg (g)			
-	10	1	0.24	17.8	C	-
-	10	1	0.24	44.8	C	-
-	8	1	0.24	75.0	C	-
99.6	8	1	0.24	46.4	C	-
99.9	8	1	0.24	76.6	VER	Vessel ruptured but not fragmented
99.86	6	1	0.24	75.1	C	-
99.99	6	1	0.24	54.1	C	-
99.99	10	1	0.24	29.7	C	-
100.00	6	1	0.24	86.8	VER	Vessel fragmented
99.97	6	1	0.24	75.2	C	-
99.97	6	1	0.24	89.1	VER	Vessel fragmented
99.99	7	1	0.24	64.1	C	-
99.97	6	1	0.24	86.5	VER	Vessel fragmented
99.97	6	1	0.24	31.4	C	-
99.95	8	1	0.24	51.3	VER	Vessel fragmented

(1) Indicative value see preceeding comments

(2) 9.5 cm corresponds to 50 % immersion

(3) In the gas phase

(4) Difference between the initial weight and remaining weight of aluminium (intact or molten) divided by initial weight

(5) VER = very energetic reaction (vessel fragmented) ; C = simple combustion (vessel intact) ;

Note : A rough calculation shows that a pressure of 1 to 1.5 MPa is necessary to rupture the thin copper test vessel used.

TABLE 1b - Tests On Immersed Packing Samples - LOX Grade "HP" (99.9 +%)

Gas Phase (1) Analysis %	LOX (2) Level (cm)	Ignitor (3)		Aluminium (4) Not Recovered %	Type (5) of Reaction	Comments
		Thermite (g)	Mg (g			
99.99	6	1	0.24	96.2	VER	Vessel fragmented
100.00	6	1	0.24	89.6	VER	Vessel fragmented
99.8	6	1	0.24	80.1	C	Sample located 9 cm over LOX level
99.96	6	1	0.24	95.1	VER	Vessel fragmented
99.99	6	1	0.24	89.5	VER	Vessel fragmented (6)
99.95	5	1	0.24	80.6	VER	Sample located 25cm over LOX level Sainless Steel Vessel, not deformed

(1) Indicative value see preceeding comments
(2) 9.5 cm corresponds to 50 % immersion
(3) In the gas phase
(4) Difference between initial weight and remaining weight of aluminium (intact or molten) divided by initial weight
(5) VER = very energetic reaction (vessel fragmented) ; C = simple combustion (vessel intact) ;
(6) Packing sample used identical to sample used for "irrigated" test (11 sheets)

Tests On Irrigated Packing Elements

The test conditions as described in Tables 1a, 1b and 1c (and as mainly performed by Dunbobbin) do not correspond at all to the actual operating conditions. In an actual cryogenic columns, packings are irrigated from the top by a liquid oxygen mixture consisting of a thin film (about 0.1 mm) of liquid oxygen mixture which flows down along the packing sheets. By distillation this film concentrates in oxygen when going down to the bottom part.

TABLE 1c - Tests On Immersed Packing Samples - LOX Grade "E" (99.999 + %) (Electrolytic)

Gas Phase (1) Analysis %	LOX (2) level (cm)	Ignitor (3)		Addition (grease)	Aluminium (4) Not Recovered %	Type of (5) Reaction	Comments
		Thermite (g)	Mg (g)				
99.96	8	1	0.24	-	46.6	VER	Vessel buldged. Contamination by GN used for LOX boiling
99.95	8	1	0.24	-	82.1	VER	Vessel fragmented
99.89	10	1	0.24	-	91.8	VER	" "
99.92	9	1	0.24	-	32.1	VER	" "
99.90	10	1	0.24	-	64.2	VER	" "
99.94	5	1	0.24	-	85.4	VER	" "
99.90	3	1	0.24	-	53.6	C	-
99.89	5	1	0.24	-	86.5	VER	5s after thermite ignition-Vessel fragmented
99.97	7	2 + 1	0	-	99.4	VER	Vessel fragmented 2 thermite pills used (2g + 1g)
99.96	9	3	0	0	92.0	VER	Vessel fragmented 3 g thermite pill
100.00	9	1	0	0	-3.6 (6)	NR	-
100.00	9	2	0	0	-4.6 (6)	NR	-
99.97	9	1 + 1	0	0	55.8	C	2 thermite pills used
100.00	9	1 + 1	0.24	0.57 g	89.3	VER	Vessel fragmented
99.98	6	1 + 1	0.24	0.15 g	68.6	VER	" "
99.99	6	1 + 1	0	0.15 g	-6.2 (6)	C	-
99.99	6	1	0.24	0.8 g	58.9	VER	Vessel fragmented
99.99	6	1	0.24	1.5 g	73.4	VER	" "
100.00	6	1	0.24	0.4 g	76.8	VER	7sec after thermite ignition-Vessel fragmented
99.95	6	1	0.24	-	84.3	VER	Vessel fragmented
99.99	6	0	0	1 g	3.0	NR	" "

(1) Indicative value see preceeding comments

(2) 9.5 cm corresponds to 50 % immersion

(3) In the gas phase

(4) Difference between initial weight and remaining weight of aluminium (intact or molten) divided by initial weight

(5) VER = very energetic reaction (vessel fragmented) ; C = simple combustion (vessel intact) ; NR = very limited reactions

(6) Molten aluminium (slightly oxidized) (Gain in weight)

Immersion of the packings in the column can easily be prevented. Dunbobbin reported that only two tests were performed with liquid oxygen distributed into the top of the cross section i.e. "irrigated" conditions. He reported that "neither test produces an explosive result and the extent of damages were less than 10 %". We then decided to perform tests under these irrigated conditions to evaluate the consequences of ignition. For these tests the following testing conditions were used :

- Packing samples : same as for "test on immersed packing elements" (IM) except that packing sample had slightly different dimensions 70 mm in height and 60 mm x 60 mm in cross section and were composed of 11 sheets. The weight of the samples was approximately 35 g.

- Ignitor : same as for IM.

- Test vessel : a thin copper vessel, 0.5 mm in thickness, 150 mm in OD, 350 mm in height, was used. This vessel had a thick copper base heated by GN to increase oxygen boiling. Fig. 2 shows a schematic of this vessel with the packing elements in it.

- Oxygen purity : the three oxygen grades P,HP and E as for the previously described tests (IM) were used. GOX was also analysed just before ignition. Gas samples were taken at the level of the thermite ignitor. For the same reasons as before, analysis results given in Table 2 should be considered as approximate and normally lower in purity than in reality.

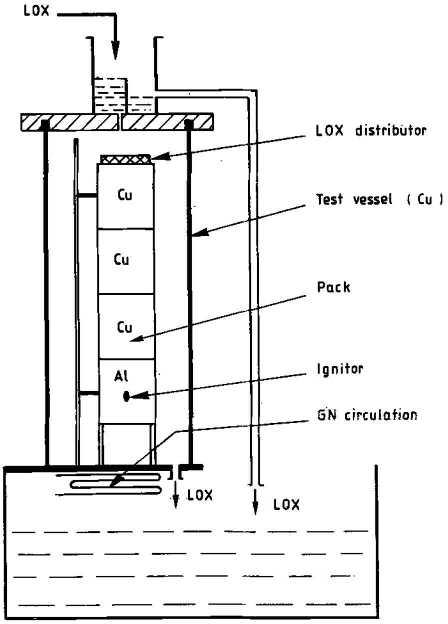

Fig. 2 - Tests on irrigated packing elements - Principle

- Experimental procedure : tests were performed at atmospheric pressure. This is close to the pressure range of actual columns where the pressure is normally lower than 0.1 MPaG. Packing samples were irrigated as illustrated in Fig. 2. A small vessel located in the upper part was fed with LOX, this vessel contained a special device to maintain a constant LOX level and consequently a constant LOX flow. A LOX distributor and 3 copper packings inserts located over the aluminium packing sample were used to insure a good irrigation of the tested aluminium packing. The thicker copper base of the test vessel was heated by GN circulation to allow vaporisation of the LOX flow and to create a certain GOX back flow as per the actual column. Special stainless steel devices are used on two sides of the copper packing to prevent LOX from going outside the packing ; the excess of LOX was collected in a large vessel located below the test vessel. Irrigation was maintained for at least 10 min before ignition to allow establishment of good oxygen purity in the test vessel. After the tests the quantity of aluminium which reacted (burned or melted) was measured and noted as was any significant damage of the test vessel. The same classification as in the previously described test (IM), was used (see Table 2).

TABLE 2 - Tests On Irrigated Packing Samples

LOX (1) Grade	Gaseous (2) Phase Analysis (%)	% of Nominal Flow	Ignitor (4)		Aluminium (5) Not Recovered %	Type of Reaction (6)
			Thermite (g)	Mg (g)		
E	-	0 (8)	1	0.24	94.9	C (8)
E	99.92	100	1	0.24	-9.1 (7)	M (and C ?)
E	99.90	100	1	0.24	-4.0 (7)	M (and C ?)
E	99.96	100	1	0.24	-14.0 (7)	M (and C ?)
HP	99.91	30	1	0.24	-19 (7)	M (and C ?)
HP	99.81	30	1	0.24	-9.6 (7)	M (and C ?)
HP	99.82	30	"	"	-9.6 (7)	M (and C ?)
HP	99.72	30	"	"	-4.7 (7)	M (and C ?)
HP	99.92	30	"	"		M (and C ?)
HP	99.76	30	"	"	-20 (7)	M (and C ?)
P	99.77	100	"	"	23.6	C
P	99.85	30	"	"	-1.7 (7)	M (and C ?)
P	99.74	30	"	"	-6.3 (7)	M (and C ?)
P	99.72	30	"	"	-6.6 (7)	M (and C ?)
P	99.78	30	"	"	-5.1 (7)	M (and C ?)
P	99.73	30	"	"	-6.5 (7)	M (and C ?)

(1) LOX grade, E : electrolytic ; HP = cryogenic high purity ; P = cryogenic current purity

(2) Indicative value, see preceding comments

(4) Ignitor located in the middle of the sample

(5) Difference between initial weight and remaining weight (intact or molten) divided by initial weight

(6) C = combustion - M = melting of aluminium

(7) Molten aluminium found in the bottom of the test vessel (slightly oxidized and often combined with molten copper from the vessel base)

(8) No more irrigation when thermite ignited - Test in GOX

RESULTS AND DISCUSSION

The main results are summarized in Tables 1 a, b and c for tests conducted on immersed elements and in Table 2 for tests conducted on irrigated elements.

Tests on immersed packing elements

In Tables 1 a, b and c, 42 tests are reported, 15 with LOX of "current purity", 6 with LOX of high purity (from cryogenic columns) and 21 with LOX of very high purity (from electrolysis and consequently without trace of argon). All together, 30 VER occurred (5, Table 1a, 5, Table 2b and 15, Table 2c). The intensity of the pressure wave, in most of the cases, fragmented the copper test vessel (see fig 3). Consequently the peak amplitude of the pressure wave is higher than 1 to 1.5 MPaG (see before) but probably lower than 6.5 MPaG because when a thicker (2 mm) stainless steel test vessel was used, it remained intact (no deformation).

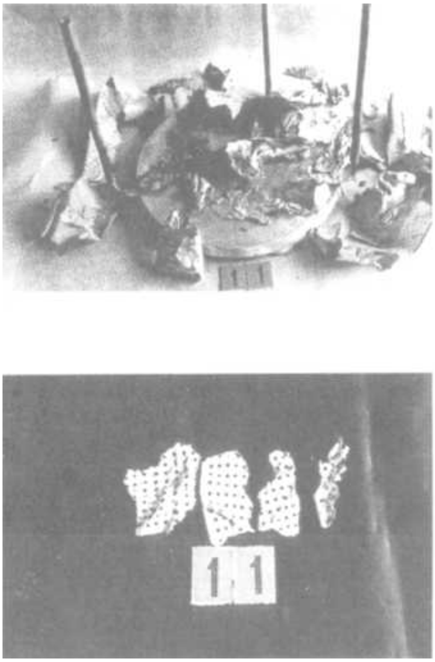

Test Vessel

Packing sample

Ignitor : 1g thermite + 0.24 Mg

Oxygen purity : 99.89 %

Fig. 3 - Tests on immersed packing elements.
State of test vessel and packing sample after testing

When the most current ignitor was used (1 g thermite + 0.24 Mg) a VER systematically occurred when oxygen of a high purity (Table 1b and Fig. 3) or oxygen of ultra high purity (Table 1c) were used. The two exceptions were, in Table 1b when the packing sample was tested not immersed but above a LOX pool and in Table 2c when the LOX level was so small (3 cm) that only the lower part of the sample (1cm) was immersed. These results are consistent with Dunbobbin results [1].

With the same ignitor (1 g thermite + 0.24 g) and with oxygen of current purity as produced from a cryogenic air separation column, VER reaction only occurs for one third (5/15) of the tests (and in one case the test vessel did not fragment).

This indicates that in this "immersed" testing condition purity is one of the most important parameters and that to 100 % reproduce VER we only need to use LOX of ultra high purity and very energetic ignitor (1 g thermite + 0.24 g Mg).

Test Vessel

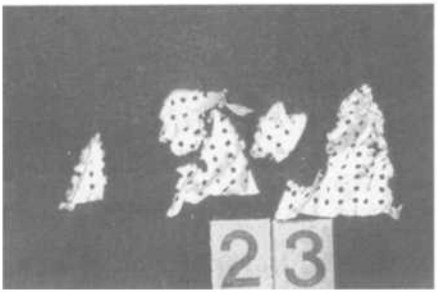

Packing sample

Ignitor : 3 g thermite

Oxygen purity : 99.96 %

Fig. 4 - Tests on immersed packing elements.
State of test Vessel and packing sample after testing

When magnesium was not used, we never succeeded in getting VER when using either 1 or 2 g of thermite (see Table 1c and Fig. 5). It was necessary to use at least 3 g of thermite to get a VER (see Fig. 4) ; in this case the intensity of the reaction was higher (99.4 % instead of 92.0 % of aluminium not recovered) when two separate thermite pills were used, the first one being ignited by the electric wire, the second one reacting during the combustion.

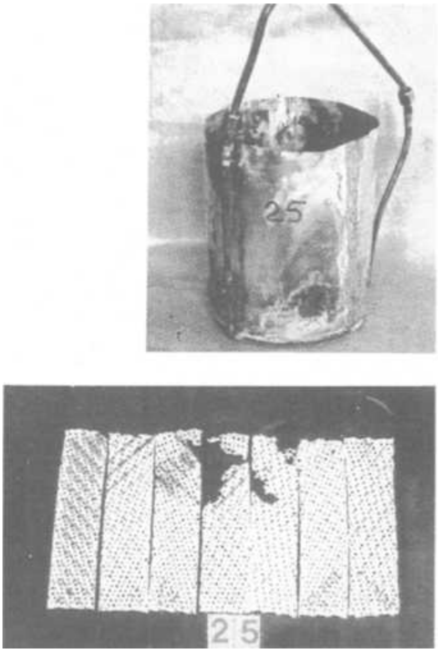

Fig. 5 - Tests on immersed packing elements.
State of test Vessel and packing sample after testing

These results seem to indicate that the proposed energy for the ignitor according to Dunbobbin is not completely relevant (i.e. 1 g thermite delivering 1850 calories and 0.24 Mg delivering 1400 calories). Ignitors made of 1 g thermite + 0.24 g magnesium are more energetic than 2 g thermite ignitor ; 1 g thermite + 0.24 g magnesium is sensibly equivalent to 3 g thermite for the consequences of ignition.

As indicated before, high LOX purity is an important condition to get VER ; consequently some tests (see Table 1c) were performed with ignitors contaminated with grease. The intention was to determine if combustion of grease, generating CO_2, thus, decreasing GOX purity inhibits VER. This was not the case for grease contamination from 0.15 g to 1.5 g and could indicate that VER occurrence mainly depends on LOX purity.

Dunbobbin [1] reports VER as "detonation". According to current terminology, detonations are understood as very fast reactions generating high pressure waves and propagating in the material. The argument used by Dunbobbin apparently was that aluminium packing samples were more or less completly destroyed after the tests.

In fact, when considering tests performed with the most current ignitor (1 g thermite + 0.24 g) the quantity of aluminium not recovered when VER occurs, varies from 46.6 % to 96.2 % ; but, the sample never did completely react, see Fig 3 showing the remaining of the packing sample (and the fragmented vessels) from one of the most complete VER and Fig 4 one of the less complete reactions when an insufficient ignitor (2 g thermite) was used. Careful examination of Table 1a shows that although the average quantity of aluminium not recovered was higher when VER occurred, simple combustion (C) led to more aluminium consumption in several cases than VER and in some cases to more than 75 % aluminium consumption. This tends to indicate that aluminium combustion mainly or only occurs before the VER occurred, normally 2 to 5 seconds after thermite ignition. The small difference in aluminium consumption could rather be explained by the fact that GOX and LOX purity is probably higher when VER occurred ; this was confirmed by test n½ 1 of Table 2, where 94.9 % of the aluminium was not recovered.

It is believed that these reactions were not "true detonation", but that VER was produced by burning molten aluminium falling at very high temperature in LOX of high or ultra high purity. The literature survey performed [2] indicates that autoignition of aluminium in oxygen can only occur at very high temperatures and most of the authors believe that this temperature is higher than the aluminium oxide melting temperature (2045½C).

In addition, to have a VER it is probably not necessary to have the packing sample immersed in LOX as reported by Dunbobbin. Molten aluminium at a sufficiently high temperatures from any source can probably react when falling in LOX of high purity. This was confirmed by tests performed by Lassmann [3] on thick (1 mm) aluminium plates used as trays for the conventional cryogenic air separation columns. Using the same energy levels ignitors, the same LOX purity (about 99.8 %) and tray samples Lassmann got VER resulting from burning molten aluminium falling in LOX. Additional tests performed in this study with packing samples located above a pool of high enough LOX level resulted in VER also (see Table 1b, last test) which showed that LOX immersion was not necessary.

Tests On Irrigated Packing Elements

In Table 2, 15 tests are reported on irrigated packing samples tested in this study. As indicated before, these tests closely reproduced the actual aluminium packing conditions found in air separation columns.

All of these tests were performed by using the same strong ignitor (1 g thermite + 0.24 g magnesium) and 10 tests were performed with high or ultra high LOX purity. Those two conditions were found to be the only necessary conditions to systematically get VER in "immersed" testing condition. Not a single VER occurred and the reaction mainly consisted of aluminium melting and probably limited oxidation/combustion. The ignitor can not be questioned, as in most of the cases a high portion of the samples was destroyed as illustrated in Fig. 6 and 7. Most of the aluminium was recovered as molten metallic aluminium (slightly oxidized) in the bottom of the test vessels.

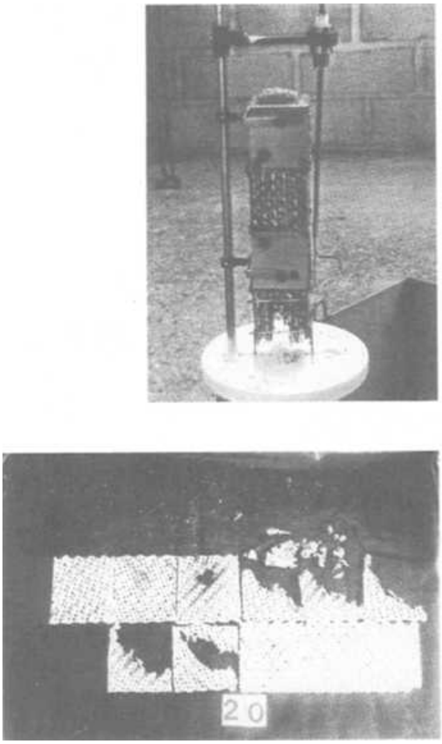

<— Packing sample

Ignitor : 1 g thermite
+ 0.24 g Mg
Flow rate : nominal

Fig. 6 - Tests on immersed packing elements
State of packing sample after testing

On purpose, the first test reported in Table 2 was performed at the end of the irrigation, no more oxygen in the upper vessel and resulted in a very extensive combustion (94.9 % of the sample having disappeared). This illustrated the beneficial effect of irrigation. However tests performed at the lowest possible service flow rates showed that irrigation was still beneficial at 30 % nominal (see Fig. 7).

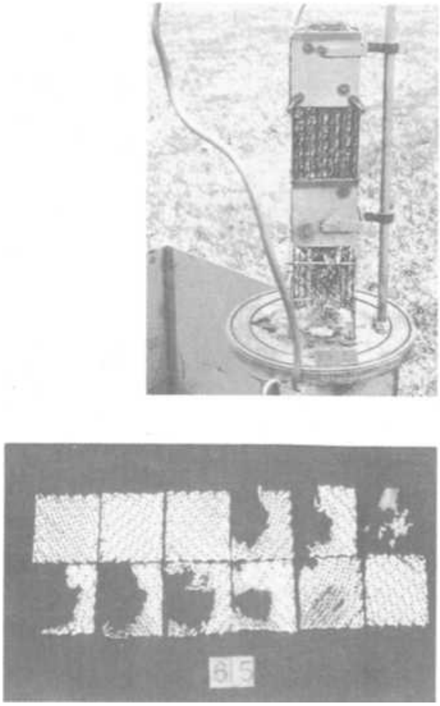

Packing sample

Ignitor : 1 g thermite
+ 0.24 g Mg

Flow rate : 30 % of nominal

Fig. 7 - Tests on irrigated packing elements.
State of packing sample after testing

Six additional tests were also performed with LOX of current purity and gave similar results as the tests performed with high purity.

The shape of the sample used for irrigated tests can not be questioned because in the immersed condition, a VER was obtained when using one of these samples (see Table 1b (6)).

CONCLUSION

The critical test results for aluminium packing sample reported by Dunbobbin have been reproduced and are now clearly understood. It is easy to systematically get the VER reactions reported when using a strong ignitor (1 g thermite + 0.24 g magnesium) in a sample partially immersed in (or located above) a LOX pool of high purity 99.9 + %.

It was shown that this strong ignitor (1 g thermite + 0.24 g Mg) is sensibly equivalent to a 3 g thermite pill without magnesium for the consequences of ignitions.

However this VER reaction does not seem to be a "true detonation" but rather a violent reaction generating pressure and occurring when burning molten aluminium at very high temperature (probably higher than aluminium oxide melting temperature) falls in high purity LOX.

This type of VER reaction has also been reproduced with tray samples and trays have been used successfully for more than 30 years in cryogenic air separation columns.

This type of VER is consequently not relevant for aluminium packing columns, but should rather be considered only for aluminium equipment used in contact with of high purity LOX pool, when strong ignitors/promoters are likely to exist.

This is not at all the case for aluminium packed columns because :

- tests have shown that VER does not occur in normal operating condition (irrigation)

- immersion of packings in columns can easily be prevented.

- strong ignitors able to ignite aluminium cannot exist in these distillation columns

REFERENCES

[1] Dunbobbin, B.R., Hansel, J.G. and Werley, B.L., "Oxygen Compatibility of High Surface Area Materials", Flammability and Sensitivity of Materials in Oxygen - Enriched Atmospheres : Fifth Volume, ASTM STP 1111, Joel M. Stoltzfus and Kenneth Mc Ilroy, Editors, American Society for Testing and Materials, Philadelphia, 1991.

[2] Werley, B.L., Barthélémy, H., Gates, R., Slusser, J. W., Wilson, K. B., and Zawierucha, R., "A Critical Review of Flammability Data for Aluminium, "Flammability and Sensitivity of Materials in Oxygen-Enriched Atmospheres : Sixth Volume, ASTM STP 1197, Dwight D. Janoff and Joel M. Stoltzlus, Eds., American Society for Testing and Materials, Philadelphia, 1993.

[3] Dr. E. Lassmann Linde AG, D-80L3 Hoellniegelshenth, private communication.

Dr. Anton Kirzinger[1]; Dr. Karl Baur[1]; Dr. Eberhard Lassmann[1]

THE BEHAVIOUR OF OIL FILMS ON STRUCTURED PACKING UNDER CRYOGENIC CONDITIONS

REFERENCE: Kirzinger, A., Baur, K., and Lassmann, E., "The Behaviour of Oil Films on Structured Packing Under Cryogenic Conditions," Flammability and Sensitivity of Materials in Oxygen-Enriched Atmospheres: 6th Volume, ASTM STP 1197, Dwight D. Janoff and Joel M. Stoltzfus, Eds., American Society for Testing and Materials, Philadelphia, 1993.

ABSTRACT: Today structured packing is commonly applied in cryogenic air separation plants. Packing is typically characterised by a high surface-to-volume-ratio. Due to the large surface of packing in comparison to common sieve trays - provided equal amounts of oil are attached to surfaces - more organic material may be present within a low pressure column of an air separation plant. Since an enrichment of organic material in an air separation plant or in liquid oxygen is a principal hazard and a major accumulation of organic material magnifies this risk, experimental tests were conducted to determine whether chipping of oil at cryogenic temperatures is possible.

Tests are discussed where single sheets of a packing segment had been coated with an oil film of definite thickness. The oil coated sheets were rinsed by moving them up and down in liquid nitrogen or in liquid oxygen. After fixed time intervals the oil content of a single sheet was determined.

It was concluded that the original oil residue on the sheets up to 250 mg/m^2 remained attached to the packing surface and no decrease of oil was found within the accuracy of the oil determination method.

KEY WORDS: Structured packing, oil film, analytical oil determination method on surfaces, cleanliness.

---

[1] LINDE AG, Process Engineering and Contracting Division
Dr.-Carl-von-Linde-Straße 6-14,
8023 Hoellriegelskreuth, Germany

INTRODUCTION

For several years structured packing have been used instead of sieve trays for the rectification of liquid air in low pressure columns and for production of argon in argon columns. Packing fabricated from 0.2 mm thick aluminium sheets are characterised by a high surface-to-volume-ratio. Packing densities up to 500 m^2/m^3 are common practice. Due to the large surface of structured packings in comparison to common sieve trays, more organic material may be present in an air separation plant. Provided that equal amounts of oil are present on surfaces measured as mg/m^2, thirty times as much oil may be present in packed columns in comparison to sieve tray columns. Since the enrichment of organic material in an air separation plant is a principal hazard, it must be assured that an oil film on a packing surface does not migrate and subsequently accumulates at other locations in the system.

KNOWLEDGE OF BEHAVIOUR OF OIL FILMS IN OXYGEN ATMOSPHERE

Flow Properties of Oil Coatings at Ambient Temperature

The flow properties of oil coatings and oil films in an oxygen enriched atmosphere were examined. The migration of oil on tube walls was examined by Wilson [1]. Oil was sprayed into a pipe and heated to selected temperatures. The pipe was then suspended vertically. At temperatures of 26°C, 38°C and 66°C drained oil was collected. With the knowledge of the original amount and the drained amount the oil quantity remaining at the pipe walls was calculated. At selected temperatures 45 percent by weight of the original amount of oil (oil quantities from 54 to 108 g/m^2) was drained. Because of the short draining time of 30 min no stationary condition was reached, but tests also showed that oil amounts > 50 g/m^2 migrate under the influence of gravity.

N-hexadecane as a model substance was used by Kehat [2] to study the ignition behaviour of oil in an oxygen atmosphere. He observed that a portion of the hexadecane film (approximately 100 g/m^2 were on the surface of the reaction tube) was running down the tube at ambient temperature.

The migration behaviour of oil films on horizontally arranged surfaces under the influence of a temperature gradient was studied by Fote [3]. On mirror finished surfaces (oil film thickness 2.15 g/m^2) and at a temperature gradient of 1.8°C/cm an unspecified amount of oil migrated to the cold end of the plate (temperature about 30°C). The author emphasized the great influence of the surface roughness to the migration behaviour. The inhibiting effect of rough surfaces is caused by capillary forces which keep oil in pores. If the thickness of an oil film is greater than the pore size the excessive oil may migrate as on a mirror finished plate.

Werley [4] presented the migration behaviour of Gulf Harmony No. 44 on vertically fixed copper plates. The copper plates were coated with oil films of various thicknesses. At an oil coating of 571 mg/m^2 484 mg/m^2 oil were found after 140 hours and 431 mg/m^2 (75 %) after 1160 hours. Regarding the total amount of oil on surfaces, the thikker the film the more oil drains off. Centrifugal forces [4] can also cause the flow of oil films: At an initial coating of 2.69 g/m^2 and after a 90-minute-centrifugation process with 5000 rpm there are only 0.215 g/m^2 oil on the surface. This is a loss of 90 %. These tests indicate a great influence of the surface roughness. In additional test series the influence of gas velocity to the migration tendency was examined by Werley [4]: On a smooth surface, which is the unfavourable case, and a gas velocity of 40 m/s the oil film decreased from an original amount of 1.08 g/m^2 to 0.215 g/m^2 within one hour. If there was 5 g/m^2 oil on the surface in the beginning 0.323 g/m^2 was present after 1 h.

Behaviour of Oil Films in Liquid Oxygen

During ignition test with n-hexadecane in liquid oxygen Kehat [2] observed that an n-hexadecane film on walls of a stainless steel tube at cryogenic temperatures solidified and a portion of the coating chipped off. Solid n-hexadecane floated on the surface of liquid oxygen caused by the lower density of the hydrocarbon. This behaviour of a n-hexadecane film was observed at oil films of > 5 g/m^2. In spite of the migration behaviour at ambient temperature and the chipping at cryogenic temperature, Kehat was unable to ignite the oil and therefore he postulated that an oil contamination of approximately 5 g/m^2 is tolerable for use in oxygen systems. In a succeeding work Ball [5] concluded, like Kehat, that because of the migration at ambient temperature and chipping in liquid oxygen only a limited oil quantity may be tolerable. Ball proposed a limit of oil contamination of 1 g/m^2 in oxygen enriched atmospheres.

Conclusions from Literature

The objective of this paper is to gain information concerning an acceptable oil content on aluminium packing in air separation plants. The following conclusions, in connection with data from the literature, can be drawn:

* Experimentally tested thicknesses of oil films are always much higher (up to 100 g/m^2) than expected in packing. Oils used are in general unspecified.

- The limit for migration of oil films under the influence of gravity is mentioned in the literature to be 430 mg/m^2. Oil films smaller than 200 mg/m^2 at ambient temperature do not migrate under the influence of gas velocity and centrifugal forces.

- Roughness of surfaces also has great influence on the migration behaviour of oil films. Oil remains in pores of rough surfaces by capillary forces. The thickness of oil films of 200 mg/m^2 is approximately 0.2 μm (density of oil 0.9 g/cm^3) and roughness-height of aluminium sheets is approximately 5 μm. An oil film that thin remains in pores of the rough surface and cannot migrate.

Data from experimental tests carried out to examine chipping of oil films with thicknesses smaller than 400 mg/m^2 at cryogenic temperatures are not available. Such tests could clarify whether with oil films of 50 - 200 mg/m^2, a detachment of oil can be observed in liquid nitrogen and liquid oxygen by chipping off solidified oil by moving the specimen in cryogenic liquids.

EXPERIMENTAL

APPARATUS

Test equipment shown in FIGURE 1 used in experimental program consists of a Dewar vessel with cover and a volume of 15 L and a stirring motor with an eccentric stroke.

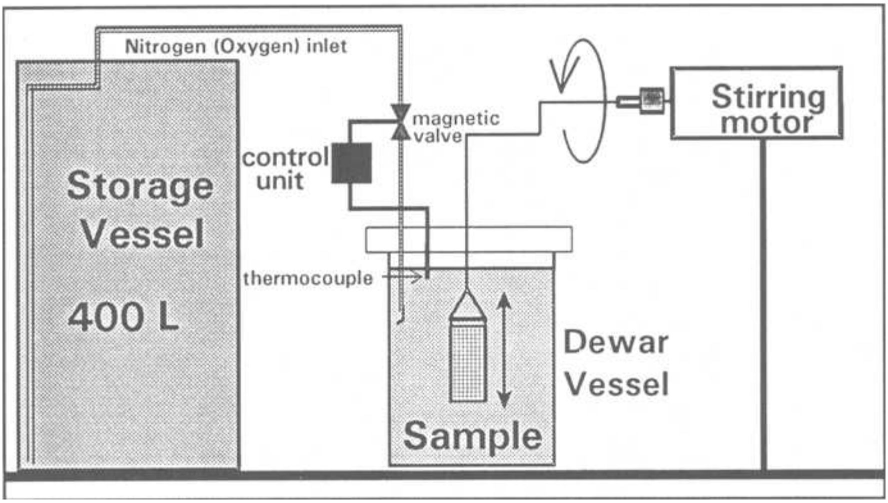

FIGURE 1: EXPERIMENTAL APPARATUS AND EQUIPMENT

A locking device for sheets was connected to the stirrer. The level of liquid nitrogen (oxygen) was maintained with a level regulating device (thermocouple, magnetic valve and controlling unit). A storage vessel with a capacity of 400 L was used for the supply of liquid nitrogen and liquid oxygen.

ANALYTICAL METHOD FOR DETERMINATION OIL ON SURFACES

For the determination of organic material on surfaces a carbon analyser C-mat 500 from Ströhlein company (FIGURE 2) was used. A sample strip with a surface of approximately 100 cm^2 (width 25 mm, length up to 150 mm) was placed in the first zone of the reaction tube, which was heated to 550°C. Organic material in the oxygen stream is oxidised to carbon dioxide and water. The second zone, which is only used for determination of inorganic carbon is insignificant for analysing organic carbon.

Traces of carbon dioxide are removed from the oxygen with sodium hydroxide fixed on a carrier material. Then the oxygen stream is fed into the reaction tube. The velocity of the gas stream is adjusted so that a portion of oxygen exits the front opening of the reaction tube to the atmosphere thereby preventing carbon dioxide traces from ambient air entering. The remaining part of oxygen flows through the reaction tube.

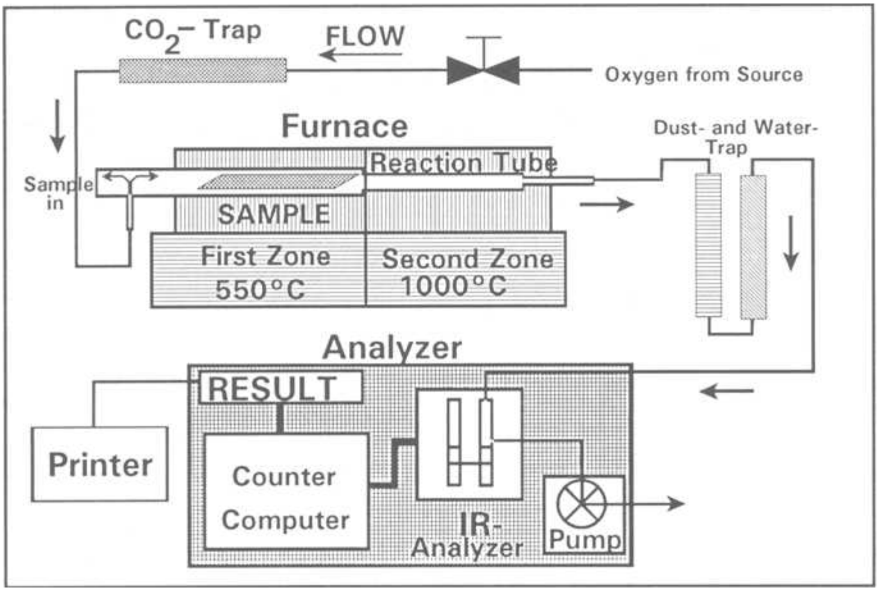

FIGURE 2: CARBON ANALYSER (SCHEMATIC)

Water is removed from the gas stream by magnesium perchlorate as drying agent. The concentration of carbon dioxide originating from the oxidation of oil in the gas stream is continuously measured. The surface of the sample is calculated from the weight of the sample taking into account the weight to surface ratio. The result of the measurement is given in mg carbon/m^2 surface.
This determination method is capable to analyse oil quantities on surfaces as low as 1 mg/m^2. Reproducibility of this method is ± 1 % and the relative error of this method is ± 5 %.

EXPERIMENTAL PROCEDURE

For these tests, structured packing sheets as commonly used in air separation plants were employed. For each test 20 single sheets with a size of 200 mm x 100 mm were coated with an oil film.

Before testing all sheets were cleaned with hexane and dried in a hot air cabinet. Coating of sheets was made with an ester-type oil (density 0.9 g/cm^3 at 20°C, viscosity 20 ± 2 cP at 20°C, burning point > 255°C, boiling point 225°C at 1 Torr). For coating with oil, sheets were immersed into an oil-hexane-mixture (approximately 10 g oil in 1 L hexane) and put in a draining stand to avoid fat-edge formation on sheets and to get uniform oil films on surfaces. Sheets were often turned around after submerging them in the oil-hexane-mixture. The coated sheets were dried in a hot air cabinet at 60°C for several minutes. Carbon content of three arbitrarily chosen sheets was analysed to get the original oil content on the sheets.

For a test, 15 single sheets were fixed with copper wires to the locking device and immersed in the Dewar vessel filled with cryogenic liquid. The liquid level was adjusted to a constant level during the duration of the test with a level regulating device and immersed sheets were moved up and down in liquid nitrogen or oxygen during all the time. The height of lift was about 12 cm. Samples were moved up and down in such a way that velocity of the movement was equal to the flow rate of the liquid gas film on the surface of packing. Daily, a single sheet was taken out of the Dewar vessel. Then the carbon content of this sheet was analysed.

RESULTS

With two tests, sheets were immersed for only 5 hours in liquid nitrogen. No significant decrease of oil was observed during this time. The initial oil content on the surface was approximately 35 mg/m^2 in the first test. See CURVE 01 in FIGURE 3. In the second test, see CURVE 02 in FIGURE 3, an oil quantity of 150 mg/m^2 was present on the surface. In both tests no migration or chipping of oil from packing surface occurred.

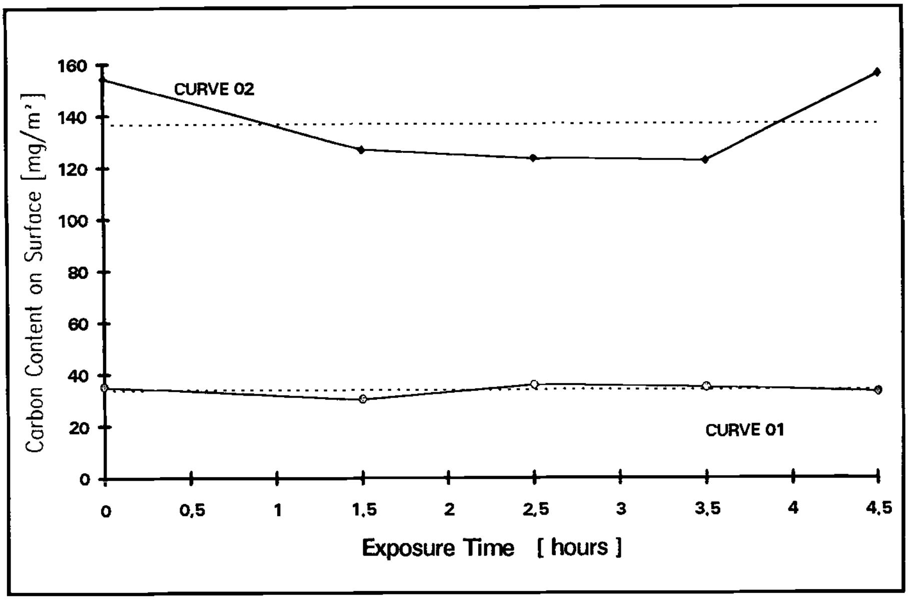

FIGURE 3: CARBON CONTENT ON SURFACE AS A FUNCTION OF TEST TIME

Since no loss in oil concentration on packing surfaces was noticed, the tests were extended to 400 hours. Two tests in liquid nitrogen were carried out. FIGURE 4 shows analysed carbon contents vs. time plots. On an specimen with an oil content of approximately 35 mg/m^2 (CURVE 03 in FIGURE 4) and an oil content of 190 mg/m^2 (CURVE 04 in FIGURE 4), no decrease of oil was observed in liquid nitrogen.

In another test (see CURVE 05 in FIGURE 4)liquid oxygen was used. For this test a relatively high content of approximately 170 mg/m^2 oil was chosen. In the liquid oxygen tests no loss of the original oil content was detected.

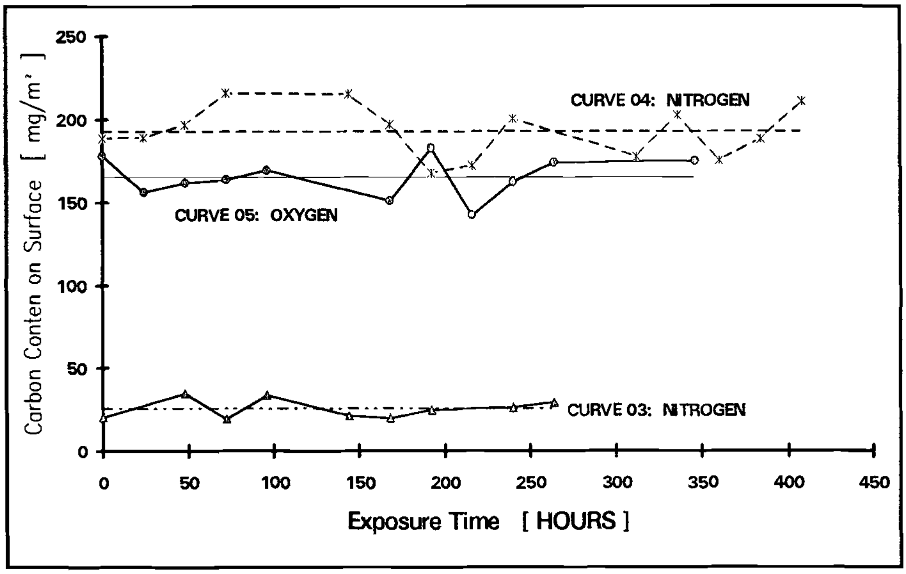

FIGURE 4: **CARBON CONTENT ON SURFACE AS A FUNCTION OF TEST TIME**

CONCLUSIONS

The behaviour of oil films on structured packing in cryogenic liquids (nitrogen or oxygen) was examined by experimental tests. For these tests single sheets of commonly used packing were coated with oil films of definite thickness.

The oil content on the surface of sheets was analysed with a carbon analyser. With this method and without any pretreatment of samples traces of oil on sheets could be analysed with high accuracy.

Within the accuracy of the oil determination method it was concluded that the original oil residue on sheets up to 250 mg/m^2 remained attached to the packing surface and no decrease of oil occurred in cryogenic liquids. Oil films are not chipped off by mechanical forces (shearing forces). An accumulation of oil in a LOX sump within a few days by chipping off is not possible. Migration of an oil film under cryogenic conditions does not occur.

REMARKS

The oil used in these tests is a typicall oil which is commonly used by the fabrication of packing, but it may not be

representative of all of the types which might be encountered in air separation destilliation columns.
Cryogenic chipping is just one of the mechanisms by wich oil films might migrate. Due to the large surface of a packing and by presence of oil residues on packing surface, this mechanism could result in an accumulations of oil which must be avoided in air separtion plants in any case.

References:

[1] Wilson, M.P, DeSouza, F. and Presti, J., Contracts NObs 4204 and 4134, General Dynamics, Groton, Conn., Nov. 1961

[2] Kehat, E., Advances in Cryogenic Engineering, Vol. 7 (1961), pp. 163-169

[3] Fote, A.A., Slade, R.A. and Feuerstein, S., Journal of Lubrication Technology, Vol. 99, No. F-2 (1977), pp. 158-162

[4] Werley, B.L., **"Oil Film Hazards in Oxygen System"**, Flammability and Sensitivity of Materials in Oxygen-Enriched Atmospheres, ASTM STP 812 (1983), B.L. Werly,Ed., American Society of Testing and Materials, 1983, pp. 108-125

[5] Ball, W.L., Safety in Air and Ammonia Plants, Vol. 4 (1965) pp. 16-23

Barry L. Werley,[1] *Hervé Barthélémy,*[2] *Robert Gates,*[3]
Joseph W. Slusser,[1] *Keith B. Wilson,*[1] *and Robert Zawierucha*[4]

A Critical Review of Flammability Data for Aluminum

REFERENCE: Werley, B. L., Barthélémy, H., Gates, R., Slusser, J. W., Wilson, K. B., and Zawierucha, R., "**A Critical Review of Flammability Data for Aluminum,**" *Flammability and Sensitivity of Materials in Oxygen-Enriched Atmospheres: Sixth Volume, ASTM STP 1197,* Dwight D. Janoff and Joel M. Stoltzfus, Eds., American Society for Testing and Materials, Philadelphia, 1993.

ABSTRACT: Aluminum is one of the more thoroughly studied metals for flammability properties. Results with aluminum in both the laboratory and the field have been mixed and experimentalists have obtained significantly differing data through the years, partly due to differing goals for application of the data. The literature contains data from ignition testing, propagation testing and heat of combustion testing. Ignition testing includes: autoignition temperature, liquid oxygen mechanical impact, friction, shock wave, resonance, promoter influence, fresh-metal exposure, and particle impact. Propagation testing includes: promoted combustion, propagation velocity, flammability limits, and alternative oxidants. Theory has been developed, but has not allowed prediction of aluminum's performance in specific applications.

Data and theory from more than one hundred sources and previously unpublished results of the contributing author's companies spanning the last forty years are abstracted and commentary is offered on experimental design, results and application to current-day loss prevention design of aluminum/oxygen systems.

KEY WORDS: fire, flammability, aluminum, ignition, propagation, combustion, adiabatic compression, autoignition, fresh metal exposure, friction, particle impact, mechanical impact, shock wave, resonance, arc, spark, promoted combustion.

At least 300 documents consider metals flammability and an assortment of additional work that has not been published. A majority of these documents include experimental data. A critical review focused on results with aluminum is presented here.

Experimental data include ignition studies, propagation studies, and heat release studies. Theoretical modeling has also been attempted. The majority of reports present ignition studies, including ignition by elevated temperatures, mechanical impact, fresh metal exposure, particle impact, friction, shock-wave exposure,

---

[1] Hazards Research Specialist, Lead Materials Engineer, and Chief Engineer - Safety and Reliability, respectively, Air Products and Chemicals Inc., 7201 Hamilton Boulevard, Allentown, PA 18195-1501.

[2] Materials Manager, L'Air Liquide Group, 75 quai d'Orsay, 75321 Paris, France.

[3] Consulting Scientist, The BOC Group, 100 Mountain Ave., Murray Hill, NJ, 07974

[4] Manager, Materials Engineering, Praxair, Inc., Linde Division, P. O. Box 44, Tonawanda, NY, 14151-0044.

resonance, electric current with arc or spark, and flammable promoters. A smaller body of work examines propagation of fires and effects of oxygen concentration or pressure. Only a few reports address heat release, however, heats of combustion are typically easy to calculate.

This paper is a collaborative effort involving representatives from four companies: Air Products, BOC, L'Air Liquide, and Praxair. Our goal is to place in perspective the large body of flammability data for aluminum that may be pertinent to oxygen systems. To this end, an effort was made to extract and highlight the most pertinent results, as well as to offer commentary about the various experimental techniques. This is not a consensus paper. The contributors were not seeking to achieve agreement. Rather, the effort was directed to incorporate all points of view and opinions. Not every paper was studied by every author, and so this review is not a substitute for careful study of each reference.

Ignition Test Results

Autoignition Temperature

Autoignition temperatures have been measured for aluminum, and they are all reported to be much higher than are observed for nonmetallic materials and most metallic materials, as well.

In early ignition studies, the most commonly measured property is autoignition temperature. Writers use inconsistent definitions of autoignition temperature. At one extreme, at which combustion is a desired goal (such as for rocket engines), the autoignition temperature is taken as the environment temperature which will guarantee spontaneous ignition and complete combustion in every test. At the other extreme, where the avoidance of ignition is desired for safety, ignition temperature is taken as the temperature below which there will be no ignition in any test. Writers frequently do not state which criterion they use.

In addition, studies are often conducted with rapid temperature rises. These studies do not yield data on critical temperatures at which low-rate exothermic reactions may occur that may lead to ignitions at lower temperatures. Further, experimental measurements of autoignition temperature frequently vary in the method used, yield wide scatter, and enable only coarse comparisons of differing metals to be made.

Autoignition temperatures of both bulk aluminum and isolated aluminum particles have been reported [*1-3*]. The most commonly reported value is the approximate melting point of the oxide (about 2045°C, 3713°F). These autoignition temperatures are relatively independent of the atmosphere and many tests are conducted in air or in combustion gases containing steam and carbon dioxide. The oxide is believed to inhibit ignition by encapsulating aluminum vapors until its structural integrity is breached during melting. When steps were taken to damage the oxide through exposure to mercury [*1*] a reduction in the ignition temperature to 1700-1800°C (3092-3272°F) resulted.

Not every experimenter measured ignition temperatures at the oxide melting point. Merzhanov et al. [*4*] reported a measurement of 1640°C (2984°F). Arguments based upon encapsulation may not be consistent with autoignition temperature measurements of aluminum fines in air: 400-700°C (752-1292°F) [*5-*

9].

Bransford [*10*] LASER-ignited aluminum 6061 and found the autoignition temperature was approximately 2210 K (3518°F) at atmospheric pressure, and that it decreased with pressure to 2150 K (3410°F) at 6.8 MPa (972 psig). However, he also found that ignition can occur at lower temperatures during the cooling of a hot specimen. Bransford's paper contains a thermogram for a test in which temperature decayed from 2150 K (3410°F) to about 1840 K (2852°F) when ignition occurred, perhaps as a result of rupture of the oxide scale.

A number of papers report extremely low autoignition temperatures (as low as 649°C, 1200°F) for aluminum through what appears to be mishap. The mishap appears to originate in one of the most important early metals flammability papers, that of Grosse and Conway [*11*]. In this work they introduced aluminum into a furnace at 1000°C (1832°F) and did not observe ignition. In the paper, they reported this fact in two tables, citing the autoignition temperature as >1000°C in one and just as 1000°C in the other. It appears that numerous writers have repeated the latter faulty value and compounded the error (reporting it as 1000°F), and it has carried thereafter to other papers as well. Among papers affected are those by Hust and Clark [*12-14*] and by Princeton researchers as discussed by Mellor [*15*] (on page 308 of his paper), and Belles [*16*]. As a result, it appears that the lowest correctly stated autoignition temperature for bulk aluminum appears to be the result of Merzhanov [*4*] of 1640°C (2984°F).

Clouds or dust layers may spontaneously ignite at temperatures below those observed for isolated specimen tests, apparently because clouds and dust layers exhibit adiabaticity. When these layered particles react with oxygen, they transfer all of the heat to the surrounding particles. Similarly, any radiation in the interior of a cloud or pile is intercepted by surrounding particles.

Poyarkov [*17*] reported that when aluminum, magnesium and alloys thereof were ground into fine powders in a low (2-6%) oxygen atmosphere, the alloys exhibited lower autoignition temperatures than did the pure metals. Layers of aluminum particles ignited in air at 694°C (1281°F), magnesium at 579°C (1074°F), and the minimum autoignition temperature of 510°C (950°F) was found near a 50-50 alloy.

In comparison, autoignition temperatures for a range of metals and alloys and for layers and dust clouds of them are shown in Table 1 [*7,18*].

Mechanical Impact

Aluminum has been sucessfully ignited by mechanical impact at lower energies than other metals, such as stainless steels.

Mechanical impact test results for aluminum are the largest database of all metals flammability testing. Thousands of LOX tests have been conducted using three mechanical impact testers operated by NASA. Fewer tests have been reported by Union Carbide Industrial Gases - Linde Div., BOC, L'Air Liquide, Convair, BAM (the German testing authority Bundesanstalt für Materialforschung und -prüfung), and Douglas Aircraft. Even fewer GOX mechanical impact tests have been accomplished mostly by NASA. These studies indicate that results can differ significantly among different apparatuses.

The size of the database for aluminum in mechanical impact tests is partly due to the use of aluminum cups in the ASTM standard test (D 2512 *Compatibility of*

TABLE 1 -- *Typical Autoignition Temperatures of Metals and Alloys.*

Metal	°C	°F	Source
magnesium	625	1157	[*18*]
iron	930	1706	[*18*]
carbon steel	900-1100	1652-2012	[*18*]
nickel alloys	1500-1600	2732-2912	[*18*]
Dust clouds and layers in air:			
iron	280-320	536-608	[*7*]
chromium	400-580	752-1056	[*7*]
zinc	460-680	860-1256	[*7*]
magnesium	490-620	914-1148	[*7*]
copper (cloud)	700	1292	[*7*]
nickel[a]	>1000	>1832	[*7*]
347 stainless steel[a]	>1000	>1832	[*7*]

[a] Did not ignite at unspecified limit of the apparatus.

Materials with Liquid Oxygen) and frequent blank runs to calibrate these systems. Aluminum is reported to produce reactions only a few percent of the time. In comparison, stainless steel typically does not ignite at the impact energies currently used (and is used as inserts in severe standard tests), while titanium yields reactions most of the time. Precise accounting of the number of reactions in the literature is difficult due to inconsistencies in descriptions and possible repetitive reporting in more than one publication.

Marshall Space Flight Center (MSFC) data in Table 2 indicate that aluminum is more mechanical-impact ignitable than is stainless steel but less mechanical-impact ignitable than magnesium and titanium [*19,20*].

MSFC [*19*] also reported that two specimens of aluminum and 301 stainless steel survived 50 consecutive impacts each at 3 kg-m (29.4 J) levels, while consecutive impacts on a single titanium specimen produced a greater fraction of ignitions on the second and third impacts than on the first. Some ignitions of titanium occurred as late as the fifth impact, and no titanium specimen in a 100-specimen lot lasted through more than five drops.

MSFC [*19*] and others indicate that the presence of grit on the impacting surfaces can aggravate aluminum ignition and MSFC installs a stainless steel insert in their aluminum cups when testing gritty materials. However, in tests of 5052 aluminum, as used in their cups, and with 0.5 g of silicon carbide grit present, they did not observe any reactions in 20 tests each at 5- and 10-kg-m (49- and 98-J) energies.

TABLE 2 -- *LOX Mechanical Impact Results of Metals and Alloys.*

Metal	Reaction/Tests or % Frequency	Energy J	ft-lb	Source
Aluminum alloys:				
2014-T6	0/400	98	72	[*19*]
2014-T6	1/420	98	72	[*20*]
5052	19/1480	98	72	[*19*]
assorted alloys	5/1056	98	72	[*20*]
assorted alloys	0/460	49	36	[*20*]
Nonaluminum metals:				
stainless steels:				
301, 302, 347 MXB1113	0/560	98	72	[*20*]
Assorted magnesium alloys	11/75	98	72	[*20*]
titanium 6Al-4V (high series)	90%	98	72	[*20*]
titanium 6Al-4V (high series)	40%	20	14	[*20*]
titanium 6Al-4V (high series)	5%	9.8	7.2	[*20*]

Keeping [*21*] reported that BOC use a 50-50 mixture by volume of polymers with carborundum grit in their LOX mechanical impact test. The plummet was a stainless steel alloy and the specimen cup was thin nickel shim stock. Aluminum was avoided as the cup material to minimize the number of aluminum ignitions that result. Ignitions of polymers occurred at lower drop energies with than without the grit present.

Lockhart et al. [*22*] also used Keeping's approach of using stainless inserts in their aluminum cups and mixing silicon-carbide with polymers. The powders also increased the rate of reactions in their test.

Barthélemy et al. [*23*] have found that aluminum ignites in their standard test (equivalent to ASTM D2512), but only if the specimens are thin (0.01mm or less).

NASA tests at Kennedy Space Center (KSC) report no reactions of 6061-T6 aluminum in 240 tests at 10 kg-m (98 J), nor in 20 tests each of René 41 (a nickel-base superalloy), 304, or 321 stainless steel [*24*]. In a separate study of surface contaminants using 6061-T6 aluminum, there were no reactions in 100 tests each of clean specimens, specimens exposed to trichloroethane, or specimens with an average 22 mg/ft^2 (237 mg/m^2) film of an impact-sensitive silicone oil (300 total tests) [*25*]. Two hundred more tests at a 43 mg/ft^2 (463 mg/m^2) contaminant level yielded two faint reactions. One hundred more tests at a 65 mg/ft^2 (700 mg/m^2) contaminant level produced two more faint reactions. Indeed, tests at still higher contaminant levels produced chars and "slight" fires, but it wasn't until contaminants of 430 mg/ft^2 (4630 mg/m^2) were tested that appreciable aluminum damage was observed.

NASA's White Sands Test Facility (WSTF) has conducted numerous LOX impact tests and has verbally commented about occasional light flashes from aluminum that do not produce noticeable damage. LOX data from WSTF were not in the authors' possession. WSTF has studied the effects of contaminants on GOX mechanical impact results at 5000 psig (34.6 MPa) [*26*]. Although the influence of pressure is not reported, NASA feels that impact sensitivity of polymers in GOX is greater than in LOX [*24*].

One difficulty with impact tests is that reactions are reported not only for ignition and propagation but also for small-scale events such as the occurrence of visible light, audible sound, or localized heat damage. Light in particular is difficult to interpret. Positive tests are often reported due to flashes of light that do not produce obvious evidence of heat or damage. Light evolution without obvious ignition has been reported in other types of tests (see *Fresh Metal Exposure*). For example, in some tests where aluminum and titanium were torn in tension, both were observed to produce flashes of light but neither ignited [*27*]. However, titanium is very impact sensitive compared to aluminum. In this case, reoxidation (and perhaps ignition) of minute particles was suspected to be the cause of the light rather than ignition.

There are numerous tests in which aluminum clearly ignites, and they tend to be at drop energy levels above those at which ignition occurs in standard polymer tests.

Bauer et al. [*28*] reported on mechanical impact testing at BAM, where metals are tested as fines (loose chips or chips pressed into pills). They report that the aluminum alloys Anticorodal 70 (G Al Si 7 Mg Ti) and Silafont 5 (G Al 10 Si Co Mg) ignite at drop energies as low as 13-38 mkp (127-372 J), but that stainless steel 4300 (X 12 CrNi 8.8), Stainless steel 4312 (GX 15 CrNi 18.8), Nickel Steel 5662 (X 8 NI 9), Bronze GBz 14, copper, and hard solder (40% Ag) did not react at impact energies to 75 mkp (735 J).

In one series of WSTF tests, a nonstandard (reduced-diameter) impact pin was used which yielded about 3-4 times the impact energy density of their standard pin [*26*]. In this series of tests at 5000 psig (34.6 MPa) in GOX, 6061-T6 aluminum was more sensitive than 304 stainless steel. Stainless steel did not react in any of 36 tests, including tests with grits or oil coatings on the surface and at 1000°F (538°C). Clean aluminum or aluminum in the presence of grits produced no reaction up to 700 ft-lb/in^2 (148 J/cm^2) in at least 96 tests (36 of which were at 500°F, 260°C); between 700 and 1200 ft-lb/in^2 (148 and 253 J/cm^2) there were 31 reactions in 96 aluminum tests including ambient and 500°F (260°C) conditions. When coated with oils, aluminum became even more sensitive and reacted to impacts as low as 300 ft-lb/in^2 (63.3 J/cm^2).

Tack et al [*29*], Reed et al. [*30,31*], Simon et al. [*32*], and Nguyen and Pham [*33*] have recently studied aluminum-lithium alloys for aerospace applications. They modified their mechanical impact system to have more rigid specimen support. Resulting damage during ignitions ranged from micro- to macro-scale (viewed with an SEM to viewed by eye). In some of these tests, the samples were substantially deformed. Many of the reactions were observed in a region of the specimens that extruded out from the impact surface. As a result, there was energy transfer to the aluminum, but there was also friction and exposure of fresh surface occurring.

In unpublished work involving about a thousand tests with impact energies in the range 67 to 134 ft-lbf (91 to 182 J, 9.6 to 19.2 kg-m), Air Products studied aluminum ignition under mechanical impact. In configurations resembling standard tests, no ignitions were observed. Ignitions were achieved when the specimens were prepared so that the impact surface could capture and collapse a volume of gas, when particles of aluminum fines were displaced by the impacting surface, or where the impact could produce shearing of the aluminum.

Promoted Ignition

Promoted ignition tests have produced mixed results with aluminum. Promoted ignition tests either use a fixed energy release from a promoter (an easily ignited fuel that is typically ignited with an electrically heated wire) to rank metals by their frequency of ignition or vary the amount of promoter and its energy release to determine how much energy is needed to obtain ignition. Results from promoted ignition tests in the literature vary widely. In promoted *combustion* tests,"strong" igniters are used. Strong igniters provide energy input that is well in excess of the minimum needed for ignition, and yield a high confidence that the metal will ignite and experience at least transient propagation. This enables promoted combustion tests to measure thresholds for propagation or "flammability limits."

Nihart and Smith [*34*] conducted one series of promoted ignition tests at 7500 psig (51.8 MPa) in which variable amounts of neoprene promoter were used to ignite standard 5-mmx30-mmx0.13-mm. specimens. Aluminum required greater promoter mass (11-16.4 mg) than did 304 stainless steel (7.1-8.5 mg), Inconel X-750 (9 mg), or copper (10.5 mg). Aluminum required less promoter mass than Inconel 600 (13.2 mg), yellow brass (11.8-15.2 mg), Monel 400 (18-19 mg), or nickel (48-56 mg). Stainless steel and aluminum were rated least satisfactory for 7500 psig (51.8 MPa) service.

Nihart and Smith also refer to an earlier series of promoted ignition tests in 2000 psi (13.9 MPa) oxygen. Details in the report are few but presumably similar to those of the 7500-psig (51.8 MPa) tests. They do not quantify the results but list an order of ranking as (best-to-worst): Monel, Inconel 600, Monel S, Tobin bronze, Duranickel, Ampco 15, Permanickel, K-Monel, Hastelloy R-235, maraging steel, beryllium copper, Elgiloy, René 41, Inconel X-750, Multimet, Hastelloy X, Haynes 25, Everdur, 18-8 stainless steel, and aluminum. Limited data for specimens at 2000 psi (13.9 MPa) in a different vessel than for the 7500 psig (51.9 MPa) test yielded combustion of 304 stainless steel at neoprene levels of 26-51 mg but no ignition of Monel up to at least 73 mg. Comparisons between the 2000 psig and 7500 psig tests are said to be invalid because of the vessel differences.

Simon [*35,36*] wrapped 3.4 g of perbunan (28 cal) with 12 grams of an apparent steel (20 kcal) and ignited the assembly inside tubes containing 16 atmospheres (1.62 MPa) of GOX pressure. Aluminum did not ignite. Copper ignited 4.8-6.4 seconds after initiation, iron ignited in 5.0-5.7 seconds, and steel ignited in 6.4-8.3 seconds.

Zawierucha et al. [*37,38*] used hydrocarbon oil or hydrocarbon oil plus carbon steel as promoters in a series of tests at pressures to 7.6 MPa (1100 psi). The hydrocarbon oil was ineffective in igniting aluminum and aluminum bronze alloys; the oil in combination with burning carbon steel was effective.

In unpublished work at Air Products, approximately 0.110- to 0.125-in. (0.28- to 0.32-cm) thick disks 2- to 2.3-in. (5.1- to 5.8-cm) diameter of 5052 aluminum, 9% nickel steel and alloy 304 stainless steel were ignited in LOX by 0.5- and 1.0-g ignition pills of mixed steel wool and aluminum wool. The tests with 1-g pills were done at 200 psig (1.48 MPa); The tests with 0.5-g pills were done at 245 psig (1.79 MPa). Complete destruction of the aluminum resulted in both cases. The 9% nickel steel was 90% destroyed in one test and 20% destroyed in the other. The stainless steel was damaged less than 50% near the igniter in both tests.

The unpublished work at Air Products also used 1-g ignition pills as above on 1- to 7.5-in^3 (16- to 123-cm^3) blocks of aluminum, stainless steel, and carbon steel. Aluminum propagation occurred at as low as 500 psig (3.55 MPa) in GOX and at as low as 25 psig (274 kPa) in LOX. In the LOX test, the vessel was sealed while containing vaporizing LOX and the pressure may have risen significantly above its initial level before propagation became well established. Stainless steel was not affected by the pill fire in LOX at 200 psig (1.48 MPa) or GOX at 850 psig (5.96 MPa). Carbon steel was not affected by the pill fire in LOX at 250 psig (1.83 MPa) or GOX at 770 psig (5.41 MPa).

Dean and Thompson [*39*] promoted ignition using AC-resistance heating of a series of metal tubes to the point of mechanical failure in static 300 psig (2.22 MPa) GOX. Aluminum resisted promoted ignition better than many other metals. In order of metal remaining, the ranking was aluminum (100% remaining), Monel (90%), Inconel (90%), copper (30%), 410 stainless steel (15%), 310 stainless steel (10%), 304 Stainless steel (5%), and 347 and 321 stainless steels and carbon steel (0%).

Fresh Metal Exposure

Although the exposure of fresh surface has been proposed to cause the ignition of aluminum, results to date do not support this. The suggested mechanism relates to the tendency of nascent aluminum surfaces to reoxidize almost immediately, releasing heat in the process. In some cases, light has been seen upon the exposure of fresh aluminum surface leading to the speculation that small regions were briefly at high temperature.

The literature reviewed does not, however, contain any instance in which the exposure of fresh aluminum surface (as opposed to the exposure of fresh surface in combination with other potential ignition influences) has produced genuine ignition of aluminum.

Most fresh metal exposure work involved only a small number of specimens, therefore the possibility of ignition cannot be ruled out. Even fewer tests considered contaminants, hence their effect is not known. Among documented fresh metal exposures in oxygen that did not produce ignitions were:

- Foils were rapidly broken in 1400 psi (9.6 MPa) GOX [*16*].

- Diaphragms of 2014-T6 and 6061-T6 aluminum up to 0.032-in (0.81-mm) thick were punctured by rods and knife edges with one atmosphere GOX on one side (47 trials) [*19*].

- Diaphragms of 2014-T6 aluminum 0.010-in. (0.25-mm) and 0.025-in. (0.64-mm) thick were punctured with 0.177 caliber ballistic darts with LOX on the reverse side [*19*].
- A 2014-T6 vessel of 0.063-in. (1.6-mm) wall was punctured with a 30-06 rifle bullet at the liquid level while containing LOX at 40-psig (377-kPa) pressure [*19*].
- Sheets of 2024-0 and 6061-T6 aluminum were punctured with a drop weight in 20 trials while immersed in LOX at atmospheric pressure (Chafey et al. [*40*]).
- Diaphragms of 2024-T3 aluminum 0.0162-in. (0.411-mm) thick were punctured with a drop weight. GOX at up to 55 psi (480 kPa) was present in 24 trials. LOX at 30 psi (308 kPa) was used in 14 trials [*40*].
- Projectiles with velocities up to 15,000 ft/s (4921 m/s) were used by Rolsten et al. [*41*] to puncture dual 2024-T3 diaphragms 0.016-in. (0.41-mm) thick while containing 60 psi (515 kPa) GOX or LOX (7 trials with up to 20 holes produced per diaphragm). Stainless steel 301 also did not ignite in seven similar mixed tests. Titanium ignited in most tests.
- Projectiles moving at up to 18,000 ft/s (5905 m/s) through vacuum punctured diaphragms containing oxygen (1 test with LOX, 1 test with GOX) [*19,40*].
- Three aluminum cylinders containing 100- to 200-psig (791- to 1480-kPa) GOX were exposed to flame impingement to the point of rupture. In similar tests, steel cylinders also did not ignite (Holyer [*42*]).
- Stress rupture in undetailed experiments at 2000 psi (13.9 MPa) GOX at 572°F [*18,43*].
- Stress rupture of aluminum under atmospheric-pressure LOX. Flashes of light were observed with both aluminum and titanium, but no damage occurred [*27*].
- Melting and flowing of molten aluminum (6060, 5052) in GOX at 60 psig (515 kPa) by Tench et al. [*44*].
- Melting and flowing of an unspecified aluminum alloy in 50, 300 and 800 psig (0.45, 2.17 and 5.62 MPa) oxygen [*39*].

In addition, the following unpublished experience and experimental attempts that produced fresh exposure of aluminum to oxygen also did not produce ignition:

- Rupture of an aluminum diaphragm containing 1000 psi (7.0 MPa) GOX at NASA (Personal Communication of Jack S. Stradling).
- Tensile tests of various aluminum alloys in GOX at 2 bar G (301 kPa), 21°C and 5 mm/s and 3 m/s strain rates and LOX at atmospheric pressure and 5 mm/s and 3m/s strain rates at L'Air Liquide.
- Fatigue-induced crack of TIG (GTA) weld joints containing 250-psig (1.83 MPa) GOX at Air Products (10 trials).
- Fatigue-induced cracks of tube-to-plate welds containing 250-psig (1.83 MPa) GOX at Air Products (about 4 trials).
- Torsional failure of TIG (GTA) welded 0.625-in. (15.9-mm) diameter, 6061 rods in 250 psig (1.83 MPa) in two tests at Air Products. Iron oxide contaminants were also included in a coaxial passage pressurized to 400 psig (2.86 MPa) in one test. Hydrochloric acid and Trichloroethane were present in the weld crevice in another test.
- Holes 0.25-in. (6.4-mm) in diameter were drilled into 0.125-in. (3.18-mm) thick 5052 alloy plate at Air Products. One in atmospheric-pressure LOX, one in 200 psig (1.48 MPa) GOX.
- A seven-inch tear was made in commercial aluminum foil under atmospheric pressure LOX at Air Products.
- Baffles in LOX tankers known to have broken in service in the presence of LOX and GOX at Air Products.
- Crevices in 5083 alloy plates that were welded were mechanically failed by repeatedly filling with LOX and warming to build pressures to 13,000 psig (89.7 MPa) at Air Products.
- A full Air Products' LOX tanker punctured by a bullet.
- Molten aluminum poured into tubing against a GOX flow at Air Products.
- Annealed 6061 aluminum extruded at room temperature through a 0.16-cm (0.063-in.) orifice to produce an extrusion approximately 0.64-cm

(0.25-in) long in GOX at 300 psig (2.17 MPa) at Air Products.

- An aluminum-to-aluminum welding arc was struck in an argon atmosphere to coat the inside of a roughly one-liter vessel with weld dust at Air Products. The vessel was cooled under argon then opened to air. The dust did not spontaneously ignite (contrary to normal welding experience in air, this dust was not pitch black but was aluminum-gray in appearance).

Only in the work of Munroe et al. [*45*] did ignition occur during a test intended to study fresh metal exposure using torsional fracture. However, the test was conducted with an electrical current flowing through the specimen to warm it. In a repeat test, with the current turned off, the aluminum did not ignite upon torsional fracture.

Electric Arc/Spark

The exposure of aluminum to electric arcs or sparks can lead to ignition. Experimentation with electric arcs and sparks is limited. Aluminum fines such as dust and particles have been ignited with ease by this method. Experiments with bulk aluminum have not achieved ignition. This may indicate that ignition of a bulk sample is difficult to achieve or is a low probability event. Fitt et al. [*46*] describe the difficulties that can occur in attempting to ignite even very easily ignited materials such as polymers with discrete sparks.

Arcing appears to have been important in the work of Munroe et al. [*45*] during which current was flowing while hot, small diameter rods were torsionally fractured. The rods were up to 0.080-in. (2.03-mm) in diameter and several hundred amperes were flowing to produce temperatures to at least 340°F (171°C). Aluminum ignited and burned at apparently 1000 psi (7.0 MPa), approximately 1400 ft/s (427 m/s) gas velocity, with the current on but not with the current off in a followup test. The effect was not evaluated for other metals.

Resistance-heated wires at Princeton [*47*] that exhibited ignition may also have been influenced by an electric current that was flowing.

NASA has exposed 0.0015- to 0.010-in. (0.038- to 0.25-mm) aluminum to 10J sparks in atmospheric pressure GOX without ignition [*19*].

Spark ignition energies have been measured for metal dust clouds in air by the Bureau of Mines [*5,6,48*]. Ignition energies for aluminum have been as low as 25 mJ, in the range 80-200 mJ for iron, 20-200 mJ for magnesium alloys, but nickel and alloy 347 stainless steel were not ignitable in their apparatus.

Kim and Colver [*49*] used an electrostatic particle suspension, said to provide very uniform distributions of particles, and measured minimum ignition energies for aluminum particles in the range 10 to 30 micrometre. They used air, oxygen and carbon dioxide oxidants. They found minimum ignition energies as low as 40 mJ in oxygen with the smallest particles. Energy required typically, but not always, increased with particle size.

In previously unpublished work, Air Products used pointed alloy 3003 aluminum rods as electrodes in 250 psig (1.83 MPa) GOX. Sparking from a high tension coil was effected at approximately 60 spark/s, estimated 25 mJ/spark energy, and for 45 minutes. A mottled surface resulted on the electrode but ignition did not occur.

Electric arcs and sparks produce temperatures well in excess of all reported autoignition temperatures for aluminum. They are highly localized and should be effective in delivering energy to the metal. However, despite the high temperature and localization of the heat, the total energy present in sparks from static charge separation or in arcs from low voltage wiring tends to be small, and aluminum, because of its high thermal conductivity, dissipates heat very effectively. Sustained and intense arcs may be necessary to ignite it.

Friction Ignition

Friction ignition has been observed during experimentation and aluminum has exhibited one of the lower thresholds. In addition, practical experience for aluminum in friction situations has resulted in many incidents.

The body of frictional-heating studies conducted at NASA [*50,51*] is the most extensive and most sophisticated in the literature. In these tests, the product of the applied force per unit area and the linear rubbing velocity (related to the power input) that produced ignition in 6.9 MPa (1000 psi) GOX was measured. Aluminum was the second most sensitive material, igniting at 0.063 W/m^2, while titanium ignited at 0.004 W/m^2, and other metals and metal pairs ignited in the range 0.09-3.38 W/m^2.

Large scale friction ignition tests were accomplished by causing rubs to occur in centrifugal LOX pumps made of aluminum and aluminum alloys [*28,52*]. Long periods (up to 30 minutes) passed before seizure or ignition occurred. The introduction of rusty nails into the suction of a LOX pump produced an immediate fire and explosion. Though the pumps being tested were initially operating at up to 450 psig (3.20 MPa) discharge pressure, friction rapidly damaged the ability of the pump to maintain a significant differential pressure. Aluminum impellers in bronze casings were also ignitable in two tests, but bronze impellers in aluminum cases did not ignite in two tests. One test of an aluminum impeller in a stainless steel casing, operating at a lower speed than the other tests, did not ignite.

Industry has experienced fires in aluminum centrifugal LOX transfer pumps and also in similar pumps made of aluminum bronze containing approximately 10% aluminum. There have also been instances where damaging rubs have occurred that did not result in ignition.

In unpublished test results, Air Products drilled holes in 0.125-in. (3.18-mm) thick aluminum plate in atmospheric-pressure, commercial-grade LOX, and in GOX at 200 psig (1.48 MPa) without ignition. Rotation of 50-mm diameter bars against each other produced flashes but no sustained combustion in one test at an unknown pressure (probably atmospheric presssure GOX). If ignition is successful in 200-psig (1.48-MPa) GOX, current data suggest massive propagation should have resulted.

Shock Wave Ignition

Aluminum is reported to have been sucessfully ignited by shock waves and to be more sensitive than stainless steel.

NASA [*19*] exposed 5052-H34 aluminum submerged in LOX and GOX at atmospheric pressure to shock waves from primacord explosive. The explosive was oriented either parallel to or below a vertical specimen. The aluminum was observed to ignite at explosive charge quantities rated to be large in comparison to those for titanium but small compared to those for stainless steel. Stainless steel alloy 301 did not ignite when used as the test specimen, and stainless steel alloy 304, which was used as the outer vessel to which the primacord was attached, and which presumably experienced much greater shock intensities, also did not ignite.

Unpublished Air Products' experiments include several attempts to ignite aluminum with explosive reactions that produced fractured surfaces but no evidence of ignition. High explosives (C4 and RDX) were set off below an aluminum plate in LOX, and in another, granulated hydrocarbon mixed with LOX was ignited in the bore of a small-diameter aluminum tube.

Resonance Ignition

Aluminum has been sucessfully ignited with acoustic resonance. The only work on igniting aluminum originates from NASA [*53,54*]. In one effort, aluminum fines, 1.5-mil x 1-mil that were up to 0.75-in. (1.91-cm) long were sucessfully ignited in a resonant cavity containing GOX at 1270 psig (8.86 MPa). A bulk heating and abrading action are felt responsible for the ignition. No other metals are known to have been studied.

Particle Impact

Particle impact has produced successful ignition of aluminum targets and particles alike. However, there are also numerous tests with particle or projectile impact of aluminum that have not caused ignition, despite severe conditions.

NASA particle impact work has employed particles moving at Mach 3.5, impacting targets at a pressure of roughly 1000 psig (7.0 MPa). To date, ignition has resulted only when either the particle or the target was aluminum [*55*].

Nihart and Smith [*34*] report on "velocity impact" in which unspecified materials are accelerated to a high velocity and impacted onto metals at 50-100 psi (446-791 kPa). A best-to-worst ranking of Monel, K-Monel, Tobin bronze, copper, steel, 18-8 stainless steel, and aluminum is reported.

Even though the above work demonstrates the ignition capability of particle impact, there are numerous data for which ignition did not result, despite severe impact conditions:

- High velocity steel projectiles puncturing aluminum diaphragms did not produce ignition (see *Fresh Metal Exposure*).

- A slug from a rifle did not cause ignition (see *Fresh Metal Exposure*).

- Single silica beads impinging onto 0.060- to 0.080-in. (1.5- to 20-mm) 1100 alloy aluminum wires at 1400 ft/s (427 m/s) in 1000-psi (7.0-MPa) GOX at up to 860°F (460°C) did not produce ignition. Numerous other alloys, including stainless steels and carbon steels also did not ignite in similar tests [*45*].

Propagation of Combustion

Many propagation studies have been accomplished. They have shown that aluminum is an extremely fast-burning material compared to other common metals, that the flammability limits for aluminum are very sensitive to even small amounts of inert impurities in the oxygen, and that under certain conditions with LOX, that aluminum can apparently detonate. Whether the observed propagation is the result of complete combustion or not is not clear. A significant fraction of the metal may not burn during some tests. In more recent papers, the more precise phrase "regression rate" (the velocity of the interface between the burning metal and specimen) is being used to describe the rate at which a rod melts and/or burns during a test.

Drew et al. [*56*] observed violent shattering from within of particles that were heated in hydrogen/oxygen flames and then passed into ambient air, and they suggested that high temperature oxide on the surface may have cause liquid superheating to occur. In a review paper, Christensen et al. [*57*] note that the fragmentation of burning particles observed by Drew is reported in many studies, and comment that the fact that fragmentation occurs in high oxygen purities suggests that fragmentation is associated with a high reaction rate which leads to a high rate of energy feedback to the particle.

Wire combustion tests by Brzustowski and Glassman [*2*] (and reviewed in Christensen et al. [*57*]) have exhibited seven distinct combustion regimes in oxygen/argon mixtures at various pressures (Fig. 1). In some instances where wires appeared to develop a skin that later ruptured, the combustion also exhibited an "explosive" nature.

Early studies of propagation rates were conducted in Germany by Kirschfeld [*58-61*]. Upward combustion of aluminum wire is reported in 0.25-1 atmosphere (25-101 kPa) GOX; rates of 3 cm/s are reported for 2-mm wire, compared to 18-cm/s for 0.5-mm (0.02-in.) wire. In the later work, horizontal combustion was studied at elevated pressure; propagation rates at 100 atmospheres (10.1 MPa) were 39 cm/s for 1-mm wires and 22 cm/s for 2-mm wire. Propagation rate increased with pressure to 16 atmospheres (1.62 MPa), decreased between 16- and 32-atmosphere (1.62- and 3.24-MPa) levels, and then increased again up to 100 atmospheres. Kirschfeld observed "explosive extinctions" that he attributed to liquid aluminum superheating. He found that events intense enough to quench the combustion only occurred when the mass burning rate of his wires exceeded 0.1g/s. He speculates that heat was not being lost to the surroundings as fast as it was being generated causing a buildup of temperature leading to superheating. The superheating may also have resulted from the condensation of aluminum oxide on the wire surface.

In comparison, the maximum combustion rates for low carbon steel were

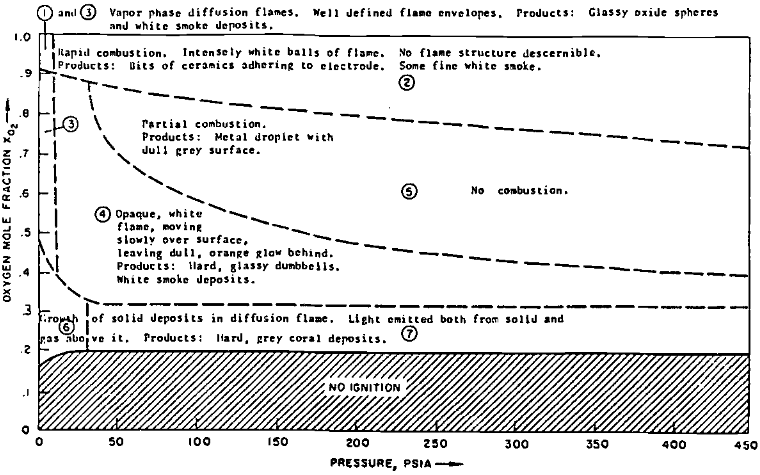

FIG. 1 -- *Observed combustion modes of aluminum wires in oxygen-argon (Brzustowski and Glassman as Reviewed in Christensen et al.* [57]).

progressively increasing with pressure to at least 100 atmospheres (10.1 MPa) at which a 4-cm/s rate was observed for 1-mm wire and a 2.6-cm/s rate for 2-mm wire. For 20%-chrome, 10%-nickel (a stainless steel similar to 304) wire at 100 atmospheres (10.1 MPa), the rates were roughly 5 cm/s for 1-mm wire and 2.3 cm/s for 2-mm wire [*61*].

Long and Sebald [62] reproduced the general nature of the aluminum propagation curve with respect to pressure that was observed by Kirschfeld (that is, increasing, decreasing, increasing rate vs pressure). They found a local maximum in the rate for 0.019-in. (0.48-mm) wire of 15-16 cm/s in the range 4-14 atmospheres (0.41-1.42 MPa), decreasing to 11 cm/s at 22 atmospheres (2.23 MPa), then increasing again to 16 cm/s at their highest tested pressure of 39 atmospheres (3.95 MPa).

Sato and associates [*63,64*] also observed the increasing, decreasing, increasing nature of aluminum combustion. However, they observed it only at 293 K (68°F) specimen temperatures; at higher temperatures of 623 K (661°F), 773 K(931°F), and 873 K (1112°F), the effect was monotonic (resembling a parabolic relationship). Data are also included for the velocity as a function of position along a specimen. Basically droplets form and periodically detach from the specimen. Just after a droplet has detached, the regression rate increases, then goes through a point of inflection and begins to decrease progressively until detachment (Fig. 2). Sato relates the inflection point to the point at which boiling is first observed on the droplet surface. This body of work tested anodized aluminum rods and found that anodizing had no effect on the velocity or nature of propagation.

Propagation rates in the detonation regime are possible for aluminum-powder/LOX mixtures and also appear to have been observed when bulk aluminum is ignited above a pool of LOX and some molten aluminum at very high temperature falls into the pool of LOX. Kirshenbaum [65] studied the

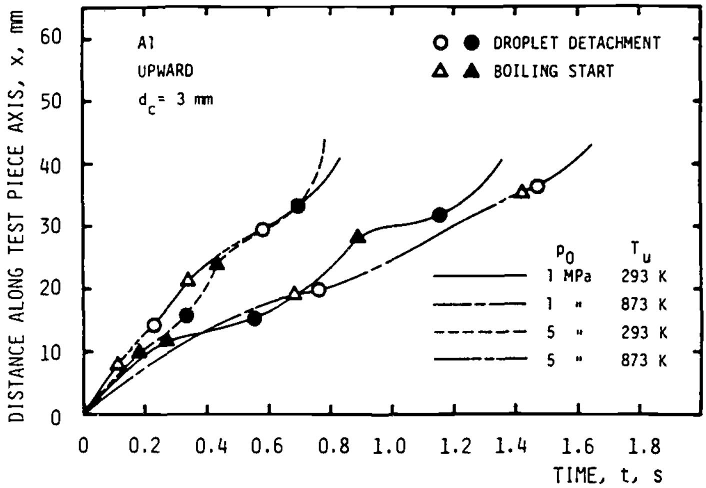

FIG. 2 -- *Position-time diagram of the leading edge of the molten mass for burning aluminum. From Sato [63].*

intensity of aluminum-powder/LOX explosions. Rozovskiy et al. [*66*] found that strong shock waves were required to initiate detonations in mixtures of aluminum powder and LOX, and that static electricity, open flames, and acoustic waves did not produce detonations even in the wake of ignition. However, these workers were studying aluminum-powder/LOX as a high explosive for which reliable detonation is important and were not focused on low-probability events that might be important in practical oxygen handling systems. In comparison, Austin [*67*], Dunbobbin et al. [*68*], and Zawierucha et al. [*69*] report violent reactions of powder or bulkier aluminum, at least several of which are believed to have been detonations, and they resulted from ignition techniques ranging from a flame to thermite powders mixtures having large energy releases. These violent reactions were not produced on every trial. In aluminum-powder/LOX systems, violent reactions occurred only a small fraction of the time. In bulk system tests, they occurred in a large fraction of tests which were directed to replicating this phenomenon. These tests used specimens which were partially immersed in high-purity LOX and for which ignition was effected in the GOX phase by a very energetic promoter, such as thermite.

Kirshenbaum [*65*] describes an assortment of materials for potential use as explosives, including a series of LOX/fuel mixtures with aluminum-powder/LOX among them. He notes that a stoichiometric mixture of aluminum and oxygen ($2Al + 1.5O_2$, Al:O ratio of 2:3) releases 3.85 times times the heat that is released by an equivalent mass of TNT. However, his experiments indicate that stoichiometric aluminum/LOX is less explosive than TNT. An excess of oxygen increases the explosive force of aluminum/LOX mixtures, and at an Al:O ratio betweeen 2:5 and 2:9 they exhibit an explosive force greater than TNT. This is partly because reaction of a stoichiometric mixture of aluminum and oxygen will result in a volume reduction (the reaction product is in a condensed phase). When oxygen-rich mixtures are used, the explosive force increases greatly due to the sudden expansion of the excess oxygen that is vaporized. Kirshenbaum notes that the explosive force of aluminum-powder/LOX increases as the particle size of the powder decreases. In only one test with excess aluminum powder (Al:O ratio 2:0.9) the explosive force was much less.

In Austin et al. [*67*], an investigation was made of an explosion that occurred during a classroom demonstration of rapid oxidation. The demonstration involved the ignition of aluminum fines in LOX. The demonstration had been accomplished several times without event, and Austin's experiments often did not yield explosions, but occasionally they produced detonations. Austin reports the energy released in the combustion of aluminum is 3.85 times that of TNT, but that the rate of aluminum reaction can vary from simply flares to destructive explosions.

In Dunbobbin et al. [*68*] specimens of distillation column packing (corrugated sheet metal) were 50% immersed in LOX of varying purity and ignited above the liquid. A threshold was observed above which apparent detonations occurred. The threshold was at a LOX/Argon purity of about 97.4% concentration of gas in equilibrium with the liquid. Above this threshold, explosive reactions frequently occurred that fragmented the open receptacle. Ignition below the liquid level did not produce the same result in several tests, nor did irrigated packing in two tests. It is estimated that less than 30% of each packing specimen melted and fell into the LOX prior to an apparent detonation. A much larger percentage appears to have reacted almost instantaneously during the "detonation." These results differ from those of Barthélémy et al. [*70*] and discussed below. These experimenters believe that detonation-like events occurred in the LOX pool and they do not report any subsequent reactions above the pool.

In unpublished work at Air Products, aluminum welding wires partially immersed in LOX were ignited in the gas phase of 99.99+% oxygen at approximately 124 kPa (3.2 psig) pressure and did not produce explosions. In one test, the combustion quenched at the liquid interface; in another it quenched prior to reaching the interface. Three ignitions below liquid did not propagate significantly, but one ignition in ambient temperature GOX did propagate completely.

Barthélémy et al. [*70*] report that they have reproduced the violent reaction results of Dunbobbin [*68*] involving distillation column packing specimens 50% immersed in LOX in some 20 tests. They looked for conditions in which the apparent detonations systematically occurred. They found these violent reactions occurred when very energetic promoters (thermite plus magnesium) were used in the gas phase and when the purity of the LOX was high (99.9+%). Twenty additional tests were also conducted at conditions that more nearly represent the normal service conditions of distillation columns. In these latter tests, the specimens were irrigated as they would be in a column, but used the same energetic promoter and high LOX purity. These specimens were only partially burned and no violent reactions occurred. These results were consistent with both the smaller amount of irrigated work in Dunbobbin [*68*] and the results of Zawierucha [*69*]. The apparent detonations of 50% immersed specimens were attributed to reaction of molten aluminum at very high temperature falling into LOX. The apparent detonations were not attributed to the distillation column packing, because similar results were obtained with thicker aluminum plates.

R. Zawierucha et al. [*69*] report on the results of 37 tests which studied the flammability and behavior of aluminum distillation packing with LOX at purities up to 99.9% and pressures up to 0.17 MPa (10 psig). The effects of various combinations of strong ignition promoters, packing immersion versus non immersion, packing irrigation (a low flow of cryogenic liquid oxidant) versus non irrigation, LOX pressure and LOX purity on packing combustion were studied. In 21 tests at atmospheric pressure there was no evidence of combustion propagation or violent energy release. A violent energy release occurred in one out of three pressurized tests conducted with packing that was 50% immersed in 98.7% purity LOX and not irrigated when a strong promoter (3-gram thermite) was ignited in the vapor phase at a pressure of 0.157 MPa (8 psig). In thirteen pressurized tests (0.17 MPa, 10 psig, max.), no combustion propagation or violent releases occurred when the packing was both irrigated and not immersed in LOX. Packing irrigation without LOX immersion was considered to be more typical of actual operating conditions.

Grosse and Conway [*11*] operated continuous combustion furnaces with molten pools of aluminum as fuel in gaseous oxygen at atmospheric pressure. The scale of the furnaces (about a cubic foot in volume) was large compared to other experimental programs. In addition, Grosse and Conway operated torches with aluminum powder as the fuel and air or oxygen as the oxidant. In torch operation, they found a lower flammability limit of 0.025 grams of metal per liter of air and an ignition temperature of 645°C (1193°F).

In comparison, Jacobsen et al. [*7*] report that ignition and propagating combustion in aluminum dust clouds was possible in 2-6% oxygen in carbon dioxide and 7-9% oxygen in nitrogen. Magnesium dust clouds ignited in pure carbon dioxide and as low as 2-4% oxygen in nitrogen. Iron dust clouds ignited in 11-17% oxygen in carbon dioxide.

Kim and Colver [*49*] used a sophisticated electrostatic suspension system to measure the lower flammability limit of 10-30 micrometre dusts in a 2.1-cm x 6.58-cm vessel. Their lowest limits in air and oxygen were 40-70 g/m^3, regardless of oxidant.

In a 1961 paper, Harrison and Yoffee [*71*] discuss the critical oxygen concentration below which combustion cannot take place. They indicate that the critical oxygen concentration increases with wire size. Their work focused only on iron alloys.

Friant [*72*] reported that in atmospheric-pressure gas, sustained combustion of 0.020-in (0.51-mm) aluminum wire occurred in 90-100% oxygen in nitrogen. Ignition without propagation occurred in 70-90% oxygen. Below 70%, ignition was not possible. A followup project [*73*] using oxygen/water-vapor instead of oxygen/nitrogen observed faster propagation and the wire became difficult to ignite below 92% oxygen/water-vapor. A second paper by Long and Sebald [*62*] found that combustion could not be accomplished beyond a moisture content of 12-15% for either of the pressures tested: 23.7 and 39.7 psi absolute (264 and 375 kPa).

A large program to study flammability limits was reported by Benning et al. [*74*]. This work studied rod and tube specimens and found:

- Even small amounts of inert diluents have a very significant effect on the propagation of aluminum. Argon in the amount 0.2%

increased the threshold for propagation of 0.25-in (0.64-cm) diameter rods from 15 to 105 psig (204 to 825 kPa).

- Argon is a much more effective diluent than nitrogen, owing apparently to nitrogen's reactivity with aluminum.
- The effect of rod dimension is much less than for steel alloys but does follow Harrison and Yoffee's [*71*] prediction.
- Variation in the magnesium content from 1-5% did not affect aluminum alloy flammability greatly.
- Aluminum very significantly altered the flammability of otherwise fire-resistant metals, such as copper, even as minority components. Aluminum bronzes with 5-10 percent aluminum burned with near the speed and near the thresholds for pure aluminum.

This appears to be the only published aluminum flammability report in which the purity of the oxygen was carefully measured and controlled. The strong influence of extreme purity on the threshold flammability was confirmed by Ken McIlroy and Robert Zawierucha of Praxair at the 1989 ASTM symposium and by Joel Stoltzfus of NASA more recently, but their results have not yet been published.

Promoted combustion data collected by NASA and reported by Tack et al. [*29*] on 3.2-mm (0.125-in) diameter rods of alloy 2219 aluminum were similar to Benning's results, exhibiting a 0.21 MPa (30 psia) threshold in high purity oxygen. However, a series of experimental aluminum-lithium alloys (of 1.2-2.5% lithium) exhibited much higher thresholds in the range 1.4-1.7 MPa (200-250 psia).

In similar work, Stoltzfus et al. [*75*] reported regression rates during combustion for aluminum 6061 that increased with pressure in the range 1.7-68.9 MPa (250-10,000 psig), increasing from 4.57 to 24.5 cm/s (1.8 to 9.65 in./s) over this range. Aluminum bronze with seven percent aluminum exhibited an increasing regression rate over the pressure range 3.5-17.2 MPa (500-2500 psig) and the rates were in the range 2.77-3.3 cm/s (1.09-1.3 in./s). The effect of pressure on the regression rates of metals such as 9% nickel steel, ductile cast iron and stainless steel was small and the regression rates were about one third of those for aluminum bronze.

Steinberg et al. [*76*] have studied the influence of microgravity on metal combustion using a free-fall tower. In general, for both aluminum and iron, the rates of regression were substantially increased in the "low gravity" condition.

Ivanov and Ultanova [*77*] reported on ignition tests of Soviet aluminum alloy tubes (10-mm O.D. x 0.5-mm wall) that were conducted to characterize their burning characteristics in oxygen gas. The oxygen purity is not specified. The pressure ranged from 0.1 to 5 MPa (14.5 to 725 psia) and flow velocities varied between 0.5 and 60 m/s. After ignition, aluminum tubes failed by rupturing near the combustion site. The burned lengths were on the order of 2-3 cm.

Dieguez et al. [78] internally ignited 80-mm diameter by 1-m long "hollow vessels" of several alloys including aluminum UNS A92017. Their study used igniters composed of a polymer combined with iron powder in oxygen gas pressures of 1-10 MPa (130-1435 psig). They measured the quantity of igniter material needed to produce a 50% probability of ignition, the duration of combustion, and the extent of combustion. Aluminum alloy was the more readily ignited and produced more extensive damage than any of the others. Metals in the study were: copper, carbon and stainless steels, cuproaluminum, and cast brass.

Aluminum Ignition and Propagation in Non-Oxygen

Aluminum burns intensely with oxygen. It also reacts intensely with numerous other materials including compounds containing oxygen (such as metal oxides), fluorinated organics (such as PTFE and CTFE), nitrogen, carbon dioxide, water, and some other metals. Since some of the materials can be present in practical oxygen systems, their potential role in ignition and propagation warrants consideration.

The Welding Handbook [79] describes thermite welding as the reaction of metal oxides of low heat of formation with metals having oxides of high heats of formation. Thermite igniters have been used in several flammability studies. Thermite reactions involving aluminum as the metal being oxidized to release a high heat of formation are as follows:

$$\text{metal oxide} + \text{aluminum} \rightarrow \text{aluminum oxide} + \text{metal}. \qquad (1)$$

Theoretically, temperatures to 3200°C (5800°F) may be possible, but practically temperatures of 2200-2400°C (4000-4350°F) are seen. In air, the reduced metal typically does not reoxidize. In oxygen, the reduced metal often recombines with oxygen to increase the heat release and, perhaps, produce higher temperatures than in air. Although these reactions are classified as "nonexplosive," the intensity of the reaction is significantly increased as the size of the fines decreases. Although compressed pills should have a small void space, loose powders at elevated pressures or in oxygen environments may also be more intense. Ignition temperatures are reported to be approximately 1200°C (2200°F). Table 3 lists several thermite reactions for aluminum.

Aluminum can react with metals, such as palladium and nickel, to produce an intermetallic compound with a substantial release of heat. Patents [*80,81*] describe this reaction and its initiation. Temperatures to 2800°C (5072°F) are reported [*82*].

Aluminum has also exhibited thermite-like reactions with fluorinated compounds. A paper [*83*] discusses the use of aluminum with PTFE as an underwater missile propellant.

Shear operations involving aluminum in combination with halogenated lubricants, such as the popular material chlorotrifluoroethylene (CTFE), under high shear in air are said (although only a few data have been located) to produce fires and perhaps detonations. Ehrenfeld [*84*] reported that jamming an aluminum needle valve closed with CTFE oil on the seat caused an explosion. Fresh

TABLE 3 -- *Typical thermite reactions involving Aluminum* [*79*].

Reaction	ΔH_f (cal/g)	ΔH_f (kJ/mol)	Temp.[1] °C
$3Fe_3O_4 + 8Al \rightarrow 9Fe + 4Al_2O_3$	- 7506	-3010	3088
$3FeO + 2Al \rightarrow 3Fe + Al_2O_3$	- 1835	- 783	2500
$Fe_2O_3 + 2Al \rightarrow 2Fe + Al_2O_3$	- 1779	- 759	2960
$3CuO + 2Al \rightarrow 3Cu + Al_2O_3$	- 2700	-1152	4866
$3Cu_2O + 2Al \rightarrow 6Cu + Al_2O_3$	- 2553	-1089	3138
$3NiO + 2Al \rightarrow 3Ni + Al_2O_3$	- 2025	- 864	3171
$Cr_2O_3 + 2Al \rightarrow 2Cr + Al_2O_3$	- 5361	-2287	2977
$3MnO + 2Al \rightarrow 3Mn + Al_2O_3$	- 3952	-1686	2427
$3MnO_2 + 4Al \rightarrow 3Mn + 2Al_2O_3$	-10211	-4356	4993

[1] Theoretical temperature.

aluminum surfaces are said to aggravate the reaction. Small scale reactions called "explosions," perhaps, bordering on detonations have been reported using a drill press to force a halogen-base-lubricated rod into aluminum. These detonations have apparently not been tested as ignition sources [*85*].

Aluminum, especially in high surface-to-volume form, is reactive with a whole range of halogenated materials, especially those containing chlorine. Some of these reactions are reported as rapid exothermic corrosions, but some are also reported to have produced explosions. Many references are cited in Bretherick [*82*] and Cutler [*86*].

Aluminum combustion can occur in gases normally thought to be relatively inert, such as nitrogen and carbon dioxide [*7, 87*]

Molten aluminum can react violently with water. This has been a safety concern in the aluminum industry for years (Long [*88*])] and for nuclear reactors with aluminum-clad fuel (Kuan and Buescher [*89*] and Nelson et al. [*90*]). These reactions are generally termed "steam explosions." Steam explosions also occur with other molten metals such as iron and steel (Long [*88*]). Many aluminum-steam explosions are believed to be caused by the rapid vaporization of the water by the molten metal with no chemical reaction between them (Kuan and Buescher [*89*]. However, in the case of aluminum at temperatures above 1672 K (2550°F), it has been suggested that aluminum vapor reacts with water. This reaction has been described as "ignition of the aluminum in the vapor phase." It is believed that a critical aluminum vapor pressure of 0.15 mm Hg ($2x10^{-4}$ atm), which corrresponds to about 1672 K (2550°F) for aluminum, is needed for the reaction to occur (Kuan and Buescher [*89*]).

It has been reported that lithium additions to aluminum dramatically increase the energy released during steam explosions (*Encyclopedia of Materials* [*91*], Jacoby et al. [*92*], and Page et al. [*93*]). The reason for the enhanced effect with lithium (even at low concentrations of about 1%) is not known, but it has been

TABLE 4 -- *Heats of combustion of typical metals and alloys.*

METAL/OXIDE	cal/g	cal/ml
Al/Al_2O_3	7425	20062
Mg/MgO	5900	10266
Ti/Ti_2O_3	4710	21195
stainless steels[a] (ferritic and martensitic)	1900-2000	14726-15500
stainless steel[a] (austenitic)	1850-1900	14850-15251
carbon steels[a]	1765-1800	13872-14147
Inconel 600[a]	1300	10960
aluminum bronzes[a]	1100-1400	8250-10500
Ni/NiO	980	8722
Monel 400	870	7682
brasses[a]	690-825	5966-6914
Cu/CuO	585	5218
Cu/Cu_2O	321	2870

[a] Oxides of alloys are assumed to be the same as the oxide of the constituent elements.

suggested that hydrogen released by reaction of water and molten Al-Li alloys increases the heat transfer through the steam blanket that surrounds the molten metal thus accelerating the vaporization of the water. The thermal conductivity of hydrogen is about ten times greater than that of steam. The quantity of hydrogen released is felt to be too small to add significantly to the energy release through a hydrogen-oxygen reaction (*Encyclopedia of Materials* [*91*]). The effect of lithium in enhancing steam explosions contrasts with its effect in reducing flammability in gaseous oxygen (see *Role of Alloy Additions*).

Heat of Combustion

Heats of combustion of metals and alloys are readily measured or can be calculated for alloys with acceptable accuracy as a linear combination of the constituent heats of combustion. Heat of combustion data are typically reported on a heat-per-unit-mass basis, and such values reported by Lowrie [*94*] are given in Table 4. These data have also been converted into heat-per-unit-volume. Aluminum possesses one of the highest heats of combustion when reported on a heat-per-mass basis (greater than copper and stainless steels by factors of 13 and 4 respectively, for example). However, due to its low density, the difference in energy release on a per-volume basis between aluminum and other common metals of construction is not as great but still significant as shown in Table 4 (greater than copper and stainless steel by factors of 3.8 and 1.3 respectively, for example). In addition, for some applications where strength properties are taken into account, the benefit of the low density of aluminum alloys is partially offset by their relatively low strength (especially in the welded and annealed conditions) and their low elastic modulus. For instance, flat plates (as might be used for the internals of vessels) in an aluminum alloy would have to be about 40% thicker than stainless steel plates to achieve the same stiffness, because the modulus of aluminum alloys is only about one-third the modulus of stainless steels. This would increase the factor of 1.3 noted above for stainless steel to 1.8.

Aluminum Flammability Theory

A substantial amount of effort has been directed towards the development of theory for aluminum flammability, but to date, the application of theory to actual situations can rarely be done with confidence. To a large extent, practical applications have been supported by empirical data, preferably from tests that relate closely to the application at hand. Nontheless, the body of understanding is increasing, as is the use of theory as a tool. This section reviews aluminum/oxygen reactions rather than aluminum reactions with oxides, fluorides or other metals.

Significance of the Combustion Phase

Perhaps the most widely analyzed and most controversial feature of metal combustion is whether the reaction occurs with the fuel in a gaseous, liquid, or even a solid state. The significance of many flammability properties is clear: the use of easily ignited materials suggests that fires will occur more frequently, and the use of energetic materials suggests that fires will be more destructive. The significance of the combustion phase is less clear.

Many of the early studies of metal flammability focused on the use of metal powders as rocket engine fuels. The current focus of metal flammability studies relates to loss prevention for bulk metals used in oxygen systems. The perceived significance of the combustion phase from these different viewpoints has been:

- Vapor-phase combustion is believed to be much faster than liquid-phase combustion. This may render vapor-phase burning materials preferable for fuel in applications such as rocket engines and explosives, but it demands extra consideration for loss-prevention when these metals are used for components in oxygen systems.

- Vapor-phase combustion is believed to be much more easily thwarted than liquid-phase combustion through control of oxidant purity and pressure. Consequently, novel fire-prevention techniques may actually render vapor-phase burning materials a preferred choice for oxygen systems in some instances.

- An understanding of the combustion nature may also lead to engineered alloys of improved compatibility.

Vapor-Phase Combustion.

Aluminum is widely, but not universally, decribed as a "vapor burning" material, that is, one that exhibits a gaseous diffusion flame. Vapor-phase burning is widely studied for many common nonmetallic materials and there is a large body of theory on the subject. Only a few of the other metals examined to date seem capable of burning in the vapor phase.

In vapor-phase combustion, a "flame" is present some distance from the material surface, and heat from the flame is transferred to the material surface and vaporizes it. The vapors migrate to the flame and provide the fuel while oxidant from the environment migrates to the flame to complete the reaction. The majority of combustion studies to date have been on organic compounds burning in this fashion.

Several criteria have been proposed to determine whether vapor-phase combustion is a possibility in a given system.

In an early work, Grosse and Conway [*11*] point out that many metal oxides, (aluminum oxide among them), limit the maximum achievable temperature through endothermic dissociation, often upon vaporization. They cite Brewer [*95*] in supporting the view that "most metallic oxides vaporize exclusively by decomposition to the gaseous elements, although some form gaseous oxide molecules." Very recently, Steinberg et al [*96*] have challenged this perspective for several metals. However, in those cases where it applies (apparently including aluminum), combustion involves the gaseous reactants condensing into molten oxide in the flame front, and the flame temperature is limited by the dissociation temperature of the oxide. As a result, there is an upper limit on the potential flame temperature.

In the same time period as Grosse and Conway's work, Glassman and associates at Princeton University [*97-101*] analyzed the relationship of dissociation temperature to flame temperature in the context of rocket engine applications. In exploring the combustion of aluminum particles as might be used in solid rocket fuel, they proposed that vapor phase combustion requires a flame temperature in excess of the metal boiling point. This condition is not met for all metals. The analysis is based upon a model for burning droplets which shrink during combustion and should easily approach the theoretical flame temperature, but may not be applicable where the heat from localized combustion may be dissipated by a much larger mass of metal.

The Princeton workers described metals whose "saturation temperature" (for example, decomposition temperature or oxide boiling point) was greater than the metal boiling point as vapor-phase burners of potential value for rocket engine uses. Through the years, the oxide boiling point has been loosely treated as the variable that limits flame temperature. Steinberg et al. [*96*] correct this tendency and call for more careful terminology to recognize that decomposition (that may not require vaporization), vaporization, or other variables may also control flame temperature.

Steinberg [*96*] surveys data from the literature which indicate for aluminum that boiling of the oxide (which appears to be the lowest temperature mechanism that would limit flame temperature) is 3800 K (6380°F), and the metal boiling temperature is 2791 K (4564°F). Clearly, aluminum is not precluded from vapor-phase combustion by limits on its potential flame temperature.

Analyses at Southern Research Institute (SRI) by Monroe, et al. [*45,102*] proposed that for metals to burn in the vapor phase, the heat of combustion, ΔH_c, must equal or exceed the heat necessary to vaporize the metal (sensible heat for the solid, $\Delta H_{rt\text{-}mp}$, plus latent heat of melting, ΔH_{mp}, plus sensible heat for the liquid, $\Delta H_{mp\text{-}bp}$, plus latent heat of vaporization, ΔH_{bp}). They have defined the ratio of these heats as the boiling-point burn ratio (BR_{BP}), as follows:

$$BR_{BP} = \Delta H_c/(\Delta H_{rt\text{-}mp} + \Delta H_{mp} + \Delta H_{mp\text{-}bp} + \Delta H_{bp}) \tag{2}$$

They also defined a similar ratio of the heat of combustion to the latent and sensible heats necessary to melt the metal as the melting point burn ratio (BR_{MP}), as follows:

$$BR_{MP} = \Delta H_c/(\Delta H_{rt\text{-}mp} + \Delta H_{mp}) \tag{3}$$

Metals with melting-point burn ratios of less than unity are taken to be nonflammable. Metals with boiling-point burn ratios of less than unity are not expected to burn as vapors. Among the metals studied by SRI, only a few satisfy the criterion for vapor burning; aluminum is among them.

Steinberg et al. [*96*] have argued that the heat of combustion is also absorbed by the oxygen that reacts with the metal, and these burn ratios should add to their denominators the sensible heat necessary to warm stoichiometric oxygen to the melting or boiling point. Regardless of whether the burn ratio formulation includes this extra heat or not, aluminum is not excluded from a prospect of vapor-phase combustion.

Indeed, most experimental observations in the literature on aluminum have been consistent with vapor phase combustion. For example, Grosse and Conway [*11*] observed "skating suns" that appeared as "clouds" above a molten aluminum surface which were taken to be burning vapors. Regression rates of combustion (the rate at which the interface between the burning metal and base metal recedes as a result of reaction, melting or boiling) are much greater for aluminum than for known liquid-burning metals. And aluminum combustion generates large quantities of fine oxide dust that is consistent with vapor phase combustion. Attempts to photograph aluminum combustion have yielded diffuse sources of bright light consistent with a burning cloud. To the authors' knowledge, no attempts have been made to date to photograph aluminum combustion with either X-ray or LASER photography, which may enable examination of the burning surface.

Several papers [*63,64,103*] indicate that aluminum may not always exhibit vapor-phase combustion. These papers report apparent direct or indirect observations of liquid-phase burning.

Liquid- or Mixed-Phase Combustion.

The thermodynamic possibility of vapor-phase combustion of aluminum and the nearly universal observation of apparent vapor-phase combustion does not preclude the possibility of liquid-phase combustion. Although the analysis by Glassman [97] argues that aluminum *will* burn in the vapor phase, within the knowledge of the authors, no one has demonstrated that liquid-phase combustion of aluminum is excluded under every circumstance.

Glassman's analysis was focused on the achievement of successful combustion for rocket applications. The focus of this paper is on loss prevention, and from this viewpoint both the flame-temperature versus boiling-temperature comparison and the burn-ratio criteria provide only coarse insights. Complete vaporization of a metal is important when the metal is a fuel, but the situation is different in loss-prevention applications, where an incompletely combusted metal that is extensively melted might be regarded as an unacceptable failure.

The burn-ratio analysis above is essentially a heat balance comparing the heat generated from burning to the heat needed to melt and/or vaporize the metal. It may be desirable to consider whether partitioning a metal's heat of combustion between melting and vaporization might allow for mixed-phase combustion of metals, especially those with boiling-point burn ratios less than unity. It can be shown that if a metal having a melting-point burn ratio (BR_{MP}) greater than unity is viewed as having two portions, one that burns at the melting point, and the other that burns at the boiling point, then the maximum Fractional Boiling-Point Combustion (FBPC) that is possible is given by:

$$FBPC = BR_{BP}[(BR_{MP}-1)/(BR_{MP}-BR_{BP})]. \qquad (4)$$

This expression considers a specimen which reacts completely. Its heat of combustion is partially absorbed in melting the entire specimen and the remaining portion, or "excess heat" is absorbed in boiling a fraction (the FBPC) of the melt. If the FBPC is between zero and unity, then there is sufficient heat from combustion to enable up to that fraction of the specimen to burn as a vapor at the boiling point. In reality, if vapor phase combustion occurs below the boiling point (that is, if it burns at a vapor pressure less than one atmosphere), then a greater fraction than the FBPC predicts might burn as a vapor. However, in real combustion, heat losses would act to suppress the fraction.

Similarly, if a metal (or alloy) has a BR_{BP} greater than unity, then only a portion need burn as a vapor in order to release sufficient heat to melt the remainder of a specimen (that is, a portion may act like an inert alloying metal of similar latent and sensible heats). In this instance, it can be shown that the Maximum NonReactive Fraction (MNRF) is given by the expression:

$$MNRF = (BR_{BP}-1)BR_{MP} / (BR_{BP}BR_{MP} - BR_{MP} + BR_{BP}) \qquad (5)$$

TABLE 5 lists burn ratios from the literature, FBPCs and MNRFs. Steinberg [96] has argued that burn ratio calculations (and related parameters such as FBPC and MNRF) include the sensible heat of stoichiometric oxygen. Generally, this effect is small. The oxygen-compensated parameters for aluminum are: BR_{MP}=19.1, BR_{BP}=1.97, FBPC=1.96, and MNRF=0.90.

TABLE 5 -- *Burn ratios and related criteria.*

METAL/OXIDE	BR_{MP}	BR_{BP}	FBPC[a]	MNRF[b]
Al/Al_2O_3	29.0	2.2	2.30	0.94
Be/BeO	12.6	1.6	1.69	0.83
Ca/CaO	17.4	3.1	3.49	0.92
Cr/Cr_2O_3	6.4	1.2	1.24	0.55
Cu/Cu_2O	2.0	0.20	0.12	N/A[c]
Cu/CuO	3.7	0.40	0.33	N/A
Fe/FeO	3.8	0.56	0.48	N/A
Pb/PbO	18.6	0.9	0.89	N/A
Li/Li_2O	41.7	1.6	1.62	0.94
Mg/MgO	22.9	3.6	4.02	0.94
Ni/NiO	3.7	0.5	0.42	N/A
Sn/SnO	44.8	0.8	0.80	N/A
Ti/Ti_2O_3	10.9	1.4	1.41	0.74
Zn/ZnO	19.3	2.4	2.59	0.92

[a] Fraction in which whole specimen reacts.
[b] Fraction for which only vapor phase reacts.
[c] Not applicable for $BR_{BP} < 1$.

These relationships presume that any vapor-phase combustion must occur at the boiling point, but this presumption may be too severe. Later analysis will consider metals with sufficient vapor pressure below the boiling point to enable vapor-phase combustion (See *Autoignition Temperature and Flash Point*). In these cases, vapor-phase combustion requires less sensible heat to achieve vaporization and the values for the burn ratios and MNRFs that would apply would be larger.

These FBPC calculations indicate that, if complete combustion occurs, a heat-balance argument cannot be used to rule out mixed-phase combustion, even for materials well established as liquid-phase burning metals such as iron. These MNRF calculations for vapor-phase combustion indicate that the burning of only a small fraction (6-10%) of aluminum releases sufficient heat to melt the remaining fraction.

The MNRF concept can be extended to binary aluminum alloys to calculate the minimum amount of aluminum needed to completely melt the alloy assuming the aluminum burns as a vapor at the boiling point and the alloy addition melts but does not react (that is the alloy addition is inert). Table 6 shows the minimum fraction of aluminum (1-MNRF) which must react to completely melt the other constituent. It is interesting that aluminum-bronze alloys having as little as 6 mass-% aluminum have been experimentally burned (in agreement with the copper-aluminum calculation of Table 6). The combustion is reported to have been rapid, and with the large production of oxide dust characteristic of vapor-

TABLE 6 -- *Minimum aluminum-combustion fraction of binary alloys.*

Binary Component X in Al-X Alloy[a]	Minimum Al Needed (atomic fraction)[b]	Minimum Al Needed (mass fraction)[b]
Cu	0.086	0.038
Fe	0.135	0.070
Ni	0.110	0.054
Mg	0.055	0.061
Zn	0.038	0.016

[a] X is assumed inert.

[b] Fractions are not compensated for sensible heats of oxygen that reacts with the aluminum.

phase combustion, despite an estimated BR_{BP} of less than unity for this alloy. The effect of aluminum on the flammability of other common alloy families (such as iron and nickel) has not been reported. However, since there are few aluminum-containing iron or nickel alloys, and those available are infrequently used in oxygen service, the effect of aluminum on nickel and iron is mostly of academic interest.

Further, these data suggest that iron (and most metals) might be capable of mixed-phase combustion or vapor-phase combustion if sufficiently preheated. Sato [*64*] presented a paper at the ASTM Fourth International Symposium which included movies of burning alloys. Some observers noted that some droplets from apparent liquid-phase burning metals grew to take on the appearance of "comets" with flaming tails as the droplets fell further away from the rod. However, these tails may have contained more volatile constituents as well as iron.

Sircar et al. [*103*], when trying to determine whether titanium burns in the vapor-, liquid- or mixed-phase condition, raised questions about the fundamental nature of aluminum combustion. This work was inspired by the properties of titanium from which one might predict vapor-phase combustion on the basis of its boiling-point burn ratio but which might be expected to be a liquid-phase burner on the basis of its flame temperature being below its boiling point (that is, the flame temperature that would be fixed by the boiling of titanium oxide is generally felt to be lower than the boiling point of the metal). Aluminum was included in the study to allow comparison of titanium with a metal widely believed to burn as a vapor, but these data suggest aluminum may also burn as a liquid in some circumstances.

Their technique involved weighing specimens as they burned. A step-function (staircase) character is expected for metals that exhibit droplet formation and detachment, with the weight decreasing by a large amount as each droplet falls away. On the plateau between drops, liquid-phase combustion should serve to add weight to the specimen as oxygen forms metal oxides. Conversely, any

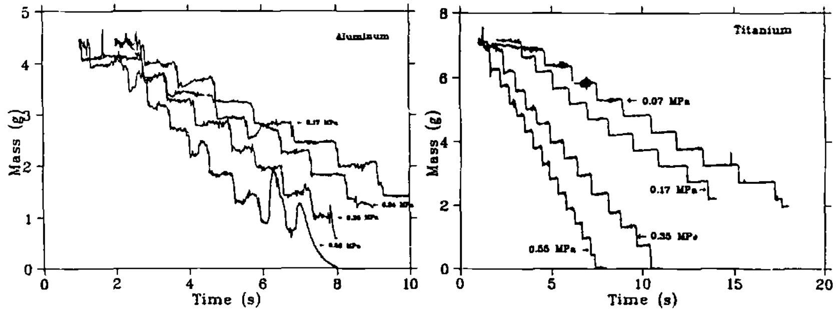

FIG 3--*Staircase plots for weight of burning aluminum (left) and titanium (right). From Sircar et al.* [*103*].

vaporization of the specimen should serve to decrease its weight. In the case of titanium (Fig. 3), the plateau weight between droplet losses was always increasing (consistent with liquid-phase burning), but for aluminum (Fig. 3) the "staircase" was erratic. Sometimes the plateau for aluminum was increasing, sometimes decreasing, sometimes with both characteristics present within a single plateau, and sometimes the weight appeared to jump upward. If those periods in which weight increased imply that aluminum can experience liquid-phase combustion, then much of the presently accepted understanding of aluminum's behavior may be seriously flawed.

During the discussion following Sircar's presentation of this paper at the Fifth ASTM Committee G-4 International Symposium on Flammability and Sensitivity of Materials in Oxygen-Enriched Atmospheres, Prof. Irvin Glassman proposed another mechanism to explain the apparently anomalous weight-gain events. It involves the migration of aluminum oxide droplets (reverse phoresis) from the flame zone back to the melt, in effect adding oxygen mass but not necessarily as a result of liquid-phase combustion.

Other weight-change mechanisms can also be identified that are only indirectly related to combustion: freezing of the oxide coating, collection of dust, and bouyancy of the specimen and apparatus.

During the combustion of metals, the extremely high temperatures produce an upward draft of hot gases, and the metal collected directly below the specimen that continues to burn would enhance this draft. In tests at Air Products, in which the specimen could be viewed from above, the first instant of ignition was accompanied by a smoke cloud that almost immediately transported debris to the top of the vessel and interfered with vision, despite a bulk downward flow of oxygen that had been deliberately designed to lessen this effect. The hot gases can provide a viscous drag on the specimen (tending to reduce the measured weight) and at high temperature, the oxygen which the specimen and sprung portion of the load cell displace has a lower density, thereby providing less buoyancy (appearing to yield a gain in weight). Also, this upward draft may transport oxides upward and deposit them on the rod or apparatus. Typically, there is a substantial dust layer on recovered unburned portions of specimens.

The staircase plots for titanium and aluminum included in Sircar et al. (Fig. 3)

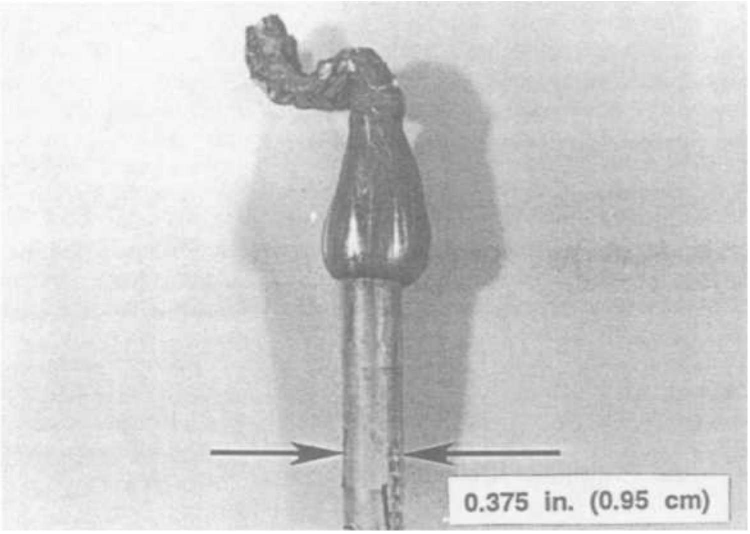

FIG 4 -- *Strength of aluminum oxide during tube ignition test.*

exhibit a small but obvious positive concavity that may be significant and indicate a progressively smaller net weight loss from each succeeding step. One possible interpretation would be that positive concavity implies decreasing combustion intensity with time (such as might occur if gas contaminants were accumulating with time). However, combustion intensity might be more likely to increase in time due to progressive preheating of successively burned segments by conduction and convection, and indeed, experimental observations tend to indicate increased intensity. Alternatively, the positive concavity would also be consistent with a progressive accumulation of weight owing to dust collection.

The curvatures within the plateaus and along the entire staircase could be accounted for on the basis of a decreasing intensity of combustion as the rod burns. However, there is also a debate on whether combustion becomes more fierce or less fierce as an attached droplet grows. Sato [*63*] and others have reported that for liquid- and vapor-phase burners, as a droplet grows the regression rate decays as molten slag or boiling interferes with the combustion. The results of Zabrenski et al. [*104*] and Steinberg et al. [*105*], however, indicate that the accumulation of slag and growth in droplet size may facilitate combustion. Variation in combustion intensity would affect all of these variables.

As the rod is consumed, heat may either accumulate in the remaining section (if it is not well heat sunk) thus accelerating combustion, or heat may be dissipated (as a result of a heat-sink mounting) that could account for a decaying regression rate.

The occasional step increases in weight observed for aluminum may be due to droplets that begin to fall away from the hot tip, momentarily appearing as a weight loss, but which are then recaptured by the tenacious aluminum oxide sack to reappear as supported mass. Numerous papers note the significant mechanical role that an oxide layer can play. Glassman et al. [2] found molten aluminum supported in a thin oxide skin during resistance-heated wire ignition tests. Air Products has observed molten aluminum within the surface oxide on aluminum foil heated by a LASER beam. Typically the result of rupture of the oxide films is extremely fast combustion of the melt. Figure 4 illustrates an aluminum tube that was top ignited, in which the molten metal appears to have been contained within its oxide coating that expanded like an elastic sack. Stretch marks on the oxide and shrink marks in the regions from which the melt drained are visible suggesting just how significant the oxide can be.

Whether the results of Sircar et al. demonstrate liquid-phase combustion is presently controversial. It might be valuable to repeat these tests with a segmented specimen, in which the lower segment is burned, and only the upper segment is weighed. This would yield insights into the buoyancy and dust collection mechanisms, and might allow ruling out liquid-phase combustion. But it might not give insight into whether debris and spatter can collect very near to the flame zone, therefore, might not rule it in.

The dynamics of the droplet reaction and variation in regression rate can be viewed in several ways. Zabrenski et al. [*104*] observed that specimens from tests that do not result in complete combustion are seldom recovered with a droplet frozen in place. Typically, there is negligible droplet present, suggesting that extinction occurred just after a droplet detached. This suggests that the loss of the high-temperature droplet may have caused the extinction. Alternatively, aluminum has shown itself very sensitive to inert diluents. The transient increase in regression rate after droplet detachment may be due to the droplet carrying accumulated diluent away (See *Role of Inert Diluents)*, thus exposing the tip to a higher local oxidant concentration.

Steinberg et al. [*105*] have found that for aluminum and iron burned in microgravity, the combustion rate increased several fold over that in normal gravity. Yet in this condition, the droplets do not detach at all.

Nontheless, the regression rate in normal gravity does increase after detachment and the new droplet that forms and grows is reported to initially be visible and "smooth" (suggestive of liquid burning). Perhaps these observations reflect reignition rather than equilibrium propagation. Following detachment of a droplet, a hot fresh surface is exposed. The new combustion of aluminum as a liquid or a flame rooted directly on the aluminum surface might transfer a greater fraction of its heat to that surface than would a similar flame located farther away. Further, because the melting-point burn ratio of aluminum is 29, only a small amount of reaction will release sufficient heat to melt a fresh droplet. In other words, it is possible that the regression rate is rapid but reflects melting rather than combustion and that the reaction rate is less than when full vapor-phase combustion is occurring.

It is worth reemphasizing that the significance of liquid- versus vapor-phase combustion is the nature of the resulting combustion. At present, it appears that vapor-burning metals will burn very rapidly, and some will be very sensitive to inert diluents.

Autoignition Temperature and Flash Point

Mellor and Glassman [*106*] have analyzed the importance of surface

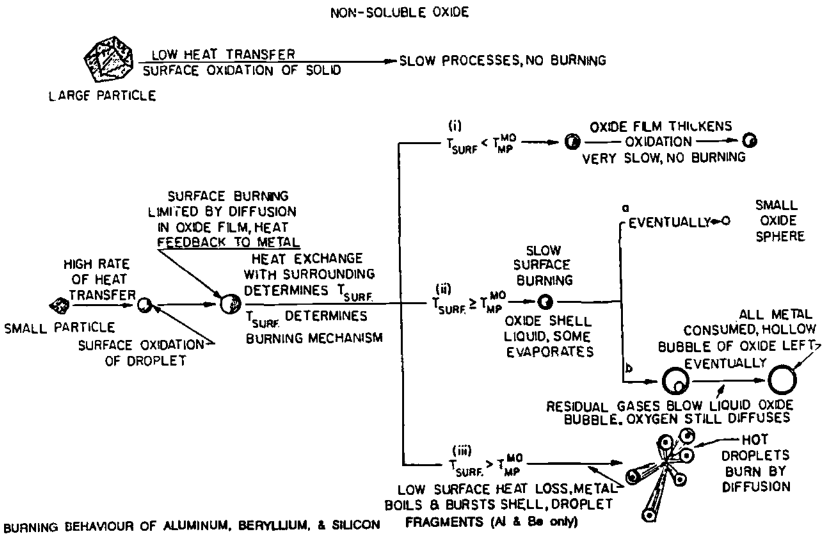

FIG. 5 -- *Combustion of nonvolatile metal particles in hot oxidizing atmospheres. From Mellor and Glassman* [*106*].

temperature in governing the mode of ignition and combustion of metals. Fig. 5 depicts their several mechanisms. Mode iii in the figure illustrates a droplet bursting into many burning fragments which may give insight into the way that reactions in intimate mixtures of aluminum and oxygen accelerate towards detonation.

Autoignition temperatures for aluminum (the system temperature at which aluminum will spontaneously ignite) are most frequently reported as being at or above the melting point of the "omnipresent" oxide that is generally assumed to surround aluminum. For materials that experience vapor-phase combustion, the concept of a flash point (the system temperature at which the vapor pressure of a material is sufficient to produce a mixture exceeding the lower flammability limit) is meaningful. Flash points for aluminum are not mentioned in the literature, presumably because oxide inhibition of autoignition would also inhibit the flash. Therefore, flash point and autoignition point might be expected to coincide. Nonetheless, the following will not consider any encapsulation that might occur and will presume that vapor-phase combustion applies for aluminum.

Flammability theory for organic vapor-burning materials [*107*] relates the autoignition temperature (temperature at which combustion spotaneously develops) and flash point (temperature at which the vapor pressure of the material is sufficient to yield a vapor-mixture which is just above the lower flammability limit).

Aluminum is far less volatile than organic materials but is volatile among metals. The measurement of its vapor pressure is experimentally challenging. Figure 6 depicts JANAF data plotted on a curve from Smithells [*108*] for vapor-pressures and boiling-points of aluminum and copper. Other sources for data are Stull [*109*], Nesmeyanov [*110*], Hultgren [*111*], Van Horn [*112*], and Van

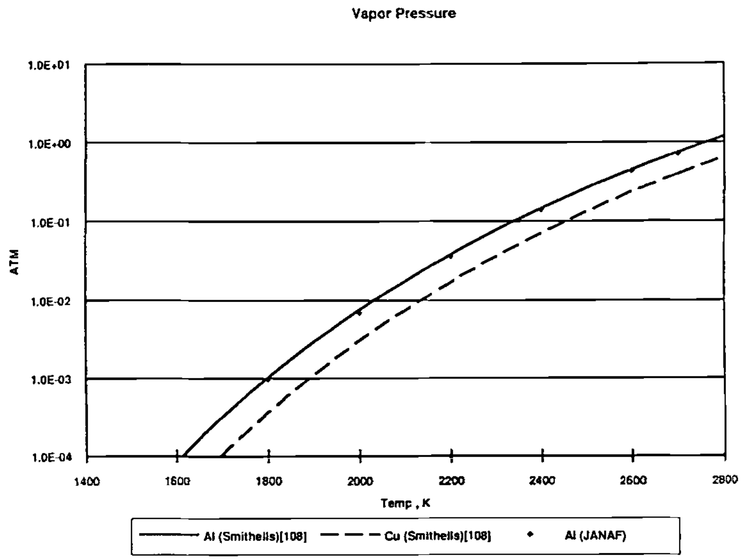

FIG. 6 - *Vapor pressure of aluminum and copper.*

Watenberg [*113*], Priselkov, [*114*], Brewer [*115*], Johnson [*116*], and Baur [*117*]. The variability among data in these papers is substantial. Nesmeyanov recommends the work of Johnson et al. and Baur et al. as the most reliable. From these curves one could estimate a flash point based upon the partial pressure necessary to achieve a lower flammability limit concentration.

Lower flammability limits are not published for aluminum vapors. However, data for less flammable aluminum dust clouds in atmospheric pressure air indicate 25-35-mg/l concentration which is equivalent to approximately 3 mol%. For hydrocarbons, good correlation of dust cloud or aerosol LFL's with flash points is obtained. If a similar correlation obtains for aluminum, then using Figure 6, a flash point approximated as the point at which a 0.02-0.03 atmosphere (2.02-3.04 kPa) partial pressure exists would be estimated at or below the 2100-2200 K (3320-3500°F) range. This is somewhat higher than the lowest autoignition temperature of 1640°C (1913 K, 2984°F) that has been measured experimentally.

Interestingly, copper is a much less volatile metal (melting point 1083°C, 1987°F, and boiling point 2595°C, 4703°F) than aluminum. This temperature range spans that for the surmised flash point range for aluminum and this may give insight into the ability of aluminum-bronze alloys to burn with the apparent vapor-phase characteristics of aluminum, despite copper having an insufficient BR_{BP} and a flame temperature apparently too low to support vapor-phase combustion.

Perhaps the aluminum evaporates from the molten bronze alloy and burns as a vapor. In this case, copper may actually facilitate combustion if it inhibits the formation of protective aluminum oxide.

Role of Inert Diluents in Oxygen

Benning et al. [*74*] discovered that small quantities of impurities in oxygen dramatically affect the threshold for propagation of aluminum combustion. Benning originally proposed that the effect was a consequence of oxygen and aluminum combining in the flame front to yield liquid aluminum oxide of relatively negligible volume, leaving behind an accumulating layer of inert gas, perhaps very near the surface. Glassman [*97,118*] and Glassman and Law [*119*] have analyzed the mechanism, and found that it is consistent with combustion theory for vapor-phase burning materials.

Benning et al. [*74*] showed that argon is much more effective in reducing flammability than is nitrogen at similar concentration. This is probably because nitrogen will react with aluminum to form aluminum nitrides and aluminum oxynitrides, consuming the nitrogen and evolving heat. The argon is, of course, essentially inert and will simply accumulate in the flame zone.

This argon effect would not manifest itself with ordinary hydrocarbon combustion. In hydrocarbon combustion the inert product gases are generated in far greater volumes than the levels to which argon might accumulate. Similarly, the flame temperatures are further above the fuel boiling point than is the case for aluminum. Finally, the boiling-point burn ratios of hydrocarbons are about an order of magnitude larger than for aluminum; many organic liquids are above their flash points even at room temperature.

Since diluents exert a significant influence on aluminum combustion, knowledge of the oxygen purity is needed to properly assess test results. Benning et al. [*74*] and Dunbobbin et al. [*68*] are explicit about the purity of oxygen used in their programs. Joel M. Stoltzfus of NASA has provided unpublished data on a series of promoted combustion tests that are consistent with Benning's results. However, most papers do not state the purity and presumably they used commercial grade oxygen or its equivalent. Typically, commercial-grade oxygen will exhibit a purity in the range 99.7-99.9+%. Argon is the principal impurity, and nitrogen the second highest impurity. Several decades ago, the purity would have been near the lower end of this range. Today, it is likely to be near the upper end of the range, as modern air separation plants recover greater fractions of the valuable argon component.

Testing accomplished with liquid will involve different purities in the liquid and gas phases. Figure 7 exhibits the relationship between equilibrium liquid and gaseous oxygen at atmospheric pressure. Indeed, experiments using oxygen from an evaporating liquid source will expose specimens to significantly different oxygen purities as the liquid is depleted as a result of the fractional vaporization that takes place.

Role of Alloying Elements

Alloying elements used in commercial aluminum alloys include copper, magnesium, manganese, zinc, and, recently, lithium. The industrial gas industry primarily utilizes the 3XXX (Al-Mn), 5XXX (Al-Mg) and the 6XXX (Al-Mg-Si) series. The aerospace industry also uses the higher strength 2XXX (Al-Cu) and

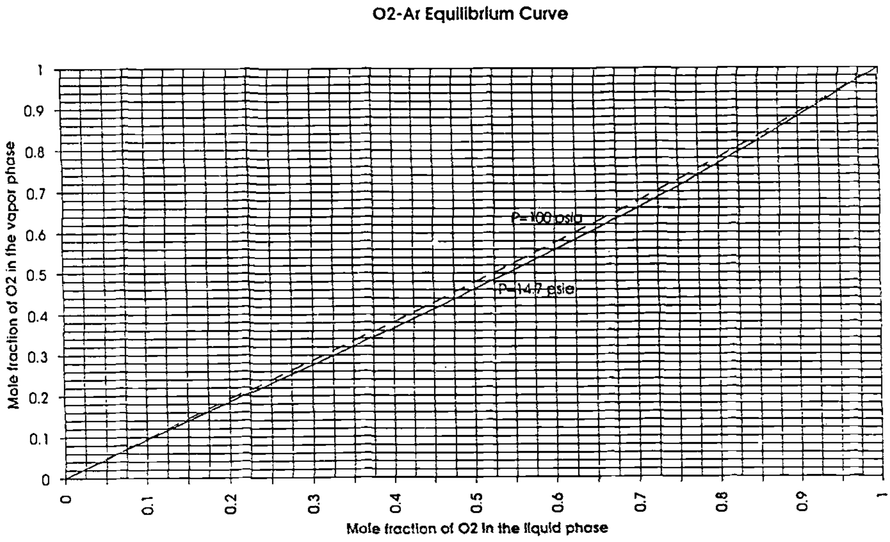

FIG. 7 -- *Oxygen purity in equilibrium liquid and gas (atmospheric pressure, oxygen-argon system).*

7XXX (Al-Zn) alloys and are investigating the newer Al-Li alloys. Most aluminum alloys contain lower levels of alloying elements than do iron, copper, and nickel alloys. Typical maximum concentrations for copper, magnesium, and zinc in commercial alloys are 5-7%. Manganese, when added, is usually at about 1% or less. Silicon levels of up to 12% are used in welding and brazing alloys, but the structural 6XXX series alloys contain only about 1% or less silicon. Most aluminum alloys contain >90% aluminum.

There has been no systematic study of the effect of alloying elements on aluminum flammability. For a variety of alloys, including commercially pure aluminum, reported threshold pressures for 0.125- and 0.250-in. (0.32- and 0.64-cm) rods are 15 to 50 psia (0.10 to 0.34 MPa) in high purity oxygen (see Table 7). Benning et al. [*74*] noted a slight reduction in flammability of high-magnesium alloy 5356 (5.0 Mg) compared to 6061 (1.0 Mg-0.6 Si) in lower purity oxygen (e.g. 99.0%). However, the alloys gave similar results in "zero-grade" oxygen (99.993%) (Table 7). In general, copper, magnesium, manganese, and silicon alloy additions appear to have little effect on flammability at levels present in commercial alloys. Indeed, Benning et al. found that even when small amounts of aluminum (6%) were in copper alloys, the flammability threshold and regression rates were not greatly different from those of aluminum alloys.

Recently, however, Tack et al. [*29*] reported threshold pressures of 200 to 250 psia (1.4 to 1.7 MPa) for Al-Li alloys (1.2-2.5% Li), showing that lithium addition makes aluminum significantly less flammable. The reason for the reduced flammability is not known. At this writing, the original workers are considering whether the lithium might lower the surface tension of the melt, causing it to drain more quickly and thus enhancing an important heat-loss mechanism. However, the reduced flammability may also be due to a shielding effect by inert Li_2O vapor generated during the burning, similar in concept to the

TABLE 7 -- *Aluminum threshold test results.*

Alloy	Nominal Composition[a]	Rod Size	Threshold Pressure(psia)	Source
Pure Al	>99.9 Al	1/8- x 6-in.	<24.65	Sircar [*103*]
2219	6.3 Cu	1/8- x 5-in.	30	Tack [*29*]
5356	5.0 Mg	1/4- x 3-in.	30	Benning [*73*]
6061	1.0 Mg-0.6 Si	1/4- x 3-in.	30	Benning [*73*]
6061	1.0 Mg-0.6 Si	1/4- x 6-in.	50	Benning [*73*]
6061	1.0 Mg-0.6 Si	1/8- x 3-in.	15	Benning [*73*]
Al-Li	1.2-2.5 Li	1/8- x 5-in.	200-250	Tack[b][*29*]

[a] Elements with nominal concentration >0.5%.

[b] Tested a series of alloys with measured Li contents varying from 1.2 to 2.5%.

gas-phase diluents described above. Magnesium oxide (MgO) is also volatile but adding up to five percent gives only an modest reduction in flammability. Lithium may be more effective than magnesium because Li_2O is more volatile than MgO (see Table 8). In addition, because Li_2O is a larger molecule than MgO, it would diffuse from the flame zone more slowly.

Surprisingly, Tack et al. [*29*] found no effect of alloy lithium concentration on threshold pressure, even though the lithium concentration was varied by a factor of two (1.2% to 2.5%). One explanation might be that Li_2O vapors in the flame zone are at the vapor pressure of molten oxide (that is, saturated). If so, the vapor pressure of Li_2O will not increase with additional Li_2O and a film of condensed Li_2O might form on the alloy. Lithium concentrations in excess of the amount needed to maintain saturation will not increase Li_2O vapor pressure. If the flame zone becomes saturated at <1.2% lithium, higher amounts of lithium may not further reduce flammability.

Lithium in aluminum appears to have little effect on mechanical impact flammability test results in LOX [*29*]. However, lithium additions to aluminum increase the severity of steam explosions which occur when liquid aluminum is mixed with water (see *Aluminum Ignition and Propagation in Non-Oxygen*). Tests of aluminum sheet-metal packing partially immersed in LOX have shown that molten aluminum-LOX reactions can also be explosive (see *Propagation of Combustion*). Similar tests with Al-Li alloys have not been conducted, and so it is not possible to surmise whether the beneficial effect of lithium additions to aluminum that were exhibited in gaseous oxygen environments would also be present for Al-Li in LOX.

We know of no measurements of the flammability of zinc-containing aluminum alloys. Zinc metal has a high volatility (boiling point of 907°C, 1665°F) and zinc oxide (ZnO) does not vaporize, but decomposes to zinc metal and oxygen at temperatures above 1000°C (1832°F). Zinc metal may act as an

TABLE 8 -- *Metal Oxide Vapor Pressures.*

	Vapor pressures[a] in atmospheres			
	1000K	2000K	3000K	4000K
Li_2O	1.3×10^{-13}	4.1×10^{-3}	2.07	31.33
MgO	1.4×10^{-25}	2.1×10^{-8}	0.01	2.56

[a]Calculated vapor pressures using JANAF data [*108*] and assuming a condensed-oxide phase is present, and the oxide vapor in the flame is saturated.

inert diluent in the high temperature flame zone surrounding the burning metal and may impede combustion. However, as the zinc diffuses from the flame zone, it will oxidize and release heat which may enhance combustion. In the absence of test data, we cannot predict if zinc additions would be beneficial, detrimental, or neutral regarding aluminum flammability.

Solubility of Oxide in the Melt / Oxide Inhibition

Most of the literature, excluding the papers by Sircar et al. [*103*] and Sato [*63,64*], appears to conclude or accept that aluminum burns in a vapor-phase reaction. Many of these reports are subjective. Nevertheless, even in instances where the aluminum was studied just above its threshold of combustion (either through increasing the diluent or the presence of less flammable alloying metals such as copper), where one might expect vapor-phase combustion to be thwarted, aluminum alloys do not appear to shift into patterns of slow combustion characteristic of liquid-phase reaction. They appear either to burn rapidly, with large amounts of dust generated, or not at all.

This may be due to the nature of the aluminum oxide-molten aluminum relationship. In the combustion of iron, which is a well established liquid-phase reaction, the melting points of the oxides are near that of the liquid metal and they are miscible. In the case of aluminum, however, the melting point of the oxide is near the boiling point of the metal, so liquid mixtures of aluminum and aluminum oxide are unlikely to form.

Therefore, any aluminum oxides that reach the surface of molten aluminum during combustion are likely to accumulate there, providing a physical barrier (perhaps encapsulation) and interfere with continued combustion. This may be why. combustion resembling a liquid-phase reaction is not observed.

Ignition Promoters

A range of materials have been used to cause aluminum ignition in laboratory tests. The kinds of igniters and promoters used can influence the test results.

Some promoters are selected to minimize this influence, while others are selected to model more acurately realistic ignition events. Igniters are sometimes used to study a materials ability to resist ignition and sometimes to study whether established combustion will sustain itself (flammability limit testing).

Certainly hydrocarbons and organics are among the contaminants most commonly present in industry, and therefore the most likely to be inadvertently introduced into oxygen systems. For this reason, some experimental work has involved hydrocarbon oils or polymers (Zawierucha et al. [*37,38*]) as igniters. However, organics exhibit relatively low adiabatic flame temperatures, and since quiescent aluminum tends to exhibit an autoignition temperature near the melting point of its oxide (2045°C, 3713°F), hydrocarbons are typically not reliable promoters for experimental purposes. In cases where these potential contaminants are, indeed, the only realistic ignition sources, tests involving hydrocabons and organics may yield the most directly applicable results.

Another point of view is to use "strong" igniters that are more likely to ensure ignition and at least transient propagation. This tactic tends to be more appropriate where the goal is to determine whether self-sustaining propagation is possible, such as in flammability-limit testing. In flammability-limit testing, a high temperature, an efficient heat transfer, and a minimum disruption of oxidant purity are desirable. To accomplish these goals, metal reactions are often chosen as promoters (for example Benning et al. [*74*] and Stoltzfus [*51*]). Depending upon test conditions, some metals (such as carbon steel or magnesium) are easily burned and can serve as igniters. In other cases, metal reactions involving aluminum itself with metal oxides (thermite) or in combination with metals such as palladium will provide the same features. Such igniters, of course, are not likely to be present in an actual oxygen system.

When these metal-based igniters burn, they achieve temperatures well above the melting point of aluminum oxide and tend to form liquid slags rather than gases (which could dilute the oxidant). The contact of the slag with a specimen provides very efficient heat transfer, in comparison to that from the carbon dioxide, steam, and radiation that are produced by hydrocarbon combustion.

The assessment of igniter significance on the application of aluminum test results to actual oxygen systems demands considerable judgement.

Industrial Experience and Incidents

Aluminum has been and continues to be used in a wide range of cryogenic applications with oxygen.

A small number of serious aluminum/oxygen reactions have occurred in aluminum LOX tanks, LOX tankers, and centrifugal LOX pumps. More, but smaller, reactions have occurred in the sump of low-pressure distillation columns. Some of these incidents are well understood, while others are less well so. To date, there do not appear to have been any incidents in certain types of hardware, such as low pressure ambient-air LOX vaporizers, and high-pressure GOX aluminum cylinders. In two severe LOX-tank incidents and several crevice ignitions in distillation columns reported by Air Products, they were unable to definitively identify a realistic ignition source. In the LOX-pump incidents, plausible ignition sources (rubs and contamination) appear to be likely critical factors.

Lainoff [*120*] reviews significant historical incidents and experimental results related to oxygen supply and storage system explosions, taking into account the mechanisms of tank burst phenomena in the case of aluminum vessels. Phenomea critical to a tank rupture event are assembled into a logical model of the rupture process. It is argued that the most critical element linking these incidents together is the introduction of contaminants into the tanks coupled with a failure to detect critical contaminant buildup. This paper uses the word "detonation" to describe rapid reaction of aluminum and oxygen. We do not believe the events surveyed in this paper actually warrant the use of this word.

A severe tanker fire in 1970 [*121*] involving extensive aluminum combustion was attributed to contamination. This incident resulted in very extensive damage and loss of aluminum.

Kilmartin [*122*] reports on a bulk tank truck containing 1300 gallons (4.9m^3) of LOX that exploded on April 22, 1969. The inner and outer vessels of the vacuum-insulated unit were fabricated from aluminum. The working pressure was 45 psig (411 kPa). The tank itself did not burn. About eight pounds of aluminum from the body of a submerged pump was consumed. The cause of the failure was attributed to a lack of lubrication in the pump bearings.

Barthélémy et al. [*123*] analyzed fire events in oxygen compressed-gas regulators and performed relevant tests. They report that these incidents are due to designs in which adiabatic compression (in combination with combustibles) can lead to ignition in regulators made of aluminum or copper alloys.

Summary

Aluminum is an extensively studied metal for use in oxygen service. Many features of its ignition, propagation of combustion, and damage potential are understood, but much more remains to be learned. Aluminum-oxygen studies are certain to continue.

Among the significant features of aluminum flammability are:

- The autoignition temperature of aluminum is reported to be higher than most other metals; it is frequently placed near the oxide melting point of about 2045°C (3713°F). However, where the oxide is disrupted or where the metal is in powder form, spontaneous ignition can occur at much lower temperatures.

- Aluminum can be ignited by mechanical impact at lower energies than most other metals, although test results vary significantly.

- Fresh-metal exposure does not cause ignition in the absence of other effects, but aluminum has one of the lower friction-ignition thresholds of all metals.

- Aluminum fines have been ignited by sparks, but bulk samples are more difficult to ignite, possibly due to the high thermal conductivity of aluminum.

- Aluminum burns quickly compared to other metals, and under some conditions, can appear to detonate. Burning rates, however, are highly variable, being affected by specimen geometry and by oxygen pressure and phase. Several researchers feel that access to a pool of relatively pure LOX is necessary for detonation.

- Aluminum will react with the oxides of other metals and with fluorinated organics.

- Aluminum is widely held to be a material that burns in the vapor phase, a mode of combustion more rapid than that involving the liquid phase.

- Thermodynamic arguments support vapor-phase burning for aluminum, but mixed-phase combustion is also seen as possible.

- Small quantities of inert diluents in oxygen significantly alter the threshold for combustion of aluminum, rendering it less flammable. Argon has a much more pronounced effect than nitrogen.

- Aluminum is volatile among metals. Its flash point can be estimated from the partial pressure corresponding to the lower flammability limit concentration of aluminum vapor.

- The effects of alloying elements on aluminum flammability have not been systematically investigated, but they can be significant. Lithium, for example, appears to raise the threshold for aluminum alloy propagation of combustion.

Aluminum is a very useful metal for oxygen systems. Among its advantages are low density, good toughness at low temperature, resistance to corrosion, ease in forming, and low cost. This paper has highlighted much of the information that is available to help evaluate it for oxygen service. The consequences of aluminum fires can be severe, nevertheless, systems employing this metal are widely used with success. Aluminum is likely to be used selectively in oxygen service in the future.

Acknowledgement

For more than a decade, Clyde McKinley tutored on the flammability of aluminum. Many of his teachings have been incorporated in this paper.

References

[1] Kuehl, D. K., "Ignition and Combustion of Small-Diameter Aluminum Wires," Western States Combustion Institute, Papers WSS/CI 64-21, 1964, 31 pages.

[2] Brzustowski, T. A., and Glassman, I., "Vapor-Phase Diffusion Flames in the Combustion of Magnesium and Aluminum - Part II Experimental Observations in the Oxygen Atmospheres," *Progress in Astronautics and Aeronautics*, 1964, pp. 117-158.

[3] Mellor, A M., and Glassman, I., Vapor-Phase Diffusion Flames in the Combustion of Magnesium and Aluminum; Part III Experimental Observations in Carbon Dioxide Atmospheres," *Progress in Astronautics and Aeronautics, 1964*, pp 159-176.

[4] Merzhanov, A., Grigorjev, Y. M., and Gal'Chenko, Y. A., "Aluminum Ignition," *Combustion and Flame,* 29, 1977, pp. 1-14.

[5] Hartman, I., "Recent Research on the Explosibility of Dust Dispersions," *Industrial and Engineering Chemistry,*" Vol. 40, No. 4, April 1948, pp. 752-758.

[6] Hartman, I., Nagy, J., and Brown, H.R., "Inflammability and Explosibility of Metal Powders," *Report of Investigations RI 3722,*" U. S. Bureau of Mines, October, 1943, 39 pages.

[7] Jacobsen, M., Cooper, A. R., and Nagy, J., "Explosibility of Metal Powders," *Report of Investigations RI 6561,* U. S. Bureau of Mines, 1964, 25 pages.

[8] Cassel, H. M., and Liebman, I., "The Cooperative Mechanism in the Ignition of Dust Dispersions," *Combustion and Flame,* Vol. 3, No. 4, December 1959, pp. 467-475.

[9] Smolenski, D. and Seweryniak, M., "Combustion of Aluminum Dust in Various Oxidizing Gases," *Biul. Wojskowej. Akad. Tech.,* Vol. 12, No. 4, 1963, pp. 43-64.

[10] Bransford, J. W., "Ignition and Combustion Temperatures Determined by Laser Heating." *Flammability and Sensitivity of Materials in Oxygen-Enriched Atmospheres: Second Volume, ASTM STP 910,* M. A. Benning, Ed., American Society for Testing and Materials, Philadelphia, 1986, pp. 78-97.

[11] Grosse, A. V., and Conway, J. B., "Combustion of Metals in Oxygen," *Industrial and Engineering Chemistry,* Vol. 50, April 1958, pp. 663-672.

[12] Clark, A. F. and Hust, J. G., *A Survey of Compatibility of Materials with High Pressure Oxygen Service, Final Report 275.03-72-11, NASA Order No. H-9 2180A,* National Bureau of Standards, Boulder, Colorado, October 1072, 45 pages plus 136-page Appendix.

[13] Clark, A. F. and Hust, J. G., "A Survey of Compatibility of Materials with High Pressure Oxygen Service," *Cryogenics,* June 1973, pp. 325-336.

[14] Clark, A. F. and Hust, J. G., "A Review of the Compatibility of Structural Materials with Liquid Oxygen," *AIAA Journal,* Vol. 12, No. 4, April 1974, pp. 441-454.

[15] Mellor, A. M., *Heterogenous Ignition of Metals: Model and Experiment,* Princeton University Department of Aerospace and Mechanical Sciences, Report 816, NASA Grant NSG-641, 1967, 367 pages.

[16] Belles, F. E., "High Pressure Oxygen Utilization by NASA," *NASA Tech Memo TMX-68203,* 1973, 17 pages.

[17] Poyarkov, V. G., "Combustibility of Powders of Aluminum-Magnesium Alloys," *Izv. Vyssh. Ucheb. Zav., Tsvetnaya Metallurgiya,* No. 4, 1967, pp. 203-209.

[18] White, E. E. and Ward, J. J., *Ignition of Metals in Oxygen, Defense Metals Information Center, DMIC Report 224,* Columbus, Ohio, February 1966, 48 pages.

[19] Riehl, W. A., Key, C. F., and Gayle, J. B., *Reactivity of Titanium with Oxygen, NASA Tech Report TR R-180,* 1963, 113 pages.

[20] Key, C. F., and Riehl, W. A., *Compatibility of Materials with Liquid Oxygen, NASA MTP-P VE-M-63-14,* 4 December 1963, p. 66.

[21] Keeping, W. O., "Compatibility of Materials with Oxygen," *CGA Oxygen Compressors and Pumps Symposium,* Compressed Gas Association, Nov. 9-11, 1971, pp. 79-86.

[22] Lockhart, B. J, Hampton, M. D., and Bryan, C. J., "The Oxygen Sensitivity/Compatibility Ranking of Several Materials by Different Test Methods," *Flammability and Sensitivity of Materials in Oxygen-Enriched Atmospheres: Fourth Volume, ASTM STP 1040,* Joel M. Stoltzfus, Frank J. Benz, and Jack S. Stradling, Eds, American Society for Testing and Materials, Philadelphia, 1989, pp. 93-105.

[23] Barthélémy, H., Delode, G., Vagnard, G., "Ignition of Materials in Oxygen

Atmospheres: Comparison of Different Testing Methods for Ranking Materials," *Flammability and Sensitivity of Materials in Oxygen-Enriched Atmospheres, Fifth Volume, ASTM STP 1111,* Joel M. Stoltzfus and Kenneth McIlroy, Eds., American Society for Testing and Materials, Philadelphia, 1991, pp. 506-515.

[24] Bryan, C. J., "NASA Mechanical Impact Testing in High-Pressure Oxygen," *Flammability and Sensitivity of Materials in Oxygen-Enriched Atmospheres, ASTM STP 812,* B. L. Werley, Ed., American Society for Testing and Materials, 1983, pp. 9-42.

[25] Bryan, C. J., "Final Report on the Effect of Surface Contamination on LOX Sensitivity," NASA KSC Letter Report MTB-306-71, 1971.

[26] Ordin, P. M., "Mechanical Impact Tests of Materials in Oxygen: Effects of Contamination," *NASA Technical Paper 1571,* April 1980.

[27] Jackson, J. D., Boyd, W. K., and Miller, P. D.,"Reactivity of Metals with Liquid and Gaseous Oxygen," Defense Metals Information Center, Battelle Memorial Institute, DMIC Report 163, January 15, 1963.

[28] Bauer, H., Wegener, W., and Windgassen, K. F. "Fire Tests on Centrifugal Pumps for Liquid Oxygen," *Cryogenics,* June 1970, pp. 241-248.

[29] Tack, W. T., McNamara, D. K., Stoltzfus, J. M., and Sircar, S., "Aluminum-Lithium Alloys: Mechanical Property and Composition Effects on Liquid Oxygen Compatibility," *Flammability and Sensitivity of Materials in Oxygen-Enriched Atmospheres: Fifth Volume, ASTM STP 1111,* Joel M. Stoltzfus and Kenneth McIlroy, Eds., American Society for Testing and Materials, Philadelphia, 1991, pp. 216-239.

[30] Reed, R. P., McCowan, C. N., McColskey, J. D., and Simon, S., "Macro- and Microreactions in Mechanical-Impact Tests of Aluminum Alloys," *Flammability and Sensitivity of Materials in Oxygen-Enriched Atmospheres: Fifth Volume, ASTM STP 1111,* Joel M. Stoltzfus and Kenneth McIlroy, Eds., American Society for Testing and Materials, Philadelphia, 1991, pp. 240-259.

[31] Reed, R. P., Simon, N. J., Berger, J. R., and McColskey, J. D., "Influence of Specimen-Absorbed Energy in LOX Mechanical-Impact Tests," *Flammability and Sensitivity of Materials in Oxygen-Enriched Atmospheres: Fifth Volume, ASTM STP 1111,* Joel M. Stoltzfus and Kenneth McIlroy, Eds., American Society for Testing and Materials, Philadelphia, 1991, pp. 381-398.

[32] Simon, N. J., McColskey, J. D., "Reaction Sensitivities of Al-Li Alloys and Alloy 2219 in Mechanical Impact Tests," *Flammability and Sensitivity of Materials in Oxygen-Enriched Atmospheres: Fifth Volume, ASTM STP 1111,* Joel M. Stoltzfus and Kenneth McIlroy, Eds., American Society for Testing and Materials, Philadelphia, 1991, pp. 193-215.

[33] Nguyen, B. K., and Pham, B. T., "Assessing LOX Compatibility for Aluminum-Lithium Alloys," *Flammability and Sensitivity of Materials in Oxygen-Enriched Atmospheres: Fifth Volume, ASTM STP 1111,* Joel M. Stoltzfus and Kenneth McIlroy, Eds., American Society for Testing and Materials, Philadelphia, 1991, pp. 463-474.

[34] Nihart, G. J., and Smith, C. P., "Compatibility of Metals with 7500 psi Oxygen," Report No, AD 608 260, conducted by Union Carbide Corporation, Linde Division, for Aerospace Medical Division, Wright Patterson Air Force Base, Ohio, October, 1964, 94 pages.

[35] Simon, W., "Studies on Combustibility and Ignitability of Metal Tubing in Stationary and Flowing Oxygen," *Verein Deutscher Eisenhunenleute Bericht,* No. 140, 1968, 116 pages.

[36] Simon, W., "The Inflammability and Combustibility of Metal Tubes in Quiet and Circulating Oxygen," *Stahl und Eisen,* Vol. 88, No. 2, 30 October 1968, pp. 1090-1097.

[37] Zawierucha, R., Drnevich, R. F., McIlroy, K., and Knecht, P., "Material Compatibility and System Considerations in Thermal EOR Environments Containing High Pressure Oxygen," SPE /DOE Paper 14922, SPE/DOE Fifth Symposium on EOR, Tulsa, Oklahoma, April, 1986, pp. 569-574 plus 7 pages of appendices.

[38] Zawierucha, R., McIlroy, K., Drnevich, R. F., and Dreisinger, D. R., "The Promoted Ignition Behavior of Engineering Alloys in High Pressure Oxygen," Canadian Western Region Conference, National Association of Corrosion Engineers, Calgary, Alberta, 25-28 Feb. 1986, 14 pages.

[39] Dean, L. E., and Thompson, W. R., "Ignition Characteristics of Metals and Alloys," *ARS Journal,* Vol. 31, No. 7, July 1961, pp. 917-923.

[40] Chafey, J. E., Witzell, W. R., and Scheck, W. G., "Titanium-Oxygen Reactivity Study,"

NASA Contract NAS 8-2664, NASA CR 518 48, General Dynamics AE 62-0674, NTIS N63 85627, July 1962, 61 pages.

[41] Rolsten, R. F., Hunt, H. H., and Wellnitz, "**Hypervelocity Impact on Pressurized Structures,**" General Dynamics Report AE62-0207, NTIS AD-660 566, January 1961, 55 pages.

[42] Holyer, N. F., "**Aluminum High Pressure Oxygen Cylinders,**" Safety Test Report 3505, British Oxygen Co., September 1964, 13 pages.

[43] Littman, F. E., and Church, F. M., "**Reaction of Metals with Oxygen and Steam,**" Final Report AECU 4092, February 1959, 21 pages.

[44] Tench, A. H., Roder, H. M., and Clark, A. F., "**Combustion of Metals in Oxygen, Phase II: Bulk Burning Experiments,**" Cryogenics Division, Institutes for Basic Standards, National Bureau of Standards, December, 1973, 45 pages.

[45] Monroe, R., Wren, J. E., and Bates, C. E., "**Structural Materials Evalaution for Oxygen Centrifugal Compressors,**" Project 3528, Report XXXVI, Dept. of Energy SORI-EAS-78-399, Southern Research Institute, Birmingham, Alabama. 1978, 226 pages.

[46] Fitt, P. W., Collings, N., and O'Neill, D., "**The Ignition of Solid Materials in Oxygen by Electric Sparks,**" Journal of Fire and Flammability, Vol. 4, July 1973, pp. 185-196.

[47] Brzustowski, T. A., and Glassman, I., "**Vapor-Phase Diffusion Flames in the Combustion of Magnesium and Aluminum - Part I,**" *Progress in Astronautics and Aeronautics*, 1964, pp. 75-117.

[48] Hartman, I., "**Explosion and Fire Hazards of Combustible Dusts,**" *Industrial Hygiene and Toxicology,*" Second Revised Ed., Chapter XVI, John Wiley and Sons, 1958, pp. 549-578.

[49] Kim, S., and Colver, G. M., "**Spark Ignition of Aluminum Powder in Mixtures of Oxygen, Nitrogen, and Carbon Dioxide-A New Testing Method**" HTD (ASME), 148 (Heat Mass Transfer Fires Combust. Syst.), 1990, pp. 97-104.

[50] Benz, F. J., and Stoltzfus, J. M., "**Ignition of Metals and Alloys in Gaseous Oxygen by Frictional Heating,**" *Flammability and Sensitivity of Materials in Oxygen-Enriched Atmospheres: Second Volume, ASTM STP* 910, M. A. Benning, Ed., American Society for Testing and Materials, Philadelphia, 1986, pp. 38-58.

[51] Stoltzfus, J. M., Homa, J. M., Williams, R. E., and Benz, F. J., "**ASTM Committee G-4 Metals Flammability Test Program: Data and Discussion,**" *Flammability and Sensitivity of Materials in Oxygen-Enriched Atmospheres: Third Volume, ASTM STP 986,* D. W. Schroll, Ed., American Society for Testing and Materials, Philadelphia, 1988, pp. 28-53.

[52] Bauer, H., Klein, G. K., Wegener, W., and Windgassen, K. F., "**Fire Tests on Centrifugal Pumps for Liquid Oxygen -- Part 2,**" *Cryogenics*, Vol. 11, 1971, pp. 469-476.

[53] Phillips, B R., and DeWitt, K. J., "**Resonance-Tube Ignition of Aluminum,**" *Combustion and Flame*, 35, 1979, pp. 249-258.

[54] Phillips, B. R., *Resonance-Tube Ignition of Metals,* Ph.D. Thesis, Universty of Toledo, July 1975, 198 pages.

[55] Benz, F. J., Williams, R. E., and Armstrong, D., "**Ignition of Metals and Alloys by High-Velocity Particles,**" *Flammability and Sensitivity of Materials in Oxygen-Enriched Atmospheres: Second Volume, ASTM STP 910,* M. A. Benning, Ed., American Society for Testing and Materials, Philadelphia, 1986, pp. 16-37.

[56] Drew, C. M., Gordon, A. S., and Knipe, R. H., "**Study of Quenched Aluminum Particle Combustion,**" *Progress in Astronautics and Aeronautics,* Vol. 15, 1963, pp. 17-39.

[57] Christensen, H. C., Knipe, R. H., and Gordon, A. S., "**Survey of Aluminum Particle Combustion,**" *Pyrodynamics,* Vol. 3, 1965, pp. 91-119.

[58] Kirschfeld, L., "**The Combustion Rate of Light-Metal Wires in Oxygen,**" *Metall,* Vol. 14, No. 3, 1960, pp 213-219.

[59] Kirschfeld, L., "**Combustion Rate of Light-Metal Wires in Oxygen High Pressures,**" *Metall,* Vol. 15, No. 9, 1961, pp. 873-878.

[60] Kirschfeld, L., "**Combustibility of Metals in Oxygen,**" From a lecture at Haus Der Technik, Essen, Federal Institute for Testing, Berlin-Dahlem, October, 27, 1960.

[61] Kirschfeld, L., "**Combustibility of Steel and Cast Iron in Oxygen at Pressures of Up to 150 Atmospheres,**" *Archiv. F. d. Eisenhüttenw,* Vol. 39, No. 7, 1968, P. 535-539.

[62] Long, G. H., and Sebald, H., "**The Burning Rate of Aluminum and Magnesium in Pure Oxygen and Oxygen Water Atmospheres at Higher Pressure,**" Western States

Combustion Institute, Preprint 68-8, April 1968, 67 pages.

[63] Sato, J., and Toshisuke H., "Behavior of Fire Spreading Along High-Temperature Mild Steel and Aluminum Cylinders in Oxygen," *Flammability and Sensitivity of Materials in Oxygen-Enriched Atmospheres: Second Volume, ASTM STP 910,* M. A. Benning, Eds, American Society for Testing and Materials, Philadelphia, 1986, pp. 118-134.

[64] Sato, J., "Fire Spread Rates Along Cylindrical Metal Rods in High Pressure Oxygen," *Flammability and Sensitivity of Materials in Oxygen-Enriched Atmospheres: Fourth Volume, ASTM STP 1040,* Joel M. Stoltzfus, Frank Benz, and Jack S. Stradling, Eds., American Society for Testing and Materials, Philadelphia, 1989, pp. 162-177.

[65] Kirshenbaum, A. D., *Fundamental Studies in New Explosive Reactions,* Office of Ordnance Research Contract DA-26-034-ORD-1489, The Research Institute of Temple University, April 30, 1956, 62 pages.

[66] Rozovskiy, A. S., Pleshakov, V. F., and Ivanov, B. A., "Detonation of Metal Powders in Oxygen," *Kislorodn. Prom-st.,* 4, January 1978, pp. 24-29.

[67] Austin, C. M., Roher, C. S., and Selfert, R. L., "Explosive Hazard of Aluminum-Liquid Oxygen Mixtures," *Journal of Chemical Education,* Vol. 36, No. 2, February 1959, pp. 54-57.

[68] Dunbobbin, B. R., Hansel, J. G., and Werley, B. L., "Oxygen Compatibility of High-Surface-Area Materials," *Flammability and Sensitivity of Materials in Oxygen-Enriched Atmospheres: Fifth Volume, ASTM STP 1111,* Joel M. Stoltzfus and Kenneth McIlroy, Eds., American Society for Testing and Materials, Philadelphia, 1991, pp. 338-353.

[69] Zawierucha, R., Million, J. F., Cooper, S. L., McIlroy, K., and Martin, J. R., "Compatibility of Aluminum Packing in Oxygen Environments Under Simulated Operating Conditions," *Flammability and Sensitivity of Materials in Oxygen-Enriched Atmospheres: Sixth Volume, ASTM STP 1197,* Dwight D. Janoff and Joel M. Stoltzfus, Eds., American Society for Testing and Materials, Philadelphia, 1993.

[70] Barthélémy, H., et al., "Compatibility of Aluminum Packing with Oxygen," *Flammability and Sensitivity of Materials in Oxygen-Enriched Atmospheres: Sixth Volume, ASTM STP 1197,* Dwight D. Janoff and Joel M. Stoltzfus, Eds., American Society for Testing and Materials, Philadelphia, 1993.

[71] Harrison, P. L. and Yoffee, A. D., "The Burning of Metals," *Proceedings of the Royal Society (London),* Series A, Vol. 261, pp. 357-370.

[72] Friant, C. W., "Determination of the Burning Rates of Small Diameter Aluminum Wires," M.S. Thesis, Virginia Polytechnic Inst., Blacksburg, VA, June 1964, 54 pages.

[73] Procter, W. L., and Long, C. H., "The Effect of Water Vapor Upon the Burning Rate of Aluminum and Magnesium Wires," Western States Section, Combustion Institute, Paper WSS-CI 66-4, Vol. 66, 1966, 35 pages.

[74] Benning, M. A., Zabrenski, J. S., and Le, N. B., "The Flammability of Aluminum Alloys and Aluminum Bronzes as Measured by Pressurized Oxygen Index," *Flammability and Sensitivity of Materials in Oxygen-Enriched Atmospheres: Third Volume, ASTM STP 986, D. W. Schroll, Ed.,* American Society for Testing and Materials, Philadelphia, 1988, pp. 54-71.

[75] Stoltzfus, J. M., These data are included in ASTM Standard G 94-90 Table X1.1.

[76] Steinberg, T. A., and Wilson, D. B., "The Burning of Metals and Alloys in Microgravity," *Combustion and Flame,* Vol. 88, 1992, pp. 309-320.

[77] Ivanov, B. A., and Ultanovam N. I., "Two Liquid Oxygen Explosions," *Fire Journal,* March, 1971, pp. 15-39.

[78] Dieguez, J., Botherel, L., De Lorenzo, A., and Faupin, A., "Ignition Testing of Hollow Vessels Pressurized with Gaseous Oxygen," *Flammability and Sensitivity of Materials in Oxygen-Enriched Atmospheres, Third Volume, ASTM STP 986,* D. W. Schroll, Ed., American Society for Testing and Materials, Philadelphia 1988, pp. 368-388.

[79] *The Welding Handbook, Eighth Edition, Volume 1,* Leonard P. Connor, Ed., American Welding Society, Miami, 1987, pp. 38,39.

[80] Cohn, J., "Fuse Member and Method of Making Same," *U. S. Patent 2,911,504,* Nov. 3, 1959, 3 pages.

[81] Dittrich, F. J., and Sheperd, A. P., "Flame-Spraying Exothermically Reacting Intermetallic Compound Forming Composites," *U. S. Patent 3,322,515,* U. S. Patent Office, May 30, 1967, 10 pages.

[82] Bretherick, L., *Bretherick's Handbook of Reactive Chemical Hazards, Fourth Edition,* Butterworth & Co., London, 1990, pp. 20-37, p. 23 (Al-Pd reactions), pp. 24-27 (Al-Halocarbon reactions).

[83] Bretherick, L., op. cit., pp. 30, referencing: Pittaluger, F. et al., *Termotechnica,* 1981, 25, pp. 332-334.

[84] Ehrenfeld, R. L. **"Polychlorotrifluoroethylene Oils as Industrial Lubricants,"** *Industrial and Engineering Chemistry,* Vol. 52, No. 2, February 1960, p. 65A.

[85] Armed Services Explosives Safety Board, **"Additional Information, Potential Incident, Report No. 38, Fluorolube - Detonation Point,"** November 6, 1967.

[86] Cutter, D. P., **"Reactions Between Halogenated Hydrocarbons and Metals - A Literature Review,"** *Journal of Hazardous Materials,* Vol. 17, Elsevier Science Publishers B. V., Amsterdam, 1987, pp. 99-108.

[87] Bouriannes, R., and Manson, N., **"Combustion of Aluminum in Pure Nitrogen,"** *Comptes Rendus de L'Academie des Sciences,* 1971, pp. 89-91.

[88] Long, G., **"Explosions of Molten Aluminum in Water - Cause and Prevention,"** *Metal Progress,* May 1957, pp. 107-112.

[89] Kuan, P., and Buescher, B. J., **"Ignition Threshold of Molten Aluminum in Water,"** *AIChE Symposium Series: Heat Transfer-Minneapolis 1991,* No. 283, Vol. 87, 1991, pp. 177-181.

[90] Nelson, L. S., Fuketa, T., Eatough, M. J., and Vigil, F. J., **"Steam Explosions of Single Drops of Molten Aluminum and 6061 Alloy,"** National Heat Transfer Symposium of Japan, May 30 - June 1, 1990, 12 pages.

[91] *Encyclopedia of Materials Science and Engineering - Supplementary Volume 2,* 1990, pp. 671-679.

[92] Jacoby, J. E., Ramser, R. A., **"Direct Chill Casting of Aluminum-Lithium Alloys,"** U. S. Patent 4,610,295, U.S. Patent Office, 1986.

[93] Page, F. M., Chamberlain, A. T., Grimes, R., **The Safety of Molten Aluminum-Lithium Alloys in the Presence of Coolants,"** 4th International Aluminum-Lithium Conference, G. Champier, B. Dubost, D. Miannay, and L. Sabetay, Eds., Editions de Physique, Les Ulis, France, 1987.

[94] Lowrie, R., **"Heat of Combustion and Oxygen Compatibility,"** *Flammability and Sensitivity of Materials in Oxygen-Enriched Atmospheres, ASTM STP 812,"* B. L. Werley, Ed., American Society for Testing and Materials, 1983, p. 84-96.

[95] Brewer, L., **"The Thermodynamic Properties of the Oxides and Their Vaporization Processes,"** *Chemical Reviews,* Vol. 52, 1953, pp. 1-75.

[96] Steinberg, T. A., Wilson, D. B., and Benz, F., **"The Combustion Phase of Burning Metals,"** *Combustion and Flame,* Vol. 91, 1992, pp. 200-208.

[97] Glassman, I., **"Combustion Fundamentals of Low Volatility Materials in Oxygen-Enriched Atmospheres,"** *Flammability and Sensitivity of Materials in Oxygen-Enriched Atmospheres: Fifth Volume, ASTM STP 1111,* Joel M. Stoltzfus and Kenneth McIlroy, Eds., American Society for Testing and Materials, Philadelphia, 1991, pp. 7-25.

[98] Glassman, I., American Rocket Society Preprint No. 938-59, New York, November, 1959, 43 pages.

[99] Mellor, A. M., **"Heterogeneous Ignition of Metals: Model and Experiment,"** Princeton University Department of Aerospace and Mechanical Sciences Report 816, NASA Grant NSG-641, Princeton University, Princeton, N. J., 1967, 362 pages.

[100] Glassman, I., Mellor, A. M., Sullivan, H. F., and Laurendeau, N. M., **"A Review of Metal Ignition and Flame Models,"** *NATO Adv. Grp. for Aerospace R&D Conference Proceedings, Paris,* Vol. 52, 1970, 39 pages.

[101] Laurendeau, N. M., and Glassman, I., *Combustion Science and Technology,* Vol.3, 1971, pp. 77-82.

[102] Monroe, R. W., Bates, C. E., and Pears, C. D., **"Metal Combustion in High- Pressure Flowing Oxygen,"** *Flammability and Sensitivity of Materials in Oxygen-Enriched Atmospheres: ASTM STP 812,* B. L. Werley, Ed., American Society for Testing and Materials, Philadelphia, 1983, pp. 126-149.

[103] Sircar, S., Gabel, H., Stoltzfus, J. and Benz, F., **The Analysis of Metals Combustion Using a Real-Time Gravimetric Technique,"** *Flammability and Sensitivity of Materials in Oxygen-Enriched Atmospheres: Fifth Volume, ASTM STP 1111,* Joel M. Stoltzfus and Kenneth McIlroy, Eds., American Society for Testing and Materials, Philadelphia, 1991, pp. 313-325.

[104] Zabrenski, J. S., Werley, B. L., and Slusser, J. W., **"Pressurized Flammability Limits of Metals,"** *Flammability and Sensitivity of Materials in Oxygen-Enriched Atmospheres: Fourth Volume, ASTM STP 1040,* Joel M. Stoltzfus, Frank J. Benz, and Jack. S. Stradling, Eds., American Society for Testing and Materials, Philadelphia, 1989, pp. 178-194.

[105] Steinberg, T. A., Wilson, D. B., and Benz, F. J., **"The Burning of Metals and Alloys in Microgravity,"** *Combustion and Flame,* Vol. 88, 1992, pp. 309-320.

[106] Mellor, A. M., and Glassman, J. A., **"A Physical Criterion for Metal Ignition,"** Western States Section, Combustion Institute, 1969 Fall Meeting, Preprint No. 64-20, October, 1964,

[107] Zabetakis, M. G., **"Flammability Characteristics of Combustible Gases and Vapors,"** *Bureau of Mines Bulletin 627,* U. S. Department of the Interior, Bureau of Mines, Washington, 1965, 121 pages.

[108] *Smithells Metals Reference Book, 6th Edition,* E. A. Brandes, Ed., Butterworths, London, 1983, pp. 8-54, 8-55.

[109] Stull, D. R., **"Vapor Pressure of Pure Substances,"** *Industrial and Engineering Chemistry,* Vol. 39, 1947, p. 517.

[110] Nesmeyanov, A. A., *Vapor Pressure of the Elements,* Academic Press, NY, 1963, pp. 29-33, 232-237, 415-426.

[111] Hultgren, R., Orr, R. L., Anderson, P. D., and Kelley, K. K., **"Selected Values of Thermodynamic Properties of Metals and Alloys,"** John Wiley and Sons, New York, 1963.

[112] Van Horn, K. R., **"Aluminum, Vol. 1, Properties, Physical Metallurgy and Phase Diagrams,"** American Society for Metals, 1967.

[113] von Wartenberg, H., **"Vapor Pressure of Metals. I.,"** *Z. Elektrochem.,* 19, 1913, pp. 482-489.

[114] Priselkov, Y. U., Yu, A., Sapozhnikov, and Tseplyaeva, A. V., **"Saturation Pressure of Aluminum Vapor,"** *Izv, Akad Nauk SSSR,* Otd Tekhn Nauk, Met i Toplivo, No. 1, 1959, pp. 106-109.

[115] Brewer, L., and Searcy, A. W., **"The Gaseous Species of the Aluminum-Alumina System,"** *Journal of the American Chemical Society,* 73, 1951, p. 5309.

[116] Johnson, R. G., Hudson, D. E., Caldwell, W. C, Spedding, F. H., and Savage, W. R., **"Mass Spectrometric Study of Phase Changes in Aluminum, Praseodymium, and Neodymium,"** *The Journal of Chemical Physics,* Vol. 25, No. 5, 1956, p. 917.

[117] Baur, E., and Brunner, R., **"Vapor-Pressure Measurements on High-Boiling Metals,"** *Helv. Chim. Acta,* 17, 1934, pp. 958-969.

[118] Glassman, I., **"Chapter Nine: Combustion of Nonvolatile Fuels: The Role of Gaseous Inert in Heterogeneous Diffusional Burning,"** *Combustion,* Academic Press, Inc., Harcourt Brace Jovanovich, Orlando, 1987, pp. 396-397.

[119] Glassman, I., and Law, C. K., **"Sensitivity of Metal Reactivity to Gaseous Impurities in Oxygen Environments,"** *Combustion Science and Technology,* Vol. 80, 1991, pp. 151-157.

[120] Lainoff, S. M., **"Potential for Catastrophic Rupture of Large Liquid Oxygen Storage Tanks,"** *Advances in Cryogenic Engineering, Vol. 27 - Proceedings of the Cryogenic Engineering Conference,* San Diego, Ca. August 11-14, 1981, Plenum Press, New York, 1982, pp. 953-961.

[121] National Traffic Safety Board, *Highway Accident Report: Liquified Oxygen Tank Truck Explosion Followed by Fires in Brooklyn, New York, May 30, 1970, Report NTSB-HAR-71-6,* May 12, 1971, 59 pages.

[122] Kilmartin, J., **Two Liquid Oxygen Explosions,"** *Fire Journal, March 1971, pp. 15-39.*

[123] Barthélémy, H., Delode, G., and Vagnard, G., **"Oxygen Compatibility of Pressure Regulators for Gas Cylinders,** *Flammability and Sensitivity of Materials in Oxygen-Enriched Atmospheres, ASTM STP 1040,* Joel M. Stoltzfus, Frank J. Benz, and Jack S. Stradling, Eds., American Society for Testing and Materials, Philadelphia, 1989, pp. 267-287.

Miscellaneous

Ulrich H. Koch[1]

OXYGEN SYSTEM SAFETY

REFERENCE: Koch, U. H., "Oxygen System Safety," Flammability and Sensitivity of Materials in Oxygen-Enriched Atmospheres: 6th Volume, ASTM STP 1197, Dwight D. Janoff and Joel M. Stoltzfus, Eds., American Society for Testing and Materials, Philadelphia, 1993.

ABSTRACT: This paper describes the hazards of high-pressure oxygen systems, lists five major causes of oxygen fires, and provides extensive references for additional information on the subject. The primary emphasis is on adiabatic compression, which has been identified as a significant but often overlooked cause of oxygen fires. The information contained in this paper was compiled from many sources; the author is not an oxygen safety expert or oxygen system design consultant. Oxygen users should obtain qualified professional assistance to establish design specifications and operating practices for the safe use of oxygen.

KEYWORDS: adiabatic compression, combustion, high-pressure oxygen, ignition, oxygen fires, oxygen service, oxygen system cleanliness, oxygen system design, oxygen system materials selection, oxygen system operating procedures, sonic velocity

OXYGEN

Pure oxygen is a colorless, odorless, and tasteless gas. It is the most abundant element, making up 21 % of the air we breathe and 55 % of the earth's crust. Oxygen supports plant and animal life. It also supports combustion, causes iron to rust, and corrodes most metals.

Oxygen has many commercial uses:

---

[1] Senior Engineer, Nupro Co., 4800 E. 345th St., Willoughby, OH 44094.

- Metals processing
  - Steelmaking
  - Flame cutting and welding
- Chemical processes
  - Synthetic gas, gasoline, methanol
  - Ammonia, aldehydes, alcohol, acetylene
  - Nitric acid, ethylene oxides, propylene oxides
  - Waste water treatment
- Life-support systems
  - SCUBA and deep-water diving
  - High-altitude flight
  - Anesthesiology
  - Firefighters
  - Ambulances

Production and Distribution

Cryogenically-produced oxygen is distilled in a five-step process in which air is:

- Filtered to remove dirt
- Compressed to high pressure
- Dried to remove water vapor
- Cooled to –160°C (–250°F) to liquefy it
- Distilled to separate each gas

The end products are oxygen, nitrogen, and inert gases, such as argon and neon. Ten grades of oxygen are produced, each to a specific purity level [*1*].

For high-volume bulk users, such as steel or chemical plants, the oxygen plant is adjacent to the user plant, and gas is delivered at low to medium pressures, usually 700 to 5500 kPa (100 to 800 psig). Cryogenic liquid oxygen also is delivered to large-volume users, who utilize storage tanks and equipment to vaporize, compress, and distribute the gas (Fig. 1).

FIG. 1—High-volume oxygen users buy the gas in bulk, storing it in an adjacent facility.

Most users buy oxygen in small amounts, 20 000-kPa or 2500-psig cylinders, and use it directly from the cylinders or through manifolds and a piping distribution system. Usually, the pressure is reduced with a regulator at the cylinder or manifold.

HAZARDS

How can oxygen be a hazard? It is all around us. It supports life and is used by hospitals to save lives. Oxygen supports combustion, but is not flammable by itself. Oxygen gas cylinders are labeled "oxidizer," but certainly do not carry a toxic warning label.

Despite its innocent appearance, oxygen is a serious fire hazard. It supports combustion, and pure oxygen makes everything burn faster and easier than it does in air.

One of the best introductions to this subject is the National Fire Protection Association Manual of Fire Hazards in Oxygen-Enriched Atmospheres (NFPA 53M). It is a concise, readable booklet that describes oxygen, its uses and hazards, design guidelines, aids to material selection, and over 100 references for more information. Chapter 3 presents more than 40 case studies of accidents caused by improper use of oxygen. Much of the material in this paper is drawn from that manual.

The major hazards of oxygen are summarized clearly in the NFPA standards Bulk Oxygen at Consumer Sites (NFPA 50), Oxygen-Fuel Gas Systems for Welding, Cutting and Allied Processes (NFPA 51), and Health Care Facilities (NFPA 99):

> Compatibility involves both combustibility and ease of ignition. Materials that burn in air will burn violently in pure oxygen at normal pressure and explosively in pressurized oxygen. Also many materials that do not burn in air will do so in pure oxygen, particularly under pressure. Metals for containers and piping must be carefully selected, depending on service conditions. The various steels are acceptable for many applications, but some service conditions may call for other materials (usually copper or its alloys) because of their greater resistance to ignition and lower rate of combustion.
>
> Similarly, materials that can be ignited in air have lower ignition energies in oxygen. Many such materials may be ignited by friction at a valve seat or stem packing or by *adiabatic compression* produced when oxygen at high pressure is rapidly introduced in a system initially at low pressure. (emphasis added)

CAUSES OF OXYGEN FIRES

Three elements are needed to create a fire: an oxidizer, fuel, and ignition. In ordinary situations, separating these three elements will prevent a fire. Oxygen systems are unique because the three elements are inseparable. The fuel—fittings, valves, and regulators—contains the oxygen and cannot be separated from it [2].

Oxygen fires need a source of ignition energy. And that energy can come from the compressed oxygen itself. When a gas flows from high to low pressure, it often reaches sonic velocity, usually at the seat of a valve or regulator. When the high-velocity gas stops at an obstruction, its temperature rises because of adiabatic compression, which occurs when gas is compressed so quickly that no heat is lost to the surroundings. The higher the initial pressure, the higher the temperature—see Table 1, condensed from ASTM Guide for Designing Systems for Oxygen Service (G 88). Anyone who has inflated a tire with a hand pump recognizes the effect: as the pressure rises in the tire, the pump gets hot. Diesel engines use the same principle. The pistons compress air in the cylinders to high pressure, the air gets hot, and injected fuel is ignited without a spark plug.

Adiabatic compression (Fig. 2) occurs in a piping system when a valve is opened and the high-velocity gas impacts at an obstruction—the next closed valve or regulator, an elbow or tee fitting, or a burr protruding into the gas stream. When that happens, the gas temperature can rise to well over 540°C (1000°F), as noted in ASTM Guide for Evaluating Nonmetallic Materials for Oxygen Service (G 63).

The gas temperature can reach the auto-ignition point of the metal and start a fire at a valve or fitting. Or the momentary heat can ignite plastics, organic contaminants, and small metal particles, while other dirt, scale, and particles become very hot. Such easily heated items act as kindling and help start a fire. ASTM G 63 contains a good technical discussion of ignition mechanisms.

Recognizing and identifying all such sources of ignition and possible causes of fire is not simple. However, ASTM G 88 summarizes the major causes of oxygen fires:

- System design errors
- Using the wrong metals
- Using the wrong plastics
- Dirty systems
- Unsafe operating procedures

TABLE 1--Theoretical Maximum Temperature Obtained When Compressing Oxygen Adiabatically from 20°C and 1 Standard Atmosphere

Final Pressure (absolute)		Final Temperature	
kPa	psi	°C	°F
690	100	234	453
6 895	1000	706	1303
13 790	2000	920	1688
27 579	4000	1181	2158
34 474	5000	1277	2330

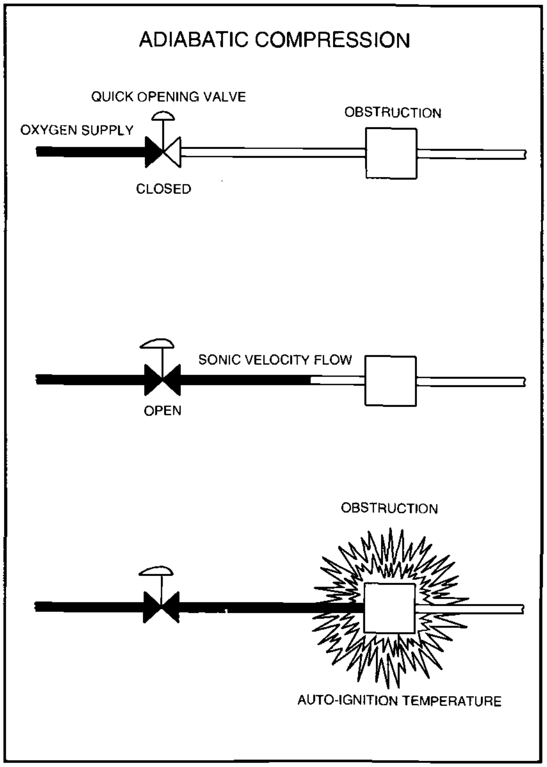

FIG. 2—Adiabatic compression can occur when oxygen under high pressure is released quickly into a low-pressure system. The gas flow can reach the speed of sound, and it if encounters an obstruction, the temperature can rise high enough to initiate ignition and cause a fire [2].

System Design

Oxygen systems require very careful and specialized design considerations. The references listed here are valuable guides, but are not handbooks. There are no textbooks, handbooks, or national codes that teach how to design oxygen systems. However, the ASTM G 4 Committee Standards Technology Training course Controlling Fire Hazards in Oxygen Handling Systems teaches the fundamentals of oxygen safety for oxygen process designers and equipment specifiers.

Excellent advice, which applies to all of these references, is given in a Linde publication [*3*]:

> This publication is not a design handbook and does not relieve the user from exercising competent engineering judgment or using *qualified professional personnel* who can tailor your design to your specific situation.
>
> In situations where qualified people are not available locally to design the system, *obtain professional assistance from a competent source.* If the oxygen supplier cannot offer assistance, he should be able to direct you to a consultant who can provide the necessary service. Remember that design of oxygen systems requires specialized knowledge. *Liability problems associated with improperly designed systems can far outweigh the cost of professional services.* (emphasis added)

In brief, the first and most important rule for safety in the use of oxygen is: **Consult an expert.**

ASTM G 88 describes an expert in this way:

> *Qualified technical personnel*—persons such as engineers and chemists who, by virtue of education, training, or experience, know how to apply physical and chemical principles involved in the reactions between oxygen and other materials.

Oxygen fire prevention starts with system design. Size piping to prevent high velocity and avoid abrupt size changes. Locate obstructions such as tees, elbows, valves, and regulators away from sources of velocity (ASTM G 88). Choose materials carefully (ASTM G 63). Carefully control construction practices such as cleaning, welding, and assembly (ASTM Practice for Cleaning Methods for Materials and Equipment used in Oxygen-Enriched Environments; G 93, and [*4*]).

Valve selection requires special care. Safety guidelines from Compressed Gas Association Industrial Practices for Gaseous Oxygen Transmission and Distribution Piping Systems (CGA G-4.4), ASTM G 88, and NFPA 51 unanimously emphasize that *valves must be opened slowly.* Opening speed is controlled by valve design, as well as operating procedures. Ball, plug, and butterfly valves are used in some low-pressure systems such as pipelines, because their straight-through design provides a lower pressure drop than a globe valve. However, full-flow valves are quick opening and create high velocity when opened. The piping system must be designed carefully to equalize the pressure across the valve before it is opened. There is no single, simple technique for designing safe systems and preventing oxygen fires. The best way to take on such a task is to remember the second rule for oxygen safety: **Consult an expert.**

Metals Selection

All common metals will burn in pure oxygen. The most familiar example is cutting steel with an oxygen torch. A torch heats the steel, and then a stream of oxygen ignites it. The heat of the burning steel continues the cutting action. The same process can happen accidentally in improperly designed oxygen piping systems (Fig. 3).

NFPA 51 and CGA G-4.4 recommend steel or stainless steel for oxygen systems, but only provide guidance for pressures up to 6900 kPa (1000 psig) or less. Further, in regions of high velocity or impingement, such as valves, orifices, branch connections, and other critical areas, copper and nickel-based alloys (brass and Monel®[2] Alloy 400) are recommended.

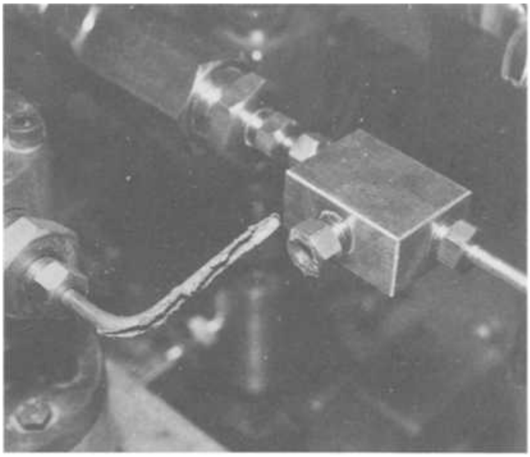

Photo courtesy NASA White Sands Test Facility, Las Cruces, NM

FIG. 3—Adiabatic compression initiated the oxygen fire that burned out this stainless steel tubing [2].

For operating pressures above 6900 kPa, CGA G-4.4 makes no general recommendations. Such systems are encountered infrequently; CGA G-4.4 recommends asking the oxygen supplier to provide specific guidance.

ASTM Guide for Evaluating Metals for Oxygen Service (G 94) provides extensive data on metal ignition in oxygen, guidance for metals selection, and several practical examples.

Non-Metals Selection

Most non-metals burn in pure oxygen, usually violently. They ignite more easily than metals and become the kindling chain that ignites the system. Also, most non-metals produce toxic gases when they decompose, which can contaminate breathing gas systems even if there is no external fire (ASTM G 63). These materials include the many polymers and elastomers used as seats, stem tips, packings, gaskets, and seals in valves, regulators, meters, and most other piping components. Chapter 5 of NFPA 53M describes the ignition and combustion properties of materials commonly used in oxygen-enriched atmospheres. No material should be used until it has been tested and proven safe for oxygen service.

ASTM G 63 presents an excellent systematic approach to selecting non-metallic materials, with numerous practical examples. It includes a compilation of test data for many

---

[2] Monel—Trademark Inco Alloys International, Huntington, WV.

non-metallic materials frequently employed in oxygen service. Teflon®[3] and Kel-F®[4] are listed by CGA G-4.4 as suitable for oxygen service and are often used in valves as seats, stem tips, packings, gaskets, and as a pipe thread sealant. Yet, even these materials will begin to decompose at 200 to 300°C (400 to 600°F) and will ignite at higher temperatures (Fig. 4).

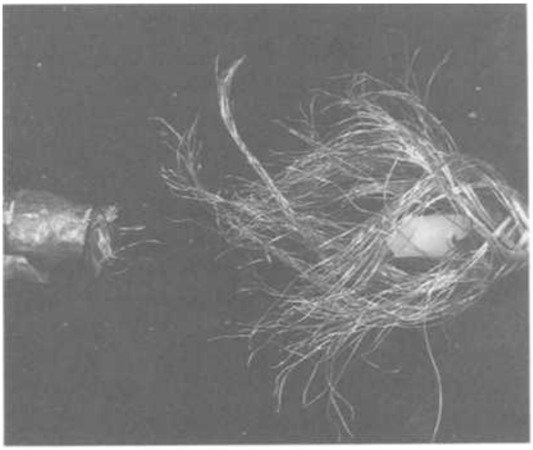

Photo courtesy NASA White Sands Test Facility, Las Cruces, NM

FIG. 4—Even PTFE-lined hose can ignite and burn violently at the temperatures generated by adiabatic compression [*2*].

As emphasized in ASTM G 63, the successful use of even the best materials depends on the design of the component. For example, PTFE-lined flexible hose has a large surface area-to-mass ratio, and many instances involving the ignition of such hoses have been reported and investigated. Safe use of PTFE-lined hose in high-pressure oxygen requires special provisions in the system design [*5*].

Several halogenated oils and greases have been tested successfully for oxygen service. ASTM G 63 includes test data on many lubricants, thread compounds, seats, and gaskets; a Linde publication [*3*] lists lubricants found suitable for low-pressure systems.

Graphite materials such as Grafoil®[5] are used as high-temperature stem packings and gaskets. Being pure carbon, they will oxidize in an oxygen-enriched atmosphere. The packing manufacturer should be consulted about specific oxygen system applications.

Oxygen System Cleanliness

Careful cleaning is essential to prevent oxygen fires (ASTM G 88, ASTM G 93, [*4*]). Organic contaminants and fine particles burn violently in pure oxygen and are the beginning of the kindling chain that starts a fire. How should a system be cleaned? When is it clean enough? ASTM G 93, CGA Cleaning Equipment for Oxygen Service (G-4.1), NFPA, and oxygen producers [*4, 6*] provide cleaning procedures, guides, and specifications.

ASTM G 93 provides special guidance for cleaning components:

> 6.1 *Disassembly:*
>
> 6.1.1 It is imperative that oxygen systems be cleaned as individual articles, preferably prior to assembly. Assembled systems *must be disassembled* for

---

[3] Teflon—Trademark DuPont Co., Wilmington, DE.

[4] Kel-F—Trademark 3M Co., St. Paul, MN.

[5] Grafoil—Trademark Union Carbide Co., Danbury, CT.

> cleaning if construction permits. Flushing an assembled system can deposit and concentrate contaminants in stagnant areas....
>
> 6.1.2 Manufactured products (for example, valves, regulators, and pumps) should preferably be *cleaned by the manufacturer* prior to final assembly and test.... The purchaser should approve the cleaning procedure and packaging to assure that they satisfy the system requirements....
>
> 6.1.3 Manufactured products that are cleaned by the purchaser *must be disassembled* for cleaning if construction permits. The purchaser should follow the manufacturer's instructions for disassembly, inspection for damage, reassembly, and testing.
>
> 6.3 *Lubricants:*
>
> 6.3.1 Mechanical components are normally assembled with lubricants on seals, threads and moving surfaces. The manufacturer should be consulted to determine the kind of lubricant originally used on the article to assure that the cleaning solutions and methods selected are effective in removing the lubricant and will not damage the component.
>
> 6.3.2 *Oxygen-compatible lubricants* should be selected in accordance with Guide G 63. The component manufacturer should also be consulted to ensure that the selected lubricant provides adequate lubrication for component performance. Oxygen-compatible lubricants often have markedly different lubricating properties from conventional lubricants. (emphasis added)

ASTM G 93 contains much additional information on cleaning methods, hindrances to effective cleaning, packaging, and inspection, including specific applications examples.

Operating Procedures

The most often neglected part of system design is how the system will be operated. Oxygen fires frequently are caused by system designs that invite operator errors. In one instance, an operator opened a ball valve on a high-pressure manifold by mistake when the system was at low pressure. The impact of the high-velocity oxygen at a tee ignited the system, violently burning the stainless steel tubing and fittings [*2*].

Another example of simple operator error: normal operating procedure required the operator to open a ball valve placed between a cylinder and a regulator first, then to turn on the oxygen with a slow-opening cylinder valve (Fig. 5). By mistake, the operator opened the cylinder valve first, then the ball valve, suddenly releasing high-pressure oxygen into a very small empty space. The adiabatic compression of the oxygen generated very high temperatures, which ignited the regulator. The system design allowed a simple operator error to cause a very serious fire [*2*].

Thorough planning and careful monitoring of operating procedures are important in oxygen fire prevention. However, safe operation should be engineered into the design of an oxygen system—with the selection and placement of valves, for example—and not rely strictly on operator compliance with procedures to prevent oxygen fires [*2*].

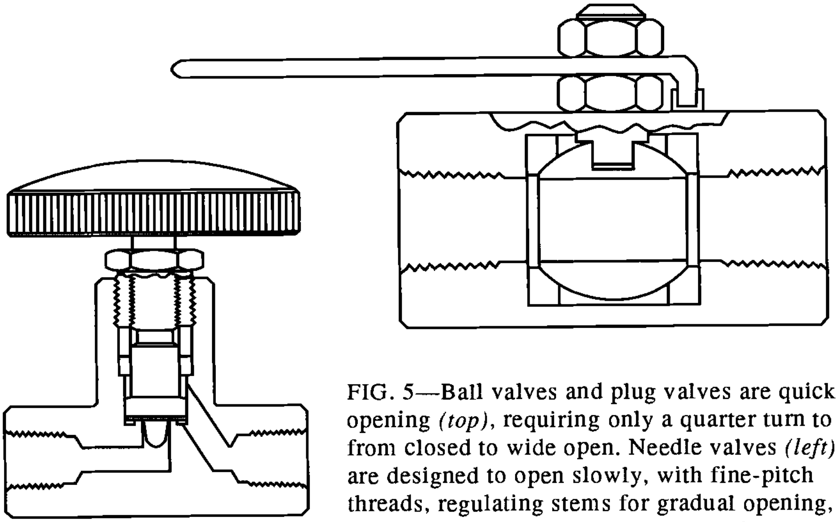

FIG. 5—Ball valves and plug valves are quick opening *(top)*, requiring only a quarter turn to go from closed to wide open. Needle valves *(left)* are designed to open slowly, with fine-pitch threads, regulating stems for gradual opening, and soft seats for gas-tight shut-off [*2*].

PRODUCT SELECTION

Most fluid system components—particularly industrial valves and fittings—are not designed for specific applications. Rather, they are versatile, general-purpose products that can be used properly in many types of applications and systems. The component manufacturer has neither the experience nor the expertise in all possible applications to select the most appropriate components for a specific use, such as an oxygen system. Only the oxygen system designer has full knowledge of the entire system and each component's function; these factors must be considered when selecting a valve or fitting. Oxygen system designers and users are responsible for product function, material compatibility, adequate ratings, and proper installation, operation, and maintenance.

ADDITIONAL INFORMATION

Much useful information is contained in the following standards and specifications:

ASTM D 2512 Test Method for Compatibility of Materials with Liquid Oxygen (Impact Sensitivity Threshold and Pass-Fail Techniques)

ASTM D 2863 Test Method for Measuring Minimum Oxygen Concentration for Candle-Like Combustion of Plastics (Oxygen Index)

ASTM D 4809 Test Method for Heat of Combustion of Liquid Hydrocarbon Fuels by Bomb Calorimeter (Intermediate Precision Method)

ASTM G 72 Test Method for Autogenous Ignition Temperature of Liquids and Solids in a High-Pressure Oxygen-Enriched Environment

ASTM G 74 Test Method for Ignition Sensitivity of Materials to Gaseous Fluid Impact

ASTM G 86 Test Method for Determining Ignition Sensitivity of Materials to Mechanical Impact in Pressurized Oxygen Environments

American Welding Society C-4.2 Operator Manual for Oxy-fuel Gas Cutting

CGA E-2 Hose Line Check Valve Standards for Welding and Cutting

CGA G-4 Oxygen

CGA G-4.3 Commodity Specification for Oxygen

CGA P-14 Accident Prevention in Oxygen-Rich and Oxygen-Deficient Atmospheres

CGA P-2.5 Transfilling of High Pressure Gaseous Oxygen Used for Respiration

CGA TB-3 Hose Line Flashback Arresters

NFPA 51B Cutting and Welding Processes

Underwriters Laboratories (UL) 252 Compressed Gas Regulators

UL 407 Manifolds for Compressed Gases

Many other sources of additional information are also available [7-27].

CITED REFERENCES

[*1*] *Handbook of Compressed Gases,* 3rd edition, Compressed Gas Association, Inc. (CGA), Arlington, VA, 1989.

[*2*] ASTM Video G 4-12-700880-31 Oxygen Safety, 1988.

[*3*] "Guidelines for Design and Installation of Industrial Gaseous Oxygen Distribution Piping Systems," L-5110N, Union Carbide Industrial Gases, Inc., Danbury, CT, 1985.

[*4*] IGC 33/86/E Cleaning of Equipment for Oxygen Service, Industrial Gas Committee (IGC), Paris, France.

[*5*] Barthelemy, H. and Vagnard, G., "Ignition of PTFE-Lined Hoses in High-Pressure Oxygen Systems: Test Results and Considerations for Safe Design and Use," *Flammability and Sensitivity of Materials in Oxygen-Enriched Atmospheres, Vol. 3, STP 986,* D.W. Schroll, Editor, ASTM, 1988.

[*6*] "Cleaning," GS-38, Union Carbide Industrial Gases, Inc., Danbury, CT, 1981.

[7] "Gaseous Oxygen," Safetygram 1, Air Products and Chemicals, Inc., Allentown, PA, 1991.

[*8*] "Liquid Oxygen," Safetygram 6, Air Products and Chemicals, Inc., Allentown, PA, 1989.

[*9*] *Flammability and Sensitivity of Materials in Oxygen-Enriched Atmospheres, STP 812,* B.L. Werley, Editor, ASTM, 1983.

[*10*] *Flammability and Sensitivity of Materials in Oxygen-Enriched Atmospheres, Vol. 2, STP 910,* M.A. Benning, Editor, ASTM, 1986.

[*11*] *Flammability and Sensitivity of Materials in Oxygen-Enriched Atmospheres, Vol. 4, STP 1040,* J.M. Stoltzfus, F.J. Benz, and J.S. Stradling, Editors, ASTM, 1989.

[*12*] *Flammability and Sensitivity of Materials in Oxygen-Enriched Atmospheres, Vol. 5, STP 1111,* J.M. Stoltzfus and K. McIlroy, Editors, ASTM, 1991.

[*13*] CGA Video AV-8 Characteristics and Safe Handling of Cryogenic Liquid Gaseous Oxygen.

[*14*] "Loss Prevention Data, Oxygen," Data Sheet 7-52, Factory Mutual Engineering Corp., Norwood, MA 02062, 1975.

[*15*] IGC 5/75/E Code of Practice for Supply Equipment and Pipelines Distributing Non-Flammable Gases and Vacuum Services for Medical Purposes, IGC, Paris, France.

[*16*] IGC 6/77 Oxygen Fuel Gas Cutting Machine Safety, IGC, Paris, France.

[*17*] IGC 8/76/E Prevention of Accidents Arising from Enrichment or Deficiency of Oxygen in the Atmosphere, IGC, Paris, France.

[*18*] IGC 10/81/E Reciprocating Compressors for Oxygen Service, IGC, Paris, France.

[*19*] IGC 12/80/E Pipelines Distributing Gases and Vacuum Services to Medical Laboratories, IGC, Paris, France.

[*20*] IGC 27/82/E Turbo Compressors for Oxygen Service, Code of Practice, IGC, Paris, France.

[*21*] "Design Guide for High Pressure Oxygen Systems," N8332990, National Technical Information Service (NTIS), Springfield, VA, 1983.

[*22*] "ASRDI Oxygen Technology Survey, Vol. IX: Oxygen Systems Engineering Review," NASA SP-3090, NTIS, Springfield, VA, 1978.

[*23*] "Safety and Health in Arc Welding and Gas Cutting and Welding," PB83-174920, NTIS, Springfield, VA, 1978.

[*24*] "Material Safety Data Sheet for Liquid Oxygen," L-4637B, Union Carbide Industrial Gases, Inc., Danbury, CT, 1985.

[*25*] "Material Safety Data Sheet for Gaseous Oxygen," L-4638A, Union Carbide Industrial Gases, Inc., Danbury, CT, 1985.

[*26*] "Precautions and Safety Practices for Gas Welding, Cutting and Heating," L-2035JJ, Union Carbide Industrial Gases, Inc., Danbury, CT, 1990.

[*27*] "Safety Precautions for Oxygen, Nitrogen, Argon, Helium, Carbon Dioxide, Hydrogen, Acetylene, FG-2, Ethylene Oxide, Sterilant Mixtures and Specialty Gases," L-3499H, Union Carbide Industrial Gases, Inc., Danbury, CT, 1988.

James A. Daniel,[1] Rollin C. Christianson,[1] Joel M. Stoltzfus,[2] and
Michelle A. Rucker[2]

A HAZARDS ANALYSIS METHOD FOR OXYGEN SYSTEMS INCLUDING SEVERAL CASE STUDIES

REFERENCE: Daniel, J. A., Christianson, R. C., Stoltzfus, J. M., and Rucker, M. A., "A Hazards Analysis Method for Oxygen Systems Including Several Case Studies," Flammability and Sensitivity of Materials in Oxygen-Enriched Atmospheres: 6th Volume, ASTM STP 1197, Dwight D. Janoff and Joel M. Stoltzfus, Eds., American Society for Testing and Materials, Philadelphia, 1993.

ABSTRACT: Oxygen systems and components have hazards associated with the ignitability and flammability of the constituent materials. The NASA Johnson Space Center White Sands Test Facility developed a method for analyzing the hazards of oxygen systems and components. Using this method, material flammability and the risks associated with various ignition modes were addressed. In addition, secondary hazards, such as those caused by seal leakage and the formation of oxygen-enriched environments exterior to pressure-retaining components were addressed. This hazards analysis method is presented as a systematic investigation tool and as a means of training individuals on the nature and level of severity of oxygen-enriched combustion. Three case studies drawn from work performed at the NASA Johnson Space Center White Sands Test Facility are presented. These case studies were conducted on a space flight component, an aircraft flight system, and a facility installation.

KEYWORDS: hazards analysis, flammability, oxygen, oxygen systems,

Fires occur in oxygen systems, therefore, safety at all phases of oxygen system design and operation must be evaluated. These fires may be characterized by rapid combustion and extreme temperatures which can be hazardous to personnel and equipment. Oxygen system safety can be enhanced by proper design to minimize the severity of the environment, proper materials selection to withstand the severe environment, and proper system operation to reduce risk during system operation.

Systematic prevention of oxygen system fires through careful design represents a front-line defense against catastrophic, life-threatening system failures. Detailed designs of oxygen systems and safe operating procedures are found in the ASTM Standard Guide for Designing Systems for Oxygen Service (G 88), *Design Guide for High-Pressure Oxygen Systems* [1], and "Techniques Employed by the NASA White Sands Test Facility to Ensure Oxygen System Component Safety" [2].

---

[1] Principal Engineer, Lockheed-ESC, White Sands Test Facility, P. O. Drawer MM, Las Cruces, NM 88004.

[2] Aerospace Technologist, NASA, White Sands Test Facility, P. O. Drawer MM, Las Cruces, NM 88004.

Proper materials selection for use in an oxygen system requires balancing operational requirements such as operating temperature, ease of assembly, and pressure sealing capability with material compatibility. Some materials are more compatible with oxygen than others. For example, nickel-copper alloys (such as Monel) are more burn-resistant [3,4], more resistant to ignition by particle impact [5,6], and more resistant to ignition by friction [7] than aluminum. Likewise, polytetrafluorethylene (PTFE), such as Teflon®, is a more oxygen-compatible soft good than silicone, because PTFE has a higher oxygen index [8], lower heat of combustion [9], higher autogenous ignition temperature (G 63), and a greater resistance to ignition by mechanical impact [10,11] and gaseous impact [12,13] than silicone. Guidelines on selecting materials for oxygen systems are found in ASTM Standard Guide for Evaluating Nonmetallic Materials for Oxygen Service (G 63) and ASTM Standard Guide for Evaluating Metals for Oxygen Service (G 94). Materials should be chosen based on compatibility for specific modes of operation.

Operational procedures for an oxygen system can enhance or defeat all efforts to select suitable materials and the use of prudent design practices. Maintaining system cleanliness is a typical operational procedure that can improve system safety. A well-designed system using compatible materials may be hazardous if not properly cleaned.[3] Guidelines for selecting methods and apparatus for cleaning oxygen equipment can be found in ASTM Standard Practice for Cleaning Methods for Material and Equipment Used in Oxygen-Enriched Environments (G 93), NFPA 50 Bulk Oxygen Systems (NFPA 50), *Oxygen* [14], and *Industrial Practices for Gaseous Oxygen Transmission and Distribution Piping Systems* [15].

The NASA Johnson Space Center White Sands Test Facility (WSTF) designs, builds, operates, and analyzes oxygen systems that have extreme operation requirements such as pressures from vacuum to 94.8 MPa (13 750 psi), temperatures from cryogenic to 538° C (1 000° F), and flow rates to 3.6 kg/s (8 lbm/s).

Based on operational experience and the reference literature, WSTF developed a method for systematic hazards analysis of oxygen components and systems. While the oxygen hazards analysis method incorporates methods similar to those found in ASTM G 88, G 63, G 94, and G 93, this method provides an alternate, faster approach to analyzing the hazards of oxygen systems. The approach can be applied to components and systems alike and can be modified to incorporate a wide range of oxygen system safety issues. This paper presents the WSTF oxygen hazards analysis method and provides case studies of its application, including a space flight component, an aircraft flight system, and a facility installation.

ANALYTICAL METHOD

The method used to perform oxygen hazards analyses at WSTF is outlined in the order that work is performed (Fig. 1).

1. Scope of Investigation

As with any project, the scope must be defined to include the available cost, manpower requirements, and schedule for completion. This scope will be used by the investigators to determine the level of detail to be used in the investigation. The analysis, using this method, can be performed at the system level, component level, and

---

[3] Incident Report on Mechanical Impact Test System Fire, Building 800, Test Cell 104, NASA Johnson Space Center White Sands Test Facility.

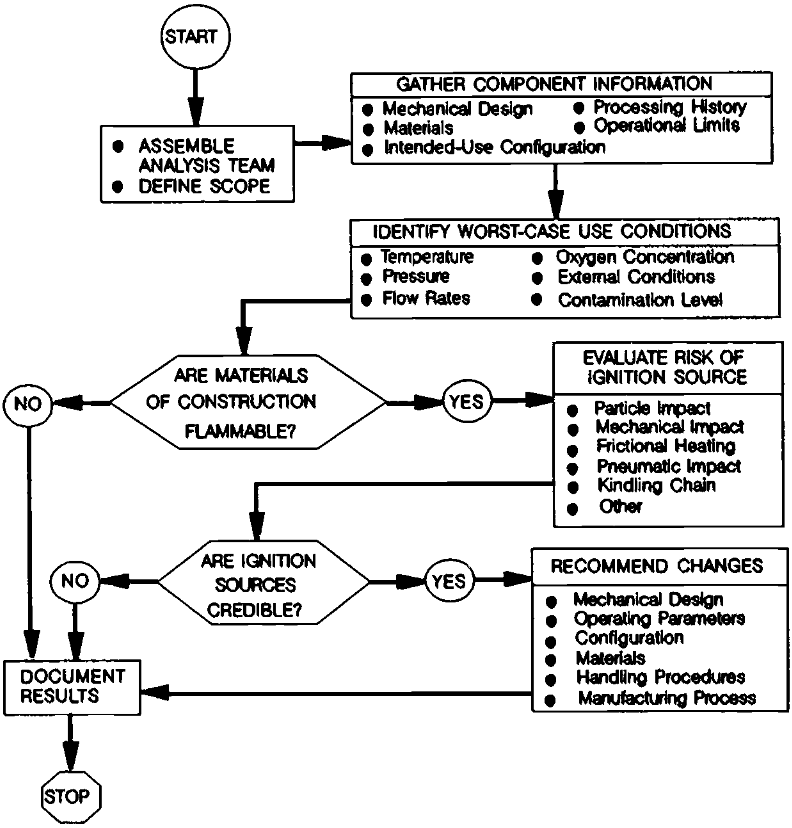

FIG. 1--Flow chart of analytical method.

individual part level. The more specific and detailed the investigation, the more useful the analysis will become.

2. Information on Components

Detailed information must be supplied for all components. Pressure ratings, temperature ratings, operating characteristics (such as relief pressures and maximum flow rates) component materials, coatings, lubricants, and processing history are identified.

The component information is necessary for two reasons. First, incorrect use of components can be hazardous. Second, materials are often flammable in oxygen-enriched environments. A cognizant choice of ignition-resistant materials coupled with a minimizing of ignition sources is critical.

Basic Functionality--Components are often selected on the basis of their pressure ratings. However, other limitations are important to consider. These limitations include maximum and minimum temperature ratings that ensure proper performance of soft goods and adequate combinations of strengths and ductility for metals. Flow capacity through components is used for determining fluid and particulate velocities. By determining the velocities, the risk of particle-impact ignition can be evaluated. A review of past operational history should be compiled for all components to eliminate any equipment which has suspect reliability. **Caution must be taken not to assume that the absence of past problems equates to oxygen compatibility.** Fortunate circumstances and the statistical nature of flammability and ignitability may have been the only reason that serious accidents have not occurred.

Configuration and Environment--Most oxygen systems are part of a larger system such as an aircraft, a spacecraft, or a facility. If a section of the oxygen system burns, other systems may be affected. These ancillary effects range from minor to catastrophic and must be considered in the course of the analysis.

Oxygen Compatibility--Thorough descriptions of the materials of construction are critical in conducting an oxygen hazards analysis. Material compatibility is important for all fluid handling systems, but with oxygen, the issue of compatibility is not simply corrosion or degradation of performance. Materials incompatibility includes the possibility of combustion of pressure-retaining parts and associated rapid venting of fluids and combustion products at extreme temperatures. Exposure to combustion in oxygen-enriched environments can be very serious to personnel and equipment. Because of the critical nature of materials compatibility, all aspects of materials processing, such as heat treating, strengths, ductility, hardness, coatings, platings, and lubricants are important for a thorough investigation. Adherence to cleanliness specifications throughout the maintenance life of the components must be considered.

3. Operating Parameters

Detailed information on all operating parameters must be supplied. This information should include realistic worst-case operating pressure, temperature, flow rates, oxygen concentration, ambient conditions, and other pertinent information. All equipment must be designed and tested to ensure that it will function safely and reliably at the extremes of anticipated operating conditions and at proof-test conditions.

4. Materials of Construction

The flammability of the materials of construction can be determined by referring to data from promoted combustion [3] and oxygen index [8] tests.

Recent investigations have produced large materials ignition and combustion data bases for polymers and metals. Data bases are maintained by WSTF, ASTM, and materials suppliers. These data bases are essential for determining the suitability of materials usage. The most preferred material is one that is not flammable over the full range of operations. However, materials can be used successfully, even though they are flammable, if the risk of ignition sources is low. The hazards analysis matrix (Fig. 2) reflects the hazards and their effects. If the materials data bases show that a material is not flammable, then the oxygen hazards are greatly reduced, and the investigation process is simplified.

Polymers--Polymers in 100-percent oxygen are flammable under most conditions. Although viewed as relatively inert in many ways, silicones are easily ignited and produce high heats of combustion, which may be sufficient to ignite metals and expand the extent of any reaction. PTFE's are the preferred soft goods because of their reduced ignition susceptibility and low heats of combustion.

Metals--Special care must be taken in evaluating metals ignition susceptibility. Ignition thresholds vary with ignition modes. For example, if a component part is subjected to friction, then the ignition data for frictional heating must be reviewed. Data for other ignition modes cannot be substituted. Ignition potentials must be considered for each ignition mode, and parts are often at risk for multiple ignition modes.

5. Ignition Sources

To determine if ignition sources exist, contamination, configurations [1], and operating procedures need to be evaluated. If investigators cannot ensure documented and sufficient ignition safety factors based on realistic extreme operating conditions, then the material should be considered flammable for the following ignition modes. These ignition modes are included in the hazards analysis matrix (Fig. 2) to ensure systematic review.

A component in an oxygen system can be ignited only if it is subjected to sufficient energy to initiate and sustain the combustion reaction. Oxygen systems may generate sufficient ignition energy through several means:

A. Particle Impact--If flow velocities are greater than 50 m/s (164 ft/s), ignition by particle impact is plausible.

B. Frictional Heating--If parts are sliding past one another, check data on materials for susceptibility to frictional (rubbing) heating and ignition in oxygen.

C. Mechanical Impact--Most polymers and many metals can be ignited when wetted by liquid or gaseous oxygen and mechanically impacted.

D. Pneumatic Impact--Fast acting valves (such as quarter-turn ball valves) can be manually opened (or closed) to adiabatically compress oxygen to high temperature. This phenomenon has been demonstrated to ignite polymers but not to ignite metals.

E. Kindling Chain and Heat of Combustion--Easily ignited parts of an oxygen system, such as polymers, may ignite and provide sufficient heat of combustion energy to cause ignition of adjacent components.

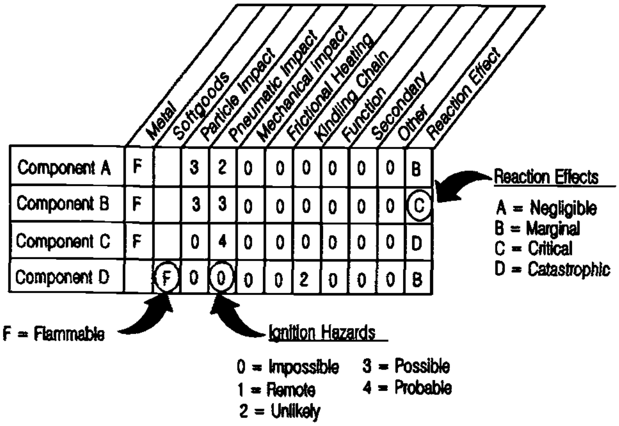

	Metal	Softgoods	Particle Impact	Pneumatic Impact	Mechanical Impact	Frictional Heating	Kindling Chain	Function	Secondary	Other	Reaction Effect
Component A	F		3	2	0	0	0	0	0	0	B
Component B	F		3	3	0	0	0	0	0	0	C
Component C	F		0	4	0	0	0	0	0	0	D
Component D		F	0	0	0	0	2	0	0	0	B

Reaction Effects

A = Negligible
B = Marginal
C = Critical
D = Catastrophic

F = Flammable

Ignition Hazards

0 = Impossible
1 = Remote
2 = Unlikely
3 = Possible
4 = Probable

FIG. 2--Typical hazards analysis matrix.

Polymeric seals provide the most common source for kindling chain ignition.

F. Other sources of ignition

1. Electrical arc/spark
2. Overheating
3. Resonance
4. Rupture/fresh metal exposure
5. Unique situations or system configurations

6. Secondary Hazards

Whether or not a component is considered at risk for ignition, secondary hazards must be addressed. For example, components can fail under normal operating conditions in many ways. These failures may be standard maintenance issues for benign fluids, but the failures may be critical when oxygen is involved. A common secondary consideration includes external fluid leakage because of seal degradation. The magnitude of fluid leakage must be considered along with the proximity of the leakage to ignition sources which would not normally be included in hazards assumptions. For example, oxygen leaking into a confined electrical control box may subject the apparatus to possible ignition from electrical arcs where materials were not selected for oxygen compatibility. In addition, if structural integrity may be compromised through off-limit handling, the effects must be considered.

7. Risk Assessment of Reaction Effects

If failures occur and result in oxygen-enriched combustion, both personnel and equipment may be at risk. Since the purpose of performing a hazards analysis is to reduce this risk, it is important to assess the outcome of a failure. After this analysis is performed, a determination of the acceptability of the potential risk must be made. For each case, these risks are designated A, B, C, and D. If the level of risk is unacceptable, the hazards analysis matrix (Fig. 2) provides the tool to identify specific items which must be corrected. After risks to personnel and equipment have been evaluated, new components will be selected, redesigned, or otherwise corrected.

8. Documentation for Hazards Analysis

The hazards analysis process is an extremely beneficial tool to ensure personnel and equipment safety, and therefore must be documented. Because system or component changes will invariably arise, another hazards review will be needed when changes occur to ensure that components are not assumed to be safe. Substitution of components can also create new hazards that must be evaluated.

CONCLUSIONS

Oxygen system safety is the goal of this hazards analysis method. This method provides oxygen system designers and users a systematic basis for risk assessment and reduction, improved system or component design, and increased operational safety.

CASE STUDIES

Case 1. Extended Duration Orbiter (EDO) Cryogenic Oxygen Shutoff Valve

Background--WSTF was asked to evaluate oxygen hazards associated with a shutoff valve used on an extended duration orbiter (EDO) life-support system. The valve was of particular concern because it is cycled between high-temperature gaseous oxygen and low-temperature cryogenic oxygen.

Analysis--An analysis team, consisting of materials and mechanical design experts, reviewed the EDO cryogenic oxygen shutoff valve schematic (Fig. 3), materials of construction, and configurational-use information. The analysis team determined the valve's most severe operating conditions to be 7.24 MPa (1 050 psi), at 65° C (150° F), in commercially pure oxygen. However, the valve was also periodically exposed to cryogenic oxygen at -183° C (-297° F). Under these operating conditions, the team determined that the majority of both metals and

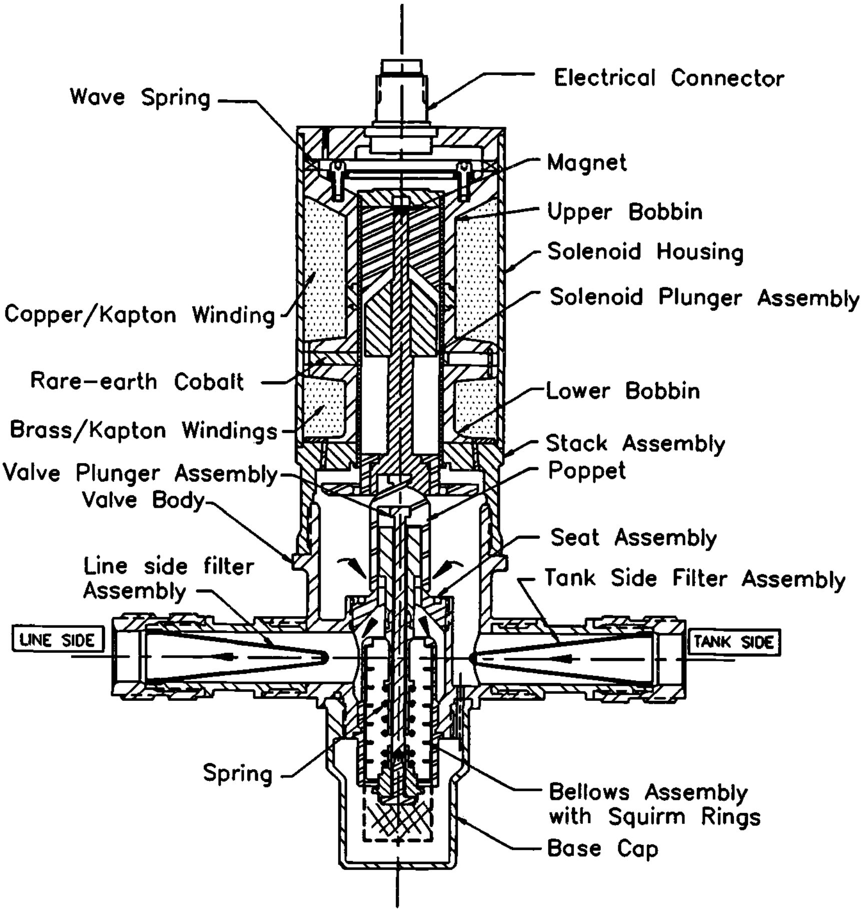

FIG. 3--EDO cryogenic oxygen shutoff valve schematic.

nonmetals used in the oxygen-wetted portions of the valve were flammable when exposed to an ignition source at maximum temperature and pressure. The valve was reviewed at the constituent parts level (poppet, filter assembly, etc.), and possible ignition sources were evaluated for each part. Electrical arc, fluid resonance, and fresh metal exposure were determined to be unlikely hazards. However, particle impact, pneumatic impact, mechanical impact, and frictional heating were all considered possible if contaminants were present in the valve (Fig. 4). The possibility of a kindling chain ignition of valve materials following ignition of the Vespel® poppet bearing was also identified.

Most of the identified hazards were rated "B" (marginal) on the reaction effect assessment scale, because the effects were primarily functional in nature and multiple-valve redundancy existed. However, ignition of either the tank-side filter or the base cap were rated "C" (critical) because of the potential of these failures to ignite nearby equipment.

Conclusions and Recommendations-- The hazards analysis team determined that, although most of the component materials of construction were flammable, no credible ignition hazards existed as long as the valve was kept clean. However, the team cautioned that particle-impact and kindling chain ignition hazards of a contaminated valve were probable under the most severe operating conditions.

The team recommended that the valve be used as designed, if the system could be kept free of contamination [16]. After stringent cleaning and inspection, several of these valves subsequently flew on Space Shuttle Columbia during NASA's first extended duration orbiter mission in the summer of 1992.

Case 2. Facility Oxygen Test System

Background--WSTF routinely performs functionality tests on oxygen components at pressures to 68.9 MPa (10 000 psi). In many cases, the test objective is to determine whether the test article can withstand repeated flow cycling or pneumatic impact in high-pressure oxygen. To guarantee accurate test results, the test system itself must not be the cause of a test article failure. During the safety review process, a WSTF hazards analysis team reviewed a new facility test system for oxygen ignition hazards. The system consisted of tubing, manual and

	Metal	Softgoods	Particle Impact	Pneumatic Impact	Mechanical Impact	Frictional Heating	Kindling Chain	Function	Secondary	Other	Reaction Effect
Filter (Line-Side)	F		3	3^a	0	0	0	0	0	0	B
Filter (Tank-Side)	F		3	3^a	0	0	0	0	0	0	C
Base Cap	F		0	3^b	0	0	0	0	0	0	C
Bellows Ass'y.	F		0	0	0	0	0	0	0	0	B
Seat Ass'y.		F	3^b	0	3^c	0	0	0	0	0	B
Plunger Ass'y.	F		3	0	3^c	0	0	0	0	0	B
Poppet	F		3	0	3^c	0	3^e	0	0	0	B
Poppet Bearing		F	0	0	0	2^d	0	0	3^e	0	B

NOTES:

[a] Clogged filter element

[b] Contaminants present

[c] Valve chatter

[d] Contaminant causes galling

[e] Vespel ignition leads to stainless steel and aluminum-bronze ignition

F = Flammable

Ignition Hazards

0 = Impossible
1 = Remote
2 = Unlikely
3 = Possible
4 = Probable

Reaction Effects

A = Negligible
B = Marginal
C = Critical
D = Catastrophic

FIG. 4--Case 1 EDO cryogenic oxygen shutoff valve hazards analysis matrix.

electrically controlled valves, check valves, filters, and relief valves.

Analysis--The hazards analysis team consisted of experts in the areas of mechanical systems, materials, safety, and test facility design. Although the system consisted of 70 individual components, the team found that many of the components could be grouped into one of nine categories (e.g. check valves of identical design and use configuration), thus reducing the number of components evaluated. Each of these component groups were then treated similarly as the valve presented in Case 1: after evaluating design and configuration data, the most severe operating conditions were identified, materials of construction were evaluated, and possible ignition sources were identified. Of the nine component groups evaluated, five were found to be of concern (3 or 4 on the risk scale, as shown in Fig. 5). An example of one component analysis, a high-pressure manual valve, is shown in Fig. 6.

Because all WSTF hazardous tests are performed remotely, most component failures were ranked no worse than "B" (marginal) on the reaction effect assessment scale. However, because filters and relief valves are typically located near the remote test area boundaries, often near a high-pressure oxygen source, failures of these components were rated "C" (critical).

Conclusions and Recommendations--Although most of the component materials are flammable, WSTF's standard contamination control practices (initial cleanliness, good assembly practices, inert gas blowdowns, and regular filter maintenance) were considered adequate to prevent most ignition hazards. However, the hazards analysis team recommended that test system operation be limited to test temperatures below 93° C (200° F) to minimize the possibility of PTFE soft good ignition.[4]

	Metal	Softgoods	Particle Impact	Pneumatic Impact	Mechanical Impact	Frictional Heating	Kindling Chain	Function	Secondary	Other	Reaction Effect
Manual Valve #1	F	F	3[a]	1	0	0	0	0	0	0	B
Filters	F		1	0	0	0	0	0[b]	0	0	C
Relief Valves	F	F	2	1[c]	0	0	1	0	0	0[d]	C
Manual Valve #2	F	F	3[a]	1	0	0	0	0	0	0	B
Manual Valve #3	F	F	3[a]	1	0	0	0	0	0	0	B
Manual Valve #4	F	F	3[a]	1	0	0	0	0	0	0	B
Manual Valve #5	F	F	3[a]	1	0	0	0	0	0	0	B
Remote Valves	F	F	2	1	0	0	0	0	0	0	B
Check Valves	F		1	0	0	2	3	0	0	0	B

NOTES:

[a] Contaminants present

[b] Clogged filter element

[c] Following catastrophic check valve failure

[d] Contaminant entry point

F = Flammable

Ignition Hazards

0 = Impossible
1 = Remote
2 = Unlikely
3 = Possible
4 = Probable

Reaction Effects

A = Negligible
B = Marginal
C = Critical
D = Catastrophic

FIG. 5--Case 2 facility oxygen test system hazards analysis matrix.

---

[4] "Hazards Analysis for Cell 110," Cell 110 Test Readiness Review, NASA Johnson Space Center White Sands Test Facility, 1992.

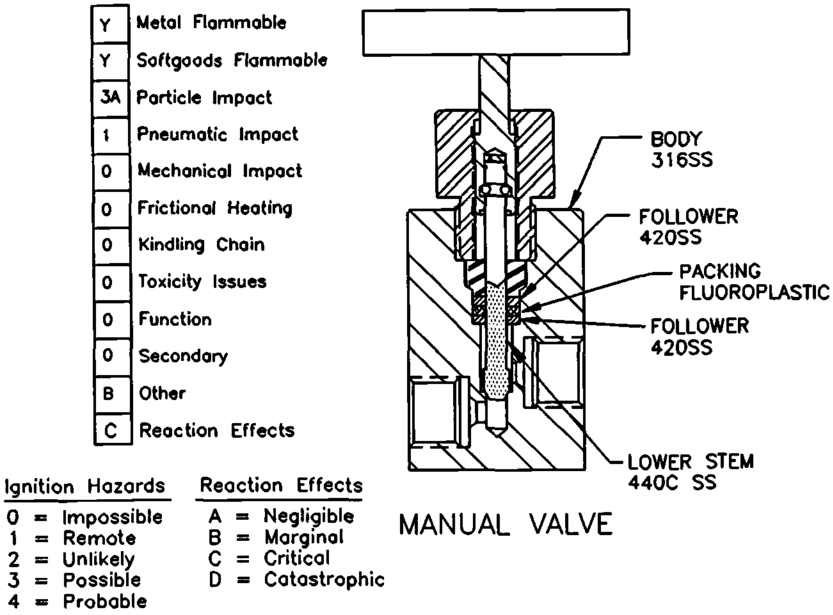

Y	Metal Flammable
Y	Softgoods Flammable
3A	Particle Impact
1	Pneumatic Impact
0	Mechanical Impact
0	Frictional Heating
0	Kindling Chain
0	Toxicity Issues
0	Function
0	Secondary
B	Other
C	Reaction Effects

Ignition Hazards	Reaction Effects
0 = Impossible	A = Negligible
1 = Remote	B = Marginal
2 = Unlikely	C = Critical
3 = Possible	D = Catastrophic
4 = Probable	

NOTES:

A. Body subject to particle impact due to sonic flow at stem/seat opening during system startup. Risk acceptable by system cleanliness, inert gas blowdowns and DMP's

B. Worst-case conditions: 10,000 psia (69 MPa) at 200° F (93° C)

FIG. 6--High-pressure manual valve hazards analysis matrix.

Case 3. USAF Aircraft Oxygen System

Background--The United States Air Force (USAF) asked WSTF to identify and evaluate potential hazards associated with an Emergency Oxygen System (EOS), which provides aviator's breathing oxygen to a single crew member during bail-out. The system consisted of an oxygen supply cylinder and an oxygen regulator containing a filter, pressure gage, relief valve, and fill valve. Oxygen fire hazards in such a system are particularly dangerous because toxic combustion or pyrolysis products may be introduced into a crew member's breathing oxygen supply. NASA was interested in evaluating this system because it is very similar to a bail-out system used by Space Shuttle astronauts.

Analysis--An analysis team, consisting of materials experts, chemists, and mechanical system designers, reviewed available design and configurational information. EOS materials of construction were identified as a carbon steel oxygen cylinder; an aluminum-bodied regulator with Torlon®, silicone, and ethylene propylene rubber (EPR) soft goods; a stainless steel check valve; a metal screen filter; and aluminum tubing. As shown in Fig. 7, four of the six components evaluated were found to be at risk (3 or 4 on the risk scale). Of particular concern was the fill valve because poor mechanical tolerances resulted in the valve producing metal particles each time the fill valve was actuated. These particles were then accelerated into the regulator, impinged on a filter at the cylinder inlet, and accumulated at the cylinder inlet until the unit was activated. At that point, the particulate was accelerated back through the regulator and into a high-velocity gas region within the regulator and into the breathing oxygen stream.

Because all of the identified hazards could lead to serious injury or death of the user (either from ignition or inhalation of toxic combustion products), all potential hazards were rated "D" (catastrophic) on the reaction effect assessment scale.

<u>Conclusions and Recommendations</u>--WSTF recommended that use of the EOS be suspended pending the following resolutions [17]:

- The fill valve should be replaced with a valve that complies with good oxygen design practices, but does not further constrict the flow.
- The EOS should be maintained clean per acceptable cleaning specifications [18]. This involves initial system cleaning as well as ensuring that oxygen servicing equipment is clean.
- The regulator filter should be moved to the inlet of the regulator to prevent it from trapping particulate at a dangerous location.
- The filter pore size should not exceed 15 um (590 microinches).
- A bayonet should be installed in the oxygen cylinder to trap any particulate in the cylinder.

As a result of WSTF's hazards analysis, the USAF initiated a program to evaluate oxygen hazards associated with their oxygen servicing equipment. Stringent cleaning procedures have been identified and are now being enforced. Additionally, the USAF issued a Safety Alert to warn government users of this particular type of fill valve of

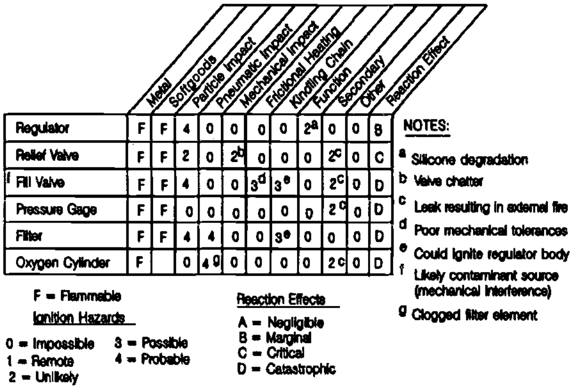

	Metal	Softgoods	Particle Impact	Pneumatic Impact	Mechanical Impact	Frictional Heating	Kindling Chain	Function	Secondary	Other	Reaction Effect
Regulator	F	F	4	0	0	0	0	2[a]	0	0	B
Relief Valve	F	F	2	0	2[b]	0	0	0	2[c]	0	C
[f] Fill Valve	F	F	4	0	0	3[d]	3[e]	0	2[c]	0	D
Pressure Gage	F	F	0	0	0	0	0	0	2[c]	0	D
Filter	F	F	4	4	0	0	3[e]	0	0	0	D
Oxygen Cylinder	F		0	4[g]	0	0	0	0	2[c]	0	D

F = Flammable

Ignition Hazards

0 = Impossible
1 = Remote
2 = Unlikely
3 = Possible
4 = Probable

Reaction Effects

A = Negligible
B = Marginal
C = Critical
D = Catastrophic

NOTES:

[a] Silicone degradation
[b] Valve chatter
[c] Leak resulting in external fire
[d] Poor mechanical tolerances
[e] Could ignite regulator body
[f] Likely contaminant source (mechanical interference)
[g] Clogged filter element

FIG. 7--EOS hazards analysis matrix.

potential ignition hazards when operated in high-pressure oxygen. Following rigorous evaluations at WSTF [19], a newly designed fill valve has been adopted for use by both the USAF and NASA.

REFERENCES

[1] Bond, Aleck C., Pohl, H. O., Chaffee, N. H., Guy, W. W., Alton, C. S., Johnston, R. L., Castner, W. J., and Stradling, J. S. Design Guide for High Pressure Oxygen Systems. Houston, Texas: NASA Johnson Space Center, 1983.

[2] Stradling, J. S., Pippen, D. L., and Frye, G. W. "Techniques Employed by the NASA White Sands Test Facility to Ensure Oxygen System Component Safety," Flammability and Sensitivity of Materials in Oxygen-Enriched Atmospheres: ASTM STP 812, B. L. Werley, Ed., Philadelphia: American Society for Testing and Materials, 1983, pp. 97-107.

[3] Benz, F. J., Shaw, R. C., and Homa, J. M., "Burn Propagation Rates of Metals and Alloys in Gaseous Oxygen," Flammability and Sensitivity of Materials in Oxygen-Enriched Atmospheres: Second Volume ASTM STP 910, M. A. Benning, Ed., Philadelphia: American Society for Testing and Materials, 1986, pp. 135-152.

[4] Stoltzfus, J. M., Homa, J. M., Williams, R. E., and Benz, F. J., "ASTM Committee G-4 Metals Flammability Test Program: Data and Discussion," Flammability and Sensitivity of Materials in Oxygen-Enriched Atmospheres: Third Volume, ASTM STP 986, D. W. Schroll, Ed., Philadelphia: American Society for Testing and Materials, 1988, pp. 28-53.

[5] Williams, R. E., Benz, F. J., and McIlroy, K., "Ignition of Steel Alloys by Impact of Low-Velocity Iron/Inert Particles in Gaseous Oxygen," Flammability and Sensitivity of Materials in Oxygen-Enriched Atmospheres: ASTM STP 986, D. W. Schroll, Ed., Philadelphia: American Society for Testing and Materials, 1988, pp. 72-84.

[6] Benz, F. J., Williams, R. E., and Armstrong, D., "Ignition of Metals and Alloys By High-Velocity Particles," Flammability and Sensitivity of Materials in Oxygen-Enriched Atmospheres: Second Volume, ASTM STP 910, M. A. Benning, Ed., Philadelphia: American Society for Testing and Materials, 1986, pp. 16-37.

[7] Benz, F. J. and Stoltzfus, J. M., "Ignition of Metals and Alloys in Gaseous Oxygen By Frictional Heating," Flammability and Sensitivity of Materials in Oxygen-Enriched Atmospheres: Second Volume, ASTM STP 910, M. A. Benning, Ed., Philadelphia: American Society for Testing and Materials, 1986, pp. 38-58.

[8] Ikeda, G. K., "Oxygen Index Tests to Evaluate the Suitability of a Given Material for Oxygen Service," Flammability and Sensitivity of Materials in Oxygen-Enriched Atmospheres: ASTM STP 812, B. L. Werley, Ed., Philadelphia: American Society for Testing and Materials, 1983, pp. 56-67.

[9] Lowrie, R., "Heat of Combustion and Oxygen Compatibility," Flammability and Sensitivity of Materials in Oxygen-Enriched Atmospheres: ASTM STP 812, B. L. Werley, Ed., Philadelphia: American Society for Testing and Materials, 1983, pp. 84-96.

[10] Key, C. F. and Riehl, W. A. Compatibility of Materials With Liquid Oxygen. NASA Headquarters: Washington, D. C., 1964.

[11] Bryan, C. J., "NASA Mechanical Impact Testing in High-Pressure Oxygen," Flammability and Sensitivity of Materials in Oxygen-Enriched Atmospheres: ASTM STP 812, B. L. Werley, Ed., Philadelphia: American Society for Testing and Materials, 1983, pp. 9-42.

[12] Schmidt, N., Moffett, G. E., Pedley, M. D., and Linley, L. J., "Ignition of Nonmetallic Materials by Impact of High-Pressure Oxygen II: Evaluation of Repeatability of Pneumatic Impact Test," Flammability and Sensitivity of Materials in Oxygen-Enriched Atmospheres: Fourth Volume, ASTM STP 1040, J. M. Stoltzfus, F. J. Benz, and J. S. Stradling, Eds., Philadelphia: American Society for Testing and Materials, 1989.

[13] Moffett, G. E., Pedley, M. D., Schmidt, N., Williams, R. E., Hirsch, D., and Benz, F. J., "Ignition of Nonmetallic Materials by Impact of High-Pressure Gaseous Oxygen," Flammability and Sensitivity of Materials in Oxygen-Enriched Atmospheres: Third Volume, ASTM STP 986, D. W. Schroll, Ed., Philadelphia: American Society for Testing and Materials, 1988, pp. 218-232.

[14] Compressed Gas Association, Inc., Oxygen, CGA G-4, Arlington, Virginia: Compressed Gas Association, Inc., 1987.

[15] Compressed Gas Association, Inc., Industrial Practices for Gaseous Oxygen Transmission and Distribution Piping Systems, Arlington, Virginia: Compressed Gas Association, 1984.

[16] Stoltzfus, J. M. Extended Duration Orbiter (EDO) Cryogenic Oxygen Shutoff Valve. WSTF-IR-91-004, NASA Johnson Space Center White Sands Test Facility, Las Cruces, NM, 1991.

[17] Plaster, M. and Rucker, M. A. Oxygen Hazard Assessment of USAF Aircraft BOS and EOS. WSTF-IR-91-001, NASA Johnson Space Center White Sands Test Facility, Las Cruces, NM, 1991, CLASSIFIED.

[18] NASA. Contamination Control Requirements Manual, JSCM 5322A, Revision B, NASA Johnson Space Center, Houston, Texas, 1982.

[19] Peterson, J. Oxygen Compatibility Tests on Fill Valves. WSTF-91-25600, NASA Johnson Space Center White Sands Test Facility, Las Cruces, NM, 1991.

Michael S. McIlroy [1]

AN INVESTIGATION OF LABORATORY METHODS FOR CLEANING TYPICAL METALLIC SURFACES USING AQUEOUS TYPE CLEANING AGENTS

REFERENCE: McIlroy, M. S., "An Investigation of Laboratory Methods for Cleaning Typical Metallic Surfaces Using Aqueous Type Cleaning Agents," Flammability and Sensitivity of Materials in Oxygen-Enriched Atmospheres: 6th Volume, ASTM STP 1197, Dwight D. Janoff and Joel M. Stoltzfus, Eds., American Society for Testing and Materials, Philadelphia, 1993.

ABSTRACT: Presently, industry places heavy reliance on the use of chlorinated solvents to achieve acceptable levels of cleanliness for systems in oxygen service. The Montreal Protocol and other restrictions will prohibit the use of these types of solvents because of potential damage to the environment. This paper discusses some of the issues involved in assessing aqueous based cleaning agents. A gravimetric test procedure has been developed to have a standard method of comparing the ability of a cleaning agent to remove oil and grease contaminants from prepared metal coupons. Data is presented to demonstrate the results of the test procedure. The testing addresses the use of a soak method and ultrasonics. The effects of time and temperature are directly addressed. Other variables are discussed in general terms such as disposal and cost considerations.

Three contaminants were selected for evaluation: hydrocarbon oil, lithium grease, and Halocarbon grease. Some of these contaminants present potential hazards in oxygen systems. The test method allows a common method for evaluation of cleaning agents and verification of contaminant levels for oxygen systems. The test procedures can also be applied to general degreasing of metal components throughout industry.

KEY WORDS: oxygen, aqueous, solvents, ultrasonics, metal cleaning

---

[1] Vice-President, McIlroy Technologies Inc. 2211 Main St. Bldg. B.
Buffalo, NY. 12214

INTRODUCTION

The 1987 Montreal Protocol[1], and subsequent 1990 amendments restrict the production and consumption of ozone depleting chemicals. The U.S. Clean Air Act (CAA) was amended in 1990, and contains several provisions pertaining to stratospheric ozone protection. Section 602 of the CAA presents a list of ozone-depleting substances that are restricted under the CAA. These ozone-depleting substances are defined as class I and class II substances. Class I substances include all fully halogenated chlorofluorocarbons (CFC's) including CFC-113. Class II substances are defined to include 33 hydrochlorofluorocarbons (HCFC's) . In order to comply with the restrictions, most of the solvents used today for cleaning will be phased out.

The disposal of chlorinated solvents requires shipping contaminated solutions to a recycler who will redistill the product, add inhibitors and resell the product. Vapor degreasers operate at elevated temperatures and although refrigeration cooling and covers are utilized to reduce the emission of solvent vapors, there is a percentage of loss each day to the atmosphere. Hand cleaning with wiping cloths, although effective, results in 100% loss of the solvents to the atmosphere. Because of the contribution of chlorinated solvents to the destruction of the ozone layer and the restrictions to the discharge of volatile organic chemicals (VOCs) to the atmosphere, new cleaning systems and cleaning agents must be developed.

Cleaning for oxygen service is similar to general degreasing except surface hydrocarbon residue must be nearly eliminated. The danger of leaving even minimal amounts of surface hydrocarbons is that these contaminants may accumulate and increase the probability of ignition or promote combustion once ignition has occurred. Major ignition mechanisms can be attributed to particle impart or adiabatic compression. Particles are always present in industrial applications and can accumulate over the years, collect in stagnant (dead) areas and be released by a sudden valve opening. Adiabatic compression is associated with a valve opening to a small dead volume. The presence of hydrocarbons or nonmetallics used in valve seats can combust and promote ignition of metals. Cleaning of metal surfaces has been a major challenge to the plating industry, however, the consequences of inadequate cleaning are discovered immediately because the plating will not adhere correctly and the parts will be scrapped. This causes a loss of productivity but does not have the hazardous consequences of fire and/or explosion in an oxygen system.

Cleaning for oxygen systems has been of prime importance since the inception of such systems and one of the difficulties is to determine " how clean is clean? ". A second determination is what is a tolerable final level of contamination? There does not appear to be an ASTM standardized method to address this problem. At this time an ASTM task force under the G-4 committee is writing such procedures which are somewhat based on this initial work. Data are presented which is a preliminary evaluation of several commercially available aqueous cleaning agents.

Several types of alternative solvents have been developed and are commercially available. Three major categories of alternative cleaning agents are aqueous, semi-aqueous, and terpenes.

Water based solutions will probably be used for the majority of cleaning in the future. This will eliminate damage to the ozone layer and eliminate VOCs. However, the use of aqueous solvents possesses other problems. The use of aqueous solutions (initially not classified as hazardous waste) may be classified as hazardous waste if it contains hydrocarbon oils and other contaminants. Eventually, systems must be designed to regenerate the fluids and have a minimal generation of hazardous waste. Systems are practical for production lines but are not practical for small cleaning jobs or on-site cleaning

With respect to cleaning systems for oxygen service, there is a wide difference in acceptable uniform contamination from 1 mg/sqft [2] to 50 mg/sqft [3]. An acceptable value is dependent on the type of oxygen service and is not discussed in this paper. To determine the efficiency of cleaning a coupon, an initial loading (contaminant) was selected as 100 mg/sqft and it is desirable to have less than 10 mg/sqft after the cleaning process. Loadings were assumed to be uniform. A loading of 100 mg/sqft is not a very heavy contamination, but for testing purposes would be representative of a machined part. Used, greasy parts require a preliminary cleaning step before final cleaning.

Aqueous cleaning was selected to demonstrate a gravimetric method for evaluation of cleaning efficiencies with standard coupons. Other cleaning agents can be evaluated using similar techniques. The choice of cleaning agents or contaminants should not be confused with the primary purpose of this paper, which is to discuss a relatively simple evaluation technique using gravimetric analysis

INITIAL PREPARATION

Test Coupons

Stainless steel (304) was selected for this test program since stainless steel is very common in cryogenic oxygen systems. Other alloys of importance are aluminum for cryogenic service and carbon steel for oxygen gas distribution systems. The coupon size (51mm x 102mm) was selected to allow complete submersion in a tall 300mL, laboratory beaker, which can be accommodated in multiples in laboratory ultrasonic cleaning tanks. A hole was made in the upper center of each coupon so that it could hang freely in a beaker and allow natural fluid circulation. The thickness of the coupon was 0.82mm and is unimportant except that the coupon weight must be within the range of the selected balance. It was desirable to have a relatively rough surface which mimics cast valve bodies. Smooth surfaces, such as encountered in stainless steel piping and tubing should be easier to clean. A bead blasted surface was selected to try to develop a "standard" surface. In practice, the surface finish can be considered to be a function of operator skill, age of beads, time of blasting, hardness of alloy and possibly other variables.

The sample coupons had varying degrees of roughness visible to the eye and were expected to influence the test results to some degree. A few samples (3 stainless steel coupons) were checked with a simple profilometer and showed a range of 34 to 56 micro inches. The use of a sophisticated surface measurement device(laser profilometer) gave results ranging from 38 to 57 micro inches [4] for the same coupons. This cannot be considered to be a scientific comparison since the selection of the specific surface location on a coupon was not the same. It merely establishes that a simple surface measurement is sufficient to give a roughness value.

Aluminum has a surface roughness of about 110 micro inches. Figure (1) shows the visual presentation of one stainless steel coupon with a measured surface roughness of 1.46 micrometers or 57 micro inches using a laser profilometer with 250 profilometer scans [4]. Subsequently a batch of 32 aluminum and 32 stainless steel coupons were measured using the simple profilometer method. The stainless steel varied from 9 to 63 micro inches with a mean of 27.4. The aluminum varied from 77 to 132 micro inches with a mean of 102 micro inches. This radical difference in surface roughness between aluminum and stainless steel is probably due to the fact that the aluminum is much softer. The significance of this data is to point out that coupon roughness must be specified when ordered to some mean value, with a tolerance range. Obviously the mean will be different for each type of alloy. This will reduce experimental error if a round robin program between laboratories is instituted.

Selection of Contaminants

During manufacture, components destined for oxygen service may have a hydrocarbon contaminant residue remaining on the surface and this residue must be removed prior to use in oxygen systems. The Castrol 10w-30 motor oil is considered to represent a light to medium weight hydrocarbon oil which may be representative of a machining fluid. Lithium grease represents a heavy grease which is unlikely to occur in an oxygen system but is nevertheless a possible contaminant in an oxygen system. Halocarbon grease is relatively expensive and is used in oxygen systems because of its relative compatibility with oxygen. At times it is required to remove such a grease in the refurbishment of equipment. Halocarbon grease is a heavy density grease and is reported to be difficult to remove. Many other contaminants can be used, however, the primary objective of this program is neither to pass judgment on a specific cleaning agent nor evaluate a contaminant, but to verify a test procedure strategy and determine the practical problems of conducting such tests.

Particle contamination, as considered by others, is not part of this program. Government cleaning specifications require verification of particles in current systems. The industrial gas industry is greatly concerned about hydrocarbon residues (especially those systems where oil can migrate and concentrate). If cleaning removes the oils, it is postulated that particles will also be removed to an acceptable degree.

Selection of Cleaning Agents

Three commercially available aqueous solvents were selected for the tests. The first aqueous solvent selected was Blue Gold. Blue Gold is a product available from the Modern Chemical Company and has been on the market for sometime. The second aqueous solvent is Beyond 2001. Beyond 2001 is available from Today and Beyond. The third was DOT 111/113 from the Delta Omega company. All three aqueous solvents are

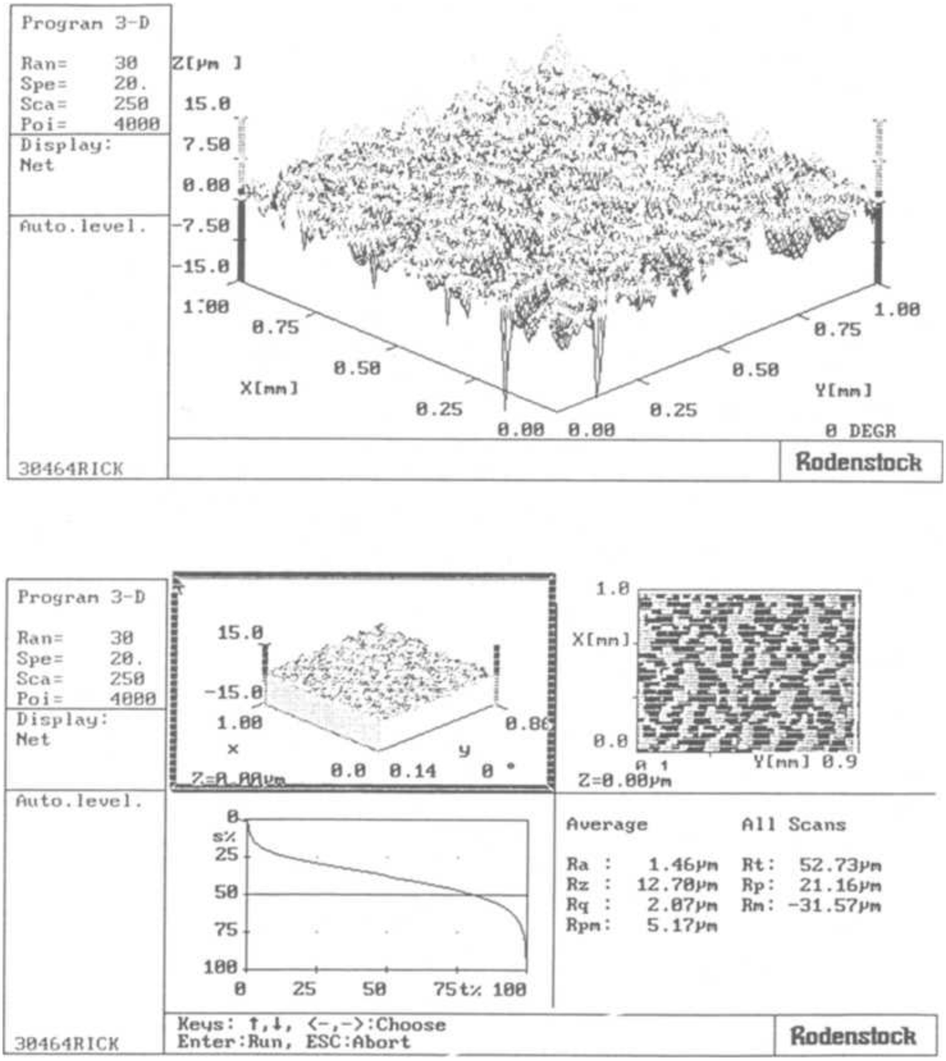

```
Program 3-D

Ran=    30
Spe=    20.
Sca=    250
Poi=    4000
Display:
Net
Auto.level.
30464RICK
```

```
Program 3-D

Ran=    30
Spe=    20.
Sca=    250
Poi=    4000
Display:
Net
Auto.level.
30464RICK
```

```
Average            All Scans

Ra  :   1.46µm    Rt:   52.73µm
Rz  :  12.70µm    Rp:   21.16µm
Rq  :   2.07µm    Rm:  -31.57µm
Rpm:    5.17µm
```

```
Keys: ↑,↓, <-,->:Choose
Enter:Run, ESC:Abort
```

Figure 1 - Laser Profilometer Reading for a Stainless Steel Coupon

available commercially and are considered environmentally safe by the manufacturers under current EPA regulations. There are many other aqueous solvents available and all can vary in performance with different contaminants and cleaning methods. In selecting an aqueous solvent it is best to consult with the manufacturers to find out in which applications their particular solvents are considered to excel. The manufacturers will have recommended time, temperature and concentration requirements to follow which means that overall performance comparisons are difficult to make especially if energy consumption and other associated aspects are considered.

Equipment Description

The two most important pieces of equipment used in this experiment are the balance and the ultrasonic cleaning tank. A Sartorius balance with a capacity of 60 grams and an accuracy of 0.0001 grams (4 place) was used. This proved to be adequate; however, in later experimental work, another balance with 0.00001 grams accuracy (5 place) proved to give better accuracy. The latter balance is very sensitive to the laboratory environment.

The ultrasonic cleaner was a Branson model 3200. It was capable of holding four 300mL beakers, which was a minimum consideration for selecting an appropriate ultrasonic cleaner. The ultrasonic cleaner has a capacity of 5.7 liters and operates at 40 MHz. The use of four beakers simultaneously help to speed the test program and cut testing costs.

TEST PROCEDURE

Application Techniques

Three methods of applying the contaminants to the coupons were considered. The first method investigated was dipping the coupon into a container of contaminant. Several drawbacks were discovered. Controlling the amount of contaminant applied was almost impossible and this method applied the contaminant to both sides of the coupon. Applying the contaminant to both sides made it impossible to place the coupon on the balance without contaminating the balance because it had to lay flat. Another problem with this method of application was that as the coupon hung vertically, the contaminant would run down and form a large bead at the base of the coupon, resulting in an uneven film distribution.

The second method investigated was simply brushing the contaminant onto one side of the coupon. This would make handling the coupon easier but again gave very little control over the amount of contaminant and the evenness of application.

The third method which proved to have the least drawbacks was combining the contaminant with a carrier solvent and applying it to one side of the coupon with a spray bottle. In the data presented, the carrier solvent chosen was 1,1,1-trichloroethane. The coupons were sprayed in the horizontal position to form a relatively even film on one side. Once the carrier solvent evaporated, the coupons could be suspended vertically until the contaminant weight stabilized. The coupons were placed horizontally on the weighing balance and thus avoided contamination of the balance pan. Contamination could be applied in the range of 0.0050 to 0.0060 grams per application by experimenting with different ratios of contaminant to carrier solvent. This translated to an average level of contaminant equal to 100 mg/sqft. On occasion, the coupons weight had to be adjusted by wiping a small amount of contaminant off the surface with a clean cloth. In the case where the weight of the contaminant was below the acceptable range, a small amount of contaminant was re-applied.

It was discovered that different contaminants took different lengths of time to stabilize at a constant weight. To determine the length of time for each of the contaminant/carrier solvent combinations to stabilize, several coupons were contaminated with each of the mixtures and their weight recorded at different times throughout the day. The data presented in Figure (2) illustrates the difference between the length of time it took for each carrier solvent, contaminant combination to stabilize.

All samples were dried in the laboratory's natural air currents. The lithium grease and Castrol oil stabilized relatively quickly (one to three hours). The Halocarbon grease behaved quite differently in that the samples continued to lose weight over a 24 hour period. The reason for the instability of the Halocarbon coated samples is not fully understood.

Residue Tests

Figure (3) shows the results of the residue test. Coupons (304SS) were weighed and then soaked in the prepared solution (5% concentration of aqueous solvent in tap water) for five minutes. The coupons were removed and no rinse cycle was performed. The coupons were then dried and reweighed. The weight difference represents a worst case condition where a rinse step is missed. The clean weight and the weight after soaking is used to determine the amount of residue remaining on the coupons surface after drying.

Solution "A" (Beyond 2001) and "B" (Blue Gold), which are quite similar, exhibited an average residue level of 16 mg/sqft. The third solution "C" (DOT 111/113) left an average residue level of 8 mg/sqft. Tap water was run as a control and exhibited a residue of 3 mg/sqft. The residue left by the tap water can be subtracted from each of the solvent results to achieve a more realistic indication of the residue remaining from each of the solvents.

Cleaning Methodology

Four clean coupons were selected of identical material. Each of the coupons was weighed on the Sartorius balance and the weight and identification number of each was recorded. The coupons were always be handled with very clean gloves (it was difficult to avoid getting contamination on the fingertips of the gloves). The preferred method of handling the coupons was with a hook through the 3.2mm hole at the top of the coupon. The coupons were then placed onto a rack that was designed to suspend the coupons vertically, and was capable of holding the coupons in a horizontal position during contamination. The rack was positioned so that the coupons were held horizontally and

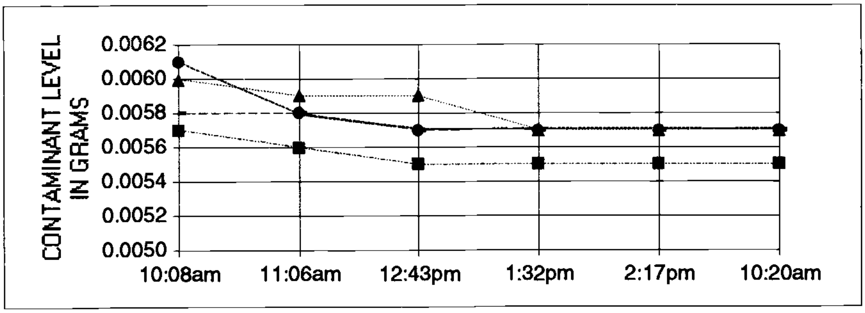

LITHIUM GREASE

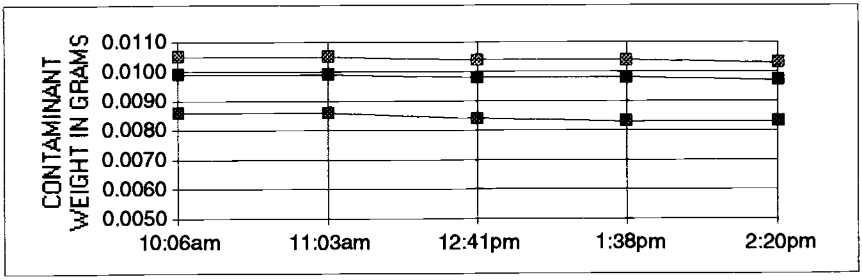

CASTROL OIL

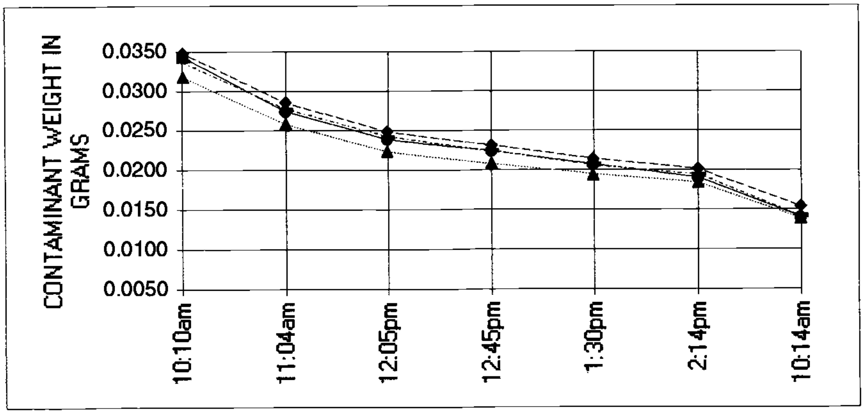

HALOCARBON GREASE

Figure 2 - Stabilization of selected contaminant weight as a function of time

SOLVENT "A" 5% SOLUTION

COUPON #	WEIGHT	WEIGHT	RESIDUE	mg/sqft
163	31.1654	31.1674	0.0020	18
55	36.8749	36.8766	0.0017	15
57	36.7942	36.7957	0.0015	14

SOLVENT "B" 5% SOLUTION

COUPON#	WEIGHT	WEIGHT	RESIDUE	mg/sqft
59	36.7428	36.7446	0.0018	16
56	36.8997	36.9015	0.0018	16
160	31.2331	31.2349	0.0018	16

SOLVENT "C" 5% SOLUTION

COUPON#	WEIGHT	WEIGHT	RESIDUE	mg/sqft
54	36.9785	36.9795	0.0010	9
53	36.8573	36.8583	0.0010	9
62	37.1207	37.1215	0.0008	7

TAP WATER

COUPON#	WEIGHT	WEIGHT	RESIDUE	mg/sqft
58	36.7993	36.7996	0.0003	3
159	31.0859	31.0862	0.0003	3
151	31.0645	31.0648	0.0003	3

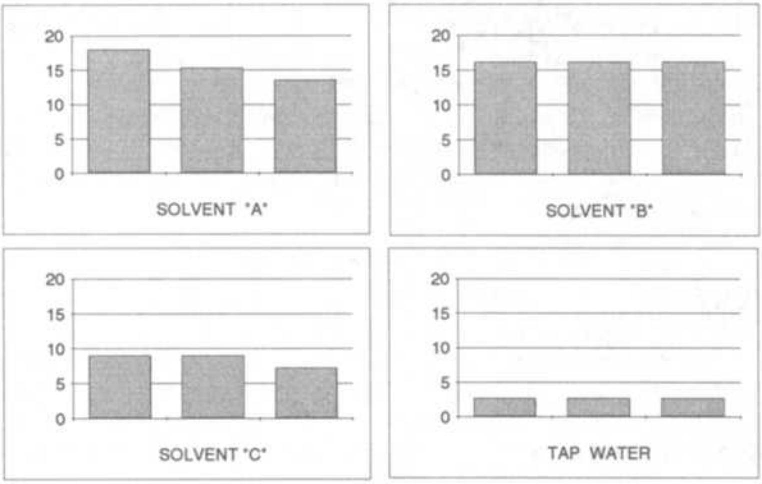

Figure 3 - Residue test summary

the mixture of contaminant is applied to one side of the coupons. The reason for applying the contaminants to the coupons when the coupon is horizontal was to prevent the contaminants from collecting at the base of the coupon while the carrier solvent evaporates. This method of applying the contaminant seemed to provide a simple way of achieving a relatively even film of contaminant on the face of the coupon. Once the contaminant was applied, the coupons remained horizontal for approximately 30 minutes and then were returned to the vertical position to allow the remainder of the carrier solvent to evaporate. The length of time it took for each of the carrier solvents to evaporate was dependent on the contaminant, the carrier solvent and the environment inside the laboratory. After the contaminant weight was stabilized (this was referenced to a test of the stabilizing time for each selected contaminant and carrier solvent combination) the weight of each coupon was recorded. If the weight of the coupon exceeded the desired target weight, a small amount of contaminant was wiped off to bring it into specification. If the coupon weight was below the desired target weight the coupon was rejected and a small amount of contaminant was reapplied following the contamination procedures described. Of course, this delayed the test while the recontaminated coupon weight was allowed to stabilize. In addition to preparing the coupons, the solvent bath must be prepared. Select the aqueous solvent to be evaluated and record it on the data sheet. Four 300mL beakers with a 5% solution of the selected aqueous solvent were prepared (or the manufacturer's recommendations were followed). Depending on the cleaning operation to be performed, ultrasonic or soak (or other), the beakers were placed into the appropriate device (the beakers sat on the bench if the test to be performed was a soak at room temperature). If the test procedure required elevated temperatures, the solutions were allowed to reach equilibrium with the bath temperature. Each of the four coupons were placed into each of the four beakers for the desired time period. Once the time has elapsed, the coupons were removed. The coupons were processed through the rinse cycle and hung vertically to dry. The coupons were placed into the drying apparatus and allowed to dry. After the coupons were thoroughly dried, the weight of each of the coupons was recorded. The data recorded was used to determine the cleaning efficiency of the selected aqueous solvent under the specified cleaning conditions and contaminant.

Rinse Methods

The same type of water was used that would be available during the actual dilution of the aqueous cleaning agent. In the data presented, two types of rinse operations were utilized. The first was ordinary tap water. The actual rinse operation consisted of swishing the coupon after it was removed from the cleaning solvent in a container of clean tap water at room temperature. The second method was identical but deionized water was used. The temperature of the rinse water was another variable considered. In the experiments performed, the tap water and deionized water was approximately 20° C .

Drying Methods

In the data presented, the rinsed coupons were dried under 250W heat lamps for a period of about one hour. The coupons were then allowed to sit at room temperature for not less than four hours. It is recommended that a desiccator be used in future experiments in order to eliminate any moisture that may have condensed or possibly penetrated the coupon material. This recommendation was taken into account and was applied to all future tests. The small amount of moisture present in the air on any given day effected the readings displayed on the balance.

RESULTS AND DISCUSSION

The test results of the efficiency of Delta Omega DOT 111/113 solution in removing lithium grease from a standard 304SS coupon are shows in Figure (4), which identifies the key parameters and test conditions used. Four coupons were tested and the percentage removed or cleaning efficiency of each single test was calculated. The simple arithmetic average was considered to be representative of the cleaning efficiency at the specific conditions. The cleaning efficiency of another cleaning agent, Beyond 2001 with Castrol Motor Oil as the contaminant is shown in Figure (5). Forty-eight tests were required to fill in all of the boxes (time, temperature and method).

The summary test data for this program are shown in Figure (6). The three cleaning agents were evaluated for their effectiveness in removing the three selected contaminants at two temperatures and three time periods (3, 6 and 9 minutes). The use of ultrasonics was also evaluated. Typically, if a cleaning agent had an acceptable performance at three minutes, it was not tested for a longer time period.

Blue Gold effectively removed the light hydrocarbon oil (Castrol oil) and lithium grease by soaking at room temperature. However, for the Halocarbon grease, Blue Gold was ineffective. All contaminants could be effectively removed using ultrasonics.

Beyond 2001 was judged to be quite similar to Blue Gold. It effectively removed the Castrol oil and the lithium grease. It appeared to be a little bit more effective for Halocarbon grease removal than Blue Gold. With the use of ultrasonics, Beyond 2001 was very effective in removing the Halocarbon grease.

Delta Omega was ineffective in removing Halocarbon grease in the soak condition as were the two other cleaning agents. It did not meet the desired cleaning efficiency of 90% for the lithium grease (74% to 89%). One very surprising result was the poor performance for light hydrocarbon oil removal. By elevating the bath temperature to 40 degrees C, the cleaning efficiency for lithium and Halocarbon grease drastically deteriorated. This is contrary to what was expected. With ultrasonics, cleaning at 40 degrees C proved to be very effective for both greases. A strange result occurred with Halocarbon grease, the efficiency was good at room temperature, but at 40 degrees C, the efficiency dropped to a lowly 26%. This behavior should be further investigated.

As for drying the coupons, several methods are applicable: 1) Laboratory ovens can be used to accelerate the drying process 2) Desiccators may be used depending on the

SOLVENT:	**DOT 111/113**	CONTAMINANT:	**LITHIUM GREASE**
CONCENTRATION:	**5%**	APPLICATION:	**SPRAYED**
TEMPERATURE:	**20 C**	TIME:	**9 MINUTES**
METHOD:	**SOAK**	MATERIAL:	**SS 304**
RINSE:	**TAP WATER 5 SEC.**	TECHNICIAN:	**M.S.M.**
		REMOVED:	**79.8 %**
DATE:	**7/5/92**	TEST # :	**34**

COUPON #	COUPON WEIGHT	COUPON W/CONT.	CONT. WEIGHT	CLEANED COUPON	CONT. REMAINING	PERCENT REMOVED
57	36.7942	36.7992	0.0050	36.7949	0.0007	86.0 %
155	31.1914	31.1966	0.0052	31.1921	0.0007	86.5 %
157	31.1256	31.1310	0.0054	31.1277	0.0021	61.1 %
158	31.0931	31.0987	0.0056	31.0939	0.0008	85.7 %

INITIAL mg/sqft (AVG.): 95.4

FINAL mg/sqft (AVG.) : 19.4

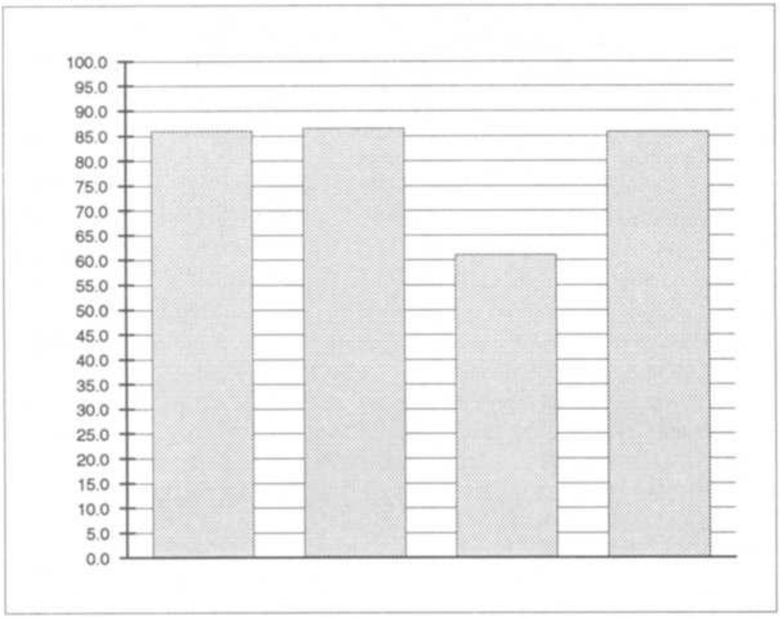

Figure 4 - Cleaning efficiency of DOT 111/113 in removal of lithium grease

************************************ TEST DATA SUMMARY ************************************

CLEANING FLUID : BEYOND 2001
CONTAMINANT : CASTROL OIL 10/30

TEMPERATURE : **20 C**

SOAK (A)

	MINUTES 3	MINUTES 6	MINUTES 9
% OF CONTAMINANT REMOVED:	89.4%	93.0%	97.4%
INITIAL CONTAMINANT mg/sqft :	113.4	105.3	110.3
FINAL CONTAMINANT mg/sqft :	12.2	7.7	2.7

ULTRASONIC (B)

	MINUTES 3	MINUTES 6	MINUTES 9
% OF CONTAMINANT REMOVED:	96.3%	86.9%	–
INITIAL CONTAMINANT mg/sqft :	109.4	105.8	–
FINAL CONTAMINANT mg/sqft :	4.1	14.0	–

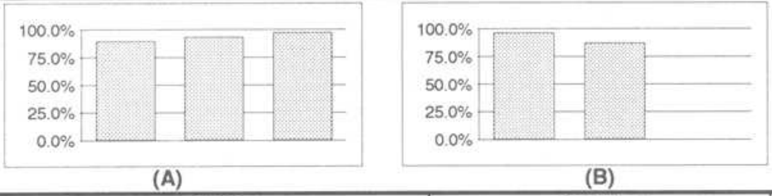

TEMPERATURE : **40 C**

SOAK (C)

	MINUTES 3	MINUTES 6	MINUTES 9
% OF CONTAMINANT REMOVED:	100.0%	100.0%	100.0%
INITIAL CONTAMINANT mg/sqft :	99.5	103.5	102.6
FINAL CONTAMINANT mg/sqft :	0.0	0.0	0.0

ULTRASONIC (D)

	MINUTES 3	MINUTES 6	MINUTES 9
% OF CONTAMINANT REMOVED:	100.0%	–	–
INITIAL CONTAMINANT mg/sqft :	98.6	–	–
FINAL CONTAMINANT mg/sqft :	0.0	–	–

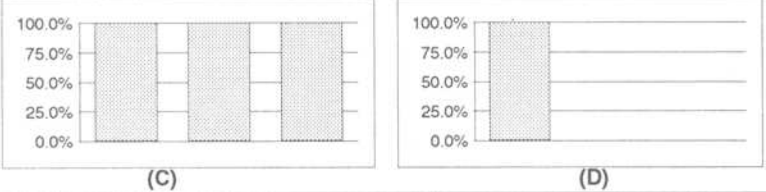

Figure 5 - Test data for Castrol oil and Beyond 2001

	CASTROL OIL			LITHIUM GREASE			HALOCARBON GREASE		
	MINUTES			MINUTES			MINUTES		
	3	6	9	3	6	9	3	6	9
BLUE GOLD									
SOAK									
20C	97%	100%	_	76%	89%	96%	55%	43%	_
40C	93%	97%	_	99%	_	_	_	_	_
ULTRASONIC									
20C	97%	100%	_	99%	_	_	96%	100%	_
40C	100%	_	_	98%	_	_	71%	99%	_
BEYOND2001									
SOAK									
20C	89%	93%	97%	88%	94%	93%	60%	60%	84%
40C	100%	100%	100%	90%	92%	_	75%	60%	72%
ULTRASONIC									
20C	96%	87%	_	100%	99%	_	98%	99%	_
40C	100%	_	_	100%	100%	_	96%	77%	_
DOT111/113									
SOAK									
20C	7%	10%	_	89%	74%	80%	42%	60%	_
40C	14%	17%	_	5%	41%	_	17%	_	_
ULTRASONIC									
20C	21%	28%	50%	99%	_	_	90%	99%	_
40C	100%	100%	_	_	_	_	26%	_	_

Figure 6 - Test data summary

accuracy required of the test results. 3) Forced hot air is another option for rapid drying the coupons. 4) Finally simply placing the coupons in the open air and allowing them to dry. This last method is of course the slowest and the results can vary dependent on the environment (relative humidity) inside the laboratory.

It must again be stressed that the test program was to verify the test techniques and not to look in depth at any specific cleaning agent or contaminant. Certain cleaning agents were not considered effective at room temperature soak conditions, especially for greases.

OTHER FACTORS

Cost Considerations of a Cleaning Agent

Typically, a cleaning agent is viewed from its initial expense ($/lb.). However, this may be a small consideration or have minimum impact on the complete picture. The cleaning agent may require expensive special equipment, special handling and special storage. If it is spent and is considered a hazardous waste, disposal is expensive and spill/cleanup measures must be considered. Other expenses will be record keeping and employee training in its use. Certain cleaning agents, solvents in particular, may require medical surveillance of the employee. Risk insurance premiums should also be considered. Finally, the use of certain cleaning agents may effect the corporate image and also generate community concerns. Thus, the evaluation of a cleaning agent goes far beyond its ability to clean.

Discharge Limits of Oil

The use of a water based agent will eventually require that it be disposed of in an environmentally acceptable manner. Many cleaning formulations are claimed to be biodegradable, however it behooves the user to verify at what limits it can be disposed by sewering to a public water treatment plant. Oil contamination levels in the discharge must be monitored, as well as pH levels. Sewer districts in the U.S. have imposed allowable limits of hydrocarbon contamination as low as 300 ppm and as high as 14,000 ppm. It is also necessary to consider the hydrocarbons in the fresh cleaning agents. Eventually, zero discharge will become mandatory and systems will be developed for each cleaning agent which will address the specific criteria.

SUMMARY AND CONCLUSIONS

This test program demonstrated the feasibility of using standardized coupons for the evaluation of cleaning agents in the removal of oil and grease. The initial contamination was selected to be 100 mg/sqft. Should the contamination level be much in excess of this value, it is recommended that precleaning be used. Stainless steel coupons were used, but the test procedure can be applied to other alloys. Corrosion was not addressed in this study and it is anticipated that in the case of carbon steel, rusting may be a problem for aqueous cleaning.

For oxygen systems, it is important to know the oxygen compatibility of any residues remaining after the rinse and dry cycles. Certain residues for cleaning agents could possibly be as hazardous or even more hazardous than the hydrocarbon contaminant.

The issue of " how clean is clean " has been briefly mentioned. Each company or agency will have different criteria.

The G-4 Task Force will use some of this initial work to develop and write test procedures. This will allow dialogue between cleaning agent suppliers and users for cleaning systems for oxygen service. The economics of cleaning systems and agents selection will require much study and trials before optimized systems can be selected.

REFERENCES

[1] ICOLP Technical Committee, Aqueous and semi-aqueous alternatives for CFC-113 and Methyl Chloroform cleaning of printed circuit boards , United States Environmental Protection Agency,
EPA/400/1-91/016, June 1991

[2] Bryan, C.J., "Final Report on the Effect of Surface Contamination on LOX Sensitivity", NASA - KSC Letter Report MTB 306-71, National Aeronautics and Space Administration, Washington, DC, 1971.

[3] CGA G-4.1, Cleaning Equipment for Oxygen Service, Compressed Gas Association, Inc., 1235 Jefferson Davis Highway, Arlington, VA 22202.

[4] Private Communication, R. J. Paciej, BOC , Murrayhill, NJ

John M. Homa[1] and Joel M. Stoltzfus[2]

THE MEASUREMENT OF THE FRICTION COEFFICIENT AND WEAR OF METALS IN HIGH-PRESSURE OXYGEN

REFERENCE: Homa, J. M. and Stoltzfus, J. M., "The Measurement of the Friction and Wear of Metals in High-Pressure Oxygen," Flammability and Sensitivity of Materials in Oxygen-Enriched Atmospheres: 6th Volume, ASTM STP 1197, Dwight D. Janoff and Joel M. Stoltzfus, Eds., American Society for Testing and Materials, Philadelphia, 1993.

ABSTRACT: The frictional forces generated during rubbing contact of metals greatly influence the ignitability of the bulk material when exposed to high-pressure oxygen environments. Previous works have ranked the ignition susceptibility of metals by frictional heating tests and by promoted combustion tests. Variations in the rankings by these two methods have been explained by differences in the friction coefficient and the resulting differences in frictional heat generation. A material with a higher coefficient of friction will produce more heat and will therefore achieve its ignition temperature at a lower PV product, where *P* is the normal load divided by the rubbing area and *V* is the relative linear velocity between the samples. A ranking of frictional ignition data taking into account the friction coefficient was shown to agree quite well with promoted combustion rankings. To further investigate the effects of the friction coefficient on ignition, a series of pin-on-disk friction tests were performed on five selected metals. These tests measured the friction and wear of each metal during the pre-ignition phase, while exposed to high-pressure oxygen. Wear characteristics appeared dramatically different for the pin-on-disk tests compared to the hollow cylinder configuration of the frictional heating test for some materials. Among the metals tested, three types of wear were observed: a severe adhesive wear resulting in high frictional forces; a mild wear characterized by a glazed oxide coating and low friction coefficients; and an adhesive-delamination wear combined with the release of many burning wear particles. The wear configuration was found to be extremely important when assessing the frictional heating properties that lead to ignition in oxygen-enriched atmospheres.

KEYWORDS: friction, wear, friction coefficient, PV product, frictional heating, ignition, oxygen

---

[1] Senior Engineer, Lockheed-ESC, White Sands Test Facility, P. O. Drawer MM, Las Cruces, NM 88004.

[2] Aerospace Engineer, NASA, White Sands Test Facility, P. O. Drawer MM, Las Cruces, NM 88004.

BACKGROUND

The NASA Johnson Space Center White Sands Test Facility has performed frictional heating tests in high-pressure oxygen to determine the relative ignition ranking of metal alloys subjected to frictional contact in oxygen environments. As a result, many alloys have been tested and a considerable database exists [1,2,3]. Some observations have been made. The relative ranking for frictional ignition of alloys differs substantially from the ranking from tests such as the promoted combustion test [4]. Protective coatings can form on the contacting surfaces as a result of heating from the rubbing processes, which can result in lower frictional heat generation and subsequent higher PV products required for ignition (where *P* is the normal load divided by the rubbing area and *V* is the relative linear velocity between the samples). This observation led to the identification of the friction coefficient as an important variable when evaluating the frictional ignition phenomenon.

EXPERIMENTAL METHOD

Test System Description

The test apparatus consists of a pin-on-disk friction rubbing configuration (see Fig. 1). The pin and disk are located in a high-pressure oxygen chamber capable of providing oxygen environments from ambient pressure to 4000 psi (27.6 MPa), at ambient temperature. The pin is 0.3125 in. (7.94 mm) in diameter with a full-radius hemispherical contact (see Fig. 2). The pin is attached to the pin arm, which is rotated by the pin-arm shaft to bring the pin into contact with the disk. The pin traces a 1.51-in. (3.84-cm)-diameter wear track on the disk surface. The disk is 2.0 in. (5.08 cm) in diameter and 0.5 in. (1.27 cm) in thickness (see Fig. 3). The disk is secured to a drive

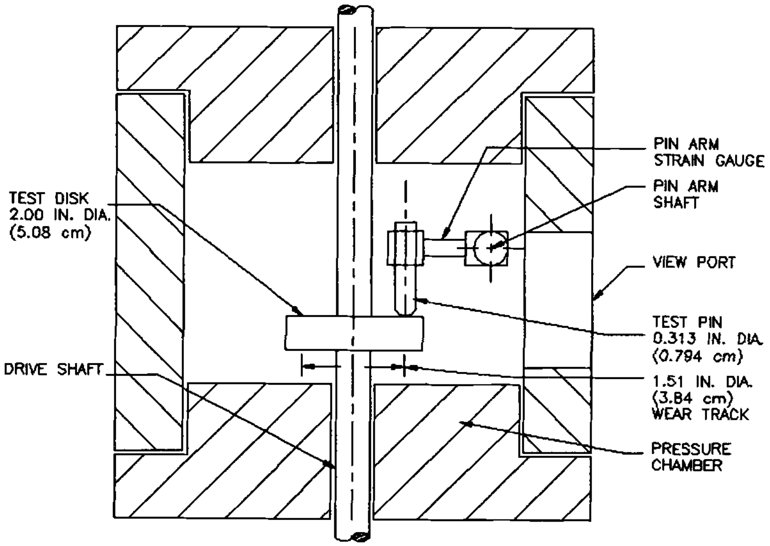

FIG. 1--Pin-on-disk test apparatus.

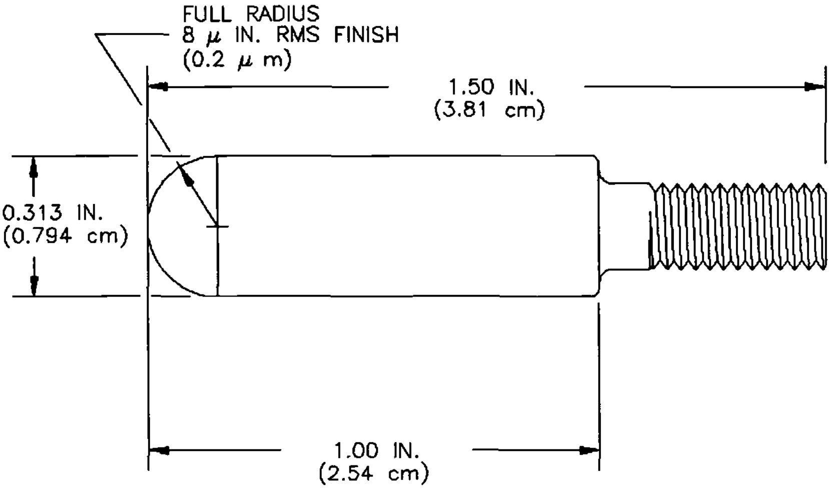

FIG. 2--Test sample: pin.

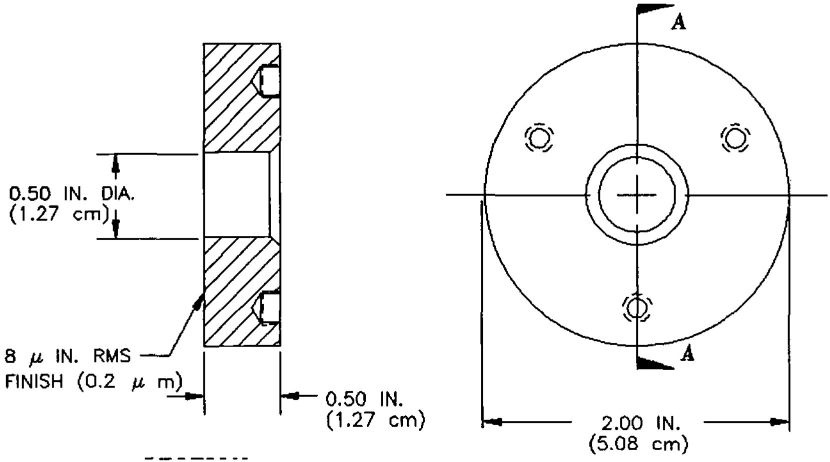

FIG. 3--Test sample: disk.

shaft that can be rotated at speeds of 2000 to 30 000 rpm (210 to 3140 rad/s) by means of a 15-hp (11.2-kW) motor and belt drive system. The pin contacts the rotating disk with a specified load. The frictional force generated by the rubbing contact is measured using a calibrated strain gauge mounted on the pin arm. The test may be monitored through a 2-in. (5.08-cm)-diameter window port using a video camera recording system. Test data consist of chamber pressure, chamber temperature, disk rpm, pin normal load, frictional load, and angular position of the pin-arm shaft; and are recorded at 100-msec intervals throughout the test duration.

Test Procedure

Test materials were obtained and fabricated into pin-on-disk samples; identical materials were used for each pin and disk pair. The samples were then polished and cleaned. The normal load and friction load readings were calibrated.

For each pin-on-disk set, several test runs were conducted in oxygen at a pressure of 1000 psia (6.89 MPa). Load and surface speed were increased successively for each subsequent test until the wear limit was reached. The initial load provided a run-in for the subsequent tests at higher loads. The maximum load was 10 lbf (44.5 N) and maximum rotational speed was 12 000 rpm (1250 rad/s).

To conduct each test, a pin-on-disk set was loaded into the test chamber. The drive motor was preset to the desired disk rotational speed. The test chamber was sealed and then pressurized with oxygen to 500 psia (3.45 MPa). The chamber was pressurized and vented three more times to ensure that air had been eliminated. The chamber was then pressurized to 1000 psia (6.89 MPa) with oxygen and isolated from the oxygen source. The desired normal load was established between the pin and disk. Data collection was initiated and the drive motor was activated for the 1-min test duration. At the completion of the test, the pin was raised from the disk and the drive motor was deactivated. The chamber was vented and the samples were removed.

A video was made of each test run, and posttest photographs were taken to document the wear results. Frictional and normal load data were used to calculate the coefficient of friction for each test sample.

Test Materials

The materials listed in Table 1 were tested for this project. All the materials selected are used or proposed for use in gaseous oxygen or liquid oxygen aerospace applications. The contact surfaces of each pin and disk were polished using a metallographic polishing wheel with a final grit size of 0.3-micron alumina particles. This resulted in a

Table 1--Composition of tested alloys.

	Weight %								
Alloy	Ni	Fe	Cr	Cu	Al	Mo	Mn	Ti	Other
Monel K-500	64.5	0.60	...	30.4	3.0	...	0.74	0.46	a
Inconel MA754	BAL	0.26	19.6	...	0.34	...	...	0.45	b
440C stainless steel	0.16	BAL	17.0	0.10	0.02	0.49	.42	...	c
Inconel 718	52.1	19.0	18.3	0.05	0.58	3.0	0.07	1.0	d
Aluminum 2219-T8511		<.3	...	6.3	BAL	...	0.3	0.06	e

a: 0.16 Si, 0.15 C, 0.001 S
b: 0.57 Y_2O_3, 0.05 C
c: 0.41 Si, 1.1 C, 0.001 S, 0.024 P
d: 5.1 Nb/Ta, 0.26 Co, 0.10 Si, 0.04 C, 0.001 S, 0.006 P, 0.004
e: 0.17 Zr, 0.10 V, <0.10 Zn, <0.02 Mg, <0.20 Si

surface finish equal to or better than 8 μin. (0.2 μm) rms. The samples were then cleaned with a detergent wash and rinsed with deionized water to a neutral pH.

RESULTS AND DISCUSSION

Among the five materials tested, three types of wear were evident. For Inconel 718 and 440C stainless steel, a mildly adhesive wear was observed; this wear resulted in a smooth oxidized layer forming on the disk surfaces, and slight overall wear. The Inconel MA754 and Monel K-500 exhibited a more severe adhesive pin wear accompanied by the release of burning particles. In addition, the disk surfaces were heavily worn with a grooved surface. The aluminum 2219 exhibited very severe adhesive wear, and could not be run for the full test duration. Typical pretest and posttest samples are show in Fig. 4.

To compare overall wear among the tested materials, pin-wear volumes were calculated for each test and are presented in Table 2.

Inconel MA754 and Monel K-500

Figs. 5 and 6 show a similar adhesive wear pattern for the Inconel MA754 and Monel K-500 pins. The disk wear in both materials appears to be a delamination wear with cracks across the wear track and flakes of material breaking off the surface. The Inconel MA754 showed no evidence of any coating on the disk surface. The Inconel MA754 pin was discolored on the trailing edge. The Monel K-500 pin was more uniformly discolored and had begun to form several glazed wear tracks with matching tracks appearing on the disk. The lower right side in Fig. 6

Table 2--Pin-wear volumes.

Test Material (Test No.)	Wear Volume (in^3)	Wear Volume (cm^3)	Sliding Distance (in.)	Sliding Distance (m)
		Monel K-500		
COF-060	.928 × 10^{-3}	.0152	.253 × 10^6	6.43 × 10^3
COF-107	1.433 × 10^{-3}	.0235	.245 × 10^6	6.22 × 10^3
		Inconel 718		
COF-059	.574 × 10^{-3}	.00941	.389 × 10^6	9.88 × 10^3
COF-078	.607 × 10^{-3}	.00995	.226 × 10^6	5.74 × 10^3
		440C Stainless Steel		
COF-061	.294 × 10^{-3}	.00482	.370 × 10^6	9.40 × 10^3
COF-096	.357 × 10^{-3}	.00585	.308 × 10^6	7.82 × 10^3
		Inconel MA754		
COF-062	1.834 × 10^{-3}	.0301	.298 × 10^6	7.57 × 10^3
COF-117	5.045 × 10^{-3}	.0827	.259 × 10^6	6.58 × 10^3
		Aluminum 2219		
COF-084	1.377 × 10^{-3}	.0226	.067 × 10^6	1.70 × 10^3

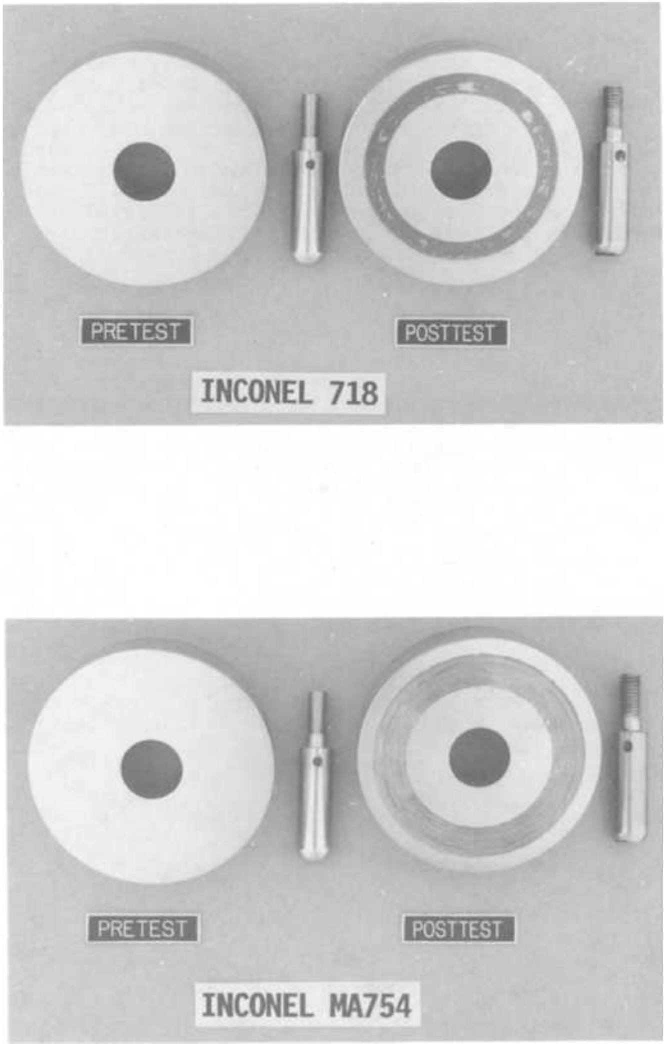

FIG. 4--Typical pretest and posttest samples.

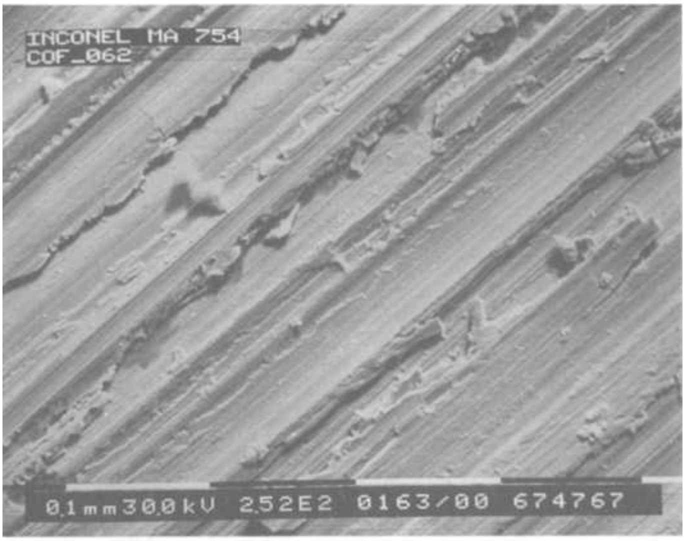

Disk

Pin

FIG. 5--Inconel MA754 posttest samples.

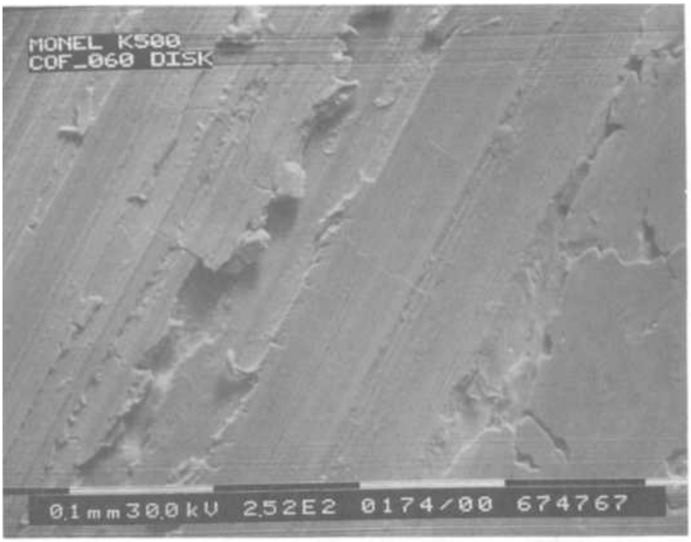

Disk

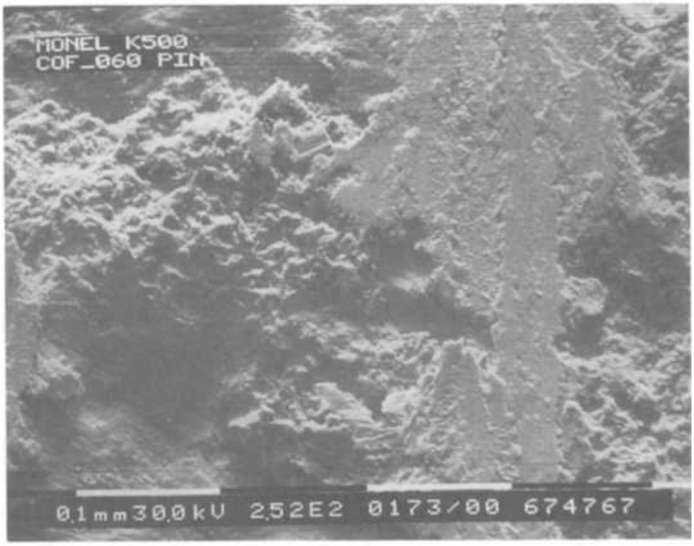

Pin

FIG. 6--Monel K-500 posttest samples.

shows a portion of the glazed track. Both materials produced a large number of burning particles from the trailing edge of the pin-disk interface.

440C Stainless Steel and Inconel 718

Figs. 7 and 8 show the 440C stainless steel and Inconel 718 posttest samples. Both of these materials were much less worn than the other test materials, with the 440C showing the least wear. Both materials formed a dark oxidized layer on both the pins and the disks.

Aluminum 2219

Aluminum 2219 had a severe adhesive wear that resulted in a rough, galled wear surface on both the pin and the disk (see Fig. 9). The total sliding distance achieved for the aluminum sample was much less than for the other samples (Table 2) because of the severe galling.

Friction Coefficient

A friction coefficient was calculated as a function of time for each material except the aluminum 2219. The severe galling of the aluminum 2219 under the test conditions did not allow a friction coefficient to be calculated. The results for a surface speed of 59.3 ft/sec (18.1 m/s) and 10 lbf (44.5 N) normal load are in Fig. 10. The sliding distances indicated in Fig. 10 are the cumulative total distances of all test runs for each sample material. Differences in the sliding distances were caused by variations in the number of test runs performed on each sample material. Despite the differences in wear characteristics, the friction coefficients for Monel K-500 and Inconel MA754 were similar to those for Inconel 718 and 440C stainless steel. The friction coefficients for Monel K-500 and Inconel MA754 appeared to be higher during the first 30 seconds of the test run, then became indistinguishable from the friction coefficients for 440C stainless steel and Inconel 718. It appears from wear data that most of the wear for each test run occurred during the first few seconds, after which a relatively steady-state wear occurred. This may indicate why the high wear materials, Monel K-500 and Inconel MA754, had higher friction coefficients during the beginning of the test run.

Comparison with Frictional Heating Test Results

The wear characteristics for Inconel MA754 in the present pin-on-disk configuration were significantly different from the previous frictional heating tests. Typical results from frictional heating tests conducted at WSTF with Inconel MA754 produced glazed-oxide coatings and no ignition at the highest PV products (1.2×10^7 psi · ft/min (410 MPa· (m/s))) available in that test. In the present test, burning particles were continuously emitted from the rubbing interface and no protective layer was developed. The maximum PV products generated for the pin-on-disk configuration after reaching a steady-state condition were estimated at 6.6×10^5 psi · ft/min (23.1 MPa · (m/s)) although higher PV products can occur during the initial wear of the pin. It has been hypothesized[3] that in the pin-on-disk configuration, the heat generation is very localized at the pin-disk interface and that the disk is principally at ambient temperature. For the hollow cylinder configuration used in the frictional heating test, high temperatures

---

[3] Personal communication with Dr. H. Julien, Professor at New Mexico State University, June 10, 1992.

Disk

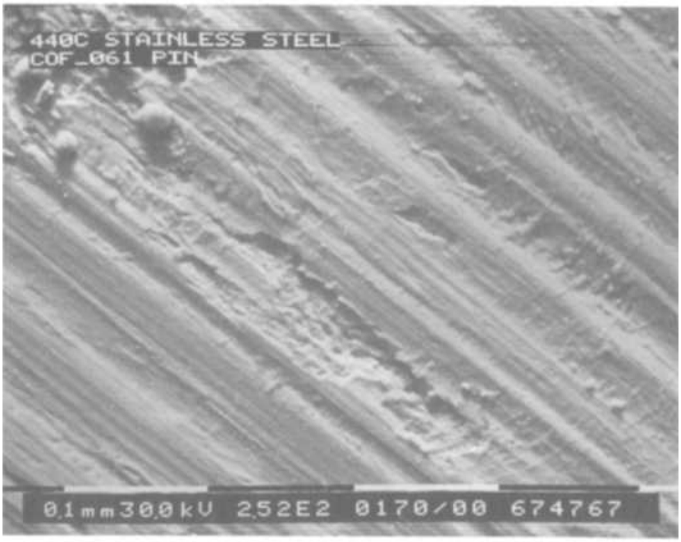

Pin

FIG. 7--440C stainless steel posttest samples.

Disk

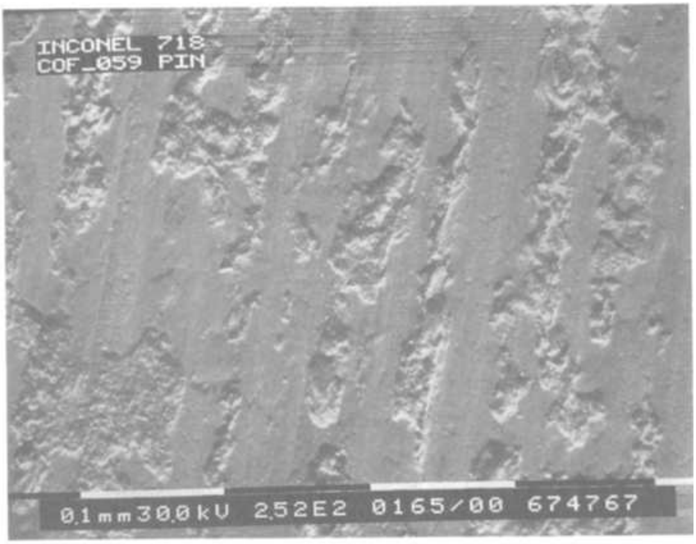

Pin

FIG. 8--Inconel 718 posttest samples.

Disk

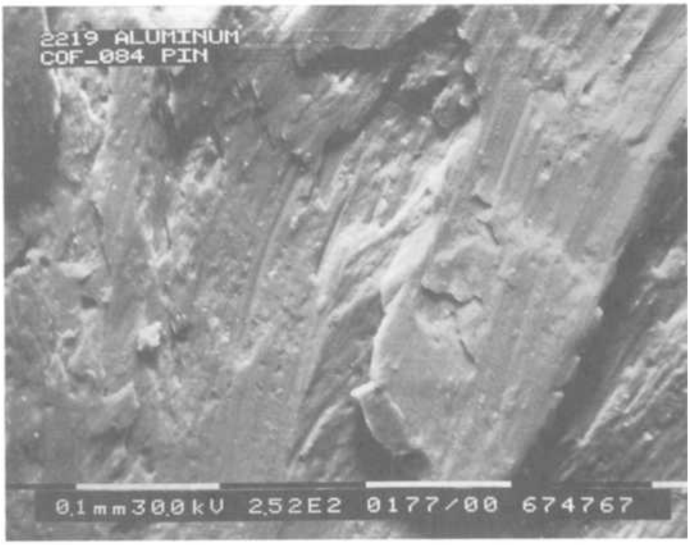

Pin

FIG. 9--Aluminum 2219 posttest samples.

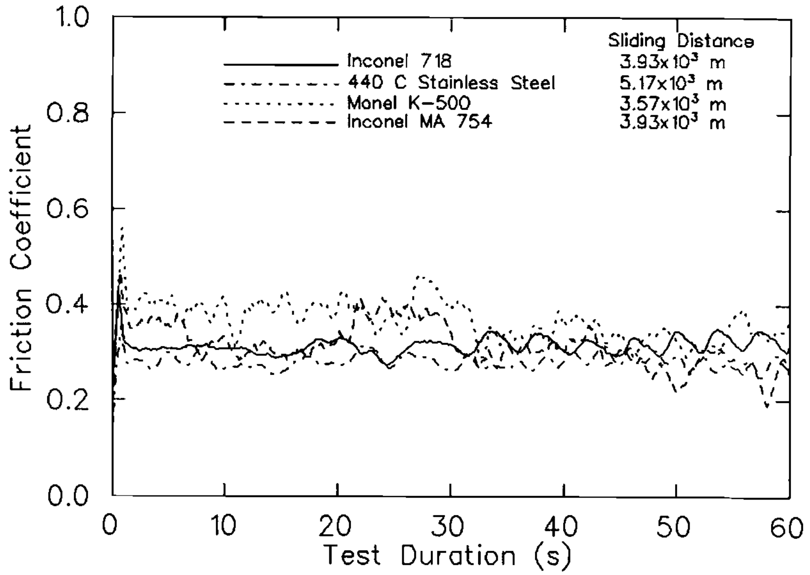

FIG. 10--Friction coefficients for tested materials.

have been measured in the stationary sample 0.20 in. (.51 cm) from the rubbing surface. It appears that the high temperatures and even surface contact of the hollow cylinder configuration promote the formation of oxide layers that would not be stable at lower temperatures while subjected to the stress concentrations at the pin-disk interface.

CONCLUSIONS

Of the materials tested, Inconel 718 and 440C stainless steel were characterized by mild adhesive wear and a smooth oxidized layer. Monel K-500 and Inconel MA754 were characterized by an adhesive/delamination wear that produced burning particles. The aluminum 2219 exhibited severe adhesive wear with high friction loads.

The use of the pin-on-disk friction configuration to evaluate the friction and wear of metals in high-pressure oxygen has led to some important insights. While the frictional heating test results have provided useful information on the ignitability of metals, the pin-on-disk test has shown that the rubbing configuration can be extremely important in assessing the wear mechanisms and surface properties that will affect the frictional heat generation and subsequent ignitability of the metal in oxygen atmospheres. Additional work should be performed to further assess the importance of wear configuration.

REFERENCES

[1] Stoltzfus, J. M., Homa, J. M., Williams, R. E., and Benz, F. J., "ASTM Committee on G-4 Metals Flammability Test Program: Data and Discussion," Flammability and Sensitivity of Materials in Oxygen-Enriched Atmospheres: Third Volume,ASTM STP 986, D. W. Schroll, Ed., ASTM, Philadelphia, PA, 1988, pp. 28-53.

[2] Benz, F. J. and Stoltzfus, J. M., "Ignition of Metals and Alloys in Gaseous Oxygen By Frictional Heating," Flammability and Sensitivity of Materials in Oxygen-Enriched Atmospheres: Second Volume, ASTM STP 910 , M. A. Benning, Ed., American Society for Testing and Materials, Philadelphia, 1986, pp. 38-58.

[3] Bryan, C. J., Stoltzfus, J. M., and Gunaji, M. V., "An Assessment of the Metals Flammability Hazard in the Kennedy Space Center Oxygen Systems," Flammability and Sensitivity of Materials in Oxygen-Enriched Atmospheres: Fifth Volume, ASTM STP 1111, Joel M. Stoltzfus and Kenneth McIlroy, Eds., American Society for Testing and Materials, Philadelphia, 1991.

[4] Stoltzfus, J. M., Benz, F. J., and Homa, J. M., "The PV Product Required for the Frictional Ignition of Alloys," Flammability and Sensitivity of Materials in Oxygen-Enriched Atmospheres: Fourth Volume, ASTM STP 1040, Joel M. Stoltzfus, Frank J. Benz, and Jack S. Stradling, Editors., American Society for Testing and Materials, Philadelphia, 1989.

Author Index

Subject Index

ISBN 0-8031-1855-4